

***Synthesis and Design of Stereogenic-at-Metal Complexes
and their Applications in Asymmetric Catalysis***

Dissertation

zur Erlangung

des Doktorgrades

der Naturwissenschaften

(Dr. rer. nat.)

dem

Fachbereich Chemie der Philipps-Universität Marburg

vorgelegt von

B.Sc.

Thomas Mietke

aus Kassel

Marburg/Lahn 2019

Original document stored on the publication server of the
Philipps University of Marburg
(German: Philipps-Universität Marburg)

<http://archiv.ub.uni-marburg.de>

Die Ergebnisse der vorliegenden Dissertation entstanden zwischen August 2013 und Oktober 2017 am Fachbereich Chemie der Philipps-Universität Marburg in der Arbeitsgruppe Meggers unter der Betreuung von Prof. Dr. Eric Meggers.

Vom Fachbereich Chemie der Philipps-Universität Marburg (Hochschulkennziffer: 1180) als Dissertation am 09.07.2019 angenommen.

Erstgutachter: Prof. Dr. Eric Meggers

Zweitgutachter: Prof. Dr. Ulrich Koert

Tag der mündlichen Prüfung: 12.07.2019

Erklärung

Ich erkläre, dass eine Promotion noch an keiner anderen Hochschule als der Philipps-Universität Marburg, Fachbereich Chemie, versucht wurde.

Ich versichere, dass ich meine vorgelegt Dissertation

*Synthesis and Design of Stereogenic-at-Metal Complexes and their Applications in
Asymmetric Catalysis*

Selbst und ohne fremde Hilfe verfasst, nicht andere als die in ihr angegebenen Quellen oder Hilfsmittel benutzt, alle vollständig oder sinngemäß übernommenen Zitate als solche gekennzeichnet sowie die Dissertation in der vorliegenden oder einer ähnlichen Form noch bei keiner anderen in- oder ausländischen Hochschule anlässlich eines Promotionsgesuchs oder zu anderen Prüfungszwecken eingereicht habe.

Ort/Datum

Unterschrift

$$\sim V \sim$$

Danksagung

Mein besonderer Dank gilt Herrn Prof. Dr. Eric Meggers für die Möglichkeit meine Promotion in seinem Arbeitskreis durchführen zu können. Ich möchte mich an dieser Stelle für die sehr interessante und offene Aufgabenstellung bedanken, die es mir ermöglicht hat, viele eigene Ideen einbringen und umsetzen zu können. Dies hat es mir ermöglicht entscheidende Erfahrungen im eigenständigen wissenschaftlichen Arbeiten zu sammeln, und meine Vorgehensweise zur Lösung wissenschaftlicher Fragestellungen weiterzuentwickeln.
– *Vielen Dank!*

Bei Herrn Prof. Dr. Ulrich Koert bedanke ich mich herzlich für die Übernahme des Zweitgutachtens der vorliegenden Arbeit. – *Vielen Dank!*

Ich danke den Mitarbeitern der NMR-Abteilung des Fachbereichs Chemie für die schnelle und kompetente Messung der benötigten NMR-Handmessungen und für den praktisch jederzeit reibungslosen Ablauf der automatisierten NMR-Messungen. Besonderer Dank geht an Herrn Gerd Häde und Frau Cornelia Mischke für das Messen zahlreicher Verbindungen.
– *Vielen Dank!*

Den Mitarbeitern der Abteilung für Massenspektrometrie und Elementaranalytik des Fachbereichs Chemie danke ich für die zügige und jederzeit zuverlässige Messung der abgegebenen MS-Proben. Ein besonderer Dank gilt besonders Dr. Uwe Linne für seine Ratschläge bezüglich kleiner und großer Probleme unserer HPLC- und LCMS-Geräte. – *Vielen Dank!*

Mein besonderer Dank gilt den Mitarbeitern der Abteilung für Kristallstrukturanalyse des Fachbereichs Chemie, Dr. Klaus Harms, Michael Marsch und Radostan Riedel, für die zügige und professionelle Messung meiner Kristalle und für die Lösung der Kristallstrukturen.
– *Vielen Dank!*

Ich bedanke mich besonders bei Dr. Thomas Cruchter und Dr. Vladimir A. Larionov für die konstruktive und professionelle Zusammenarbeit bei verschiedenen Projekten (siehe Publications) und danke beiden darüber hinaus für die wertvollen fachlichen Diskussionen ohne die die vorliegende Arbeit wahrscheinlich weit weniger erfolgreich ausgefallen wäre.
– *Vielen Dank!*

Mein besonderer Dank gilt Dr. Michael Schween und Dr. Carsten Auel für den reibungslosen Ablauf der organischen Grund-, Fortgeschrittenen- und Masterpraktika. – *Vielen Dank!*

Ich bedanke mich bei allen Mitgliedern des AK Meggers, des AK Vázquez und des AK Höhenreich für eine angenehme und konstruktive Zusammenarbeit. – *Vielen Dank!*

Ich danke meinen Bachelorstudenten Jannick Meinecke, Erik Winterling und Marc Paul Fischer sowie meinen Vertiefungsstudenten Leon Maser, Patrick Peschke, Jannick Meinecke, Erik Winterling, Theodor Peez, Fabian Daus, Frederik Buck, Martin Arnold, Andre Schmiegel, Anna Reuter, Matthias Tripp, Tabea Faber für ihre Beiträge zur vorliegenden Arbeit sowie die gute Arbeitsatmosphäre. Darüber hinaus danke ich meinen Studenten aus den organischen Grund-, Fortgeschrittenen- und Masterpraktika, die durch ihre Synthesestufen zu dieser Arbeit beigetragen haben. – *Vielen Dank!*

Dr. Jens Henker möchte ich für eine angenehme und gute Boxenpartnerschaft danken. – *Vielen Dank!*

Ich bedanke mich bei Dr. Elisabeth Martin, Dr. Melanie Helms, Dr. Nathalie Nett, Dr. Paul Nikodemiak, Dr. Thomas Cruchter, Erik Winterling, Felix Klein, Franziska Nousch, Johanna Schepp, Julia Hartmann, Tabea Faber, Thomas Dörr ausdrücklich für das Korrekturlesen von Teilen der vorliegenden Arbeit. – *Vielen Dank!*

Bei Ina Pinnschmidt, Andrea Tschirch und Dr. Lili Zhang bedanke ich mich für ihre unkomplizierte und schnelle Hilfe in allen organisatorischen Fragen. – *Vielen Dank!*

Großer Dank gebührt meinen Eltern, die mich zu jeder Zeit nicht nur in den Jahren meines Studiums jeder Lebenslage unterstützt haben und ohne deren Unterstützung mein Studium und meine Promotion nicht möglich gewesen wären. – *Vielen Dank!*

$$\sim X \sim$$

Für meine Freunde und Familie

Publications

Parts of the research results presented in this dissertation have already been published in following peer-review-article.

1. *Asymmetric Nazarov Cyclizations Catalyzed by Chiral-at-Metal Complexes*
T. Mietke, T. Cruchter, V. A. Larionov, T. Faber, K. Harms, E. Meggers
Adv. Synth. Catal. **2018**, 360, 2093–2100 (*Communication*).
 - Highlighted as VIP article by the editorial office and the referees.
 - Highlight in Synfacts (M. Lautens, A. Whyte, *Synfacts* **2018**, 14, 0729).
2. *Asymmetric Nucleophilic Catalysis with an Octahedral Chiral-at-Metal Iridium(III) Complex*
T. Cruchter, M. G. Medvedev, X. Shen, T. Mietke, K. Harms, M. Marsch, E. Meggers,
ACS Catal. **2017**, 7, 5152–5162 (*Research Article*).
 - Highlight in Synfacts (M. Lautens, I. Franzoni, *Synfacts* **2017**, 13, 0945).
3. *Suzuki Cross-Coupling for Post-Complexation Derivatization of Non-racemic Bis-Cyclometalated Iridium(III) Complexes*
T. Mietke, T. Cruchter, E. Winterling, M. Tripp, K. Harms, E. Meggers
Chem. Eur. J. **2017**, 23, 12363–12371 (*Full Paper*).
 - This Article is part of a *Chem. Eur. J.* special edition on the occasion of the 150th anniversary of the GDCh.
4. *Polymer-Supported Chiral-at-Metal Lewis Acid Catalysts*
V. A. Larionov, T. Cruchter, T. Mietke, E. Meggers
Organometallics **2017**, 36, 1457–1460 (*Communication*).

Kurzdarstellung

Teil 1: Kreuzkupplungsreaktionen in der Ligandensphäre von Iridium(III) Komplexen

Eine unkomplizierte Methode zur Modifikation von diastereomeren reinen Benzoxazol- und Benzthiazol-Iridium(III)-Komplexen im Anschluss zur Komplexierung wurde entwickelt.

Triflat- und bromfunktionalisierte Iridium(III)-Dimer-Komplexe (sieben Beispiele mit bis zu 89% Ausbeute), wurden mit Hilfe von einfach zugänglichen, chiralen Salicyloxazolin und Salicylthiazolin Hilfsliganden zu den korrespondierenden Diastereomer-Komplexen umgesetzt (Elf Beispiele mit bis zu 40% Ausbeute pro Diastereomer). Die als Diastereomengemisch erhaltenen Komplexe wurden säulenchromatografisch getrennt und im Anschluss durch SUZUKI-Kreuzkupplung modifiziert (18 Beispiele mit bis zu 94% Ausbeute).

Unter Zuhilfenahme von CD Spektroskopie und HPLC Analyse wurde ermittelt, dass die Kreuzkupplungsreaktionen an den Iridium(III)-Komplexen unter Erhalt der metallzentrierten Chiralität ablaufen. Dies ermöglicht die Synthese von enantiomerenreinen Komplexen, die mit vorherigen Methoden nur schwer zugänglich waren.

Die vorgestellte Strategie erweitert bisherige Synthesemethoden zur Herstellung von nicht racemischen Iridium(III)-Komplexen mit Anwendungen in Gebieten wie: *Life Sciences*, Material-Wissenschaft und Katalyse z. B. „Synthese eines an der Festphase immobilisierten Katalysators mit metallzentrierter Chiralität.“

Teil 2: Asymmetrische Nazarov Cyclisierung

Die Anwendung von LEWIS sauren Iridium(III)- und Rhodium(III)-Komplexen mit metallzentrierter Chiralität als Katalysatoren für die asymmetrische, polarisierte NAZAROV-Cyclisierung von 3,4-Dihydropyran- und Indol-funktionalisierten α -ungesättigten β -Ketoestern wurde entwickelt (24 Beispiele).

Bereits mit 2.0 mol% Katalysatorladung konnten hohe Ausbeuten und hohe Enantioselektivität erreicht werden. Die cyclisierten 3,4-Dihydropyran-Produkte wurden mit Ausbeuten von 85%→98%, einem *ee* von 89%→99% sowie einem *trans/cis*-Verhältnis von 15:1–50:1 isoliert (neun Beispiele), Indol-Produkte wurden mit Ausbeuten über 70%, einem *ee* von bis zu 97% sowie einem *trans/cis*-Verhältnis von 12:1→28:1 isoliert (15 Beispiele).

Im Fall der Indol-Substrate, wurde eine starke Lösungsmittelabhängigkeit zu Hexafluoro-*iso*-propanol festgestellt.

Abstracts

Part 1: Post Complexation Cross-Coupling Reactions

A straight forward method for post-complexation derivatizations of diastereomerically pure bis-cyclometalated benzoxazole and benzothiazole iridium(III) complexes was developed.

Triflate- and bromide-functionalized iridium(III) complex dimers (seven examples, up to 89% yield), were converted to the corresponding diastereomeric complexes (eleven examples up to 40% yield for each diastereomer), using readily available chiral salicyloxazolines and salicylthiazolines as ancillary ligands. The diastereomer complexes, formed as mixtures of diastereomers, were then resolved by flash chromatography and the diastereomerically pure complexes subjected to SUZUKI cross-coupling reactions (18 examples up to 94% yield).

Using CD spectroscopy and HPLC analysis it was evaluated that the post-complexation cross-coupling reactions proceed without affecting the metal-located stereocenter and hence provide post-complexation derivatized non-racemic iridium(III) complexes, which were not easily accessible with previous methods.

This strategy expands the toolbox to access functionalized non-racemic iridium(III) complexes for diverse applications in life sciences, materials sciences, and catalysis i.e.: “Synthesis of a stereogenic-at-metal catalyst immobilized on solid support.”

Part 2: Asymmetric Nazarov Cyclization Reactions

The application of LEWIS acidic stereogenic-at-metal complexes of iridium(III) and rhodium(III) as catalysts for the asymmetric polarized NAZAROV cyclization of 3,4-dihydropyran- and indole-functionalized α -unsaturated β -ketoesters was developed (overall 24 examples).

For both substrate classes, catalyst loadings of 2.0 mol% were found to be sufficient for achieving high yields and high stereoselectivities. The cyclized 3,4-dihydropyran products were isolated in 85→98% yield, with 89%→99% ee, and trans/cis ratios of 15:1→50:1 (nine examples). The cyclized indole products were isolated in more than 70% yield, up to 97% ee, and trans/cis ratios of 12:1→28:1 (15 examples).

In case of the indole substrates, a strong solvent dependence on hexafluoro-*iso*-propanol was observed.

Table of Content

1	Post Complexation Cross-Coupling Reactions.....	1
1.1	Introduction	1
1.1.1	Asymmetric Catalysis with Octahedral Stereogenic-Only-at-Metal Complexes	1
1.1.2	Stereogenic-Only-at-Metal Transition Metal Catalysts by Fontecave	2
1.1.3	Stereogenic-Only-at-Metal Complexes for Hydrogen-Bond Catalysis by Gladysz	3
1.1.4	Stereogenic-Only-at-Metal Complexes as Organocatalysts by Meggers and Gong	4
1.1.5	Synthesis of Stereogenic-Only-at-Metal Complexes from the Meggers Group	6
1.1.6	Cross-Coupling Reactions on Enantiopure Binaphthols and Applications	10
1.1.7	Cross-Coupling Reactions in the Ligand Sphere of Metal Complexes	14
1.2	Motivation	17
1.3	Results and Discussion	19
1.3.1	First Cross-Coupling Attempts Using Λ -(<i>S</i>)-C2a as Test System	27
1.3.2	Investigation of the Stereochemistry	31
1.3.3	Extending the Scope of the Cross-Coupling Procedure	37
1.3.4	Modifications on the Annulated Phenyl Ring	38
1.3.5	Modifications on the Cyclometalating Phenyl Ring	41
1.3.6	Peculiarities in the ^{19}F NMR Spectra of Diastereomer Complex Λ -(<i>S</i>)-C2e	49
1.3.7	Modifications on the Heterocycle	50
1.3.8	Experiments Towards Orthogonal Multifunctionalization	55
1.3.9	Experiments Towards Inversed Functionality	58
1.4	Applications	60
1.4.1	Attachment of Linkers for Immobilization on Solid Support	60
1.4.2	Cross-Coupling Products as Precursors for Enantiopure Lewis Base Catalysts	63
1.4.3	Access to Structural Diverse Rhodium(III) Complexes	66
1.5	Summary	68
1.6	Outlook	73
2	Asymmetric Nazarov Cyclization Reactions	75
2.1	Introduction	75
2.1.1	Nazarov Cyclization with Substrate Type A	77
2.1.2	Nazarov Cyclization with Substrate Type B	80
2.1.3	Nazarov Cyclization with Substrate Type C	83
2.1.4	Nazarov Cyclization with Substrate Type D	85
2.1.5	Iridium(III) Complexes in Nazarov Cyclization Reactions	88
2.1.6	Examples for Asymmetric Lewis Acid Catalysis from the Meggers Group	88

2.2	Motivation	92
2.3	Results and Discussion.....	93
2.3.1	Synthesis of 3,4-Dihydropyran Substrate N1	93
2.3.2	Initial Experiments and Screening Results	94
2.3.3	Exploring the Scope of Substrates N1 Yielding Nazarov Products N2	97
2.3.4	Synthesis of Indole Substrates N3	100
2.3.5	Condition Screening for Indole Substrates N3	103
2.3.6	Observed Differences in Relative Configuration	104
2.3.7	Exploring the Scope of Substrates N3 Yielding Nazarov Products N4	108
2.3.8	Absolute Configuration Assignments.....	110
2.3.9	Rationalization of the Reaction Mechanism.....	111
2.4	Summary	114
2.5	Outlook.....	115
3	Experimental Section	119
3.1	General Aspects.....	119
3.2	Chromatography	120
3.3	Spectroscopy and Spectrometry	120
3.4	Procedures	122
3.4.1	Procedure A): Br- and TfO Functionalized Dimer Complexes <i>rac</i> - C1	122
3.4.2	Procedure B): Br- and TfO-Functionalized Diastereomer Complexes C2	122
3.4.3	Procedure C): Cross-Coupling Reaction to Yield Complexes C3	123
3.4.4	Ancillary Ligand (<i>S</i>)-AL1	124
3.4.5	Ligand L1c , Dimer <i>rac</i> - C1a , Diastereomers Λ -(<i>S</i>)- C2a and Λ -(<i>S</i>)- C2a	126
3.4.6	Cross-Coupling Products Λ -(<i>S</i>)- C3a-d	133
3.4.7	Ligand L2c , Dimer <i>rac</i> - C1b , Diastereomers Λ -(<i>S</i>)- C2b and Λ -(<i>S</i>)- C2b	137
3.4.8	Cross-Coupling Products Λ -(<i>S</i>)- C3f , Λ -(<i>S</i>)- C3g and Λ -(<i>S</i>)- C3h	142
3.4.9	Ligand L3c , Dimer <i>rac</i> - C1c , Diastereomers Λ -(<i>S</i>)- C2c and Λ -(<i>S</i>)- C2c	145
3.4.10	Cross-Coupling Products Λ -(<i>S</i>)- C3h and Λ -(<i>S</i>)- C3i	153
3.4.11	Ligand L4c and Dimer <i>rac</i> - C1d	155
3.4.12	Ligand L6c , Dimer <i>rac</i> - C1e , and Diastereomers Λ -(<i>S</i>)- C2h	159
3.4.13	Ligand L5 , Dimer <i>rac</i> - C1f and Diastereomers Λ -(<i>S</i>)- C2i and Λ -(<i>S</i>)- C2i	162
3.4.14	Cross-Coupling Products Λ -(<i>S</i>)- C3l , Λ -(<i>S</i>)- C3m , Λ -(<i>S</i>)- C3n , and Λ -(<i>S</i>)- C3o	166
3.4.15	Pyreneboronic Ester P2	172
3.4.16	Acetylacetonate Complex 4d and 4e	174
3.4.17	Ligand L0a	177
3.4.18	Ligand L9 , Dimer <i>rac</i> - C1h , Diastereomers Λ -(<i>S</i>)- C2n , Λ -(<i>S</i>)- C2n and Cat. Λ - C5d	178
3.4.19	Procedure D): Synthesis of Nazarov Substrates N1 and N3	183

3.4.20	Procedure E): Synthesis of Nazarov Substrates N1 and N3	183
3.4.21	Procedure F): Nazarov Cyclizations N1 → N2	183
3.4.22	Procedure G): Nazarov Cyclizations N3 → N4	184
3.4.23	Procedure H): Synthesis of Racemic References	184
3.4.24	3,4-Dihydropyran-Functionalized α -Unsaturated β -Ketoesters	185
3.4.25	Nazarov Cyclizations with α -Unsaturated β -Ketoesters N1	192
3.4.26	Indole-Functionalized α -Unsaturated β -Ketoesters N3	210
3.4.27	Nazarov Cyclizations with α -Unsaturated β -Ketoesters N3	228
4	Appendix	263
4.1	Representative ^1H NMR and ^{13}C NMR Spectra	263
4.2	Crystallographic Data	278
4.3	CD Spectra	298
4.4	Synthesized Ligands L and Building Blocks S	301
4.5	Synthesized Ligands L , Ancillary Ligands AL and Building Blocks	302
4.6	Synthesized Racemic Complexes <i>rac</i> - C1	303
4.7	Synthesized Diastereomer Complexes Λ -(<i>S</i>)- C2 and Λ -(<i>S</i>)- C2	304
4.8	Cross-Coupling Product Complexes Λ -(<i>S</i>)- C3 and Λ -(<i>S</i>)- C3	305
4.9	Cross-Coupling Product Complexes Λ -(<i>S</i>)- C3 , Λ -(<i>S</i>)- C3 and C4e	306
4.10	Other Complexes <i>rac</i> - C4d and Λ - C5d	306
4.11	Synthesized Nazarov Substrates N1 and Building Blocks S12	307
4.12	Synthesized Nazarov Products N2	308
4.13	Synthesized Building Blocks S13 to S15	308
4.14	Synthesized Nazarov Substrates N3	309
4.15	Synthesized Nazarov Products N4	310
4.16	List of Abbreviations	311
5	Literature	321

1 Post Complexation Cross-Coupling Reactions

1.1 Introduction

The following chapters serve to provide an insight into the development of stereogenic-only-at-metal complexes, previously reported design strategies, and recent applications in asymmetric catalysis. Subsequently, a chapter on design strategies for enantiopure binaphthol scaffolds using palladium(0)/nickel(0)-catalyzed cross-coupling reactions is discussed and how these strategies can be used in affords to design stereogenic-at-metal complexes in a straightforward fashion. In the final introductory chapter, previous examples for cross-coupling reactions in the ligand sphere of metal complexes are discussed, which serve as inspiration for this project to extend the synthetic toolbox for stereogenic-at-metal complexes.

1.1.1 Asymmetric Catalysis with Octahedral Stereogenic-Only-at-Metal Complexes

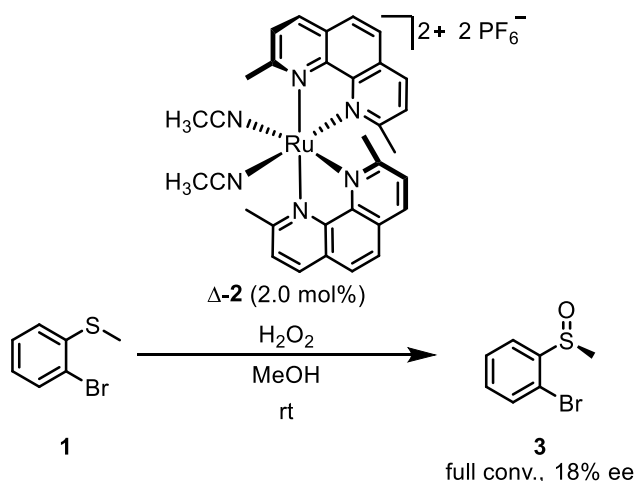
One key aspect of asymmetric catalysis is the development of new catalyst designs in order to obtain more efficient catalytic systems. In 2006 a definition for “asymmetric catalyst” was provided in a review article in “Chemie unserer Zeit”:^[1]

Complex containing a metal center and one or more ligands, from which at least one [ligand] has to be chiral. Those complexes can either be synthesized directly by inorganic or metal organic methods or be generated in-situ by multiple components. For a range of asymmetric catalysts, the structure of the active catalytic species is unknown; the (isolated) precatalyst is therefore, often mistakenly called catalyst.”

However, catalysts where exclusively achiral ligands are used, where the metal center is providing the only source of chirality through propeller-shaped arrangements of ligands, are less known.

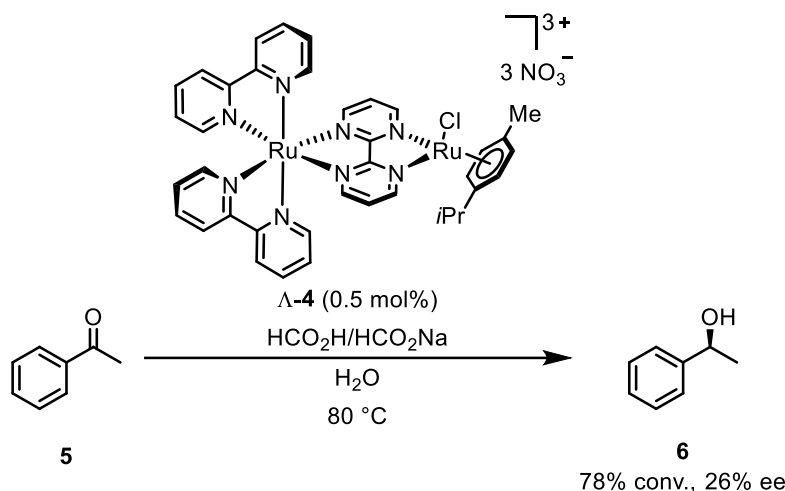
1.1.2 Stereogenic-Only-at-Metal Transition Metal Catalysts by Fontecave

Pioneering work in the field of stereogenic-only-at-metal complexes as reactive transition metal catalysts was published in 2003 by FONTECAVE and co-workers.^[2a-b] In the first work, oxidation of aryl-alkyl thioethers **1** was catalyzed by 2.0 mol% of Δ -configured ruthenium(II) complex **Δ -2** at ambient temperature using hydrogen peroxide in MeOH as oxidant. Dicationic ruthenium(II) complex **Δ -2** used as transition metal catalyst for the oxidation consists of two chelating phenanthroline and two labile acetonitrile ligands. Indeed, thioether **1** was completely converted to chiral sulfoxide **3**, however the enantiomeric excess of sulfoxide **3** was comparably low with 18% ee. Nonetheless, this work introduced the concept of octahedral stereogenic-at-metal complexes to the field of asymmetric catalysis (Scheme 1).^[2a]



Scheme 1: First application of a stereogenic-only-at-metal complex as an asymmetric catalyst in the oxidation of thioethers **1** to sulfoxides **3**. Substrate **1** was treated with 2.0 mol% of ruthenium(II) complex **Δ -2** to furnish sulfoxides **3** with 18% ee.^[2a]

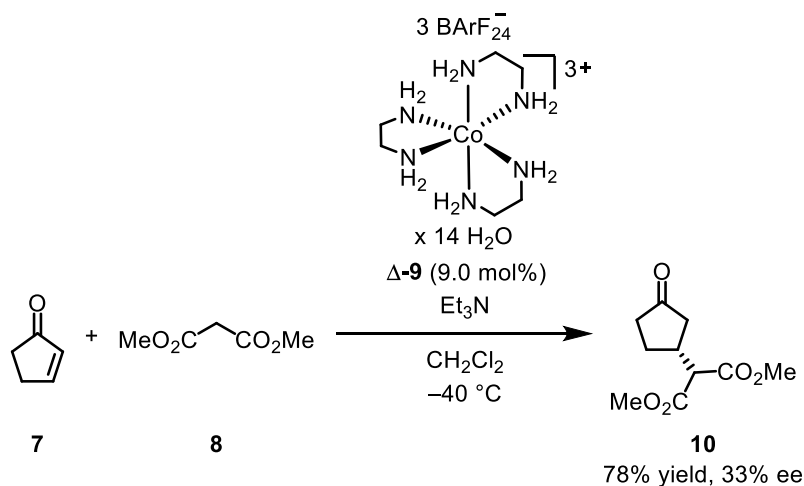
A second example was published in 2007, 0.5 mol% of binuclear complex **Δ -4** comprising two ruthenium(II) centers, was used for the asymmetric transfer hydrogenation of acetophenone (**5**) in aqueous solution of HCO_2H/HCO_2Na at 80 °C. In that case, the two ruthenium(II) center served two distinct roles: The inert octahedral Δ -configured ruthenium(II) fragment exclusively provides the chiral information which is transferred to secondary alcohol **6** upon reduction. In contrast, the ruthenium(II) half sandwich fragment provides the reactive site where the reaction takes place. Using this catalytic system, secondary alcohol **6** was obtained with 26% ee (Scheme 2).^[2b]



Scheme 2: Stereogenic-only-at-metal binuclear complex $\Delta\text{-4}$ as asymmetric catalyst for a transfer hydrogenation. Acetophenone (**5**) was treated with 0.5 mol% of complex $\Delta\text{-4}$ to furnish secondary alcohol **6** with 26% ee.^[2b]

1.1.3 Stereogenic-Only-at-Metal Complexes for Hydrogen-Bond Catalysis by Gladysz

Another early example for a reaction catalyzed by a stereogenic-at-metal catalyst is the asymmetric MICHAEL addition of dimethyl malonate (**8**) to cyclopentenone (**7**) from GLADYSZ and co-workers published in 2008 (Scheme 3).^[3]

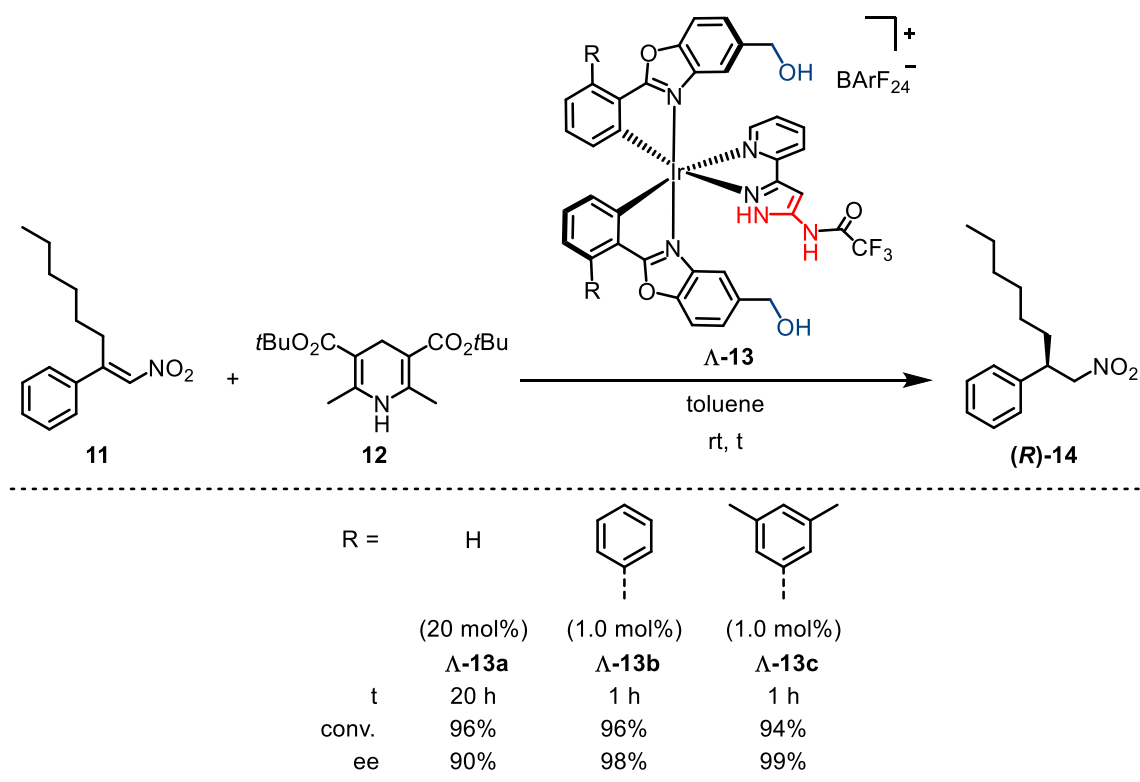


Scheme 3: Stereogenic-only-at-metal cobalt(III) complex $\Delta\text{-9}$ as hydrogen-bond catalyst. Malonate (**8**) and cyclopentenone (**7**) were treated with 9.0 mol% of complex $\Delta\text{-9}$ to furnish MICHAEL product **10** with 33% ee.^[3]

In this study, enantiopure trishomoleptic cobalt(III) ethylenediamine complex $\Delta\text{-9}$ was used as organocatalyst with 9.0 mol% loading in the presence of Et_3N in CH_2Cl_2 . The inert metal center of complex $\Delta\text{-9}$ provides the only source of chirality, the hydrogen-bond catalysis itself takes place in the ligandsphere, not at the metal-center. Using a reaction temperature of $-40\text{ }^\circ\text{C}$ and the capability of catalyst $\Delta\text{-9}$ to form hydrogen bonds to dimethyl malonate (**8**), MICHAEL addition product **10** could be obtained with 33% ee and 78% yield (Scheme 3).^[3]

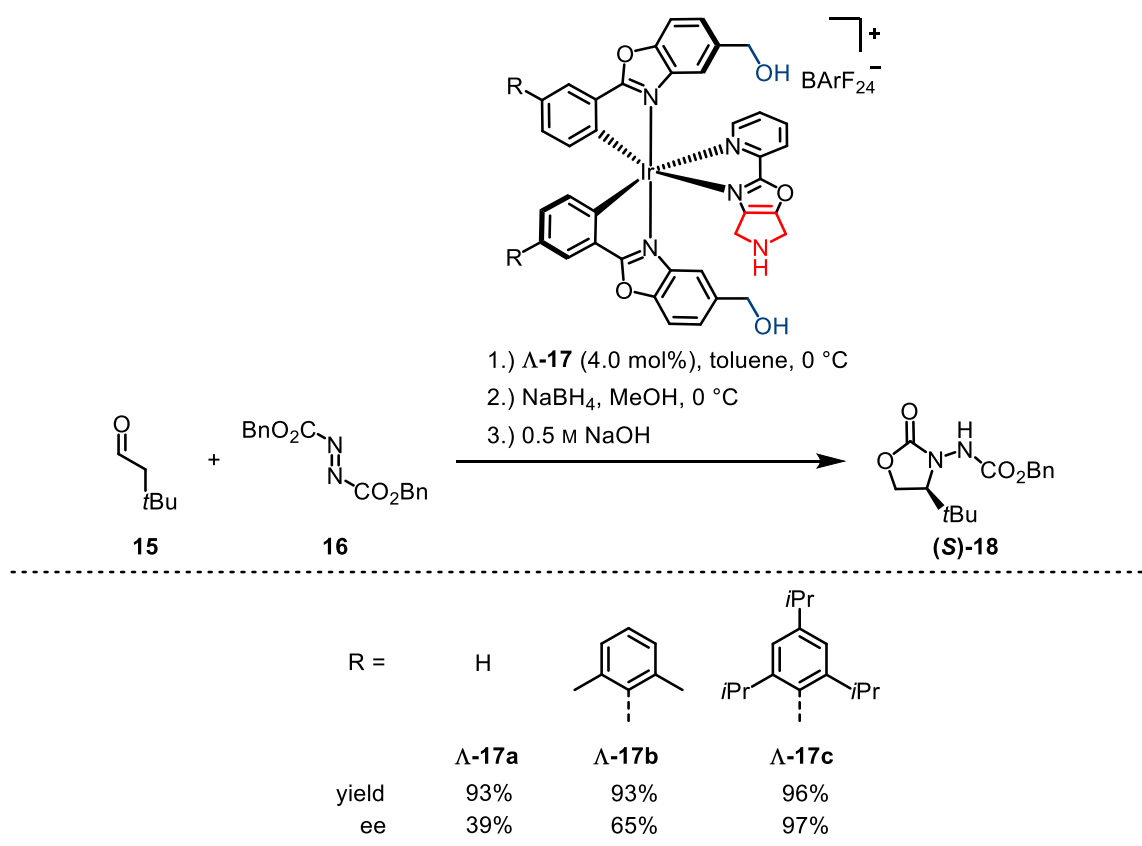
1.1.4 Stereogenic-Only-at-Metal Complexes as Organocatalysts by Meggers and Gong

In 2013, MEGGERS and co-workers reported about bifunctional stereogenic-at-metal hydrogen bonding catalysts **13** comprising two hydroxy (highlighted in blue, scheme 4) and an amidine-resembling moiety (highlighted in red, scheme 4) simultaneously activating α,β -unsaturated nitro styrene **11** and HANTZSCH ester **12**.^[4a] Through simultaneous activation and arrangement of the reactants into close proximity of each other, the transfer hydrogenation was reported to furnish β,β -difunctionalized nitroalkane (**R**)-**14** with a conversion of 94% and an excellent enantioselectivity of 99% ee within only one hour using 1.0 mol% of catalyst **13c** (Scheme 4).^[4a] The three catalysts **A-13a-c** were investigated to understand if modified cyclometalated rings would have an influence on the reaction outcome.^[4a] Indeed, the introduction of phenyl (R = Ph, catalyst **A-13b**) and 3,5-dimethyl phenyl (R = 3,5-Me₂Ph, catalyst **A-13c**) was able to reduce the necessary reaction time from 20 h to 1 h while the catalyst loading could be lowered from 20 mol% to 1.0 mol% (Scheme 4).^[4a] Moreover, introduction of phenyl (**A-13b**) and, even more, 3,5-dimethylphenyl (**A-13c**) considerably improved the enantioselectivity from 90% to 99% ee, compared to unmodified catalyst **A-13a**.^[4a] In conclusion, the modification of the cyclometalated ring is a worthwhile improvement in many aspects concerning catalyst performance (Scheme 4).^[4a]



Scheme 4: Influence of modifications of R on reaction time, conversion and enantioselectivity of the transfer hydrogenation reaction yielding nitroalkane (**R**)-**14**.^[4a]

Another catalytic system that uses a similar catalyst design is depicted in scheme 5.^[4b] Bifunctional catalysts **Λ-17** designed by H. HUO rely on hydroxy groups (highlighted in blue, scheme 5) for the activation of azodicarboxylate **16** through hydrogen bonding.^[4b] In contrast to catalysts **Λ-13**, a ligand which features a secondary amine is used to activate enolizable aldehydes **15** for reaction via enamine formation (highlighted in red, scheme 5).^[4b] In this investigated reaction sequence, aldehydes **15** were α -hydrazinated through enamine catalysis, subsequently reduced with NaBH₄ to the corresponding alcohols and then cyclized under basic conditions to chiral carbamates (**S**)-**18** (Scheme 5).^[4b] Again, significant improvement in terms of enantioselectivity was observed when the catalysts were modified on the cyclometalated ring additional hydrophobic moieties (Scheme 5).^[4b]

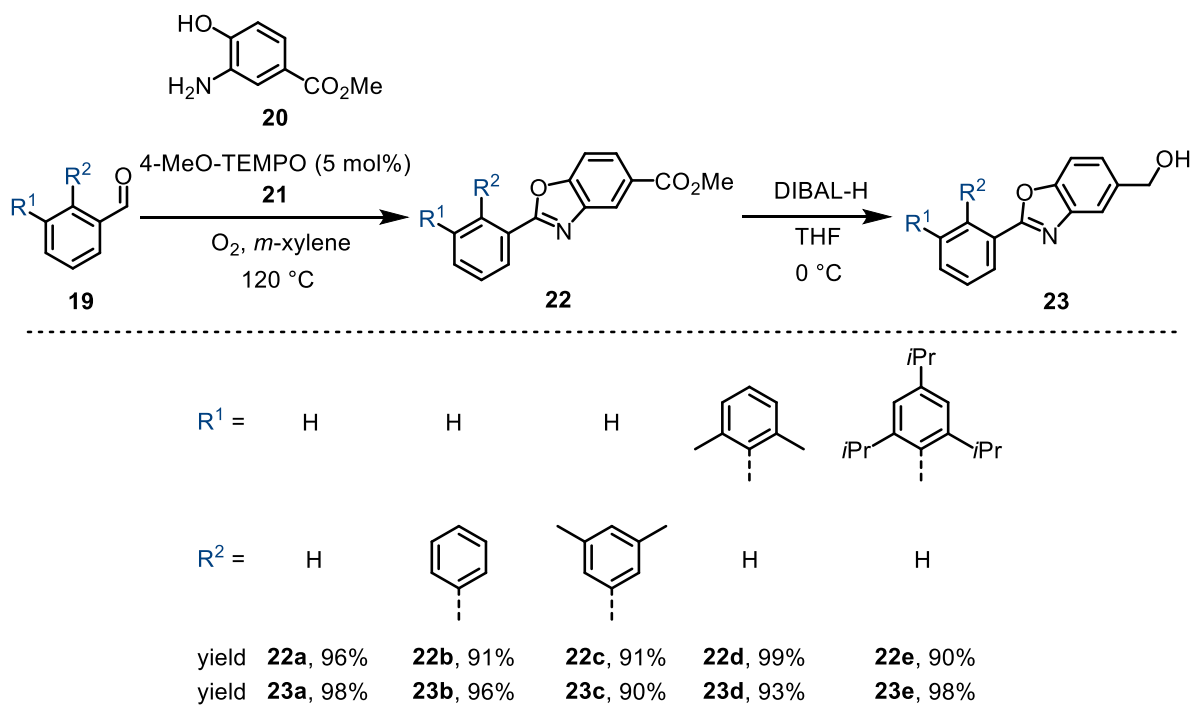


Scheme 5: Influence of moiety R on yield and enantioselectivity of the α -amination reaction yielding chiral carbamates (**S**)-**18**.^[4b] Significant improvement in selectivity is seen when R is increased in size from R = H (**Λ-17a**) via R = 2,6-Me₂Ph (**Λ-17b**) to R = 2,4,6-*i*Pr₃Ph (**Λ-17c**).^[4b]

Starting the study with catalyst **Λ-17a** (R = H) carbamate (**S**)-**18** was obtained with 39% ee. By replacing the proton with a 2,6-dimethylphenyl group (catalyst **Λ-17b**) the selectivity could be raised to 65% ee. Further improvement is achieved with the introduction of a 2,4,6-tri-*iso*-propylphenyl group (catalyst **Λ-17c**), which raised the enantioselectivity to 97% (Scheme 5).^[4b]

1.1.5 Synthesis of Stereogenic-Only-at-Metal Complexes from the Meggers Group

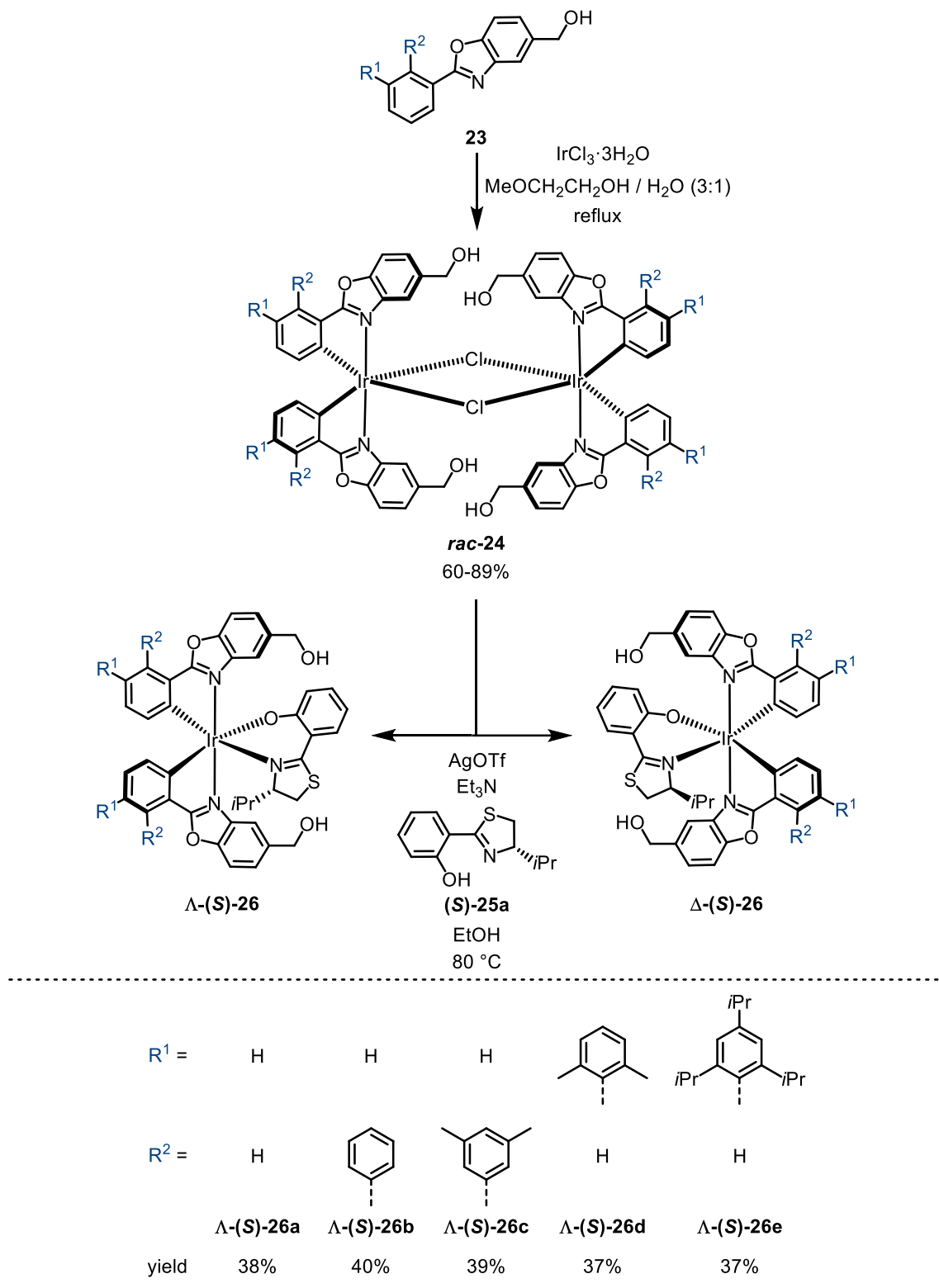
The following paragraph shall provide an insight into the synthesis strategies that were applied for the stereogenic-at-metal complexes developed in the MEGGERS group. Usually, the synthesis of such stereogenic-at-metal complexes starts off with ligand synthesis. In case a 2-phenylbenzoxazole-based ligand is used, a protocol from HAN and co-workers is utilized to assemble the according 2-phenylbenzoxazole core structure (Scheme 6).^[5a] According to this procedure, functionalized benzaldehyde **19** and 2-aminophenol **20** are *in-situ* transformed into SCHIFF bases and cyclized under aerobic conditions with 4-MeO-TEMPO (**21**) as a catalyst to obtain the desired 2-phenylbenzoxazoles **22** with yields ranging from 90% to 99%.^[4] To obtain ligands for catalysts **13** and **17**, resulting carboxylate-functionalized ligands **22** were reduced to alcohols **23** with yields ranging from 90 % to 98% using DIBAL-H as a reductant (Scheme 6).^[4]



Scheme 6: Typical example for the synthesis of a 2-phenylbenzoxazole ligand as performed in the MEGGERS group, starting with 4-MeO-TEMPO (**21**) catalyzed ring closing reaction under aerobic conditions yielding desired 2-phenylbenzoxazole **22** which is further modified by reduction to alcohol **23**.^[4]

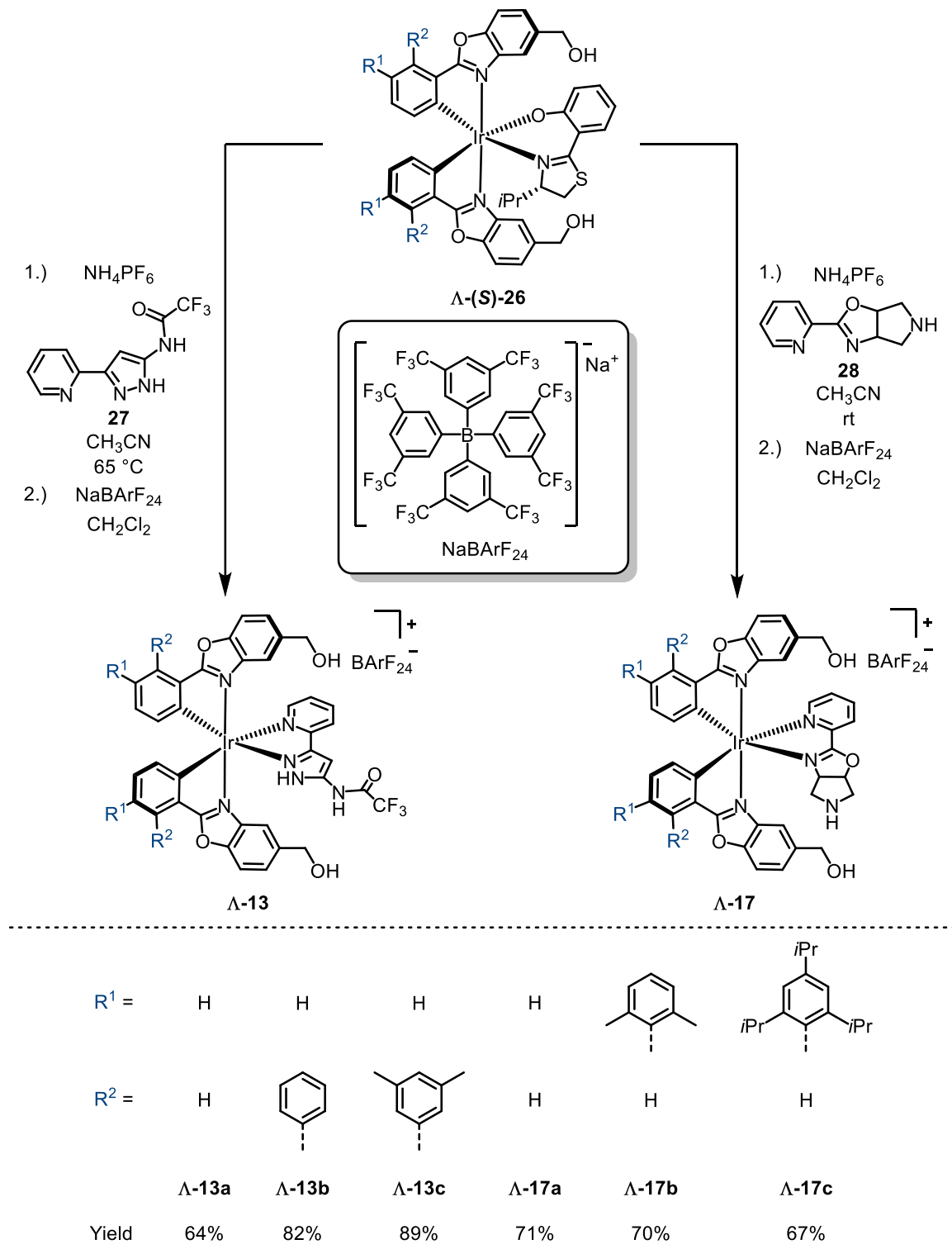
In the subsequent step, each of the ligands **23** and iridium(III) trichloride hydrate were reacted to the according racemic mixture of iridium(III) dimer complexes *rac*-**24** with yields of 60% to 89% using established NONOYAMA conditions (Scheme 7).^[6] Subsequently, dimer complexes *rac*-**24** were converted into diastereomeric complexes Λ -(*S*)-**26** and Δ -(*S*)-**26** using ancillary

ligand **(S)**-**25** in the presence of AgOTf and Et₃N.^[7e] Diastereomer complexes Λ -(**S**)-**26** and Δ -(**S**)-**26** could be readily separated by silica gel column chromatography (Scheme 7).^[4]



Scheme 7: Synthesis of diastereomerically pure stereogenic-at-metal complexes Λ -(**S**)-**26** and Δ -(**S**)-**26b** used in the MEGGERS group.^[4]

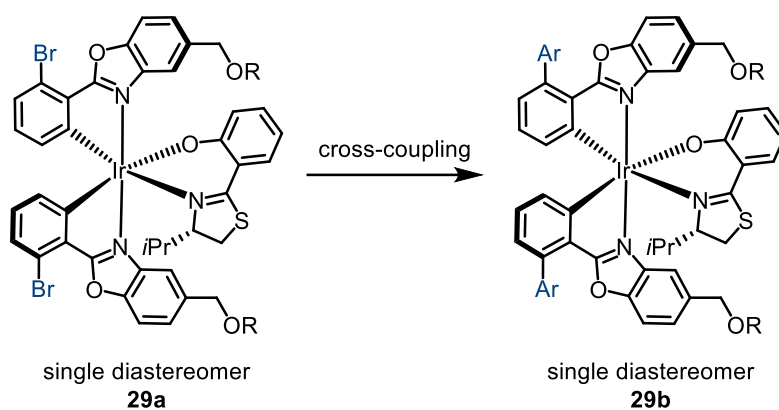
In the last step, complexes Λ -(*S*)-**26** were converted into respective catalysts Λ -**13** or Λ -**17**.^[4] To achieve this, Λ -(*S*)-**26** were treated with catalytically relevant ligands **27** or **28** under acidic conditions substituting ancillary ligand (*S*)-**25a**.^[4] For both types of catalysts, counterion metathesis (PF_6^- to BArF_{24}^-) served to enhance solubility and reactivity (Scheme 8).^[4]



Scheme 8: Applied protocol used to convert diastereomer complexes Λ -(*S*)-**26** into the respective catalysts Λ -**13** and Λ -**17**.^[4]

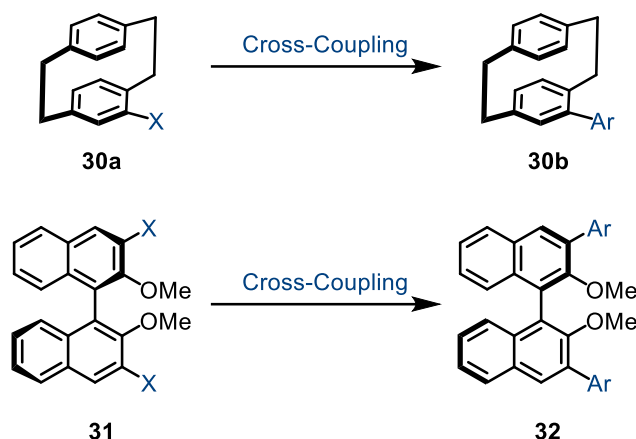
Significant advantage of this catalyst is the modular design. The functionality of ligands **23**, **27** and **28** can be finetuned independently from each other.

In metal organic chemistry, it is a common strategy to synthesize new ligands from scratch for each new complex.^[6-8] However, this strategy accumulates a large number of steps and work, in case many different complexes have to be synthesized and evaluated (Scheme 4 and 8). Moreover, the more hydrophobic the functionality of the ligands sphere becomes, the more difficult it becomes to separate diastereomers and to solely isolate one defined complex species.^[4] To avoid unnecessary steps and a tedious separation, well-resolvable (non-racemic) precursor complexes **29a** were developed. They allow derivatizations after complex formation by cross-coupling reactions to obtain modified complexes **29b** (Scheme 9). Since attachment of hydrophobic aromatic rings to the ligand sphere proofed to be beneficial in case of catalysts **13** and **17** (Scheme 4 and 5).^[4-9] Consequently, introduction of such aromatic rings by cross-coupling after complexation reactions was envisioned to be a valuable strategy (Scheme 9).



Scheme 9: Envisioned strategy: Modification after complex formation and diastereomer separation.

Inspirations for this strategy were drawn from works on other enantiopure scaffolds like planar chiral [2,2]paracyclophanes **30** and axial chiral binaphthols **31-33** (Scheme 10).^[10,11]

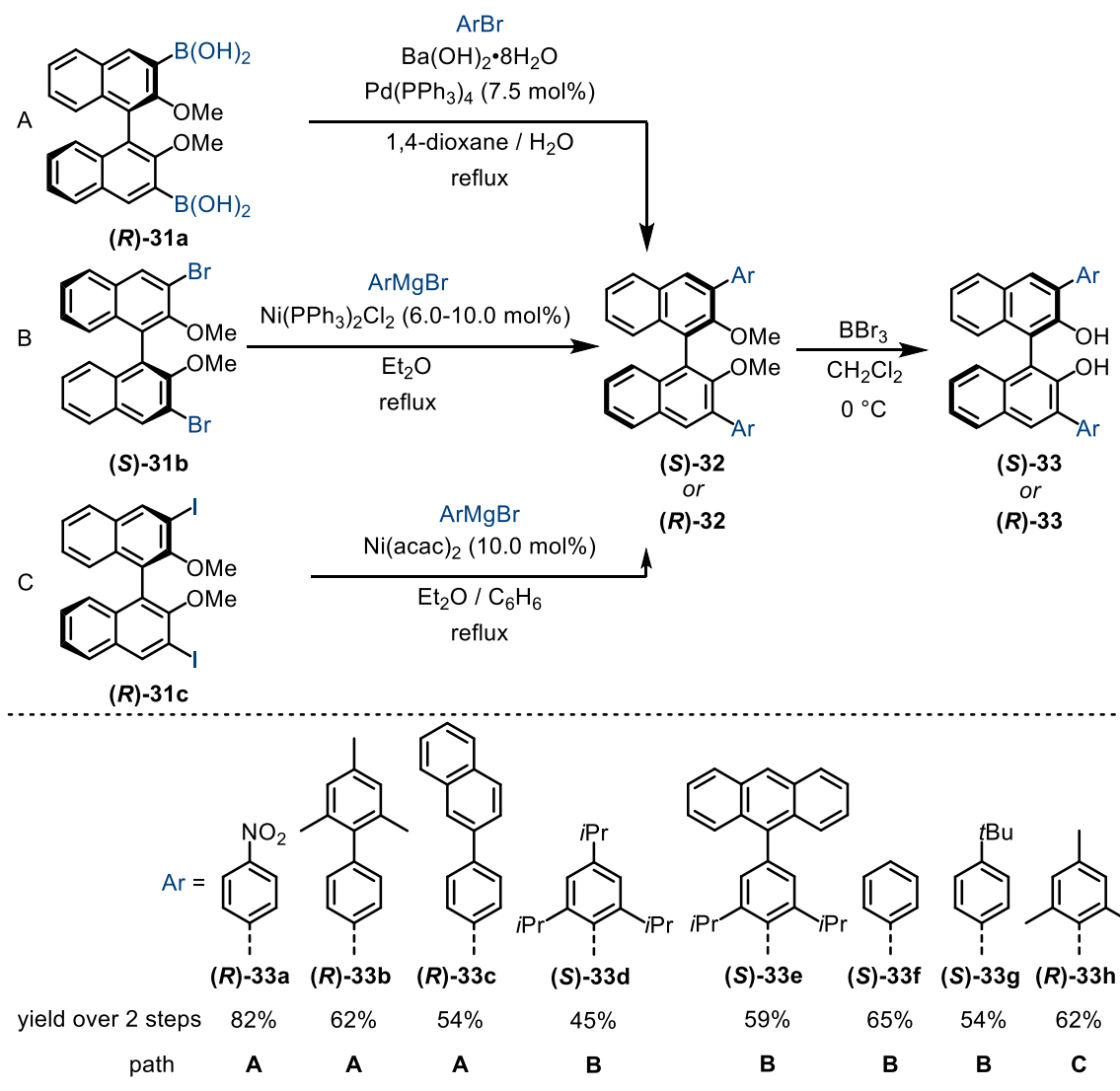


Scheme 10: Modification on enantiopure [2,2]paracyclophanes **30a** and binaphthol **31**.^[10,11]

The following section provides insights how enantiopure binaphthol derivatives **33** were modified by cross-coupling and how they were applied in the formal total synthesis of (+)-Diepoxin σ (**34**) and in the synthesis of organocatalysts **41**.^[10a,d]

1.1.6 Cross-Coupling Reactions on Enantiopure Binaphthols and Applications

A common approach to obtain structurally diverse and enantiopure binaphthol compounds is to rely on cross-coupling reactions.^[10] Common strategies are: A) An enantiopure boronic-acid-functionalized binaphthol (**R**)-**31a** is used in a palladium(0)-catalyzed SUZUKI cross-coupling reaction.^[10a,d] B) and C): Enantiopure binaphthols (**R**)-**31b** or (**S**)-**31c** functionalized with bromine ((**R**)-**31b**)^[10a,b,f] or iodine ((**S**)-**31c**)^[10b] are used in a nickel(0)-catalyzed KUMADA cross-coupling reaction. The crude cross-coupling products (**R**)-**32** or (**S**)-**32** are subsequently deprotected with BBr₃. Using these procedures, enantiopure binaphthol derivatives (**R**)-**33** or (**S**)-**33** could be obtained with yields up to 82% over two steps (Scheme 11).^[10a,b,d,f]



Scheme 11: Enantiopure binaphthol derivatives **(R)-32** and **(S)-32** were modified by cross-coupling reactions and subsequent deprotection to access an array of binaphthol derivatives **(R)-33** or **(S)-33**.^[10a,b,d,f]

For the total synthesis of (+)-Diepoxin **σ** (**34**, figure 1), JUNG and co-workers used this approach to rapidly screen binaphthol derivatives as chiral auxiliaries in an asymmetric DIELS-ALDER reaction.

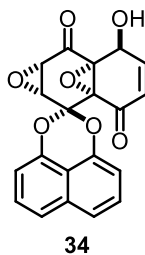
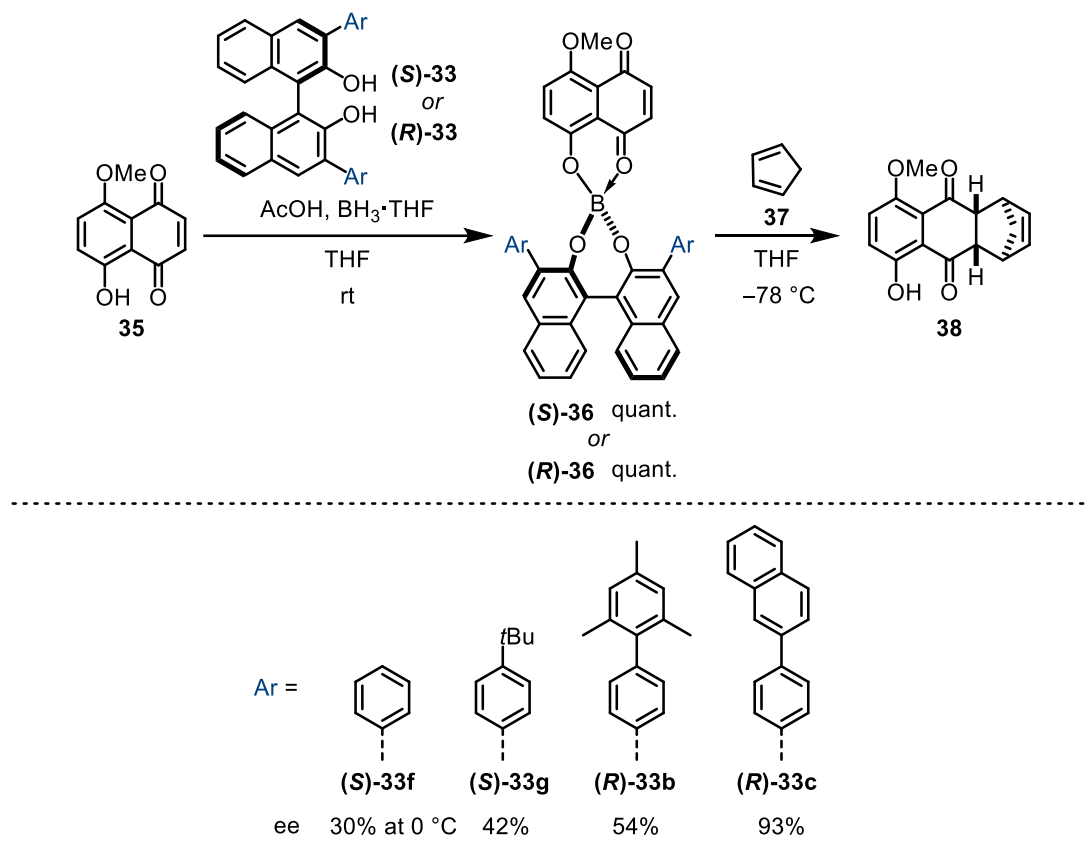


Figure 1: Synthetic (+)-Diepoxin (**34**) σ by JUNG and co-worker.

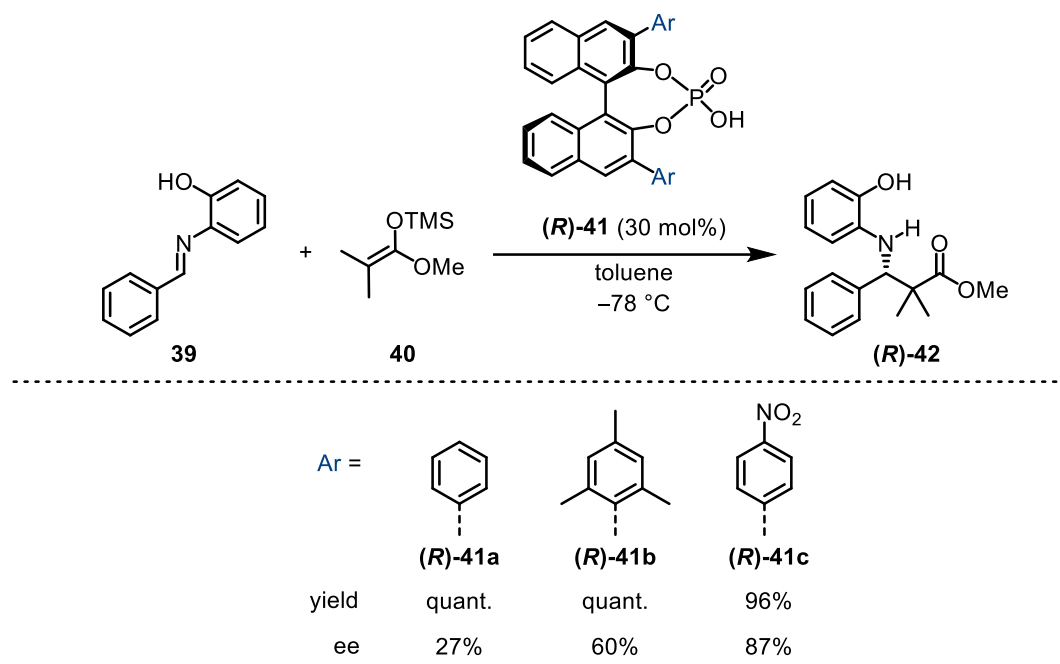
The auxiliary binaphthols **33** were quantitatively attached to the substrate **35** forming boronic acid ester **36** using acetic acid and $\text{BH}_3 \cdot \text{THF}$. Boronic acid ester **36** was then reacted with

cyclopentadiene **37** to furnish cyclization product **38**. The enantioselectivity of the reaction could be raised significantly by using appropriately modified binaphthol auxiliaries ((*R*)-**33b**, (*R*)-**33c**, (*S*)-**33f**, (*S*)-**33g**). The best enantioselectivity was obtained with *para*-(2-naphthyl)phenyl-substituted binaphthol (*R*)-**33c** providing cyclization product **38** with 93% ee (Scheme 12).^[10a]



Scheme 12: Application of enantiopure binaphthol derivatives (*R*)-**33** and (*S*)-**33** as chiral auxiliaries for an asymmetric DIELS-ALDER reaction.^[10a]

Another study where this cross-coupling strategy was used has been published in 2007 by AKIYAMA and co-workers.^[10d] In this report, binaphthol derivatives (*R*)-**33** and (*S*)-**33** were converted into chiral phosphoric acids (*R*)-**41** and (*S*)-**41**. Organocatalysts (*R*)-**41** and (*S*)-**41** were used in asymmetric-counterion-directed-catalysis (ACDC) to form chiral amino esters **42** using imine **39** and silyl ketene acetals **40**. A considerable improvement in enantioselectivity was observed by substituting the phenyl ring of catalyst (*R*)-**41a** (27% ee) with either 2,4,6-trimethylphenyl ((*R*)-**41b**, 60% ee) or *para*-nitrophenyl ((*R*)-**41c**, 87% ee) (Scheme 13).^[10d]



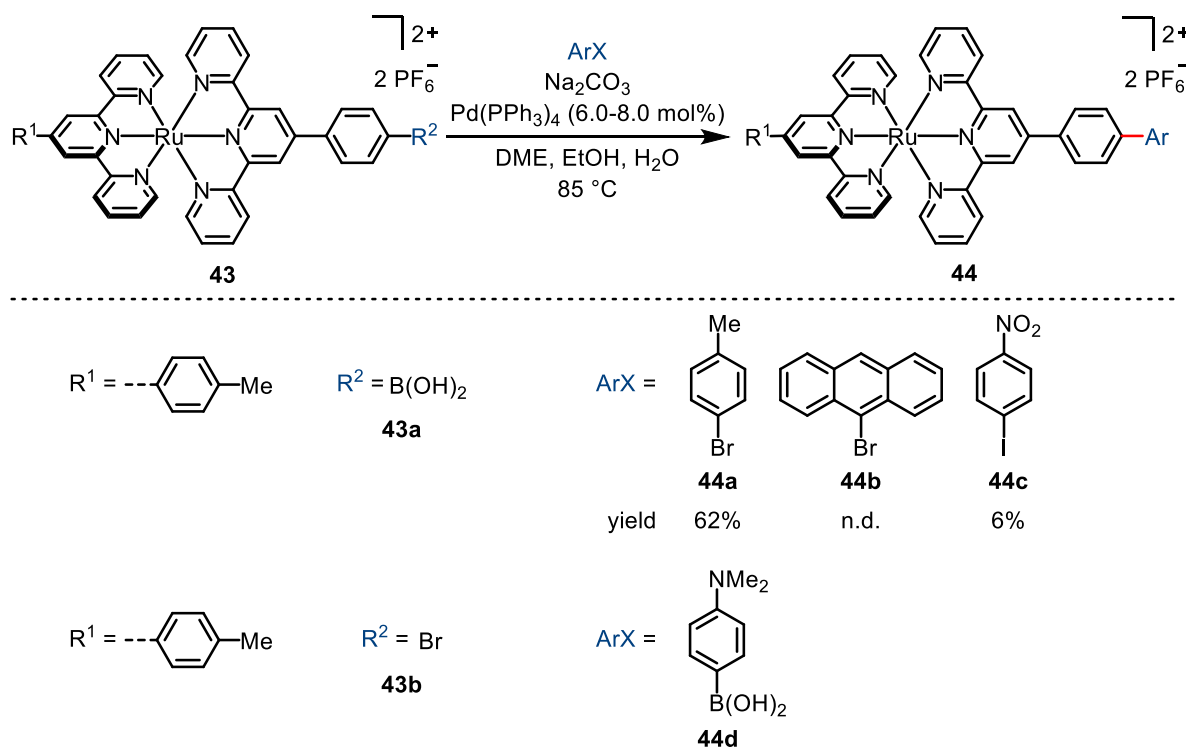
Scheme 13: Enantiopure binaphthol derivatives **(R)-31** were modified by cross-coupling reactions and subsequently converted into phosphoric acids **(R)-41**.^[10d]

Since cross-coupling reactions were successfully used in the synthesis of a diverse array of enantiopure binaphthol compounds for asymmetric follow-up chemistry, it seemed reasonable to transfer this cross-coupling strategy from axial chiral binaphthol derivatives to stereogenic-at-metal iridium(III) complexes.

The next section deals with the pioneering works from WILLIAMS and co-workers using cross-coupling reactions to modify the ligand sphere of metal complexes after complexation.^[12]

1.1.7 Cross-Coupling Reactions in the Ligand Sphere of Metal Complexes

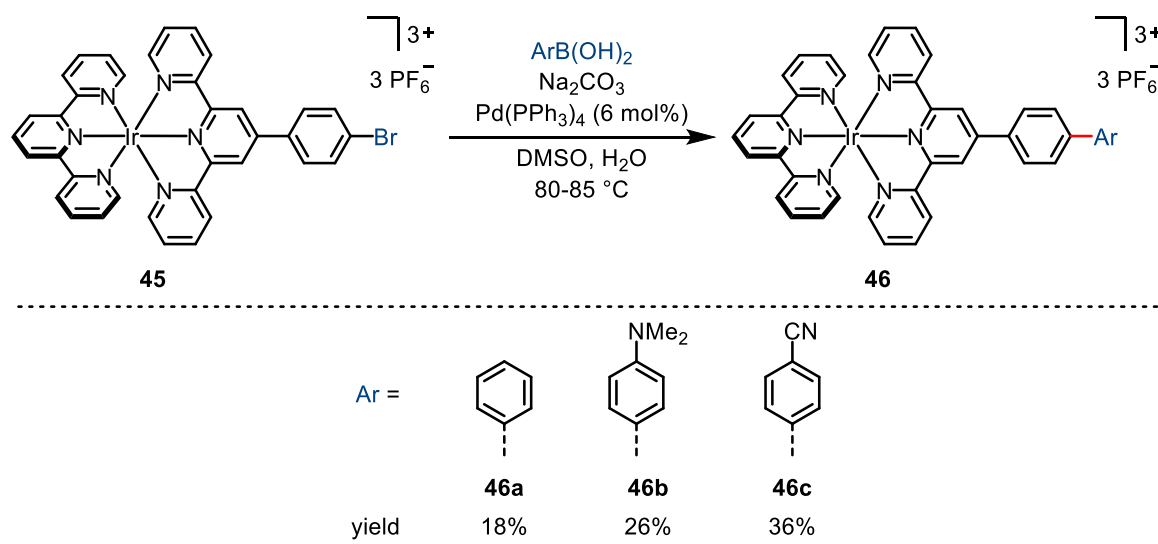
In 2001, WILLIAMS and co-workers published a method to modify ruthenium(II) complexes by SUZUKI cross-coupling reactions after the complexation step.^[12a] First, complex **43a** comprising a boronic-acid-functionalized phenylterpyridine ligand ($R^2 = \text{B(OH)}_2$) was used as trans-metalating species and bromo- and iodo-functionalized arenes were used as reagents for the oxidative addition step. The reaction was catalyzed by 6.0-8.0 mol% of $\text{Pd(PPh}_3)_4$ in presence of Na_2CO_3 in a solvent mixture of DME, EtOH, and water. The modified complexes **44** were obtained with yields ranging from 6% to 62%. In case of anthracenyl-modified complex **44b** it was reported that the cross-coupling reaction proceeded smoothly but the product decomposed afterwards. Since the ruthenium(II) complexes **43** and **44** are also photo sensitizers, it is anticipated that singlet oxygen is formed which reacts with the anthracenyl moiety in a DIELS-ALDER reaction (Scheme 14).^[12a]



Scheme 14: Study by WILLIAMS and co-workers showcasing two strategies to modify complexes by SUZUKI cross-coupling reactions using ruthenium(II) complexes **43** as substrates.^[12a]

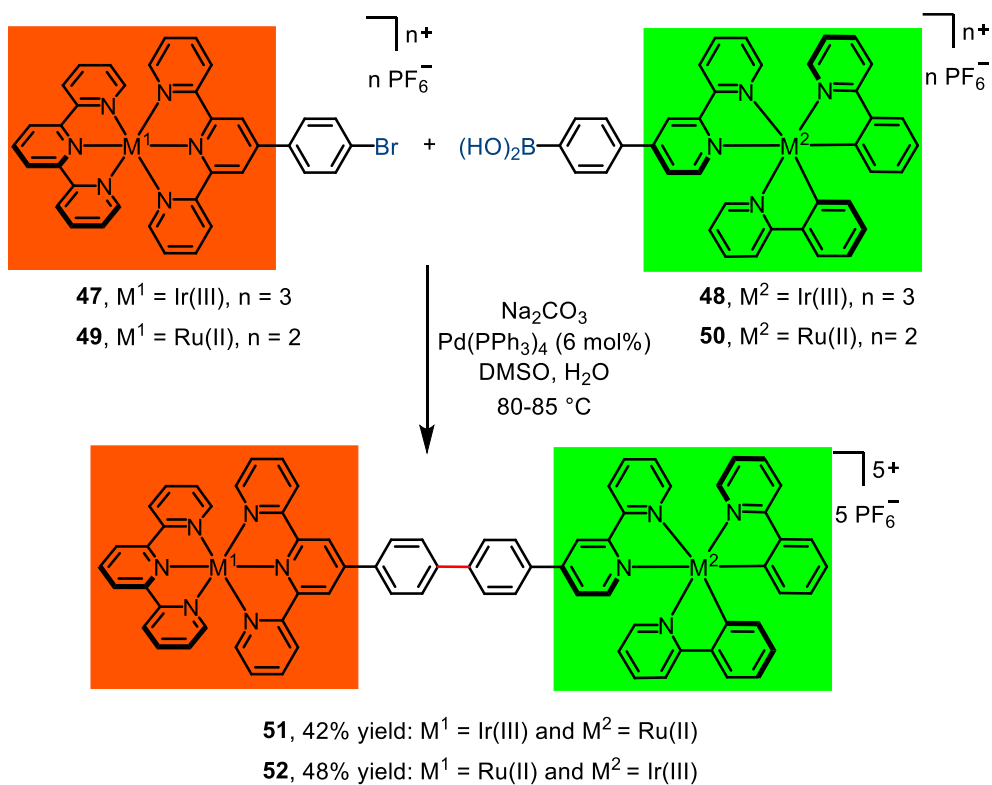
To further improve this concept, the role of the reaction partners was inverted. Therefore, a ruthenium(II) complex **43b** comprising a bromo-functionalized phenyl terpyridine ligand was reacted with *N,N*-dimethylamino phenyl boronic acid under identical reaction conditions to obtain complex **44d** with 61% yield (Scheme 14).^[12a]

In 2004, WILLIAMS and co-workers extended this cross-coupling concept to iridium(III) complexes **45** with brominated phenyl-terpyridine ligands.^[12b] The reaction was performed in a similar fashion as previously reported with ruthenium(II) complexes **43b** using DMSO/water instead of DME/EtOH/water. A set of three modified complexes was synthesized with yields ranging from 18% for phenyl-modified complex **46a**, 26% for dimethylamine-functionalized complex **46b**, and up to 36% for benzonitrile-functionalized complex **46c** (Scheme 15).^[12b]



Scheme 15: Study by WILLIAMS and co-workers extending the strategies to modify complexes by SUZUKI cross-coupling reactions using iridium(III) complexes **45** as substrates.^[12b]

In 2006, this cross-coupling reaction method was applied to appropriately functionalized mononuclear iridium(III) complexes **47** and **48** as well as to ruthenium(II) complexes **49** and **50** to obtain binuclear complexes **51** and **52** comprising two different metals.^[12d] For this reaction, the same conditions were used (Scheme 15 and 16). For the oxidative addition step, brominated phenyl-terpyridine complexes containing iridium(III) complex **47** and ruthenium(II) complex **49** were used. Iridium(III) complex **48** and ruthenium(II) complexes **50** comprising two phenylpyridine- and a phenylboronic-acid-functionalized bipyridine ligand were used as transmetalating reagents. The binuclear complexes **51** and **52** were obtained with yields of 42% (complex **51**) and 48% (complex **52**), respectively (Scheme 16).^[12d]



Scheme 16: Study by WILLIAMS and co-workers using SUZUKI cross-coupling reactions to obtain binuclear complexes **51** and **52**.^[12d]

It is important to note that the cross-coupling reaction does not take place at the backbone of each of the coordinating ligands but instead at an attached phenyl spacer (e.g. scheme 16).

1.2 Motivation

Stereogenic-at-metal iridium(III)- and rhodium(III)-complexes were successfully used as catalysts in asymmetric organic reactions by the groups of MEGGERS and GONG. Catalyst performance was improved by modifying the ligand sphere of those complexes with bulky hydrophobic groups.^[4]

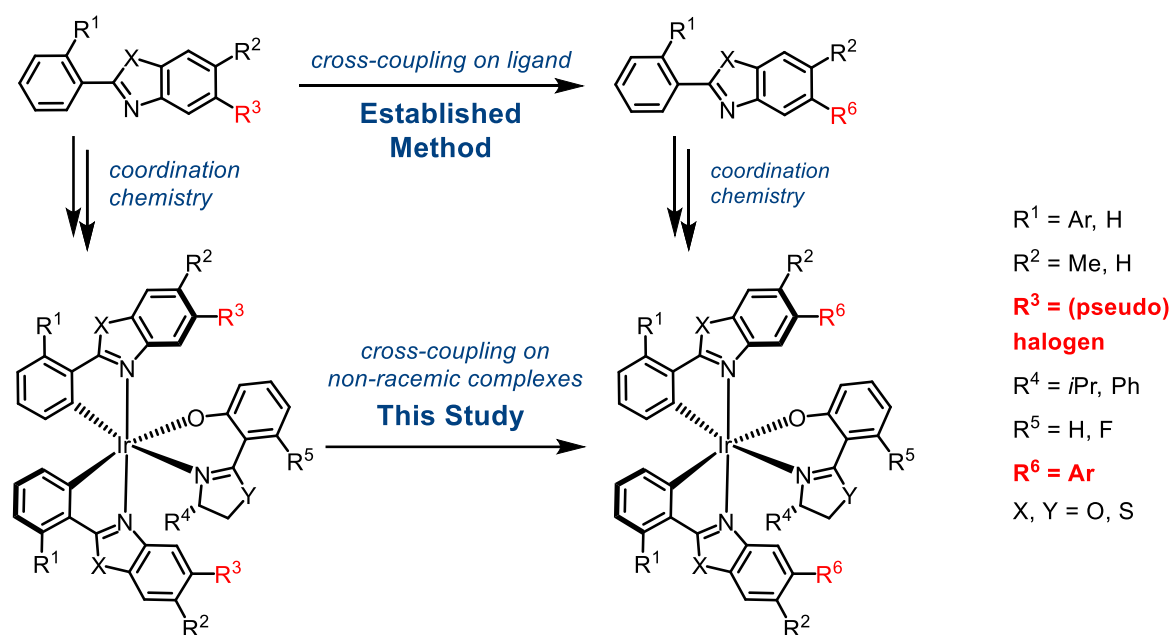
To obtain the required stereogenic-at-metal catalysts enantiomerically pure, acid-labile salicyloxazoline and salicylthiazoline ancillary ligands, which typically allow a convenient resolution of the initially formed diastereomeric precursor complexes by standard flash chromatography, are used.^[7] Subsequently, the acid-labile ancillary ligands are cleaved off to finally provide the desired enantiopure stereogenic-at-metal catalysts.^[4,9,13] However, limitations of this approach to design new catalysts were encountered. It was experienced that excessive attachment of bulky hydrophobic groups to the benzoxazole or benzothiazole core structure, often necessary for obtaining catalysts with tailored properties, frequently entails a tedious diastereomer separation as the elution of the diastereomers converges.^[4,9] Other issues involve tailing of the diastereomers, which renders it comparably challenging to isolate the second eluting diastereomer fully separated.^[4,12]

Moreover, it is a common approach in the field of cyclometalated iridium(III) complexes referring to the synthesis of libraries to modify the relevant ligands for each derivative before complexation, which accumulates in a lot of steps and work.^[8]

To avoid unnecessary steps and a tedious separation, the development of well-resolvable, (non-racemic) precursor complexes, which allow derivatizations after complex formation is desirable.

Aim of this project is to develop a method to modify isomerically pure iridium(III) complexes to gain access to a library of complexes that are difficult to obtain by conventional methods.^[4,8,9]

Using this method, it should be possible to attach unpolar aromatic groups to complexes under retention of the configuration of the metal center. Therefore, palladium(0)-catalyzed cross-coupling reactions were chosen for the modification. Accordingly, ligands containing either (pseudo-) halides for the oxidative addition step or transmetalating moieties have to be designed (Scheme 17).



Scheme 17: Synthesis of isomerically pure, biscyclometalated iridium(III) complexes with (pseudo) halide functionalized ligand sphere for post complexation modification by palladium(0)-catalyzed cross-coupling reactions.

The following section provides an overview of the applied synthetic strategy.

1.3 Results and Discussion

Starting the project, the complexes should comply with following requirements: 1.) The complexes should be functionalized at both ligands for later derivatization; 2.) The complexes should be soluble in solvents commonly used for cross-coupling reactions (xylenes, toluene, DMF, 1,4-dioxane); 3.) The precursor complexes should therefore remain neutral complexes species, favorably complexes containing chiral ancillary ligand; 4.) The diastereomer complex mixtures should be easily resolvable into single diastereomers; 5.) The ligands as well as the complexes should be readily available in just a few steps from commercially available starting materials.

Following these premises, it was at first envisioned to introduce halogen functionality into the ligand sphere of the iridium(III) complexes. Therefore, ligands **L0a-d** were utilized for complexation reactions (Figure 2).

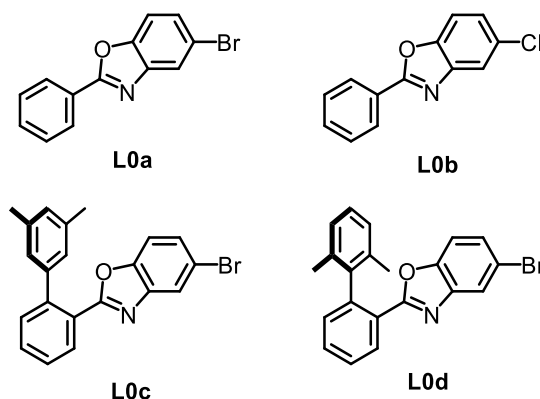
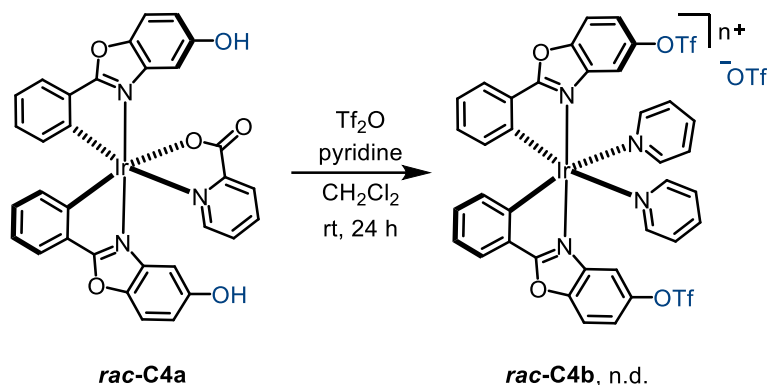


Figure 2: Initially investigated halogenated ligands **L0a-d** utilized for dimer formation und later functionalization through cross-coupling reactions.

Synthesis of dimer complexes *rac*-**C0a-d** with halogenated ligands **L0a-d** lead to the formation of yellow solids as expected. However, the obtained solids were poorly soluble in common solvents. Due to their solubility and therefore limited characterization, different moieties for the oxidative addition step of the desired cross-coupling reaction were considered. A literature known alternative is the preparation of acid esters, most notably the pseudo halogen triflate (TfO), for usage in cross-coupling reactions.^[14]

Due to the potential danger of losing the triflate groups by hydrolysis utilizing NONOYAMA's procedures,^[6] initial test reactions were carried out to functionalize racemic complexes containing hydroxy groups after complexation with Tf₂O. To establish a test system saving chiral ancillary ligand (**S**)-**AL**, complex *rac*-**C4a** was synthesized with commercially available

picolinic acid as achiral ancillary ligand (Figure 3).¹ Hydroxy complex **rac-C4b** in CH₂Cl₂ was stirred in the presents of Tf₂O and dry pyridine (Scheme 18).



Scheme 18: Initially test reaction to introduce TfO-groups into the ligand sphere of iridium(III) complexes.

Both hydroxy groups in the ligands sphere were converted into the respective triflate group (see **rac-C4b**, scheme 18). However, the chelate ligand picolinic acid was replaced by pyridine ligands in the process, leading to a mono cationic complex with two mono dentate pyridine ligands. Strikingly, triflated complex **rac-C4b** was highly soluble in CH₂Cl₂ despite the charge. Single crystals suitable for X-ray diffraction from starting complex **rac-C4a** were obtained by slow evaporation of CH₂Cl₂ and from product complex **rac-C4b** by slow diffusion of *n*-hexane into a solution of **rac-C4b** in CH₂Cl₂ (Figure 4).

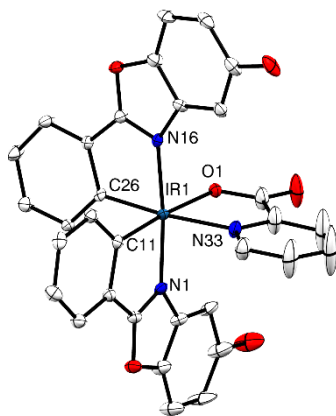


Figure 3 Structure of **rac-C4a**. ORTEP drawing with 50% probability of thermal ellipsoids, co-crystallized solvent molecules omitted for clarity. Selected bond lengths [Å] and angles [°]: C11-Ir1 2.006(5), C26-Ir1 2.009(5), N1-Ir1 2.034(4), N16-Ir1 2.042(4), N33-Ir1 2.121(4), O1-Ir1 12.168(3); C11-Ir1-C26 86.93(19), C11-Ir1-N1 80.07(18), C26-Ir1-N1 95.14(17), C11-Ir1-N16 96.26(18), C26-Ir1-N16 80.31(17), N1-Ir1-N16 174.35(15), C11-Ir1-N33 100.66(18), C26-Ir1-N33 172.27(17), N1-Ir1-N33 87.67(17), N16-Ir1-N33 97.27(17), C11-Ir1-O1 175.50(16), C26-Ir1-O1 95.67(15), N1-Ir1-O1 96.01(14), N16-Ir1-O1 87.82(14) N33-Ir1-O1 76.85(15).

¹ Racemic Dimer for the synthesis of **rac-C4a** was provided by HAOHUA HUO.

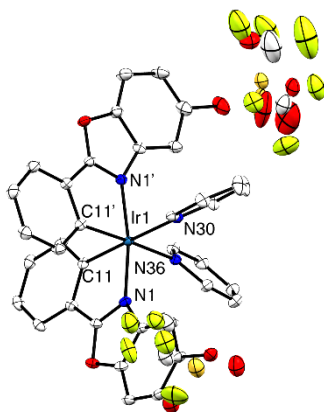
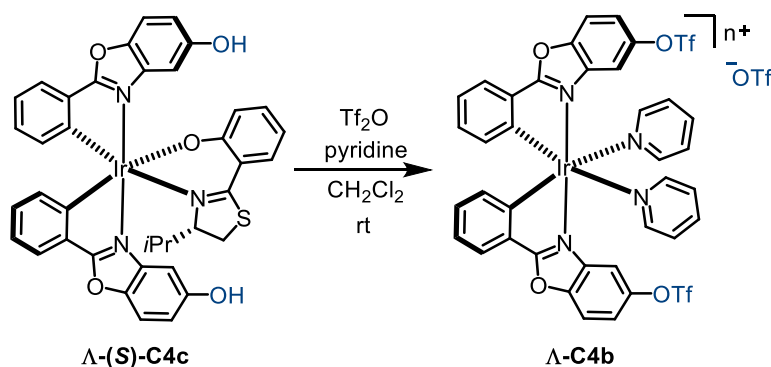


Figure 4: Structure of *rac*-**C4b**. ORTEP drawing with 50% probability of thermal ellipsoids, co-crystallized solvent molecules omitted for clarity. Selected bond lengths [Å] and angles [°]: C11-Ir1 2.026(4), C11'-Ir1 2.039(4), N1-Ir1 2.052(3), N1'-Ir1 2.057(3), N36-Ir1 2.165(3), N30-Ir1 2.169(3); C11-Ir1-C11' 85.89(14), C11-Ir1-N1 79.46(14), C11'-Ir1-N1 91.02(14), C11-Ir1-N1' 95.74(14), C11'-Ir1-N1' 80.09(14), N1-Ir1-N1' 170.22(12), C11-Ir1-N36 89.61(13), C11'-Ir1-N36 175.43(13), N1-Ir1-N36 88.92(12), N1'-Ir1-N36 99.62(13), C11-Ir1-N30 179.04(13), C11'-Ir1-N30 94.91(13), N1-Ir1-N30 99.98(12), N1'-Ir1-N30 84.92(12), N36-Ir1-N30 89.60(12).

Since the modifiable complexes *rac*-**C4b** were supposed to be obtained in an enantiopure fashion in later studies, the achiral picolinic acid would be replaced by the acid labile, chiral ancillary ligand (*S*)-**AL** to receive diastereomerically pure iridium(III) complex Λ -(*S*)-**C4c**. Since it was expected, that complex Λ -(*S*)-**C4c** would react in a similar fashion with Tf₂O under aforementioned conditions as *rac*-**C4a**, a cationic complex Λ -**C4b** would be obtained (Scheme 19).



Scheme 19: Potential side reaction for post complexation triflation.

Since good solubility of the precursor complexes is a key-criteria for the post complexation modification, different strategies were considered. Therefore, two strategies were fleshed out. One of the strategies was inspired by work of MC MURRY and COMINS.^[15] Both groups published methods and reagents **T1-4** for mild and regioselective functionalization of enolates with triflate groups (Figure 5).^[15] These achievements lead to the conclusion that mild aryl

triflimides **T1-4** could potentially tolerate the ancillary ligands on complexes *rac*-**C4a** and Λ -(*S*)-**C4c** (Scheme 18 and 19).

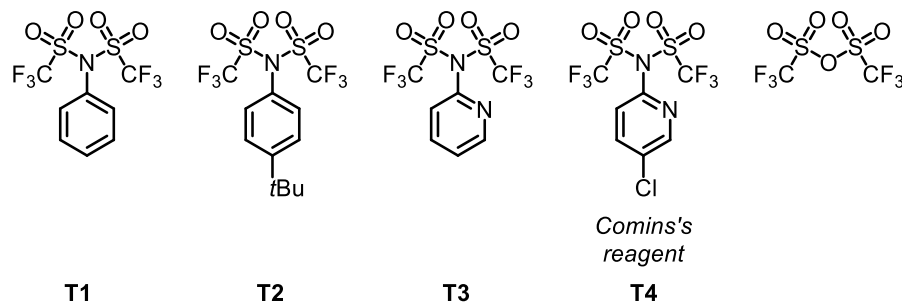
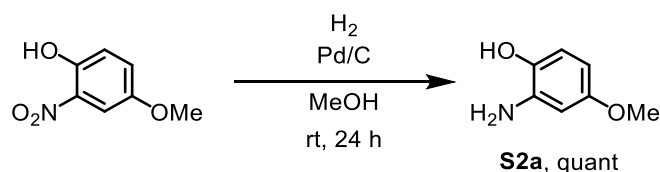


Figure 5: Reagents **T1-4** were considered for post complexation triflation of complex *rac*-**C4a** and Λ -(*S*)-**C4c**.^[15]

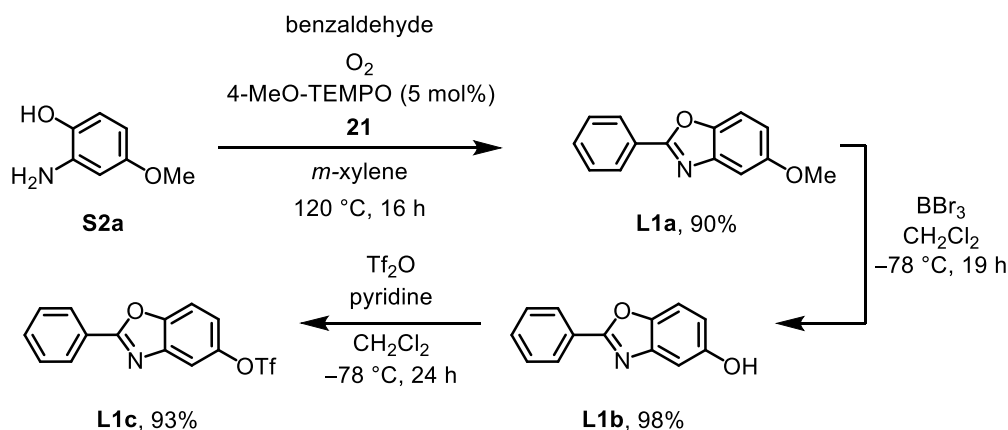
The second strategy dealt with the synthesis of an TfO functionalized ligand **L1c** (Scheme 21) in a four-step procedure to investigate, if a triflate functionalized ligand could maintain intact during dimer formation (Scheme 21 and 22).

Therefore, 2-amino-4-methoxyphenol (**S2a**) was obtained in quantitative yield by catalytic reduction of commercially available 4-methoxy-2-nitrophenol in the presents of Pd/C and hydrogen gas in MeOH solution at room temperature (Scheme 20).^[16]



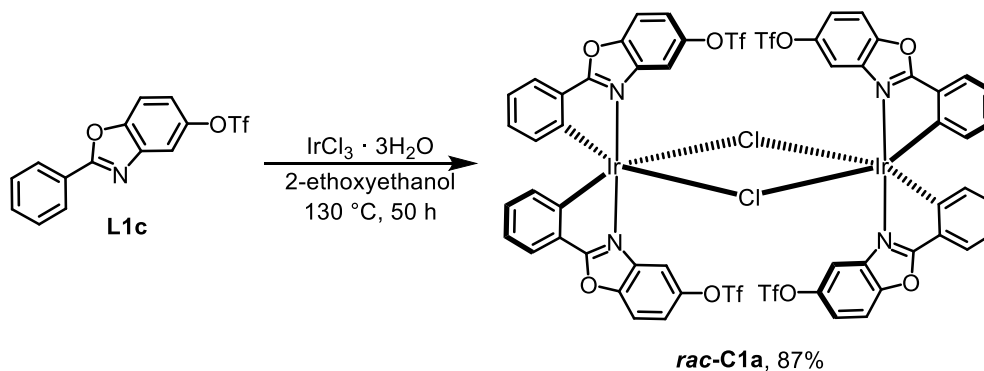
Scheme 20: Synthesis of 2-amino-4-methoxyphenol **S2a** from commercially available 4-methoxy-2-nitrophenol by hydrogenation.^[16]

Phenol **S2a** was then reacted with benzaldehyde to form the respective SCHIFF base intermediate. The ring closing reaction of intermediate was achieved in the presents of catalytic amounts of 4-MeO-TEMPO (**21**) and oxygen atmosphere to furnish ligand **L1a** with 90% as off white crystalline solid.^[5a] Ligand **L1a** was then deprotected by BBr₃ in CH₂Cl₂ at –78 °C to furnish hydroxy ligand **L1b** with 98% yield^[4b] and subsequently esterified with Tf₂O in the presents of pyridine in CH₂Cl₂ at –78 °C to obtain ligand **L1c** with 93% (81% yield over four steps, scheme 20 and 21).



Scheme 21: Synthesis of the TfO functionalized phenyl benzoxazole **L1c** in a three-step protocol.^[4b,5a,16]

Ligand **L1c** was initially subjected to standard NONOYAMA conditions to furnish iridium(III) dimer complex **rac-C1a**.^[6] Therefore, ligand **L1c** and iridium(III)chloride hydrate were suspended in a degassed 3:1 mixture of 2-ethoxyethanol and water and heated to 130 °C under exclusion of light to avoid side reactions. As expected, the complex was not obtained as the desired triflate complex. Instead, a dark substance mixture was obtained. To solve the issue, the reaction was carried out without the commonly used amount of water, instead in pure ethoxyethanol under otherwise identical reaction conditions (Scheme 22).^[6]



Scheme 22: Synthesis of the TfO functionalized iridium(III) dimer complex **rac-C1a** by modified NONOYAMA conditions.^[6]

Indeed, a red reaction mixture was obtained indicating qualitatively that complex formation took place. The solution was concentrated and dried excessively to obtain the crude product **rac-C1a** as solid.

After column chromatography, the dimer **rac-C1a** was obtained as orange powder with 87% yield based on ligand **L1c**. The received complex **rac-C1a** was well soluble in CH_2Cl_2 , rendering it possible to obtain proper analytical data. By comparison of ^1H NMR spectra with literature known complexes^[13b] it was possible to identify that the dimer **rac-C1a** was obtained

as a single diastereomer, with nitrogen atoms oriented *trans* to each other, hence only one set of seven signals is present due to all four ligands being chemically and magnetically identical. The ^1H NMR spectrum is shown in figure 6.

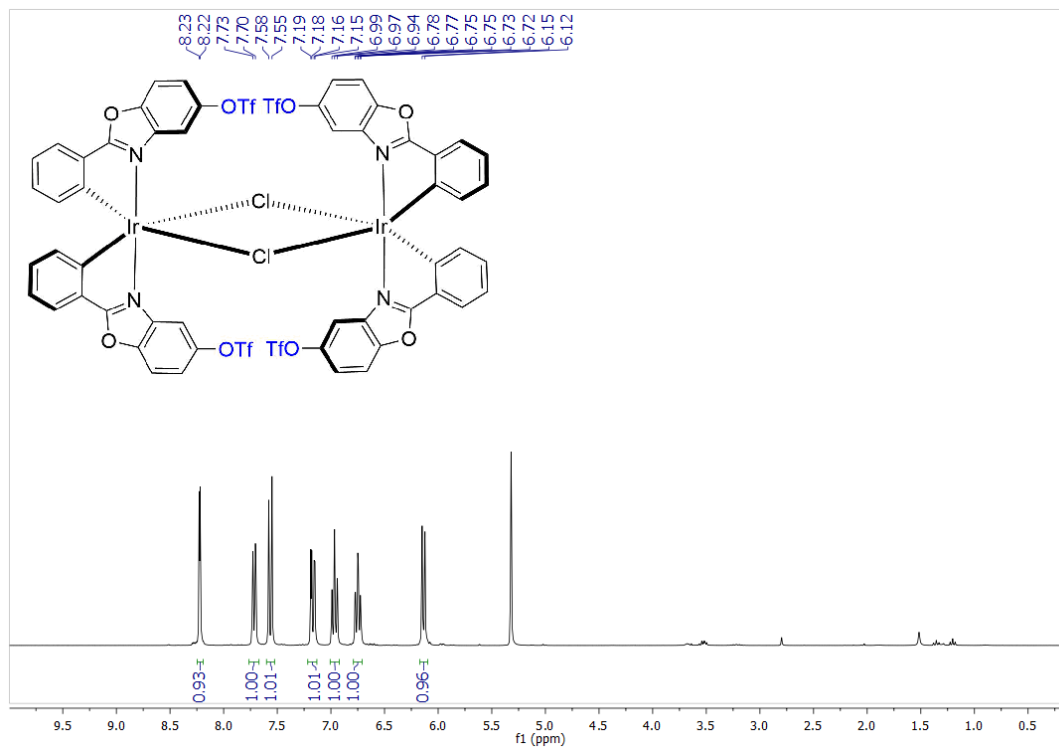
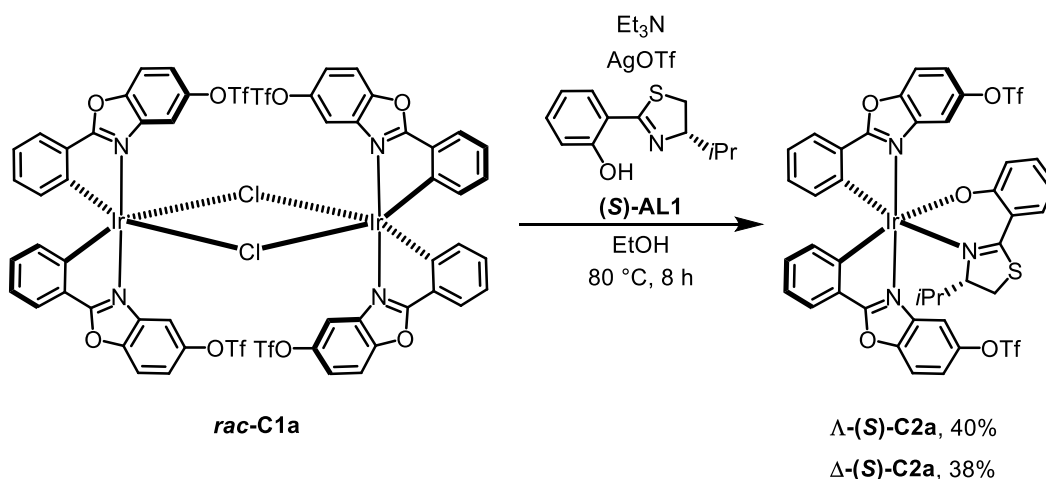


Figure 6: ^1H NMR of the triflate functionalized iridium(III) dimer complex ***rac*-C1a** in CD_2Cl_2 recorded with a Bruker Avance III at 300 MHz.

From a *cis* iridium(III) dimer complex, a set of 14 signals would be expected, since two pairs of ligands would be present.

With the confidence to have the correct complex in hand, dimer complex ***rac*-C1a** was converted into the diastereomer complexes Λ -(***S***)-C2a and Δ -(***S***)-C2a using ancillary ligand (***S***)-AL1.^[7e] Doing so, dimer ***rac*-C1a** was suspended in an EtOH solution containing ancillary ligand (***S***)-AL1 (Scheme 23).



Scheme 23: Synthesis of the diastereomeric, TfO functionalized iridium(III) complexes $\Lambda\text{-(S)-C2a}$ and $\Delta\text{-(S)-C2a}$ by established method. The diastereomeric complexes are separated by silica gel column chromatography.^[7e]

AgOTf was added to precipitate AgCl as driving force to split the dimer.^[7e] Since the chiral ancillary ligand **(S)-AL1** is acid labile and can be exchanged easily by other ligands in the presents of weak acids like NH_4PF_6 in later steps,^[13] Et_3N was applied in excess to scavenge protons released upon ligand coordination. The suspension was heated to $80\text{ }^\circ\text{C}$ and shielded from light to avoid photoinduced side reactions. Reaction control by TLC indicated early the formation of two new separable complex species.

Those complexes could be resolved by standard silica gel column chromatography to furnish complex $\Lambda\text{-(S)-C2a}$ with 40% yield and $\Delta\text{-(S)-C2a}$ with 38% yield as orange solids. Single crystals from these complexes were obtained by slow liquid-liquid diffusion of *n*-hexane into a solution of the respective complex in CH_2Cl_2 . X-ray diffraction was used to determine the metal-centered configuration of the complexes $\Lambda\text{-(S)-C2a}$ and $\Delta\text{-(S)-C2a}$ (Figure 7 and 8). Since both crystal structures illustrated nicely, that the benzoxazole ligands coordinated with nitrogen atoms trans to each other and, more importantly, remain triflate functionalized, the strategy for post complexation triflation with aryl triflimides was discontinued.

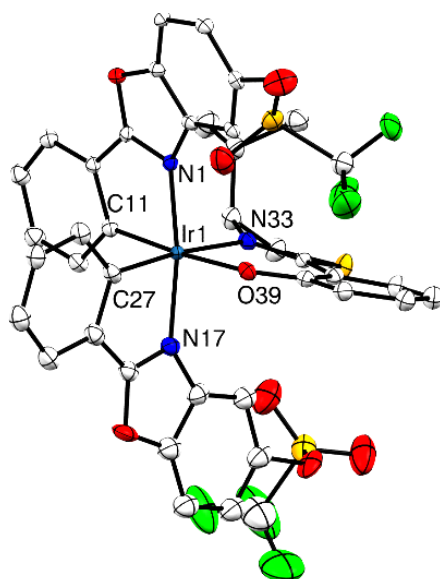


Figure 7: Structure of Λ -(*S*)-C2a. ORTEP drawing with 70% probability of thermal ellipsoids, co-crystallized solvent molecules omitted for clarity. Selected bond lengths [Å] and angles [°]: C11-Ir1 2.012(11), C27-Ir1 2.024(11), N1-Ir1 2.026(9), N17-Ir1 2.077(10), O39-Ir1 2.115(8), N33-Ir1 2.152(8); C11-Ir1-C27 88.0(4), C11-Ir1-N1 80.2(4), C27-Ir1-N1 90.2(4), C11-Ir1-N17 96.7(4), C27-Ir1-N17 80.4(4), N1-Ir1-N17 170.2(4), C11-Ir1-O39 175.0(4), C27-Ir1-O39 91.1(4), N1-Ir1-O39 94.9(3), N17-Ir1-O39 88.0(3), C11-Ir1-N33 93.4(4), C27-Ir1-N33 174.1(4), N1-Ir1-N33 95.7(3), N17-Ir1-N33 93.7(4), O39-Ir1-N33 87.9(3).

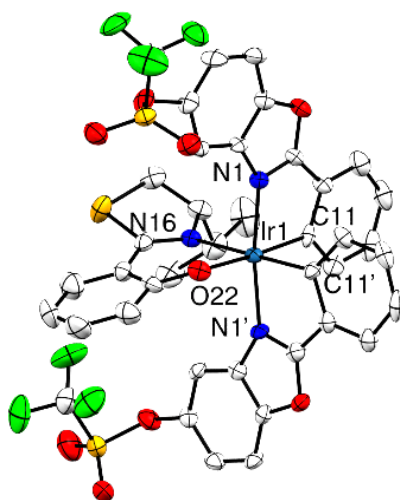


Figure 8: Structure of Λ -(*S*)-C2a. ORTEP drawing with 70% probability of thermal ellipsoids, co-crystallized solvent molecules omitted for clarity. Selected bond lengths [Å] and angles [°]: C11-Ir1 2.023(7), C11'-Ir1 2.027(4), N1-Ir1 2.035(6), N1'-Ir1 2.048(5), O22-Ir1 2.126(4), N1-Ir1 6 2.146(3); C11-Ir1-C11' 85.1(3), C11-Ir1-N1 79.5(2), C11'-Ir1-N1 92.2(3), C11-Ir1-N1' 96.7(2), C11'-Ir1-N1' 79.9(3), N1-Ir1-N1' 171.5(2), C11-Ir1-O22 175.0(2), C11'-Ir1-O22 92.6(2), N1-Ir1-O22 96.2(2), N1'-Ir1-O22 87.20(16), C11-Ir1-N16 95.8(2), C11'-Ir1-N16 178.9(4), N1-Ir1-N16 87.3(2), N1'-Ir1-N16 100.7(2), O22-Ir1-N16 86.47(19).

The assignment was further confirmed by comparison of the circular dichroism spectra (Figure 9). The depicted curve shapes act almost like mirror images, meaning that the local minima and maxima for the first diastereomer are inverted for the second diastereomer. This observation indicated that both metal centers inhabit opposite configuration. A perfect mirror image of both curve shapes cannot be expected, since both complexes are diastereomers, not enantiomers. In accordance with our previous results, it turned out that the first eluting diastereomer is Λ -(*S*) and the second Δ -(*S*) configured.^[4,13]

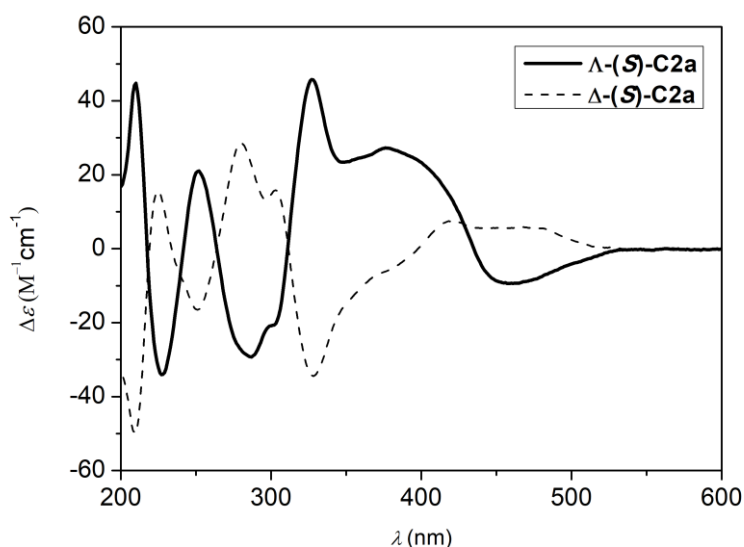


Figure 9: CD spectra of the diastereomers Λ -(*S*)-C2a and Δ -(*S*)-C2a (MeCN; 0.20 μ M).

1.3.1 First Cross-Coupling Attempts Using Λ -(*S*)-C2a as Test System

With this diastereomerically pure, triflate functionalized precursor complexes Λ -(*S*)-C2a in hand, initial cross-coupling experiments were conducted. From the subsequent post-complexation cross-coupling following features were expected: 1.) Both (pseudo)halides in the complex should take part in the cross-coupling process leading to only a single bis-derivatized product; 2.) The coupling process should require comparably mild reaction conditions to avoid decomposition of the participating complexes; 3.) The reaction should work with a broad range of commercially available, ideally bench stable, least harmful reagents and take place under easily reproducible reaction conditions.

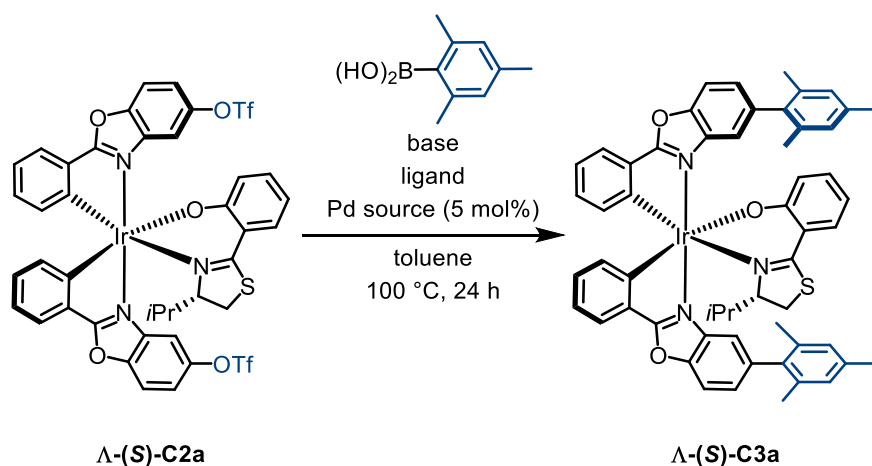
The cross-coupling method of choice was the SUZUKI coupling due to several positive features: 1.) A broad range of compounds is commercially available from a multitude of vendors. 2.) Boronic acids are air and moisture stable compared to organozinc compounds^[17a] (NEGISHI

coupling) and GRIGNARD reagent^[17b] (KUMADA coupling). 3.) Boronic acids tend to be of low toxicity compared to organotin compounds (STILLE coupling).^[18]

With the goal, to obtain complexes with bulky groups in the ligand sphere in mind, 2,4,6-trimethylphenylboronic acid was chosen as the trans metalating species for the optimization. Doing so, it was aimed to directly optimize the conditions towards sterically demanding boronic acids.

At first, SUZUKI cross-coupling reactions were performed with iridium(III) complexes **Λ-(S)-C2a** in toluene at 100 °C for 24 h. Reactions with the commonly utilized Pd-catalyst Pd(PPh₃)₄ and K₂CO₃ were neither clean nor complete after 24 h (Entry 1, table 1). In contrast, P(*t*Bu)₃ and Pd(OAc)₂ with KO^{*t*}Bu as base cleaved the Tf groups of complex **Λ-(S)-C2a** (Entry 2, table 1). Finally, complete and clean spot-to-spot cross-coupling was found with SPhos and Pd(OAc)₂ as catalyst and K₃PO₄ as base (Entry 3, table 1).

Table 1: Initial screening for suitable cross-coupling conditions.^[a]



Entry	Pd Source	Ligand	Base	Yield ^[a]	Observation
1	Pd(PPh ₃) ₄	-	K ₂ CO ₃	n.d.	incomplete reaction, sluggish conversion
2	Pd(OAc) ₂	P(<i>t</i> Bu) ₃ ^[b]	KO ^{<i>t</i>} Bu	n.d.	triflates were cleaved from complex
3	Pd(OAc) ₂	SPhos ^[c]	K ₃ PO ₄	82%	clean, spot-to-spot reaction

[a] After 24 h at 100 °C the reaction was stopped. [b] 20 mol% catalyst loading were used. [c] 10 mol% catalyst loading were used.

Since SPhos as ligand provided good yields,^[19a-b] other biaryl mono phosphine ligands like XPhos^[19c] and BI DIME^[19d] were considered (Figure 10). However, those ligands were not further considered due to higher cost factor and the optimization was continued with SPhos.^[19a-b]

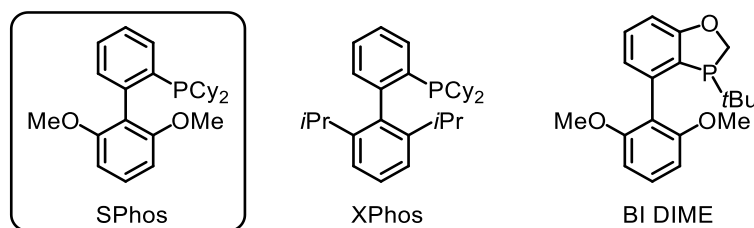
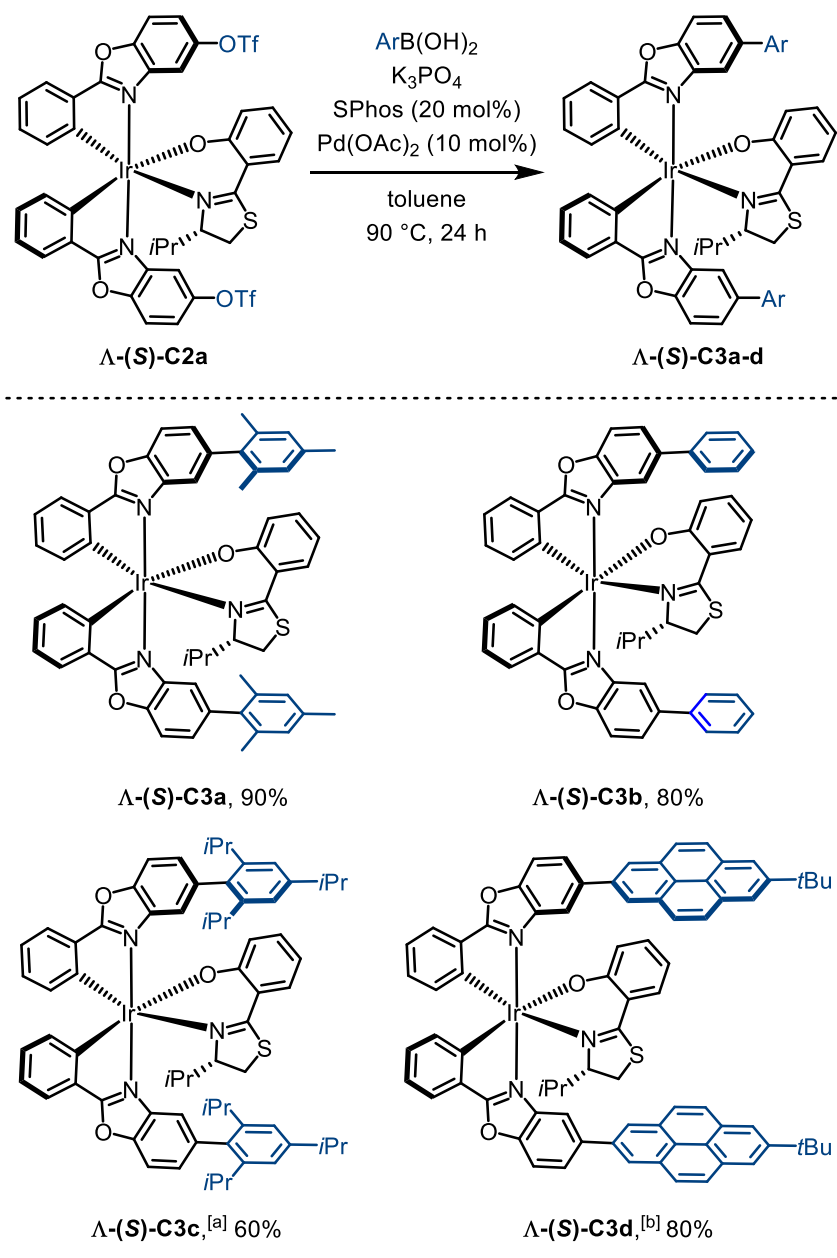


Figure 10: Considered mono phosphine ligands for cross-coupling.^[19]

In difference to the initial literature known conditions from BUCHWALD and co-workers, the catalyst loading was raised to 10 mol% of $\text{Pd}(\text{OAc})_2$ and 20 mol% SPhos to decrease the reaction time and to account for the two cross-coupled functional groups in complex **Λ -(S)-C2a**. In addition, the temperature was lowered to 90 °C to avoid side reactions and complex decomposition. Drastically improved reaction times were observed when the required potassium phosphate was employed finely grounded and thoroughly flame-dried. If potassium phosphate was used directly from the storage container, no conversion could be observed at all, instead starting material was recovered. A 200 mM concentration of pseudo-halide-functionalized iridium(III) complex **Λ -(S)-C2a** in dry and degassed toluene resulted in a good compromise between reaction time and solubility. With these optimized reaction conditions for the SUZUKI cross-coupling on iridium(III) complexes in hand, the scope of derivatives with regard towards iridium(III) complex **Λ -(S)-C2a** and different boronic acids was investigated.

Therefore, iridium(III) complex **Λ -(S)-C2a** was combined with 2,4,6-trimethylphenylboronic acid, powdered potassium phosphate, $\text{Pd}(\text{OAc})_2$, and SPhos and set under inert gas atmosphere. The heterogenous mixture was suspended in dry, thoroughly degassed toluene and heated to 90 °C over night. The reaction vessel was shielded from light to avoid photoinduced side reactions. Subsequently, complex **Λ -(S)-C3a** was obtained as orange solid after flash column chromatography with a yield of 90% (Scheme 24). These reaction conditions were repeated with phenyl boronic acid to obtain **Λ -(S)-C3b** with 80% yield (Scheme 24). Consequentially, to increase the scope towards sterically more demanding functionalization, additional cross-coupling reactions were conducted on iridium(III) complex **Λ -(S)-C2a** with different boronic acids under otherwise identical conditions. Notably, complex **Λ -(S)-C2a** could be functionalized with a considerably bulky 2,4,6-tri-*iso*-propylphenyl moiety to furnish complex **Λ -(S)-C3c** in 60% yield (Scheme 24). Thinking along these lines, introduction of an extended polycyclic aromatic functionality using this method is possible.

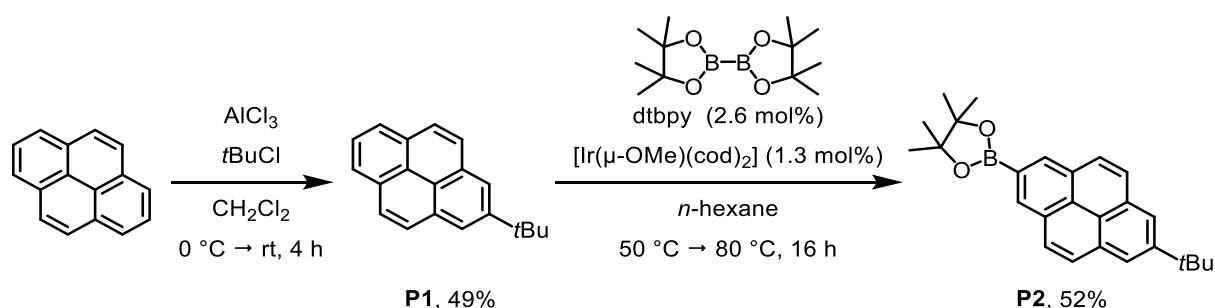


Scheme 24: Scope of cross-coupling experiments with Λ -(S)-C2a. [a] For this reaction, 6.0 eq. of the boronic acid were used instead of 4.0 eq. [b] For this reaction, boronic acid ester **P2** and 10% water as additive were used.

The attempt to cross-couple 2-(7-*tert*-butylpyren-2-yl)-4,4,5,5-tetramethyl-1,3,2-dioxaborolane (**P2**) with iridium(III) complex Λ -(S)-C2a proceeded smoothly, which demonstrates that pinacol boronic ester can be applied to this procedure if a slight amount of degassed water is present, yielding complex Λ -(S)-C3d with 80% (Scheme 24).

Following a protocol from TODD MARDER and co-workers, pinacol boronic ester **P2** was synthesized in a two-step synthesis starting from commercially available pyrene.^[20] In accordance with this procedure, pyrene was functionalized with *tert*-butyl chloride and AlCl_3 as LEWIS acid in a FRIEDEL-CRAFTS-alkylation reaction yielding pyrene **P1** with 49% yield

followed by a regioselective iridium(I) catalyzed CH borylation.^[20] For the CH activation, the commercial methoxy bridged $[(\text{Ir}-\mu\text{-OCH}_3)(\text{cod})]_2$ iridium(I) dimer complex and dtbpy as ligand were used as catalyst, with pinacol diboron as borylation agent in dry *n*-hexane as unpolar solvent (Scheme 25).^[20]



Scheme 25: Synthesis of the pyrene boronic acid ester **P2** by established method from MARDER.^[20]

1.3.2 Investigation of the Stereochemistry

Since the method should be applied to obtain catalysts with tailored properties, it is crucial that the cross-coupling reaction in the ligand sphere proceeds under retention of the metal centered configuration. Since the cross-coupling products contain two stereocenters, two sets of signals would appear in ^1H NMR spectra, if one of the stereocenter, either the chiral carbon on the ancillary ligand or the metal center, would racemize. Suitable probes to determine diastereomeric ratio are the methyl groups of the aromatic rings, displayed as strong, baseline separated singlets. Since no second diastereomer can be observed in the ^1H NMR spectrum of complex $\Lambda\text{-(S)-C3a}$ two conclusions can be drawn: 1.) The amount of second diastereomer $\Lambda\text{-(R)-C3a}$ and/or $\Lambda\text{-(S)-C3a}$ is below the detection limit of the chosen ^1H NMR experiment. 2.) Both stereocenter racemized, therefore the enantiomer $\Lambda\text{-(R)-C3a}$ of the desired product would provide an identical set of signals as $\Lambda\text{-(S)-C3a}$ (Figure 11).

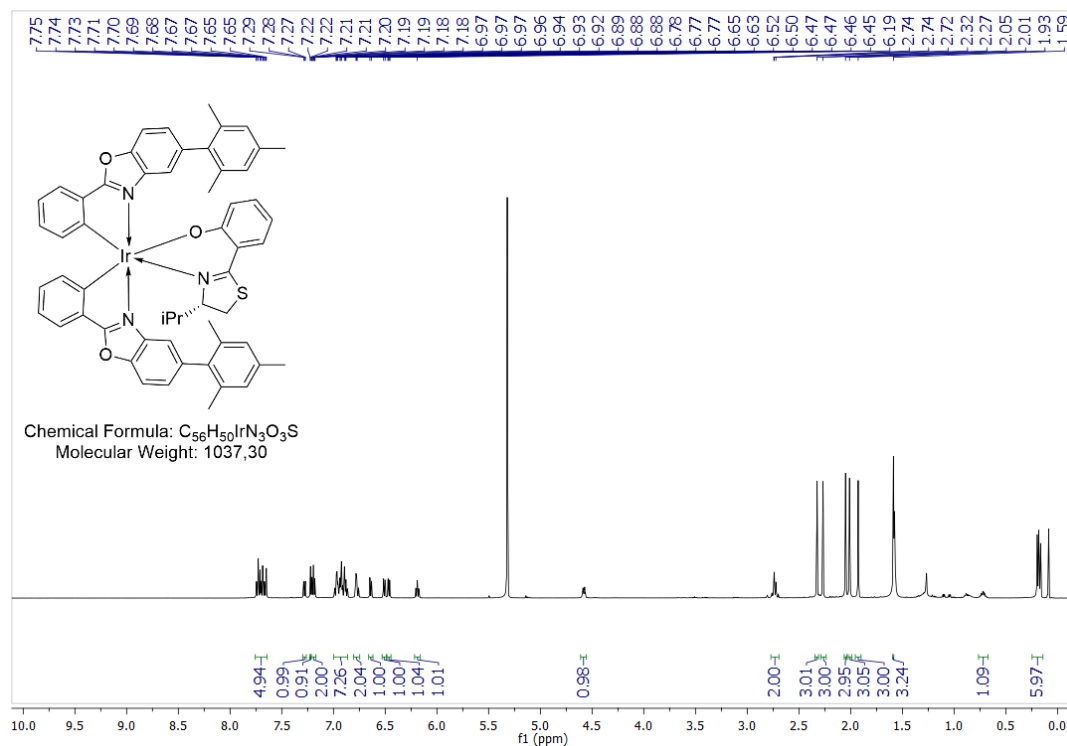


Figure 11: 1H NMR of the modified iridium(III) complex Λ -(S)-C3a in CD_2Cl_2 recorded with a *Bruker Avance III* at 300 MHz.

To investigate if both stereocenters did racemize, CD spectra of the cross-coupling product complexes Λ -(S)-C3a and Λ -(S)-C3c were superimposed with precursor complex Λ -(S)-C2a. Since all three complexes lead to the same characteristic curves with minima and maxima at comparable wavelengths, it can be assumed that all three complexes Λ -(S)-C3a, Λ -(S)-C3c and Λ -(S)-C2a share the same metal centered configuration (Figure 12).

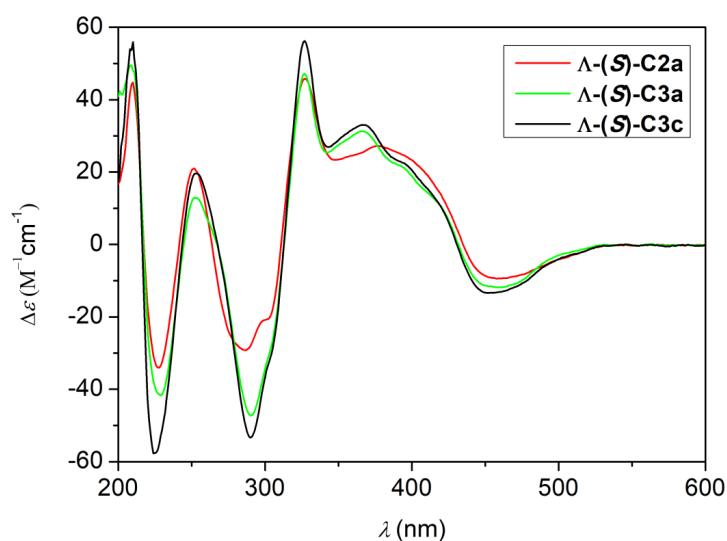
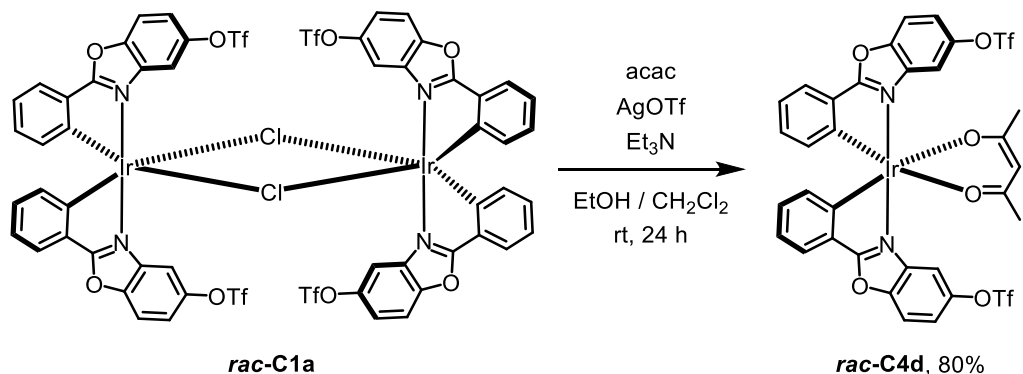


Figure 12: Superimposed CD spectra of the product complexes Λ -(S)-C2a (red), Λ -(S)-C3a (green) and the precursor complex Λ -(S)-C3c (black) (MeCN; 0.20 mM).

However, CD spectra were not considered to give quantitative information about potential, partial racemization of either stereocenter. Since ^1H NMR and CD spectroscopy did not exclude partial racemization of the complex, a representative HPLC experiment was carried out. The HPLC experiment should deliver the necessary information to showcase that the developed post-complexation cross-coupling approach is capable to furnish enantiopure complexes. Therefore, the cross-coupled diastereomer complex was converted into a stereogenic-only-at-metal complex.

The racemic reference for this experiment was obtained by converting the racemic dimer complex *rac*-C1a into the racemic triflate functionalized acetylacetone complex *rac*-C4d (Scheme 26). The utilized protocol for this kind of reaction is analogue to the synthesis of the diastereomer complexes, using CH_2Cl_2 as co-solvent for better solubility and therefore lower temperature.



Scheme 26: Synthesis of the racemic stereogenic-only-at-metal acetylacetone complex *rac*-C4d.

A crystal structure of the racemic complex **rac-C4d** was obtained by slow diffusion of *n*-hexane into a solution of **rac-C4d** in CH₂Cl₂ (Figure 13).

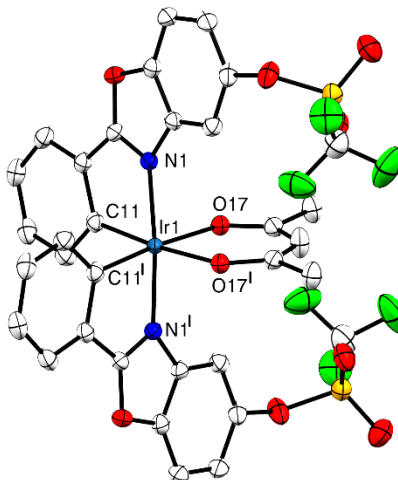
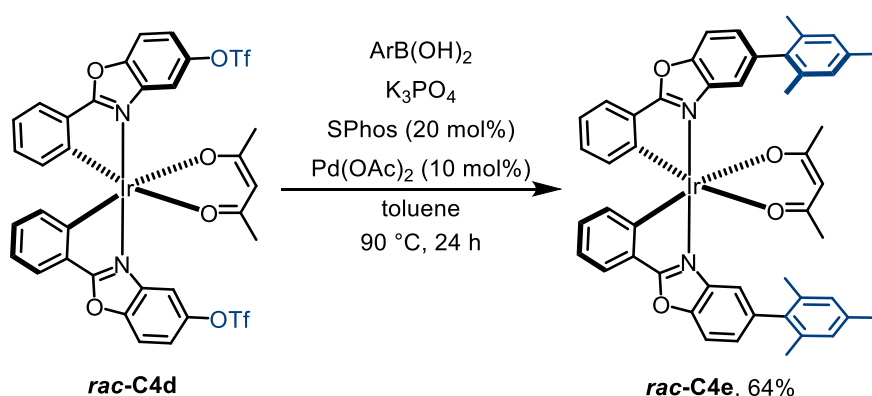


Figure 13: Structure of **rac-C4d**. ORTEP drawing with 70% probability of thermal ellipsoids, co-crystallized solvent molecules omitted for clarity. Selected bond lengths [Å] and angles [°]: C11-Ir1 2.0086(17), N1-Ir1 2.0371(14), O17-Ir1 2.1375(12); C11'-Ir1-C11 92.06(9), C11'-Ir1-N1 96.67(6), C11-Ir1-N1 79.79(6), C11'-Ir1-N1' 79.79(6), C11-Ir1-N1' 96.67(6), N1-Ir1-N1' 174.96(8), C11'-Ir1-O17 175.01(6), C11-Ir1-O17 89.74(6), N1-Ir1-O17 88.22(5), N1'-Ir1-O17 95.38(5), C11'-Ir1-O17' 89.74(6), C11-Ir1-O17' 175.01(6), N1-Ir1-O17 95.38(5), N1-Ir1-O17 88.22(5), O17-Ir1-O17 88.85(7).

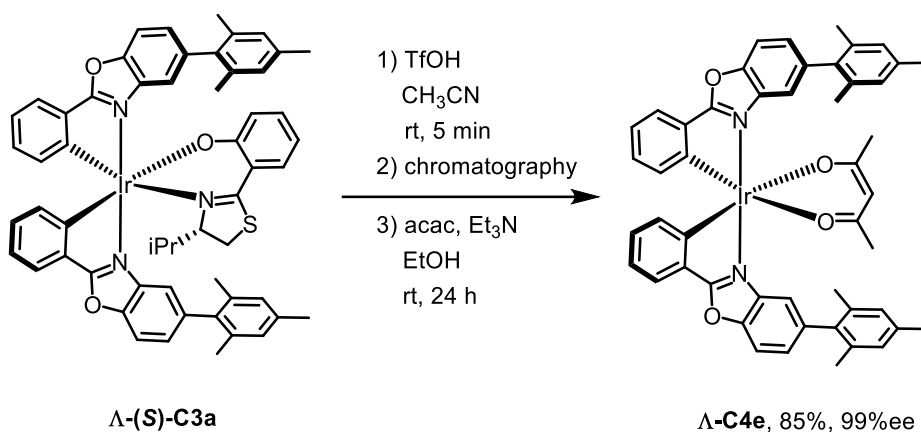
Racemic precursor complex **rac-C4d** was subsequently used in a SUZUKI cross-coupling reaction following the optimized method. The obtained racemic iridium(III) complex with mesityl group functionalization **rac-C4e** was obtained as a yellow powder with 64% yield (Scheme 27).



Scheme 27: Synthesis of the stereogenic-only-at-metal complex **rac-C4e**.

To obtain the enantiopure complex, the chiral ancillary ligand (**S**)-**AL1** of diastereomerically pure iridium(III) complex **Λ-(S)-C3a** was replaced with an achiral acetylacetonate (acac) ligand to obtain stereogenic-only-at-metal complex **Λ-C4e** with 85%. To achieve this, diastereomer

complex Λ -(*S*)-**C3a** was dissolved in CH₃CN and treated with TfOH to replace the acid labile ancillary ligand (*S*)-**AL1** with two CH₃CN ligands. The course of the reaction could be monitored visually, since the solution turned from orange to yellow in a matter of seconds. The free ancillary ligand (*S*)-**AL1** was removed by column chromatography. The acetonitrile complex was isolated and dissolved in EtOH and treated with achiral acac ligand and Et₃N (Scheme 28).



Scheme 28: Synthesis of the stereogenic-only-at-metal complex Λ -**C4e**.

This kind of ligand exchange is already well investigated in the MEGGERS group and proceeds under retention of the metal centered configuration.^[7e]

The HPLC experiment was conducted using cellulose tris-(3,5-dimethylphenyl-carbamate) as stationary and acetonitrile/water as mobile phase.^[21] Separation of the enantiomers was achieved with an isocratic 82:18 ratio of acetonitrile/water with a flow rate of 0.5 mL/min at 40 °C column temperature. From this HPLC experiment we can judge that the cross-coupling approach to synthesis structural divers stereogenic-at-metal complexes is suitable to obtain complexes with up to 99% ee (Figure 14).

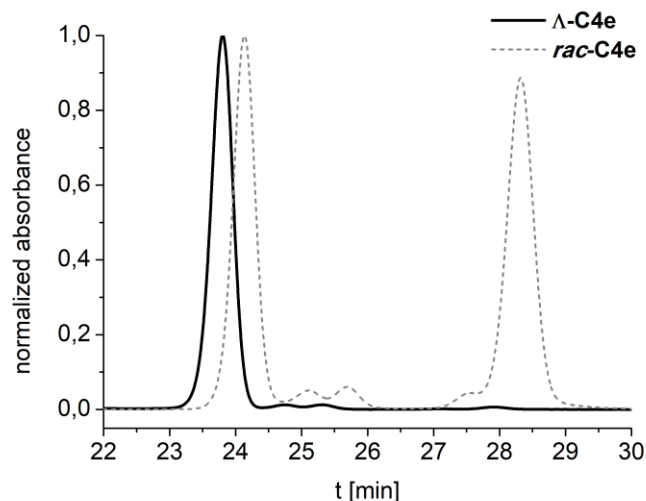


Figure 14: Chiral HPLC traces of *rac*-C4e (grey) and Λ -C4e (black). HPLC conditions: Daicel Chiralpak IB column (250×4.6 mm), solvent A: 0.1% TFA in water, solvent B: MeCN, isocratic ratio A/B 18:82, flow rate: $0.5 \text{ mL} \cdot \text{min}^{-1}$, column temperature: 40°C , UV absorption detected at $\lambda = 254 \text{ nm}$.

Based on the results of the discussed ^1H NMR, CD spectra as well as the HPLC experiment, it can be concluded that the investigated post complexation cross-coupling method does proceed under retention of the metal centered configuration. Thus, the post complexation cross-coupling approach provides a useful method to synthesis structurally divers iridium(III) complexes with well-defined stereo information. Therefore, more experiments should be conducted to better understand the scope and limitations of this method.

1.3.3 Extending the Scope of the Cross-Coupling Procedure

Since it was possible to demonstrate, that a single diastereomer precursor material could be used as a starting point to generate a small library of complexes under retention of the stereo information, it felt compelling to extend the scope towards structurally more diverse precursor material. Potential modifications of the initial test system evolve around following aspects:

- 1.) Further functionalization of the annulated phenyl ring would give further insight into reactivity of the precursor material. Incorporate more steric hindrance next to the cross-coupling position could potentially be detrimental to overall yield (Figure 15, no highlight).
- 2.) Due to the unique shape of octahedral complexes and arrangement of functional groups in the ligand sphere, it might be questionable if modifications on the cyclometalating phenyl ring could be detrimental for post complexation modifications. (Figure 15, green highlight)
- 3.) An exchange of the heteroaromatic building block could increase the scope nicely (Figure 15, red highlight).

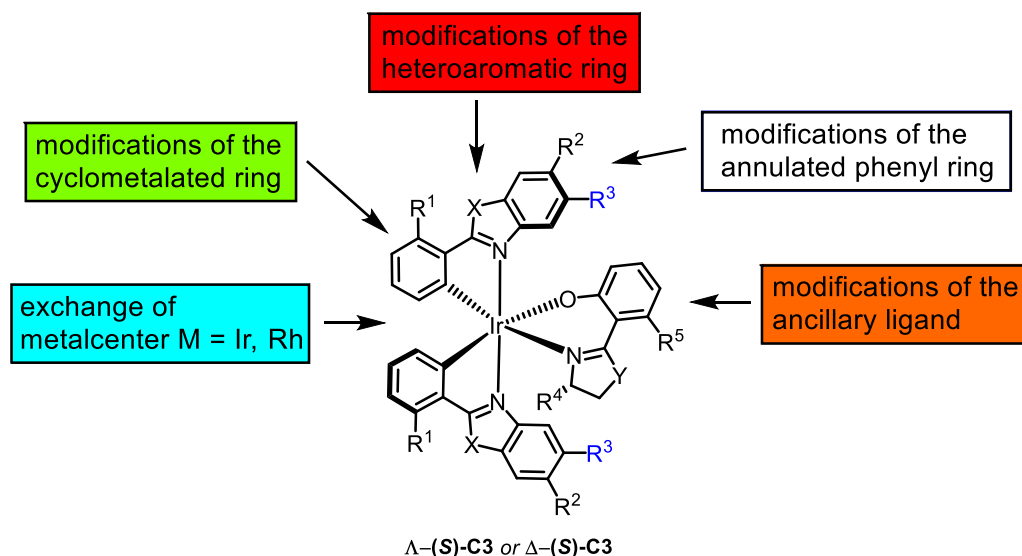


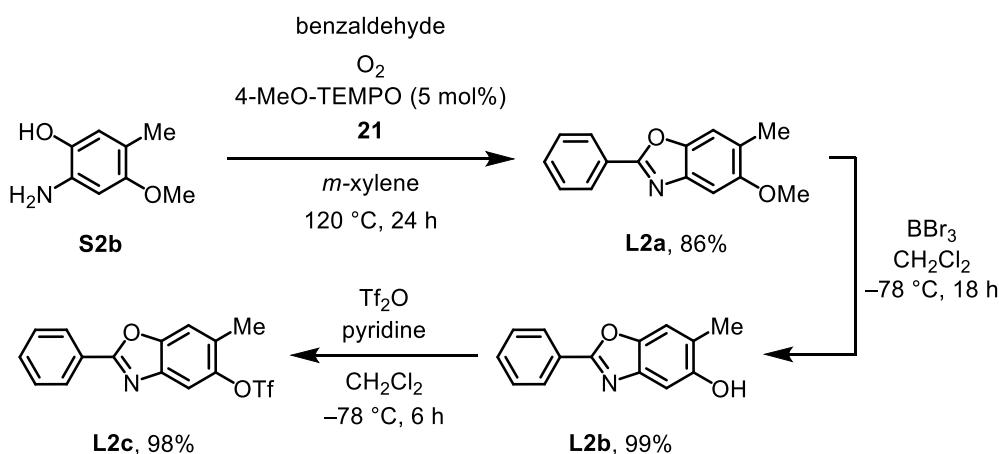
Figure 15: Illustration to highlight moieties for modifications on complex C3.

- 4.) As a result of previous studies about the synthesis of diastereomerically pure complexes it is known, that the chiral ancillary ligand has to provide tailored properties to match the complex.^[7e] Only a match results in sufficiently separable diastereomers and stability high enough to be separated without loss of material. Thinking along this line, it is reasonable to investigate distinct types of chiral ancillary ligands and their suitability for the new approach (Figure 15, orange highlight).^[7e]
- 5.) Since the establishment of stereogenic-at-rhodium-complexes had been successful,^[22] an exchange of chiral iridium(III) center with rhodium(III) could give further insight into the general usefulness of the designed method (Figure 15, cyan highlight). From those studies it is known, that the synthesis of a single rhodium complex

diastereomer can turn out to be particularly tricky, due to the sensitive nature of the rhodium complexes.

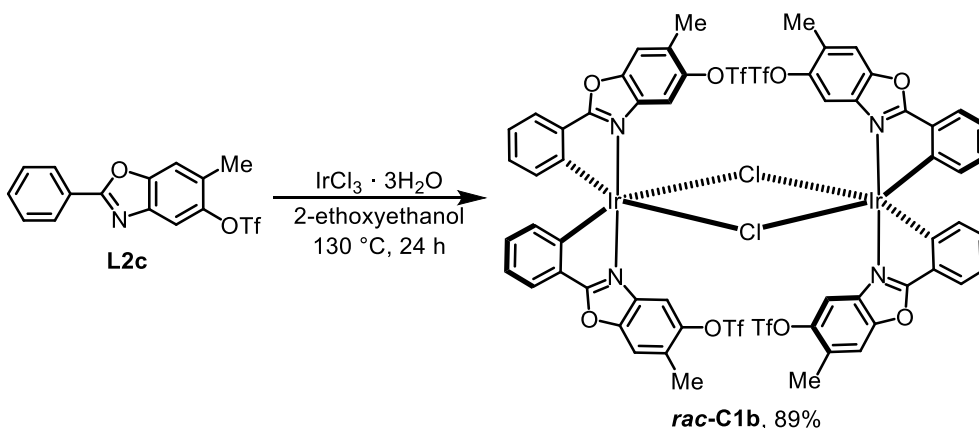
1.3.4 Modifications on the Annulated Phenyl Ring

Inspired by the previous results, the question rose, if the method would still life up to the expectations, if the *ortho* position to the TfO group is occupied by a methyl group, rendering the cross-coupling position more crowded. Therefor phenol derivative **S2b** was synthesized by THOMAS CRUCHTER in a three-step synthesis according to a literature known protocol.^[23] Phenol **S2b** was subsequently converted into methyl protected ligand **L2a** (86% yield),^[5a] deprotected by BBr₃ to form product **L2b** (99% yield)^[4b] and esterified with Tf₂O similarly to ligand **L1c** to obtain ligand **L2c** with a yield of 98% (83% yield over three-steps, scheme 29).^[16]



Scheme 29: Synthesis of the TfO functionalized phenyl benzoxazole **L2c** in a three-step protocol.^[4b,5a,16]

Ligand **L2c** was then applied to the adjusted NONOYAMA reaction conditions to furnish dimer **rac-C1b** (89% yield based on ligand **L2c**, scheme 30).^[6]



Scheme 30: Synthesis of the TfO functionalized iridium(III) dimer complex **rac-C1b**.^[6]

Single crystals suitable for X-ray diffraction from dimer complex ***rac*-C1b** could be obtained by slow evaporation of a solution of ***rac*-C1b** in CH₂Cl₂. This crystal structure illustrates nicely, that complex ***rac*-C1b** formed as racemic single diastereomers with the two benzoxazole ligands coordinated *trans* to each other and all four ligands remain TfO functionalized (Figure 16).

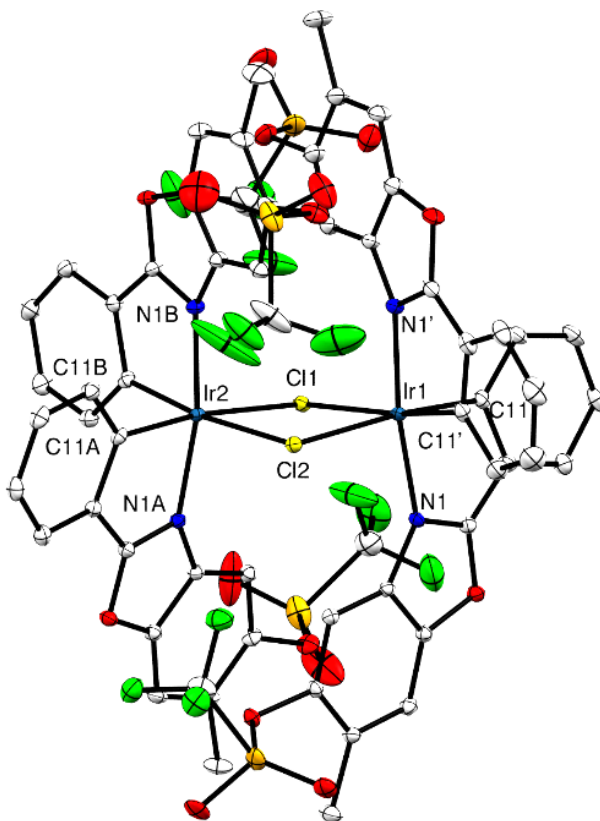
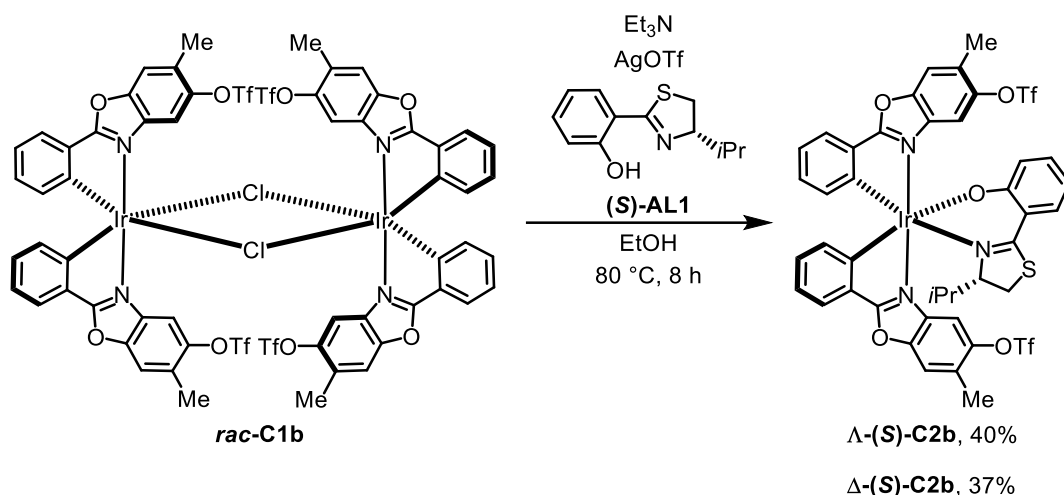


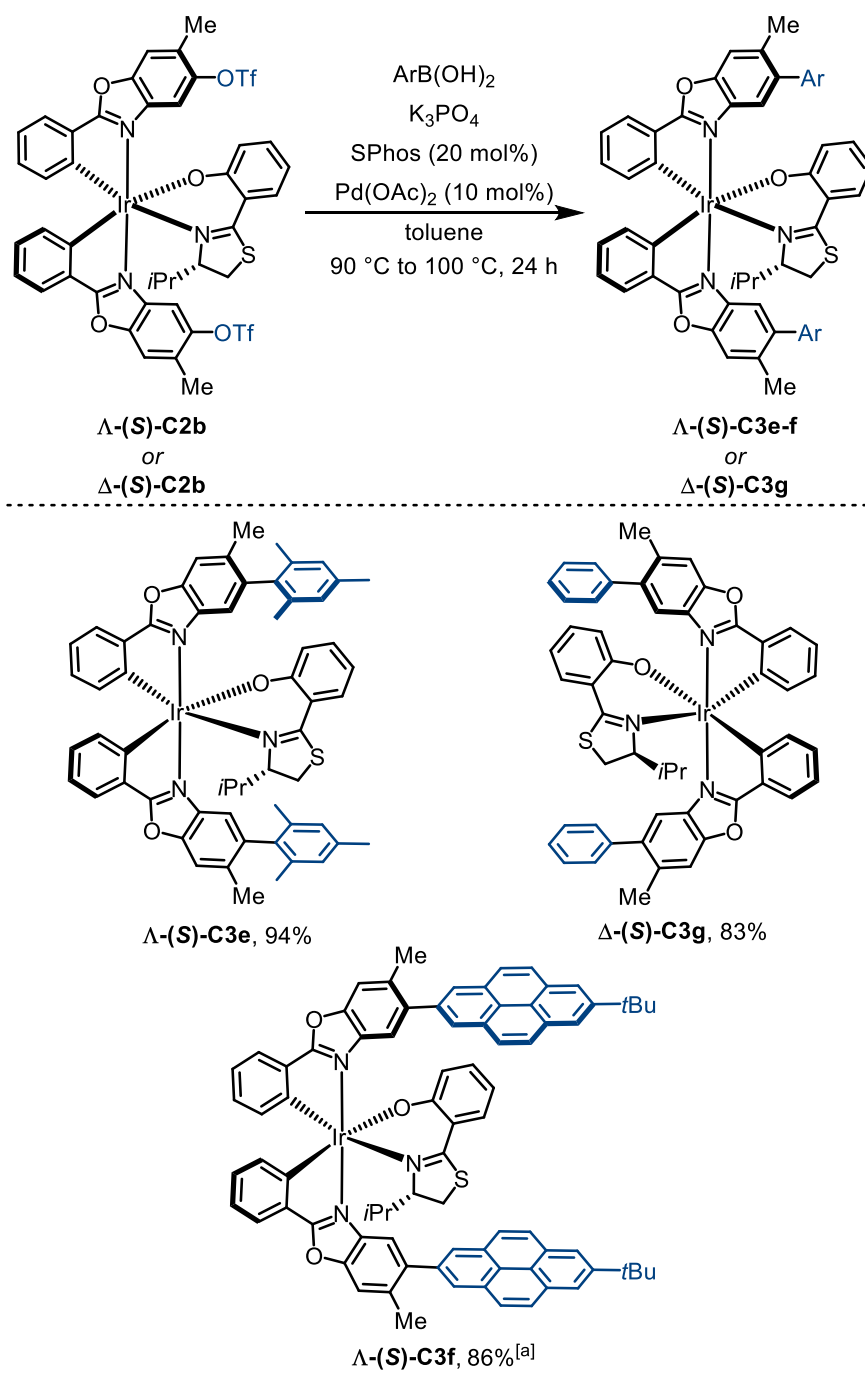
Figure 16: Structure of ***rac*-C1b**. ORTEP drawing with 30% probability of thermal ellipsoids, co-crystallized solvent molecules omitted for clarity. Selected bond lengths [Å] and angles [°]: Ir1-C11' 2.005(3), Ir1-C11 2.008(3), Ir1-N1' 2.035(2), Ir1-N1 2.059(2), Ir1-Cl1 2.4944(6), Ir1-Cl2 2.5032(6), Ir2-C11B 2.004(2), Ir2-C11A 2.009(3), Ir2-N1A 2.041(2), Ir2-N1B 2.043(2), Ir2-Cl2 2.4824(6), Ir2-Cl1 2.5129(6); C11'-Ir1-C11 92.93(10), C11'-Ir1-N1' 79.80(10), C11'-Ir1-N1 91.99(9), C11'-Ir1-N1 97.91(10), C11'-Ir1-N1 80.17(9), N1'-Ir1-N1 171.76(8), C11'-Ir1-Cl1 169.15(8), C11'-Ir1-Cl1 95.74(7), N1'-Ir1-Cl1 93.37(6), N1'-Ir1-Cl1 89.99(6), C11'-Ir1-Cl2 88.66(8), C11'-Ir1-Cl2 174.37(7), N1'-Ir1-Cl2 93.60(6), N1'-Ir1-Cl2 94.27(6), C11'-Ir1-Cl2 83.330(19), C11B-Ir2-C11A 93.51(10), C11B-Ir2-N1A 92.26(9), C11A-Ir2-N1A 80.42(9), C11B-Ir2-N1B 80.44(9), C11A-Ir2-N1B 91.71(9), N1A-Ir2-N1B 168.97(8), C11B-Ir2-Cl2 172.88(7), C11A-Ir2-Cl2 91.60(7), N1A-Ir2-Cl2 93.48(6), N1B-Ir2-Cl2 94.47(6), C11B-Ir2-Cl1 92.04(7), C11A-Ir2-Cl1 172.16(7), N1A-Ir2-Cl1 93.84(6), N1B-Ir2-Cl1 94.67(6), Cl2-Ir2-Cl1 83.374(19), Ir1-Cl1-Ir2 95.70(2), Ir2-Cl2-Ir1 96.25(2).

Consequently, dimer complex ***rac*-C1b** was converted with ancillary ligand (***S***)-AL1 to diastereomer complex Λ -(***S***)-C2b (40% yield) and Δ -(***S***)-C2b (37% yield, scheme 31).^[7e]



Scheme 31: Synthesis of the TfO functionalized, diastereomer iridium(III) complexes **Δ -(S)-C2b** and **Δ -(S)-C2b** by established method. The diastereomers are separable by standard column chromatography.^[7e]

Surprisingly, the desired cross-coupling products were obtained in excellent yields. The investigated cross-coupling conditions were applied to complex **Δ -(S)-C2b** using mesitylene-2-boronic and 2-(7-*tert*-butylpyren-2-yl)-4,4,5,5-tetramethyl-1,3,2-dioxaborolane (**P2**) to receive **Δ -(S)-C3e** (94%) and **Δ -(S)-C3f** (86%) in excellent yields. Additionally, complex **Δ -(S)-C2b** was converted to **Δ -(S)-C3g** with 83% yield using phenylboronic acid (Scheme 32). In conclusion, it could be demonstrated, that even though the 5-position is less accessible, the cross-coupling still proceeds nicely.

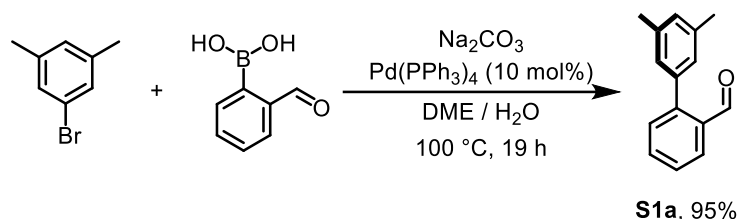


Scheme 32: Scope of cross-coupling experiments with Λ -(S)-C2b. [a] For this reaction, boronic acid ester **P2** and 10% water as additive were used.

1.3.5 Modifications on the Cyclometalating Phenyl Ring

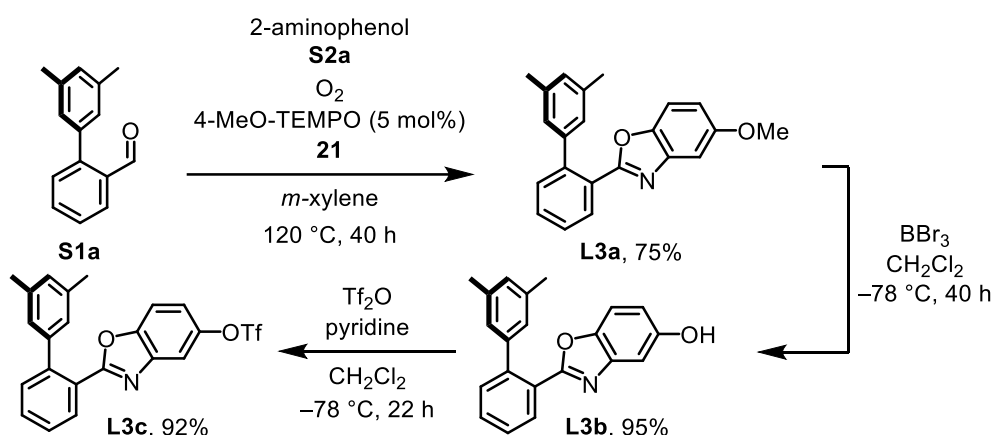
Since complexes with functionalization at the 2'-position of the cyclometalated phenyl ring showed great promise in LEWIS base as well as hydrogen-bond catalysis,^[4a] complexes with 2,6-xylyl and 3,5-xylyl functional groups were designed. Therefore, benzaldehyde derivatives **S1a** and **S1b** were synthesized by cross-coupling reactions using established methods.^[24]

Modified benzaldehyde **S1a** was accessible by Pd(PPh₃)₄ catalyzed cross-coupling reaction of 2-formylphenylboronic acid with 3,5-dimethylbromobenzene in the presence of Na₂CO₃ in a DME/water solvent mixture (95% yield, scheme 33).^[24a]



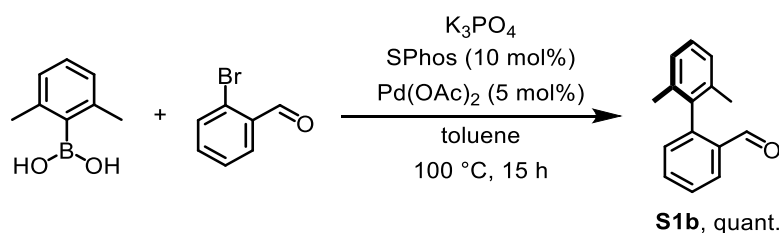
Scheme 33: Synthesis of the biphenyl carbaldehyde **S1a** by SUZUKI cross-coupling.^[24a]

Carbaldehyde **S1a** was then converted into the triflate functionalized ligand under the aforementioned conditions utilized for ligand **L1c** and **L2c**. Methyl protected ligand **L3a** obtained from carbaldehyde **S1a** and phenol **S2a** (75% yield),^[5a] was deprotected by BBr₃ to obtain hydroxy ligand **L3b** (95% yield)^[4b] which was successfully esterified with Tf₂O (92% yield) to obtain triflated ligand **L3c** with 62% yield^[16] over five steps (Scheme 20, 33 and 34).



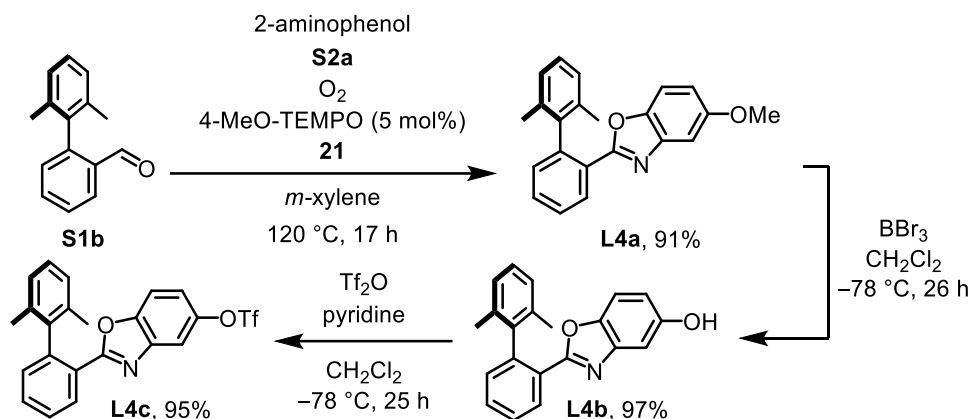
Scheme 34: Synthesis of the TfO functionalized phenyl benzoxazole **L3c** in a three-step protocol.^[4b,5a,16]

Modified carbaldehyde **S1b** however, was obtained by Pd(OAc)₂/SPhos catalyzed cross-coupling reaction of (2,6-dimethylphenyl) boronic acid with 2-bromobenzaldehyde in the presence of K₃PO₄ in toluene with quantitative yield (Scheme 35).^[24b]



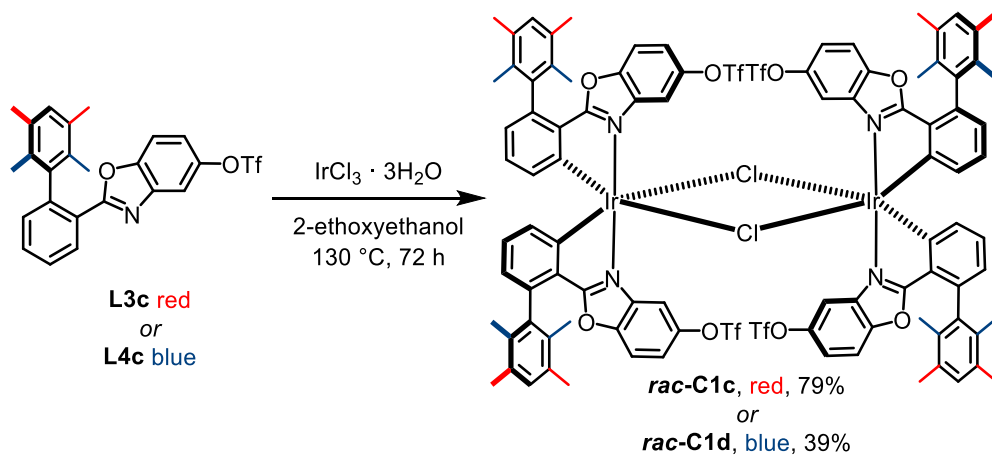
Scheme 35: Synthesis of the biphenyl carbaldehyde **S1b** by SUZUKI cross-coupling.^[24b]

Carbaldehyde **S1b** was converted into the methyl protected ligand **L4a** (91% yield),^[5a] deprotected with BBr₃ to form the hydroxy ligand **L4b** (97% yield)^[4b] and esterified with Tf₂O to yield ligand **L4c** (95% yield)^[16] using established methods (82% yield over five-steps, see scheme 20, 35 and 36).



Scheme 36: Synthesis of the TfO functionalized phenyl benzoxazole **L4c** in a three-step protocol.^[4b,5a,16]

Both ligands were successfully converted into racemic dimer complexes **rac-C1c** and **rac-C1d** (Scheme 37, ligand **L3c** and dimer **rac-C1c** (79% yield) highlighted red, ligand **L4c** and dimer **rac-C1d** (39% yield) highlighted blue).^[6] Single crystals suitable for X-ray diffraction from complex **rac-C1d** could be obtained by slow evaporation of an *n*-hexane solution containing **rac-C1d** (Figure 17).



Scheme 37: Synthesis of the TfO functionalized dimer complexes **rac-C1c** and **rac-C1d**.^[6]

Crystal structure of **rac-C1d** reinforces the observations made with complex **rac-C1b**. It could be observed that dimer **rac-C1d** was obtained as racemic mixture of a single diastereomer, with ligand coordinated *trans* and all four TfO groups intact (Figure 17).

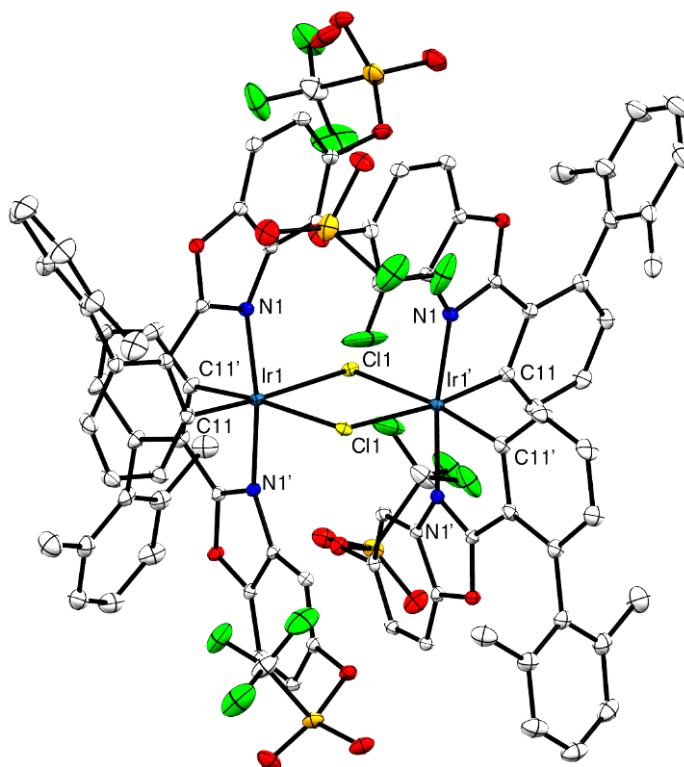
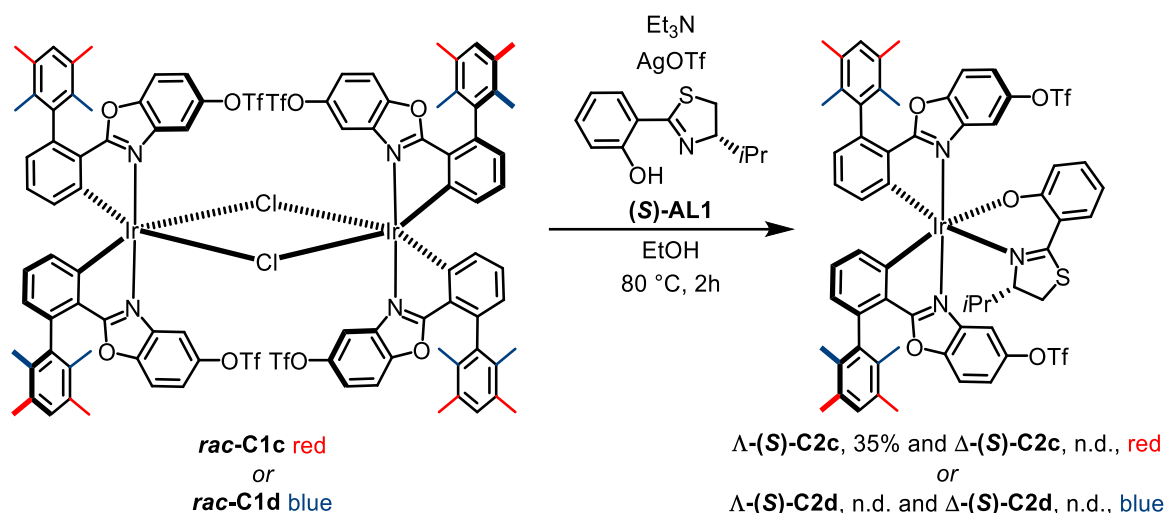


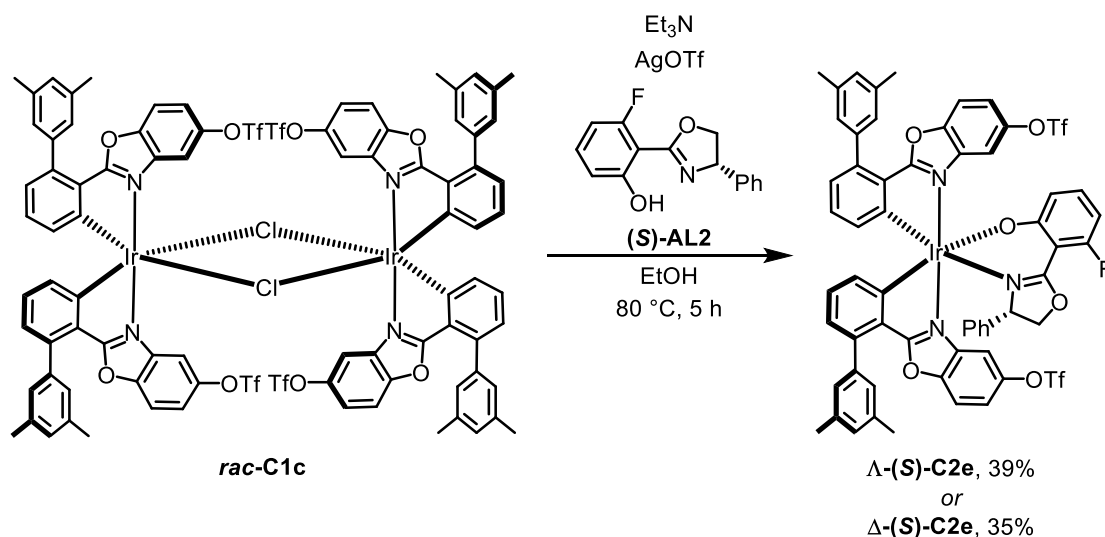
Figure 17: Structure of *rac*-**C1d**. ORTEP drawing with 30% probability of thermal ellipsoids, co-crystallized solvent molecules omitted for clarity. Selected bond lengths [Å] and angles [°]: Ir1-C11 2.004(2), Ir1-C11' 2.010(2), Ir1-N1 2.0399(19), Ir1-N1' 2.0403(19), Ir1-Cl1 2.4955(6), Ir1-Cl1' 2.5024(6), Cl1-Ir1' 2.5025(6); C11-Ir1-C11' 90.71(10), C11-Ir1-N1 80.06(9), C11'-Ir1-N1 93.66(9), C11-Ir1-N1' 94.31(8), C11'-Ir1-N1' 80.02(9), N1-Ir1-N1' 171.55(8), C11-Ir1-Cl1 172.65(7), C11'-Ir1-Cl1 94.33(7), N1-Ir1-Cl1 94.26(6), N1'-Ir1-Cl1 91.83(5), C11-Ir1-Cl1' 92.45(7), C11'-Ir1-Cl1' 172.72(7), N1-Ir1-Cl1' 93.35(6), N1'-Ir1-Cl1' 93.19(5), Cl1-Ir1-Cl1' 83.170(19), Ir1-Cl1-Ir1' 96.746(19).

Those complexes *rac*-**C1c** and *rac*-**C1d** were converted into the respective mixtures of diastereomers utilizing the established method and ancillary ligand **AL1**. It is noteworthy, that the diastereomer complexes Λ -(*S*)-**C2c** (35% yield) and Δ -(*S*)-**C2c** could be separated by column chromatography but tend to decompose in solution. In case of diastereomers Λ -(*S*)-**C2d** and Δ -(*S*)-**C2d** however, it remained impossible to separate them by column chromatography due to retention times becoming too much alike (Scheme 38).^[7e]



Scheme 38: Synthesis of the TfO functionalized, diastereomer iridium(III) complexes $\Delta\text{-(S)-C2c-d}$ and $\Delta\text{-(S)-C2c-d}$ by established method.^[7e] Diastereomer complexes with the 2,6-dimethylphenyl modification $\Delta\text{-(S)-C2d}$ and $\Delta\text{-(S)-C2d}$ are unresolvable. Complexes with the 2,6-dimethylphenyl modification $\Delta\text{-(S)-C2c}$ and $\Delta\text{-(S)-C2c}$ are resolvable but prone for decomposition in solution.

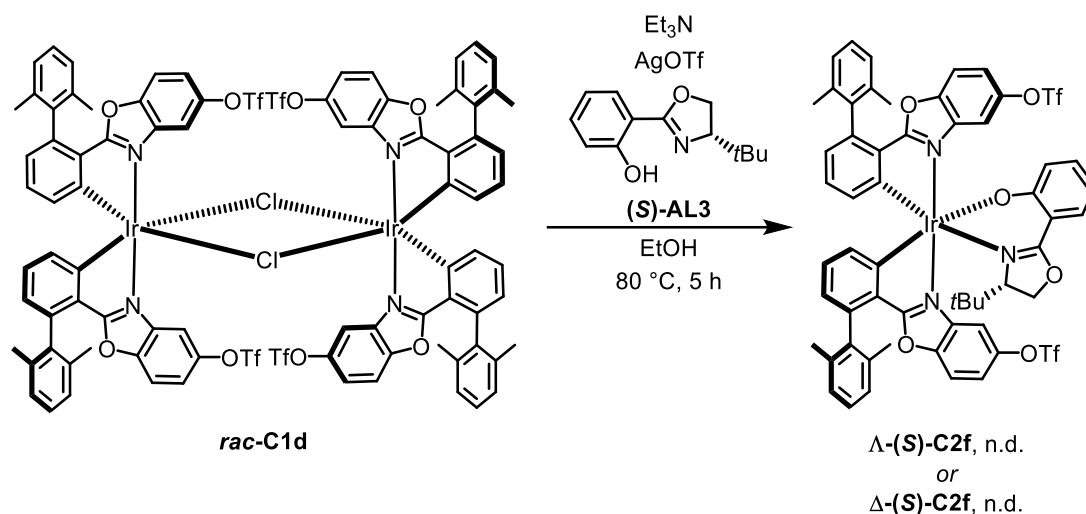
To enhance the stability of the diastereomer complexes derived from dimer **rac-C1c**, an alternative ancillary ligand **(S)-AL2** was applied during complex formation.^[7c] Indeed, using fluorinated ancillary ligand **(S)-AL2** diastereomer complexes $\Delta\text{-(S)-C2e}$ (39% yield) and $\Delta\text{-(S)-C2e}$ (35% yield) were obtained (Scheme 39).



Scheme 39: Synthesis of the TfO functionalized, diastereomer iridium(III) complexes $\Delta\text{-(S)-C2e}$ and $\Delta\text{-(S)-C2e}$ by established method. The diastereomers are separable by standard column chromatography.^[7c]

In case of the dimer **rac-C1d**, the respective diastereomer complexes could be obtained with ancillary ligand **(S)-AL3**.^[7e] The change to ancillary ligand **(S)-AL3** yielded complexes very

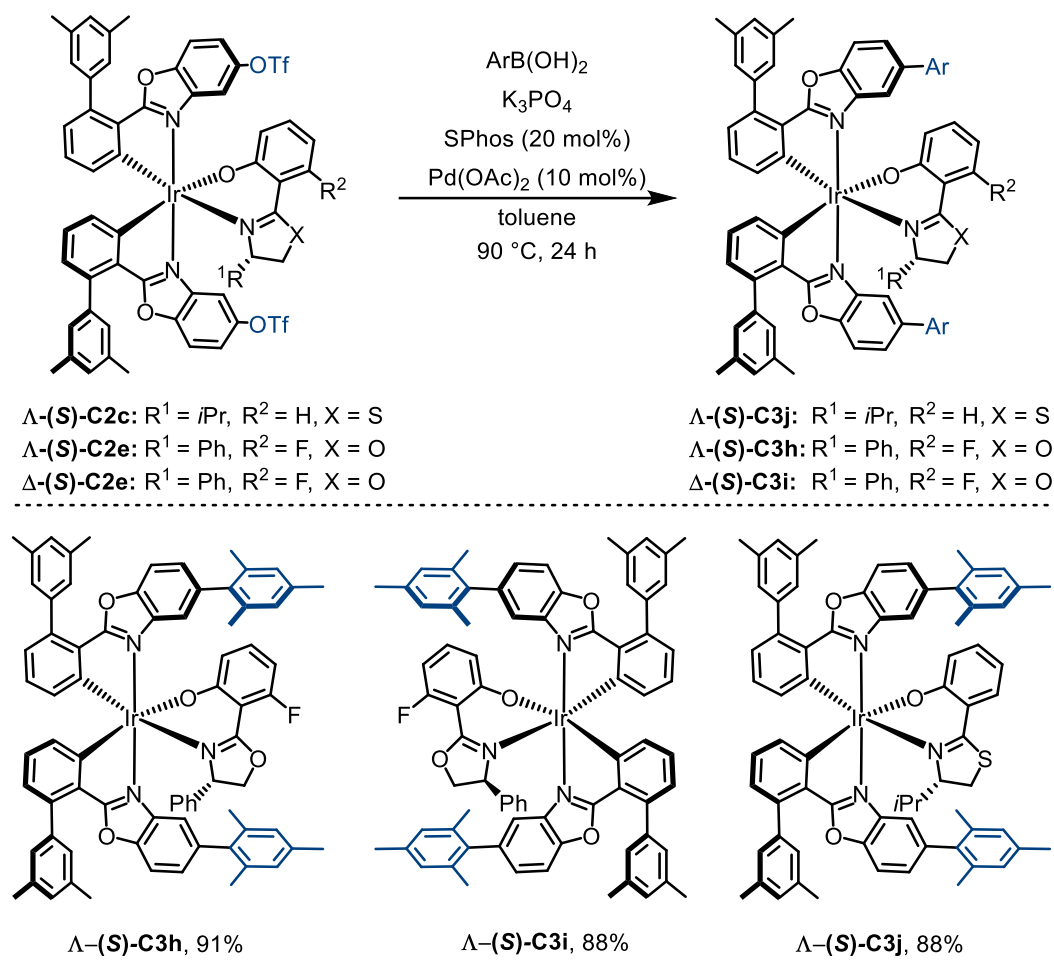
sensitive towards heat and acidity, rendering complexes Λ -(*S*)-C2f and Δ -(*S*)-C2f challenging to separate in higher quantities (Scheme 40).



Scheme 40: Synthesis of the TfO functionalized, diastereomer iridium(III) complexes Λ -(*S*)-C2f and Δ -(*S*)-C2f by established method.^[7c]

Since the issues with diastereomers Λ -(*S*)-C2e and Δ -(*S*)-C2e turned out to be manageable with the use of the proper ancillary ligand (*S*)-AL2, focus shifted on applying the designed approach on Λ -(*S*)-C2e and Δ -(*S*)-C2e. Strikingly, both diastereomers could be applied to the investigated cross-coupling procedure, furnishing mesityl functionalized complexes Λ -(*S*)-C3h (91% yield) and Δ -(*S*)-C3i (88% yield) with excellent yields. Encouraged by this result, the sensitive complex Λ -(*S*)-C2c was subjected to the cross-coupling method as well.

Surprisingly, mesityl functionalized complex Λ -(*S*)-C3j was still obtained with a yield of 88%, hinting that the degradation of the precursor material happens on a smaller timescale than the conversion to the mesitylated complex Λ -(*S*)-C3j. This is further supported by the observation that functionalized complex Λ -(*S*)-C3j remained stable in solution and showed no signs of degradation (Scheme 41).



Scheme 41: Scope of the cross-coupling experiments with $\Delta\text{-(S)-C2c}$, $\Delta\text{-(S)-C2e}$ and $\Delta\text{-(S)-C2e}$.

From these results, it was judged that the modifications on the phenyl ring had unexpected adverse impact on the stability of the triflated diastereomer complexes. Ancillary ligand (**S**)-**AL2** provided sufficient stability but lead to smaller difference in retention times.

The higher stability could be rationalized by two effects. First of all, ancillary ligand (**S**)-**AL2** contains an electron withdrawing group (fluorine) on the phenol moiety, reducing the electron density of the ring making the phenol more acidic. Consequentially, diastereomer complexes containing ancillary ligand (**S**)-**AL2** were less basic and therefore less prone for protonation and labilization. The second effect that should be discussed, might cohere with the phenyl ring on the oxazoline's chiral center. Potential π -stacking of this phenyl ring with the benzoxazole backbone from diastereomer complexes $\Delta\text{-(S)-C2e}$ and $\Delta\text{-(S)-C2e}$ could contribute to the higher stability as well. Evidence was given by a crystal structure of PAOLA and co-workers.^[7c] Unfortunately, no crystals suitable for single crystal X-ray analysis was obtained for complexes $\Delta\text{-(S)-C2e}$ and $\Delta\text{-(S)-C2e}$, further investigations should therefore be considered.

However, important conclusions can be drawn from the experiments on complexes with modified phenyl rings concerning the ancillary ligand. The experiments demonstrate nicely yet again, that the properties of the ancillary ligand must be tailored properly to find the an optimum between stability and difference in retention time. From a stability point of view, fluorinated ancillary ligand **(S)-AL2** was favorable over ligand **(S)-AL1** and **(S)-AL3**. However, from a preparative point of view, separation appeared to be better, introducing *tert*-butyl ligand **(S)-AL3**, rendering it favorable over fluorinated ligand **(S)-AL2** and *iso*-propyl ligand **(S)-AL1**. From these results it can be concluded, that ancillary ligand **(S)-AL1** takes the middle ground in terms of stability as well as separability (Figure 18).

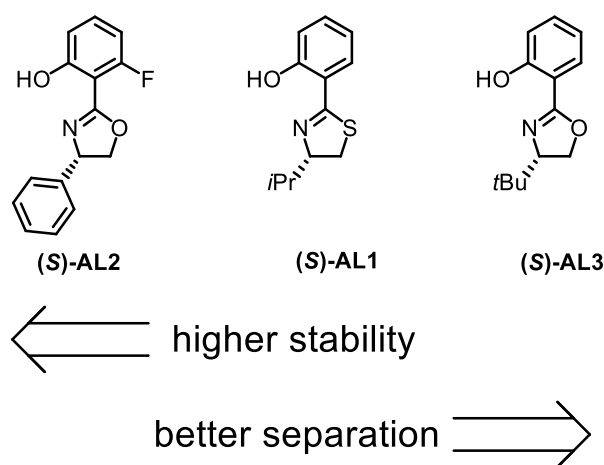


Figure 18: Illustration for the compromise between separation und stability in regard towards the chosen ancillary ligand **(S)-AL1**.

This observation matches previous results by former MEGGERS group member MELANIE HELMS, rendering it hardly possible to find the ultimate ancillary ligand suitable for all needs and complexes.^[7e]

1.3.6 Peculiarities in the ^{19}F NMR Spectra of Diastereomer Complex Λ -(*S*)-C2e

^{19}F NMR analysis of diastereomer complexes Λ -(*S*)-C2e and Λ -(*S*)-C2e provided an interesting insight. From initial assumption it was expected that three singlet signals with an integral ratio of 3:3:1 are generated by both CF_3 groups of the benzoxazole ligand as well as the single fluorine atom on the ancillary ligand (*S*)-AL2. What we observed however, was a doublet with an integral of three and coupling constant of $J = 2.9$ Hz, a singlet with an integral of three, and quartet with an integral of one and coupling constant of $J = 2.9$ Hz (Figure 19).

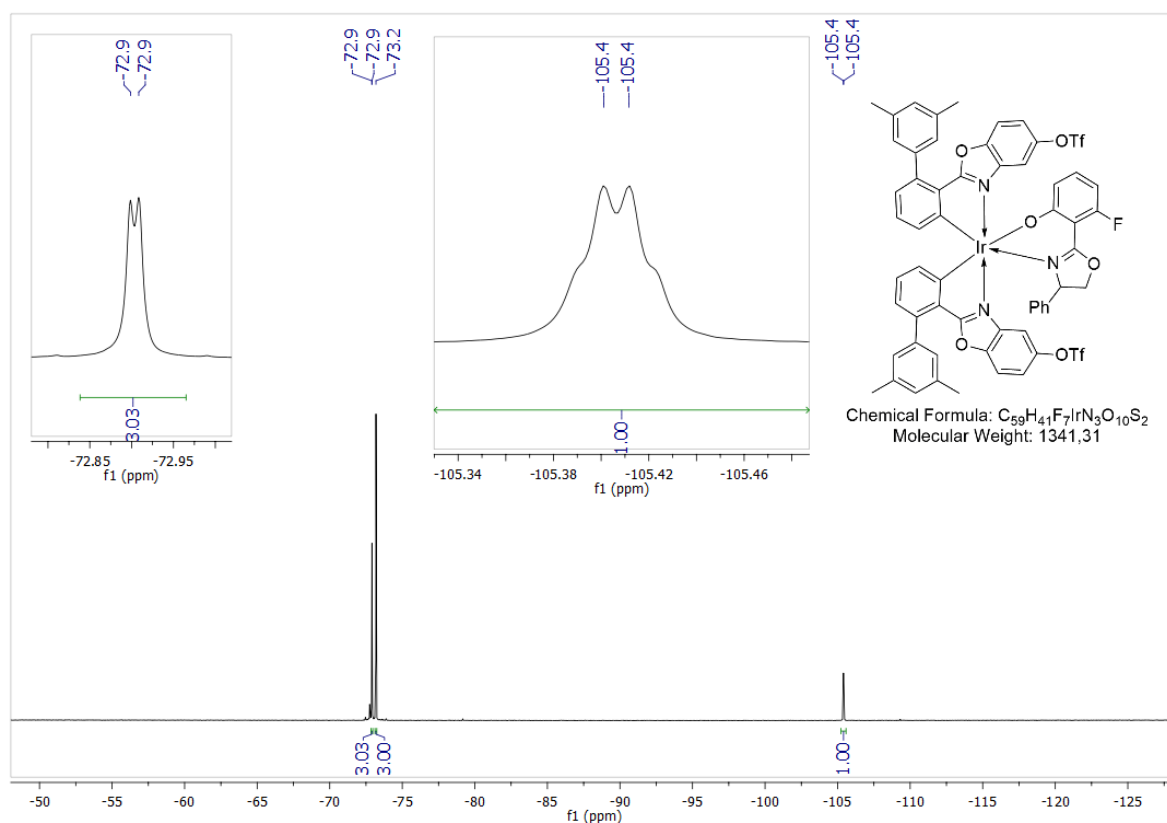
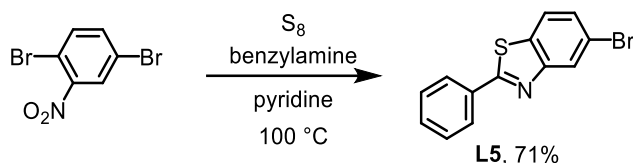


Figure 19: ^{19}F NMR of complex Λ -(*S*)-C2e in CD_2Cl_2 recorded with a *Bruker Avance III HD* at 283 MHz illustrating fluorine through space coupling.

This phenomenon is known as through space coupling of nuclei.^[25] This occurs, if the nuclei are in close proximity to each other and is no sign of contamination or an incorrect compound.

1.3.7 Modifications on the Heterocycle

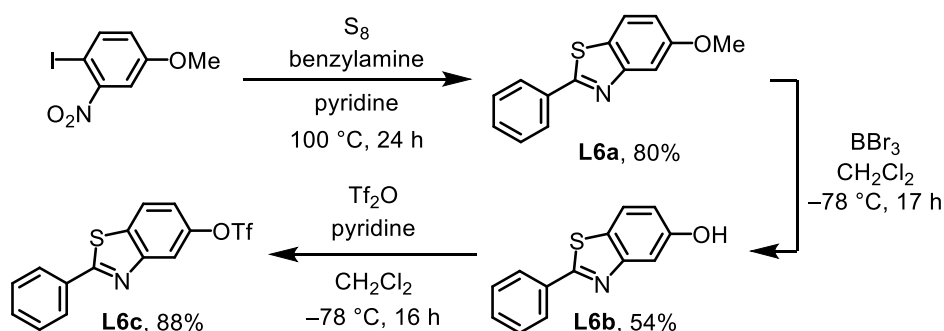
Since it is known from previous work of the MEGGERS group, that complexes based on benzothiazoles ligands inhabit different reactivity than benzoxazole congeners, the idea to synthesize complexes with functionalized benzothiazole ligands gained significant interest.^[13c] Therefore, two different types of benzothiazole ligands were synthesized. Both, a bromo functionalized ligand **L5** and a MeO functionalized ligand **L6a** were synthesized by a literature reported method (Scheme 42 and 43).^[5b]



Scheme 42: Synthesis of the Br functionalized phenyl benzothiazole **L5** in one step.^[5b]

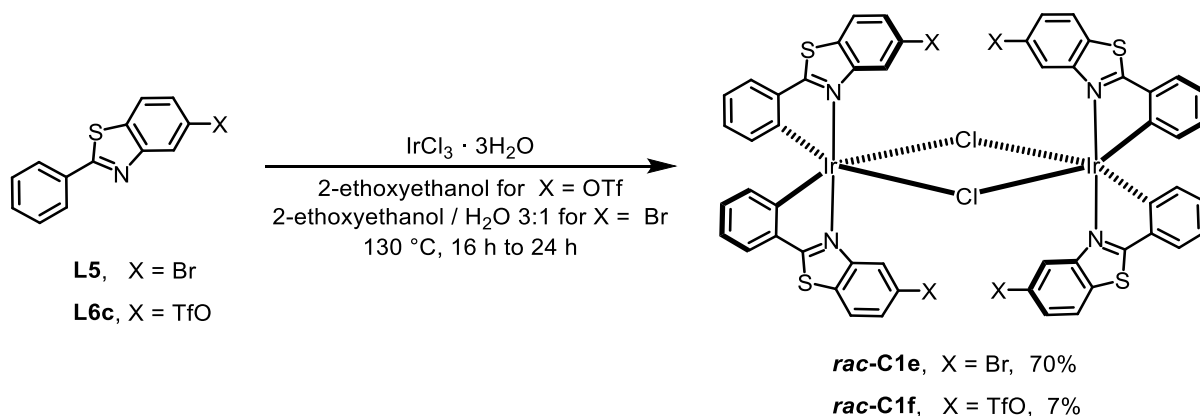
In this reaction, the respective nitro compound was reacted with elemental sulfur and benzylamine in the presents of pyridine. In case of brominated ligand **L5**, it turned out to be beneficial for the dimer formation to recrystallize the ligand from MeOH, furnishing the ligand with 71% yield (Scheme 42).^[5b]

Methoxy ligand **L6a** was obtained with 80% yield^[5b] and further converted into the hydroxy ligand **L6b** (54% yield)^[4b] and the TfO functionalized ligand **L6c** (88% yield)^[16] as mentioned beforehand (Scheme 43).



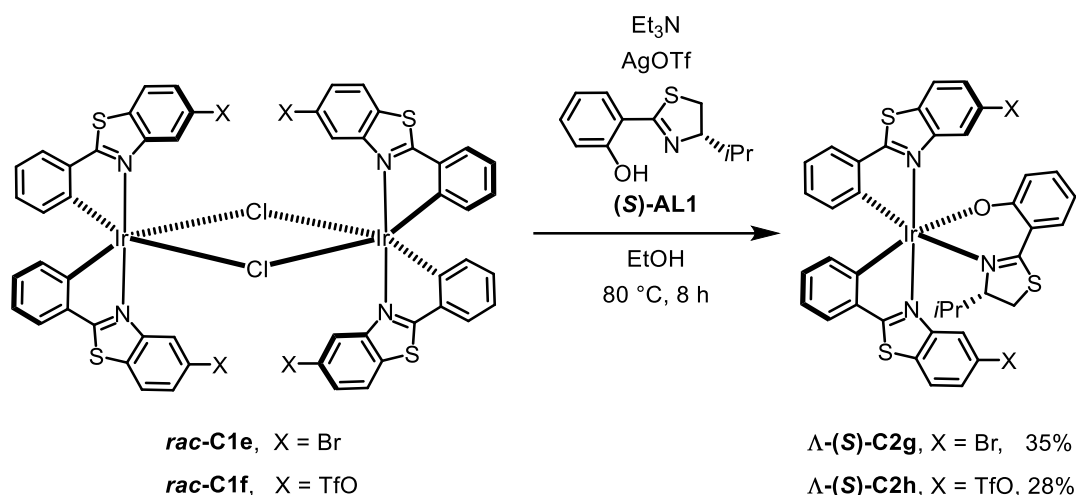
Scheme 43: Synthesis of the TfO functionalized phenyl benzothiazole **L6c** in a three-step protocol.^[4b,5b,16]

Both ligands were successfully converted to the respective dimer *rac*-**C1e** (70% yield) and *rac*-**C1f** (7% yield). For the synthesis of *rac*-**C1e**, the reaction performed cleaner, if standard NONOYAMA conditions were met, applying a solvent mixture of 3:1 ethoxyethanol/water to the dimer formation (Scheme 44).^[6]



Scheme 44: Synthesis of the TfO functionalized dimer complexes **rac-C1e** and **rac-C1f**.^[6]

Surprisingly, complex **rac-C1e** was comparably soluble in commonly used solvents, therefore it was possible to obtain proper analytic data as well as to do follow up chemistry. From the previous experience with complexes Λ -(*S*)-**C2c-f** and Δ -(*S*)-**C2c-f**, both complexes **rac-C1e** and **rac-C1f** were at first converted to the diastereomer complexes with ancillary ligand (*S*)-**AL1** (Scheme 45).^[7e]



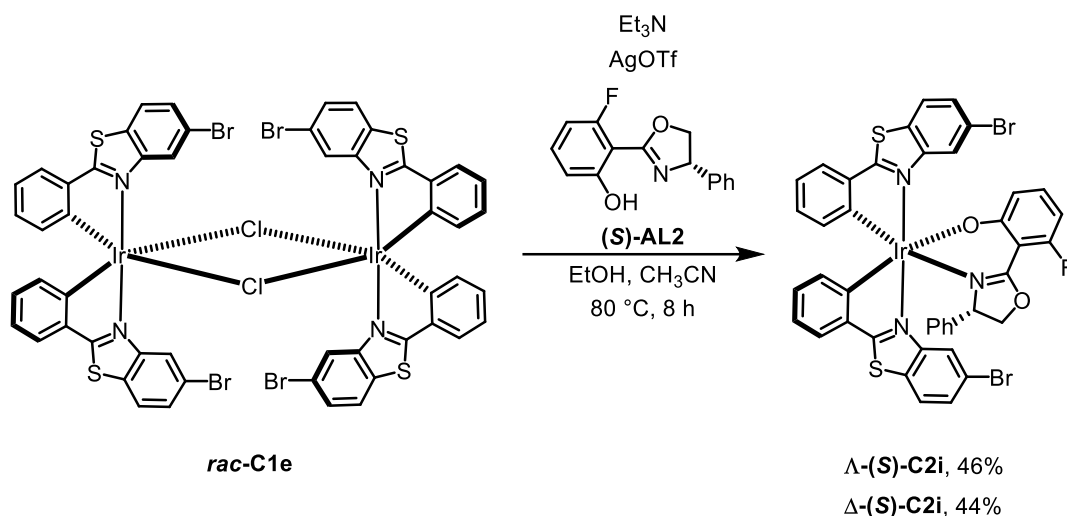
Scheme 45: Synthesis of the TfO functionalized, diastereomer iridium(III) complexes Λ -(*S*)-**C2g** and Λ -(*S*)-**C2h** by established method.^[7e]

In case of the dimer **rac-C1e**, CH_3CN turned out to be beneficial to obtain Λ -(*S*)-**C2g** and Δ -(*S*)-**C2g** using ancillary ligand (*S*)-**AL1**. On the other hand, CH_3CN was not necessary for the formation of diastereomers Λ -(*S*)-**C2h** and Δ -(*S*)-**C2h**. However, in both cases, the Δ -(*S*)-diastereomer was not stable in solution and decomposed quickly during column chromatography.

Surprisingly, Λ -(*S*)-**C2g** was successfully cross coupled with mesityl boronic acid to obtain complex Λ -(*S*)-**C3k** (64% yield, scheme 47). Since the synthesis of the brominated derivative

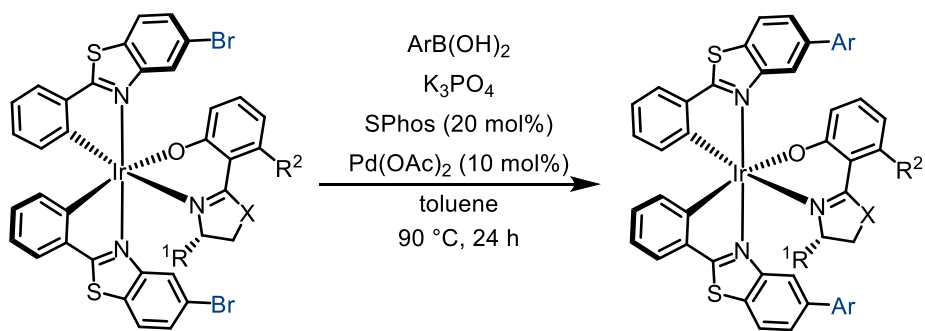
L5 proceeded in a more streamlined fashion than the TfO congener **L6c**, the focus of the stability issue was shifted towards complexes with brominated ligands Λ -(*S*)-**C2g**.

From the previous results concerning Λ -(*S*)-**C2e** and Λ -(*S*)-**C2e** could be concluded, that ancillary ligand (*S*)-**AL2** might lead to sufficiently stable, brominated benzothiazole precursors complexes. Indeed, conversion of dimer *rac*-**C1e** with ancillary ligand (*S*)-**AL2** to the diastereomer complexes Λ -(*S*)-**C2i** (46% yield) and Λ -(*S*)-**C2i** (44% yield) was possible with CH₃CN as additive. Both diastereomers could be isolated with excellent yields and turned out to be stable in solution (Scheme 46).^[7c]



Scheme 46: Synthesis of the bromo functionalized, diastereomer iridium(III) complexes Λ -(*S*)-**C2i** and Δ -(*S*)-**C2i** by established method.^[7c]

Accordingly, Λ -(*S*)-**C2i** and Δ -(*S*)-**C2i** were applied to the cross-coupling method to obtain mesityl functionalized benzothiazole complexes in excellent yields Λ -(*S*)-**C3l** (94% yield); Δ -(*S*)-**C3m** (92% yield) applying mesitylene-2-boronic acid. To further extend the scope of the benzothiazole derivatives complex Λ -(*S*)-**C2i** was cross-coupled with 2-(7-*tert*-butylpyren-2-yl)-4,4,5,5-tetramethyl-1,3,2-dioxaborolane (**P2**) to obtain Λ -(*S*)-**C3n** with 92% yield. To demonstrate, that both diastereomers undergo cross-coupling, complex Δ -(*S*)-**C2i** was cross-coupled with (3-(dimethylamino)phenyl)boronic acid to receive complex Δ -(*S*)-**C3o** with 55% yield (Scheme 47). Fortunately, a single crystal suitable for X-ray diffraction of Δ -(*S*)-**C3o** was obtained by slow liquid-liquid diffusion of *n*-hexane into a solution of Δ -(*S*)-**C3o** in CH₂Cl₂ (Figure 20).



$\Lambda\text{-(S)-C2g}$: $\text{R}^1 = i\text{Pr}$, $\text{R}^2 = \text{H}$, $\text{X} = \text{S}$

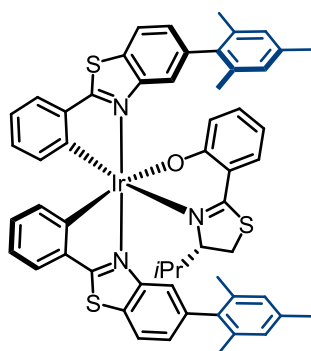
$\Lambda\text{-(S)-C2i}$: $\text{R}^1 = \text{Ph}$, $\text{R}^2 = \text{F}$, $\text{X} = \text{O}$

$\Delta\text{-(S)-C2i}$: $\text{R}^1 = \text{Ph}$, $\text{R}^2 = \text{F}$, $\text{X} = \text{O}$

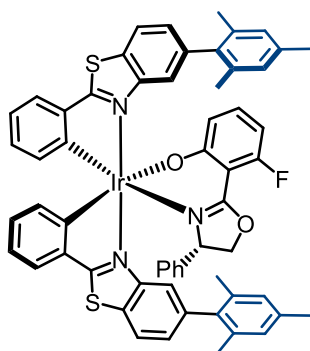
$\Lambda\text{-(S)-C3k}$: $\text{R}^1 = i\text{Pr}$, $\text{R}^2 = \text{H}$, $\text{X} = \text{S}$

$\Lambda\text{-(S)-C3l}$, $\Lambda\text{-(S)-C3n}$: $\text{R}^1 = \text{Ph}$, $\text{R}^2 = \text{F}$, $\text{X} = \text{O}$

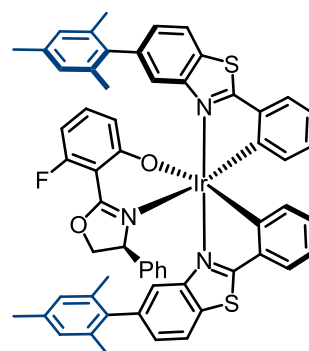
$\Delta\text{-(S)-C3m}$, $\Delta\text{-(S)-C3o}$: $\text{R}^1 = \text{Ph}$, $\text{R}^2 = \text{F}$, $\text{X} = \text{O}$



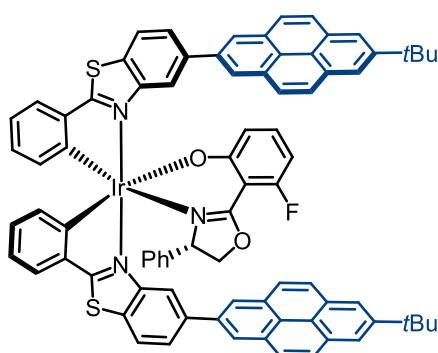
$\Lambda\text{-(S)-C3k}$, 64%



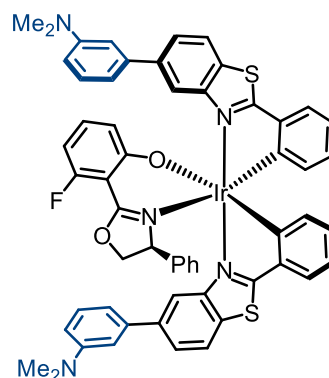
$\Lambda\text{-(S)-C3l}$, 94%



$\Delta\text{-(S)-C3m}$, 92%



$\Lambda\text{-(S)-C3n}$, 92%



$\Delta\text{-(S)-C3o}$, 55%

Scheme 47: Scope of the cross-coupling experiments with $\Lambda\text{-(S)-C2g}$, $\Lambda\text{-(S)-C2i}$ and $\Delta\text{-(S)-C2i}$.

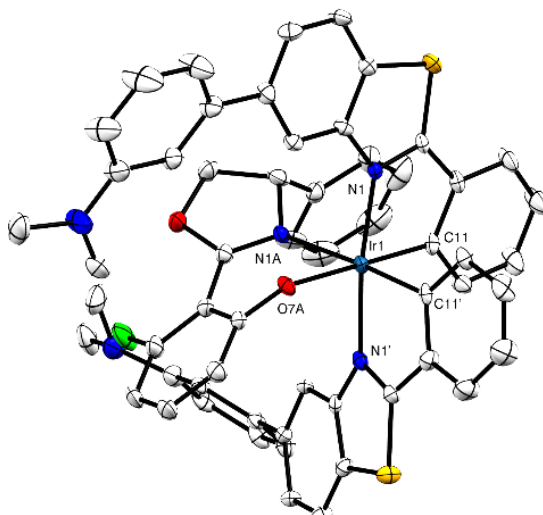
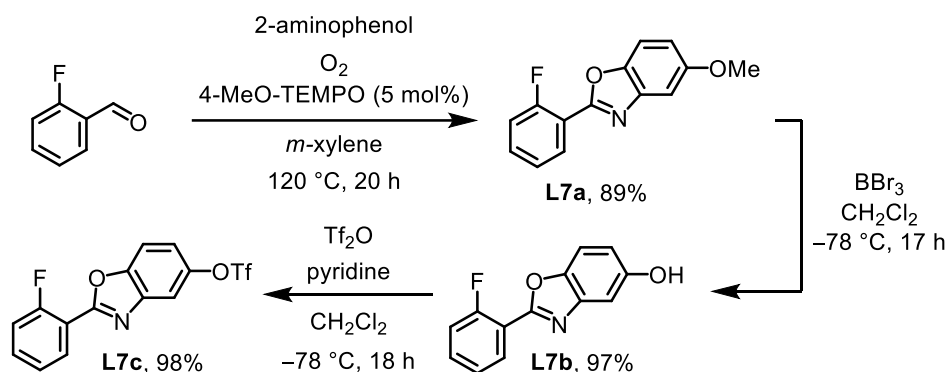


Figure 20: Structure of Δ -(*S*)-C3o. ORTEP drawing with 30% probability of thermal ellipsoids, co-crystallized solvent molecules omitted for clarity. Selected bond lengths [Å] and angles [°]: Ir1-C11 1.993(6), Ir1-C11' 2.009(5), Ir1-N1 2.048(5), Ir1-N1' 2.064(5), Ir1-N1A 2.161(4), Ir1-O7A 2.167(4); C11-Ir1-C11' 88.7(2), C11-Ir1-N1 79.8(2), C11'-Ir1-N1 93.4(2), C11-Ir1-N1' 95.8(2), C11'-Ir1-N1' 79.8(2), N1-Ir1-N1' 172.09(19), C11-Ir1-N1A 99.8(2), C11'-Ir1-N1A 171.43(19), N1-Ir1-N1A 87.19(17), N1'-Ir1-N1A 100.12(17), C11-Ir1-O7A 177.6(2), C11'-Ir1-O7A 89.26(19), N1-Ir1-O7A 99.12(17), N1'-Ir1-O7A 84.95(16), N1A-Ir1-O7A 82.21(16).

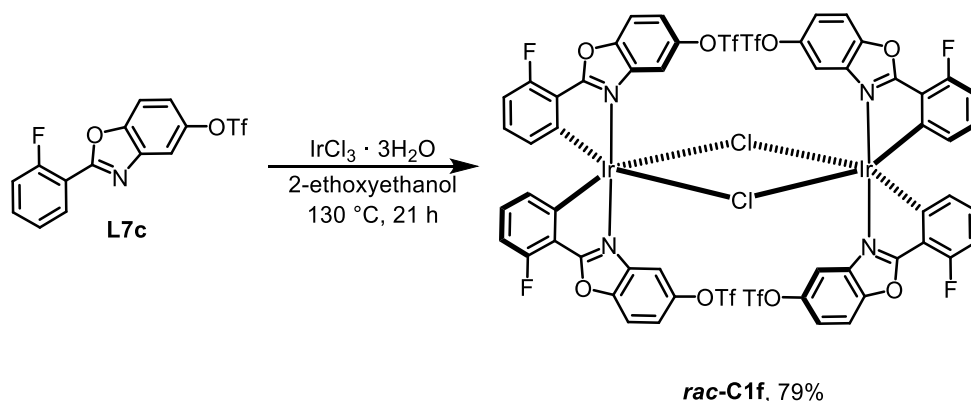
1.3.8 Experiments Towards Orthogonal Multifunctionalization

To circumvent the issue of inseparable diastereomers faced with complexes Λ -(*S*)-**C2f** and Λ -(*S*)-**C2f**, it came to mind to introduce the functional groups to the 2'-position of the cyclometalated ring after complexation as well. This part of the project was developed by ERIK WINTERLING within the context of a bachelor thesis under my supervision.^[26] The idea evolved around a method to address both the 2'-position and the 5-position in an orthogonal fashion. The 5-position would be addressed with the new cross-coupling method and the 2'-position by a different kind of cross-coupling or different reaction all together. Therefore, fluorinated ligand **L7c** was synthesized according to the established method. Commercially available fluorinated carbaldehyde was converted into the methyl protected ligand **L7a** (89% yield),^[5a] deprotected with BBr₃ to form the hydroxy ligand **L7b** (97% yield)^[4b] and esterified with Tf₂O to yield ligand **L7c** (98% yield)^[16] using established methods (84% yield over three-steps, scheme 48).



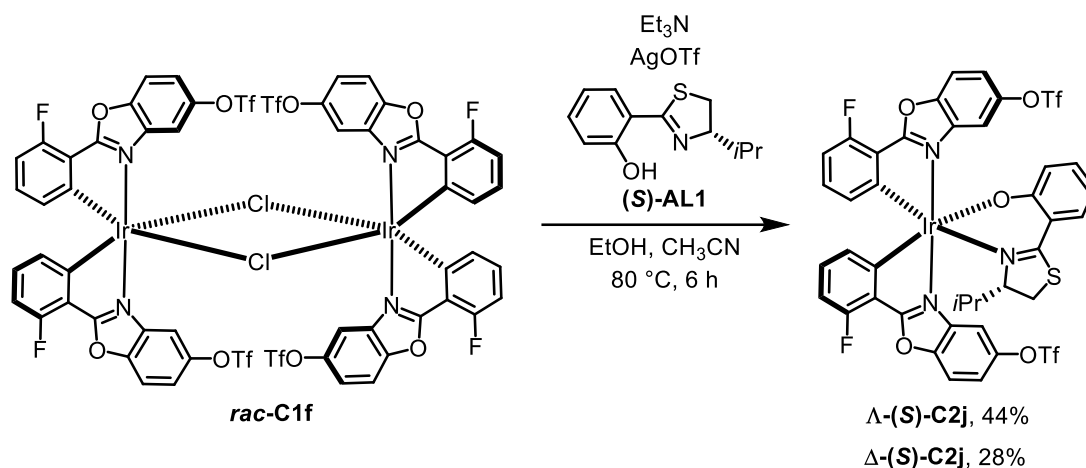
Scheme 48: Synthesis of the TfO functionalized phenyl benzoxazole **L7c** in a three-step protocol.^[4b,5a,16]

The ligand **L7c** was subjected to modified NONOYAMA conditions to synthesize dimer complex *rac*-**C1f** (79%, scheme 49).^[6]



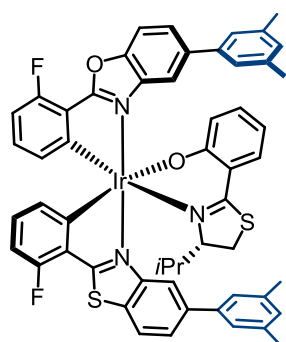
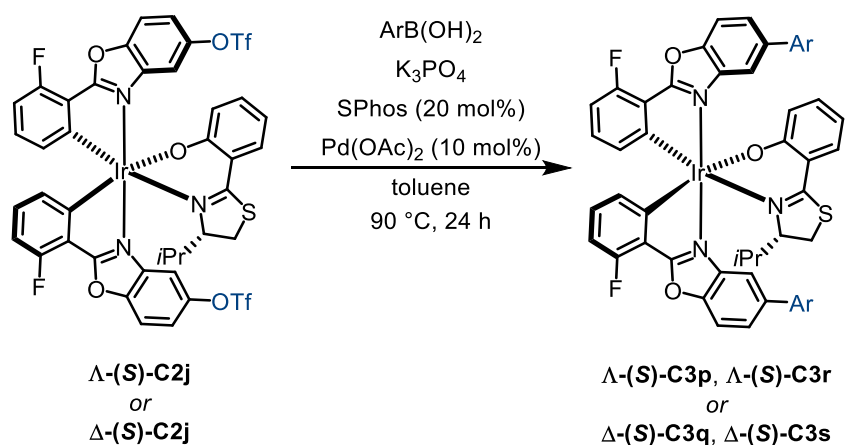
Scheme 49: Synthesis of the TfO functionalized dimer complex *rac*-**C1f**.^[6]

Complex **rac-C1f** inhabited similar solubility properties like dimer complexes **rac-C0** derived from halogenated ligands. This became very much apparent upon the synthesis of the respective diastereomer complexes **Λ-(S)-C2j** and **Δ-(S)-C2j**. To obtain these complexes it turned out to be beneficial to add CH₃CN as an additive to the reaction mixture. This additive and prolonged reaction times lead to the formation of the desired complexes **Λ-(S)-C2j** (44% yield) and **Δ-(S)-C2j** (28% yield, scheme 50).^[7e]

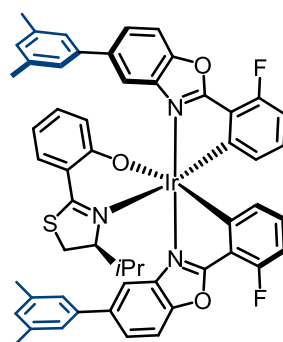


Scheme 50: Synthesis of the fluorine functionalized, diastereomer iridium(III) complexes **Λ-(S)-C2j** and **Δ-(S)-C2j** by established method.^[7e]

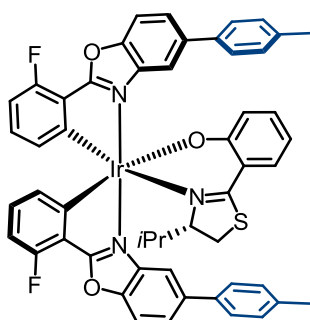
Those fluorinated complexes were successfully used in cross-coupling reactions to furnish complexes **Λ-(S)-C3p** (86% yield) and **Λ-(S)-C3q** (92% yield) using 3,5-dimethylphenylboronic acid as well as **Λ-(S)-C3r** (66% yield) and **Λ-(S)-C3s** using *para*-tolylboronic acid (Scheme 51). It remains to be investigated for future projects, if the fluorinated position can be functionalized after complexation by any means.



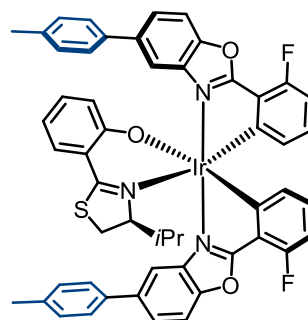
Λ -(S)-C3p, 86%



Δ -(S)-C3q, 92%



Λ -(S)-C3r, 66%

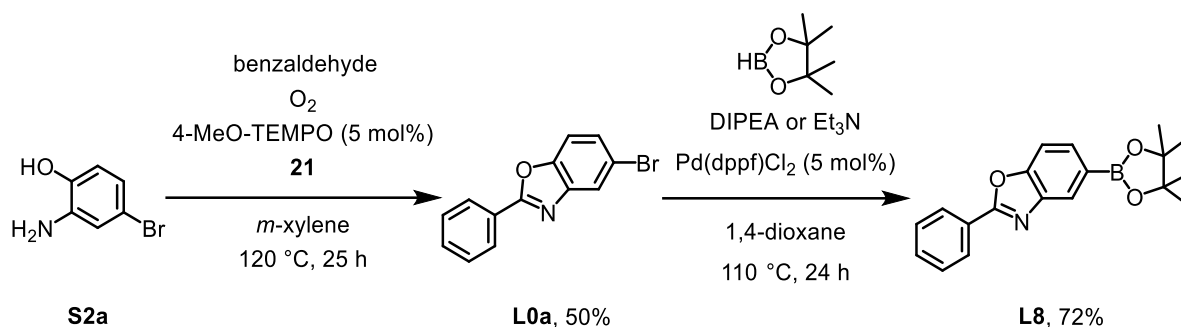


Δ -(S)-C3s

Scheme 51: Scope of the cross-coupling experiments with Λ -(S)-C2j and Δ -(S)-C2j.

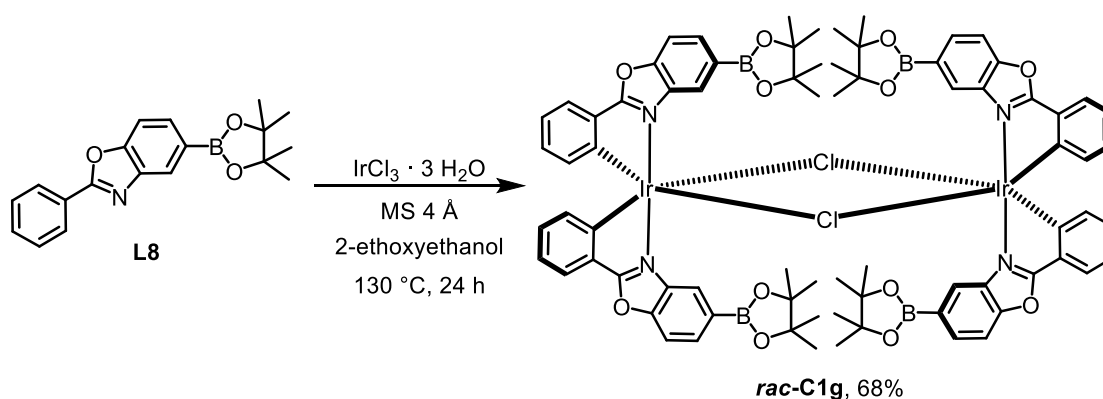
1.3.9 Experiments Towards Inversed Functionality

This part of the project was developed by JANNICK MEINECKE within the context of a bachelor thesis under my supervision.^[27] Encouraged by the previous results and inspired by the work of WILLIAMS and co-workers,^[12a] questions rose, if the reactivity in the cross-coupling reaction can be inverted. Therefore, a Bpin-functionalized benzoxazole ligand was synthesized starting with aminophenol **S2a**, which was reacted with benzaldehyde and 4-MeO-TEMPO under aerobic conditions to form brominated benzoxazole **L0a** (50% yield).^[5a] Bpin-functionalized ligand **L8** was obtained with 72% yield using MASUDA borylation (Scheme 52).^[27]



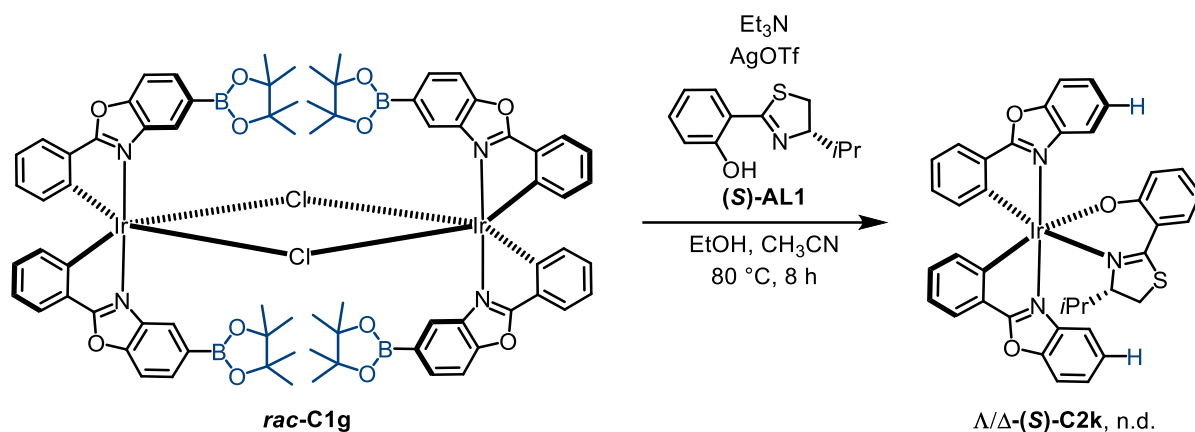
Scheme 52: Synthesis of the Bpin functionalized phenyl benzoxazole **L8** in a two-step protocol.^[5a,27]

To ensure, that all four pinacol boronic acid ester remain intact applying water free NONOYAMA conditions, molecular sieves were added to the reaction mixture to trap trace amounts of water (Scheme 53).^[6]



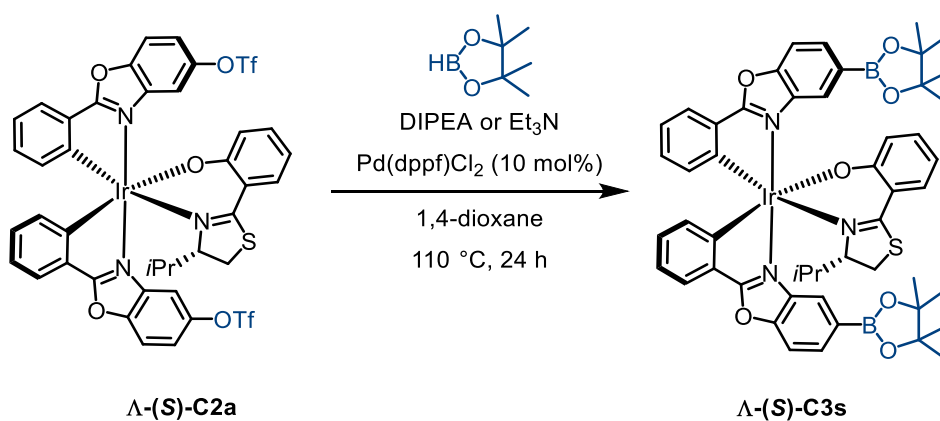
Scheme 53: Synthesis of the Bpin functionalized phenyl benzoxazole iridium(III) dimer **rac-C1g**.^[6]

Indeed, it was possible to obtain borylated dimer complex **rac-C1g** as pale yellowish solid with 68% yield. Unfortunately, both diastereomer complexes were defunctionalized yielding iridium(III) complex species **Λ-(S)-C2k** and **Λ-(S)-C2k** (Scheme 54).^[7e]



Scheme 54: Approach towards Bpin functionalized phenyl benzoxazole iridium(III) diastereomers **Λ-(S)-C2k**.^[7e]

For further investigation, the borylation could take place after complexation yielding complex **Λ-(S)-C3s** circumventing defunctionalization (Scheme 55).



Scheme 55: Potential approach towards Bpin functionalized phenyl benzoxazole iridium(III) diastereomers **Λ-(S)-C3s**.

1.4 Applications

The developed cross-coupling method was successfully applied to other research topics in the MEGGERS group, providing examples for the usefulness of the late stage modification.^[29]

1.4.1 Attachment of Linkers for Immobilization on Solid Support

A common downside faced in the field of homogenous catalysis is the separation of the catalyst from the desired product. Especially for applications in the pharmaceutical industry trace amounts of residual catalyst have to be lowered to acceptable levels.^[30] An example currently faced, can be seen in the contamination of pharmaceutical compound with traces of palladium catalyst after cross-coupling reactions, diming it necessary to further process the desired material.^[30] An issue of equal importance can be seen in the limited “world’s supply of economically accessible of precious metals”.^[31] Solutions to these problems evolve around key aspects like: 1.) Low catalysts loadings lead to less contamination.^[32] 2.) Utilizing different transition metals like nickel^[33] or copper.^[34,35] 3.) Immobilization of the catalyst on (solid) support for easy separation and recycling.^[30] Thinking along these lines, it felt challenging to immobilize chiral LEWIS acid catalysts from the MEGGERS group. Considered methods were covalent bond formation, adsorption on surfaces, ion-pair-formation, and entrapment of the catalyst into a bigger molecule (ship-in-a-bottle).^[36] Due to the competition between solvent/ions/substrate and catalyst occurring with the adsorption and ion-pair-formation methods, leaching of the supported catalyst may be observed.^[36] To avoid this, covalent binding of the catalyst was picked as the method of choice.^[36]

In this context, standard LEWIS acid catalysts^[13] was modified with different linkers. In a cooperative project with VLADIMIR LARIONOV and THOMAS CRUCHTER, linkers **S5a** and **S5b** were designed (Figure 21).^[29a]

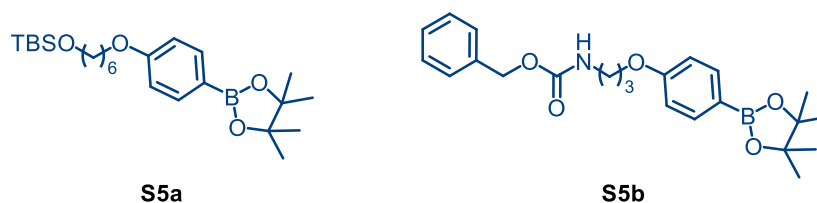
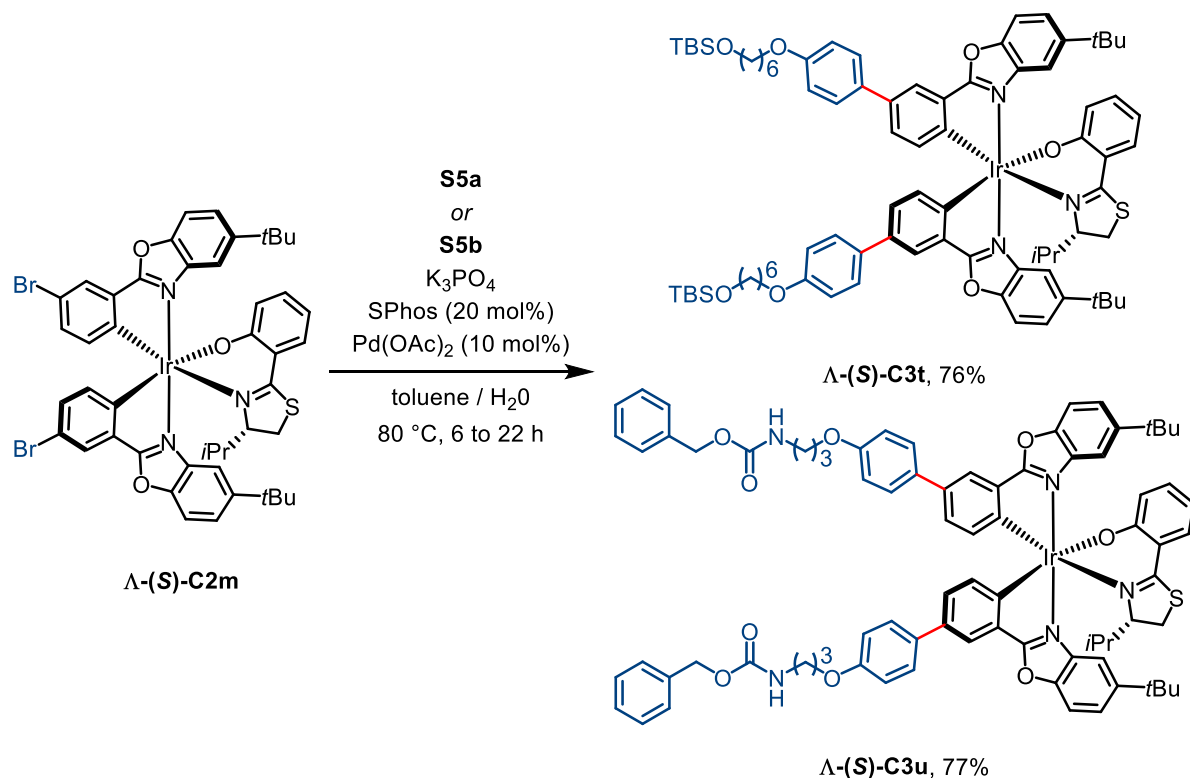


Figure 21: Protected linkers **S5a** and **S5b** functionalized with boronic acid ester for post complexation cross-coupling reactions.^[29a]

These linkers were cross-coupled to the brominated diastereomer complex Λ -(S)-C2m yielding complex Λ -(S)-C3t (76% yield) and Λ -(S)-C3u (77% yield) respectively (Scheme 56).^[29a]



Scheme 56: Functionalization of complex Λ -(S)-C2m with linker **S5a-b** moieties by developed cross-coupling method.^[29a]

After deprotection of the linkers, these complexes were immobilized on functionalized polystyrene (PS) beads and treated with TfOH in acetonitrile to furnish the first literature known stereogenic-at-metal catalysts on solid support (Figure 22).^[29a]

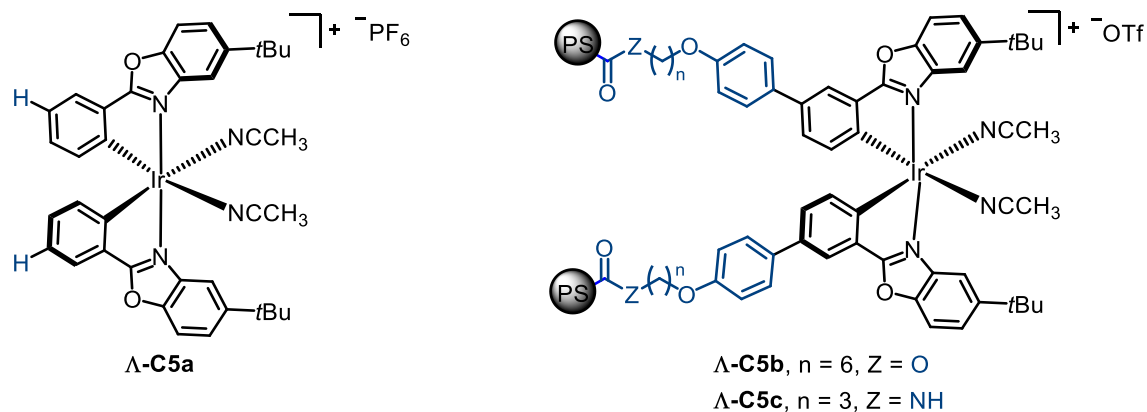


Figure 22: Illustration of the immobilized stereogenic-at-metal LEWIS acid catalysts Λ -C5b-c compared with one of the standard catalysts Λ -C5a.^[29a]

Successful immobilization could already be judged visually in a qualitative fashion due to the bright color of the iridium(III) complexes (Figure 23).²

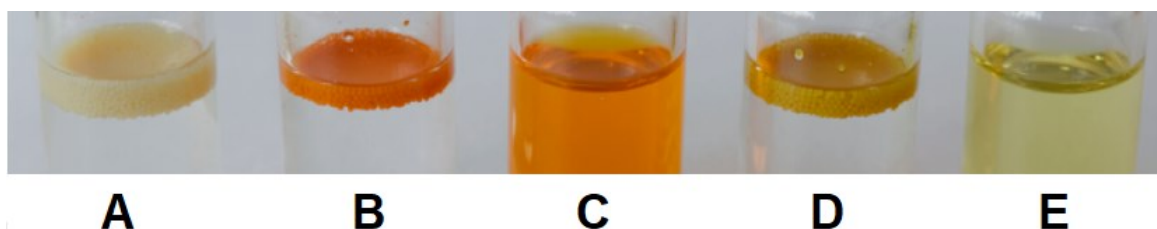
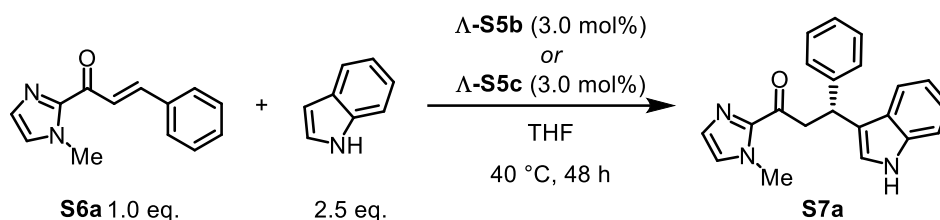


Figure 23: Illustration of iridium complex immobilization on polystyrene. **A** Solid support without complex, **B** Solid support linked with precatalyst, **C** Precatalyst in solution, **D** Solid support linked to LEWIS acid catalyst, **E** LEWIS acid catalyst in solution. All samples in CH₂Cl₂.^[29a]

The chosen model reaction was a FRIEDEL-CRAFTS-alkylation reaction (Scheme 57).



Scheme 57: FRIEDEL-CRAFTS-alkylation reactions as model reaction for the immobilized stereogenic-only-at-metal catalysts **Λ-C5b** and **Λ-C5c** using acyl imidazole **S6a** and indole.^[29a]

It was possible to recycle the immobilized catalyst up to fifteen times for FRIEDEL-CRAFTS-alkylation reactions and still obtain yields up to 99% with an enantiomeric excess of 96% for all runs (Table 2).^[29a]

Table 2: Recycling Experiments with immobilized catalysts for enantioselective FRIEDEL-CRAFTS-alkylation.^[a]

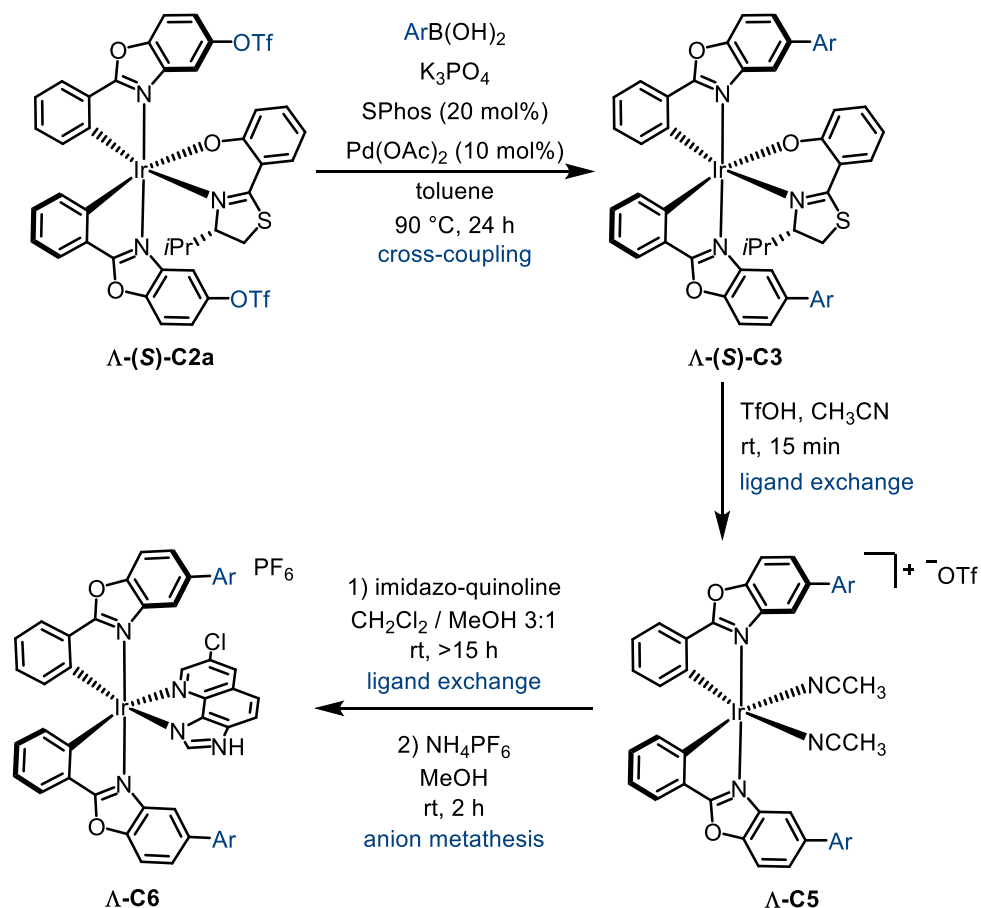
Entry	Run	Conversion (%) ^[b] S7a	ee (%) ^[c]	Conversion (%) ^[b] S7a	ee (%) ^[c]
		Catalyst Λ-C5b		Catalyst Λ-C5c	
1	1	91	96	>99	95
2	2	92	96	>99	96
3	3	80	97	>99	96
4	4	47 (88) ^[d]	96 (96) ^[d]	>99	96
5	5	47 (80) ^[e]	96 (96) ^[e]	95	96
6	15	n.a.	n.a.	>99 ^[f]	96 ^[f]

[a] Reaction conditions: Imidazole **S6a** (0.15 mmol), indole (0.38 mmol), and catalyst **Λ-C5b** or **Λ-C5c** (3.0 mol%) in 0.2 mL (**Λ-C5c**) or 0.4 mL of THF (**Λ-C5b**) were stirred 48 h at 40 °C under nitrogen. n.a. = not applied. [b] Conversion determined by ¹H NMR. [c] Determined by chiral HPLC analysis. [d] Conversion and ee after 96 h are given in parentheses. [e] Conversion and ee after 112 h are given in parentheses. [f] Conversion and ee after 72 h at 50 °C.

² For spectroscopic analysis see supporting information [29a]

1.4.2 Cross-Coupling Products as Precursors for Enantiopure Lewis Base Catalysts

The investigated method displayed its usefulness in supporting the efforts of THOMAS CRUCHTER to screen iridium(III) scaffolds for LEWIS base catalysis **Λ-C6**, especially when pyrene groups were involved (Scheme 58).^[29b]



Scheme 58: Application of the cross-coupling products as scaffolds for LEWIS base precatalysts **Λ-C6**.^[29b]

A small library of catalyst was accessible from common precursor. This was achieved by functionalizing the precursor **Λ-(S)-C2a** by cross-coupling reaction forming **Λ-(S)-C3**, followed by exchanging the chiral ligand with a functional, achiral imidazo-quinoline ligand and counterion metathesis leading to LEWIS base precatalysts **Λ-C6** (Figure 24).^[29b]

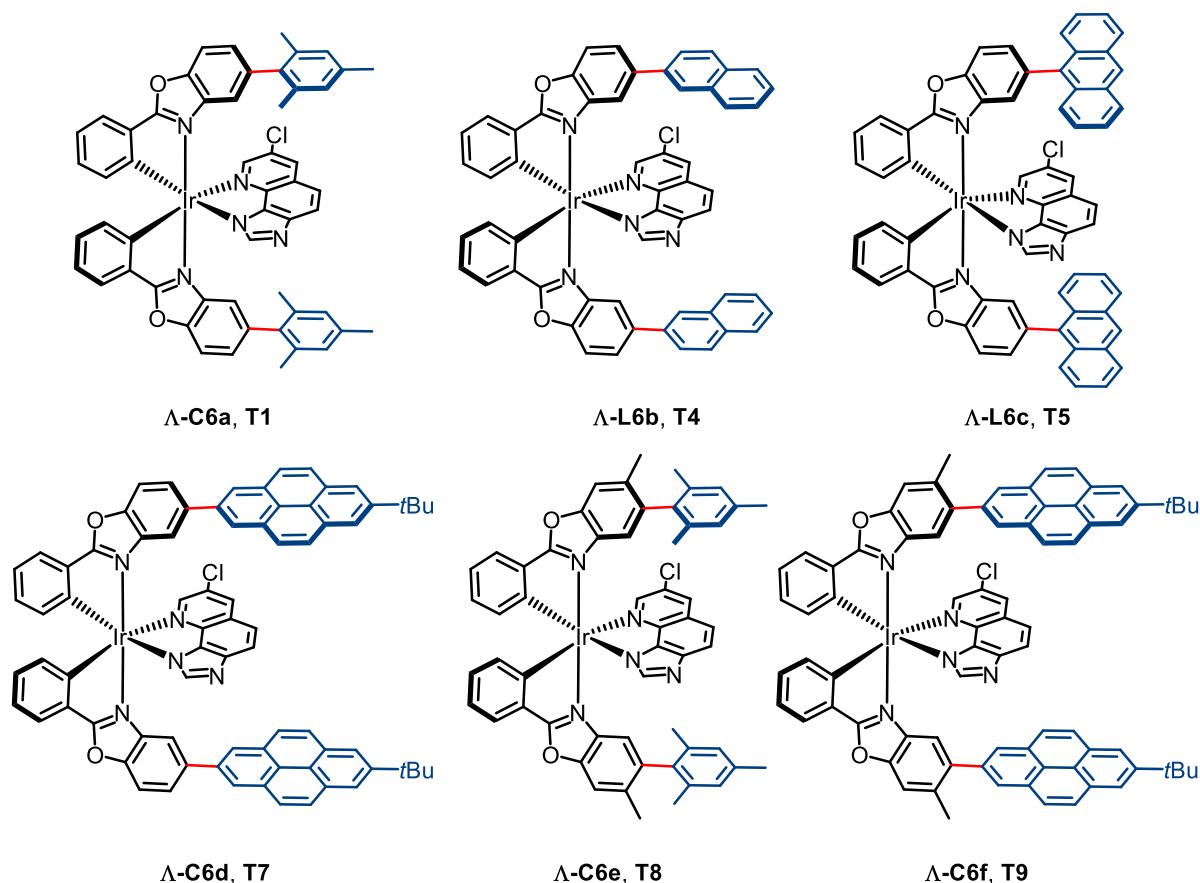


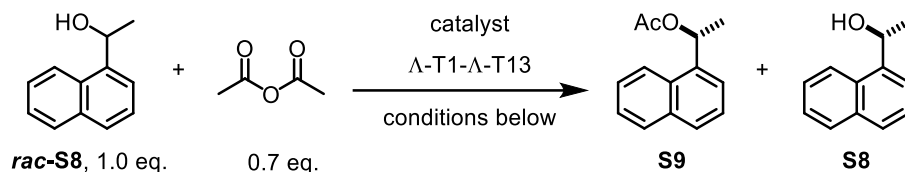
Figure 24: Representative precatalysts Λ -C6 that are accessible with the developed cross-coupling method.^[29b]

Those catalysts were used for kinetic resolution of *rac*-1-(1-naphthyl)ethanol (***rac*-S8**) with acetic anhydride as resolving agent. The complete catalyst screening is displayed in table 3 to compare the results of precatalysts Λ -C6a-f (**T1**, **T4**, **T5**, **T7-9**), that were prepared with the cross-coupling strategy with those precatalysts **T2**, **T3**, **T6**, **T10-13** that were synthesized by the classic approach.^[29b]

For sake of clarity, only catalysts prepared with the cross-coupling strategy are displayed in this thesis. For further details see: *Design, Synthesis, and Application of a Nucleophilic Octahedral Stereogenic-Only-at-Metal Iridium(III) Catalyst* by THOMAS CRUCHTER.^[29b]

With those precatalysts Λ -C6, selectivity factors ranging from $S = 1.64$ to $S = 3.21$ were achieved. It has to be pointed out, that those results are in the same margin as selectivity factors received by precatalysts **T2**, **T3**, **T6**, **T10-13** that were prepared with classic procedures.^[29b]

Table 3: Kinetic resolution of *rac*-1-(1-naphthyl)ethanol (*rac*-**S8**) with acetic anhydride as resolving agent and catalysts **Λ-T1–Λ-T13**. Experiment conducted by co-worker THOMAS CRUCHTER.^[a] Entries with precatalysts prepared by the cross-coupling approach are: 1 to 6 and 8 to 12, entry with the best result: 7.^[29b]



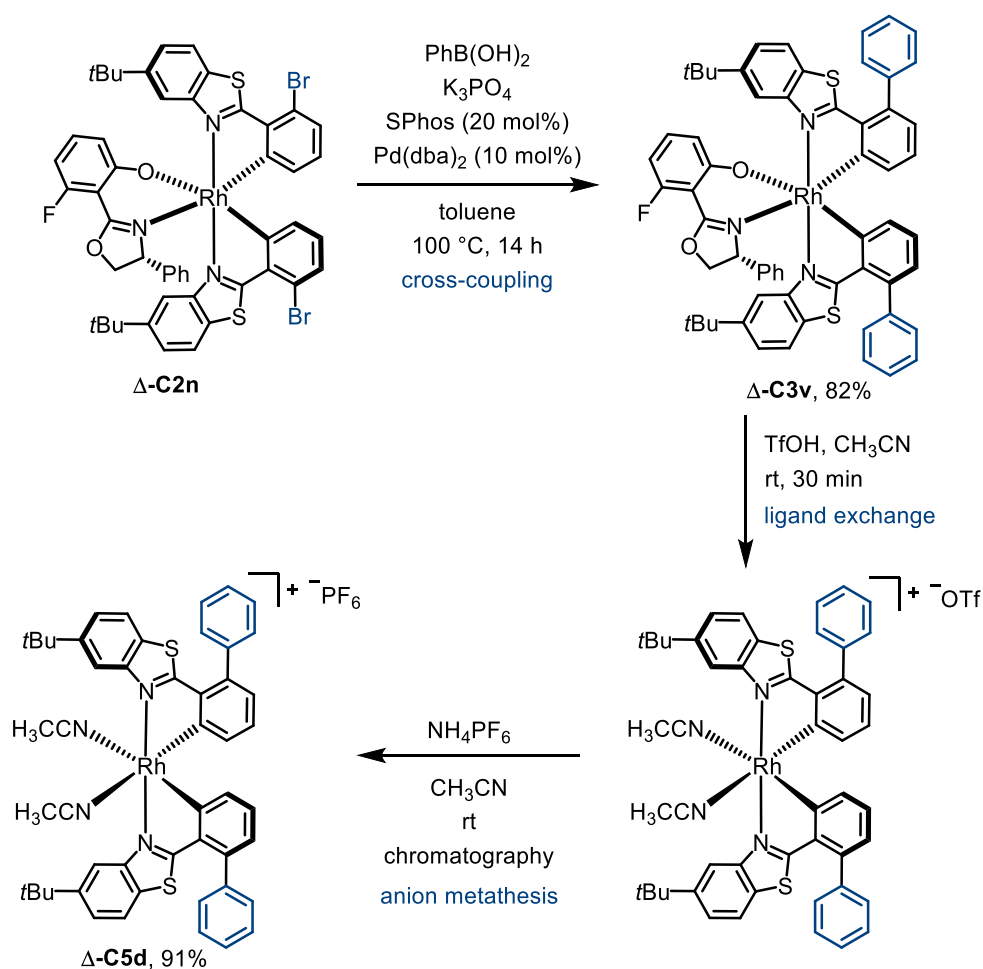
Entry	Complex	Cat. Loading (mol%)	T (°C)	Solvent	Time (min)	C ^[b] (%)	ee of S9/S8 ^[c] (%)	S ^[b]
1 ^[d]	Λ-T1 (\triangleq Λ-X2)	0.2	0	TAA	50 / 100	45 / 62	30 / 49	2.92 / 2.89
2 ^[d]	Λ-T1 (\triangleq Λ-X2)	0.2	0	TAA	50 / 110	48 / 65	36 / 56	3.22 / 3.15
3	Λ-T2	1	0	TAA	50 / 100	~25 / ~50	< 3 / < 3	~1.0 / ~1.0
4 ^[e]	<i>rac</i> - T3	0.5	rt	TAA	125	trace ^[f]	— ^[f]	— ^[f]
5	Λ-T4	0.2	0	TAA	50 / 110	11 / 37	3 / 11	1.65 / 1.64
6 ^[g]	Λ-T5	— ^[g]	— ^[g]	— ^[g]	— ^[g]	— ^[g]	— ^[g]	— ^[g]
7	Λ-T6	0.2	0	TAA	50 / 100	19 / 37	13 / 30	3.80 / 3.92
8	Λ-T7	0.3	0	TAA	50 / 100	22 / 48	8 / 22	1.99 / 1.97
9 ^[d]	Λ-T8	0.3	0	TAA	50 / 100	53 / 60	42 / 51	3.21 / 3.19
10 ^[d]	Λ-T8	0.3	0	TAA	50 / 100	55 / 65	43 / 56	3.06 / 3.05
11	Λ-T9	0.3	0	TAA	50 / 100	22 / 45	10 / 25	2.35 / 2.36
12	Λ-T9	0.6	0	TAA	50 / 100	28 / 56	14 / 34	2.35 / 2.35
13	Λ-T10	0.6	0	TAA	50 / 100	31 / 45	14 / 22	2.16 / 2.14
14	Λ-T10	1.8	0	TAA	50 / 100	51 / 60	26 / 33	2.11 / 2.08
15	Λ-T11	0.3	0	TAA	50 / 100	10 / 21	6 / 13	3.11 / 3.35
16	Λ-T12	0.6	0	TAA	50 / 100	32 / 53	19 / 38	2.84 / 2.86
17	Λ-T13	0.6	0	TAA	50 / 100	69 / 69	51 / 52	2.49 / 2.49
18	Λ-T13	0.3	0	TAA	50 / 100	63 / 67	44 / 49	2.52 / 2.51
19	Λ-T13	0.1	0	TAA	50 / 100	45 / 59	28 / 41	2.62 / 2.56

[a] Standard reaction conditions: Substrate *rac*-**S8** (1.0 eq; 200–400 μ mol), 0.7 eq acetic anhydride, and 0.7 eq *i*Pr₂NEt with catalysts **Λ-T1–Λ-T13** in the indicated solvent at conc = 0.7 M at the indicated temperature.

[b] Calculated according to KAGAN's equation. [c] Enantioselectivities of **S8** and **S9** determined from crude product mixtures by chiral HPLC analysis (Chiralpak IB (5 μ m, 25 cm x 4.6 mm); *n*-hexane/*i*PrOH 90:10, λ = 254 nm, flow = 0.5 mL/min, *t* (column) = 40 °C: **S9**: t_R = 7.7 min and 8.3 min; **S8**: t_R = 11.8 min and 14.2 min). [d] Two different freshly prepared batches of catalysts were used. [e] 1.1 eq Ac₂O and 1.1 eq *i*Pr₂NEt were added. [f] Direct comparison with a reference batch without any complex indicated that the trace formation of **S9** exclusively originated from the uncatalyzed racemic background reaction. [g] Not tested, **Λ-T5** was found to be unstable.

1.4.3 Access to Structural Diverse Rhodium(III) Complexes

During research on stereogenic-only-at-metal rhodium(III) complexes, the MEGGERS group faced increasing demand to finetune those catalysts to further improve their performance. The introduction of diverse groups attached to the cyclometalating phenyl ring by traditional means (modification on the ligand followed by complex chemistry) led to difficulties in dimer formation and challenging purification. To circumvent these problems, co-worker JIAJIA MA applied the post complexation cross-coupling method to brominated diastereomer rhodium(III) precursor complex Δ -(*S*)-C2n. The phenylated rhodium(III) complex Δ -(*S*)-C3v was obtained after 14 h reaction time with 82% yield using 10 mol% of Pd(dba)₂, 20 mol% of SPhos, K₃PO₄ and PhB(OH)₂ in toluene. The modified LEWIS acid catalyst Δ -C5d was obtained after ligand exchange and anion metathesis with 91% yield (Scheme 59).^[29c]

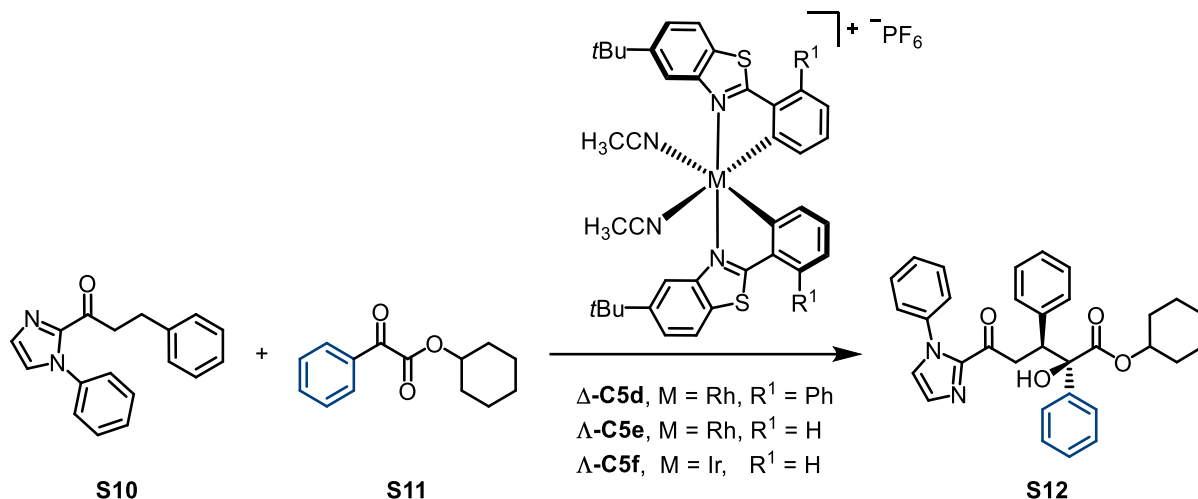


Scheme 59: Synthesis of structural divers stereogenic-only-at-metal rhodium(III) LEWIS acid catalysts Δ -C5d by using the developed cross-coupling method.^[29c]

Functionalized catalyst Δ -C5d showed particular usefulness compared to the unfunctionalized catalyst Δ -C5e and Δ -C5f for the visible-light-activated asymmetric β -C–H functionalization

of 2 acceptor-substituted ketones with 1,2-dicarbonyl (Table 4). Indeed, it was possible to increase diastereoselectivity from 6.4:1 to 10:1 as well as enantiomeric excess from 98% to >99% (compare entry 1 and 2, table).^[29c]

Table 4: Catalyst comparison for the visible-light-activated asymmetric β -C–H functionalization of 2 acceptor-substituted ketones with 1,2-dicarbonyl compounds devised by JIAJIA MA.^[a] ^[29c]



Entry	Catalyst	M	R ¹	NMR yield (%) ^[b]	d.r. ^[c]	ee (%) ^[d]
1	$\Delta\text{-C5e}$	Rh	H	98	6.4:1	98
2	$\Delta\text{-C5d}$	Rh	Ph	98	10.0:1	>99
3	$\Delta\text{-C5f}$	Ir	H	0	n.a.	n.a.

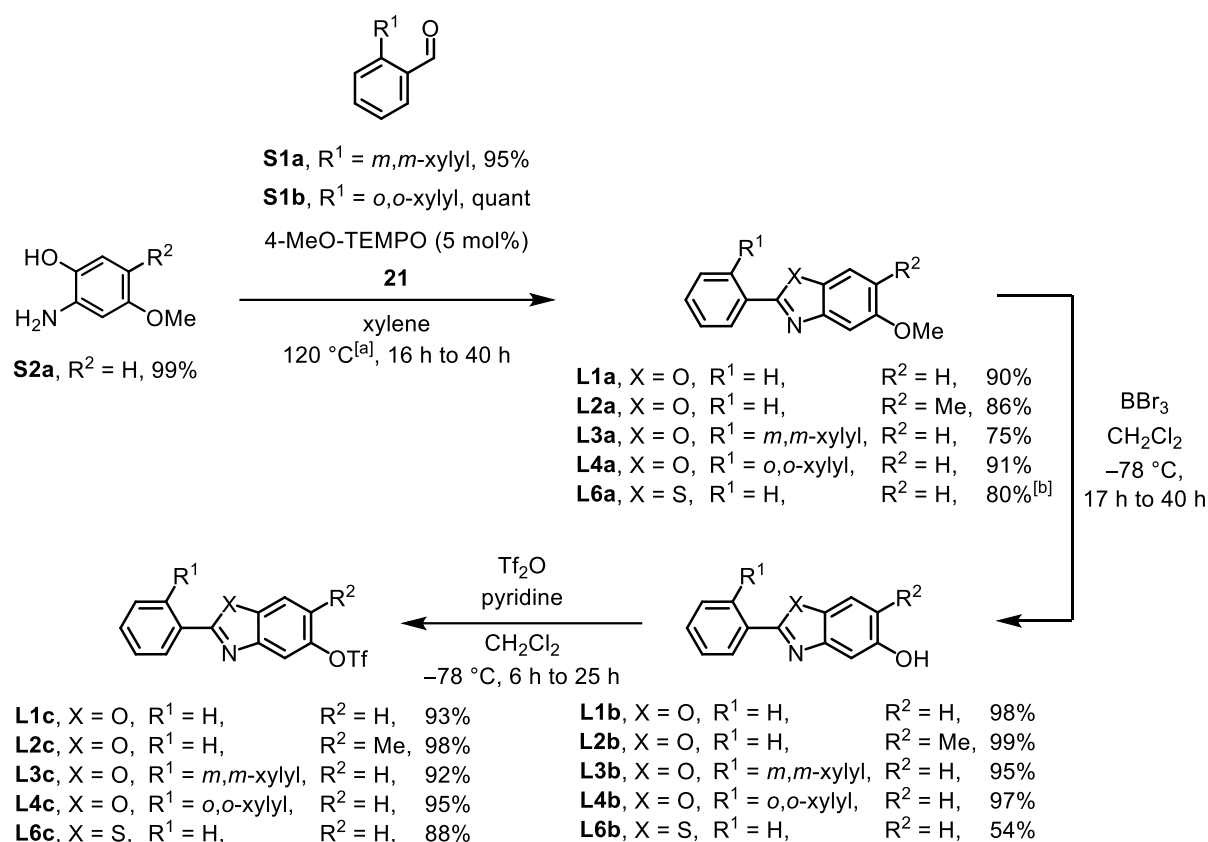
[a] Reaction conditions: **S10** (0.1 mmol), **S11** (0.3 mmol), chiral LEWIS acid catalyst $\Delta\text{-C5}$ (0.004 mmol), and DABCO (0.02 mmol) in acetone (1 mL) stirred at rt for 16 h under N₂ and irradiated with blue LEDs (24 W).

[b] Determined by ¹H NMR of the crude products. [c] Determined by ¹H NMR analysis of the crude main product.

[d] Determined by HPLC analysis of the crude main product on a chiral stationary phase; ee of major diastereomer is shown. n.a. = not applicable.

1.5 Summary

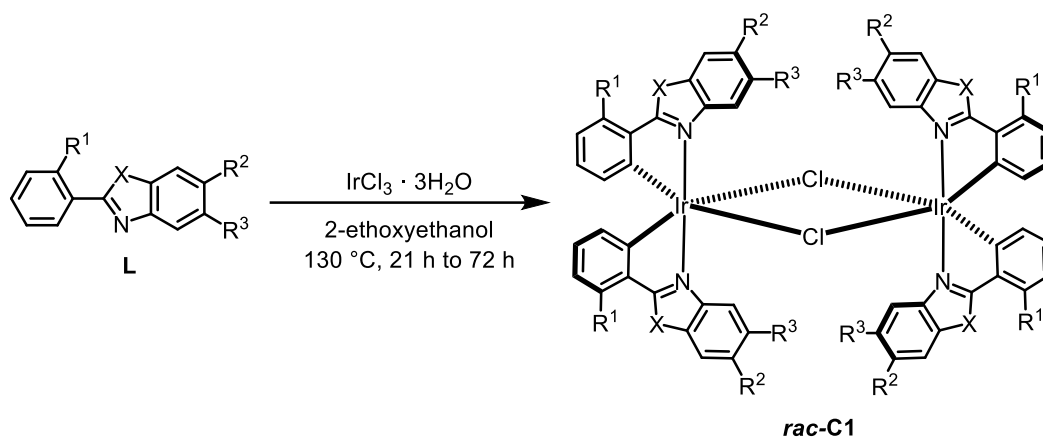
Goal of this project was to develop a method for post complexation modifications by cross-coupling reactions on diastereomerically pure bis-cyclometalated iridium(III) complexes after their separation. The protocol provides access to an array of different complexes from one common precursor, rendering it a useful tool in the life sciences, materials sciences, and in asymmetric catalysis. To gain access to these complexes, appropriately functionalized ligands were designed. Six different literature-unknown triflate-functionalized phenyl benzoxazole and phenyl benzothiazole ligands **L** were synthesized in a three-step protocol from easily accessible benzaldehydes **S1** and 2-aminophenols **S2** (Scheme 60).



Scheme 60: Synthesis of TfO-functionalized benzoxazole ligands. [a] For ligand **L2a** 135 °C was used. [b] Ligand **L6a** was synthesized with a different protocol (Scheme 42 and 43).

Those ligands were successfully reacted with iridium(III) chloride under modified NONOYAMA conditions to furnish six new racemic iridium(III) dimer complexes **rac-C1** with yields up to 89% (Entry 2, table 5). It is worth noting that such triflated dimer complexes were well-soluble in chlorinated solvents and alcohols.

Table 5: Synthesis of racemic iridium(III) dimer complexes **rac-C1** bearing triflate and bromide substituents.^[a]



Entry	Ligand	Dimer	R ¹	R ²	R ³	X	Yield ^[b] [%]
1	L1c	rac-C1a	H	H	TfO	O	87
2	L2c	rac-C1b	H	Me	TfO	O	89
3	L3c	rac-C1c	<i>m,m</i> -xylyl	H	TfO	O	79
4	L4c	rac-C1d	<i>o,o</i> -xylyl	H	TfO	O	39
5	L5 ^[c]	rac-C1e	H	H	Br	S	70
6	L6c	rac-C1f	H	H	TfO	S	7

[a] Reaction conditions: Iridium(III) chloride hydrate (1.00 eq.) and **L** ligand (2.00 eq.) in 2-ethoxyethanol (c = 25 – 100 mM) at 130 °C under exclusion of light. [b] Isolated yield. [c] 2-Ethoxyethanol and water were used as solvent in a 3:1 ratio.

To obtain the desired diastereomer iridium(III) complexes, the dimer complexes **rac-C1** were cleaved with chiral ancillary ligands (**S**)-**AL1** or (**S**)-**AL2** in the presence of AgOTf and Et₃N (Table 6).

Table 6: Synthesis of diastereomeric precursor complexes with salicylthiazolinato (**(S)**-AL1 and salicyloxazolinato (**(S)**-AL2 ligands.^[a]

Entry	Dimer	R ¹	R ²	R ³	X	R ⁴	Y	R ⁵	AL	Dia	Yield	Dia	Yield
	<i>rac</i>								(S)	Δ-(S)	[%] ^[b]	Δ-(S)	[%] ^[b]
1	C1a	H	H	TfO	O	<i>i</i> Pr	S	H	1	C2a	40	C2a	38
2	C1b	H	Me	TfO	O	<i>i</i> Pr	S	H	1	C2b	40	C2b	37
3	C1c	<i>m,m</i> -xylyl	H	TfO	O	<i>i</i> Pr	S	H	1	C2c	35	C2c	0 ^[c]
4	C1c	<i>m,m</i> -xylyl	H	TfO	O	Ph	O	F	2	C2e	39	C2e	35
5 ^[d]	C1e	H	H	Br	S	<i>i</i> Pr	S	H	1	C2g	35	C2g	0 ^[c]
6	C1f	H	H	TfO	S	<i>i</i> Pr	S	H	1	C2h	28	C2h	0 ^[c]
7 ^[d]	C1e	H	H	Br	S	Ph	O	F	2	C2i	46	C2i	44

[a] Reaction conditions: Racemic iridium(III) dimer complex **rac-C1** (1.00 eq.) and ancillary ligand (2.10 eq.) salicylthiazoline (**(S)**-AL1 or salicyloxazoline (**(S)**-AL2) in the presents of AgOTf (2.10 eq.) and Et₃N (10.0 eq.) in EtOH (15–30 mM) at 80 °C. Resolution of the resulting diastereomeric complexes was achieved by simple flash column chromatography.^[4] [b] Isolated yield. [c] Δ-(S)-C2c, Δ-(S)-C2g and Δ-(S)-C2h were found to be unstable on silica and basic aluminium oxide as stationary phase. [d] Acetonitrile was added.

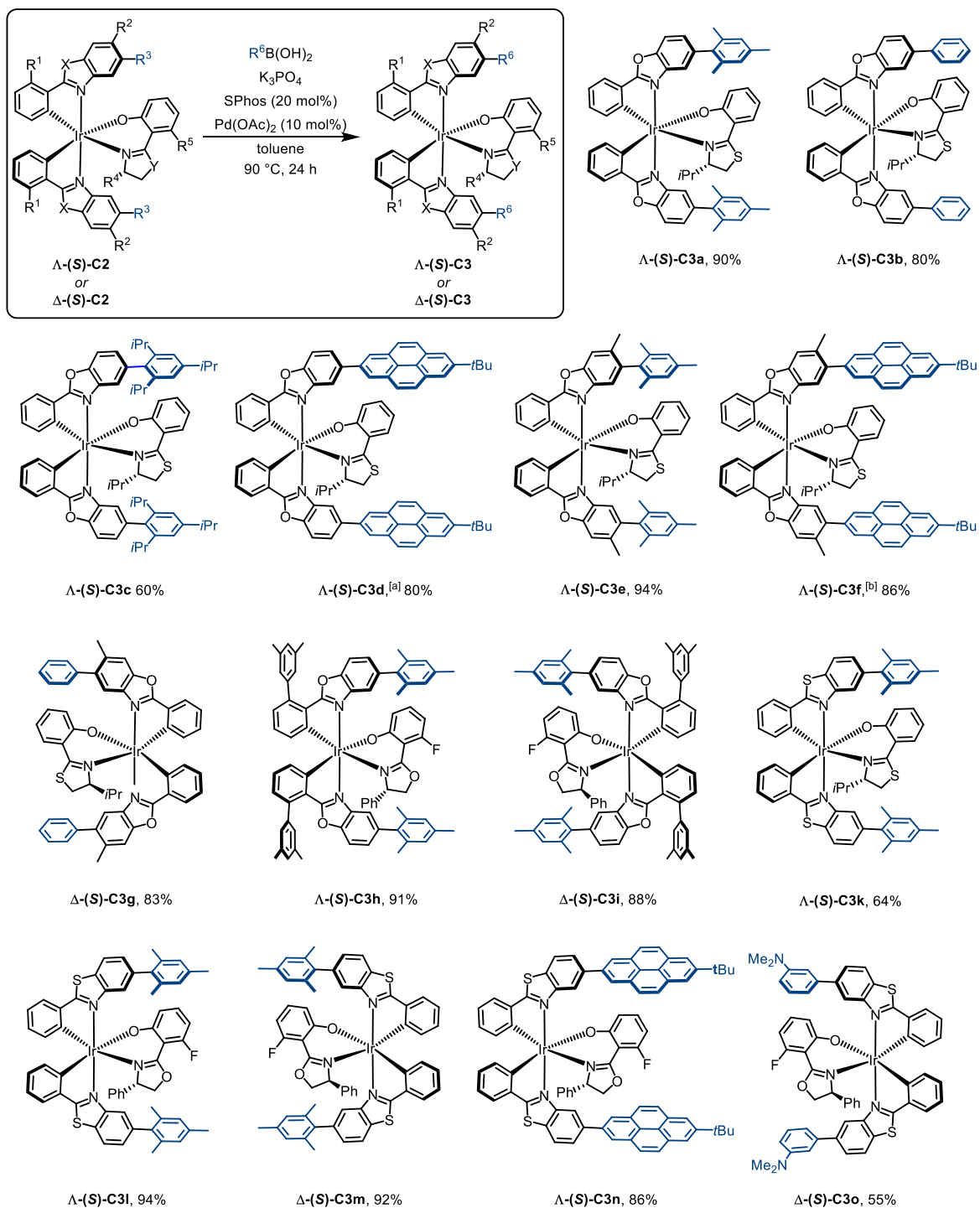
In total, eleven new diastereomer iridium(III) complexes **C2** suitable for modifications by cross-coupling were obtained as single diastereomers with yields up to 46% (Table 6).

In the course of these experiments it was possible to get valuable insights into the influence of chiral ancillary ligands (**(S)**-AL1-3 with regard to stability and separability. Fluorinated ancillary ligand (**(S)**-AL2 turned out to be the ligand of choice, when *iso*-propyl-functionalized ancillary (**(S)**-AL1 formed unstable complexes. On the other hand, *tert*-butyl-functionalized ancillary ligand (**(S)**-AL3 turned out to be superior in terms of separability. From these observations it was concluded that the *iso*-propyl-functionalized ancillary ligand (**(S)**-AL1 strikes a good compromise between stability and separability of the diastereomer iridium(III) complexes **C2**.

The absolute configuration of the synthesized precursor complexes **C2** was determined by X-ray diffraction and CD spectra comparisons. The results matched with previous observations made in the MEGGERS group, namely that Λ -(*S*) configured complexes **C2** always eluate before Δ -(*S*) configured complexes **C2**, making a general trend apparent.

This precursor complexes **C2** were then modified by post complexation SUZUKI cross-coupling reactions, giving access to 18 aryl-functionalized, diastereomerically pure iridium(III) complexes **C3** with yields up to 94%. Representative HPLC experiments demonstrated that these complexes can be obtained with 99% *ee* using this method. This rendered the investigated approach suitable to screen catalytic properties in asymmetric synthesis (Scheme 61).

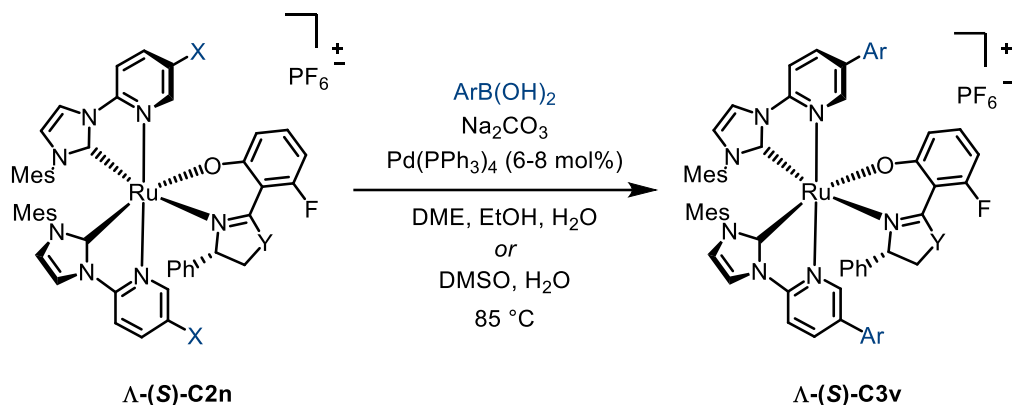
In cooperation with other group members it was demonstrated that this approach is of high synthetic value, namely by the synthesis of the first stereogenic-at-metal catalyst on a solid support (see figure 22 Λ -**C5b** and Λ -**C5c**),^[29a] in the field of asymmetric LEWIS base catalysis (catalyst Λ -**C6**)^[29b] and in finetuning rhodium(III) complexes for LEWIS acid catalysis.^[29c]



Scheme 61: Representative examples for the scope of post-complexation SUZUKI cross-couplings on functionalized iridium(III) precursor complexes $\Lambda\text{-(S)-C3}$ and $\Delta\text{-(S)-C3}$. Isolated yields. [a] Pinacol boronic ester was used instead of free boronic acid.

1.6 Outlook

Since iridium(III) and rhodium(III) complexes were successfully modified by the presented cross-coupling strategy, it would be reasonable to extend the scope towards ruthenium(II) complexes. Due to the fact that ruthenium(II) complexes **Λ -(S)-C2n** are cationic and therefore potentially poorly soluble in toluene, it might be appropriate to use polar solvent mixtures applied by WILLIAMS and co-workers (compare scheme 14, 15 and 16).^[12]

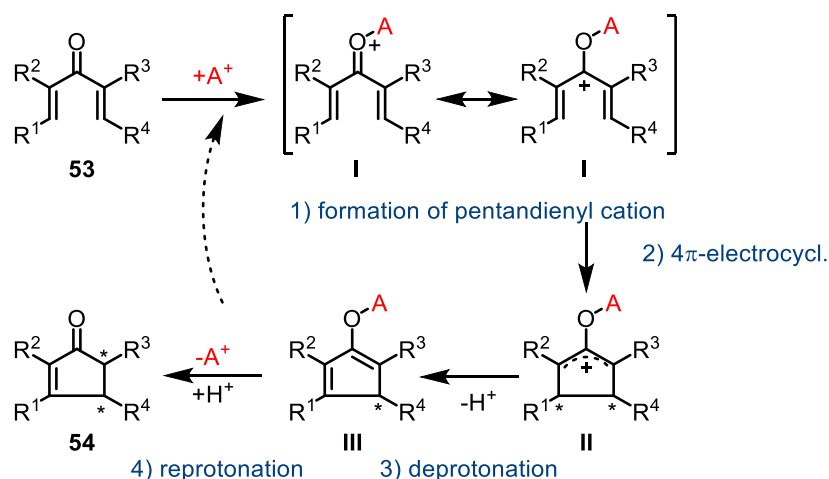


Scheme 62: Potential reaction path towards functionalized ruthenium(II) complexes **Λ -(S)-C3v** by cross-coupling strategy.^[12]

2 Asymmetric Nazarov Cyclization Reactions

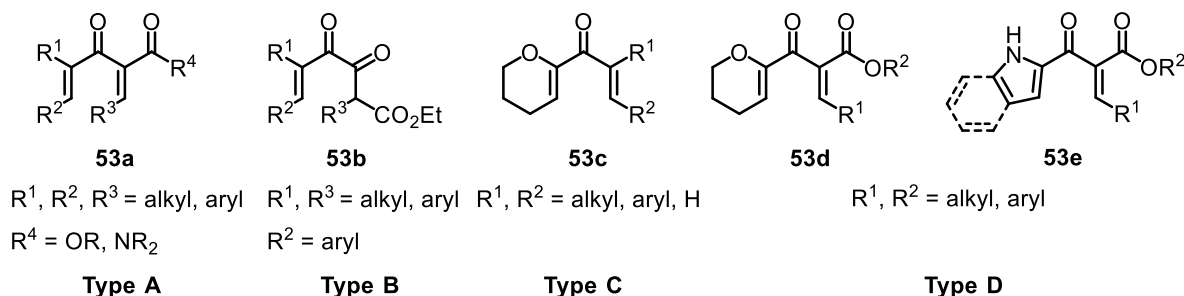
2.1 Introduction

The NAZAROV cyclization is a powerful tool in organic chemistry to generate cyclopentenones^[37-40] and cyclopenta[*b*]indoles.^[41] Most commonly, the reaction is activated by BRØNSTED- or LEWIS acids and proceeds under thermal conditions via a 4 π -electrocyclization mechanism: 1.) Activation of divinyl ketone or aryl vinyl ketone **53** by the LEWIS acid A^+ to form cation **I**. 2.) Conrotatory 4 π -electrocyclization reaction under thermal conditions to form cyclopentenyl cation **II**. 3.) Deprotonation to form intermediate **III**. 4.) Re-protonation under formation of cyclopentenyl **54** and release of the LEWIS acid A^+ for new turnover (Scheme 63).^[37b]



Scheme 63: General mechanism of the LEWIS acid catalyzed NAZAROV cyclization. Stereocenters are marked with an asterix.

The substrates suitable for this reaction can be categorized into different classes. A proposal for four representative substrate types was made by TANG (Scheme 64).^[42]



Scheme 64: Representative substrate types commonly investigated in enantioselective NAZAROV cyclization reactions.

Type A substrates are acyclic and distinguished by a lag of polarizing and for that matter activating groups, whereas acyclic **Type B** diketoester substrates get complementary polarized

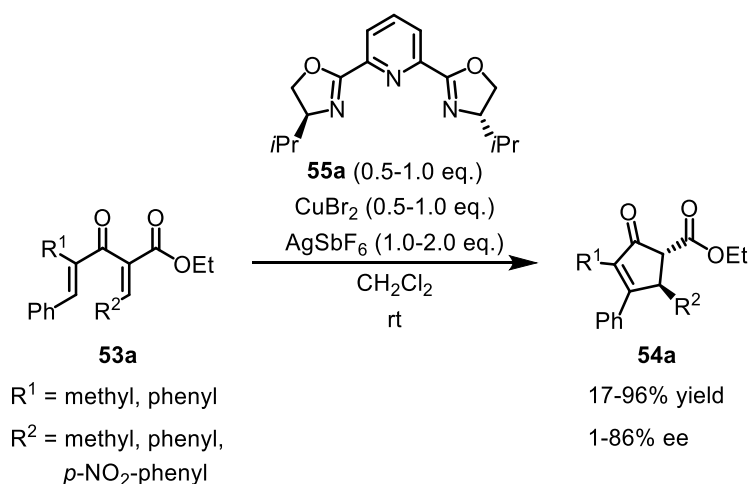
upon coordination to the catalyst. **Type C** and **D** substrates contain negatively polarized cyclic moieties, favoring a rapid cyclization. **Type D** substrates contain an additional electron withdrawing group, further complementary polarizing the substrate and providing a second coordination site for the catalyst.^[42]

In recent years, significant efforts have been devoted to catalytic methods for asymmetric NAZAROV cyclization reactions.^[40-48] However, the combination of low catalyst loadings, short reaction times, high enantioselectivity and high diastereoselectivity is still a formidable challenge, even for favorably activated substrates from **Type C** and **D**.^[40-48]

The following section should provide an overview on the progress and challenges faced in the field of the enantioselective NAZAROV cyclization for substrate classes **Type A** to **D**.

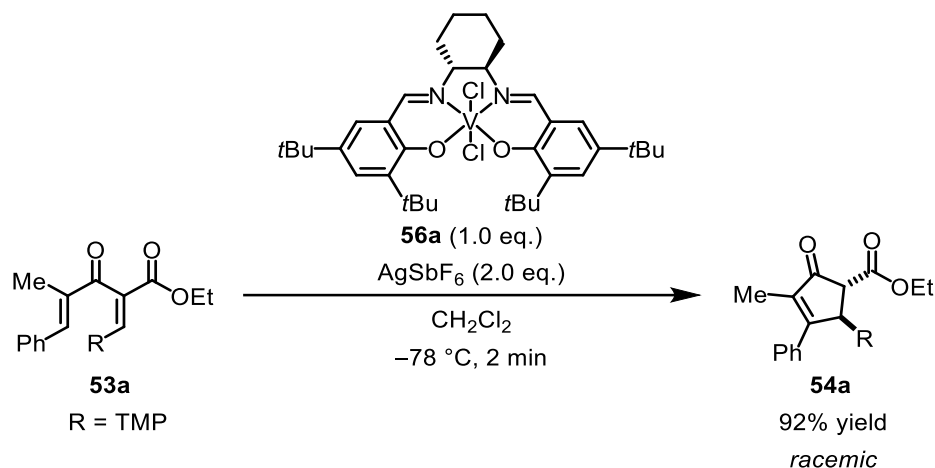
2.1.1 Nazarov Cyclization with Substrate Type A

After TRAUNER and co-workers published first results in the field of asymmetric NAZAROV in 2003,^[43] one of the first studies dealing exclusively with the asymmetric NAZAROV cyclization was published 2003 by BELFIELD and co-workers.^[44a] The ring closing reaction of substrates **53a** (Type A) was catalyzed by a Cu-PyBOX complex which was formed previously from PyBOX ligand **55a**, CuBr₂ and two equivalents AgSbF₆. This catalyst showed better performance if precipitated AgBr was removed by filtration and if the complex was purified by column chromatography. The reaction was conducted with 0.5 to 1.0 equivalents catalyst in CH₂Cl₂ at ambient temperature. The term promoter is therefore more appropriate than catalyst in case of reactions with 1.0 equivalent complex. Even though considerable amounts of LEWIS acid complex must be used, the results are nonetheless astonishing since the products **54a** were obtained with yields up to 96% and selectivity up to 86% ee observed as a single diastereomer (Scheme 65).^[44a]



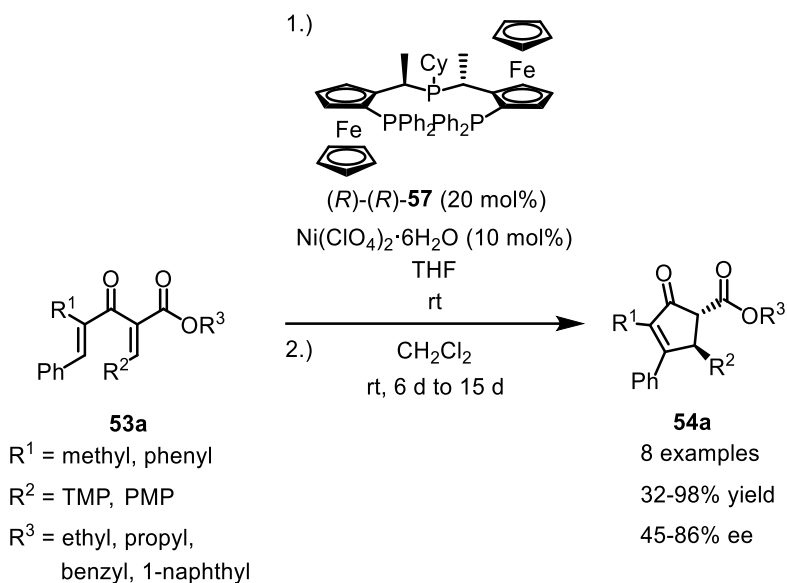
Scheme 65: First study dealing exclusively with the catalytic asymmetric NAZAROV cyclization. The substrates **53a** were treated with up to equimolar ratios of Cu-PyBOX complex to furnish cyclization products **54a**.^[44a]

The same substrate class was investigated in 2007 by TOGNI and co-workers, using a cationic vanadium(IV) salen complex as catalyst at ambient temperature.^[44b] All NAZAROV cyclization reactions were carried out inside a glove box due to the sensitive nature of the dicationic catalyst. Substrate **53a** was treated with one equivalent of vanadium salen complex **56a** and two equivalents AgSbF₆ in CH₂Cl₂ to obtain product **54a** with 92% yield observed as a single diastereomer. However, no matter what temperature, solvent or molar ratio of catalyst was used, the product was obtained as a racemic mixture (Scheme 66).^[44b]



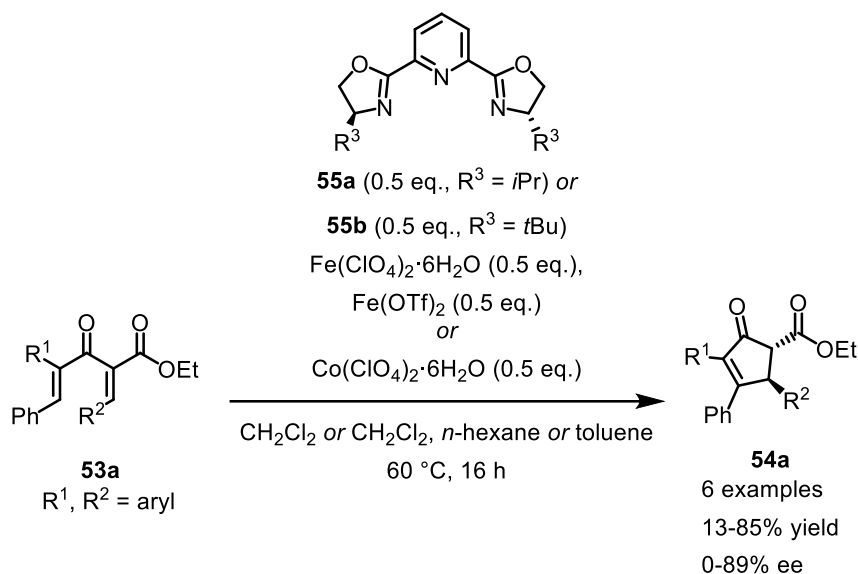
Scheme 66: Attempts by TOGNI and co-workers to perform catalytic asymmetric NAZAROV cyclization with vanadium(IV) salen complexes **56a**. The Substrates **53a** were treated with up to equimolar ratios of catalyst to furnish cyclization product **54a** as racemic mixture.^[44b]

In 2008 TOGNI and co-workers followed up with a dicationic nickel(II)-triphosphine complex as LEWIS acid catalyst.^[44c] The catalyst was formed from nickel(II) perchlorate hydrate and the pigiphos ligand **57** in dry THF. The preformed catalyst was then concentrated to dryness and mixed with the substrate **53a** in dry CH_2Cl_2 . The reaction was carried out at ambient temperature with reaction times varying from six to fifteen days. Eight different substrates **53a** were tested resulting in the cyclization products **54a** with yields ranging from 32% to 98% and low to high selectivity ranging from 45% to 86% ee for only one diastereomer found (Scheme 67).^[44c]



Scheme 67: Catalytic asymmetric NAZAROV cyclization with nickel(II)-pigiphos complexes **57** by TOGNI and co-workers. The substrates **53a** were treated with 20 mol% of catalyst to furnish cyclization product **54a** with good enantioselectivity as a single diastereomer.^[44c]

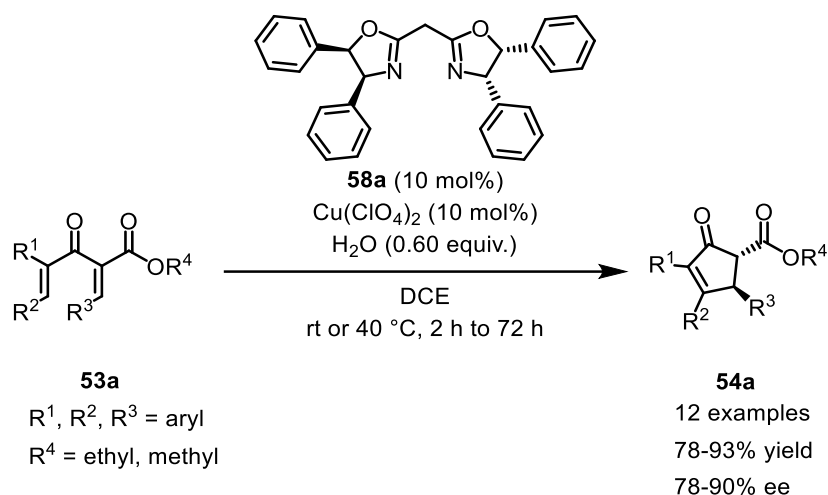
In 2010, ITOH and co-workers published methods using iron(II)- and cobalt(II)-salts and PyBOX ligands **55a** and **55b** as chiral LEWIS acid catalysts in varying solvents like CH₂Cl₂, CH₂Cl₂/*n*-hexane or toluene at 60 °C (Scheme 68).^[44d]



Scheme 68: Overview of methods for enantioselective NAZAROV cyclization with iron(II)- and cobalt(II) salts and PyBOX ligands **55a** and **55b** by ITOH and co-workers.^[44d]

Indeed, the cyclization products **54a** were obtained with yield up to 85% and an enantioselectivity of 89%. However, the catalyst loading of 50 mol% remains uncomfortably high albeit reaction times remained around 16 h.^[44d]

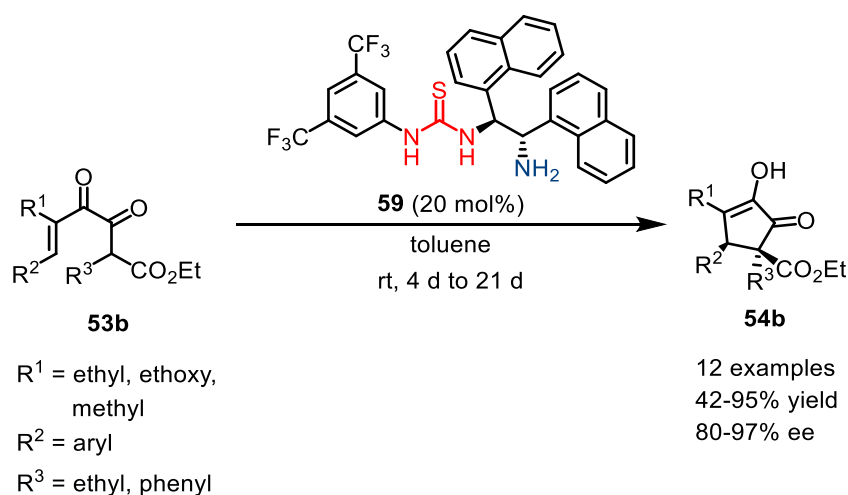
In 2015 TANG and co-workers succeeded lowering the catalyst loading to 10% for the substrate **Type A** using Cu(ClO₄)₂, box ligand **58a** as catalyst and water as additive. With this catalyst system, 12 substrates **53a** could be converted to the desired cyclization product **54a** with good to excellent yields and enantioselectivity, all while maintaining the reaction time between 2 h and 72 h (Scheme 69).^[44e]



Scheme 69: Catalytic system by TANG and co-workers using $\text{Cu}(\text{ClO}_4)_2$ and box ligand **58a** as catalyst for the enantioselective NAZAROV cyclization. The substrates **53a** were treated with a catalyst loading of 10 mol% to furnish cyclization product **54a** with excellent selectivity up to 90% ee.^[44c]

2.1.2 Nazarov Cyclization with Substrate Type B

For substrate **Type B**, two reported catalysts by TIUS and co-workers have to be highlighted. In 2010, an organocatalytic asymmetric NAZAROV cyclization using bifunctional BRØNSTED acid (thiourea highlighted in red, scheme 70) and LEWIS base (amine highlighted in blue, scheme 70) catalyst **59** was reported.^[45a] This catalyst was applied with 20 mol% catalyst loading at ambient temperature in toluene. 12 Substrates **53b** were converted to the desired products **54b** with yields up to 95% and an excellent selectivity of 80% to 97% ee with only one diastereomer observed (Scheme 70).^[45a]



Scheme 70: Catalytic system by TIUS and co-workers using bifunctional organocatalyst **59** for the enantioselective NAZAROV cyclization. The substrates **53b** were treated with a catalyst loading of 20 mol% to furnish cyclization product **54b** with excellent selectivity up to 97% ee.^[45a]

A magnificent feature of this bifunctional catalyst is the weak activation through hydrogen bonding/weak BRØNSTED acidity and LEWIS basicity polarizing the substrate in a complementary fashion leading to the cyclization (Figure 25).^[45a]

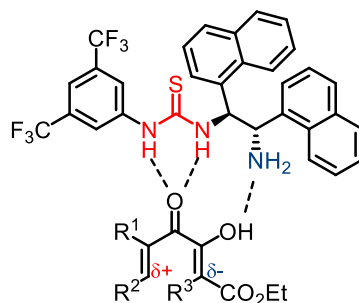
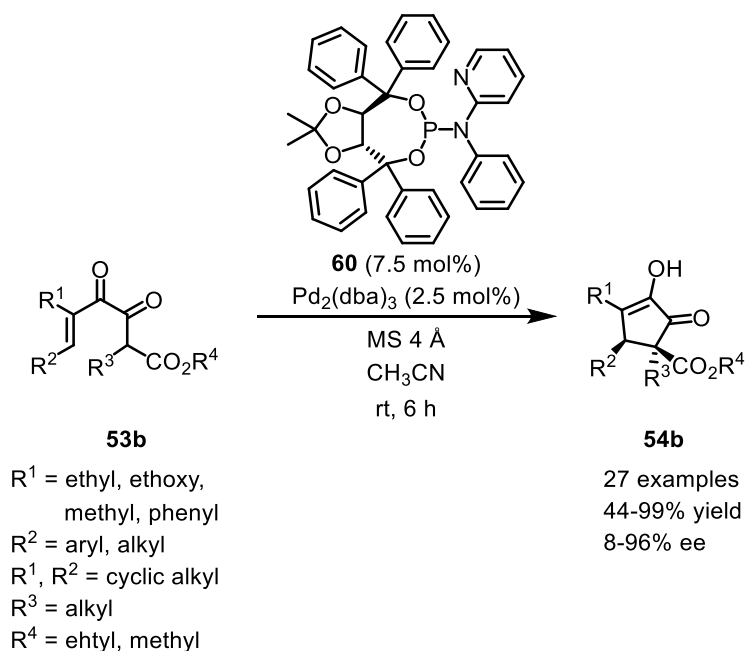


Figure 25: Postulated transition state by TIUS and co-workers illustrating both modes of activation with the bifunctional catalyst.^[45a]

A deeper insight into the reaction mechanism was gained in 2015 by TIUS, HOUK and co-workers, rationalizing the relation between the absolute configuration of the catalyst **59** and the products **54b** by computational studies.^[45b] However, the reaction times with 4 to 21 days are comparable extensive.^[45a]

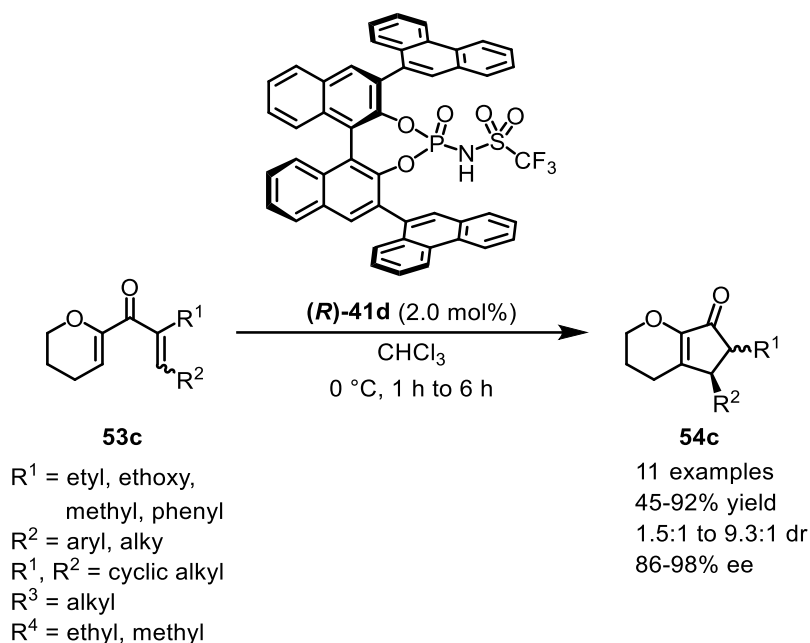


Scheme 71: Catalytic system by TIUS and co-workers using a neutral palladium TADDOL **60** complex as catalyst for the enantioselective NAZAROV cyclization. The substrates **53b** were treated with a catalyst loading of 5.0 mol% palladium(0) to furnish cyclization product **54b** with excellent selectivity up to 96% ee.^[45c]

The second example represents a neutral variant of the NAZAROV cyclization. This system, published in 2015, uses $\text{Pd}_2(\text{dba})_3$ as palladium(0)-source and TADDOL ligand **60** in acetonitrile at ambient temperature. It must be acknowledged that approximately 100 different ligands were screened to identify optimum conditions for this type of NAZAROV reaction. With these conditions in hand, 27 different substrates **53b** were readily converted to the cyclopentenones **54b** with yield up to 99% yield and high selectivity up to 96% ee (Scheme 71).^[45c]

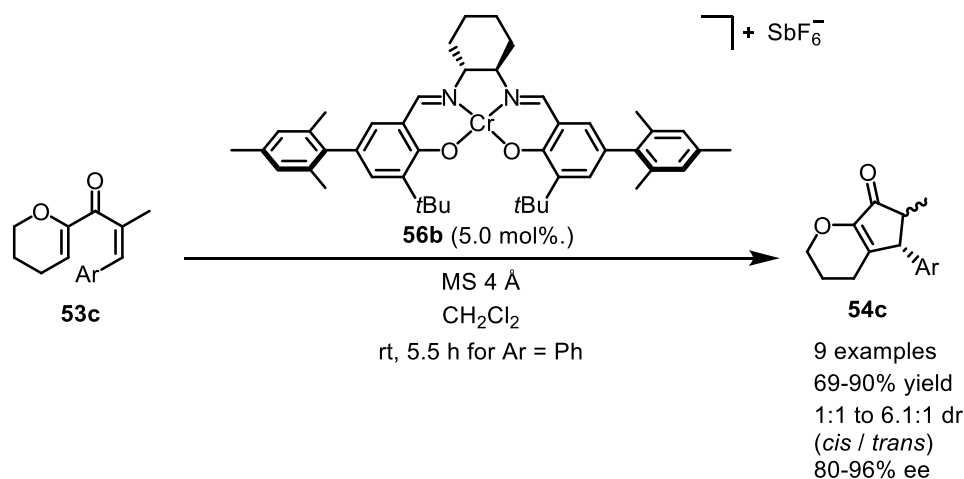
2.1.3 Nazarov Cyclization with Substrate Type C

In terms of activated substrates **Type C**, the decisive breakthrough was made by RUEPING and co-workers in 2007 with the development of the first organocatalytic enantioselective NAZAROV cyclization using 9-phenanthryl-functionalized binaphthol phosphate **41d** as catalyst.^[46a] Not only is this reaction the first example for an enantioselective BRØNSTED acid catalyzed NAZAROV cyclization, but also the first example for an enantioselective electrocyclic reaction using a chiral BRØNSTED acid. The reaction was conducted with a catalyst loading as low as 2.0 mol% in chloroform at 0 °C. Those conditions were applied to eleven activated 3,4-dihydropyran based substrates **53c** with yields varying from 45% to 92% and diastereomeric ratios of up to 9.3:1. Enantiomeric excess was determined for both diastereomers of products **54c** ranging from 86% to 98% (Scheme 72).^[46a]



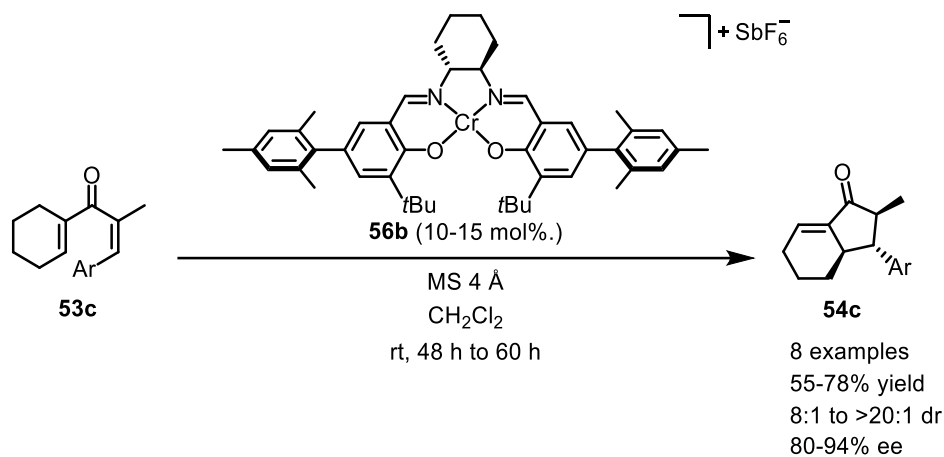
Scheme 72: Breakthrough by RUEPING and co-workers with binaphthol phosphate **(R)-41d** as catalyst for the enantioselective NAZAROV cyclization. The Substrates **53c** were treated with a catalyst loading as low as 2.0 mol% to furnish cyclization product **54c** with excellent selectivity up to 98% ee.^[46a]

In 2013 RAWAL and co-workers successfully applied a LEWIS acidic chromium(III) salen complex **56b** to those activated substrates of **Type C**.^[46b] For this strategy, 5.0 mol% of chromium (III) salen complex were used in CH_2Cl_2 in the presence of molecular sieves (4 Å) at ambient temperature. With this strategy in hand, nine cyclopentenone products **54c** were obtained with yield up to 90% and excellent selectivity ranging from 80% to 96% ee for both diastereomers (d.r. 1.2:1 to 2.8:1). It is worth mentioning that the reaction time remain in the range of one to six hours despite the low catalyst loading (Scheme 73).^[46b]



Scheme 73: Chromium(III) salen complex **56b** developed by RAWAL and co-workers for the enantioselective NAZAROV cyclization. The substrates **53c** were treated with a catalyst loading as low as 5.0 mol% to furnish cyclization products **54c** with excellent selectivity up to 96% ee.^[46b]

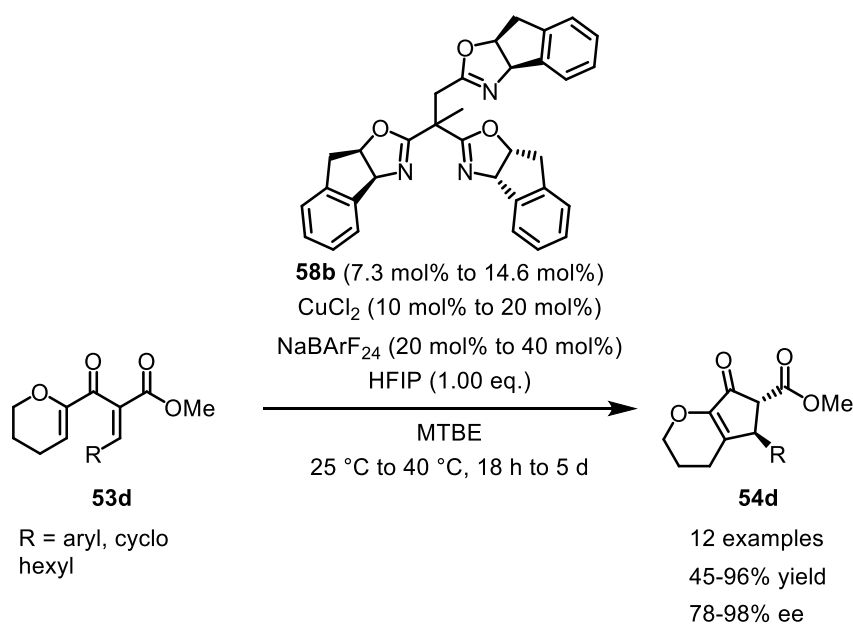
Furthermore, this catalyst system could be used to facilitate cyclization for non-activated circular substrates **53c** (Scheme 74). For non-activated substrates **53c**, the catalyst loading had to be raised to 10 mol% to 15 mol% and the reaction times had to be prolonged up to 60 h, providing the NAZAROV products **54c**. Indeed, the payoff is considerably huge, since three stereocenters are generated in this process, providing products with yields up to 78% and selectivity up to 94% ee and a diastereomeric ratio higher than 20:1.^[46b]



Scheme 74: Chromium(III) salen complex **56b** catalyze non-activated substrates **53c** to furnish cyclization products **54c** containing three stereocenters with excellent selectivity up to 94% ee.^[46b]

2.1.4 Nazarov Cyclization with Substrate Type D

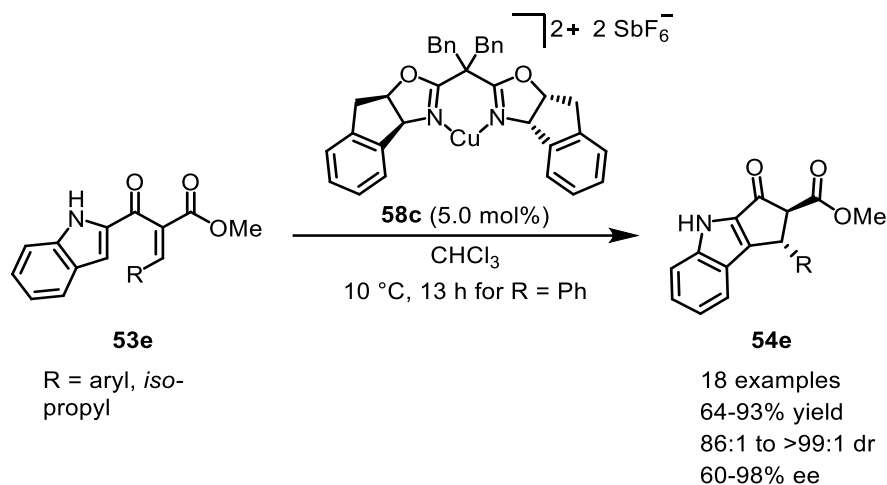
In 2010, TANG and co-workers showcased a catalytic system utilizing CuCl_2 , box ligand **58b** and NaBARF_{24} in a 0.73:1.00:2.00 ratio. Twelve polarized substrates **53d** established by FRONTIER and co-workers were used to determine the scope.^[47a] These substrates could be converted to the desired products **54d** using MTBE as solvent and hexafluoro-2-*iso*-propanol (HFIP, 1.00 eq.) as additive at 25 °C to 40 °C with yields of 45% to 96% and high selectivity up to 96% ee for only one observed diastereomer. However, for substrates **53d** with electron withdrawing groups, like *para*-bromo-, *para*-fluorophenyl or alkyl moieties, that are known to undergo the reaction in a sluggish way,^[47a] catalyst loadings up to 20 mol% of CuCl_2 have to be used leading to 40 mol% NaBARF_{24} . Still, reaction times for those substrates are as long as 30 h for the fluoro, 57 h for the bromo or even five days for the cyclohexyl derivatives (Scheme 75).^[47a]



Scheme 75: Catalytic system by TANG and co-workers using CuCl_2 , modified box ligand **58b** and NaBARF_{24} as catalyst for the enantioselective NAZAROV cyclization. The polarized substrates **53d** were treated with a catalyst loading of 10 to 20 mol% of CuCl_2 to furnish cyclization products **54d** with excellent selectivity up to 98% ee.^[47a]

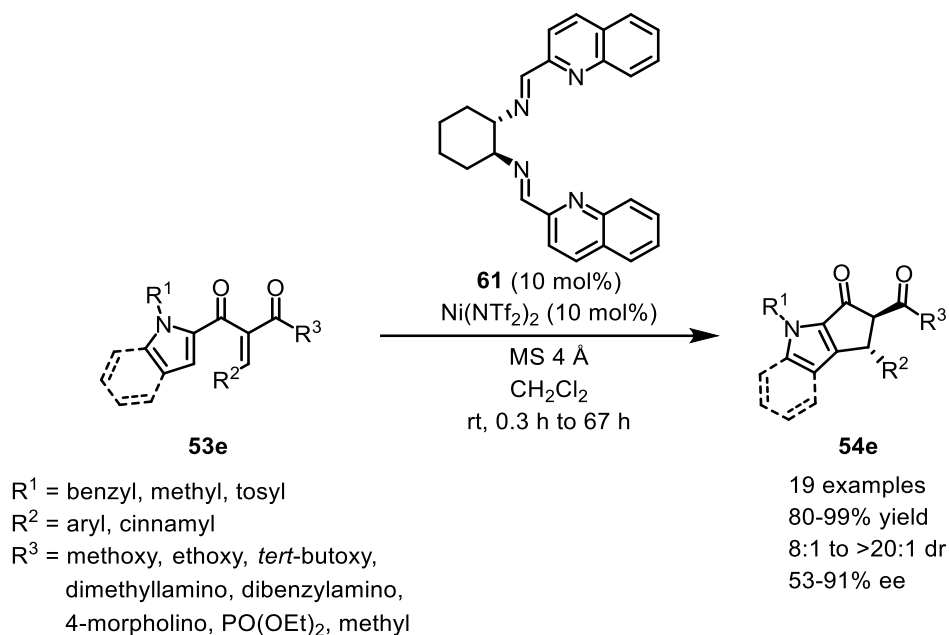
In 2015, first RUEPING then NISHIDA and co-workers published enantioselective NAZAROV cyclization reactions of aryl-vinyl ketones **53e** (Type D) containing an indole moiety as negatively polarized vinyl equivalent.^[47b,47c] In RUEPING's case, a copper(II)/box/ SbF_6 complex **58c** was used with a loading of 5.0 mol% in chloroform at 10 °C.^[47b] The box ligand of **58c** closely resembles box ligand **58b** used by TANG's group, providing 18 cyclization products **54e**

with yield up to 93% and excellent diastereo- as well as enantioselectivity up to 98% ee (Scheme 76).^[47b]



Scheme 76: Catalytic system by RUEPING and co-workers using copper(II)/box/ SbF_6 complex **58c** as catalyst for the enantioselective NAZAROV cyclization of polarized substrates **53e** containing indole moieties. The polarized substrates **53e** were treated with a catalyst loading of 5.0 mol% to furnish cyclization products **54e** with excellent selectivity up to 98% ee.^[47b]

In NISHIDA's lab, 10 mol% of $\text{Ni}(\text{NTf}_2)_2$ and bisimino-bisquinoline ligand **61** were used in CH_2Cl_2 at ambient temperature to catalyze the cyclization of substrate **53e** (Scheme 77). Key-feature of this catalyst can be seen in the structure of the catalytically active species. It was assumed, that two equivalents of each $\text{Ni}(\text{NTf}_2)_2$, ligand **61** and substrate **53e**, form a defined binuclear complex with each nucleus forming a Δ -configured octahedral stereogenic-at-metal complex (see crystal structure in figure 26).^[47c]



Scheme 77: Catalytic system by NISHIDA and co-workers using $\text{Ni}(\text{NTf}_2)_2$ and bisimino-bisquinoline **61** as catalyst for the enantioselective NAZAROV cyclization of polarized substrates **53e** containing indole moieties. The polarized substrates **53e** were treated with a catalyst loading of 10 mol% to furnish cyclization product **54e** with high selectivity up to 91% ee.^[47c]

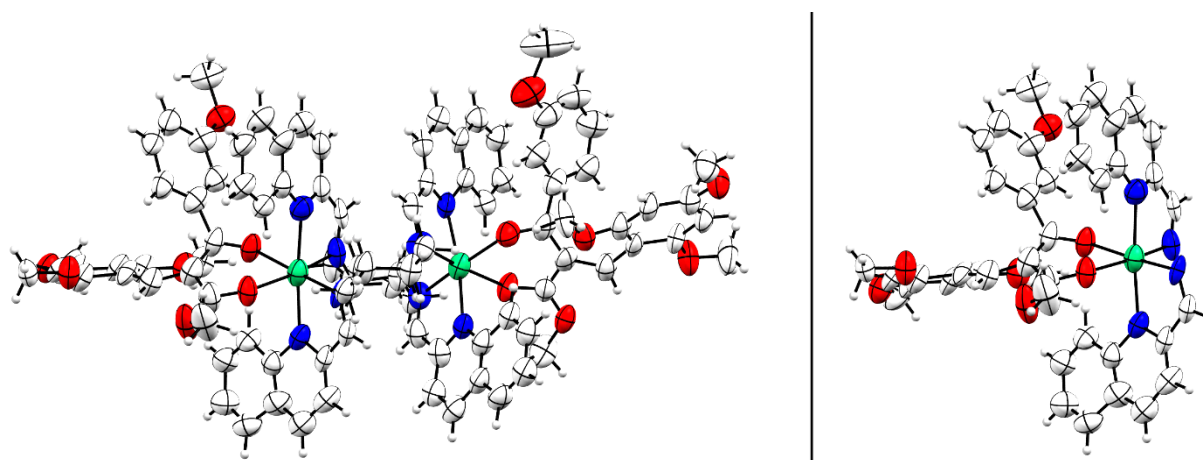
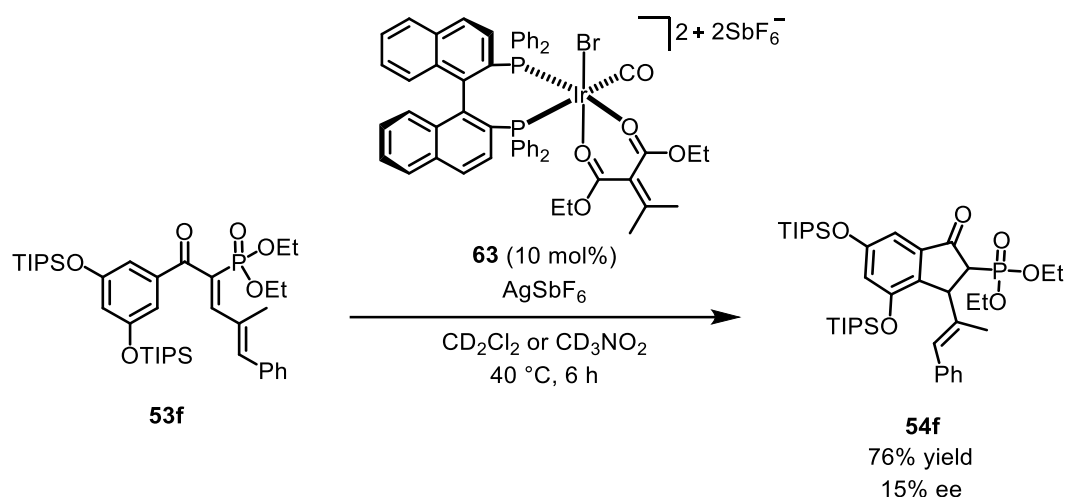


Figure 26: Crystal structure of the binuclear nickel(II) complex **62** (left) and a cut-out showcasing the Δ -configured octahedral geometry of one nucleus for better clarity (right). Solvent molecules and counterions omitted for clarity. Ellipsoids are drawn at the 50% probability level.^[47c]

With this nickel(II)-catalyst, 19 NAZAROV products with yields up 99% and high selectivity up to 91% ee and diastereomeric ratio greater 20:1 were obtained.^[47c]

2.1.5 Iridium(III) Complexes in Nazarov Cyclization Reactions

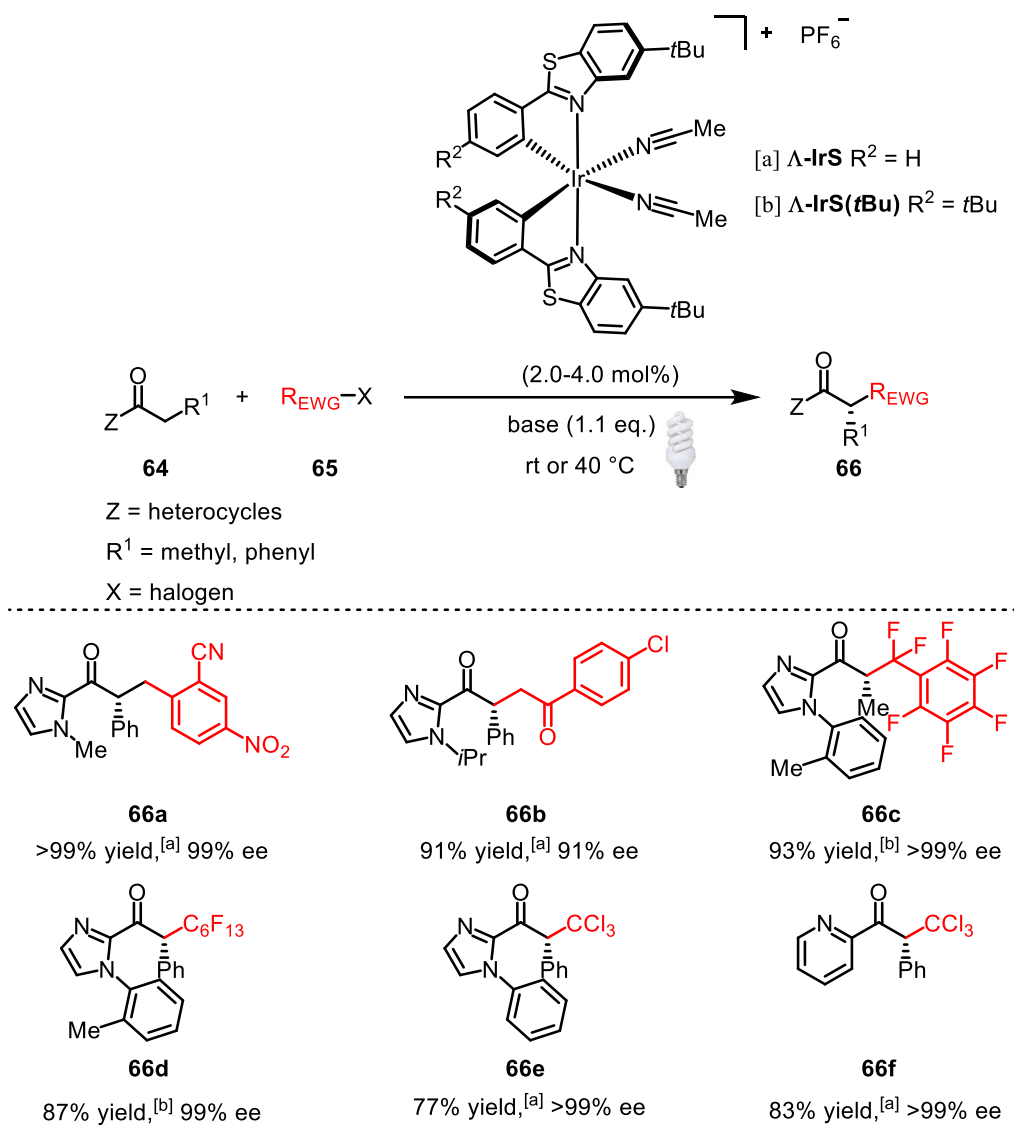
In 2010 EISENBERG, FRONTIER and co-workers developed a highly reactive, dicationic iridium(III) complex **63** for the polarized NAZAROV cyclization of **Type D**. It was assumed that the catalytically active species is tricationic through addition of AgSbF_6 . Even though the catalysts **63** contains a chiral (*R*)-binap ligand, no significant enantioselectivity was achieved (15% ee) with 10 mol% catalyst loading in the presents of AgSbF_6 at 40 °C (Scheme 78).^[48]



Scheme 78: Catalytic system by EISENBERG, FRONTIER and co-workers using a tricationic iridium(III) complex **63** as catalyst for the enantioselective NAZAROV cyclization of polarized substrate **53f**. The polarized substrates **53f** were treated with a catalyst loading of 10 mol% to furnish cyclization product **54f** without significant stereo control.^[48]

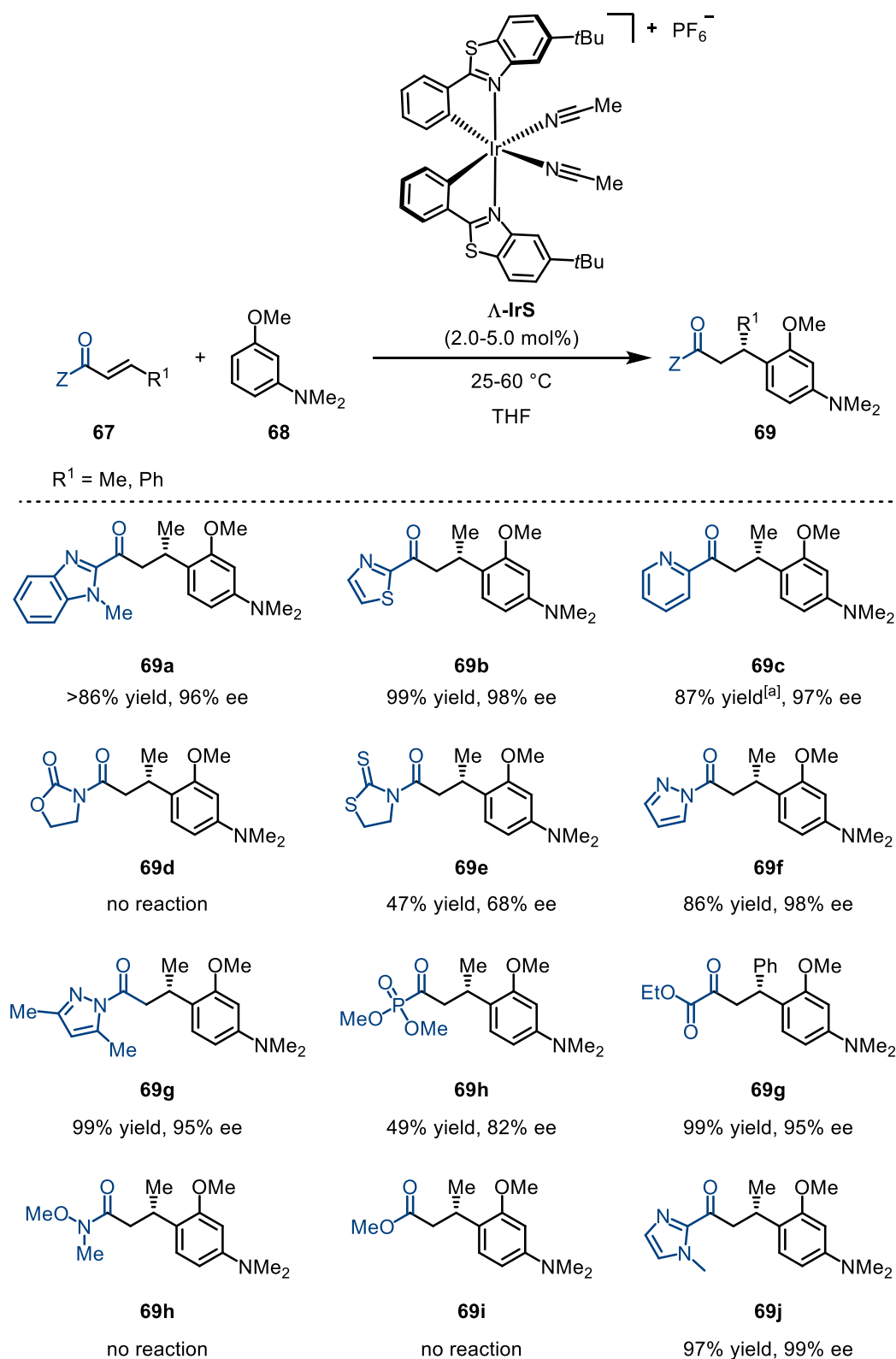
2.1.6 Examples for Asymmetric Lewis Acid Catalysis from the Meggers Group

Iridium(III) stereogenic-at-metal complexes like **Λ -IrS** from the MEGGERS have proven to be useful 3 in 1 catalysts. Those catalysts provided LEWIS acidity, the center of chirality as well as photo redox properties. Using catalysts **Λ -IrS** and **Λ -IrS (*t*Bu)** for example, asymmetric benzylation, perfluoro alkylation as well as trichloromethylation was performed with high yields and enantioselectivity. Substrate of choice for those reactions were *N,O*-coordinating substrates like 2-acyl imidazoles and 2-acyl pyridines **64** yielding functionalized 2-acyl imidazoles and 2-acyl pyridines **66** (Scheme 79).^[49]



Scheme 79: Reactions performed in the MEGGERS group using stereogenic-at-metal complexes Λ -IrS.^[49]

In a study by XIAODONG CHEN, twelve α,β -unsaturated substrates **69** with different coordinating groups were investigated for the asymmetric FRIEDEL-CRAFTS-alkylation (Scheme 80).^[13c]



Scheme 80: Substrates **69** investigated by XIAODONG CHEN.^[13c]

XIAODONG CHEN's study showcased, that products **69** with ee >95% could be obtained with *N,O*-coordinating substrates like 2-acyl benzimidazole **67a**, 2-acyl thiazole **67b**, 2-acyl pyridine **67c**, *N*-acyl pyrazole **67f** and **67g** as well as 2-acyl imidazole **67j**, whereas *O,O*- and

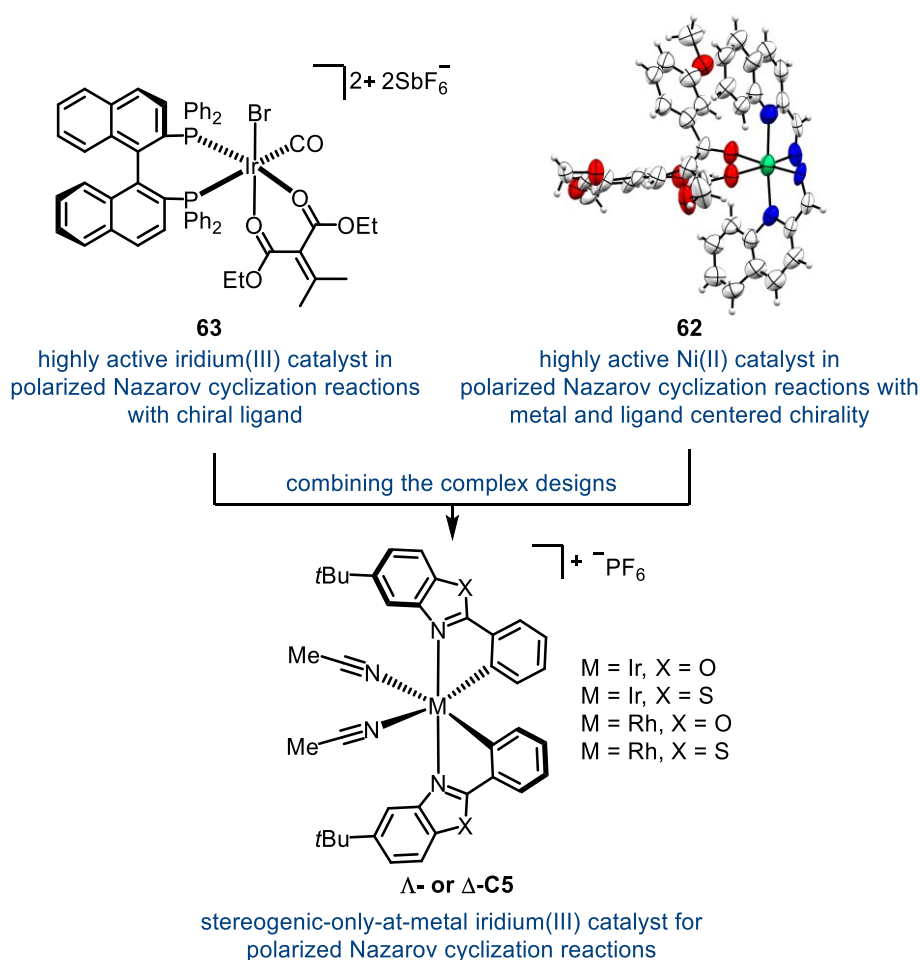
S,O-coordinating substrates like *N*-acyl thioxothiazolidine **67e**, α -keto phosphoric esters **67h** and α -keto carboxylic acid esters **67g** yielded products **69** with ee <95%. Indeed, *O,O*-coordinating substrates *N*-acyl oxazolidine **69d**, WEINREB amide **69h** and carboxylic acid esters **69i** did not yield any products at all.

For most following studies in the MEGGERS group, *N,O*-coordinating substrates 2-acyl pyridine **67c**, *N*-acyl pyrazole **67f**, and 2-acyl imidazole **67j** remained the go-to substrate for reactions catalyzed stereogenic-at-metal complexes like **Λ -IrS**.

2.2 Motivation

In the recent years, the MEGGERS group could demonstrate that the stereogenic-at-metal LEWIS acid catalysts **A-C5** are capable to promote several transformations with excellent yields and enantioselectivity.^[13c,49] The substrate type of choice used is commonly *N,O*-coordinating like 2-acyl imidazoles, 2-acyl pyridines and *N*-acyl pyrazoles.^[49] Examples where *O,O*-coordinating substrates are used remain scarce.^[13c]

Since the enantioselective NAZAROV cyclization remains a formidable challenge, even with favorable polarized substrates of **Type D** they remain an exciting target. From work by FRONTIER, EISENBERG and NISHIDA it could be rationalized, that stereogenic-only-at-metal **A-C5** from the MEGGERS group should be a suitable catalyst for this reaction (Scheme 81).^[47c,48]



Scheme 81: Rationalization of the planned approach towards enantioselective NAZAROV cyclization using stereogenic-only-at-metal complexes **A-C5** from the MEGGERS group.

The complexes should be tested with range of different polarized α -unsaturated- β -keto esters **TYPE D** derived from 3,4-dihydropyran **N1** and indole **N3** to obtain NAZAROV products **N2** and **N4** (Figure 27).

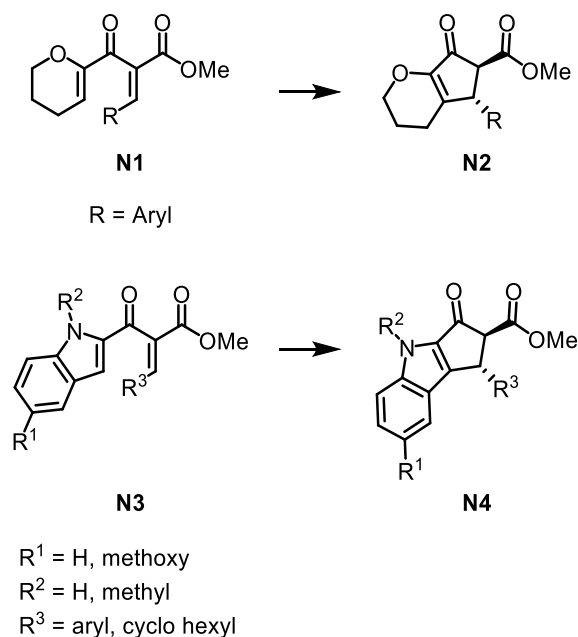


Figure 27: Polarized α -unsaturated- β -keto esters derived from 3,4-dihydropyran **N1** and indole **N3** as substrate for complexes **A-C5**.

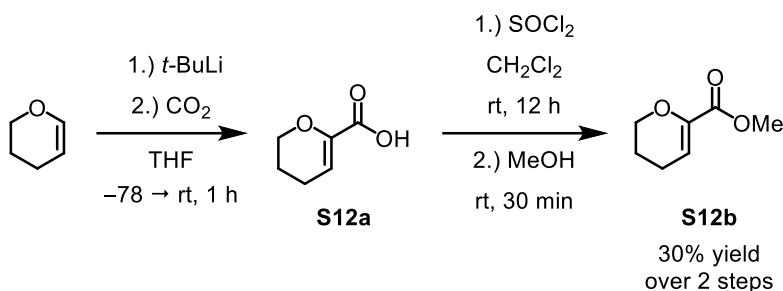
This way, the substrate scope of catalysts **A-C5** could be further extended towards *O,O*-coordinating substrates.

2.3 Results and Discussion

Since the recently developed stereogenic-at-metal LEWIS acids **A-C5** were successfully applied to broad range of substrate, they might be suitable catalysts for the asymmetric NAZAROV cyclization of vinyl-vinyl ketones **N1** and aryl-vinyl ketones **N3** (TYPE D) through bidentate coordination to the dicarbonyl unit. Since condition screening should be conducted rapidly, 3,4-dihydropyran derivative **N1a** containing a *para*-methoxyphenyl group was used that is known to undergo NAZAROV cyclization reactions swiftly.^[47a] The following section provides an insight into typical synthesis of 3,4-dihydropyrane substrates **N1**, the optimization of the reaction conditions and finally the scope of the catalyst system.

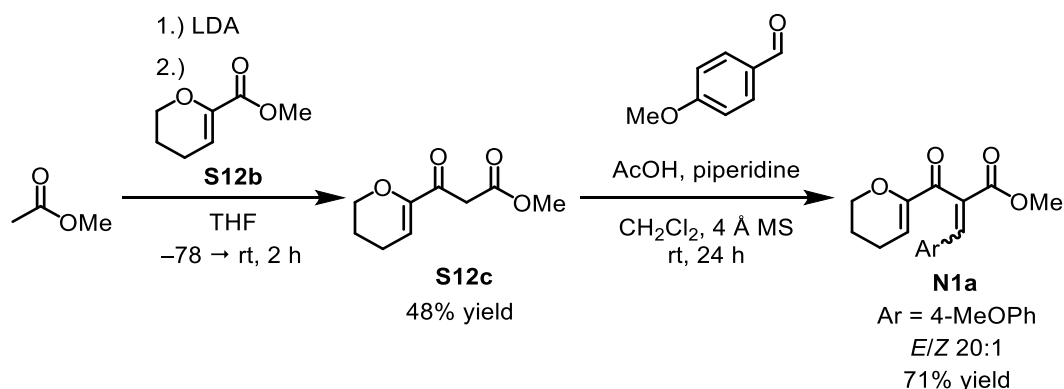
2.3.1 Synthesis of 3,4-Dihydropyran Substrate N1

Starting from commercially available 3,4-dihydropyran, *t*-BuLi solution in pentane was used for a directed lithiation. The resulting anion equivalent was trapped with gaseous CO₂ to furnish the carboxylic acid **S12a** after aqueous workup. The crude product **S12a** was first treated with thionyl chloride in CH₂Cl₂ to provide reactive acid chloride which was further reacted with excess MeOH to obtained ester **S12b** with 30% yield over to steps after column chromatography (Scheme 82).^[50]



Scheme 82: Synthesis of ester **S12b** in a two-step protocol from commercially available 3,4-dihydropyran.

In the next step, ester **S12b** and methylacetate were applied to a CLAISEN condensation reaction. Therefore, a freshly prepared LDA solution in THF was used to form an enolate of acetate which was further treated with ester **S12b** to furnish the desired β -keto ester **S12c** with 48% yield and a keto/enol ratio of 5:1 (Scheme 83). In the last step, β -keto ester **S12c** and commercial anisic aldehyde were reacted in the presence of acetic acid and piperidine to form divinyl ketone **N1a** with 71% yield after KNOEVENAGEL condensation (Scheme 83).^[50]



Scheme 83: Synthesis of β -keto ester **S12c** by CLAISEN condensation (only keto form of ester **S12c** displayed) which was further used in a KNOEVENAGEL condensation with anis aldehyde to furnish divinyl ketone **N1a**.

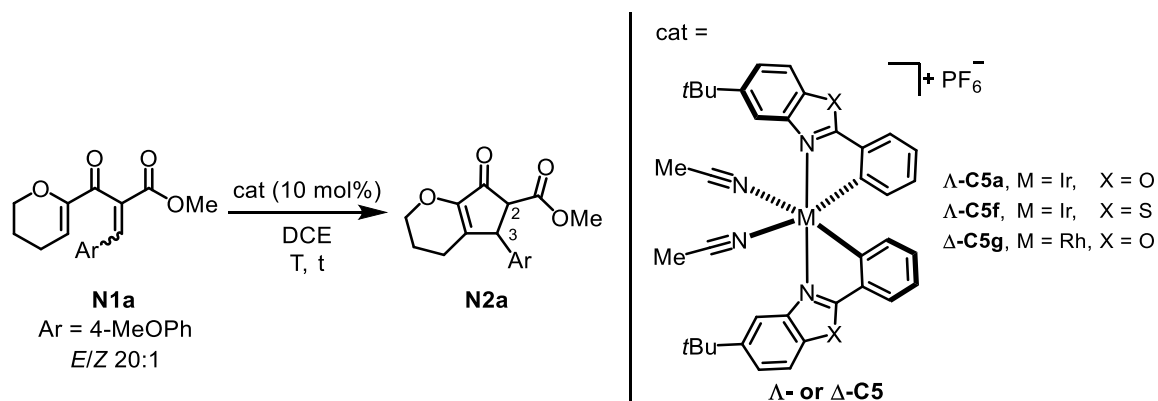
With substrate **N1a** in hand, conditions were screened to find suitable reaction conditions as presented in the next section.

2.3.2 Initial Experiments and Screening Results

To investigate the reactivity of stereogenic-at-metal complexes **A-C5**, a solution of substrate **N1a** in DCE containing 10 mol% of the respective complex was heated to 50 °C or kept at ambient temperature and monitored by TLC and HPLC. Gratifyingly, both the bis-cyclometalated iridium(III) complexes **A-C5a**^[13a] and **A-C5f**^[13c] (Entry 1 and 2, table 7), as well as the bis-cyclometalated rhodium(III) complex **A-C5g**^[51] (Entry 3, table 7) provided the cyclopentenone derivative **N2a** with enantiomeric excess of 91% to 93%. The reactivity of rhodium catalyst **A-C5g** with respect to reactivity and stereoselectivity is slightly superior and

allows to execute the reaction at room temperature whereas the iridium(III) complexes **Λ-C5a** and **Λ-C5f** showed sluggish conversion at room temperature (compare entries 4-6, table 7).

Table 7: Initial experiments to investigate the reactivity of LEWIS acid **Λ-C5a**, **Λ-C5f**, and **Δ-C5g** towards NAZAROV cyclization reactions.^[a]



Entry	Catalyst	Time t (h)	T (°C)	Conversion ^[b]	ee (%) ^[c]
1	Λ-C5a	24	50	near completion	91 (2 <i>S</i> ,3 <i>S</i>)
2	Λ-C5f	24	50	near completion	91 (2 <i>S</i> ,3 <i>S</i>)
3	Δ-C5e	24	50	full	−93 (2 <i>R</i> ,3 <i>R</i>)
4	Λ-C5f	44	rt	partial	n.d. ^[d]
5	Λ-C5a	44	rt	partial	n.d. ^[d]
6	Δ-C5g	12	rt	full	−93 (2 <i>R</i> ,3 <i>R</i>)

[a] Reaction conditions: *E/Z*-mixture of substrate **N1a** (16.5 μmol) and catalyst **C5** (1.65 μmol) in DCE at the indicated temperature. [b] Estimated by a combination of TLC and HPLC analysis. [c] Determined from crude product mixtures by HPLC on a chiral stationary phase. [d] n.d. = not determined.

Since **Λ-C5f** was synthetically the most accessible complex, the study was continued with iridium catalyst **Λ-C5f**^[13c] to screen for suitable reaction conditions. When the concentration of substrate **N1a** was decreased from 0.5 M (Table 7) to 0.3 M (table 8) in DCE and the temperature was reduced from 50 °C (Table 7) to 40 °C (Table 7), while maintaining a catalyst loading of 10 mol%, the enantioselectivity increased slightly from 91% to 93% ee (compare entry 1, table 7 with entry 1, table 8). The addition of 10% (v/v) water did not change the result in terms of conversion and stereoselectivity (Entry 2, table 8), dry solvent and SCHLENK technic showed no influence on selectivity and yield either (Entry 3, table 8), which indicates that dry solvents are neither necessary nor beneficial. However, catalyst loading was decreased from 10 mol% to 2.0 mol% without decrease in ee, facilitating further optimization (Entry 4, table 8).

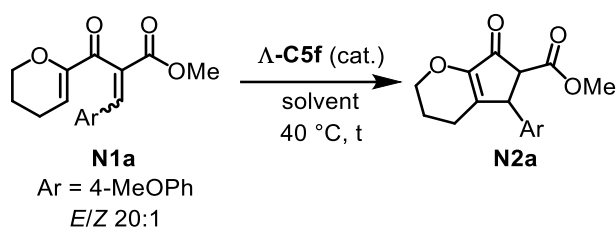


Table 8: Optimization of reaction conditions with catalyst **A-C5f** and focus on enantioselectivity and full conversion.^[a]

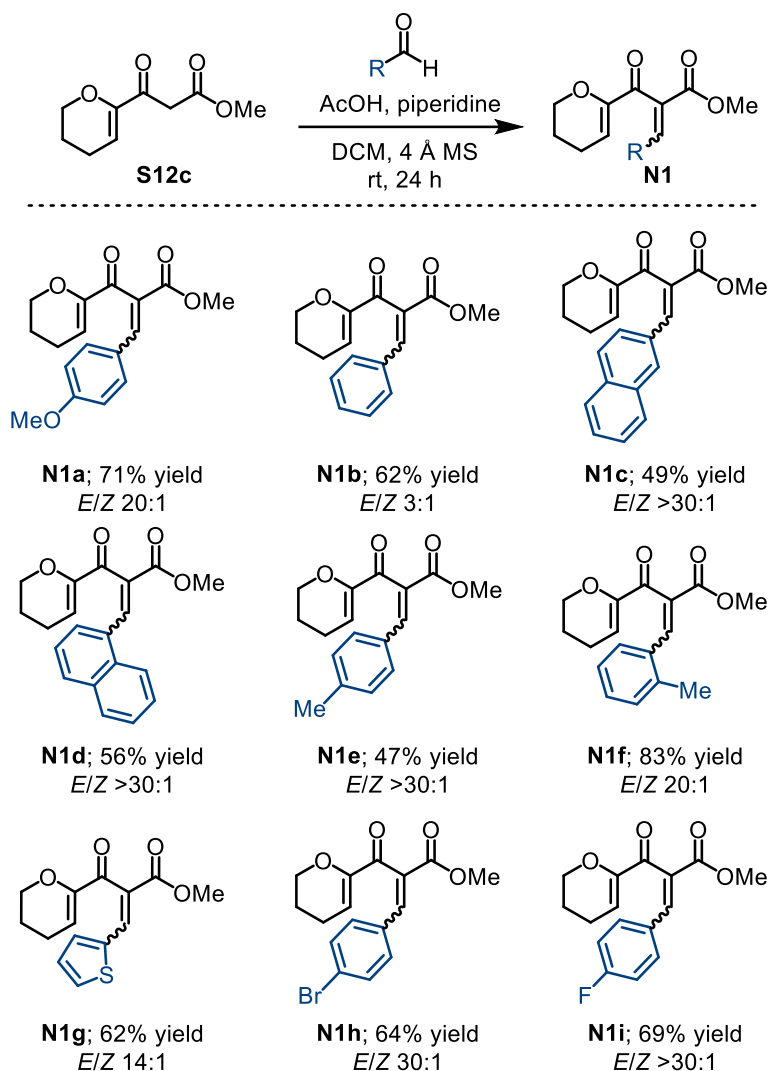
Entry	A-C5f (mol%)	Solvent	Time t (h)	Conversion ^[c]	ee (%) ^[d]
1	10	DCE	13	full	93
2	10	DCE + 10% H ₂ O	13	full	93
3 ^[b]	10	DCE	13	full	93
4	2.0	DCE	13	full	93
5	2.0	HFIP	7	full	90
6	2.0	DCE + HFIP (1.0 eq.)	7	full	93
7	2.0	CHCl ₃	14	near completion	92
8	2.0	EtOAc	14	low	80
9	2.0	DME	14	low	30
10	2.0	MeCN	14	low	30
11	2.0	toluene	7	low	30
12	2.0	THF	7	low	20
13	2.0	MTBE	7	low	20
14	2.0	MeOH	14	low	3

[a] Reaction conditions: *E/Z*-mixture of substrate **N1a** (14.5–56.0 μmol) and **A-C5f** (0.70–1.45 μmol) in the indicated solvent at 40 °C and for the indicated time. [b] Reaction was performed under inert gas atmosphere in dry solvent. [c] Estimated by a combination of TLC and HPLC analysis. [d] Determined from crude product mixtures by HPLC on a chiral stationary phase.

When replacing the solvent DCE with HFIP, the enantioselectivity slightly deteriorated but the reaction was significantly accelerated (Entry 5, table 8). Optimal conditions were found to be DCE as a solvent with the addition of one equivalent of HFIP (Entry 6, table 8). At a catalyst loading of 2.0 mol% **A-C5f**, the reaction was completed within 7 hours at 40 °C and provided the cyclopentenone **N2a** with 93% ee for the major diastereomer. Other investigated solvents turned out to be less suitable (Entries 7-14, table 8).

2.3.3 Exploring the Scope of Substrates N1 Yielding Nazarov Products N2

To investigate the possible scope of that catalyst, nine vinyl-vinyl ketones **N1a-i** were obtained with yields ranging from 47% to 83% yield with *E/Z* selectivity ranging from 3:1 to >30:1 (Scheme 84).^[50]



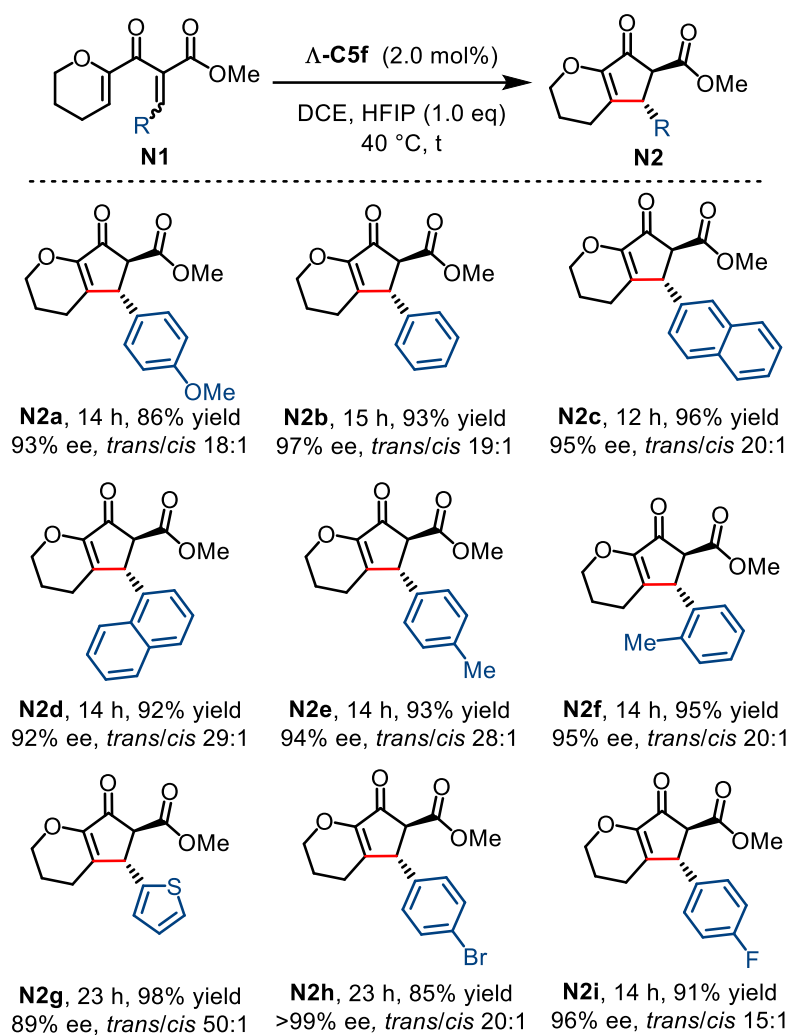
Scheme 84: Overview of the synthesis of 3,4-dihydropyran-functionalized divinyl ketones **N1a-i** by KNOEVENAGEL condensation reaction between β -keto ester **S12c** and various aldehydes with isolated yields and product *E/Z* ratios.

For the typical NAZAROV cyclization procedure using vinyl-vinyl ketones, a rubber-sealed screw-capped vial (1.5 mL) was charged with an *E/Z*-mixture of substrate **N1** (1.0 eq.; approx. 80–90 μ mol), catalyst **A-C5f** (2.0 mol%) and stock solution of HFIP (1.0 eq.) in DCE to obtain a 0.3 M solution with respect to substrate **N1**. The vial was kept at 40 °C for the indicated time, full conversion for each reaction was determined by TLC analysis. Given d.r. values (*trans/cis*) were determined by ¹H NMR analysis of the crude product mixtures. Yields and

enantioselectivity were determined from isolated products. Enantioselectivities were determined by chiral HPLC analysis for *trans* products exclusively.

For substrates **N1b–d** with electronically neutral aromatic substituents R = Ph (product **N2b**), R = 1-naphthyl (product **N2c**), and R = 2-naphthyl (product **N2d**) full conversion was found after reaction times of 12–15 h and products **N2b–d** were isolated in yields of 92–96% with ee values ranging from 92%–97% (ee values for the *trans* diastereomers) and d.r. values in the range of 19:1–29:1 (*trans*:*cis*). Substrates **N1a** and **N1e–f** with electron-rich aromatic substituents *p*-MeO-Ph (product **N1a**), *p*-Me-Ph (product **N1e**), and *o*-Me-Ph (product **N1f**) gave comparable results (86%–95% yield; 93%–95% ee (ee values for the *trans* diastereomers); *trans*/*cis* 18:1–28:1; full conversion found for all three after 14 h). Substrate **N1g** containing electron rich heteroaromatic substituent R = thiophen-2-yl (product **N2g**) was also tested. In this case, full conversion was found after 23 h and the product isolated in 98% yield with 89% ee (*trans* diastereomer) and a *trans*:*cis* ratio of 50:1. Finally, substrates **N1h** and **N1i** with electron-deficient substituents R = *p*-Br-Ph (product **N2h**) and R = *p*-F-Ph (product **N2i**) were tested which also yielded in good results (85% and 91% yield; >99% ee and 96% ee; *trans*/*cis* ratios of 20:1 and 15:1; full conversion after 23 and 14 h) (Scheme 85).

As all screened substrates **N1** were readily converted to **N2** with just 2.0 mol% of catalyst **Δ-C5f** under the applied reaction conditions, there was no immanent reason to change to the faster rhodium(III) catalyst **Δ-C5g** which is somewhat more difficult to prepare.

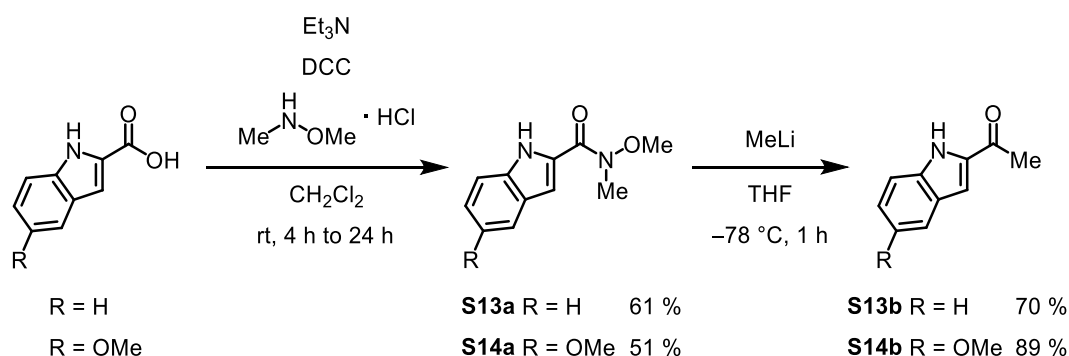


Scheme 85: Scope with 3,4-dihydropyran-functionalized α -unsaturated β -Ketoesters **N1**.

Since vinyl-vinyl ketones **N1** were suitable substrates for stereogenic-at-metal complexes Δ -**C5f**, indole-functionalized aryl-vinyl ketones **N3** were investigated. Analogous to the electron-rich double bond of 3,4-dihydropyran **N1**, the electron-donating indole has been demonstrated to activate the NAZAROV cyclization. The following section should provide an overview of the substrate synthesis, screening experiments and scope of the indole substituted aryl-vinyl ketones **N3**.

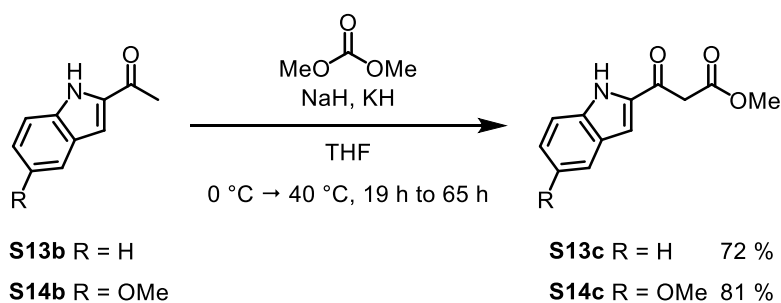
2.3.4 Synthesis of Indole Substrates N3

For the synthesis of aryl-vinyl ketone **N3** two approaches were used to synthesize β -keto ester **S13c** and **S14c**. The first strategy discussed is a modified synthesis by LEONORI and co-workers.^[50] Commercially available indole-2-carboxylic acids were converted to the corresponding WEINREB amide **S13a** and **S14a** with 51% to 61% yield using DCC as coupling reagent in the presence of Et₃N at ambient temperature. These WEINREB amides **S13a** and **S14a** were treated with MeLi in THF to furnish the 2-acyl-indoles **S13b** and **S14b** with yield of 70% and 89% respectively (Scheme 86).



Scheme 86: Synthesis of the acylated indole derivatives **S13b** and **S14b** from commercially available indole-2-carboxylic acids using WEINREB amides **S13a** and **S14a**.

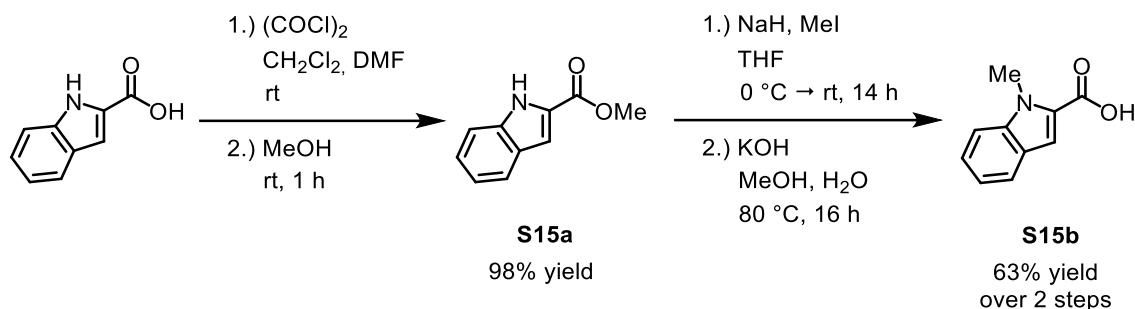
In the following step, 2-acyl-indoles **S13b** and **S14b** were converted to the β -keto esters **S13c** and **S14c** using NaH and KH as base in THF and dimethyl carbonate with 72% to 81% yield (Scheme 87).



Scheme 87: Synthesis of β -keto ester **S13c** and **S14c** by CLAISEN condensation.

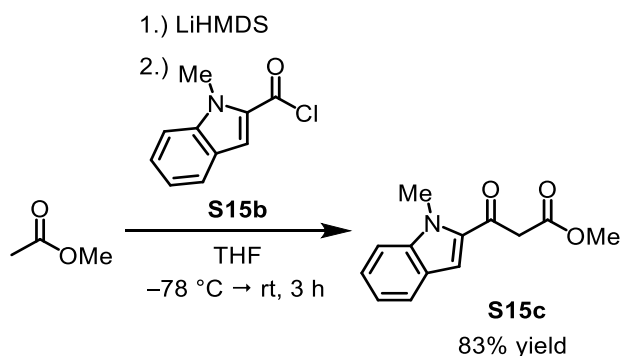
The second strategy applied shows similarities to the method used to obtain 3,4-dihydropyran functionalized β -keto ester **S12c** (compare scheme 82, 83, 88 and 89). Starting from indole-2-carboxylic acids, oxalyl chloride was used to obtain the more reactive acid chloride, which reacted in MeOH to methyl ester **S15a** with 98% yield in a clean fashion with no need for further purification. Then, crude ester **S15a** was methylated with iodo methane in the presence of NaH in THF to furnish the *N*-protected indole derivative. After saponification with KOH in

aqueous MeOH at 80 °C, *N*-methyl-indole-2-carboxylic acid **S15b** was obtained with 63% over two steps (Scheme 88).



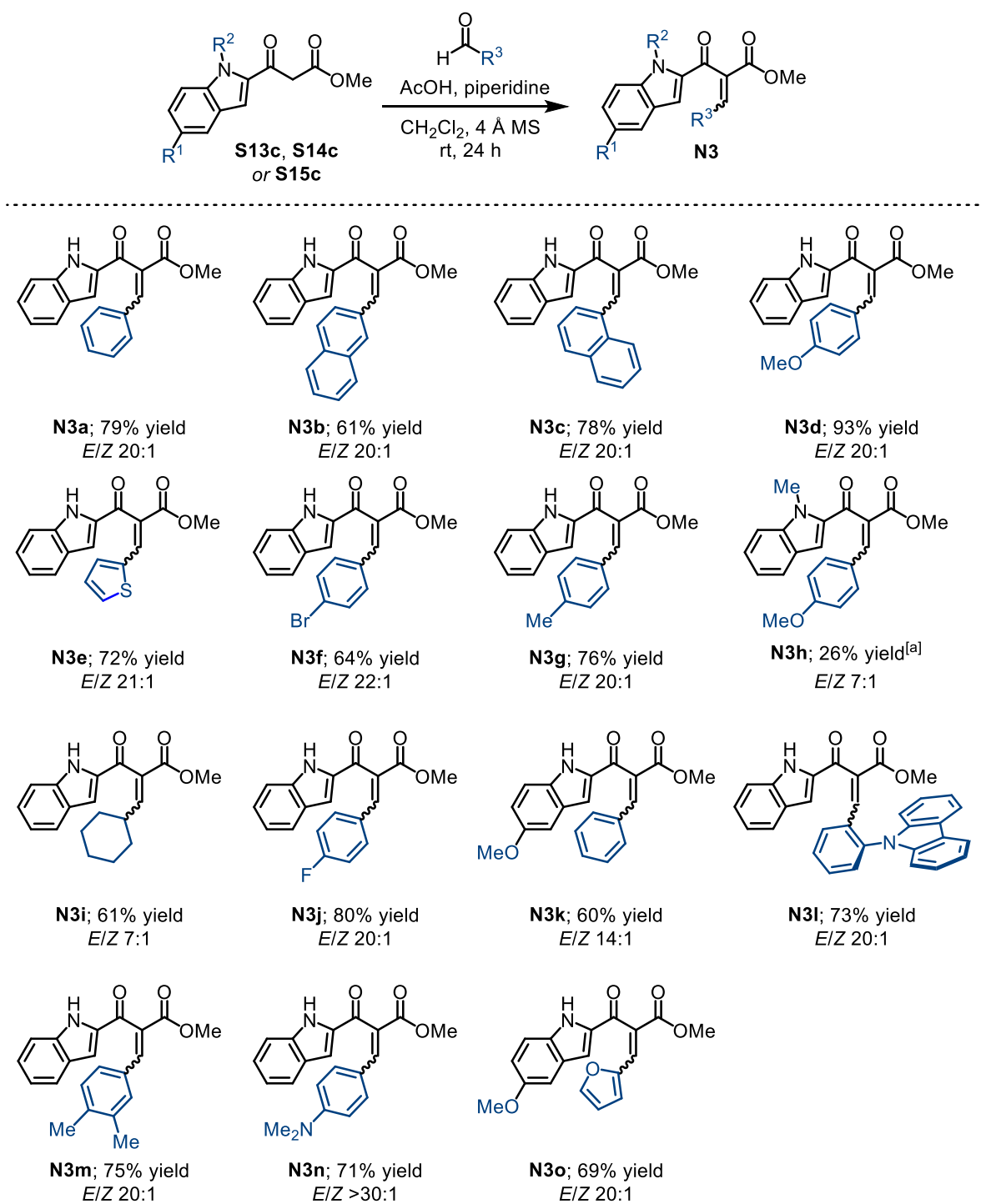
Scheme 88: Synthesis of *N*-methyl-indole-2-carboxylic acid **S15b** from commercially available indole-2-carboxylic acid.

Finally, methyl acetate was converted into a lithium enolate using LiHMDS in THF which was then treated with a freshly prepared solution of acid chloride **S15b** in THF to obtain the *N*-protected β -keto ester **S15c** with 83% yield (Scheme 89).



Scheme 89: Synthesis of β -keto ester **S15c** by CLAISEN condensation.

To obtain a library of aryl-vinyl substrates **N3**, β -keto ester **S13c**, **S14c** and **S15c** were reacted as previously mentioned by KNOEVENAGEL condensation (compare scheme 84 and 90).^[50] Aryl-vinyl substrates **N3** were obtained with yields ranging from 60% to 93% with an *E/Z* ratio ranging from 7:1 to 22:1 (Scheme 90).

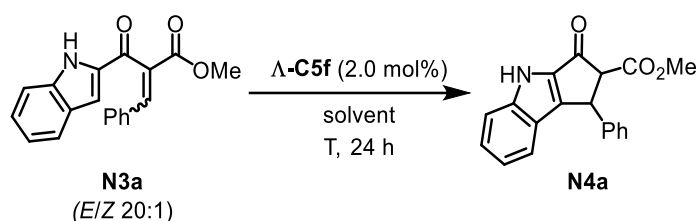


Scheme 90: Overview of the synthesis of indole-functionalized α -unsaturated β -ketoesters **N3** by KNOEVENAGEL condensations between β -keto esters and various aldehydes with isolated yields and product *E/Z* ratios. [a] Toluene was used as solvent instead of CH₂Cl₂.

2.3.5 Condition Screening for Indole Substrates **N3**

Optimization of the reaction conditions is shown in table 9. Interestingly, compared to the 3,4-dihydropyran substrates, the **Λ-C5f**-catalyzed NAZAROV cyclization with the indole substrate **N3** displayed a distinct solvent dependence. DCE as well as a variety of tested other solvents are not suitable for this reaction (Entries 1-9, table 9). A 1:1 mixture of DCE and HFIP provided the major diastereomer with 90% ee (Entry 10, table 9). Pure HFIP turned out to be the solvent of choice which provided full conversion at 50 °C after 24 hours and a satisfactory enantioselectivity of 93% ee (Entry 11, table 9).

Table 9: Optimization of reaction conditions for indole substrates with catalyst **Λ-C5f** with a focus on enantioselectivity and full conversion.^[a]



Entry	Solvent	T (°C)	Conversion (%) ^[b]	ee (%) ^[c]
1	DCE	40	none	n.a. ^[d]
2	DCE	50	trace	n.d. ^[d]
3	CHCl ₃	60	none	n.d.
4	MeNO ₂	60	trace	n.a.
5	DMF	60	trace	n.a.
6	THF	60	none	n.a.
7	toluene	60	none	n.a.
8	EtOAc	60	trace	n.d.
9	1,4-dioxane	60	trace	n.d.
10	DCE/HFIP 1:1	50	near completion	90
11	HFIP	50	full	93

[a] Reaction conditions: Substrate **N3** (28.5 μmol) and **Λ-C5f** (0.6 μmol) in the indicated solvent and at the indicated temperature for 24 hours. [b] Estimated by a combination of TLC and HPLC analysis. [c] Determined from crude product mixtures by HPLC on a chiral stationary phase. [d] n.a. = not applicable, n.d. = not determined.

2.3.6 Observed Differences in Relative Configuration

To establish the relative configurations of products **N4**, $^3J_{\text{HH}}$ couplings between their methine protons were compared with literature reported values.^[47a-b,50] According to the KARPLUS relation,^[52] larger $^3J_{\text{HH}}$ coupling constants around 7.0 Hz are expected for the *cis* products as they possess smaller dihedral angles with respect to the methine protons. When compared to the *cis* product, *trans* products have a smaller coupling constant around $^3J_{\text{HH}} = 2.0$ Hz. In case of NAZAROV product **N4d**, ^1H NMR analysis of the crude product directly after complete ring closing reaction revealed that the methine signals of the initial main diastereomer had a coupling constant of $^3J_{\text{HH}} = 7.2$ Hz, leading to the conclusion that *cis* isomers are formed in a significant quantity. The minor *trans* product however, showed coupling constants with $^3J_{\text{HH}} = 2.8$ Hz (Figure 28).

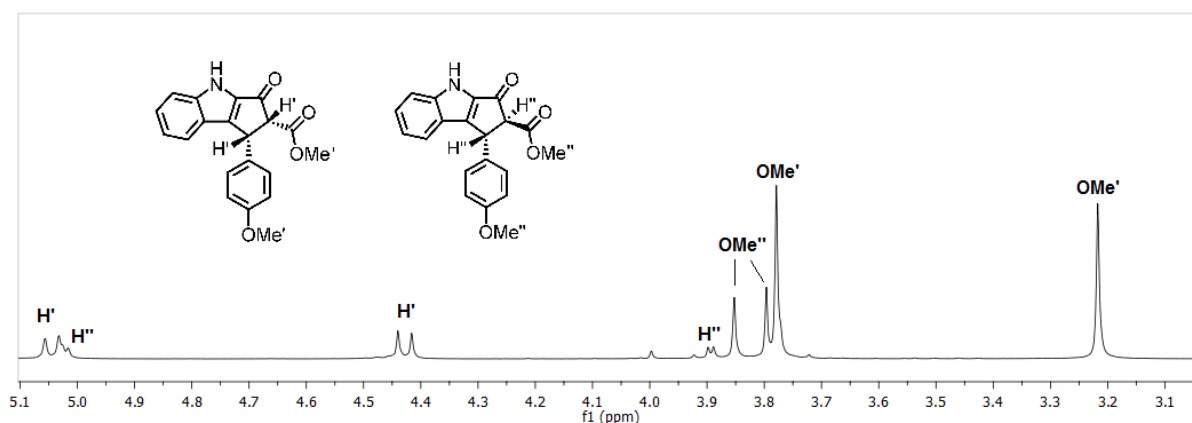
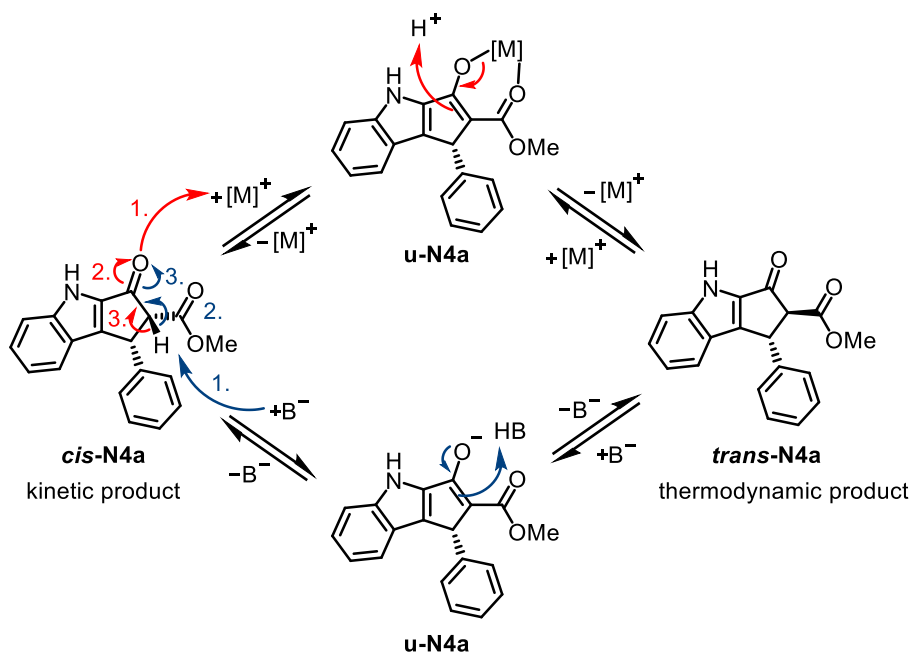


Figure 28: Excerpts from crude ^1H NMR spectra of product **N4d** in CDCl_3 recorded with a *Bruker Avance III* at 300 MHz directly after cyclization *trans/cis* 1:2.4).

Notably, in case of experiments with indole substrates **N4d**, and **N4g** it was observable that the *cis* diastereomer was initially predominant in the reaction mixture (kinetic product). In case of the other substrates **N4**, initially low *trans/cis* ratios were observed when reaction times were short. *Cis*-selectivity for cyclization products has been reported for binol phosphates as organocatalysts^[46a] whereas metal-based LEWIS acidic catalysts are usually known for providing the *trans* product.^[44,47] However, after prolonged reaction times the *trans* diastereomer became the predominant species, at the same time being the thermodynamic product. A potential LEWIS acid induced equilibration mechanism is depicted in scheme 91 (top pathway). As the *trans/cis* equilibrations were partially found to be very slow under the given reaction conditions which lead to partial decomposition of the products, a modified general equilibration protocol from RUEPING and co-workers^[46a] was applied for all reactions with

indole substrates (**N3** → **N4**) which relies on basic aluminium oxide as weak insoluble base. A potential base induced equilibration mechanism is depicted in scheme 91 (bottom pathway).



Scheme 91: Potential mechanism for LEWIS acid induced equilibration by catalyst (top pathway) and for base induced equilibration by basic Al₂O₃ (bottom pathway).

Consequently, all cyclization products **N4**, derived from aryl-vinyl ketones, were analyzed by ¹H NMR after ring closing reaction (before base induced equilibration) and after treatment with basic Al₂O₃.

In case of substrate **N3d**, product **N4d** was initially formed with a *trans/cis* ratio of 1:2.4 (Figure 29, top). Upon treatment with basic aluminum oxide, the thermodynamically favored *trans* product became the main product with a final *trans/cis* ratio of 14:1 (Figure 29, bottom).

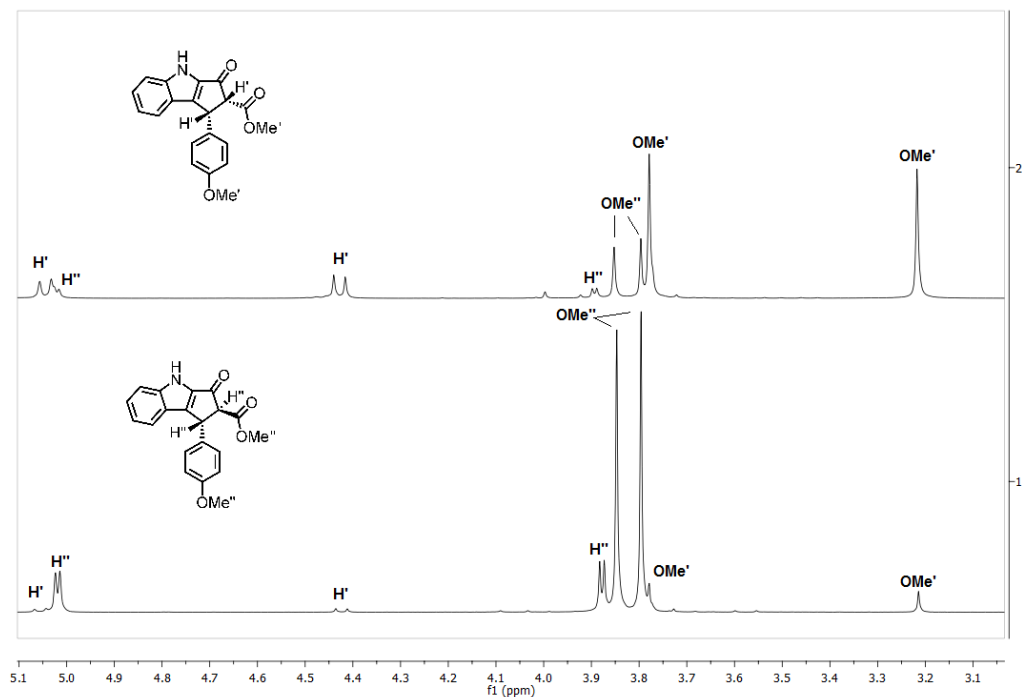


Figure 29: Excerpts from the crude ¹H NMR spectra of crude product **N4d** in CDCl₃ recorded with a *Bruker Avance III* at 300 MHz before (top; major: *cis*, *trans/cis* 1:2.4) and after equilibration (bottom; major: *trans*, *trans/cis* 14:1) with basic aluminum oxide.

Figure 30 illustrates product **N4g** before equilibration (*trans/cis* ratio 1:1, top) and afterwards (*trans/cis* ratio 14:1, bottom).

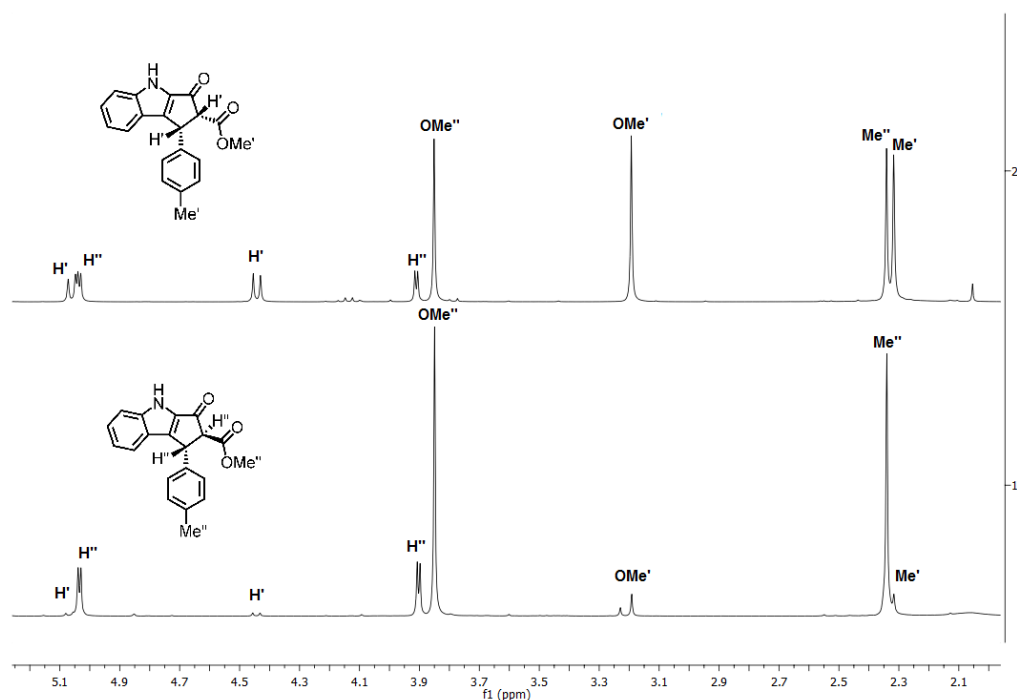


Figure 30: Excerpts from the crude ^1H NMR spectra of product **N4g** in CDCl_3 recorded with a *Bruker Avance III* at 300 MHz before (top; major: *cis*, *trans/cis* 1:1) and after equilibration (bottom; major: *trans*, *trans/cis* 14:1) with basic aluminum oxide.

These results are in accordance with recent literature reports.^[47,50] To reaffirm the assignment of the relative configuration, the chemical shifts of both methyl groups of both diastereomers of product **N4d** were compared: While both signals of the methyl groups of the *trans* product only differ by about 0.05 ppm, the corresponding signals of the *cis* product differ by about 0.55 ppm (Figure 28). This can be traced back to an upfield shift of the ester's methyl group of the *cis* product due to an aromatic ring current effect, since the methyl ester and the *p*-methoxyphenyl group share the same half space (Figure 28, 30 and 31).

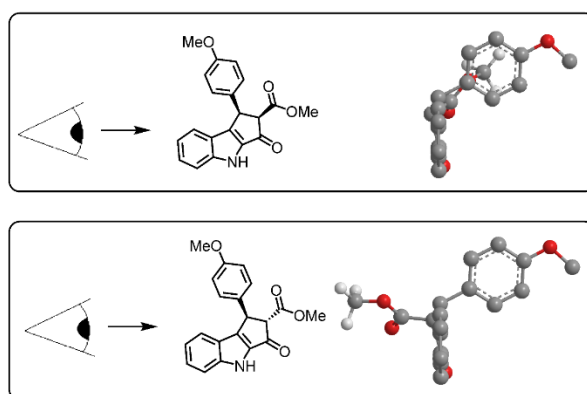
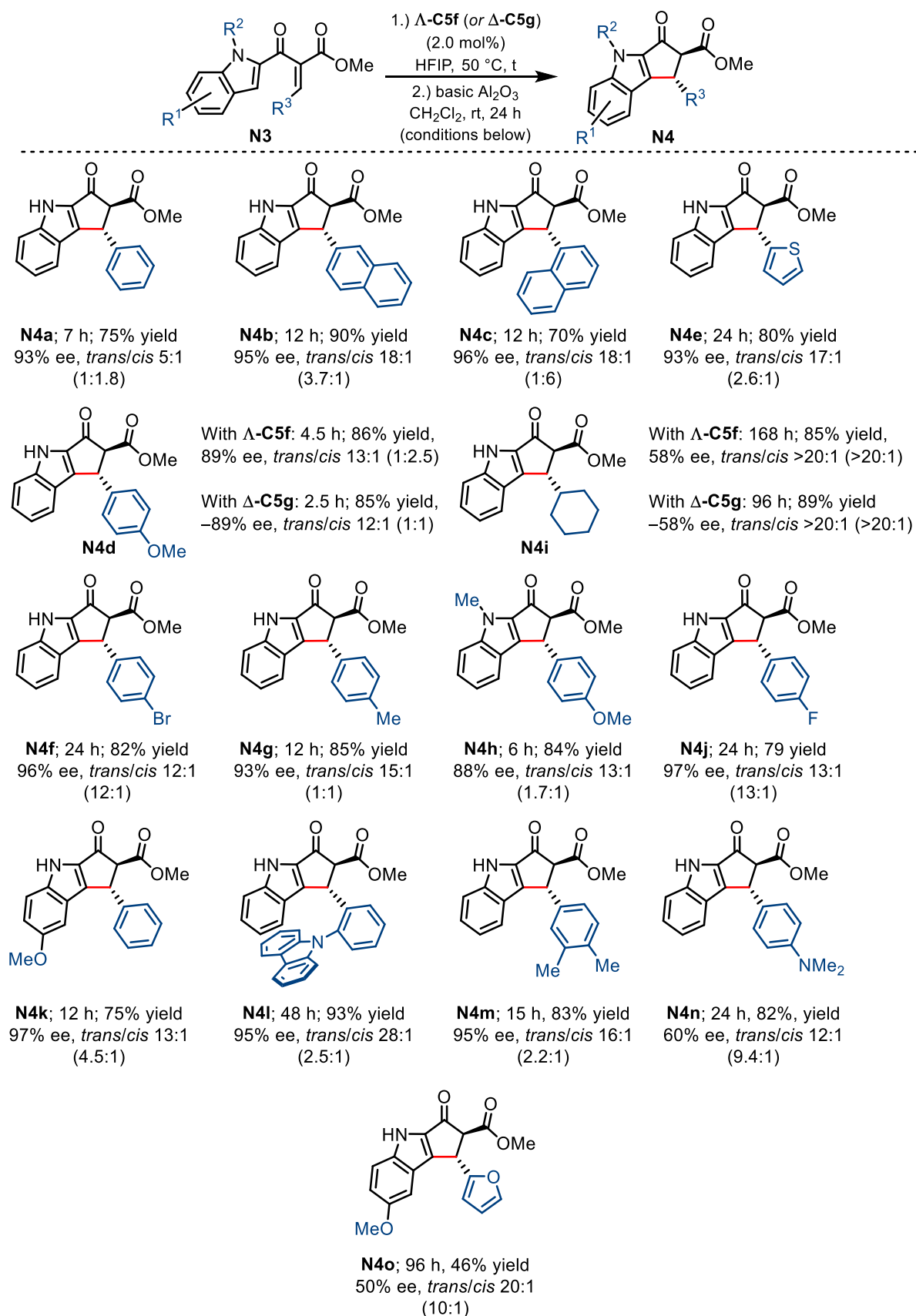


Figure 31: View alongside the edge of the planar indole moiety of product **N4d** with methyl ester and PMP sharing the same half space (*cis*; top) and ester and PMP in different half spaces (*trans*; bottom).

2.3.7 Exploring the Scope of Substrates **N3** Yielding Nazarov Products **N4**

For the typical NAZAROV cyclization procedure using aryl-vinyl ketones **N3**, a rubber-sealed screw-capped vial (1.5 mL) was charged with an *E/Z*-mixture of substrate **N3** (1.0 equivalent, approx. 70–90 μ mol), catalyst **Δ -C5f** (or **Δ -C5g**, each 2.0 mol%) and HFIP (*c* = 0.3 M) and kept at 50 °C for the indicated reaction time. Full conversion for each reaction was determined by TLC analysis. Given d.r. values (*trans/cis*) determined by ^1H NMR analysis of the crude product mixtures before and after basic aluminum oxide induced equilibration. Provided yields and ee values were determined from isolated, equilibrated products. Enantioselectivity was determined by chiral HPLC analysis (*trans* only).

With optimized reaction conditions (Entry 11, table 9) and a straightforward *trans/cis* equilibration procedure in hands, the scope for the indole substrates (**N3a–o**) were investigated (Scheme 92). For most of the indole-functionalized substrates (**N3a–o**), apart from a few exceptions (products **N4i**, **N4n**, and **N4o**), comparable results in terms of selectivity (88%–97% ee) were obtained as for the 3,4-dihydropyran-substituted substrates **N1**. Moreover, the indole-functionalized products were, apart from one exception (product **N4o**), obtained in good albeit slightly lower yields compared to the dihydropyran-functionalized products **N2** (70%–93% yield). Also, the observed d.r. values were, after the described basic aluminum oxide induced *cis/trans* equilibration procedure, in the same range as the d.r. values of the 3,4-dihydropyran-substituted products **N2** (*trans/cis* 12:1–28:1). In terms of isolated yields, *p*-MeO-Ph substituted products **N4d** and **N4h**, 2-thiophenyl substituted **N4e**, *p*-Br-Ph substituted **N4f**, *p*-Me-Ph substituted **N4g**, *p*-F-Ph substituted product **N4j**, *p*-(*N*-carbazolyl)-Ph substituted **N4l**, 3,4-(Me)₂-Ph substituted **N4m**, and *p*-NMe₂-Ph substituted **N4n** were all obtained in yields larger than 80%. Ph substituted products **N4a** and **N4k**, 2-naphthyl substituted **N4b**, and 1-naphthyl substituted **N4c** were obtained with yields in the range of 70%–80% (Scheme 92). In terms of enantioselectivity, ee values of more than 95% were found for 1-naphthyl substituted **N4c**, *p*-Br-Ph substituted **N4f**, *p*-F-Ph substituted **N4j**, phenyl substituted **N4k**, and *o*-(*N*-carbazolyl)-Ph substituted **N4l**. It is striking that the cyclization reaction of sterically congested substrate **N4l** worked so well. Enantioselectivities of 90%–95% were found for Ph substituted **N4a**, 2-naphthyl substituted **N4b**, 2-thiophenyl substituted **N4e**, *p*-(Me)-Ph substituted **N4g** and 3,4-(Me)₂-Ph substituted **N4m**. In case of *p*-MeO-Ph substituted **N4d** and **N4g** ee values of 88% were obtained in both cases. Cyclohexyl substituted **N4i** was obtained with a modest ee: 41% (in case **Δ -IrS** was used) and 58% (in case **Δ -RhO** was used). However, this is a notable result for an alkylated NAZAROV product in consideration of previous literature reports (Scheme 92).^[44a,50]



Scheme 92: Scope for the NAZAROV cyclization of aryl-vinyl ketones **N3**. The d.r. values in parentheses determined by ^1H NMR analysis of the crude product mixtures before Al_2O_3 induced equilibration (before step 2.).

As initially expected, rhodium(III) complex **Δ-S5g** catalyzed the reaction much faster than iridium(III) complex **Δ-S5f**. For product **N4i** full conversion was reached after 168 h in case catalyst **Δ-S5f** and after 98 h in case catalyst **Δ-S5g** was used. This demonstrates the usefulness of the rhodium(III) congener for substrates which react slowly. The *p*-NMe₂-Ph substituted **N4n** was obtained with modest 60% ee, too. Finally, 2-furyl substituted **N4o** was obtained in 46% yield with an ee of 50%. In case of this last substrate from scheme 90, formation of an considerable amount of side products was observed by TLC analysis, which was not observed in case of all other substrates **N4a-n**.

2.3.8 Absolute Configuration Assignments

Absolute configurations of NAZAROV cyclization products **N2** and **N4** were assigned by comparison of the chiral HPLC elution orders of individual products (major / minor enantiomer) with the literature reported elution orders of the same products and by comparison of optical rotation values of individual products with literature reported values of the same products. Literature reported elution orders/optical rotation values were utilized where the absolute configurations of the products of interest are directly linked to X-ray diffraction-based absolute configuration assignments.^[44a-b]

In case of the dihydropyran products **N2**, TANG and co-workers assigned 5*S*,6*R* configuration to their major enantiomer of product **N2e**. They observed consistency in terms of the sense of optical rotation of all their products **N2** and consequently assigned 5*S*,6*R* configuration to all these products.^[44a] When Λ -configured catalyst **Δ-S5f** was used, the chiral HPLC enantiomer elution order of **N2a** and **N2i** was found to be inverted (same chiral HPLC column as TANG) and, moreover, an opposite sense of optical rotation was found for products **N2a**, **N2b**, **N2e**, **N2f**, **N2h** and **N2i**. Consequently, 5*R*,6*S* configuration was assigned to 3,4-dihydropyran products **N2**.

In case of indole products **N4**, RUEPING and co-workers assigned 1*R*,2*S* configuration to the major enantiomers of their products.^[44b] When Λ -configured catalyst **Δ-C5f** was used, the same enantiomer elution orders was observed for products **N4a**, **N4c**, **N4g**, and **N4j** (same chiral HPLC column as RUEPING), and, moreover, the same senses of optical rotation of products **N4a**, **N4c–g**, and **N4j**. consequently, 1*R*,2*S* configuration was assigned to products **N4**. As expected, in cases where Δ -configured rhodium catalyst **Δ-C5g** was used, an inverted elution order was observed, and the products obtained with the opposite sense of optical rotation. Consequently, 1*S*,2*R* configuration was assigned to products **N4d** and **N4i** for which rhodium catalyst **Δ-C5g** was used.

In conclusion, related products **N2a** and **N4a** were obtained with a consistent absolute configuration when catalysts with an identical configuration (Λ or Δ) are used (Figure 32).

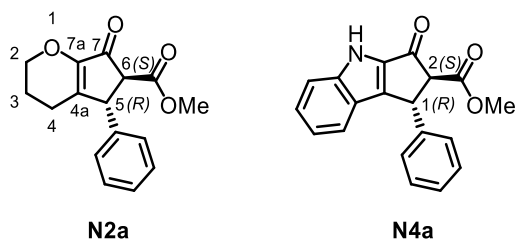


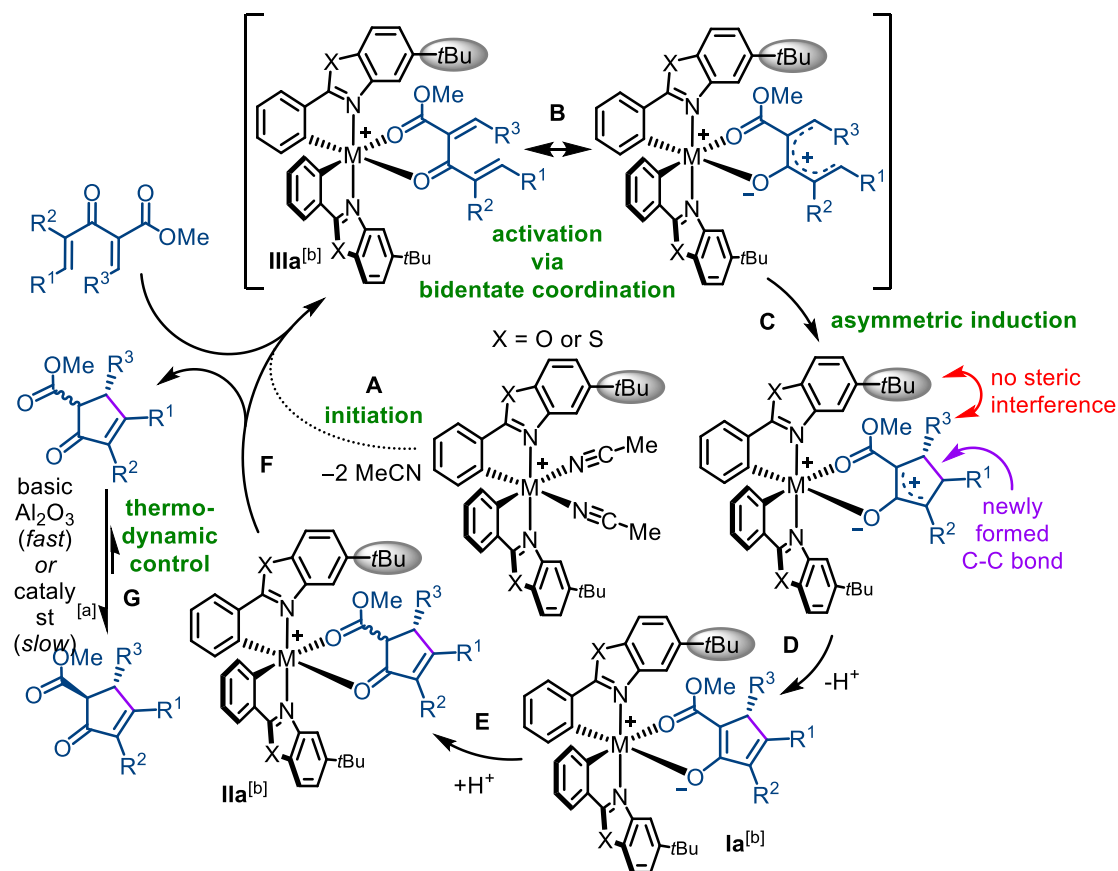
Figure 32: Products (5*R*,6*S*)-**N4a** and (1*R*,2*S*)-**N4a** are obtained when Λ -**C5f** is used as catalyst.

2.3.9 Rationalization of the Reaction Mechanism

A mechanistic proposal for the NAZAROV cyclization reactions of α -unsaturated β -ketoesters with the here presented stereogenic-at-metal catalysts is shown in scheme 93, which is based on previous works on the mechanisms of NAZAROV cyclization reactions^[40–48] and on the well-established properties of LEWIS acidic stereogenic-at-metal catalysts of iridium(III) and rhodium(III) **C5**.^[4,7,9,13,49,51,53]

At first, an α -unsaturated β -ketoester replaces both semi-labile acetonitrile ligands and coordinates to the metal center in an *O,O*-bidentate fashion (Step **A**, scheme 93).^[37] It should be noted here that the LEWIS acidic bis-cyclometalated chiral-at-metal fragment has a C_2 symmetry, which entails that there exists only one possibility to coordinate the substrate to the metal center in an *O,O*-bidentate fashion. Coordination to the metal center goes along with electronic activation of the substrate (Step **B**, scheme 93), which triggers a conrotatory 4π -electrocyclization^[37] to give a catalyst-bound cyclopentadienyl cation (Step **C**, scheme 93). Step **C** constitutes the stereogenic step of the reaction in which the stereo information of the stereogenic-at-metal catalyst is transferred to the emerging product. Subsequent deprotonation (Step **D**, scheme 93) and re-protonation (Step **E**, scheme 93) provides the catalyst-bound NAZAROV product. Release of the NAZAROV product allows a new catalytic cycle to be started (Step **F**, scheme 93). In case of the indole products (**N4**) it was apparent, that the *cis* diastereomers were initially formed as kinetic products, which then either slowly epimerize to the respective predominantly *trans*-configured products under the conditions of the reaction or, faster and milder, upon treatment with powdered basic aluminum oxide in CH_2Cl_2 at rt (Step **G**). In contrast, 3,4-dihydropyran products (**N2**) were found to be predominantly *trans*-configured right after the cyclization. Nonetheless, it is well possible that the *cis*-products

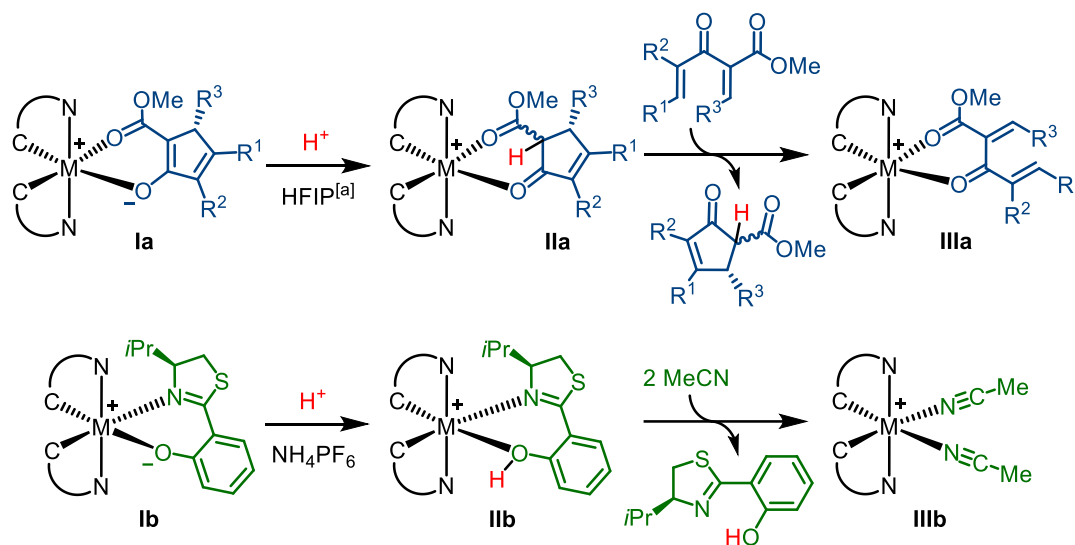
are also initially formed in these cases and that a fast epimerization occurs under the applied reaction conditions (Scheme 93).



Scheme 93: Proposed mechanism for NAZAROV cyclization reactions of α -unsaturated β -ketoesters with the here presented stereogenic-at-metal catalysts **A-C5f** and **A-C5g**. [a] Only observed for indole-functionalized products **N4**. In case of 3,4-dihydropyran-functionalized products **N2**, predominantly *trans*-enriched products were found right after the cyclization. [b] Identifiers **Ia**, **IIa**, **IIIa**: See scheme 94 below.

It is striking that the use of HFIP as additive or solvent was found to be beneficial in case of 3,4-dihydropyran substrates **N1** (Table 8) and even crucial in case of indole substrates **N3** (Table 9). In this regard, it was previously revealed in the course of extensive research on stereogenic-at-metal complexes^[53] that bidentate salicylthiazoline (**S**)-**AL1** and salicyloxazoline (**S**)-**AL2** ancillary ligands in bis-cyclometalated complexes of iridium(III) and rhodium(III) are readily cleaved in the presence of acids as weak as NH_4PF_6 . Since HFIP is known for its weak acidity^[54] and catalysis intermediate **Ia** is structurally similar to such salicyloxazolinato and salicylthiazolinato complexes (see **Ib** in scheme 94),^[4,7,9,13,49,51,53] it can be rationalized that re-protonation of intermediate **Ia** to form **IIa** is facilitated by the presence of weakly acidic HFIP, which enhances or even enables product dissociation and hence catalytic turnover (Scheme 94). Note that H^+ is actually not consumed in the course of the catalytic cycle

(see step **D** and **E** of scheme 93) and that HFIP rather seems to increase the steady-state concentration of H^+ .

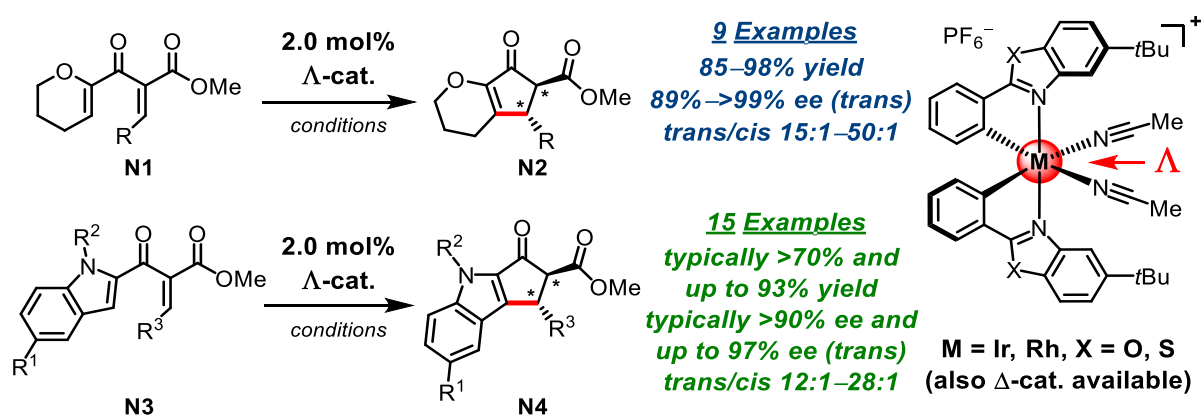


Scheme 94: Comparison of the anticipated product dissociation enhancement by HFIP (**Ia**–**IIIa**; *top*) with the already established salicylthiazoline cleavage with NH_4PF_6 in MeCN (**Ib**–**IIIb**; *bottom*).^[4,7,9,13,49,51,53] [a] Note that H^+ is actually not consumed in the course of the catalytic cycle (see scheme 93, Step D and E).

2.4 Summary

With this project it was demonstrated that stereogenic-at-metal LEWIS acid complexes **C5** from the MEGGERS group serve as powerful catalysts for asymmetric NAZAROV cyclization reactions. Moreover, it could be demonstrated with this work that the scope of catalysts **C5** is extendable to *O,O*-coordinating substrates.

Key features of the NAZAROV cyclization reaction with catalyst **A-C5f** are: 1.) a low catalyst loading; 2.) no need to rely on expensive counterions like BArF_{24}^- , NTf_2^- or SbF_6^- anions; 3.) no need for anhydrous solvents and SCHLENK technique; 4.) therefore a convenient setup 5.) the option to address two differently functionalized substrates of **Type D**, namely 3,4-dihydropyran- and indole-functionalized substrates **N2** and **N4**) short reaction times as well as competitive selectivity and yield (Scheme 95).^[47]



Scheme 95: Overview of NAZAROV products **N2** and **N4** with obtained yields and selectivity.

Even though iridium complex **A-C5f** was used with only 2.0 mol% catalyst loading at 40 °C, reaction times for the 3,4-dihydropyran substrates **N2** remained below 24 h while still providing excellent yields and enantioselectivity, even for more challenging compounds like *p*-Br-Ph functionalized substrate **N2h** and *p*-F-Ph functionalized substrate **N2i** (Scheme 84). On the contrary, it took established catalyst system $\text{BOX}/\text{Cu}^{\text{II}}(\text{BArF}_{24})_2$ more than 24 h with a catalyst loading of 20 mol% to furnish **N2h** and **N2i** with comparable selectivity but lower yields (**N2h**, 57 h, 76% yield, 96% ee; **N2i**, 30 h, 69% yield, 96% ee).^[47a]

A similar trend can be recognized in case of indole substrates **N3**. Using the same catalyst **A-C5f** with 2.0 mol% catalyst loading at 50 °C, products **N4** were obtained with yields and selectivity in the same order of magnitude as reported in literature for established catalyst system $\text{BOX}/\text{Cu}^{\text{II}}(\text{SbF}_6)_6$ (5.0 mol%) at 10 °C.^[47b] Remarkably, substituted indole product **N4l** containing the *o*-(*N*-carbazolyl)-Ph moiety is still obtained with excellent yields and high selectivity despite the sheer size of the substrate.

The herein reported stereogenic-at-metal complexes **A-C5f** and **A-C5g** therefore represent a useful tool to catalyze NAZAROV substrates that are known for sluggish cyclization with previously reported methods.

2.5 Outlook

One way to extent the usefulness of the stereogenic-at-metal catalysts **C5** in the field of NAZAROV cyclization would be to address lesser activated substrates of **Type A** and **B** (Figure 33).^[44,45]

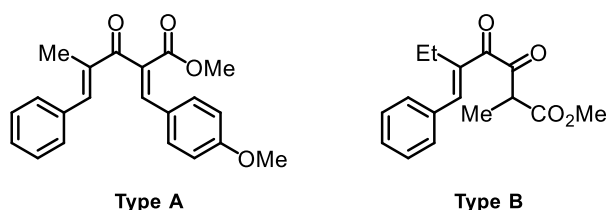
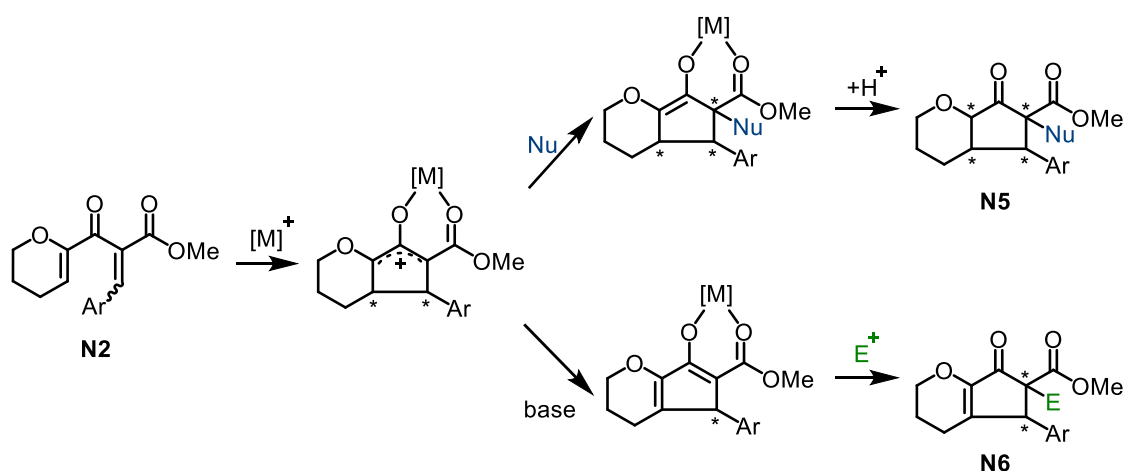


Figure 33: Examples for lesser activated substrates of **Type A** and **B**.

Another possibility to extend the developed strategy is to interrupt the NAZAROV reaction after ring closing reaction. It is literature known that cyclopentenyl cation can be trapped by nucleophiles (Nu^-) to obtain products **N5** with up to four stereocenters (Scheme 96, top). Furthermore, it could also be possible to interrupt the NAZAROV reaction by addition of base to form enolate which could be used to trap electrophiles (E^+) yielding product **N6** (Scheme 96, bottom).



Scheme 96: Possible approaches towards an asymmetric, interrupted NAZAROV cyclization: Interruption by attack of a nucleophile (Nu^-) on the cyclopentenyl cation (top). Interruption through enol formation which can be used to trap electrophiles (E^+ , bottom).

For both scenarios it would be a reasonable approach to generate the nucleophile or electrophile by photochemistry.

A third approach to harness the full potential of the developed catalytic system is the application in natural product synthesis or pharmaceutical chemistry. Examples are the synthesis of (+)-Indatraline **N7** and (+)-Irindaline **N8** (Figure 34).

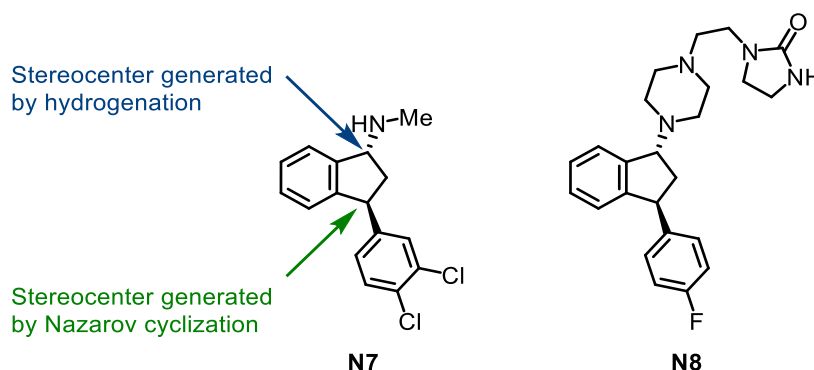
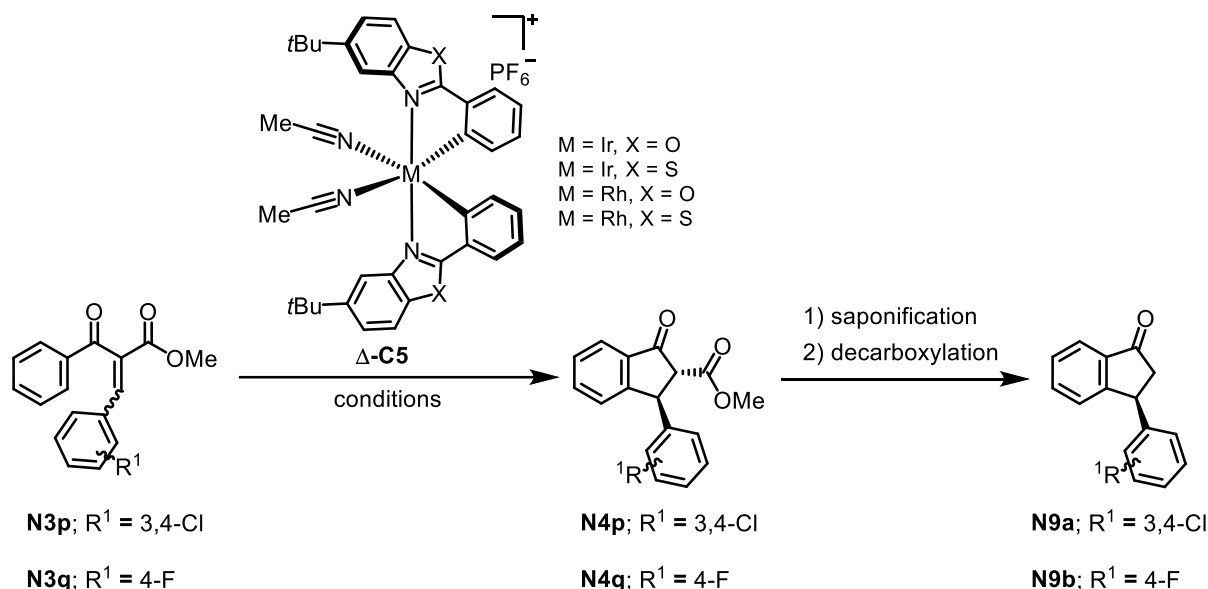


Figure 34: Structure of (+)-Indatraline **N7** and (+)-Irindaline **N8**.

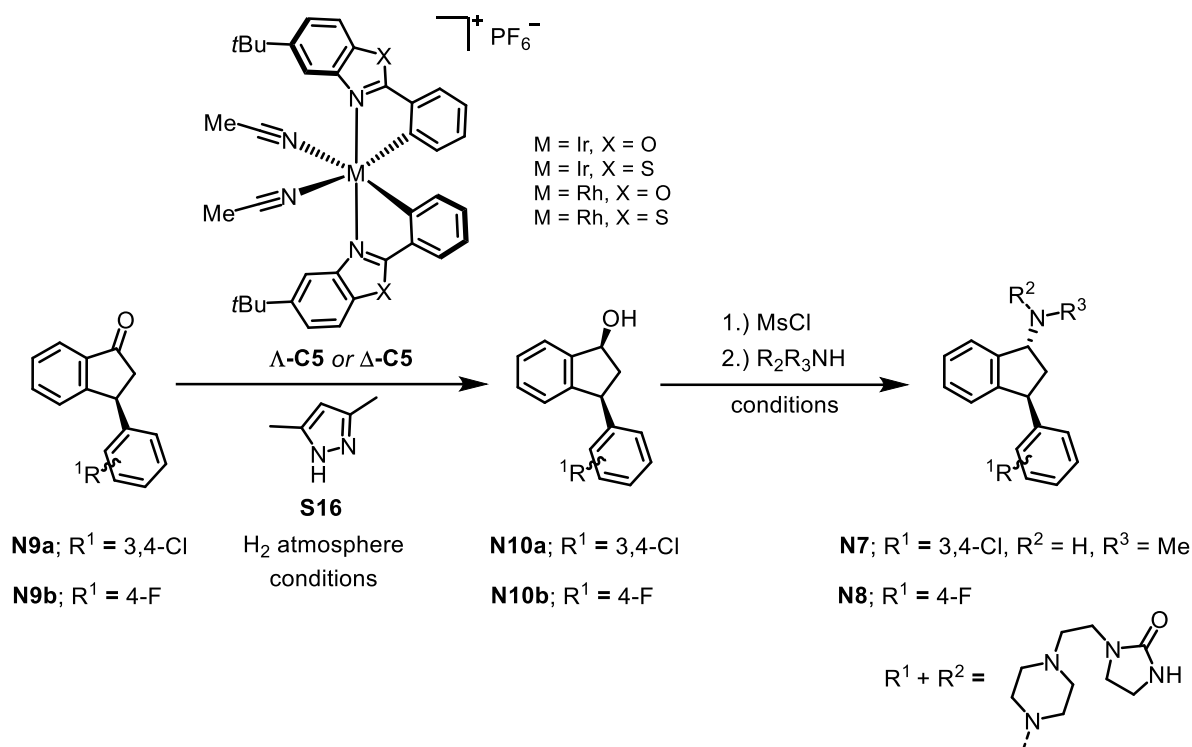
Key steps of the synthesis are asymmetric NAZAROV cyclization and asymmetric transfer hydrogenation reactions. Aryl-vinyl ketone **N3p** and **N3q** could be utilized in the NAZAROV cyclization reaction key step to generate the first stereocenter in products **N4p** and **N4q**. Subsequently, the ancillary ester could be removed by saponification and decarboxylation to obtain pentanone **N9a** and **N9b** (Scheme 97).



Scheme 97: Synthesis of chiral cyclopentanone **N9** by NAZAROV cyclization.

In the next key step, catalyst **C5** could be used for asymmetric transfer hydrogenation in kinetic resolution. Doing so, a matched pair of catalyst control and substrate control must be identified, to exclusively reduce enriched cyclopentanone **N9** to chiral alcohol **N10** with high selectivity.

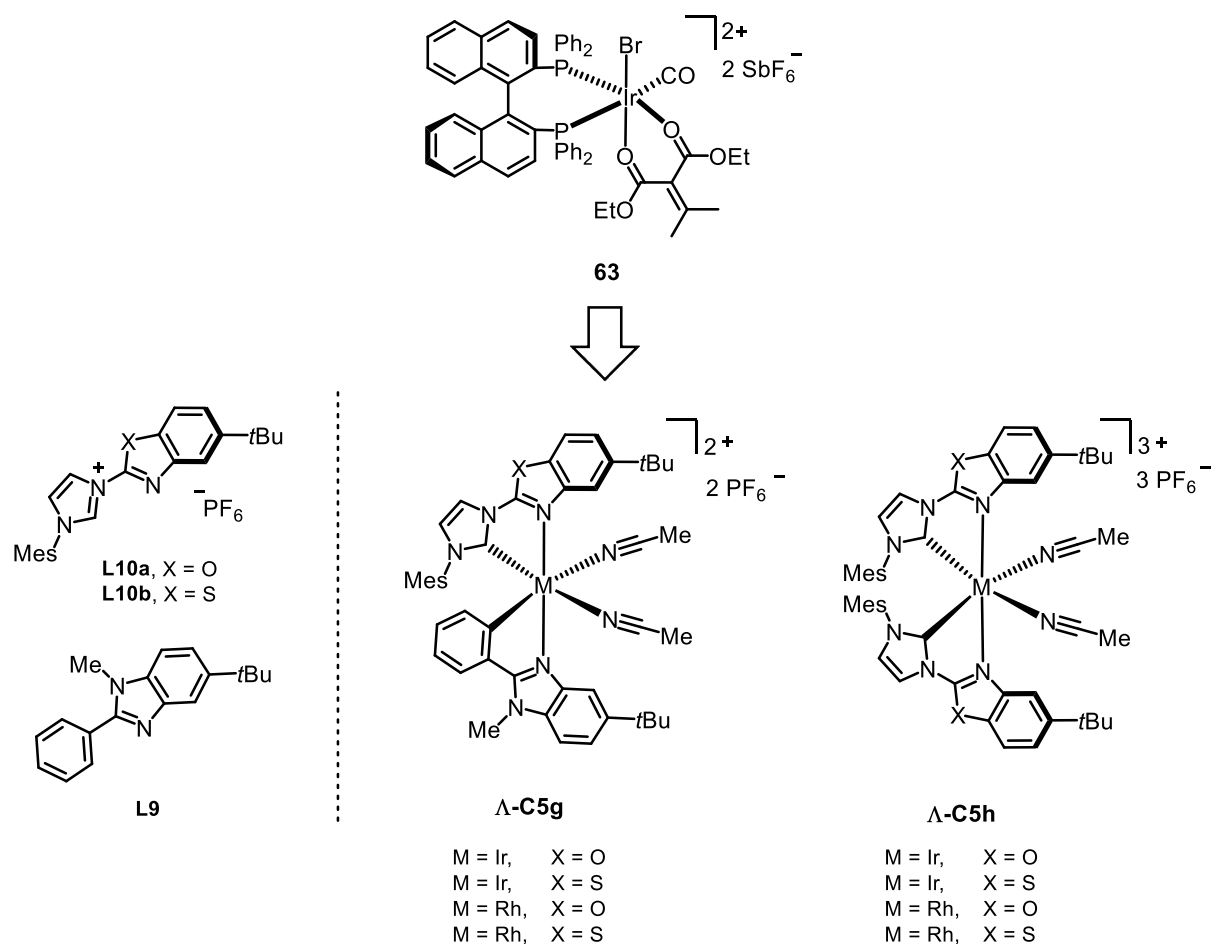
In the last step, mesylation of alcohol **N10** and subsequent nucleophilic attack of amines does provide chiral amines **N7** and **N8** under inversion of the stereochemistry (Scheme 98).



Scheme 98: Transfer hydrogenation to obtain enriched alcohol **N10** as substrate for amination.

A fourth approach to harness the full potential of the developed catalytic system is the application of catalyst with higher reactivity. Initial test reaction showed that rhodium(III) complex $\Delta\text{-C5e}$ catalyzes the NAZAROV cyclization up to three times faster than the iridium(III) congener $\Delta\text{-C5f}$ (see table 7 and scheme 92). Inspiration might be taken by work of FRONTIER and EISENBERG. In this studies, biscationic and tricationic iridium(III) complexes **63** (tricationic species is generated *in-situ* by use of silver salts) showed great potential due to short reaction times and high yields.^[48]

Since first examples for trisheteroleptic complexes are currently investigated by the MEGGERS group using phenylbenzimidazo ligands **L9**, biscationic $\Delta\text{-C5g}$ could potentially be obtained by using a neutral bidentate NHC ligand like **L10**. Tricationic complex $\Delta\text{-C5h}$ could be obtained by using NHC ligand **L10** two times (Scheme 99).



Scheme 99: Design for potential biscationic and tricationic iridium(III) or rhodium(III) complexes.

Similarly, ruthenium(II) complex **Λ-C5i** might be favorable for the NAZAROV cyclization (Figure 35).

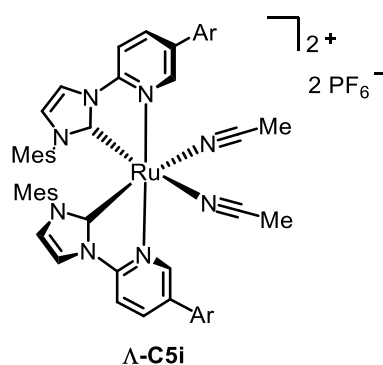


Figure 35: Structure of the biscationic ruthenium(II) complex **Λ-C5i** from the MEGGERS group.

3 Experimental Section

3.1 General Aspects

General methods: All reactions were performed in oven-dried and previously evacuated glassware, if not stated otherwise.

All coordination chemistry and modifications on iridium(III) complexes were performed in the dark as precaution against light-induced decomposition and side reactions. When iridium(III) complexes were adsorbed on silica gel or aluminium oxide, the temperature was not raised higher than 40 °C and the adsorbed material was shielded from light before chromatography.

Whenever the term 'room temperature' (rt) is used, it means that the reaction or operation was performed at an ambient temperature of 25 °C without active thermostatzation.

All reactions below 100 mg of substrate and / or product were conducted using a *Mettler Toledo XP204* high precision analytical balance. The purified product solutions were filtered through a rinsed pipette equipped with a small cotton plug in each case to remove possible traces of dust and silica to ensure accurate yields. All other chemicals were weighed with an *Ohaus Pioneer P114C* analytical balance

Solvents: CH₂Cl₂, pyridine, triethylamine and diisopropylethylamine were distilled under nitrogen from calcium hydride. Toluene, diethyl ether, THF and 1,4-dioxane were distilled under nitrogen from sodium and MeOH was distilled under nitrogen from iodine activated magnesium. Toluene was degassed via freeze-pump-thaw method in five cycles prior to use in cross-coupling reactions. All solvents for reactions were at least HPLC grade and purchased from *Merck*. Ethoxyethanol and MeOH were degassed by purging with nitrogen gas before use for complex chemistry or reactions with hydrogen gas. Solvents for column chromatography were distilled prior to use.

Reagents: Potassium phosphate was grounded and dried under vacuum at 600 °C and stored under nitrogen atmosphere for later use. Piperidine was freshly filtered over basic aluminium oxide prior to use. All aldehydes were purified by short path distillation *or* short column on basic aluminium oxide. Iridium(III)chloride was purchased from *Precious Metals Online*. Other reagents were purchased from *Alfa Aesar*, *Acros Organics*, *Sigma Aldrich* or *TCI* and used without further purification.

The chiral ancillary ligands (*S*)-4-*iso*-propyl-2-(2'-hydroxyphenyl)-2-thiazoline ((**S**)-**AL1**) was prepared according to published procedures.^[13c] (*S*)-4-phenyl-2-(4'-fluoro-2'-hydroxyphenyl)-

2-oxazoline ((**S**)-**AL1**) was provided by JIAJIA MA and (*S*)-4-*tert*-buthyl-2-(-2'-hydroxyphenyl)-2-oxazoline ((**S**)-**AL3**) and 2-Amino-4-methoxy-5-methylphenol were provided by THOMAS CRUCHTER.

3.2 Chromatography

Column chromatography was performed with silica gel 60 M from *Macherey–Nagel* (irregularly shaped, 230–400 mesh) and basic aluminium oxide (powder, 58 Å pore size, pH 9.5±0.5 in water) from *Sigma Aldrich*. A uniform column packing was achieved by loading the column with a suspension of dry immobile phase in the respective eluent (wet packing). The packing was optimized by applying compressed air.

Thin layer chromatography was carried out on aluminium TLC plates *silica gel 60 F₂₅₄* from *Merck*. The detection was carried out by fluorescence quenching (UV-light: $\lambda = 254$ nm), fluorescence (vis-light: $\lambda = 633$ nm), permanganate stain and HANESSIAN's stain.

HPLC Analysis: Enantiopurities were determined with an *Agilent 1200 Series* and an *Agilent 1260 Series* HPLC system under indicated conditions (temperature, flowrate, solvents, solvent ratio, wavelength). The following chiral HPLC columns were used: *Daicel Chiralpak AS-H* (5 μ m, 250 mm x 4.6 mm); *Daicel Chiralpak AD-H* (5 μ m, 250 mm x 4.6 mm); *Daicel Chiralcel OJ-H* (5 μ m, 250 mm x 4.6 mm); *Daicel Chiralpak IA* (5 μ m, 250 mm x 4.6 mm); *Daicel Chiralpak IB* (5 μ m, 250 mm x 4.6 mm).

3.3 Spectroscopy and Spectrometry

Nuclear magnetic resonance spectroscopy: ^1H NMR and ^{13}C NMR spectra were recorded with a *Bruker Avance III* (300 MHz, automatization), *Avance III* (500 MHz) or an *Avance II* (600 MHz) spectrometer at a temperature of 300 K if not stated otherwise. The *Avance III* (500 MHz) and *Avance II* (600 MHz) were operated by the service department of the PHILIPPS UNIVERSITY OF MARBURG. Chemical shifts δ are expressed in parts per million (ppm) relative to tetramethylsilane (TMS). The NMR standards used were as follows: ^1H NMR spectroscopy: $\delta = 7.26$ ppm (CDCl_3), $\delta = 5.32$ ppm (CD_2Cl_2), $\delta = 2.50$ ppm ($\text{DMSO}-d_6$), $\delta = 2.05$ ppm (acetone- d_6), $\delta = 3.31$ ppm (CD_3OD). ^{13}C NMR spectroscopy: $\delta = 77.0$ ppm (CDCl_3), $\delta = 53.8$ ppm (CD_2Cl_2), $\delta = 39.5$ ppm ($\text{DMSO}-d_6$), $\delta = 29.8, 206.3$ ppm (acetone- d_6), $\delta = 49.0$ ppm (CD_3OD). For the assignments of the signal in ^1H NMR spectra following abbreviations were used: H_{Ar} - aromatic protons, H_{Aliph} - aliphatic protons. ^{13}C NMR spectra are given as observed. ^{19}F NMR spectra were recorded with a *Bruker Avance III HD* (300 MHz with respect to ^1H)

spectrometer at a temperature of 300 K. CFCl_3 was used as NMR standard: $\delta = 0.00$ ppm (CFCl_3). All coupling constants (J) are absolute values and are expressed in hertz (Hz). The description of signals includes: br = broad, s = singlet, d = doublet, dd = doublet of doublets, t = triplet, m = multiplet.

Mass spectrometry: HR-MS spectra were recorded with an *LTQ-FT Ultra* (Thermo Fischer Scientific) instrument by electrospray ionization (ESI) and an *AccuTOF GCv* (Jeol) instrument by liquid injection field desorption ionization (LIFDI) by the service department of the PHILIPPS UNIVERSITY OF MARBURG. The peaks are given as mass-to-charge-ratio (m/z). Every reported isotopic pattern was in accordance with the calculated isotopic pattern. The molecule peak is given as $[\text{M}]^+$, $[\text{M}+\text{H}]^+$, $[\text{M}+\text{Na}]^+$ if ionized by a proton or sodium ion respectively or as $[\text{M}-\text{Cl}]^+$ if a chloride ion is removed. For the high-resolution mass (HR-MS), the following abbreviations were used: calcd = calculated data, found = measured data.

IR-spectroscopy: IR-spectra were recorded on a *Bruker Alpha ATR FT-IR* spectrometer. Absorption bands are given as wave numbers $\tilde{\nu}$ in the unit cm^{-1} in a range of $4000\text{--}400\text{ cm}^{-1}$. The intensities of the bands were characterized as follows: br = broad, s = strong, m = medium, w = weak.

Circular dichroism spectroscopy: CD spectra were recorded with a *JASCO J-810* CD spectropolarimeter (200 to 600 nm, 1 nm bandwidth, scanning speed of $50\text{ nm}\cdot\text{min}^{-1}$, accumulation of 5 scans). CD spectra were smoothed with the SAVITZKY-GOLAY-Filter.

Optical rotation spectroscopy: Optical activity of isolated chiral products was determined using a *P8000-T* polarimeter (*A. Kruess Optronic GmbH*) and a 50.0 mm polarimeter cell, optical activity is given as specific rotation $[\alpha]_{\text{D}}^{27}(c, \text{solvent})$ at the sodium D line ($\lambda = 589\text{ nm}$) at $27\text{ }^\circ\text{C}$ in the indicated solvent and the concentration c is given in the unit g/100 mL.

X-Ray crystallography: X-Ray diffraction data was collected with a *Bruker D8 Quest* diffractometer by the service department. Refinement and analysis of the data was conducted by KLAUS HARMS.

3.4 Procedures

3.4.1 Procedure A): Br- and TfO Functionalized Dimer Complexes *rac*-C1

The reactions were performed according to a slightly modified reported procedure.^[6] A flame dried flask equipped with nitrogen inlet, condenser and stirr bar was charged with the benzoxazole or benzothiazole ligand **L** (2.00 eq.) and ethoxyethanol ($c \approx 50$ mM based on 1.00 eq. ligand). The solution was purged with nitrogen for 30 min before iridium(III) chloride hydrate (1.00 eq.) was added. The mixture was heated to 130 °C under reflux and exclusion of light overnight. The reaction was monitored by TLC every 12 h. In case that the ligand was not completely consumed after 24 h, iridium(III) chloride hydrate (0.10 eq.) was added and the reaction time was prolonged. If the ligand was consumed, the mixture was cooled to room temperature. The resulting orange solution was filtered through a thin pad of silica gel to remove insoluble compounds. The filter cake was washed with CH₂Cl₂ thoroughly, the solvent was removed under reduced pressure and the crude product was dried overnight. The crude product was adsorbed on basic aluminium oxide with CH₂Cl₂ and purified by filter column on silica to afford the dimer *rac*-**1** as bright orange solid.

3.4.2 Procedure B): Br- and TfO-Functionalized Diastereomer Complexes **C2**

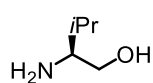
The reaction was performed according to a slightly modified reported procedure.^[7e] A SCHLENK tube (threaded PTFE plug) equipped with stir a bar was charged with the respective dimer *rac*-**C1** (1.00 eq.), ancillary ligand (**S**)-**AL** (2.20 eq.), and EtOH (90 mM). This mixture was homogenized by sonication for 10 min before AgOTf (2.20 eq.) and Et₃N (10.0 eq.) were added. Afterwards, the mixture was further diluted with EtOH ($c = 45$ mM) and again homogenized by sonication. The mixture was heated to 80 °C for 5 h to 8 h and monitored by TLC. After completion, the flask was cooled to rt, and the mixture filtered through a plug of celite which was rinsed with CH₂Cl₂. The filtrate was concentrated under reduced pressure and the crude product was adsorbed on basic aluminium oxide with CH₂Cl₂ and subjected to silica gel flash column chromatography (*n*-hexane/CH₂Cl₂) to separate the Λ -(**S**)-**C2** and Λ -(**S**)-**C2** diastereomer iridium(III) complexes. Each complex was further purified by silica gel flash column chromatography (*n*-hexane/EtOAc) to obtain bright orange-red solids as diastERICALLY pure compounds.

3.4.3 Procedure C): Cross-Coupling Reaction to Yield Complexes C3

The reaction was performed according to a slightly modified reported procedure.^[19a-b] A SCHLENK tube (10 mL; threaded PTFE plug) equipped with stir bar was charged with diastereomerically pure iridium(III) complex Λ -(*S*)-C2 or Λ -(*S*)-C2 (1.00 eq.), boronic acid (4.00 eq.), K₃PO₄ (4.00 eq.), Pd(OAc)₂ (10 mol%) and SPhos (20 mol%). The mixture was evacuated and refilled with nitrogen (3x). Toluene (200 mM), thoroughly degassed by freeze-pump-thaw in five cycles, was used to suspend the solids. The suspension was sonicated for 10 min and placed in a preheated oil bath (90 °C). The reaction was stirred for 12 h and monitored by TLC. The solvent was removed under reduced pressure, the crude product dissolved in CH₂Cl₂, adsorbed on basic aluminum oxide and purified by silica gel flash chromatography (*n*-hexane/EtOAc) to afford the cross-coupled, diastereomerically pure iridium(III) complex Λ -(*S*)-C3 or Λ -(*S*)-C3 as orange-red solid.

3.4.4 Ancillary Ligand (S)-AL1

L-Valinol ((S)-AL3)

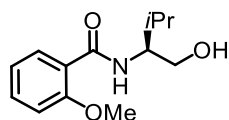


The reaction was performed according to a slightly modified reported procedure.^[55] A 1 L three-neck flask equipped with condense, dropping funnel, nitrogen inlet and stir bar was charged with NaBH₄ (7.75 g, 204.9 mmol, 2.40 eq.), L-valine (10.0 g, 85.4 mmol, 1.00 eq.), dry THF (200 mL) and cooled to 0 °C. To this suspension, a solution of iodine (21.6 g, 85.4 mmol, 2.00 eq.) in THF (60 mL) was added dropwise over 1 h. **Caution:** Violent generation of hydrogen gas upon rapid addition or to elevated temperature! When gas formation ceased, the mixture was heated to 80 °C and stirred for 40 h. After cooling to rt, the reaction was terminated by careful addition of MeOH (200 mL). After gas formation ceased, the mixture was stirred further for 30 min before all volatiles were removed under reduced pressure, and the residue was stirred in aqueous KOH solution (20% m/m, 150 mL) for 12 h. The aqueous layer was extracted with CH₂Cl₂ (5x150 mL), the combined organic layers were washed with brine (50 mL), dried over Na₂SO₄, filtered and concentrated. The crude product was purified by fractional distillation. Volatiles at 32 °C and 700 mbar were discarded. L-Valinol ((S)-AL3) was collected at 75 °C at 8 mbar and obtained as colorless crystalline solid (3.48 g, 33.7 mmol, 39%) upon cooling.

¹H NMR (300 MHz, CDCl₃): δ = 3.63 (dd, *J* = 10.6, 4.0 Hz, 1H, CH), 3.29 (dd, *J* = 10.6, 8.7 Hz, 1H, CH), 2.61–2.50 (m, 1H, CH), 2.08 (s br, 3H, NH₂, OH), 1.65–1.49 (m, 1H, CH), 0.91 (dd, *J* = 6.8, 4.1 Hz, 6H, 2xCH₃) ppm.

¹³C NMR (75 MHz, CD₂Cl₂): δ = 78.3, 77.8, 77.4, 65.3, 59.2, 32.2, 19.9, 19.0 ppm.

((S)-N-(1-Hydroxy-3-methylbutan-2-yl)-2-methoxybenzamide ((S)-AL4)



The reaction was performed according to a slightly modified reported procedure.^[13c] A 500 mL flask equipped with a stir bar was charged with L-valinol ((S)-AL3, 2.64 g, 25.6 mmol, 1.00 eq.), Et₃N (3.90 mL, 2.85 g, 28.1 mmol, 1.10 eq.), DMAP (160 mg, 1.31 mmol, 5.0 mol%), dry THF (150 mL) and cooled to 0 °C. To this solution, *O*-Methylsalicylic acid chloride (4.19 mL, 4.80 g, 28.1 mmol, 1.10 eq.) was added dropwise. The reaction was allowed to warm up to rt and stirred over night for 16 h. Complete conversion was indicated by TLC and permanganate stain. All volatiles were removed under reduced pressure and the residue diluted with water and EtOAc (100 mL

each). The aqueous layer was extracted with EtOAc (3x50 mL). The combined organic layers washed with brine (50 mL), dried over Na₂SO₄, filtered, concentrated under reduced pressure and adsorbed on silica gel. Filter column (*n*-hexane/EtOAc 2:1) furnished amid (**S**)-**AL4** as colorless oil (5.07 g, 21.4 mmol, 83%) which crystallized upon cooling.

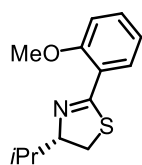
TLC (*n*-hexane/EtOAc 1:1): *R*_f = 0.75.

¹H NMR (300 MHz, CH₂Cl₂): δ = 8.19–7.98 (m, 3H, *H*_{Ar}, *NH*), 7.54–7.44 (m, 1H, *H*_{Ar}), 7.13–7.01 (m, 2H, *H*_{Ar}), 3.99–3.88 (m, 4H, *CH*, *CH*₃), 3.80–3.63 (m, 2H, *CH*₂), 3.18 (dd, *J* = 6.5, 4.6 Hz, 1H, *H*_{Aliph}), 2.09–1.93 (m, 1H, *CH*), 1.01 (t, *J* = 7.0 Hz, 6H, *OCH*₃) ppm.

¹³C NMR (75 MHz, CD₂Cl₂): δ = 166.7, 158.1, 133.2, 132.4, 122.0, 121.6, 111.9, 65.4, 58.5, 56.5, 29.6, 20.0, 18.5 ppm.

HR-MS (ESI): *m/z* calcd. for C₁₃H₂₀N₁O₃ [*M*+*H*]⁺: 238.1438, found 238.1421.

(**S**)-4-*Iso*-propyl-2-(2-methoxyphenyl)-4,5-dihydrothiazole ((**S**)-**AL5**)



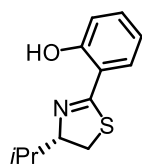
The reaction was performed according to a slightly modified reported procedure.^[13c] A 250 mL three-neck flask equipped with stir bar was charged with amid (**S**)-**AL4** (4.20 g, 17.7 mmol, 1.00 eq.), P₄S₁₀ (6.18 g, 27.8 mmol, 1.57 eq.), dry CH₂Cl₂ (120 mL) and heated to reflux (40 °C) for 5 d. After full conversion was indicated by TLC, the mixture was filtered, and the solid residue was rinsed thoroughly with CH₂Cl₂ and discarded. The filtrate was washed with aqueous NaOH solution (2 M, 50 mL), and brine, dried over Na₂SO₄, filtered, concentrated under reduced pressure and adsorbed on silica gel. Filter column (*n*-hexane/EtOAc 10:1) furnished thiazoline (**S**)-**AL5** as colorless oil (3.33 g, 14.1 mmol, 80%).

TLC (*n*-hexane/EtOAc 5:1): *R*_f = 0.61.

¹H NMR (300 MHz, CH₂Cl₂): δ = 7.89–7.80 (m, 1H, *H*_{Ar}), 7.44–7.36 (m, 1H, *H*_{Ar}), 7.03–6.93 (m, 2H, *H*_{Ar}), 4.32–4.21 (m, 1H, *H*_{Aliph}), 3.31 (dd, *J* = 10.9, 8.7 Hz, 1H, *CH*), 3.02 (dd, *J* = 10.7, 10.2 Hz, 1H, *CH*), 2.12–1.96 (m, 1H, *CH*), 1.10 (d, *J* = 6.7 Hz, 3H, *CH*₃), 1.01 (d, *J* = 6.7 Hz, 3H, *CH*₃) ppm.

HR-MS (ESI): *m/z* calcd. for C₁₃H₁₈N₁O₁Si₁ [*M*+*H*]⁺: 236.1104, found 236.1092.

(*S*)-2-(4-*Iso*-propyl-4,5-dihydrothiazol-2-yl) phenol ((*S*)-AL1)



The reaction was performed according to a slightly modified reported procedure.^[13c] A 100 mL flask equipped with nitrogen inlet and stir bar was charged with thiazoline (**(S)-AL5**) (1.00 g, 4.25 mmol, 1.00 eq.), dry CH₂Cl₂ (100 mL) and cooled to –78 °C. BBr₃ (0.48 mL, 1.28 g, 5.10 mmol, 1.20 eq., neat) was added dropwise and the solution was stirred for 12 h and allowed to warm up to rt. After full conversion was indicated by TLC, triethanolamine (10 mL) was added to the mixture at 0 °C. The mixture was heated to 50 °C for 5 h, diluted with MeOH (70 mL) and stirred for 1 h. All volatiles were removed under reduced pressure, the residue diluted with water and EtOAc (50 mL each), the aqueous layer was extracted with EtOAc (3x50 mL), the combined organic layer washed with brine, dried over Na₂SO₄, filtered, concentrated under reduced pressure and adsorbed on silica gel. Filter column (*n*-hexane/EtOAc 40:1) furnished the ancillary ligand (**(S)-AL1**) as yellow oil (579 mg, 2.62 mmol, 62%).

TLC (*n*-hexane/EtOAc 20:1) *R*_f = 0.42.

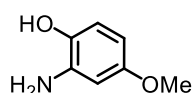
¹H NMR (300 MHz, CH₂Cl₂): δ = 12.8 (s, 1H, OH), 7.44–7.38 (m, 1H, *H*_{Ar}), 7.38–7.30 (m, 1H, *H*_{Ar}), 7.00–6.93 (m, 1H, *H*_{Ar}), 6.92–6.84 (m, 1H, *H*_{Ar}), 4.52–4.41 (m, 1H, *H*_{Aliph}), 3.40 (dd, *J* = 11.0, 8.7 Hz, 1H, CH), 3.11 (dd, *J* = 11.0, 9.6 Hz, 1H, CH), 2.13–1.95 (m, 1H, *H*_{Aliph}), 1.10 (d, *J* = 6.7 Hz, 3H, CH₃), 1.04 (d, *J* = 6.7 Hz, 3H, CH₃) ppm.

¹³C NMR (75 MHz, CD₂Cl₂): δ = 171.0, 159.7, 133.1, 130.8, 119.1, 117.2, 116.9, 83.1, 34.5, 33.7, 19.8, 19.5 ppm.

HR-MS (ESI): *m/z* calcd. for C₁₂H₁₅N₁O₁S₁[M+H]⁺: 222.0947, found 222.0948.

3.4.5 Ligand L1c, Dimer *rac*-C1a, Diastereomers Λ-(*S*)-C2a and Λ-(*S*)-C2a

2-Amino-4-methoxyphenol (S2a)



The reaction was performed according to a slightly modified reported procedure.^[16] A 1 L flask equipped with septum and stir bar was charged with 4-methoxy-2-nitrophenol (14.6 g, 86.6 mmol, 1.00 eq.) and nitrogen saturated MeOH (550 mL). To this solution, Pd/C (10 wt%, 50 wt % water, 2.00 g, 1.88 mmol, 0.02 eq.) was added and the flask was set under an atmosphere of hydrogen gas (H₂ filled balloon). After stirring vigorously for 40 h, the mixture was filtered through a plug of celite and rinsed with

EtOAc/MeOH (85:15) until the filtrate remained colorless. The solvent was removed under reduced pressure to obtain **S2a** (12.0 g, 86.2 mmol, 99%) as a dark brown solid, which was used without further purification.

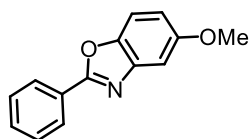
¹H NMR (300 MHz, DMSO-*d*₆): δ = 8.43 (s, 1H, *OH*), 6.51 (d, *J* = 8.9 Hz, 1H, *H*₆), 6.20 (d, *J* = 2.6 Hz, 1H, *H*₃), 5.95 (dd, *J* = 8.4, 2.9 Hz, 1H, *H*₅), 4.52 (s, 2H, *NH*₂), 3.58 (s, 3H, *OCH*₃) ppm.

¹³C NMR (75 MHz, DMSO-*d*₆): δ = 153.0, 138.0, 137.5, 114.5, 100.9, 100.3, 54.9 (CH₃) ppm.

IR (ATR): $\tilde{\nu}$ = 3380 (m), 3288 (m), 2985 (w), 2184 (w), 1596 (w), 1508 (m), 1459 (m), 1430 (m), 1393 (m), 1307 (w), 1223 (s), 1194 (s), 1160 (m), 1083 (w), 1026 (s), 946 (w), 833 (s), 794 (s), 704 (s), 622 (w), 521 (w), 455 (m) cm⁻¹.

HR-MS (ESI): *m/z* calcd. for C₇H₁₀NO₂ [M+H]⁺: 140.0706, found 140.0711.

5-Methoxy-2-phenylbenz[*d*]oxazole (**L1a**)



The reaction was performed according to a slightly modified reported procedure.^[5a] A 250 mL three-necked flask equipped with nitrogen inlet, condenser and stir bar was charged with benzaldehyde (3.90 mL, 37.7 mmol, 1.00 eq.), amino-phenol **S2a** (5.20 g, 37.7 mmol, 1.00 eq.), *m*-xylene (80 mL) and heated to 120 °C. After 1 h, the mixture was allowed to cool to rt, 4-MeO-TEMPO (0.70 g, 3.76 mmol, 10 mol%) was added carefully and the atmosphere was set under oxygen gas (O₂-balloon). After stirring vigorously for 15 h at 120 °C, complete conversion was indicated by TLC. The mixture was cooled to rt, the solvent removed under reduced pressure, the crude product adsorbed on silica gel with CH₂Cl₂ and purified by flash chromatography (*n*-hexane/EtOAc 12:1 → 8:1) to obtain **L1a** (7.90 g, 33.7 mmol, 90%) as a beige solid.

TLC (*n*-hexane/EtOAc 8:1) *R*_f = 0.26.

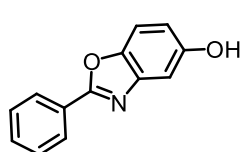
¹H NMR (300 MHz, CD₂Cl₂): δ = 8.25–8.19 (m, 2H, *H*_{Ar}), 7.57–7.51 (m, 3H, *H*_{Ar}), 7.48 (d, *J* = 8.9 Hz, 1H, *H*_{Ar}), 7.25 (d, *J* = 2.4 Hz, 1H, *H*_{Ar}), 6.95 (dd, *J* = 8.9, 2.4 Hz, 1H, *H*_{Ar}), 3.87 (s, 3H, *OCH*₃) ppm.

¹³C NMR (75 MHz, CD₂Cl₂): δ = 164.2, 157.9, 145.9, 143.5, 131.8, 129.3 (2C), 127.8 (2C), 114.0, 111.1, 103.3, 56.3 (CH₃) ppm.

IR (ATR): $\tilde{\nu}$ = 3064 (w), 3000 (w), 2934 (w), 2827 (w), 1967 (w), 1904 (w), 1846 (w), 1721 (w), 1589(m), 1550 (s), 1475 (m), 1427 (w), 1342 (m), 1276 (s), 1186 (m), 1146 (s), 1103 (m), 1056 (m), 1018 (s), 926 (m), 825 (s), 796 (w), 773 (w), 693 (vs), 618 (w), 551 (w), 485 (w), 427 (w) cm^{-1} .

HR-MS (ESI): m/z calcd. for $\text{C}_{14}\text{H}_{12}\text{NO}_2$ $[\text{M}+\text{H}]^+$: 226.0868, found 226.0874.

2-Phenylbenz[d]oxazole-5-ol (**L1b**)



The reaction was performed according to a slightly modified reported procedure.^[4b] A 1 L flask equipped with nitrogen inlet, septum and stir bar was charged with a solution of BBr_3 (20.9 g, 83.2 mmol, 2.50 eq.) in dry CH_2Cl_2 (400 mL) and cooled to -78°C . Ligand **L1a** (7.50 g, 33.3 mmol, 1.00 eq) was dissolved in dry CH_2Cl_2 (50 mL) and added dropwise at -78°C . The resulting green solution was allowed to warm up to rt and stirred for 19 h. Reaction control by TLC indicated full conversion, the reaction was quenched by careful addition of triethanolamine (30 mL). After stirring for 10 min at rt, the resulting white paste was diluted with water (100 mL) and EtOAc (100 mL). The aqueous layer was separated and extracted with EtOAc (6x100 mL). The combined organic layers were washed with brine (100 mL), dried over MgSO_4 , and adsorbed on silica gel. Short-column chromatography (*n*-hexane/EtOAc 3:1) yielded **L1b** (6.86 g, 32.5 mmol, 98%) as a beige, crystalline solid. Crystals suitable for X-ray analysis were obtained by slow evaporation from CH_2Cl_2 .

TLC (*n*-hexane/EtOAc 3:1): R_f = 0.23.

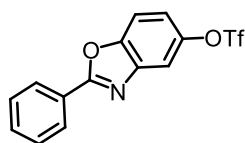
^1H NMR (300 MHz, $\text{DMSO}-d_6$): δ = 9.52 (s, 1H, OH), 8.19–8.10 (m, 2H, H_{Ar}), 7.63–7.58 (m, 3H, H_{Ar}), 7.56 (d, J = 8.8 Hz, 1H, H_{Ar}), 7.11 (d, J = 2.3 Hz, 1H, H_{Ar}), 6.85 (dd, J = 8.8, 2.4 Hz, 1H, H_{Ar}) ppm.

^{13}C NMR (75 MHz, $\text{DMSO}-d_6$): δ = 162.6, 155.0, 143.9, 142.4, 131.6, 129.2 (2C), 127.0 (2C), 126.6, 113.8, 110.8, 104.7 (CH_3) ppm.

IR (ATR): $\tilde{\nu}$ = 3156 (m, br), 2740 (w), 2663 (w), 2185 (w), 2069 (w), 1690 (m), 1599 (s), 1542 (w), 1442 (vs), 1377 (m), 1284 (m), 1230 (w), 1188 (w), 1145 (s), 1063 (m), 1026 (w), 944 (w), 918 (w), 837 (m), 805 (m), 774 (m), 701 (w) 675 (vs, br), 484 (m), 432 (m) cm^{-1} .

HR-MS (ESI): m/z calcd. for $\text{C}_{13}\text{H}_{10}\text{NO}_2$ $[\text{M}+\text{H}]^+$: 212.0712, found 212.0717.

2-Phenylbenz[d]oxazole-5-yl-trifluoromethanesulfonate (**L1c**)



A flame dried 500 mL flask equipped with nitrogen inlet, septum and stir bar was charged with ligand **L1b** (6.80 g, 32.2 mmol, 1.00 eq.) and dry pyridine (26.3 mL, 326 mmol, 10.0 eq.) in dry CH_2Cl_2 (325 mL) and cooled to -78°C . To this suspension, Tf_2O (13.2 mL, 78.6 mmol, 2.44 eq.) was added dropwise at -78°C . The resulting dark solution was allowed to warm up to rt overnight. After stirring for 24 h, reaction control by TLC indicated full conversion. The reaction was stopped by addition of saturated, aqueous NH_4Cl (100 mL). The aqueous layer was removed and extracted with EtOAc (3x80 mL). The combined organic layers were washed with brine (100 mL), dried over MgSO_4 , and adsorbed on silica gel. Short-column chromatography (*n*-hexane/EtOAc 3:1) of the brown crude product yielded ligand **L1c** (10.3 g, 30.1 mmol, 93%) as colorless, crystalline scales.

TLC (*n*-hexane/EtOAc 3:1): $R_f = 0.63$.

^1H NMR (300 MHz, CD_2Cl_2): $\delta = 8.29\text{--}8.19$ (m, 2H, H_{Ar}), 7.70 (d, $J = 2.3$ Hz, 1H, H_{Ar}), 7.64 (d, $J = 8.9$ Hz, 1H, H_{Ar}), 7.61–7.47 (m, 3H, H_{Ar}), 7.29 (dd, $J = 8.9, 2.3$ Hz, 1H, H_{Ar}) ppm.

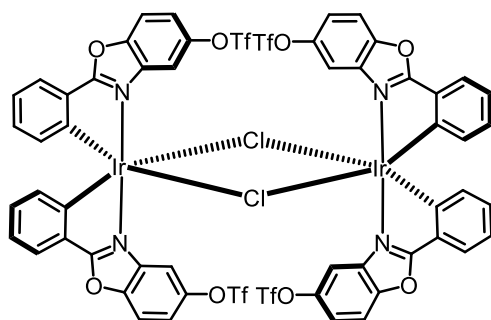
^{13}C NMR (75 MHz, CD_2Cl_2): $\delta = 166.0, 150.4, 146.8, 143.8, 132.7, 129.5$ (2C), 128.3 (2C), 126.9, 119.2 ($J = 322.2$ Hz, CF_3), 118.8, 113.7, 112.0 ppm.

^{19}F NMR (283 MHz, CD_2Cl_2): $\delta = -73.2$ ppm.

IR (ATR): $\tilde{\nu} = 3080$ (w, br), 1598 (w), 1548 (w), 1465 (w), 1418 (s), 1341 (w), 1200 (s), 1131 (s), 1091 (w), 1056 (w), 942 (m), 873 (m), 815 (m), 704 (s), 597 (vs), 491 (s), 430 (w) cm^{-1} .

HR-MS (ESI): m/z calcd. for $\text{C}_{14}\text{H}_9\text{F}_3\text{NO}_4\text{S}$ [$\text{M}+\text{H}$] $^+$: 344.0204, found 344.0199.

Dimer *rac*-**C1a**



According to procedure A, ligand **L1c** (2.00 g, 5.82 mmol, 1.85 eq.), iridium(III) chloride hydrate (1.11 g, 3.17 mmol, 1.00 eq.) and ethoxyethanol (60 mL) were used. After 12 h additional iridium(III)chloride hydrate (200 mg) was added and the reaction was prolonged for additional 48 h. The crude product was purified with flash chromatography

n-hexane/MTBE (2:1) as eluent to remove side products. The main product was eluted with CH₂Cl₂/MeOH (75:1). The iridium(III) dimer complex ***rac*-C1a** (2.32 g, 1.27 mmol, 87% based on the amount of starting ligand **L1c**) was obtained as an orange powder.

TLC (*n*-hexane/CH₂Cl₂ 1:1): *R*_f = 0.33.

¹H NMR (300 MHz, CD₂Cl₂): δ = 8.22 (d, *J* = 2.5 Hz, 4H), 7.72 (d, *J* = 7.0 Hz, 4H), 7.56 (d, *J* = 9.1 Hz, 4H), 7.17 (dd, *J* = 9.0, 2.6 Hz, 4H), 6.97 (t, *J* = 7.3 Hz, 4H), 6.75 (td, *J* = 7.8, 1.3 Hz, 4H), 6.14 (d, *J* = 7.8 Hz, 4H) ppm.

¹³C NMR (75 MHz, CD₂Cl₂): δ = 180.5 (4C), 149.5 (4C), 146.5 (4C), 144.6 (4C), 140.9 (4C), 133.2 (4C), 132.8 (4C), 128.7 (4C), 127.3 (4C), 122.9 (4C), 119.1 (q, *J* = 319.9 Hz, 4C, CF₃), 118.6 (4C), 113.0 (4C), 111.3 (4C) ppm.

¹⁹F NMR (282 MHz, CD₂Cl₂) δ = −73.4 ppm.

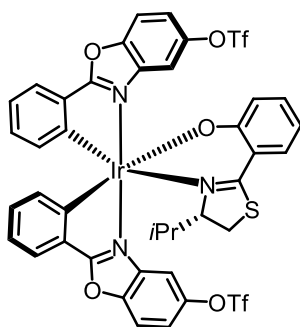
IR (ATR): $\tilde{\nu}$ = 3077 (w), 1623 (w), 1589 (m), 1513 (w), 1465 (w), 1425 (m), 1339 (w), 1296 (w), 1212 (s), 1135 (m), 1106 (m), 1038 (w), 978 (w), 943 (m), 864 (m), 810 (w), 775 (w), 737 (m), 705 (w), 665 (w), 625 (w), 599 (m), 506 (w), 448 (w) cm^{−1}.

HR-MS (ESI): *m/z* calcd. for C₅₆H₂₈Cl₂F₁₂Ir₂N₄O₁₆S₄Na₁ [M+Na]⁺: 1846.8697, found 1846.8691.

Diastereomers **Λ-(S)-C2a** and **Δ-(S)-C2a**

According to procedure B, dimer ***rac*-C1a** (1.33 g, 0.73 mmol, 1.00 eq.), ancillary ligand **(S)-AL1** (0.34 g, 1.53 mmol, 2.10 eq.), AgOTf (0.39 g, 1.53 mmol, 2.10 eq.), Et₃N (1.01 mL, 0.74 g, 7.30 mmol, 10.0 eq.), and EtOH (25 mL) were used. The resulting diastereomers were separated by flash column chromatography (CH₂Cl₂/*n*-hexane 13:2 → CH₂Cl₂). The separated diastereomers were once again purified by flash chromatography (*n*-hexane/EtOAc 5:2) to obtain the first eluting diastereomer **Λ-(S)-C2a** (640 mg, 0.58 mmol, 40%) and the second diastereomer **Δ-(S)-C2a** (608 mg, 0.55 mmol, 38%) as orange solids. Single crystals suitable for X-ray analysis from each complex were grown by slow diffusion of *n*-hexane into a solution of the respective diastereomer in CH₂Cl₂.

Diastereomer Λ -(S)-C2a



TLC (*n*-hexane/EtOAc 5:2): $R_f = 0.29$, (CH_2Cl_2 /*n*-hexane 13:2) $R_f = 0.09$.

^1H NMR (300 MHz, CD_2Cl_2): $\delta = 7.85$ (d, $J = 2.5$ Hz, 1H, H_{Ar}), 7.77–7.68 (m, 2H, H_{Ar}), 7.66–7.58 (m, 2H, H_{Ar}), 7.43 (dd, $J = 8.2, 1.6$ Hz, 1H, H_{Ar}), 7.35–7.32 (m, 2H, H_{Ar}), 7.27 (dd, $J = 9.1, 2.5$ Hz, 1H, H_{Ar}), 7.16–7.07 (m, 1H, H_{Ar}), 6.96–6.73 (m, 4H, H_{Ar}), 6.66 (d, $J = 8.7$ Hz, 1H, H_{Ar}), 6.58 (d, $J = 8.0$ Hz, 1H, H_{Ar}), 6.34–6.24 (m, 2H, H_{Ar}), 4.64–4.55 (m, 1H, CH_{aliph}), 3.33 (dd, $J = 11.9, 9.8$ Hz, 1H, CH_{aliph}), 2.96 (dd, $J = 11.9, 1.7$ Hz, 1H, CH_{aliph}), 0.72–0.55 (m, 1H, CH_{iPr}), 0.19 (t, $J = 6.9$ Hz, 6H, $2 \times \text{CH}_3$) ppm.

^{13}C NMR (75 MHz, CD_2Cl_2): $\delta = 181.2, 180.8, 169.6, 167.5, 151.7, 150.8, 149.9, 149.6, 147.9, 147.4, 140.0, 139.9, 135.2, 134.3, 133.8, 133.2, 132.8, 132.0, 130.3, 129.9, 127.4, 127.0, 124.1, 122.6, 121.7, 119.4, 119.4$ (q, $J = 321.0$ Hz, CF_3), 119.1 (q, $J = 321.4$ Hz, CF_3), 118.6, 118.3, 114.2, 113.4, 113.0, 111.8, 110.2, 85.1, 32.4, 27.3, 19.0, 14.1 ppm.

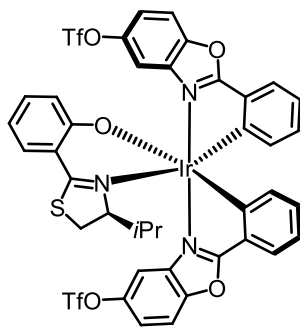
^{19}F NMR (282 MHz, CD_2Cl_2): $\delta = -72.8, -72.9$ ppm.

IR (ATR): $\tilde{\nu} = 3054$ (w), 2962 (w), 1592 (m), 1557 (w), 1517 (w), 1463 (m), 1421 (m), 1345 (w), 1297 (w), 1206 (s), 1135 (s), 1104 (m), 1037 (w), 1013 (w), 981 (w), 943 (m), 870 (s), 814 (w), 776 (w), 739 (m), 706 (w), 663 (w), 626 (m), 601 (m), 560 (w), 509 (w), 432 (w) cm^{-1} .

HR-MS (ESI): m/z calcd. for $\text{C}_{40}\text{H}_{28}\text{F}_6\text{Ir}_1\text{N}_3\text{O}_9\text{S}_3\text{Na}_1$ $[\text{M}+\text{Na}]^+$: 1120.0411, found 1120.0455.

CD (MeCN): λ ($\Delta\epsilon$, $\text{M}^{-1}\cdot\text{cm}^{-1}$) = 210 (+45), 227(−34), 252 (+21), 287 (−29), 327 (+46), 347 (+23), 376 (+27), 458 (−9) nm.

Diastereomer Δ -(S)-C2a



TLC (*n*-hexane/EtOAc 5:2): R_f = 0.26; (CH_2Cl_2 /*n*-hexane 13:2): R_f = 0.05.

^1H NMR (300 MHz, CD_2Cl_2): δ = 7.86–7.66 (m, 5H, H_{Ar}), 7.44–7.37 (m, 2H, H_{Ar}), 7.35–7.28 (m, 2H, H_{Ar}), 7.06–6.92 (m, 3H, H_{Ar}), 6.89–6.75 (m, 2H, H_{Ar}), 6.73–6.67 (m, 1H, H_{Ar}), 6.60–6.53 (m, 1H, H_{Ar}), 6.40–6.26 (m, 2H, H_{Ar}), 3.67–3.58 (m, 1H, CH_{aliph}), 2.99 (dd, J = 11.5, 1.6 Hz, 1H, CH_{aliph}), 2.82 (dd, J = 11.3, 10.0 Hz, 1H, CH_{aliph}), 2.11–1.96 (m, 1H, $\text{CH}_{i\text{Pr}}$), 1.10 (d, J = 6.8 Hz, 3H, CH_3), 0.08 (d, J = 6.8 Hz, 3H, CH_3) ppm.

^{13}C NMR (75 MHz, CD_2Cl_2): δ = 181.5, 169.5, 167.5, 152.4, 151.1, 150.0, 149.4, 148.0, 147.2, 140.6, 139.7, 136.3, 133.5, 132.7 (2C), 132.6, 131.8, 129.9, 129.3, 127.6, 127.0, 123.8, 122.5, 121.5, 119.7, 119.5, 119.1 (q, J = 320.6 Hz, CF_3), 119.0 (q, J = 321.4 Hz, CF_3), 118.7, 114.0, 113.1, 111.5, 110.5, 81.8, 32.4, 30.5, 20.4, 16.5 ppm.

^{19}F NMR (282 MHz, CD_2Cl_2): δ = –73.0, –73.2 ppm.

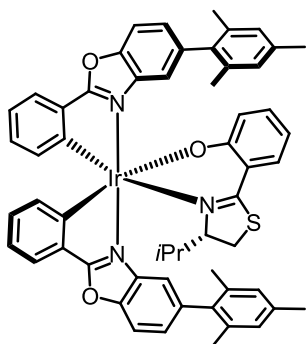
IR (ATR): $\tilde{\nu}$ = 3051 (w), 2962 (w), 2052 (w), 1593 (m), 1562 (w), 1517 (w), 1463 (m), 1422 (m), 1340 (w), 1297 (w), 1208 (s), 1135 (s), 1105 (m), 1036 (w), 1014 (w), 983 (w), 943 (m), 871 (m), 812 (m), 777 (w), 740 (m), 707 (w), 665 (w), 626 (w), 601 (m), 561 (w), 509 (w), 450 (w) cm^{-1} .

HR-MS (ESI): m/z calcd. for $\text{C}_{40}\text{H}_{28}\text{F}_6\text{Ir}_1\text{N}_3\text{O}_9\text{S}_3\text{Na}_1$ $[\text{M}+\text{Na}]^+$: 1120.0411, found 1120.0457.

CD (MeCN): λ ($\Delta\epsilon$, $\text{M}^{-1}\cdot\text{cm}^{-1}$) = 210 (–50), 225 (+16), 251 (–17), 280 (+29), 297 (+13), 303 (+16), 328 (–35), 420 (+7) nm.

3.4.6 Cross-Coupling Products Λ -(S)-C3a-d

Cross-Coupling Product Λ -(S)-C3a



According to procedure C, iridium(III) complex Λ -(S)-C2a (90.0 mg, 82.0 μ mol, 1.00 eq.), 2,4,6-trimethylphenylboronic acid (54.0 mg, 328 μ mol, 4.00 eq.), K_3PO_4 (70.0 mg, 323 μ mol, 4.00 eq.), $Pd(OAc)_2$ (1.8 mg, 8.2 μ mol, 10 mol%), SPhos (6.7 mg, 16.4 μ mol, 20 mol%), and toluene (400 μ L) were used. The crude product was purified by flash chromatography *n*-hexane/EtOAc (15:2 \rightarrow 5:1) to yield iridium(III) complex Λ -(S)-C3a (76.6 mg, 73.6 μ mol, 90%) as an orange solid.

TLC (*n*-hexane/EtOAc 15:2): R_f = 0.16; (*n*-hexane/EtOAc 5:1): R_f = 0.30.

1H NMR (500 MHz, CD_2Cl_2): δ = 7.76–7.64 (m, 5H, H_{Ar}), 7.28 (dd, J = 8.2, 1.7 Hz, 1H, H_{Ar}), 7.23–7.22 (m, 1H, H_{Ar}), 7.22–7.17 (m, 2H, H_{Ar}), 7.00–6.86 (m, 7H, H_{Ar}), 6.81–6.75 (m, 2H, H_{Ar}), 6.66–6.62 (m, 1H, H_{Ar}), 6.53–6.49 (m, 1H, H_{Ar}), 6.48–6.44 (m, 1H, H_{Ar}), 6.22–6.16 (m, 1H, H_{Ar}), 4.60–4.56 (m, 1H, CH_{aliph}), 2.77–2.69 (m, 2H, CH_{aliph}), 2.32 (s, 3H, CH_3), 2.27 (s, 3H, CH_3), 2.05 (s, 3H, CH_3), 2.01 (s, 3H, CH_3), 1.93 (s, 3H, CH_3), 1.59 (s, 3H, CH_3), 0.76–0.67 (m, 1H, CH_{iPr}), 0.19 (d, J = 7.1 Hz, 3H, CH_3), 0.17 (d, J = 7.1 Hz, 3H, CH_3) ppm.

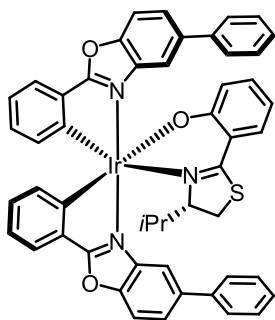
^{13}C NMR (125 MHz, CD_2Cl_2): δ = 178.5, 178.2, 168.7, 167.5, 151.1, 149.9, 149.6, 149.4, 140.0, 139.7, 139.2, 138.9, 138.2, 138.0, 137.2, 137.0, 136.6, 136.3, 136.0, 135.7, 134.8, 133.5 (2C), 132.3, 132.1, 131.6, 131.4, 130.9, 128.5 (2C), 128.4, 128.2, 127.4, 126.7, 126.5, 126.2, 123.8, 122.1, 121.0, 119.5, 118.3, 116.9, 113.4, 112.0, 111.2, 84.9, 32.0, 30.1, 27.6, 21.2 (3C), 21.0, 20.9, 20.5, 19.0, 14.2 ppm.

IR (ATR): $\tilde{\nu}$ = 3054 (w), 2969 (w), 2855 (w), 1592 (m), 1556 (m), 1517 (m), 1438 (s), 1378 (m), 1285 (w), 1254 (m), 1191 (m), 1153 (m), 1125 (m), 1074 (w), 1035 (m), 1011 (m), 979 (w), 950 (w), 910 (m), 848 (m), 814 (m), 773 (w), 736 (s), 707 (m), 655 (w), 626 (w), 596 (w), 563 (w), 524 (w), 436 (w) cm^{-1} .

HR-MS (LIFDI): m/z calcd. for $C_{56}H_{50}IrN_3O_3S$ $[M]^+$: 1037.3205, found 1037.3193.

CD (MeCN): λ ($\Delta\epsilon$, $M^{-1} cm^{-1}$) = 209 (+50), 229 (−42), 259 (+13), 290 (−47), 327 (+47), 342 (+25), 366 (+31), 459 (−12) nm.

Cross-Coupling Product Λ -(*S*)-C3b



According to procedure C, iridium(III) complex Λ -(*S*)-C2a (90.0 mg, 82.0 μmol , 1.00 eq.), phenylboronic acid (40.0 mg, 323 μmol , 4.0 eq.), K_3PO_4 (70.0 mg, 323 μmol , 4.00 eq.), $\text{Pd}(\text{OAc})_2$ (1.8 mg, 8.2 μmol , 10 mol%), SPhos (6.7 mg, 16.4 μmol , 20 mol%), and toluene (400 μL) were used. The crude product was purified by flash chromatography *n*-hexane/EtOAc (5:1 \rightarrow 5:2) to yield iridium(III) complex Λ -(*S*)-C3b (62.5 mg, 65.6 μmol , 80%) as an orange solid.

TLC (*n*-hexane/EtOAc 5:1): R_f = 0.19; (*n*-hexane/EtOAc 5:2) R_f = 0.31.

^1H NMR (500 MHz, CD_2Cl_2): δ = 8.10–8.06 (m, 1H, H_{Ar}), 7.79–7.65 (m, 9H, H_{Ar}), 7.56 (dd, J = 8.1, 1.7 Hz, 1H, H_{Ar}), 7.52–7.48 (m, 2H, H_{Ar}), 7.45–7.34 (m, 5H, H_{Ar}), 7.33–7.28 (m, 1H, H_{Ar}), 7.25–7.20 (m, 1H, H_{Ar}), 6.95–6.90 (m, 1H, H_{Ar}), 6.89–6.84 (m, 1H, CH_{aliph}), 6.82–6.74 (m, 2H, CH_{aliph}), 6.72–6.67 (m, 1H, CH_{aliph}), 6.43–6.36 (m, 2H, CH_{aliph}), 4.92–4.83 (m, 1H, CH_{aliph}), 3.19 (dd, J = 11.8, 10.0 Hz, 1H, CH_{aliph}), 2.94 (dd, J = 11.8, 1.8 Hz, 1H, CH_{aliph}), 0.92–0.83 (m, 1H, $\text{CH}_{i\text{Pr}}$), 0.21 (d, J = 7.2 Hz, 3H, CH_3), 0.16 (d, J = 7.2 Hz, 3H, CH_3) ppm.

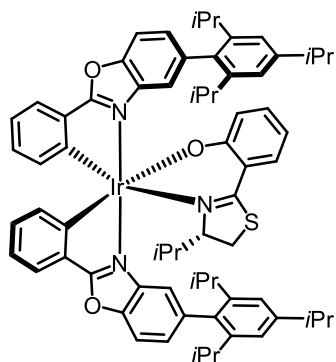
^{13}C NMR (125 MHz, CD_2Cl_2): δ = 178.9, 178.7, 168.1, 166.8, 150.8, 150.3, 150.1, 149.9, 141.0, 140.4, 140.0, 139.8, 139.6, 139.3, 135.1, 134.0, 133.8, 132.2, 131.8, 131.4, 130.9, 129.3 (2C), 129.1 (2C), 128.1, 127.9 (3C), 127.7 (2C), 126.5, 126.2, 125.1, 124.5, 124.3, 122.3, 121.2, 118.5, 116.3, 114.4, 113.6, 112.3, 111.7, 86.0, 31.9, 27.9, 18.9, 14.2, 1.2 ppm.

IR (ATR): $\tilde{\nu}$ = 3054 (w), 2970 (w), 2855 (w), 1593 (m), 1556 (m), 1517 (m), 1442 (s), 1381 (m), 1351 (w), 1296 (m), 1256 (m), 1189 (w), 1154 (m), 1109 (s), 1073 (m), 1034 (m), 1011 (m), 916 (m), 887 (w), 821 (m), 763 (m), 736 (s), 697 (s), 640 (w), 596 (w), 554 (w), 517 (w), 449 (w), 417 (w) cm^{-1} .

HR-MS (LIFDI): m/z calcd. for $\text{C}_{50}\text{H}_{38}\text{IrN}_3\text{O}_3\text{S}$ $[\text{M}]^{+}$: 953.2265, found 953.2289.

CD (MeCN): λ ($\Delta\epsilon$, $\text{M}^{-1}\cdot\text{cm}^{-1}$) = 205 (+11), 218 (+56), 235 (–23), 243 (–12), 257 (–31), 269 (–15), 292 (–53), 336 (+35), 346 (+32), 367 (+36), 463 (–10) nm.

Cross-Coupling Product Λ -(S)-C3c



According to procedure C, iridium(III) complex Λ -(S)-C2a (90.0 mg, 82.0 μ mol, 1.00 eq.), 2,4,6-tri-*iso*-propylphenylboronic acid (124 mg, 500 μ mol, 6.00 eq.), K_3PO_4 (106 mg, 500 μ mol, 6.00 eq.), $Pd(OAc)_2$ (1.8 mg, 8.2 μ mol, 10 mol%), SPhos (6.7 mg, 164 μ mol, 20 mol%), and toluene (600 μ L) were used. The crude product was purified by flash chromatography *n*-hexane/EtOAc (15:2 \rightarrow 5:1) to yield the iridium(III) complex Λ -(S)-C3c (59.3 mg, 49.2 μ mol, 60%) as an orange solid.

TLC (*n*-hexane/EtOAc 15:2): R_f = 0.21; (*n*-hexane/EtOAc 5:1): R_f = 0.42.

1H NMR (500 MHz, CD_2Cl_2): δ = 7.76–7.72 (m, 1H, H_{Ar}), 7.72–7.67 (m, 3H, H_{Ar}), 7.66–7.64 (m, 1H, H_{Ar}), 7.26 (dd, J = 8.4, 1.6 Hz, 1H, H_{Ar}), 7.24–7.19 (m, 3H, H_{Ar}), 7.10 (d, J = 1.6, 1H, H_{Ar}), 7.06–7.02 (m, 2H, H_{Ar}), 7.01–6.97 (m, 1H, H_{Ar}), 6.95–6.86 (m, 4H, H_{Ar}), 6.79–6.74 (m, 1H, H_{Ar}), 6.61–6.56 (m, 2H, H_{Ar}), 6.45 (dd, J = 8.6, 1.2 Hz, 1H, H_{Ar}), 6.13–6.08 (m, 1H, CH_{aliph}), 4.58–4.52 (m, 1H, CH_{aliph}), 2.99–2.84 (m, 2H, CH_{aliph}), 2.73–2.58 (m, 4H, CH_{aliph}), 2.28–2.17 (m, 1H, CH_{aliph}), 1.30 (d, J = 6.9 Hz, 6H, CH_3), 1.26 (d, J = 6.9 Hz, 6H, CH_3), 1.16 (d, J = 6.8 Hz, 3H, CH_3), 1.15 (d, J = 6.8 Hz, 3H, CH_3), 1.10 (d, J = 6.8 Hz, 3H, CH_3), 1.04 (d, J = 7.0 Hz, 3H, CH_3), 1.03 (d, J = 7.0 Hz, 3H, CH_3), 1.00 (d, J = 6.8 Hz, 3H, CH_3), 0.86 (d, J = 6.9 Hz, 3H, CH_3), 0.70–0.62 (m, 1H, CH_{aliph}), 0.5 (d, J = 6.8 Hz, 3H, CH_3), 0.15 (d, J = 7.0 Hz, 3H, CH_3), 0.14 (d, J = 7.1 Hz, 3H, CH_3) ppm.

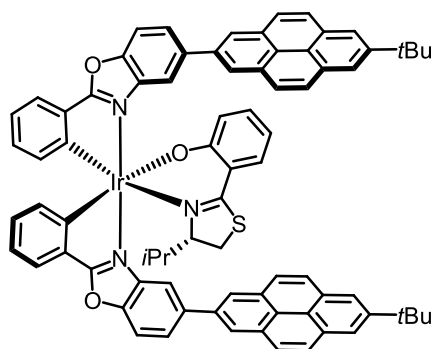
^{13}C NMR (125 MHz, CD_2Cl_2): δ = 178.6, 178.4, 168.6, 167.3, 151.3, 150.0, 149.7, 149.6, 148.9, 148.5, 147.1, 147.0, 146.9, 146.8, 139.6, 139.5, 138.9, 138.7, 136.4, 136.3, 134.7, 133.8, 133.5, 132.5, 132.0, 131.7, 131.6, 130.9, 127.5, 127.3, 126.5, 126.0, 123.8, 121.1 (2C), 120.9, 120.8, 120.7, 120.5, 119.6, 118.2, 117.3, 113.7, 111.6, 110.8, 84.9, 34.7 (2C), 31.8, 30.9, 30.8, 30.7, 30.4, 26.9, 24.7, 24.6, 24.4, 24.3, 24.2 (3C), 24.1, 24.0, 23.9, 23.8, 18.8, 13.9 ppm.

IR (ATR): $\tilde{\nu}$ = 3050 (w), 2958 (w), 2926 (w), 2867 (w), 1728 (w), 1594 (m), 1557 (m), 1517 (m), 1430 (s), 1381 (m), 1299 (w), 1208 (s), 1136 (s), 1105 (m), 1036 (w), 1012 (w), 979 (w), 941 (m), 871 (m), 813 (m), 776 (w), 737 (s), 705 (w), 657 (s), 626 (w), 600 (m), 558 (w), 507 (w), 449 (w) cm^{-1} .

HR-MS (LIFDI): m/z calcd. for $C_{68}H_{74}IrN_3O_3S$ $[M]^+$: 1205.5085, found 1205.5106.

CD (MeCN): λ ($\Delta\epsilon$, $\text{M}^{-1}\cdot\text{cm}^{-1}$) = 209 (+56), 224 (−58), 253 (+20), 290 (−53), 327 (+56), 343 (+27), 367 (+33), 452 (−13) nm.

Cross-Coupling Product Λ -(*S*)-C3d



According to procedure C, iridium(III) complex Λ -(*S*)-C2a (90.0 mg, 82.0 μmol , 1.00 eq.), 2-(7-(*tert*-butyl)pyren-2-yl)-4,4,5,5-tetramethyl-1,3,2-dioxaborolane (**P2**; 126 mg, 328 μmol , 4.00 eq.), K_3PO_4 (70.0 mg, 328 μmol , 4.00 eq.), $\text{Pd}(\text{OAc})_2$ (1.8 mg, 8.2 μmol , 10 mol%), SPhos (6.7 mg, 16.4 μmol , 20 mol%), toluene (400 μL), and water (40 μL , degassed) were used. The crude product was purified by flash chromatography *n*-hexane/EtOAc (15:2 \rightarrow 5:2) to yield the iridium(III) complex Λ -(*S*)-C3d (86.2 mg, 66.0 μmol , 80%) as an orange solid.

TLC (*n*-hexane/EtOAc 5:1): R_f = 0.10, (*n*-hexane/EtOAc 5:2) R_f = 0.34.

^1H NMR (500 MHz, CD_2Cl_2): δ = 8.54–8.46 (m, 3H, H_{Ar}), 8.31 (s, 2H, H_{Ar}), 8.27 (s, 2H, H_{Ar}), 8.25 (s, 2H, H_{Ar}), 8.17–8.02 (m, 9H, H_{Ar}), 7.96–7.72 (m, 7H, H_{Ar}), 7.37–7.28 (m, 1H, H_{Ar}), 7.06–6.87 (m, 4H, H_{Ar}), 6.82–6.72 (m, 2H, H_{Ar}), 6.56–6.46 (m, 2H, H_{Ar}), 4.98–4.87 (m, 1H, CH_{aliph}), 3.24–3.11 (m, 1H, CH_{aliph}), 2.94–2.80 (m, 1H, CH_{aliph}), 1.63–1.56 (m, 18H, 2 x $\text{C}(\text{CH}_3)_3$), 0.98–0.89 (m, 1H, CH_{aliph}), 0.28 (d, J = 7.0 Hz, 3H, CH_3), 0.10 (d, J = 7.0 Hz, 3H, CH_3) ppm.

^{13}C NMR (125 MHz, CD_2Cl_2): δ = 179.2, 178.8, 168.0, 167.2, 150.9, 150.6, 150.3, 150.1, 149.8 (2C), 149.8, 140.6, 140.4, 139.9, 139.7, 138.1, 137.5, 135.2, 134.4, 134.3, 132.4 (2C), 132.3, 132.0, 131.9 (2C), 131.6 (2C), 131.5 (2C), 131.4 (2C), 131.1, 128.5 (2C), 128.4 (2C), 128.0 (2C), 127.9 (2C), 127.5 (2C), 126.6, 126.3, 125.9, 125.5, 124.8, 124.3, 124.2, 124.0, 123.9, 123.1, 123.0, 122.9, 122.4, 121.3, 118.7, 117.2, 115.1, 114.0, 112.4, 112.1, 86.3, 35.6 (2C), 32.1 (6C), 30.2, 27.8, 25.3, 18.9, 14.4 ppm.

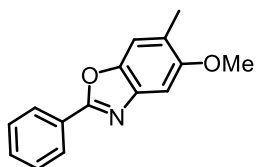
IR (ATR): $\tilde{\nu}$ = 3040 (w), 2956 (m), 2867 (w), 1594 (m), 1558 (m), 1518 (m), 1439 (s), 1379 (m), 1296 (w), 1257 (m), 1224 (m), 1197 (m), 1145 (m), 1124 (m), 1076 (m), 1037 (m), 1010 (m), 940 (m), 878 (s), 812 (s), 738 (s), 709 (s), 661 (w), 631 (w), 598 (w), 557 (w), 504 (w), 447 (w) cm^{-1} .

HR-MS (LIFDI): m/z calcd. for $C_{78}H_{62}IrN_3O_3S$ $[M]^{+}$: 1313.4147, found 1313.4120.

CD (MeCN): λ ($\Delta\epsilon$, $M^{-1}\cdot cm^{-1}$) = 218 (+64), 230 (+32), 257 (+185), 283 (–233), 316 (–91), 325 (–130), 332 (–65), 340 (–185), 365 (+49), 447 (–18) nm.

3.4.7 Ligand L2c, Dimer *rac*-C1b, Diastereomers Δ -(*S*)-C2b and Δ -(*S*)-C2b

5-Methoxy-6-methyl-2-phenylbenzo[*d*]oxazole (L2a)



The reaction was performed according to a slightly modified reported procedure.^[5a] A 250 mL nitrogen flask equipped with stir bar was charged with compound **S2b** (1.30 g, 8.49 mmol, 1.00 eq.), benzaldehyde (0.91 mL, 8.95 mmol, 1.05 eq.), and *m*-xylene (28 mL).

This mixture was heated to 135 °C for 30 min. After cooling to rt, 4-MeO-TEMPO (86 mg, 0.46 mmol, 5.4 mol%) was added carefully. The mixture was set under oxygen atmosphere (O_2 -balloon) and stirred at 135 °C for 24 h. After cooling to RT, all volatiles were removed under reduced pressure. The residue was dissolved in CH_2Cl_2 , adsorbed on silica gel, and purified by flash chromatography (*n*-hexane/EtOAc 20:1 → 15:1). After drying under reduced pressure, desired methylated ligand **L2a** was obtained as an off-white, crystalline solid (1.75 g, 7.31 mmol, 86%).

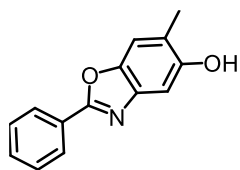
1H NMR (300 MHz, $CDCl_3$): δ = 8.28-8.13 (m, 2H, H_{Ar}), 7.54-7.46 (m, 3H, H_{Ar}), 7.33 (s, 1H, H_{Ar}), 7.19 (s, 1H, H_{Ar}), 3.89 (s, 3H, OCH_3), 2.34 (s, 3H, CH_3) ppm.

^{13}C NMR (75 MHz, $CDCl_3$): δ = 162.9, 155.8, 145.2, 140.8, 131.2, 129.0 (2C), 127.6, 127.4 (2C), 125.6, 111.7, 100.6, 56.0, 17.3 ppm.

IR (ATR): $\tilde{\nu}$ = 1552, 1480, 1466, 1423, 1334, 1295, 1198, 1152, 1111, 1055, 1017, 927, 862, 828, 778, 704, 694, 492, 433 cm^{-1} .

HR-MS (ESI): m/z calcd. for $C_{15}H_{14}NO_2$ $[M+H]^+$: 240.1019, found: 240.1018.

6-Methyl-2-phenylbenzo[d]oxazole-5-ol (**L2b**)



The reaction was performed according to a slightly modified reported procedure.^[4b] A 250 mL nitrogen flask equipped with stir bar was charged with compound **L2a** (1.74 g, 7.27 mmol, 1.00 eq.) and dried for 1 h under reduced pressure. Dry CH₂Cl₂ (52 mL) was added under nitrogen atmosphere. The resulting solution was cooled to –78 °C and BBr₃ (2.50 mL, 25.9 mmol, 3.57 eq.) was added dropwise over 15 min. The mixture was then allowed to warm to rt and stirred for 18 h. Then, the mixture was cooled to 0 °C, carefully quenched with sat. Na₂CO₃ solution and diluted with EtOAc and water. The organic layer was separated and the aqueous layer extracted with EtOAc (3x). The combined organic layers were washed with brine and dried over Na₂SO₄. All volatiles were removed and the residue was dried under reduced pressure. The desired product **L2b** was obtained as an off-white, crystalline solid (1.66 g, 7.37 mmol, >99%) and used without further purification.

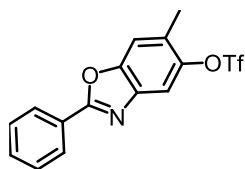
¹H NMR (500 MHz, DMSO-*d*₆): δ = 9.52 (s, 1H, OH), 8.16-8.10 (m, 2H, *H*_{Ar}), 7.62-7.53 (m, 3H, *H*_{Ar}), 7.47 (s, 1H, *H*_{Ar}), 7.12 (s, 1H, *H*_{Ar}), 2.25 (s, 3H, CH₃) ppm.

¹³C NMR (125 MHz, DMSO-*d*₆): δ = 161.7, 153.1, 143.9, 140.1, 131.4, 129.2 (2C), 126.8 (3C), 123.4, 111.4, 103.7, 16.8 ppm.

IR (ATR): $\tilde{\nu}$ = 3219, 1545, 1455, 1430, 1331, 1282, 1191, 1160, 1101, 1062, 1024, 992, 860, 775, 681, 622, 506, 429 cm^{–1}.

HR-MS (ESI): *m/z* calcd. for C₁₄H₁₂NO₂ [M+H]⁺: 226.0863, found: 226.0861.

6-Methyl-2-phenylbenzo[d]oxazol-5-yl trifluoromethanesulfonate (**L2c**)



A 250 mL nitrogen flask equipped with stir bar was charged with compound **L2b** (1.64 g, 7.28 mmol, 1.00 eq.), dry CH₂Cl₂ (96 mL) and dry pyridine (5.50 mL, 68.0 mmol, 9.34 eq.). The mixture was cooled to –78 °C and Tf₂O (1.80 mL, 10.7 mmol, 1.47 eq.) was added dropwise. The mixture was stirred at –78 °C for 30 min then allowed to warm to 0 °C and stirred for 1 h. Then, the reaction was allowed to warm to rt and stirred for another 5 h. The reaction was quenched by addition of water and stirred for 10 min. The organic layer was separated, and the aqueous layer was extracted with CH₂Cl₂ (4x). The combined organic layers were dried over

Na₂SO₄ and the solvent removed under reduced pressure. The crude product was dissolved in CH₂Cl₂, adsorbed on silica gel and purified by short-column flash chromatography (*n*-hexane/EtOAc 6:1). After drying under reduced pressure, desired ligand **L2c** was obtained as an off-white, crystalline solid (2.55 g, 7.14 mmol, 98%).

¹H NMR (300 MHz, acetone-*d*₆): δ = 8.27-8.18 (m, 2H, *H*_{Ar}), 7.78 (s, 1H, *H*_{Ar}), 7.74 (s, 1H, *H*_{Ar}), 7.69-7.56 (m, 3H, *H*_{Ar}), 2.53 (s, 3H, CH₃) ppm.

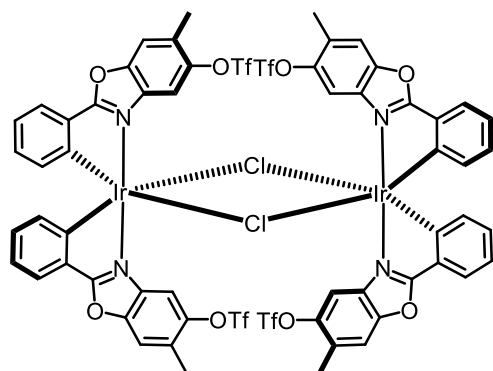
¹³C NMR (75 MHz, acetone-*d*₆): δ = 165.6, 150.8, 146.2, 142.1, 133.1, 130.1 (2C), 129.5, 128.5 (2C), 127.4, 119.6 (q, *J* = 319 Hz, CF₃), 114.0, 113.5, 17.1 ppm.

¹⁹F NMR (282 MHz, acetone-*d*₆): δ = −73.3 (s, CF₃) ppm.

IR (ATR): $\tilde{\nu}$ = 1550, 1460, 1414, 1246, 1206, 1133, 1054, 883, 834, 777, 697, 598, 502, 438 cm^{−1}.

HR-MS (ESI): *m/z* calcd. for C₁₅H₁₁F₃N₁O₄S₁ [M+H]⁺: 358.0355, found: 358.0354.

Dimer *rac*-C1b



According to procedure A, a 50 mL flask equipped with nitrogen inlet, condenser and stir bar, iridium(III) chloride hydrate (246 mg, 698 μmol, 1.00 eq.), ligand **L2c** (510 mg, 1.43 mmol, 2.04 eq.), and 2-ethoxyethanol (25.0 mL) were used. The crude product was purified by short-column flash chromatography (*n*-hexane/CH₂Cl₂ 1:1). The desired dimer *rac*-C1b (584 mg, 310 μmol, 89% based on the

amount of starting ligand **L2c**) was obtained as an orange crystalline solid. A single crystal suitable for X-ray analysis was obtained by slow evaporation of CH₂Cl₂.

¹H NMR (500 MHz, CD₂Cl₂): δ = 8.10 (s, 4H, *H*_{Ar}), 7.70–7.62 (m, 4H, *H*_{Ar}), 7.45 (s, 4H, *H*_{Ar}), 7.00–6.89 (m, 4H, *H*_{Ar}), 6.78–6.66 (m, 4H, *H*_{Ar}), 6.17–6.11 (m, 4H, *H*_{Ar}), 2.47 (s, 12H, 4xCH₃) ppm.

^{13}C -NMR (125 MHz, CD_2Cl_2): δ = 179.9 (4C), 149.7 (4C), 145.4 (4C), 144.4 (4C), 139.1 (4C), 133.1 (4C), 132.8 (4C), 129.2 (4C), 129.0 (4C), 127.0 (4C), 122.8 (4C), 119.0 (q, $J_{\text{C-F}}$ = 320 Hz, 4x CF_3), 113.7 (4C), 111.5 (4C), 17.5 (4C, CH_3) ppm.

^{19}F NMR (282 MHz, CD_2Cl_2): δ = -74.0 (s, 12 F, 4x CF_3) ppm.

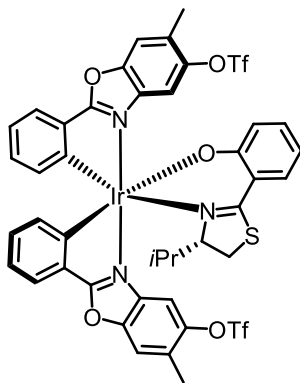
IR (ATR): $\tilde{\nu}$ = 1590, 1516, 1457, 1416, 1213, 1130, 1063, 962, 883, 850, 772, 735, 701, 604, 569, 506, 443 cm^{-1} .

HR-MS (ESI): m/z calcd. for $\text{C}_{60}\text{H}_{36}\text{Cl}_2\text{F}_{12}\text{Ir}_2\text{N}_4\text{O}_{16}\text{S}_4\text{Na}_1$ $[\text{+Na}]^+$: 1902.9324, found: 1902.9318.

Diastereomers Δ -(*S*)-C2b and Δ -(*S*)-C2b

According to procedure B, a 50 mL nitrogen flask equipped with stir bar was charged with dimer *rac*-C1b (585 mg, 311 μmol , 1.00 eq.), chiral ancillary ligand (*S*)-AL1 (154 mg, 696 μmol , 2.24 eq.), AgOTf (168 mg, 653 μmol , 2.10 eq.), EtOH (20 mL), and Et_3N (430 μL , 3.10 mmol, 9.97 eq.). The mixture was stirred at reflux (80 $^\circ\text{C}$) for 8 h. Both diastereomers were separated and purified by flash chromatography (*n*-hexanes/ CH_2Cl_2 1:3 (elution of Δ -(*S*)-C2b) \rightarrow *n*-hexanes/ CH_2Cl_2 1:1 \rightarrow CH_2Cl_2 (elution Δ -(*S*)-C2b)). Both diastereomers were obtained as red-orange solids (Δ -(*S*)-C2b: 282 mg, 250 μmol , 40%; Δ -(*S*)-C2b: 257 mg, 228 μmol , 37%, combined yield: 77%).

Diastereomer Δ -(*S*)-C2b



^1H NMR (500 MHz, CD_2Cl_2): δ = 7.89 (s, 1H, H_{Ar}), 7.73 (dd, J = 7.8, 1.0 Hz, 1H, H_{Ar}), 7.68 (s, 1H, H_{Ar}), 7.65–7.59 (m, 1H, H_{Ar}), 7.57–7.51 (m, 1H, H_{Ar}), 7.49–7.43 (m, 1H, H_{Ar}), 7.40 (s,

^1H NMR (500 MHz, CD_2Cl_2): δ = 7.16–7.07 (m, 1H, H_{Ar}), 6.98–6.91 (m, 2H, H_{Ar}), 6.91–6.84 (m, 1H, H_{Ar}), 6.84–6.79 (m, 1H, H_{Ar}), 6.71–6.66 (m, 1H, H_{Ar}), 6.66–6.63 (m, 1H, H_{Ar}), 6.37–6.32 (m, 1H, H_{Ar}), 6.32–6.26 (m, 1H, H_{Ar}), 4.63–4.55 (m, 1H, $\text{NCH}(i\text{Pr})$), 3.46–3.39 (m, 1H, $\text{S}(\text{CH})_2$), 3.00–2.95 (m, 1H, H_{aliph} , $\text{S}(\text{CH})_2$), 2.55 (s, 3H, $\text{C}_{\text{Ar}}\text{CH}_3$), 2.48 (s, 3H, $\text{C}_{\text{Ar}}\text{CH}_3$), 0.77–0.62 (m, 1H, $\text{CH}(\text{CH}_3)_2$), 0.27 (d, J = 7.0 Hz, 3H, $\text{CH}(\text{CH}_3)_2$), 0.24 ppm (d, J = 7.0 Hz, 3H, $\text{CH}(\text{CH}_3)_2$).

^{13}C NMR (125 MHz, CD_2Cl_2): δ = 180.5, 180.0, 169.7, 167.9, 151.6, 150.5, 150.0, 149.6, 147.1, 145.7, 138.0, 137.9, 135.4, 134.1, 133.9, 133.1, 132.5, 132.0, 130.6, 130.4, 129.9, 129.3, 127.2, 126.9, 124.5, 122.6, 121.6, 119.2 (q, $J_{\text{C-F}}$ = 320 Hz, CF_3), 119.0 (q, $J_{\text{C-F}}$ = 321 Hz, CF_3), 118.5, 114.8, 114.4, 114.1, 111.7, 110.3, 85.0 ($\text{NCH}(i\text{Pr})$), 32.4 ($\text{CH}(\text{CH}_3)_2$), 27.3 ($\text{S}(\text{CH})_2$), 19.2 (CH_3), 17.9 (CH_3), 17.3 (CH_3), 14.3 (CH_3) ppm.

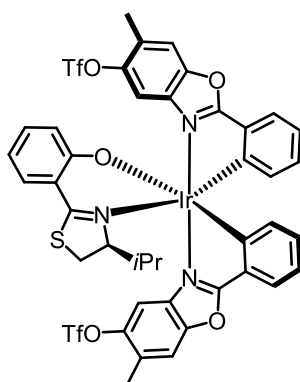
^{19}F NMR (283 MHz, CD_2Cl_2): δ = –73.9 (s, CF_3), –74.2 (s, CF_3) ppm.

IR (ATR): $\tilde{\nu}$ = 1594, 1557, 1518, 1463, 1414, 1205, 1130, 1063, 1012, 961, 882, 851, 735, 607, 508, 446 cm^{-1} .

HR-MS (ESI): m/z calcd. for $\text{C}_{42}\text{H}_{32}\text{F}_6\text{Ir}_1\text{N}_3\text{O}_9\text{S}_3\text{Na}_1$ $[\text{M}+\text{Na}]^+$: 1148.0724, found: 1148.0725.

CD (MeCN): λ ($\Delta\epsilon$, $\text{M}^{-1}\cdot\text{cm}^{-1}$) = 209 (+54), 228 (–41), 252 (+23), 287 (–46), 329 (–62), 348 (+34), 374 (+38), 455 (–15) nm.

Diastereomer Δ -(S)-C2b



^1H NMR (500 MHz, CD_2Cl_2): δ = 7.80 (s, 1H, H_{Ar}), 7.75 (dd, J = 7.7, 1.2 Hz, 1H, H_{Ar}), 7.69 (dd, J = 7.6, 1.2 Hz, 1H, H_{Ar}), 7.67 (s, 1H, H_{Ar}), 7.57 (s, 1H, H_{Ar}), 7.38 (s, 1H, H_{Ar}), 7.33 (dd, J = 8.0, 1.7 Hz, 1H, H_{Ar}), 7.05–7.01 (m, 1H, H_{Ar}), 6.97–6.91 (m, 2H, H_{Ar}), 6.84–6.80 (m, 1H, H_{Ar}), 6.78–6.74 (m, 1H, H_{Ar}), 6.67–6.63 (m, 1H, H_{Ar}), 6.58 (dd, J = 8.5, 1.0 Hz, 1H, H_{Ar}), 6.35–6.29 (m, 2H, H_{Ar}), 3.64–3.60 (m, 1H, $\text{NCH}(i\text{Pr})$), 2.97 (dd, J = 11.4, 1.8 Hz, 1H, $\text{S}(\text{CH})_2$), 2.83

(dd, $J = 11.3, 10.0$ Hz, 1H, S(CH)₂), 2.54 (s, 3H, CH₃), 2.48 (s, 3H, CH₃), 2.07-1.96 (m, 1H, CH(CH₃)₂), 1.08 (d, $J = 6.8$ Hz, 1H, CH(CH₃)₂), 0.05 (d, $J = 7.0$ Hz, 1H, CH(CH₃)₂) ppm.

¹³C NMR (125 MHz, CD₂Cl₂): $\delta = 180.6$ (2C), 169.0, 167.4, 152.0, 150.9, 150.0, 149.4, 147.1, 145.7, 138.5, 137.5, 136.0, 133.4, 132.5, 132.3, 132.2, 130.1, 129.9, 129.6, 129.3, 127.3, 126.7, 123.9, 122.3, 121.3, 119.0 (q, $J_{C-F} = 320$ Hz, CF₃), 118.9 (q, $J_{C-F} = 320$ Hz, CF₃), 114.4, 114.3, 113.7, 111.2, 110.4, 81.9 (NCH(*i*Pr)), 32.3 (CH(CH₃)₂), 30.4 (S(CH)₂), 20.4 (Me), 17.8 (Me), 17.4 (Me), 16.3 (Me) ppm.

¹⁹F NMR (283 MHz, CD₂Cl₂): $\delta = -73.8$ (s, CF₃), -73.9 (s, CF₃) ppm.

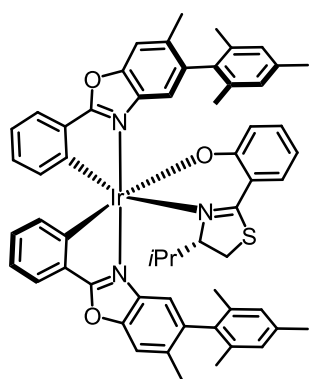
IR (ATR): $\tilde{\nu} = 1594, 1562, 1517, 1463, 1414, 1337, 1205, 1130, 1065, 1038, 1010, 882, 852, 735, 605, 508, 442$ cm⁻¹.

HR-MS (ESI): m/z calcd. for C₄₂H₃₂F₆IrN₃O₉S₃Na [M+Na]⁺: 1148.0724, found: 1148.0716.

CD (MeCN): λ ($\Delta\epsilon$, M⁻¹·cm⁻¹) = 209 (−75), 225(+23), 252 (−23), 281 (+46), 298 (+22), 305 (+27), 330 (−52), 419 (+12) nm.

3.4.8 Cross-Coupling Products Λ -(*S*)-C3f, Λ -(*S*)-C3g and Λ -(*S*)-C3h

Cross-Coupling Product Λ -(*S*)-C3f



According to procedure C, iridium(III) complex Λ -(*S*)-C2b (30.2 mg, 26.8 μ mol, 1.00 eq.), 2,4,6-trimethylphenylboronic acid (17.7 mg, 108 μ mol, 4.02 eq.), K₃PO₄ (22.7 mg, 107 μ mol, 3.98 eq.), Pd(OAc)₂ (0.7 mg, 3.1 μ mol, 10 mol%), SPhos (2.3 mg, 5.6 μ mol, 20 mol%), and toluene (600 μ L) were used. The crude product was purified by flash chromatography *n*-hexane/CH₂Cl₂ (1:3 \rightarrow CH₂Cl₂) to yield the iridium(III) complex Λ -(*S*)-C3f (26.8 mg, 25.2 μ mol, 94%) as an orange solid.

¹H NMR (300 MHz, CD₂Cl₂): $\delta = 7.74$ –7.68 (m, 1H, *H*_{Ar}), 7.68–7.62 (m, 1H, *H*_{Ar}), 7.61 (s, 1H, *H*_{Ar}), 7.58 (s, 1H, *H*_{Ar}), 7.48 (s, 1H, *H*_{Ar}), 7.24 (dd, $J = 8.1, 1.7$ Hz, 1H, *H*_{Ar}), 7.11 (s, 1H, *H*_{Ar}), 7.01–6.97 (m, 1H, *H*_{Ar}), 6.97–6.83 (m, 5H, *H*_{Ar}), 6.81 (s, 1H, *H*_{Ar}), 6.79–6.72 (m, 1H, *H*_{Ar}), 6.63–6.58 (m, 1H, *H*_{Ar}), 6.55–6.47 (m, 1H, *H*_{Ar}), 6.44–6.38 (m, 1H, *H*_{Ar}), 6.18–6.11 (m, 1H, *H*_{Ar}), 4.58–4.48 (m, 1H, NCH(*i*Pr)), 2.77–2.56 (m, 2H, S(CH)₂), 2.34 (s, 3H, CH₃), 2.29 (s, 3H,

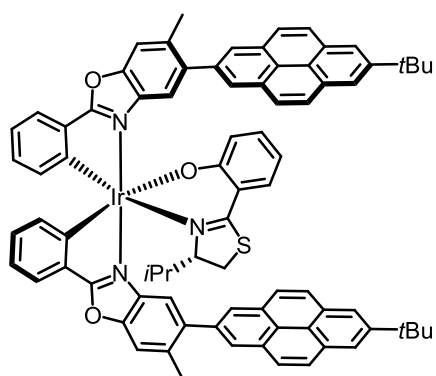
CH_3), 2.10 (s, 3H, CH_3), 2.08 (s, 3H, CH_3), 1.94 (s, 3H, CH_3), 1.93 (s, 3H, CH_3), 1.87 (s, 3H, CH_3), 1.54 (s, 3H, CH_3), 0.83-0.62 (m, 1H, $CH(CH_3)_2$), 0.20 (d, $J = 7.0$ Hz, 1H, $CH(CH_3)_2$), 0.18 (d, $J = 7.0$ Hz, 1H, $CH(CH_3)_2$) ppm.

^{13}C NMR (75 MHz, CD_2Cl_2): $\delta = 178.0, 177.8, 169.0, 168.3, 151.1, 150.4, 150.2, 149.9, 139.9, 139.8, 137.6, 137.6, 137.5, 137.5, 137.3, 137.1, 136.7, 136.2, 136.1, 135.7, 135.0, 134.9, 134.7, 133.6, 133.5, 132.6, 132.0, 131.9, 131.6, 131.4, 128.8, 128.6, 128.5, 128.5, 126.4, 126.0, 124.1, 122.2, 121.1, 119.1, 118.7, 116.7, 113.3, 113.1, 112.5, 85.1$ ((NCH(*i*Pr))), 32.2 ($CH(CH_3)_2$), 27.7 ($S(CH)_2$), 21.5 (CH_3), 21.4 (CH_3), 20.8 (CH_3), 20.6 (3x CH_3), 20.3 (CH_3), 20.3 (CH_3), 19.2 (CH_3), 14.5 (CH_3) ppm.

IR (ATR): $\tilde{\nu} = 2957, 2917, 1596, 1557, 1518, 1441, 1378, 1280, 1194, 1153, 1036, 1011, 849, 736, 445$ cm^{-1} .

HR-MS (ESI): m/z calcd. for $C_{58}H_{54}Ir_1N_3O_3S_1Na_1$ $[M+Na]^+$: 1088.3410, found: 1088.3456.

Cross-Coupling Product Λ -(*S*)-C3g



According to procedure C, iridium(III) complex Λ -(*S*)-C2b (70.1 mg, 62.3 μ mol, 1.00 eq.), boronic ester **P2** (72.6 mg, 189 μ mol, 3.03 eq.), K_3PO_4 (53.2 mg, 251 μ mol, 4.02 eq.), $Pd(OAc)_2$ (1.7 mg, 7.6 μ mol, 12 mol%), SPhos (5.2 mg, 12.7 μ mol, 20 mol%), toluene (900 μ L), and water (90 μ L, degassed) were used. The crude product was purified by flash chromatography *n*-hexane/ CH_2Cl_2 (1:3 \rightarrow 1:6) to yield the iridium(III) complex Λ -(*S*)-C3g (71.5 mg, 53.3 μ mol, 86%) as an orange solid.

1H NMR (600 MHz, CD_2Cl_2): $\delta = 8.32$ (s, 2H, H_{Pyrene}), 8.31 (s, 2H, H_{Pyrene}), 8.29 (s, 2H, H_{Pyrene}), 8.17 (d, $J = 9.0$ Hz, 2H, H_{Pyrene}), 8.15-8.11 (m, 4H, H_{Pyrene}), 8.08 (d, $J = 9.0$ Hz, 2H, H_{Pyrene}), 8.05 (s, 2H, H_{Pyrene}), 7.99 (s, 1H, H_{Ar}), 7.78–7.76 (m, 1H, H_{Ar}), 7.75–7.72 (m, 1H, H_{Ar}), 7.70 (s, 1H, H_{Ar}), 7.61 (dd, $J = 8.2, 1.7$ Hz, 1H, H_{Ar}), 7.61 (s, 1H, H_{Ar}), 7.57 (s, 1H, H_{Ar}), 7.05–7.00 (m, 1H, H_{Ar}), 6.98-6.91 (m, 2H, H_{Ar}), 6.84-6.77 (m, 3H, H_{Ar}), 6.57 (dd, $J = 8.2, 1.1$ Hz, 1H, H_{Ar}), 6.52–6.49 (m, 1H, H_{Ar}), 6.33–6.29 (m, 1H, H_{Ar}), 4.83–4.79 (m, 1H, NCH(*i*Pr)), 2.69 (dd, $J = 11.4, 9.9$ Hz, 1H, $S(CH)_2$), 2.63-2.55 (m, 4H, $S(CH)_2$), 2.49 (s, 3H, CH_3), 1.64 (s, 9H,

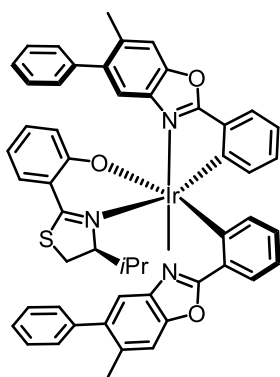
$C(CH_3)_3$, 1.63 (s, 9H, $C(CH_3)_3$), 0.99-0.89 (m, 1H, $CH(CH_3)_2$), 0.26 (d, $J = 7.0$ Hz, 3H, $CH(CH_3)_2$), 0.09 (d, $J = 7.0$ Hz, 3H, $CH(CH_3)_2$) ppm.

^{13}C NMR (150 MHz, CD_2Cl_2): $\delta = 178.3, 178.1, 168.4, 167.4, 151.0, 150.5, 150.3, 150.2, 150.0, 149.8, 141.4, 141.2, 138.9, 138.7, 137.4, 137.2, 135.4, 134.5, 134.5, 134.0, 133.6, 132.4, 132.1, 131.9, 131.7, 131.6$ (3C), 131.6 (2C), 131.4 (2C), $131.3, 131.3$ (2C), 128.6 (2C), 128.3 (2C), 128.0 (2C), 127.8 (2C), 126.5 (2C), $126.5, 126.7, 126.1, 124.4, 124.2, 124.0, 123.2, 123.1$ (2C), 123.0 (2C), $122.3, 121.2, 120.1, 118.7, 117.7, 113.6, 113.4, 113.0, 86.0$ ((NCH(*i*Pr))), 35.8 ($C(CH_3)_3$), 35.8 ($C(CH_3)_3$), 32.3 (9C, $C(CH_3)_3$), 32.1 ($CH(CH_3)_2$), 27.6 (S(CH_2)), 22.1 (Me), 21.7 (Me), 19.0 (Me), 14.5 (Me) ppm.

IR (ATR): $\tilde{\nu} = 3041, 2956, 2867, 1595, 1556, 1517, 1441, 1378, 1254, 1226, 1192, 1150, 1126, 1033, 1009, 874, 848, 801, 715, 444$ cm^{-1} .

HR-MS (ESI): m/z calcd. for $C_{80}H_{66}Ir_1N_3O_3S_1Na_1$ $[M+Na]^+$: 1364.4353, found: 1364.4386.

Cross-Coupling Product Δ -(*S*)-C3h



According to procedure C, iridium(III) complex Δ -(*S*)-C2b (55.1 mg, 49.0 μ mol, 1.00 eq.), phenylboronic acid (23.8 mg, 196 μ mol, 4.00 eq.), K_3PO_4 (41.6 mg, 196 μ mol, 4.00 eq.), $Pd(OAc)_2$ (1.1 mg, 5.0 μ mol, 10 mol%), SPhos (4.1 mg, 10.0 μ mol, 20 mol%), and toluene (250 μ L) were used. The crude product was purified by flash chromatography *n*-hexane/EtOAc (5:1 \rightarrow 5:2) to yield the iridium(III) complex Δ -(*S*)-C3h (40.2 mg, 41.0 μ mol, 83%) as an orange solid.

TLC (*n*-hexane/EtOAc 5:1): $R_f = 0.14$, (*n*-hexane/EtOAc 5:2) $R_f = 0.43$.

1H NMR (500 MHz, CD_2Cl_2): $\delta = 7.74$ – 7.71 (m, 1H, H_{Ar}), 7.71 (s, 1H, H_{Ar}), 7.69 – 7.67 (m, 1H, H_{Ar}), 7.61 (s, 1H, H_{Ar}), 7.50 (s, 1H, H_{Ar}), 7.43 – 7.38 (m, 2H, H_{Ar}), 7.37 – 7.27 (m, 6H, H_{Ar}), 7.23 – 7.19 (m, 2H, H_{Ar}), 7.18 – 7.13 (m, 2H, H_{Ar}), 6.97 – 6.93 (m, 2H, H_{Ar}), 6.92 – 6.88 (m, 1H, H_{Ar}), 6.83 – 6.78 (m, 1H, H_{Ar}), 6.75 – 6.69 (m, 2H, H_{Ar}), 6.48 – 6.42 (m, 2H, H_{Ar}), 6.36 – 6.32 (m, 1H, H_{Ar}), 3.61 – 3.35 (m, 1H, CH_{aliph}), 2.84 – 2.74 (m, 2H, CH_{aliph}), 2.42 (s, 3H, CH_3), 2.33 (s, 3H, CH_3), 2.00 – 1.93 (m, 1H, CH_{aliph}), 0.92 – 0.83 (m, 1H, CH_{iPr}), 0.56 (d, $J = 6.8$ Hz, 3H, CH_3), -0.05 (d, $J = 7.0$ Hz, 3H, CH_3) ppm.

^{13}C NMR (125 MHz, CD_2Cl_2): δ = 178.4 (2C), 168.1, 167.9, 150.8, 150.4, 150.2, 149.7, 141.2, 141.1, 140.3, 137.5, 136.8, 135.9, 134.2, 133.8, 133.1, 132.7, 131.6, 131.4, 131.3, 130.9, 130.5, 129.8 (2C), 129.7 (2C), 128.4 (2C), 128.3 (2C), 127.4 (2C), 126.5, 125.9, 123.9, 121.9, 120.9, 120.4, 118.7, 117.9, 113.3, 112.7, 112.5, 81.6, 32.2, 30.5, 30.1, 21.7, 21.2, 20.4, 16.1 ppm.

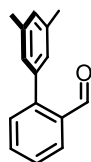
IR (ATR): $\tilde{\nu}$ = 3049 (w), 2955 (w), 2923 (w), 2858 (w), 1722 (w), 1594 (m), 1562 (m), 1518 (m), 1438 (s), 1380 (m), 1338 (m), 1284 (w), 1243 (w), 1197 (m), 1153 (w), 1132 (w), 1072 (w), 1034 (m), 1009 (m), 951 (w), 864 (m), 806 (w), 764 (m), 737 (s), 700 (s), 648 (w), 586 (w), 547 (w), 511 (w), 445 (w), 399 (w) cm^{-1} .

HR-MS (LIFDI): m/z calcd. for $\text{C}_{52}\text{H}_{42}\text{IrN}_3\text{O}_3\text{S}$ $[\text{M}]^{+}$: 981.2576, found 981.2563.

CD (MeCN): λ ($\Delta\epsilon$, $\text{M}^{-1}\cdot\text{cm}^{-1}$) = 205 (−64), 232(+33), 243 (+18), 249 (+20), 267 (+7), 287 (+40), 333 (−41), 417 (+11) nm.

3.4.9 Ligand L3c, Dimer *rac*-C1c, Diastereomers Λ -(*S*)-C2c and Λ -(*S*)-C2c

3',5'-Dimethyl-[1,1'-biphenyl]-2-carbaldehyde (S1a)



The reaction was performed according to a slightly modified reported procedure.^[24a] A 50 mL flask equipped with nitrogen inlet, septum and stir bar was charged with Na_2CO_3 (1.56 g, 14.7 mmol, 2.50 eq.), 2-formylphenylboronic acid (1.11 g, 7.42 mmol, 1.26 eq.), water (6 mL) and DME (24 mL). The resulting suspension was purged with N_2 gas for 30 min before $\text{Pd}(\text{PPh}_3)_4$ (443 mg, 0.38 mmol, 6.5 eq.) and 1-bromo-3,5-dimethylbenzene (0.80 mL, 1.09 g, 5.89 mmol, 1.00 eq.) were added. The mixture was heated to 80 °C for 19 h. Reaction control by TLC indicated full conversion. The product mixture was diluted with water and EtOAc and the aqueous layer was extracted (4x) with EtOAc. The combined organic layers were washed with brine (50 mL), dried over Na_2SO_4 , concentrated, and adsorbed on silica gel with CH_2Cl_2 . The crude product was purified by flash chromatography (*n*-hexane/EtOAc 50:1) to yield product **S1a** as a colorless, crystalline solid. (1.17 g, 5.54 mmol, 95%).

TLC (*n*-hexane/EtOAc 20:1): R_f = 0.39.

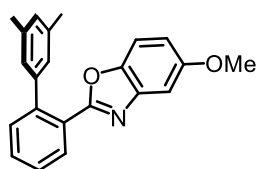
^1H NMR (300 MHz, CD_2Cl_2): δ = 9.96 (s, 1H, H_{CHO}), 7.97 (dd, J = 7.7, 1.2 Hz, 1H, H_{Ar}), 7.64 (td, J = 7.5, 1.5 Hz, 1H, H_{Ar}), 7.52–7.42 (m, 2H, H_{Ar}), 7.11–7.08 (m, 1H, H_{Xy}), 7.03–6.99 (m, 2H, H_{Xy}), 2.38 (s, 6H, 2x CH_3) ppm.

^{13}C NMR (75 MHz, CD_2Cl_2): δ = 192.7 (C_{CHO}), 146.8 (C_{Ar}), 138.5 (C_{Ar}), 138.1 (C_{Ar}), 134.2 (C_{Ar}), 133.8 (C_{Ar}), 131.2 (C_{Ar}), 130.0 ($2\times\text{C}_{\text{Ar}}$), 128.4 ($2\times\text{C}_{\text{Ar}}$), 127.9 (C_{Ar}), 127.6 (C_{Ar}), 21.4 ($2\times\text{CH}_3$) ppm.

IR (ATR): $\tilde{\nu}$ = 3025 (w), 2919 (w), 2851 (w), 2750 (w), 1692 (s), 1597 (m), 1460 (w), 1391 (w), 1268 (w), 1200 (w), 1159 (w), 1106 (w), 1037 (w), 855 (w), 820 (m), 766 (m), 706 (w), 667 (w), 635 (w), 595 (w), 448 (w) cm^{-1} .

HR-MS (ESI): m/z calcd. for $\text{C}_{15}\text{H}_{14}\text{O}_1\text{Na}_1$ [$\text{M}+\text{Na}$] $^+$: 233.0937, found 233.0940.

2-(3',5'-Dimethyl-[1,1'-biphenyl]-2-yl)-5-methoxybenzo[d]oxazole (**L3a**)



The reaction was performed according to a slightly modified reported procedure.^[5a] A 50 mL flask equipped with nitrogen inlet, condenser and stir bar was charged with phenol **S2a** (447 mg, 3.21 mmol, 1.00 eq.), aldehyde **S1a** (675 mg, 3.21 mmol, 1.00 eq.), and *m*-xylene (20 mL). The resulting suspension was stirred at 120 °C for 1 h, then 4-MeO-TEMPO (30 mg, 0.16 mmol, 5.0 mol%) was added and stirred at 120 °C under O_2 -atmosphere (O_2 -balloon) for 40 h. The mixture was cooled to rt, concentrated, and adsorbed on silica gel. Purification by flash chromatography (*n*-hexane/EtOAc 6:1) yielded product **L3a** as pale-yellow, viscous oil (788 mg, 2.41 mmol, 75%).

TLC (*n*-hexane/EtOAc 5:1): R_f = 0.30.

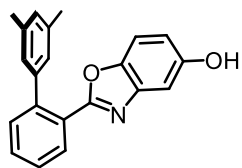
^1H NMR (300 MHz, CD_2Cl_2): δ = 8.07-8.02 (m, 1H, H_{Ar}), 7.61-7.45 (m, 3H, H_{Ar}), 7.23 (d, J = 8.8 Hz, 1H, H_{Ar}), 7.18 (d, J = 2.5 Hz, 1H, H_{Ar}), 6.99–6.95 (m, 1H, H_{Ar}), 6.92–6.85 (m, 3H, H_{Ar}), 3.83 (s, 3H, OCH_3), 2.38 (s, 6H, $2\times\text{CH}_3$) ppm.

^{13}C NMR (75 MHz, CD_2Cl_2): δ = 164.9 (C_{Ar}), 157.7 (C_{Ar}), 145.8 (C_{Ar}), 143.1 (C_{Ar}), 143.0 (C_{Ar}), 141.2 (C_{Ar}), 137.9 (C_{Ar}), 131.6 (C_{Ar}), 131.2 (C_{Ar}), 129.2 (C_{Ar}), 127.7 (C_{Ar}), 127.1 ($2\times\text{C}_{\text{Ar}}$), 126.8 (C_{Ar}), 113.9 (C_{Ar}), 110.9 (C_{Ar}), 103.9 (C_{Ar}), 56.3 (OCH_3), 21.4 ($2\times\text{CH}_3$) ppm.

IR (ATR): $\tilde{\nu}$ = 3003 (w), 2917 (w), 2835 (w), 1599 (m), 1575 (m), 1475 (s), 1437 (s), 1377 (w), 1340 (w), 1275 (m), 1192 (m), 1150 (s), 1114 (w), 1026 (s), 935 (w), 835 (m), 761 (m), 705 (m), 630 (w), 559 (w), 523 (w), 483 (w), 432 (w) cm^{-1} .

HR-MS (ESI): m/z calcd. for $\text{C}_{22}\text{H}_{19}\text{NO}_2$ [$\text{M}+\text{H}$] $^+$: 330.1489, found 330.1471.

2-(3',5'-Dimethyl-[1,1'-biphenyl]-2-yl)benzo[d]oxazole-5-ol (**L3b**)



The reaction was performed according to a slightly modified reported procedure.^[4b] A flame dried 250 mL flask equipped with nitrogen inlet, septum and stir bar was charged with ligand **L3a** (788 mg, 2.39 mmol, 1.00 eq.) and dry CH₂Cl₂ (100 mL). BBr₃ (0.90 mL, 2.40 g, 9.57 mmol, 4.00 eq.) was added dropwise at –78 °C. The solution was allowed to warm to rt and stirred for 40 h after which TLC indicated full conversion. The mixture was cooled to 0 °C and quenched carefully with triethanolamine (14 mL). The slurry was stirred at rt for 90 min, then diluted with water until phase separation occurred. The aqueous layer was separated and extracted with EtOAc (3x75 mL). The combined organic layers were washed with brine (150 mL), dried over Na₂SO₄, and concentrated to dryness yielding the product **L3b** as off-white solid (719 mg, 2.27 mmol, 95%) without the need for further purification.

TLC (*n*-hexane/EtOAc 3:1): *R*_f = 0.34.

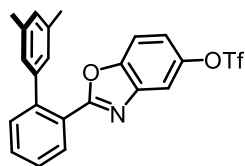
¹H NMR (300 MHz, DMSO-*d*₆): δ = 9.46 (s, 1H, OH), 7.97 (dd, *J* = 7.6, 1.0 Hz, 1H, *H*_{Ar}), 7.63 (dt, *J* = 7.5, 1.4 Hz, 1H, *H*_{Ar}), 7.68-7.45 (m, 2H, *H*_{Ar}), 7.26 (d, *J* = 8.8 Hz, 1H, *H*_{Ar}), 7.04 (d, *J* = 2.4 Hz, 1H, *H*_{Ar}), 6.93 (s, 1H, *H*_{Ar}), 6.82 (s, 2H, *H*_{Ar}), 5.77 (dd, *J* = 8.8, 2.4 Hz, 1H, *H*_{Ar}), 2.38 (s, 6H, 2xCH₃) ppm.

¹³C NMR (75 MHz, DMSO-*d*₆): δ = 163.6, 154.7, 143.9, 142.0, 141.7, 140.1, 136.9, 131.0, 130.8, 130.6, 128.7, 127.5 (2C), 126.3, 125.9, 113.6, 110.4, 104.6, 20.8 (2xCH₃) ppm.

IR (ATR): $\tilde{\nu}$ = 3186 (m, br), 3072 (m), 2919 (m), 2861 (m), 2746 (m), 1601 (m), 1472 (s), 1449 (s), 1377 (m), 1314 (m), 1273 (m), 1216 (m), 1154 (s), 1113 (m), 1036 (w), 951 (w), 845 (m), 806 (m), 762 (m), 705 (m) cm^{–1}.

HR-MS (ESI): *m/z* calcd. for C₂₁H₁₇NO₂ [M+H]⁺: 316.1332, found 316.1324.

2-(3',5'-Dimethyl-[1,1'-biphenyl]-2-yl)benzo[d]oxazol-5-yl trifluoromethanesulfonat (**L3c**)



An oven dried 100 mL flask equipped with nitrogen inlet, septum and stir bar was charged with hydroxy ligand **L3b** (713 mg, 2.26 mmol, 1.00 eq.), dry pyridine (1.82 mL, 1.79 g, 22.6 mmol, 10.0 eq.), and dry CH₂Cl₂ (40 mL). Triflate anhydride (0.76 mL, 1.28 g, 4.52 mmol, 2.00 eq.) was added dropwise at –78 °C. The solution was allowed to gradually warm to rt and stirred for 22 h

after which TLC indicated full conversion. The organic layer was washed with saturated aqueous NH_4Cl (2x40 mL), dried over Na_2SO_4 , and concentrated. The resulting oil was diluted with CH_2Cl_2 , adsorbed on silica, and purified by flash chromatography (*n*-hexane/EtOAc 20:1) to obtain ligand **L3c** as a white, crystalline solid (0.93 g, 2.08 mmol, 92%).

TLC (*n*-hexane/EtOAc 5:1) R_f = 0.46.

^1H NMR (300 MHz, CD_2Cl_2): δ = 8.17–8.00 (m, 1H, H_{Ar}), 7.67 (d, J = 2.5 Hz, 1H, H_{Ar}), 7.65–7.58 (m, 1H, H_{Ar}), 7.56–7.48 (m, 2H, H_{Ar}), 7.41 (d, J = 8.9 Hz, 1H, H_{Ar}), 7.24 (dd, J = 8.9, 2.5 Hz, 1H, H_{Ar}), 7.00 (s, 1H, H_{Xy}), 6.91 (s, 2H, H_{Xy}), 2.26 (s, 6H, 2x CH_3) ppm.

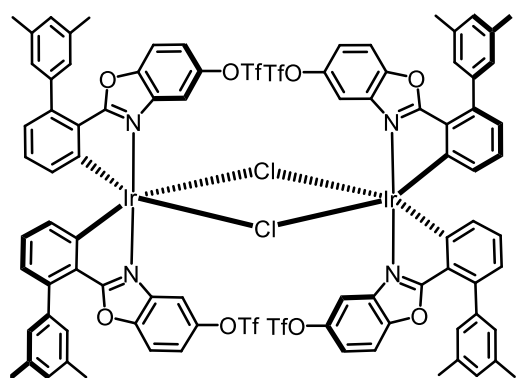
^{13}C NMR (75 MHz, CD_2Cl_2): δ = 166.9, 150.3, 146.6, 143.5, 143.3, 141.0, 138.1, 131.9, 131.8, 131.5, 129.5, 127.9, 127.1 (2C), 125.9, 119.3 (q, J = 320.7 Hz, CF_3), 118.7, 112.9, 111.8, 21.4 (2x CH_3) ppm.

^{19}F NMR (283 MHz, CD_2Cl_2): δ = –73.1 (s, CF_3) ppm.

IR (ATR): $\tilde{\nu}$ = 3026 (w), 2921 (w), 1601 (w), 1572 (w), 1549 (w), 1463 (m), 1424 (m), 1344 (w), 1304 (w), 1211 (s), 1141 (m), 1097 (m), 1029 (m), 951 (m), 880 (m), 815 (w), 763 (w), 730 (w), 660 (w), 604 (w), 562 (w), 509 (w), 427 (w) cm^{-1} .

HR-MS (ESI): m/z calcd. for $\text{C}_{22}\text{H}_{16}\text{F}_3\text{NO}_4\text{S}$ $[\text{M}+\text{H}]^+$: 448.0825, found 448.0822.

Dimer *rac*-C1c



According to procedure A, a 100 mL flask equipped with nitrogen inlet, condenser and stir bar, ligand **L3c** (0.60 g, 1.34 mmol, 1.95 eq.), iridium(III) chloride hydrate (0.24 g, 690 μmol , 1.00 eq.), and ethoxyethanol (50 mL) were used. The mixture was heated to 130 $^\circ\text{C}$ for 22 h. The crude product was purified by flash chromatography (*n*-hexane/ CH_2Cl_2 1:1) to yield dimer *rac*-**C1c** as an orange, crystalline solid (594 mg, 265 μmol , 79% based on the amount of starting ligand **L3c**).

TLC (*n*-hexane/EtOAc 1:1): $R_f = 0.30$.

^1H NMR (300 MHz, CD_2Cl_2): $\delta = 8.29$ (d, $J = 2.5$ Hz, 1H, H_{Ar}), 7.21 (d, $J = 9.0$ Hz, 1H, H_{Ar}), 7.13 (s, 1H, H_{Ar}), 7.05 (s, 2H, H_{Ar}), 6.99 (dd, $J = 9.0, 2.5$ Hz, 1H, H_{Ar}), 6.83–6.77 (m, 1H, H_{Ar}), 6.72 (t, $J = 7.6$ Hz, 1H, H_{Ar}), 6.25–5.99 (m, 1H, H_{Ar}), 2.42 (s, 6H, $2 \times \text{CH}_3$) ppm.

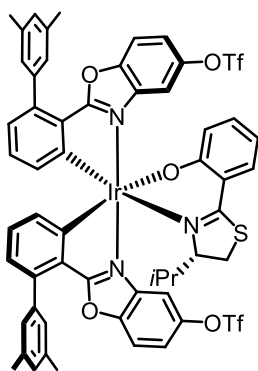
^{13}C NMR (75 MHz, CD_2Cl_2): $\delta = 180.7, 149.2, 146.4, 146.2, 144.7, 140.7, 139.9, 137.7, 132.4, 131.5, 129.7, 127.6, 125.9, 125.7, 119.1$ (q, $J = 321.6$ Hz, CF_3), 118.5, 112.5, 111.7, 21.4 ($2 \times \text{CH}_3$) ppm.

^{19}F NMR (283 MHz, CD_2Cl_2): $\delta = -72.5$ (s, CF_3) ppm.

IR (ATR): $\tilde{\nu} = 3046$ (w), 2922 (w), 1601 (w), 1572 (w), 1565 (m), 1501 (w), 1465 (m), 1429 (m), 1344 (w), 1272 (w), 1214 (s), 1138 (m), 1109 (m), 1052 (m), 980 (w), 945 (m), 888 (m), 862 (m), 814 (w), 741 (w), 709 (w), 603 (w), 567 (m), 509 (w), 438 (w) cm^{-1} .

HR-MS (LIFDI): m/z calcd. for $\text{C}_{88}\text{H}_{60}\text{Cl}_1\text{F}_{12}\text{N}_4\text{O}_{16}\text{S}_4$ $[\text{M}-\text{Cl}]^+$: 2205.1632, found 2205.1753.

Diastereomers Λ -(*S*)-C2c



According to procedure B, dimer ***rac*-C1c** (150 mg, 66.9 μmol , 1.00 eq.), ancillary ligand (***S***)-AL1 (29.7 mg, 134 μmol , 2.00 eq.), AgOTf (34.5 mg, 134 μmol , 2.00 eq.), Et_3N (93 μL , 670 μmol , 10.0 eq.), and EtOH (6.5 mL) were added. The mixture was stirred for 2 h at 80°C . The diastereomers were separated by silica gel flash chromatography (CH_2Cl_2 /*n*-hexane 3:2) to obtain the diastereomers Λ -(*S*) and Λ -(*S*) as orange solids (Λ -(*S*)-C2c: 85 mg, 65.1 μmol , 39%, Λ -(*S*)-C2c: 80 mg, 61.3 μmol , 35%). Both complexes decompose in solution. Second diastereomer decomposes quicker.

TLC (CH_2Cl_2 /*n*-hexane 5:1): R_f (dia 1) = 0.33, R_f (dia 2) = 0.19.

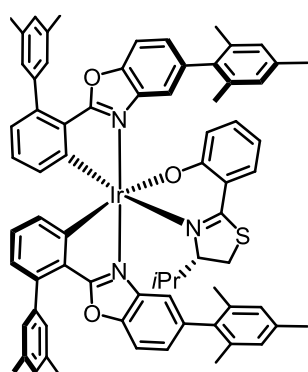
^1H NMR (300 MHz, CD_2Cl_2): $\delta = 7.86$ (d, $J = 2.5$ Hz, 1H, H_{Ar}), 7.64–7.59 (m, 1H, H_{Ar}), 7.64–7.59 (m, 1H, H_{Ar}), 7.48–7.45 (m, 1H, H_{Ar}), 7.44–7.39 (m, 1H, H_{Ar}), 7.39–7.35 (m, 1H, H_{Ar}), 7.34–7.30 (m, 2H, H_{Ar}), 7.23–7.21 (m, 1H, H_{Ar}), 7.13–7.05 (m, 3H, H_{Ar}), 7.02–6.99 (m, 1H, H_{Ar}), 6.97 (br, 2H, H_{Ar}), 6.94 (br, 2H, H_{Ar}), 6.83 (d, $J = 7.3$ Hz, 1H, H_{Ar}), 6.80 (d, $J = 1.3$ Hz, 1H, H_{Ar}), 6.76–6.72 (m, 2H, H_{Ar}), 6.70–6.65 (m, 1H, H_{Ar}), 6.51 (dd, $J = 6.5, 2.4$ Hz, 1H, H_{Ar}), 6.29 (dd, $J = 7.3, 1.4$ Hz, 1H, H_{Ar}), 6.27–6.20 (m, 1H, H_{Ar}), 4.64–4.60 (m, 1H, H_{aliph}), 3.35–

3.30 (m, 1H, H_{aliph}), 2.98–2.95 (m, 1H, H_{aliph}), 2.33 (s, 6H, 2xCH₃), 2.28 (s, 6H, 2xCH₃), 0.30 (d, $J = 7.0$ Hz, 3H, CH₃), 0.12 (d, $J = 7.0$ Hz, 3H, CH₃) ppm.

IR (ATR): $\tilde{\nu} = 2959$ (w), 2925 (w), 2860 (w), 1601 (m), 1564 (m), 1529 (w), 1500 (w), 1464 (s), 1429 (w), 1341 (w), 1214 (s), 1140 (m), 1107 (m), 1044 (w), 1016 (w), 946 (m), 867 (m), 800 (m), 744 (w), 710 (w), 603 (m), 563 (w), 510 (w), 434 (w) cm⁻¹.

HR-MS (ESI): m/z calcd. for C₅₆H₄₄F₆Ir₁N₃O₉S₃Na₁ [M+Na]⁺: 1328.1665, found 1328.1679.

Cross-Coupling Product Λ -(S)-C3j



According to procedure C, iridium(III) complex Λ -(S)-C2c (40.0 mg, 30.7 μmol , 1.00 eq.), 2,4,6-trimethylphenylboronic acid (19.8 mg, 122 μmol , 4.00 eq.), K₃PO₄ (25.7 mg, 122 μmol , 4.00 eq.), Pd(OAc)₂ (0.7 mg, 3.12 μmol , 10 mol%), SPhos (2.5 mg, 6.1 μmol , 20 mol%), and toluene (600 μL) were used. Full conversion was indicated after 18 h by TLC. The crude product was purified by silica gel flash chromatography (CH₂Cl₂/*n*-hexane 2:1) to yield the iridium(III) complex Λ -(S)-C3j (34.0 mg, 27.0 μmol , 88%) as an orange solid.

TLC (CH₂Cl₂/*n*-hexane, 2:1): $R_f = 0.31$.

¹H NMR (300 MHz, CD₂Cl₂) $\delta = 7.74$ – 7.72 (m, 1H, H_{Ar}), 7.43 (d, $J = 8.5$ Hz, 1H, H_{Ar}), 7.38 (d, $J = 8.5$ Hz, 1H, H_{Ar}), 7.30 (dd, $J = 8.2, 1.7$ Hz, 1H, H_{Ar}), 7.30 (d, $J = 1.1$ Hz, 1H, H_{Ar}), 7.02–6.85 (m, 6H, H_{Ar}), 6.85–6.72 (m, 3H, H_{Ar}), 6.62 (dd, $J = 7.3, 1.5$ Hz, 1H, H_{Ar}), 6.55 (dd, $J = 7.3, 1.4$ Hz, 1H, H_{Ar}), 6.26–6.17 (m, 1H, H_{Ar}), 4.70–4.61 (m, 1H, H_{Aliph}), 2.80–2.64 (m, 2H, H_{Aliph}), 2.44 (s, 6H, 2xCH₃), 2.42 (s, 6H, 2xCH₃), 2.33 (s, 3H, CH₃), 2.27 (s, 3H, CH₃), 2.02 (s, 3H, CH₃), 1.99 (s, 3H, CH₃), 1.94 (s, 3H, CH₃), 1.54 (s, 3H, CH₃), 0.81–0.70 (m, 1H, H_{Aliph}), 0.31 (d, $J = 7.0$ Hz, 3H, CH₃), 0.16 (d, $J = 7.0$ Hz, 3H, CH₃) ppm.

¹³C NMR (75 MHz, CD₂Cl₂): $\delta = 178.6, 178.2, 169.0, 167.9, 167.7, 153.3, 152.4, 149.2, 149.1, 143.8, 143.3, 140.7, 140.6, 139.9, 139.6, 138.7, 138.7, 138.2, 138.0, 137.7$ (2C), 137.5 (2C), 137.2, 136.9, 136.6, 136.3, 135.9, 135.7, 133.9, 133.6, 133.4, 131.3, 131.3, 131.0, 130.7, 129.5, 129.4, 129.1, 128.8, 128.5, 128.4, 128.4, 128.3, 128.2, 127.7, 127.6, 127.3, 126.5, 124.9, 124.1, 123.7, 119.6, 118.3, 116.7, 113.3, 111.8, 110.9, 84.8, 68.4, 39.3, 32.1, 30.8, 29.4, 27.6, 24.2, 23.4, 21.6, 21.5, 21.2, 21.1, 21.0, 20.9, 20.4, 19.2, 14.3, 14.2, 11.2 ppm.

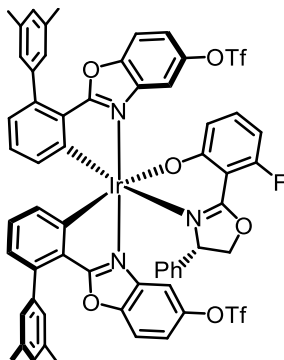
IR (ATR): $\tilde{\nu}$ = 3034 (m), 2957 (m), 2922 (m), 2862 (m), 1729 (w), 1603 (m), 1561 (s), 1523 (m), 1501 (w), 1464 (m), 1439 (m), 1402 (m), 1356 (w), 1267 (w), 1195 (w), 1146 (w), 1076 (w), 1044 (w), 1011 (w), 950 (w), 851 (w), 816 (w), 791 (w), 743 (w), 711 (w), 414 (w) cm^{-1} .

HR-MS (ESI): m/z calcd. for $\text{C}_{72}\text{H}_{66}\text{Ir}_1\text{N}_3\text{O}_3\text{S}_1$ $[\text{M}+\text{Na}]^+$: 1268.4351, found 1268.4378.

Diastereomers Λ -(*S*)-C2e and Λ -(*S*)-C2e

According to procedure B, dimer *rac*-C1c (245 mg, 109 μmol , 1.00 eq.), ancillary ligand (*S*)-AL2 (65.7 mg, 241 μmol , 2.20 eq.), AgOTf (61.9 mg, 241 μmol , 2.20 eq.), Et₃N (149 μL , 1.09 mmol, 10.0 eq.), and EtOH (250 μL) were added. The mixture was stirred for 5 h at 80°C. The diastereomers were separated by silica gel flash chromatography ($\text{CH}_2\text{Cl}_2/n$ -hexane 2:1 \rightarrow 13:2) to obtain the diastereomers Λ -(*S*) and Λ -(*S*). Each complex was once again purified by silica gel flash column chromatography (n -hexane/EtOAc 10:1 \rightarrow 5:1) to obtain both diastereomers as orange solids (Λ -(*S*)-C2e: 114 mg, 84.0 μmol , 39%, Λ -(*S*)-C2e: 102 mg, 76.0 μmol , 35%).

Diastereomer Λ -(*S*)-C2e



TLC ($\text{CH}_2\text{Cl}_2/n$ -hexane 3:1): R_f = 0.30, (n -hexane/EtOAc 5:1): R_f = 0.30.

^1H NMR (500 MHz, CD_2Cl_2): δ = 7.86 (d, J = 2.5 Hz, 1H, H_{Ar}), 7.47 (d, J = 2.4 Hz, 1H, H_{Ar}), 7.45 (d, J = 9.0 Hz, 1H, H_{Ar}), 7.33 (dd, J = 9.0, 2.4 Hz, 1H, H_{Ar}), 7.24 (dd, J = 9.0, 2.5 Hz, 1H, H_{Ar}), 7.18 (d, J = 9.0 Hz, 1H, H_{Ar}), 7.14–7.08 (m, 3H, H_{Ar}), 7.06–6.94 (m, 4H, H_{Ar}), 6.91–6.80 (m, 4H, H_{Ar}), 6.78–6.74 (m, 1H, H_{Ar}), 6.62 (dd, J = 6.6, 2.2 Hz, 1H, H_{Ar}), 6.58–6.54 (m, 1H, H_{Ar}), 6.34 (dd, J = 7.4, 1.4 Hz, 1H, H_{Ar}), 6.32–6.25 (m, 2H, H_{Ar}), 6.06 (ddd, J = 12.5, 7.9,

0.9 Hz, 1H, H_{Ar}), 4.95 (dd, $J = 9.4, 3.6$ Hz, 1H, H_{aliph}), 4.81 (t, $J = 9.4$ Hz, 1H, H_{aliph}), 4.18 (dd, $J = 9.4, 3.6$ Hz, 1H, H_{aliph}), 2.43 (s (br), 6H, $2 \times CH_3$), 2.36 (s, 6H, $2 \times CH_3$) ppm

^{13}C NMR (125 MHz, CD_2Cl_2): $\delta = 181.0, 180.1, 173.7$ (2C), 164.4, 162.9 (2C), 162.4, 156.0, 150.6, 149.3, 149.1, 147.4 (2C), 144.5, 144.4, 140.6, 140.1, 140.0, 139.7, 139.5, 137.7, 137.6, 134.0, 133.9, 133.8, 132.1, 131.7, 130.8, 129.6, 128.2, 127.8, 127.5, 127.3, 125.2, 124.3, 120.4 (2C), 120.3, 120.2, 118.7, 118.6, 117.9, 117.8, 113.4, 112.5, 111.3, 108.9, 101.3 (2C), 100.8, 100.6, 75.6, 69.9, 21.5 (2C) ppm.

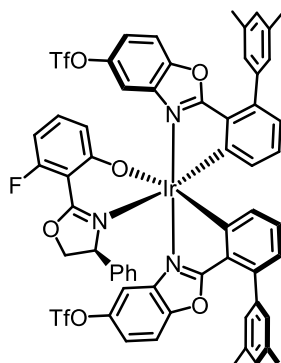
^{19}F NMR (283 MHz, CD_2Cl_2): $\delta = -72.9$ (d, $J = 2.9$ Hz, CF_3), -73.2 (s, CF_3), -105.4 (q, 2.9 Hz, CF) ppm.

IR (ATR): $\tilde{\nu} = 3030$ (w), 2956 (w), 2918 (w), 2857 (w), 1617 (m), 1564 (m), 1532 (w), 1499 (w), 1425 (m), 1212 (s), 1138 (m), 1105 (m), 1038 (w), 944 (m), 865 (m), 794 (m), 744 (w), 698 (w), 626 (w), 601 (m), 569 (w), 536 (w), 508 (w), 433 (w) cm^{-1} .

HR-MS (LIFDI): m/z calcd. for $C_{59}H_{41}F_7IrN_3O_{10}S_2 [M]^{+}$: 1341.1751, found 1341.1747.

CD (MeCN): λ ($\Delta\epsilon$, $M^{-1} \cdot cm^{-1}$) = 213 (+37), 231(−20), 249 (+6), 288 (−45), 332 (+52), 355 (+31), 381 (+45), 447 (−11) nm.

Diastereomer Δ -(S)-C2e



TLC (CH_2Cl_2/n -hexane 13:2): $R_f = 0.31$, (n -hexane/EtOAc 5:1): $R_f = 0.27$.

1H NMR (500 MHz, CD_2Cl_2): $\delta = 8.03$ (d, $J = 2.5$ Hz, 1H, H_{Ar}), 7.58 (d, $J = 9.0$ Hz, 1H, H_{Ar}), 7.40–7.35 (m, 2H, H_{Ar}), 7.31 (d, $J = 9.0$ Hz, 1H, H_{Ar}), 7.21–7.13 (m, 4H, H_{Ar}), 7.12–7.06 (m, 4H, H_{Ar}), 7.01 (s br, 2H, H_{Ar}), 6.97–6.91 (m, 1H, H_{Ar}), 6.89–6.84 (m, 2H, H_{Ar}), 6.78–6.72 (m, 3H, H_{Ar}), 6.45–6.37 (m, 3H, H_{Ar}), 6.07–6.01 (m, 2H, H_{Ar}), 4.52 (dd, $J = 8.9, 5.6$ Hz, 1H, H_{aliph}),

4.28 (t, $J = 9.4$ Hz, 1H, H_{aliph}), 4.20 (dd, $J = 9.8, 5.6$ Hz, 1H, H_{aliph}), 2.46 (s, 6H, CH_3), 2.35 (s, 6H, CH_3) ppm.

^{13}C NMR (125 MHz, CD_2Cl_2): $\delta = 181.7, 180.9, 173.8$ (2C), 163.7, 163.1, 161.7, 153.9, 152.4, 149.6, 148.7, 147.8, 147.0, 144.7, 144.2, 140.3, 140.1, 140.0, 139.7, 139.5, 137.9, 137.7, 135.3, 133.3, 133.2, 131.8, 131.7, 131.1, 129.8, 129.6, 129.0, 128.5, 127.5, 127.1, 126.0, 125.2, 124.1, 123.0, 122.8, 120.4, 120.3, 119.4 (2C), 119.2, 118.2, 117.8, 117.7, 115.3, 115.2, 113.1, 112.7, 111.2, 110.3, 103.3, 103.2, 100.6, 100.4, 76.3, 68.7, 21.6, 21.5 ppm.

^{19}F NMR (283 MHz, CD_2Cl_2): $\delta = -73.0$ (s, CF_3), -73.2 (d, $J = 3.9$ Hz, CF_3), -108.0 (q, $J = 4.0$ Hz, CF) ppm.

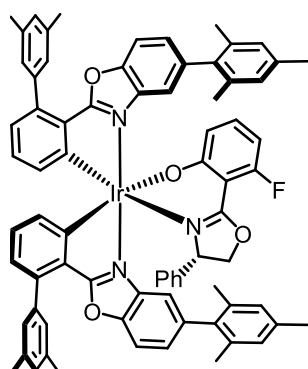
IR (ATR): $\tilde{\nu} = 3036$ (w), 2916 (w), 1620 (m), 1564 (m), 1499 (w), 1424 (s), 1348 (w), 1273 (w), 1211 (s), 1137 (m), 1103 (m), 1037 (m), 983 (w), 943 (m), 862 (m), 815 (m), 790 (m), 743 (m), 700 (m), 625 (m), 600 (s), 534 (m), 507 (m), 434 (s) cm^{-1} .

HR-MS (LIFDI): m/z calcd. for $\text{C}_{59}\text{H}_{41}\text{F}_7\text{IrN}_3\text{O}_{10}\text{S}_2 [\text{M}]^{+}$: 1341.1751, found 1341.1723.

CD (MeCN): λ ($\Delta\epsilon$, $\text{M}^{-1} \cdot \text{cm}^{-1}$) = 208 (−77), 225 (−12), 241 (−48), 289 (+40), 327 (−31), 359 (−3), 382 (−8), 455 (+6) nm.

3.4.10 Cross-Coupling Products Λ -(*S*)-C3h and Λ -(*S*)-C3i

Cross-Coupling Product Λ -(*S*)-C3h



According to procedure C, iridium(III) complex Λ -(*S*)-C2c (64.4 mg, 49.0 μmol , 1.00 eq.), 2,4,6-trimethylphenylboronic acid (32.2 mg, 196 μmol , 4.00 eq.), K_3PO_4 (41.6 mg, 196 μmol , 4.00 eq.), $\text{Pd}(\text{OAc})_2$ (1.1 mg, 5.0 μmol , 10 mol%), SPhos (4.1 mg, 10.0 μmol , 20 mol%), and toluene (250 μL) were used. The crude product was purified by flash chromatography *n*-hexane/EtOAc (12:1 \rightarrow 5:1) to yield the iridium(III) complex Λ -(*S*)-C3h (57.7 mg, 45.0 μmol , 91%) as an orange solid.

TLC (*n*-hexane/EtOAc, 10:1): $R_f = 0.24$, (*n*-hexane/EtOAc, 5:1): $R_f = 0.47$

¹H NMR (500 MHz, CD₂Cl₂) δ = 7.66 (d, J = 1.5 Hz, 1H, H_{Ar}), 7.43 (d, J = 8.5 Hz, 1H, H_{Ar}), 7.31 (d, J = 1.3 Hz, 1H, H_{Ar}), 7.20–7.15 (m, 2H, H_{Ar}), 7.12–7.07 (m, 5H, H_{Ar}), 7.04–6.99 (m, 3H, H_{Ar}), 6.99–6.93 (m, 2H, H_{Ar}), 6.92–6.88 (m, 2H, H_{Ar}), 6.87–6.78 (m, 5H, H_{Ar}), 6.73–6.44 (m, br, 4H, H_{Ar}), 6.40–6.35 (m, 1H, H_{Ar}), 6.23–6.18 (m, 2H, H_{Ar}), 5.99 (ddd, J = 12.9, 7.9, 0.9 Hz, 1H, H_{Ar}), 5.02 (dd, J = 9.3, 3.6 Hz, 1H, H_{aliph}), 4.21 (t, J = 9.3 Hz, 1H, H_{aliph}), 3.93 (dd, J = 9.3, 3.6 Hz, 1H, H_{aliph}), 2.44 (s br, 6H, 2xCH₃), 2.39 (s, 6H, 2xCH₃), 2.33 (s, 3H, CH₃), 2.30 (s, 3H, CH₃), 2.08 (s, 3H, CH₃), 2.00–1.97 (m, 6H, 2xCH₃), 1.87 (s, 3H, CH₃) ppm.

¹³C NMR (125 MHz, CD₂Cl₂): δ = 178.6, 177.6, 173.4 (2C), 164.3, 162.4 (2C), 162.3, 155.3, 150.0, 149.3, 149.0, 143.5, 143.4, 140.8, 140.5, 140.4, 139.7, 139.2, 138.9, 138.7, 138.2 (2C), 137.6, 137.4 (2C), 136.9, 136.4, 136.0 (2C), 135.9, 133.8, 133.4, 133.3, 131.3, 131.1, 130.8, 129.4, 129.3, 128.7, 128.6, 128.5, 128.4 (2C), 128.3 (2C), 127.7 (br), 127.6, 126.9, 126.8, 125.2 (br), 124.9, 124.0, 120.3 (2C), 118.9, 116.5, 112.1, 110.9, 101.0, 100.9, 100.3, 100.1, 75.3, 70.3, 21.5 (2C), 21.2, 21.1 (3C), 20.7, 20.5 (2C) ppm.

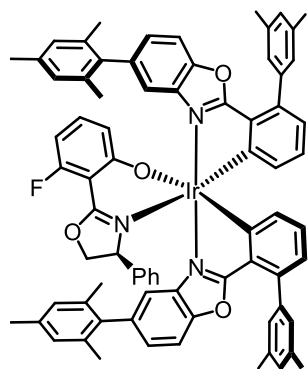
¹⁹F NMR (283 MHz, CD₂Cl₂): δ = –105.3 (s, CF) ppm.

IR (ATR): $\tilde{\nu}$ = 3031 (w), 2915 (w), 2858 (w), 1615 (m), 1566 (s), 1531 (m), 1501 (w), 1438 (s), 1399 (m), 1317 (w), 1263 (w), 1219 (m), 1176 (w), 1146 (w), 1101 (w), 1038 (m), 950 (w), 919 (w), 850 (m), 816 (m), 789 (m), 746 (m), 694 (m), 661 (w), 608 (w), 575 (w), 534 (w), 489 (w), 434 (w), 405 (w) cm^{–1}.

HR-MS (LIFDI): m/z calcd. for C₇₅H₆₃FIrN₃O₄ [M]⁺: 1281.4432, found 1281.4406.

CD (MeCN): λ ($\Delta\epsilon$, M^{–1}·cm^{–1}) = 226 (+6), 242 (–35), 291 (+42), 329 (–34), 361 (–5), 377 (–6), 432 (+9) nm.

Cross-Coupling Product Δ -(*S*)-C3i



According to procedure C, iridium(III) complex Δ -(*S*)-C2c (64.4 mg, 49.0 μ mol, 1.00 eq.), 2,4,6-trimethylphenylboronic acid (32.2 mg, 196 μ mol, 4.00 eq.), K₃PO₄ (41.6 mg, 196 μ mol, 4.00 eq.), Pd(OAc)₂ (1.1 mg, 5.0 μ mol, 10 mol%), SPhos (4.1 mg, 10.0 μ mol, 20 mol%), and toluene (250 μ L) were used. The crude product was purified by flash chromatography *n*-hexane/EtOAc (12:1 \rightarrow 5:1) to

yield the iridium(III) complex **A-(S)-C3i** (55.1 mg, 43.0 μmol , 88%) as an orange solid.

TLC (*n*-hexane/EtOAc 10:1): $R_f = 0.18$, (*n*-hexane/EtOAc 5:1): $R_f = 0.41$.

^1H NMR (500 MHz, CD_2Cl_2): $\delta = 7.76$ (d, $J = 1.2$ Hz, 1H), 7.53 (d, $J = 8.5$ Hz, 1H), 7.29–7.22 (m, 3H), 7.21–7.16 (m, 2H), 7.10 (s br, 3H), 7.04 (s br, 1H), 7.00 (s br, 1H), 6.96–6.80 (m, 9H), 6.73 (dd, $J = 7.5, 1.2$ Hz, 1H), 6.54–6.49 (m, 2H), 6.46–6.40 (m, 3H), 6.33–6.30 (m, 1H), 6.18 (dd, $J = 7.8, 0.9$ Hz, 1H), 5.99–5.93 (m, 1H), 4.43 (dd, $J = 8.3, 3.6$ Hz, 1H), 4.03–3.93 (m, 2H), 2.49 (s, 6H), 2.41–2.38 (m, 9H), 2.27 (s, 3H), 2.03 (s, 3H), 1.88 (s, 3H), 1.81 (s, 3H), 1.72 (s, 3H) ppm.

^{13}C NMR (125 MHz, CD_2Cl_2): $\delta = 179.5, 178.3, 174.1$ (2C), 163.4, 162.6, 161.4, 153.5, 151.8, 149.5, 148.6, 144.1, 143.3, 140.7, 140.6, 140.2, 140.1, 139.3, 138.8, 138.7, 138.4, 138.1, 137.9, 137.6, 137.3, 137.2, 136.6, 136.5, 136.1, 136.0, 135.9, 132.7, 132.6, 131.7, 130.8, 130.6, 129.7, 129.4, 128.8, 128.6, 128.5, 128.4, 128.3, 128.2, 127.7 (br), 127.4, 127.3, 127.2, 126.7, 125.0, 123.7, 119.4 (2C), 118.6, 117.1, 111.6, 111.3, 103.7 (2C), 100.1, 100.0, 76.4, 68.1, 21.6, 21.5, 21.3, 21.1 (3C), 20.5, 20.4 (2C) ppm.

^{19}F NMR (283 MHz, CD_2Cl_2): $\delta = -108.4$ (s, CF) ppm.

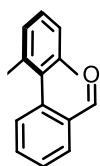
IR (ATR): $\tilde{\nu} = 3033$ (w), 2956 (w), 2914 (w), 2858 (w), 1619 (m), 1565 (s), 1533 (w), 1501 (w), 1442 (m), 1400 (m), 1352 (m), 1317 (w), 1263 (m), 1223 (m), 1176 (w), 1146 (w), 1092 (w), 1035 (m), 984 (w), 949 (w), 915 (w), 882 (w), 849 (m), 815 (m), 789 (s), 758 (m), 699 (s), 661 (w), 616 (w), 578 (w), 534 (w), 437 (w), 397 (w) cm^{-1} .

HR-MS (LIFDI): m/z calcd. for $\text{C}_{75}\text{H}_{63}\text{FIrN}_3\text{O}_4$ $[\text{M}]^{+}$: 1281.4432, found 1281.4450.

CD (MeCN): λ ($\Delta\epsilon$, $\text{M}^{-1}\cdot\text{cm}^{-1}$) = 232 (–27), 250 (–35), 256 (–11), 269 (–5), 295 (–42), 334 (+43), 352 (+31), 376 (+39), 444 (–12) nm.

3.4.11 Ligand L4c and Dimer *rac*-C1d

2',6'-Dimethyl-[1,1'-biphenyl]-2-carbaldehyde (S1b)



The reaction was performed according to a slightly modified reported procedure.^[24b]

A 50 mL flask equipped with nitrogen inlet, septum and stirr bar was charged with (2,6-dimethylphenyl)boronic acid (1.62 g, 10.8 mmol, 2.00 eq.), K_3PO_4 (2.28 g, 10.8 mmol, 2.00 eq.), $\text{Pd}(\text{OAc})_2$ (60.0 mg, 0.27 mmol, 5.0 mol%), SPhos (220 mg,

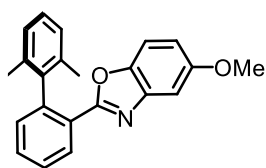
0.54 mmol, 10mol%), and toluene (20 mL). To the resulting suspension 2-bromobenzaldehyde (628 mL, 5.40 mmol, 1.0 eq.), was added and the mixture was heated to 100 °C for 15 h until reaction control by TLC indicated full conversion. The suspension was cooled to rt and directly subjected to flash chromatography (*n*-hexane/EtOAc 50:1) to yield product **S1b** as a colorless solid. (1.14 g, 5.40 mmol, quantitative).

TLC (*n*-hexane/EtOAc 10:1) R_f = 0.64.

¹H NMR (300 MHz, CD₂Cl₂): δ = 9.63 (d, J = 0.8, 1H, H_{CHO}), 8.04–7.97 (m, 1H, H_{Ar}), 7.73–7.66 (m, 1H, H_{Ar}), 7.56–7.48 (m, 1H, H_{Ar}), 7.27–7.19 (m, 2H, H_{Ar}), 7.17–7.14 (m, 1H, H_{Ar}), 7.14–7.11 (m, 1H, H_{Ar}), 1.96 (s, 6H, 2xCH₃) ppm.

HR-MS (ESI): m/z calcd. for C₁₅H₁₄O₁Na₁ [M+Na]⁺: 233.0937, found 233.0940.

2-(2',6'-Dimethyl-[1,1'-biphenyl]-2-yl)-5-methoxybenzo[d]oxazole (**L4a**)



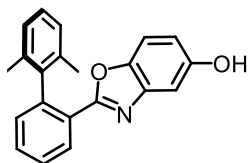
The reaction was performed according to a slightly modified reported procedure.^[5a] A 50 mL flask equipped with nitrogen inlet, condenser and stir bar was charged with phenol **S2a** (925 mg, 5.47 mmol, 1.00 eq.), aldehyde **S1b** (1.15 g, 5.47 mmol, 1.00 eq.), and *m*-xylene (20 mL). The resulting suspension was stirred at 120 °C for 2 h, 4-MeO-TEMPO (51 mg, 0.27 mmol, 5.0 mol%) added and stirred at 120 °C under O₂-atmosphere (O₂-balloon) for 15 h. The mixture was cooled to rt, concentrated, and adsorbed on silica gel. Purification by flash chromatography (*n*-hexane/EtOAc 6:1) yielded product **L4a** as pale-yellow, viscous oil (1.64 g, 4.98 mmol, 91%) that solidifies upon cooling.

TLC (*n*-hexane/EtOAc 5:1): R_f = 0.30.

¹H NMR (300 MHz, CD₂Cl₂): δ = 8.23–8.16 (m, 1H, H_{Ar}), 7.56–7.41 (m, 2H, H_{Ar}), 7.17–7.12 (m, 1H, H_{Ar}), 7.12–7.03 (m, 2H, H_{Ar}), 7.02–6.96 (m, 3H, H_{Ar}), 6.74 (dd, J = 8.9, 2.6 Hz, 1H, H_{Ar}), 3.71 (s, 3H, OCH₃), 1.85 (s, 6H, 2xCH₃) ppm.

HR-MS (ESI): m/z calcd. for C₂₂H₁₉NO₂ [M+H]⁺: 330.1489, found 330.1490.

2-(2',6'-Dimethyl-[1,1'-biphenyl]-2-yl)benzo[d]oxazole-5-ol (**L4b**)



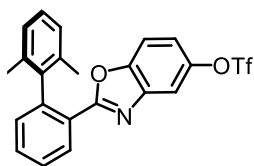
The reaction was performed according to a slightly modified reported procedure.^[4b] A flame dried 250 mL flask equipped with nitrogen inlet, septum and stir bar was charged with ligand **L4a** (1.64 g, 4.98 mmol, 1.00 eq.) and dry CH₂Cl₂ (100 mL). BBr₃ (1.42 mL, 14.9 mmol, 3.00 eq.) was added dropwise at –78 °C. The solution was allowed to warm to rt and stirred for 24 h after which TLC indicated full conversion. The mixture was cooled to 0 °C and quenched carefully with triethanolamine (~10 mL). The slurry was diluted with MeOH (50 mL) stirred at rt for 2 h, then diluted with water until phase separation occurred. The aqueous layer was separated and extracted with EtOAc (3x75 mL). The combined organic layers were washed with brine (150 mL), dried over Na₂SO₄, and concentrated to dryness yielding the product **L4b** as brown foam (1.53 mg, 4.85 mmol, 97%) without the need for further purification.

TLC (*n*-hexane/EtOAc 3:1): *R*_f = 0.34.

¹H NMR (300 MHz, CD₂Cl₂): δ = 8.22–8.15 (m, 1H, *H*_{Ar}), 7.56–7.41 (m, 2H, *H*_{Ar}), 7.17–7.12 (m, 1H, *H*_{Ar}), 7.12–7.03 (m, 1H, *H*_{Ar}), 7.02–6.96 (m, 3H, *H*_{Ar}), 6.95–6.93 (m, 1H, *H*_{Ar}), 6.66 (dd, *J* = 8.7, 2.5 Hz, 1H, *H*_{Ar}), 1.85 (s, 6H, 2xCH₃) ppm.

HR-MS (ESI): *m/z* calcd. for C₂₁H₁₇N₁O₂ [M+H]⁺: 316.1332, found 316.1334.

2-(2',6'-Dimethyl-[1,1'-biphenyl]-2-yl)-benzo[d]oxazol-5-yl-trifluoromethanesulfonate (**L4c**)



An oven dried 250 mL flask equipped with nitrogen inlet, septum and stir bar was charged with hydroxy ligand **L4b** (1.53 mg, 4.85 mmol, 1.00 eq.), dry pyridine (3.92 mL, 3.84 g, 48.5 mmol, 10.0 eq.), and dry CH₂Cl₂ (60 mL). Triflate anhydride (2.74 mL, 1.64 g, 9.70 mmol, 2.00 eq.) was added dropwise at –78 °C. The solution was allowed to gradually warm to rt and stirred for 24 h after which TLC indicated full conversion. The reaction was terminated with saturated aqueous NH₄Cl (40 mL), the aqueous layer separated and extracted with CH₂Cl₂ (3x25 mL), the combined organic layers dried over Na₂SO₄, and concentrated. The resulting brown oil was diluted with CH₂Cl₂, adsorbed on silica, and purified by flash chromatography (*n*-hexane/EtOAc 20:1) to obtain ligand **L4c** as a colorless oil (2.05 g, 4.59 mmol, 95%).

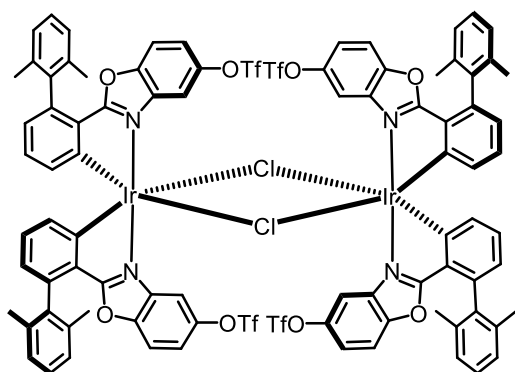
TLC (*n*-hexane/EtOAc 5:1): *R*_f = 0.47

¹H NMR (300 MHz, CD₂Cl₂): δ = 8.26–8.19 (m, 1H, *H*_{Ar}), 7.61–7.52 (m, 1H, *H*_{Ar}), 7.50–7.43 (m, 2H, *H*_{Ar}), 7.26–7.20 (m, 1H, *H*_{Ar}), 7.20–7.15 (m, 1H, *H*_{Ar}), 7.12–7.05 (m, 2H, *H*_{Ar}), 7.02–6.99 (m, 1H, *H*_{Ar}), 6.99–6.95 (m, 1H, *H*_{Ar}), 1.84 ppm (s, 6H, 2xCH₃).

¹³C NMR (75 MHz, CD₂Cl₂): δ = 166.1, 150.2, 146.4, 143.2, 142.0, 140.8, 136.1, 132.4, 131.6, 130.8, 128.0, 127.6, 127.4 (2C), 126.0, 119.1 (q, *J*_{CF} = 320 Hz, CF₃), 118.5, 113.5, 111.6, 20.7 (2C).

HR-MS (ESI): *m/z* calcd. for C₂₂H₁₇F₃N₁O₄S [M+H]⁺: 448.0824, found 448.0824.

Dimer *rac*-C1d



According to procedure A, a 100 mL flask equipped with nitrogen inlet, condenser and stir bar, ligand **L4c** (0.60 g, 1.34 mmol, 1.95 eq.), iridium(III) chloride hydrate (0.24 g, 690 μmol, 1.00 eq.), and ethoxyethanol (50 mL) were used. The mixture was heated to 130 °C for 72 h. Cooled to rt, the reaction mixture was diluted with 50 mL CH₂Cl₂, washed with water (4x50 mL) and brine (1x50 mL), dried

over Na₂SO₄, filtered and concentrated. The crude product was purified by flash chromatography (*n*-hexane/CH₂Cl₂ 1:1) to yield dimer *rac*-C1d as a yellow solid (290 mg, 129 μmol, 39% based on the amount of starting ligand **L4c**). Single crystals suitable for X-ray analysis from each complex were grown by evaporating a *n*-hexane/CH₂Cl₂ solution of **L4c**.

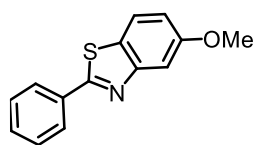
TLC (*n*-hexane/ CH₂Cl₂ 1:1): *R*_f = 0.30

¹H NMR (300 MHz, CD₂Cl₂): δ = 7.89 (d, *J* = 2.5 Hz, 1H, *H*_{Ar}), 7.29–7.25 (m, 2H, *H*_{Ar}), 7.16–7.11 (m, 1H, *H*_{Ar}), 7.08 (d, *J* = 9.1 Hz, 1H, *H*_{Ar}), 6.95 (dd, *J* = 9.0, 2.5 Hz, 1H, *H*_{Ar}), 6.72–6.60 (m, 2H, *H*_{Ar}), 5.95 (dd, *J* = 7.5, 1.4 Hz, 1H, *H*_{Ar}), 2.11 (s, 3H, CH₃), 1.80 (s, 3H, CH₃) ppm.

HR-MS (LIFDI): *m/z* calcd. for C₈₈H₆₀Cl₁F₁₂N₄O₁₆S₄ [M-Cl]⁺: 2205.1632, found 2205.1703.

3.4.12 Ligand L6c, Dimer *rac*-C1e, and Diastereomers Λ -(*S*)-C2h

5-Methoxy-2-phenylbenz[*d*]thiazole (L6a)



The reaction was performed according to a slightly modified reported procedure.^[5b] A 10 mL flask equipped with nitrogen inlet, condenser and stir bar was charged with 1-iodo-4-methoxy-2-nitrobenzene (500 mg, 1.79 mmol, 1.00 eq.), benzylamine (0.49 mL 480 mg, 4.48 mmol, 2.50 eq.), sulphur (S₈, 0.69 mg, 2.69 mmol, 1.50 eq.), dry pyridine (0.5 mL) and heated to 100 °C. After 24 h, the mixture was allowed to cool to rt, the formed solid triturated with CH₂Cl₂, adsorbed on silica gel, and purified by flash chromatography (*n*-hexane/EtOAc 25:1) to obtain **L6a** (344 mg, 1.43 mmol, 80%) as a beige solid.

TLC (*n*-hexane/EtOAc 25:1): *R*_f = 0.20.

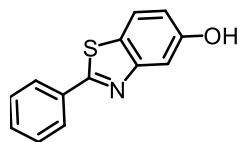
¹H NMR (300 MHz, CD₂Cl₂): δ = 8.13–8.04 (m, 2H, *H*_{Ar}), 7.77 (d, *J* = 8.8 Hz, 1H, *H*_{Ar}), 7.56 (d, *J* = 2.4 Hz, 1H, *H*_{Ar}), 7.54–7.45 (m, 3H, *H*_{Ar}), 7.04 (dd, *J* = 8.7, 2.5 Hz, 1H, *H*_{Ar}), ppm.

¹³C NMR (75 MHz, CD₂Cl₂): δ = 169.4, 159.6, 155.9, 134.2, 131.3, 129.4 (2C), 127.7 (2C), 127.3, 122.7, 115.7, 106.0, 56.0 (*C*_{Aliph}) ppm.

IR (ATR): $\tilde{\nu}$ = 3071 (w), 2997 (w), 2940 (w), 1597 (m), 1552 (w), 1506 (w), 1456 (s), 1421 (m), 1322 (m), 1277 (m), 1242 (m), 1194 (m), 1160 (m), 1134 (m), 1074 (m), 1019 (m), 964 (m), 832 (m), 805 (m), 764 (m), 693 (m), 640 (m), 607 (m), 472 (m), 436 (m) cm⁻¹.

HR-MS (ESI): *m/z* calcd. for C₁₄H₁₂S₁N₁O₁ [*M*+*H*]⁺: 242.0634, found 226.0636.

2-Phenylbenz[*d*]thiazole-5-ol (L6b)



The reaction was performed according to a slightly modified reported procedure.^[4b] A 50 mL flask equipped with nitrogen inlet, septum and stir bar was charged with a solution of BBr₃ (0.16 mL, 0.42 mg, 83.2 mmol, 4.00 eq.) in dry CH₂Cl₂ (5.00 mL) and cooled to –78 °C. Ligand **L6a** (100 mg, 4.14 μ mol, 1.00 eq) was dissolved in dry CH₂Cl₂ (2 mL) and added dropwise at –78 °C. The resulting green solution was allowed to warm up to rt and stirred for 17 h. Reaction control by TLC indicated full conversion, the reaction was quenched by careful addition of triethanolamine (1 mL) at 0 °C. After stirring for 10 min at rt, the resulting white paste was dissolved with aqueous HCl (36% w/w, 1 mL), adjusted to pH = 2 and heated to 75 °C for 2 h. The aqueous solution was

adjusted to pH 7 and extracted with EtOAc (3x50 mL). The combined organic layers were washed with brine (50 mL), dried over MgSO₄, and purified by column chromatography (*n*-hexane/EtOAc 1:1) yielding **L6b** (52.0 mg, 22.4 μmol, 54%) as a colorless solid.

TLC (*n*-hexane/EtOAc 1:1): *R*_f = 0.58.

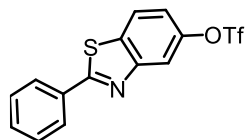
¹H NMR (300 MHz, DMSO-*d*₆): δ = 9.76 (s, 1H, OH), 8.10–8.01 (m, 2H, *H*_{Ar}), 7.89 (d, *J* = 8.7 Hz, 1H, *H*_{Ar}), 7.61–7.51 (m, 3H, *H*_{Ar}), 7.38 (d, *J* = 2.3 Hz, 1H, *H*_{Ar}), 6.97 (dd, *J* = 8.7, 2.3 Hz, 1H, *H*_{Ar}) ppm.

¹³C NMR (75 MHz, DMSO-*d*₆): δ = 167.9, 156.8, 155.0, 133.1, 131.1, 129.3 (2C), 126.9 (2C), 124.6, 122.4, 115.6, 107.8 ppm.

IR (ATR): $\tilde{\nu}$ = 3132 (m, br), 3052 (w), 2922 (w), 2851 (w), 1604 (m), 1507 (w), 1450 (s), 1385 (m), 1315 (m), 1231 (s), 1177 (m), 1101 (m), 1072 (m), 1026 (w), 977 (m), 954 (m), 873 (m), 846 (m), 801 (m), 758 (s), 681 (s), 641 (m), 611 (m), 502 (w), 470 (m), 436 (m) cm⁻¹.

HR-MS (ESI): *m/z* calcd. for C₁₃H₁₀SiN₁O₁ [M+H]⁺: 228.0478, found 228.0480.

2-Phenylbenz[*d*]thiazole-5-yl-trifluoromethanesulfonate (**L6c**)



A flame dried 10 mL flask equipped with nitrogen inlet, septum and stir bar was charged with ligand **L6b** (36.8 mg, 162 μmol, 1.00 eq.) and dry pyridine (150 μL, 1.85 mmol, 11.4 eq.) in dry CH₂Cl₂ (2.5 mL) and cooled to –78 °C. To this suspension, Tf₂O (41.0 mL, 243 μmol, 1.5 eq.) was added dropwise at –78 °C. The resulting dark solution was allowed to warm up to rt overnight. After stirring for 16 h, reaction control by TLC indicated full conversion. The reaction was stopped by addition of saturated, aqueous NH₄Cl (15 mL). The aqueous layer was removed and extracted with EtOAc (4x20 mL). The combined organic layers were dried over MgSO₄, concentrated and purified by column chromatography (*n*-hexane/EtOAc 6:1) yielding ligand **L6c** (514 mg, 143 μmol, 88%) as colorless solid.

TLC (*n*-hexane/EtOAc 6:1): *R*_f = 0.50.

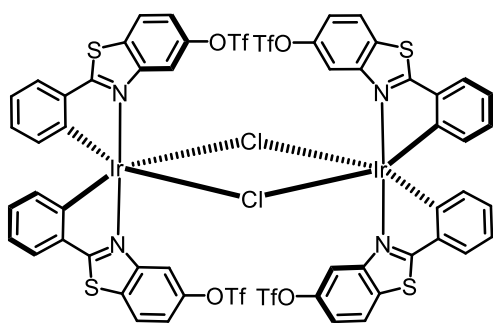
¹H NMR (300 MHz, CD₂Cl₂): δ = 8.11–8.01 (m, 2H, *H*_{Ar}), 7.97 (d, *J* = 2.3 Hz, 1H, *H*_{Ar}), 7.92 (d, *J* = 8.9 Hz, 1H, *H*_{Ar}), 7.56–7.45 (m, 3H, *H*_{Ar}), 7.31 (dd, *J* = 8.9, 2.3 Hz, 1H, *H*_{Ar}) ppm.

^{13}C NMR (75 MHz, CD_2Cl_2): δ = 171.8, 155.2, 148.6, 135.6, 133.4, 132.1, 129.6 (2C), 128.0 (2C), 123.3, 119.2 (q, J_{CF} = 320 Hz, CF_3), 118.8, 116.2 ppm.

IR (ATR): $\tilde{\nu}$ = 3083 (w), 2924 (w), 1444 (m), 1407 (m), 1318 (w), 1210 (s), 1134 (s), 1099 (m), 1031 (w), 940 (m), 878 (w), 847 (m), 817 (m), 768 (m), 742 (m), 681 (m), 620 (s), 587 (s), 501 (m), 491 (w), 430 (w) cm^{-1} .

HR-MS (ESI): m/z calcd. for $\text{C}_{14}\text{H}_9\text{S}_2\text{N}_1\text{O}_3\text{F}_3$ $[\text{M}+\text{H}]^+$: 359.9974, found 344.9974.

Dimer *rac*-C1e



According to procedure A, ligand **L6c** (39.9 mg, 111 μmol , 1.80 eq.), iridium(III) chloride hydrate (21.8 mg, 61.7 μmol , 1.00 eq.) and ethoxyethanol (2.5 mL) were used. After 16 h, the crude product was purified with flash chromatography $\text{CH}_2\text{Cl}_2/n$ -hexane (7:1) as eluent to remove side products. The main product was eluted with $\text{CH}_2\text{Cl}_2/\text{MeOH}$ (75:1). The

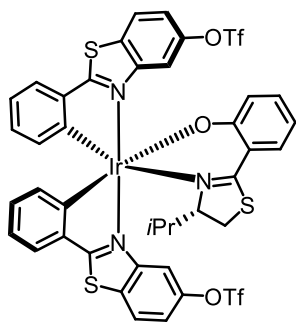
iridium(III) dimer complex *rac*-C1e (7.08 mg, 3.75 μmol , 7% based on the amount of starting ligand **L6c**) was obtained as an orange powder.

TLC ($\text{CH}_2\text{Cl}_2/n$ -hexane 7:1): R_f = 0.68.

^1H NMR (300 MHz, CD_2Cl_2): δ = 8.92 (d, J = 2.4 Hz, 4H), 7.72–7.61 (m, 8H, H_{Ar}), 7.17 (dd, J = 8.8, 2.4 Hz, 4H, H_{Ar}), 6.91–6.83 (m, 4H, H_{Ar}), 6.57–6.48 (m, 4H, H_{Ar}), 5.94–5.88 (m, 4H, H_{Ar}) ppm.

HR-MS (ESI): m/z calcd. for $\text{C}_{56}\text{H}_{28}\text{Cl}_1\text{F}_{12}\text{Ir}_2\text{N}_4\text{O}_{12}\text{S}_8$ $[\text{M}-\text{Cl}]^+$: 1852.8225, found 1852.8235.

Diastereomer Δ -(S)-C2h



According to procedure B, dimer *rac*-C1e (50.0 g, 26.5 mmol, 1.00 eq.), ancillary ligand (S)-AL1 (11.7 mg, 52.9 μ mol, 2.00 eq.), AgOTf (13.6 mg, 52.9 mmol, 2.00 eq.), Et₃N (33.0 mL, 238 mmol, 9.0 eq.), and EtOH (1 mL) were used. The resulting diastereomers were separated by flash column chromatography (CH₂Cl₂/*n*-hexane 13:2 \rightarrow CH₂Cl₂). The separated, first eluting diastereomer was further purified by flash chromatography (CH₂Cl₂/*n*-hexane 15:1) to obtain diastereomer Δ -(S)-C2h (16.6 mg, 14.7 μ mol, 28%) as red solid. The second eluting diastereomer was unstable on silica gel.

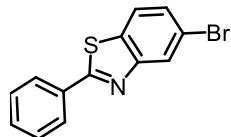
TLC (CH₂Cl₂/*n*-hexane 15:1): *R*_f = 0.30.

¹H NMR (300 MHz, CD₂Cl₂): δ = 9.06 (d, *J* = 2.5 Hz, 1H, *H*_{Ar}), 8.02 (d, *J* = 8.8 Hz, 1H, *H*_{Ar}), 7.92–7.84 (m, 1H, *H*_{Ar}), 7.84–7.77 (m, 1H, *H*_{Ar}), 7.71–7.64 (m, 2H, *H*_{Ar}), 7.39 (dd, *J* = 8.8, 2.5 Hz, 1H, *H*_{Ar}), 7.34 (dd, *J* = 8.8, 2.5 Hz, 1H, *H*_{Ar}), 7.20–7.14 (m, 1H, *H*_{Ar}), 7.02–6.90 (m, 3H, *H*_{Ar}), 6.80–6.70 (m, 3H, *H*_{Ar}), 6.57–6.50 (m, 1H, *H*_{Ar}), 6.20–6.08 (m, 2H, *H*_{Ar}), 4.41–4.31 (m, 1H, *CH*_{aliph}), 3.35 (dd, *J* = 12.1, 9.8 Hz, 1H, *CH*_{aliph}), 3.02 (dd, *J* = 12.1, 1.9 Hz, 1H, *CH*_{aliph}), 0.64–0.47 (m, 1H, *CH*_{*i*Pr}), 0.39 (d, *J* = 6.9 Hz, 3H, *CH*₃), 0.19 (d, *J* = 6.9 Hz, 3H, *CH*₃). ppm.

HR-MS (ESI): *m/z* calcd. for C₄₀H₂₉F₆IrN₃O₇S₅ [*M*+*H*]⁺: 1130.0132, found 1130.0138.

3.4.13 Ligand L5, Dimer *rac*-C1f and Diastereomers Δ -(S)-C2i and Δ -(S)-C2j

5-Bromo-2-phenylbenz[d]thiazole (L5)



The reaction was performed according to a slightly modified literature procedure.^[5b] A 25 mL flask equipped with nitrogen inlet, condenser and a strong stir bar was charged with a suspension of 1,4-dibromo-2-nitrobenzene (2.54 g, 9.04 mmol, 1.00 eq.), benzylamine (2.5 mL, 22.6 mmol, 2.50 eq.), sulphur (3.47 g, 13.6 mmol, 1.50 eq.), and pyridine (2 mL, freshly distilled). The resulting black suspension was heated to 100 °C and stirred at reflux for 24 h. After cooling the mixture to rt, the solidified red mixture was triturated with CH₂Cl₂. The insoluble remains were filtered, rinsed with CH₂Cl₂ until colorless, and discarded. The filtrate was concentrated under reduced

pressure, adsorbed on silica gel, and purified by flash column chromatography (*n*-hexane/EtOAc 100:1 → 80:1). The obtained yellow solid was recrystallized from MeOH to afford ligand **L5** as colorless, crystalline solid (1.87 g, 6.44 mmol, 71%).

TLC (*n*-hexane/EtOAc 50:1): R_f = 0.20.

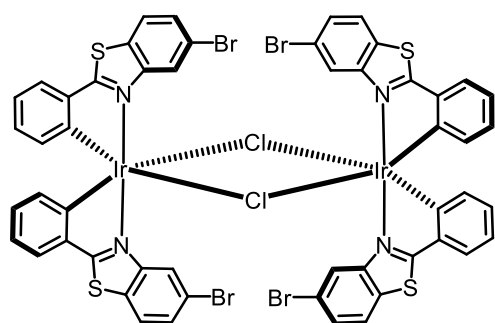
^1H NMR (300 MHz, CDCl_3): δ = 8.23 (d, J = 1.7 Hz, 1H, H_{Ar}), 8.09–8.06 (m, 2H, H_{Ar}), 7.77 (d, J = 8.9 Hz, 1H, H_{Ar}), 7.52–7.48 (m, 4H, H_{Ar}) ppm.

^{13}C NMR (75 MHz, CDCl_3): δ = 169.8, 155.5, 134.0, 133.4, 131.5, 129.3, 128.4, 127.8, 126.3, 122.8 120.1 ppm.

IR (ATR): $\tilde{\nu}$ = 3074 (w), 3020 (w), 1960 (w), 1888 (w), 1747 (w), 1688 (w), 1574 (w), 1536 (w), 1507 (w), 1469 (m), 1418 (m), 1309 (m), 1255 (m), 1219 (m), 1154 (w), 1104 (w), 1067 (m), 959 (m), 917 (m), 879 (m), 801 (m), 758 (s), 724 (m), 682 (s), 622 (s), 554 (m), 467 (m), 428 (w) cm^{-1} .

HR-MS (ESI): m/z calcd. for $\text{C}_{13}\text{H}_8\text{BrNS}$ $[\text{M}+\text{H}]^+$: 291.9624, found 291.9615.

Dimer *rac*-**C1f**



According to procedure A, ligand **L5** (1.00 g, 3.45 mmol, 1.00 eq.) and iridium(III) chloride trihydrate (608 mg, 1.72 mmol, 1.00 eq.) were used. Instead of pure ethoxyethanol a 3:1 mixture of ethoxyethanol (50 mL) and water (17 mL) was used to provide a cleaner reaction. To completely consume the ligand, additional iridium(III)chlorate trihydrate (183 mg, 0.51 mmol, 0.30 eq.) was added. After cooling to rt, the mixture was diluted with CH_2Cl_2 (100 mL) and filtered through a plug of celite which was rinsed with CH_2Cl_2 (600 mL). After purification by silica gel column chromatography (*n*-hexane/ CH_2Cl_2 1:1 → 1:3) dimer *rac*-**C1f** was obtained as an orange solid (973 mg, 604 μmol , 70% based on the amount of starting ligand **L5**).

TLC (*n*-hexane/ CH_2Cl_2 1:1): R_f = 0.23.

¹H NMR (300 MHz, CD₂Cl₂): δ = 9.18 (d, *J* = 1.7 Hz, 1H, *H*_{Ar}), 7.65 (dd, *J* = 7.6, 1.0 Hz 1H, *H*_{Ar}), 7.49 (d, *J* = 8.6 Hz, 1H, *H*_{Ar}), 7.30 (dd, *J* = 8.6, 1.8 Hz, 1H, *H*_{Ar}), 6.90–6.84 (m, 1H, *H*_{Ar}) 6.55 (dt, *J* = 7.2, 0.4 Hz, 1H, *H*_{Ar}), 5.90 (d, *J* = 7.7 Hz, 1H, *H*_{Ar}) ppm.

¹³C NMR (125 MHz, CD₂Cl₂): δ = 182.2, 152.4, 145.0, 141.1, 133.2, 131.1, 130.9, 128.1, 126.5, 125.1, 123.5, 122.5, 120.6 ppm.

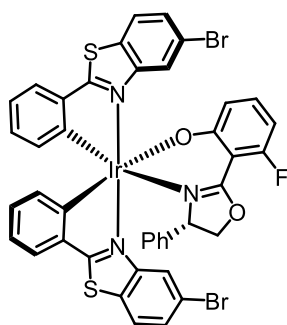
IR (ATR): $\tilde{\nu}$ = 3085 (w), 3053 (w), 1572 (m), 1460 (m), 1434 (m), 1398 (s) 1282 (m), 1158 (w), 1122 (w), 1062 (m), 1026 (m), 986 (m), 876 (m), 784 (m), 725 (s), 644 (m), 456 (m), 439 (m) cm⁻¹.

HR-MS (ESI): *m/z* calcd.: C₅₂H₂₈Br₄Cl₂Ir₂N₄S₄ [M]⁺: 1611.6498, found 1611.6497.

Diastereomers Λ -(*S*)-C2i and Λ -(*S*)-C2i

According to procedure B, dimer *rac*-C1f (424 mg, 263 μmol, 1.00 eq.), ancillary ligand (*S*)-AL2 (158 mg, 579 μmol, 2.20 eq.), AgOTf (151 mg, 579 μmol, 2.20 eq.), Et₃N (0.913 mL, 675 mg, 2.63 mmol, 10.0 eq.), CH₃CN (83 μL), and EtOH (10.0 mL) were used. The resulting diastereomers were separated by flash column chromatography (CH₂Cl₂/*n*-hexane 9:1, two runs). Both diastereomers were once again purified by flash column chromatography (*n*-hexane/EtOAc 5:2) to yield Λ -(*S*)-C2i (248.5 mg, 242 μmol, 46%) and Λ -(*S*)-C2i (237.2 mg, 231 μmol, 44%) as a red solid.

Diastereomer Λ -(*S*)-C2i



TLC (CH₂Cl₂/*n*-hexane 9:1): *R*_f = 0.40, (*n*-hexane/EtOAc 5:2) *R*_f = 0.33.

¹H NMR (300 MHz, CD₂Cl₂): δ = 8.91 (d, *J* = 1.5 Hz, 1H, *H*_{Ar}), 8.12 (d, *J* = 1.7 Hz, 1H, *H*_{Ar}), 7.74 (d, *J* = 8.6 Hz, 1H, *H*_{Ar}), 7.66–7.63 (m, 1H, *H*_{Ar}), 7.57–7.53 (m, 2H, *H*_{Ar}), 7.50 (dd, *J* = 8.6, 1.8 Hz, 1H, *H*_{Ar}), 7.47–7.44 (m, 1H, *H*_{Ar}), 6.98–6.86 (m, 4H, *H*_{Ar}), 6.78–6.64 (m, 5H, *H*_{Ar}), 6.42–

6-37 (m, 3H, H_{Ar}), 5.97 (d, $J = 7.7$ Hz, 1H, H_{Ar}), 5.94–5.89 (m, 1H, H_{Ar}), 5.00 (t, $J = 9.3$ Hz, 1H, H_{aliph}), 4.89 (dd, $J = 9.4, 3.5$ Hz, 1H, H_{aliph}), 4.15 (dd, $J = 9.3, 3.5$ Hz, 1H, H_{aliph}) ppm.

^{13}C NMR (75 MHz, CD_2Cl_2): $\delta = 183.2, 182.2, 174.1, 174.0, 165.0, 164.4, 161.5, 155.0, 152.5, 151.8, 148.8, 141.9$ (2C), 140.6, 135.7, 133.7, 133.5, 132.9, 131.4, 131.3, 130.7, 128.5, 128.4, 128.0, 127.0, 126.8, 125.7, 125.0, 124.5, 123.3, 122.1, 121.5, 121.4, 121.3, 120.0 (2C), 102.4, 102.3, 100.6, 100.3, 76.3, 69.7, 30.1 ppm.

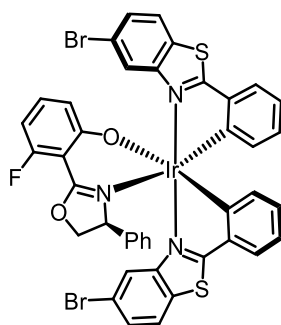
^{19}F NMR (283 MHz, CD_2Cl_2): $\delta = -106.1$ (s, CF) ppm.

IR (ATR): $\tilde{\nu} = 3048$ (w), 2969 (w), 2921 (w), 2898 (w), 1614 (s), 1578 (s), 1531 (m), 1436 (s), 1404 (s), 1379 (m), 1318 (w), 1284 (m), 1218 (s), 1153 (m), 1101 (w), 1033 (m), 990 (m), 934 (w), 903 (m), 788 (s), 730 (s), 692 (s), 647 (w), 622 (w), 579 (s), 531 (m), 447 (m), 403 (w).

HR-MS (LIFDI): m/z calcd. for $\text{C}_{41}\text{H}_{25}\text{Br}_2\text{F}_1\text{IrN}_3\text{O}_2\text{S}_2 [\text{M}]^{+}$: 1026.9341, found 1026.9355.

CD (MeCN): λ ($\Delta\epsilon$, $\text{M}^{-1}\cdot\text{cm}^{-1}$) = 216 (+105), 231(−50), 256 (+12), 280 (−16), 339 (+49), 459 (−14) nm.

Diastereomer Δ -(*S*)-C2i



TLC ($\text{CH}_2\text{Cl}_2/n$ -hexane 9:1): $R_f = 0.22$, (n -hexane/EtOAc 5:2): $R_f = 0.23$.

^1H NMR (300 MHz, CD_2Cl_2): $\delta = 9.13$ (d, $J = 1.8$ Hz, 1H, H_{Ar}), 8.25 (d, $J = 1.7$ Hz, 1H, H_{Ar}), 7.89 (d, $J = 8.5$ Hz, 1H, H_{Ar}), 7.70-7.67 (m, 1H, H_{Ar}), 7.64-7.58 (m, 3H, H_{Ar}), 7.45 (dd, $J = 8.6, 1.8$ Hz, 1H, H_{Ar}), 7.07–7.05 (m, 3H, H_{Ar}), 6.92–6.68 (m, 6H, H_{Ar}), 6.27–6.21 (m, 1H, H_{Ar}), 6.18–6.15 (m, 2H, H_{Ar}), 6.03 (d, $J = 7.7$ Hz, 1H, H_{Ar}), 5.93–5.87 (m, 1H, H_{Ar}), 4.53 (dd, $J = 9.1, 6.2$ Hz, 1H, H_{aliph}), 4.34 (dd, $J = 10.0, 9.1$ Hz, 1H, H_{aliph}), 4.08 (dd, $J = 10.0, 6.2$ Hz, 1H, H_{aliph}) ppm.

^{13}C NMR (75 MHz, CD_2Cl_2): δ = 182.9, 182.7, 174.4, 163.9, 160.9, 152.6, 152.1 (2C), 150.6, 141.5, 140.8, 139.8, 136.2, 133.1, 132.9, 132.8, 131.1, 131.0 (2C), 130.0, 129.3, 128.9, 128.6, 128.1, 127.8 (br), 127.3, 126.4, 124.7, 124.1, 123.7 (2C), 123.1, 122.4, 121.2, 120.9, 118.6, 100.3, 100.0, 76.7, 69.4, 30.1 ppm.

^{19}F NMR (283 MHz, CD_2Cl_2): δ = -109.3 (s, CF) ppm

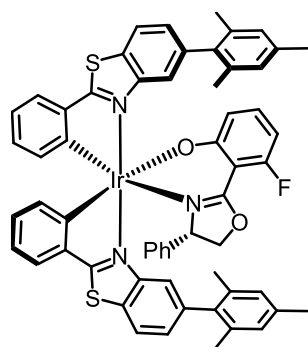
IR (ATR): $\tilde{\nu}$ = 3040 (w), 2952 (w), 2918 (w), 2852 (w), 1619 (s), 1578 (m), 1537 (m), 1438 (s), 1403 (s), 1347 (m), 1284 (m), 1224 (s), 1153 (m), 1123 (w), 1097 (m), 1030 (s), 986 (m), 945 (m), 904 (m), 859 (w), 787 (s), 728 (s), 696 (s), 620 (m), 579 (m), 531 (m), 446 (m) cm^{-1} .

HR-MS (LIFDI): m/z calcd. for $\text{C}_{41}\text{H}_{25}\text{Br}_2\text{F}_1\text{IrN}_3\text{O}_2\text{S}_2 [\text{M}]^{+}$: 1026.93413, found 1026.9253.

CD (MeCN): λ ($\Delta\epsilon$, $\text{M}^{-1}\cdot\text{cm}^{-1}$) = 217 (-114), 232 (+34), 258(-3), 280 (+13), 339 (-30), 499 (+7) nm.

3.4.14 Cross-Coupling Products Λ -(*S*)-C3l, Λ -(*S*)-C3m, Λ -(*S*)-C3n, and Λ -(*S*)-C3o

Cross-Coupling Product Λ -(*S*)-C3l



According to procedure C, iridium(III) complex Λ -(*S*)-C2i (50.0 mg, 49.0 μmol , 1.00 eq.), 2,4,6-trimethylphenylboronic acid (32.2 mg, 195 μmol , 4.00 eq.), K_3PO_4 (41.6 mg, 196 μmol , 4.00 eq.), $\text{Pd}(\text{OAc})_2$ (1.1 mg, 5.0 μmol , 10 mol%), SPhos (4.1 mg, 10.0 μmol , 20 mol%), and toluene (245 μL) were used. The crude product was purified by flash chromatography *n*-hexane/EtOAc (10:1 \rightarrow 5:1) to yield the iridium(III) complex Λ -(*S*)-C3l (51.0 mg, 46.0 μmol , 94%)

as an orange solid.

TLC (*n*-hexane/EtOAc 5:1): R_f = 0.33.

^1H NMR (500 MHz, CD_2Cl_2) δ = 8.45 (d, J = 1.2 Hz, 1H, H_{Ar}), 7.97 (d, J = 8.2 Hz, 1H, H_{Ar}), 7.73 (dd, J = 4.6, 3.4 Hz, 2H, H_{Ar}), 7.66 (dd, J = 7.6, 0.7 Hz, 1H, H_{Ar}), 7.35 (d, J = 7.5 Hz, 1H, H_{Ar}), 7.26 (dd, J = 8.2, 1.4 Hz, 1H, H_{Ar}), 7.20 (dd, J = 8.2, 1.5 Hz, 1H, H_{Ar}), 7.01 (s, 1H, H_{Ar}), 6.98–6.77 (m, 8H, H_{Ar}), 6.74–6.65 (m, 4H, H_{Ar}), 6.20–6.14 (m, 3H, H_{Ar}), 6.08 (d, J = 8.8 Hz, 1H, H_{Ar}), 5.92–5.89 (m, 1H, H_{Ar}), 4.72 (dd, J = 8.9, 3.4 Hz, 1H, H_{aliph}), 3.65 (dd, 1H, J = 8.9,

3.4 Hz, H_{aliph}), 3.61 (t, $J = 3.4$ Hz, 1H, H_{aliph}), 2.31 (s, 4H, H_{aliph}), 2.28 (s, 6H, CH_3), 2.06 (s, 6H), 2.02 (s, 3H), 1.95 (s, 6H), 1.79 (s, 3H) ppm.

^{13}C NMR (125 MHz, CD_2Cl_2) $\delta = 181.6, 180.7, 172.7$ (2C), 164.1, 163.2 (2C), 162.1, 154.4, 151.2, 151.1, 148.7, 142.7, 142.3, 141.0, 140.9, 140.6, 138.2, 138.0, 137.4, 136.7, 136.6, 136.0, 135.9, 135.8, 134.9, 133.2, 133.1, 133.0, 130.8, 130.6, 130.3, 130.2, 128.5, 128.3 (3C), 127.9, 127.2, 126.8, 126.5, 126.2, 125.4 (br), 123.4, 123.1, 121.9, 121.7, 121.1, 120.4, 120.3, 120.1, 100.8 (2C), 100.1, 99.9, 75.2, 70.0, 30.0, 21.2 (3C), 21.0, 20.5 (2C), 20.4 ppm.

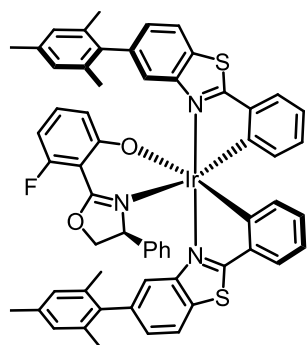
^{19}F NMR (283 MHz, CD_2Cl_2): $\delta = -105.2$ (s, CF) ppm.

IR (ATR): $\tilde{\nu} = 3050$ (w), 2920 (w), 2853 (w), 1730 (w), 1614 (m), 1580 (s), 1529 (m), 1491 (w), 1437 (s), 1409 (m), 1377 (m), 1319 (w), 1283 (m), 1218 (m), 1154 (w), 1099 (w), 1032 (m), 992 (m), 949 (w), 915 (w), 849 (w), 791 (m), 731 (s), 692 (m), 623 (w), 581 (w), 532 (w), 452 (w), 410 (w) cm^{-1} .

HR-MS (LIFDI): m/z calcd. for $\text{C}_{59}\text{H}_{47}\text{FIrN}_3\text{O}_2\text{S}_2$ $[\text{M}]^{+}$: 1105.2725, found 1105.2720.

CD (MeCN): λ ($\Delta\epsilon$, $\text{M}^{-1}\cdot\text{cm}^{-1}$) = 215 (+74), 232 (−42), 256 (0), 301 (−12), 339 (+32), 448 (−10) nm.

Cross-Coupling Product Δ -(S)-C3m



According to procedure C, iridium(III) complex Δ -(S)-C2i (50.0 mg, 49.0 μmol , 1.00 eq.), 2,4,6-trimethylphenylboronic acid (32.2 mg, 195 μmol , 4.00 eq.), K_3PO_4 (41.6 mg, 196 μmol , 4.00 eq.), $\text{Pd}(\text{OAc})_2$ (1.1 mg, 5.0 μmol , 10 mol%), SPhos (4.1 mg, 10.0 μmol , 20 mol%), and toluene (245 μL) were used. The crude product was purified by flash chromatography *n*-hexane/EtOAc (10:1 \rightarrow 5:2) to yield the iridium(III) complex Δ -(S)-C3m (49.7 mg, 45.0 μmol ,

92%) as an orange solid.

TLC (*n*-hexane/EtOAc 5:2): $R_f = 0.33$.

^1H NMR (500 MHz, CD_2Cl_2) $\delta = 8.66$ –8.64 (m, 1H, H_{Ar}), 8.07 (dd, $J = 8.2, 0.5$ Hz, 1H, H_{Ar}), 7.83–7.79 (m, 2H, H_{Ar}), 7.70 (ddd, $J = 7.6, 0.8, 0.5$ Hz, 2H, H_{Ar}), 7.52 (dd, $J = 1.1, 0.4$ Hz, 1H, H_{Ar}), 7.32 (dd, $J = 8.2, 1.6$ Hz, 1H, H_{Ar}), 7.10 (s br, 1H, H_{Ar}), 7.04 (dd, $J = 8.2, 1.4$ Hz, 1H, H_{Ar}), 7.02 (s br, 1H, H_{Ar}), 6.97–6.93 (m, 1H, H_{Ar}), 6.90 (s br, 1H, H_{Ar}), 6.85–6.29 (m, 2H, H_{Ar}),

6.82 (s br, 1H, H_{Ar}), 6.80–6.74 (m, 2H, H_{Ar}), 6.48–6.42 (m, 3H, H_{Ar}), 6.39–6.32 (m, 4H, H_{Ar}), 6.11–6.07 (m, 1H, H_{Ar}), 5.93–5.88 (m, 1H, H_{Ar}), 4.31 (dd, $J = 8.1, 4.6$ Hz, 1H, H_{aliph}), 4.03–3.92 (m, 2H, H_{aliph}), 2.44 (s, 3H, H_{aliph}), 2.28 (s, 3H, CH_3), 2.06 (s, 6H, CH_3), 1.85 (s, 3H), 1.68 (s, 3H) ppm.

^{13}C NMR (125 MHz, CD_2Cl_2): $\delta = 181.5, 180.9, 174.0, 173.9, 163.2, 163.1, 161.1, 151.7, 151.4, 151.1, 150.6, 142.5, 141.5$ (2C), 140.9, 139.5, 138.4, 137.8, 137.2, 137.0, 136.7 (2C), 136.4, 136.0, 135.8, 132.9, 132.6, 132.5, 130.4, 130.1, 129.3, 128.6, 128.5, 128.4 (2C), 128.2, 127.8, 127.6, 127.1, 127.0, 125.9, 122.7 (2C), 122.5, 122.2, 121.0, 120.3, 118.6 (2C), 104.1 (2C), 99.9, 99.7, 76.5, 68.8, 21.3, 21.2, 21.1, 21.0, 20.5, 20.4, 20.3 ppm.

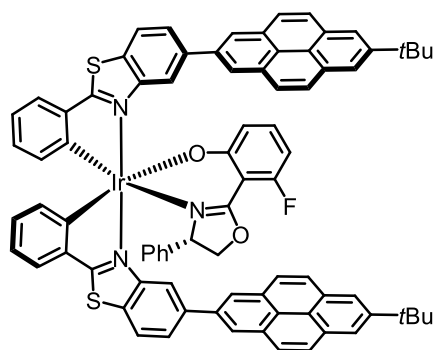
^{19}F NMR (283 MHz, CD_2Cl_2): $\delta = -108.1$ (s, CF) ppm.

IR (ATR): $\tilde{\nu} = 3049$ (w), 2955 (w), 2917 (w), 2853 (w), 1619 (s), 1582 (s), 1535 (m), 1441 (s), 1407 (m), 1377 (m), 1284 (m), 1224 (m), 1155 (w), 1096 (w), 1030 (m), 990 (m), 948 (w), 908 (w), 849 (w), 814 (w), 788 (m), 730 (s), 697 (s), 620 (w), 581 (m), 532 (w), 451 (w) cm^{-1} .

HR-MS (LIFDI): m/z calcd. for $C_{59}H_{47}FIrN_3O_2S_2$ $[M]^{+}$: 1105.2724, found 1105.2723.

CD (MeCN): λ ($\Delta\epsilon, M^{-1}\cdot cm^{-1}$) = 215 (–126), 230 (+63), 281 (+14), 338 (–35), 443 (+12) nm.

Cross-Coupling Product Λ -(S)-C3n



According to procedure C, iridium(III) complex Λ -(S)-C2i (50.0 mg, 49.0 μ mol, 1.00 eq.), 2-(7-(*tert*-butyl)-pyren-2-yl)-4,4,5,5-tetramethyl-1,3,2-dioxaborolane (**P2**, 75.3 mg, 196 μ mol, 4.00 eq.), K_3PO_4 (62.4 mg, 196 μ mol, 4.00 eq.), $Pd(OAc)_2$ (1.1 mg, 5.00 μ mol, 10 mol%), SPhos (4.1 mg, 10.0 μ mol, 20 mol%), toluene (250 μ L), and water (25 μ L, degassed)

were used. The crude product was purified by flash chromatography *n*-hexane/EtOAc (10:1 \rightarrow 5:1 \rightarrow 5:2 \rightarrow EtOAc) to yield the iridium(III) complex Λ -(S)-C3n (62.2 mg, 45.0 μ mol, 92%) as an orange solid.

TLC (*n*-hexane/EtOAc 5:2): $R_f = 0.15$.

1H NMR (500 MHz, CD_2Cl_2): $\delta = 9.49$ (d, $J = 1.4$ Hz, 1H, H_{Ar}), 8.50–8.47 (m, 3H, H_{Ar}), 8.47–8.43 (m, 1H, H_{Ar}), 8.28 (s, 2H, H_{Ar}), 8.24 (s, 2H, H_{Ar}), 8.21 (s, 1H, H_{Ar}), 8.19 (s, 1H, H_{Ar}), 8.13–

8.05 (m, 6H, H_{Ar}), 7.98–7.92 (m, 1H, H_{Ar}), 7.89 (d, $J = 8.3$ Hz, 1H, H_{Ar}), 7.86–7.80 (m, 1H, H_{Ar}), 7.68 (d, $J = 7.5$ Hz, 1H, H_{Ar}), 7.33 (d, $J = 7.5$ Hz, 1H, H_{Ar}), 7.22–7.15 (m, 1H, H_{Ar}), 7.06–5.92 (m, 12H, H_{Ar}), 4.87 (dd, $J = 9.4, 3.8$ Hz, 1H, H_{Ar}), 4.49 (t, $J = 9.4$ Hz, 1H, H_{aliph}), 3.89 (dd, $J = 9.1, 3.8$ Hz, 2H, H_{aliph}), 1.61 (s, 9H, $C(CH_3)_3$), 1.58 (s, 9H, $C(CH_3)_3$) ppm.

^{13}C NMR (125 MHz, CD_2Cl_2): $\delta = 182.4, 181.1, 173.0$ (2C), 164.4, 163.2 (2C), 162.3, 153.8, 152.0, 151.9, 149.4 (2C), 148.1, 142.2, 141.9, 140.7, 140.5, 138.5, 137.3, 134.6, 133.4, 133.3, 132.5, 131.6, 131.4 (2C), 131.0 (2C), 130.7, 130.5, 130.4, 128.3, 127.8, 127.6 (2C), 127.1, 126.3, 125.0, 124.7, 123.9, 123.8 (2C), 123.6, 123.3, 122.6 (2C), 122.5, 122.4, 121.8, 121.7, 120.8, 120.4, 118.5, 101.5 (2C), 100.4, 100.2, 75.2, 70.0, 35.2 (2C), 31.7 (2C), 29.7 ppm.

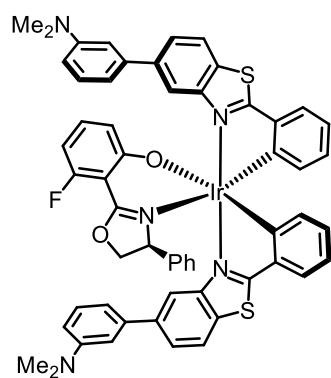
^{19}F NMR (283 MHz, CD_2Cl_2): $\delta = -103.9$ (s, CF) ppm.

IR (ATR): $\tilde{\nu} = 3045$ (w), 2956 (w), 2923 (m), 2856 (w), 1725 (w), 1615 (s), 1585 (s), 1531 (w), 1442 (s), 1410 (m), 1380 (m), 1319 (w), 1285 (m), 1250 (w), 1222 (m), 1154 (w), 1101 (w), 1035 (m), 995 (m), 925 (m), 881 (m), 813 (m), 793 (m), 760 (m), 719 (m), 694 (m), 626 (w), 587 (w), 533 (w), 495 (w), 450 (w), 403 (w) cm^{-1} .

HR-MS (LIFDI): m/z calcd. for $C_{81}H_{59}IrN_3O_2S_2$ $[M]^{+}$: 1381.3662, found 1381.3666.

CD (MeCN): λ ($\Delta\epsilon$, $M^{-1}\cdot cm^{-1}$) = 214 (+33), 229 (+4), 259 (+69), 292 (−106), 318 (−30), 326 (−46), 333 (−22), 342 (−97), 376 (+15), 454 (−91) nm.

Cross-Coupling Product Δ -(S)-C3o



According to procedure C, iridium(III) complex Δ -(S)-C2i (50.0 mg, 49.0 μ mol, 1.00 eq.), (3-(dimethylamino)phenyl)boronic acid (32.2 mg, 196 μ mol, 4.00 eq.), K_3PO_4 (41.6 mg, 196 μ mol, 4.00 eq.), $Pd(OAc)_2$ (1.1 mg, 5.0 μ mol, 10 mol%), SPhos (4.1 mg, 10.0 μ mol, 20 mol%), and toluene (245 μ L) were used. The crude product was purified by flash chromatography *n*-hexane/EtOAc (5:1 \rightarrow 5:2 \rightarrow EtOAc) to yield the iridium(III) complex Δ -(S)-C3o (30.3 mg, 27.0 μ mol, 55%) as

an orange solid.

TLC (*n*-hexane/EtOAc 5:2): $R_f = 0.15$.

¹H NMR (500 MHz, CD₂Cl₂): δ = 9.20 (d, J = 1.7 Hz, 1H, H_{Ar}), 8.22 (d, J = 1.6 Hz, 1H, H_{Ar}), 8.06 (d, J = 8.4 Hz, 1H, H_{Ar}), 7.84 (dd, J = 8.4, 1.7 Hz, 1H, H_{Ar}), 7.81 (d, J = 8.2 Hz, 1H, H_{Ar}), 7.64–7.59 (m, 2H, H_{Ar}), 7.54 (dd, J = 8.2, 1.7 Hz, 1H, H_{Ar}), 7.43–7.39 (m, 1H, H_{Ar}), 7.16–7.12 (m, 1H, H_{Ar}), 6.99–6.97 (m, 1H, H_{Ar}), 6.94–6.91 (m, 1H, H_{Ar}), 6.90–6.82 (m, 5H, H_{Ar}), 6.78–6.68 (m, 3H, H_{Ar}), 6.66–6.63 (m, 1H, H_{Ar}), 6.55–6.51 (m, 2H, H_{Ar}), 6.41–6.36 (m, 2H, H_{Ar}), 6.30–6.26 (m, 2H, H_{Ar}), 6.26–6.22 (m, 1H, H_{Ar}), 6.00–5.95 (m, 2H, H_{Ar}), 4.34 (dd, J = 8.9, 7.0 Hz, 1H, H_{aliph}), 4.22 (dd, J = 9.9, 8.9 Hz, 1H, H_{aliph}), 4.13 (dd, J = 9.9, 7.0 Hz, 1H, H_{aliph}), 3.04 (s, 6H, H_{aliph}), 2.79 ppm (s, 6H, H_{aliph}).

¹³C NMR (125 MHz, CD₂Cl₂): δ = 181.7, 181.6, 174.0, 173.9, 163.6, 163.3 (2C), 161.6, 152.1, 151.8, 151.6, 151.5, 150.2, 142.8, 142.4, 142.1 (2C), 141.3, 140.6, 139.2, 135.8, 133.1, 133.0, 132.8, 130.6, 130.5 (2C), 129.9, 129.8, 129.7, 128.2, 127.9, 127.7, 126.8, 125.9 (2C), 125.1, 123.0, 122.5, 122.2, 120.9, 119.6, 119.5, 119.3, 119.2, 117.5 (2C), 115.8, 112.6, 112.4 (2C), 111.5, 104.2, 104.1, 100.2, 100.1, 76.2, 69.7, 41.0, 40.7, 30.1 ppm.

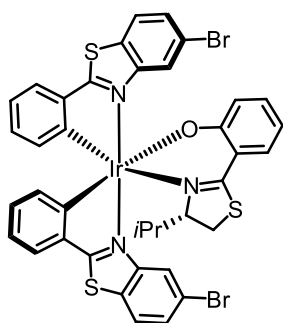
¹⁹F NMR (283 MHz, CD₂Cl₂): δ = –107.9 ppm (s, CF).

IR (ATR): $\tilde{\nu}$ = 3050 (w), 2958 (w), 2921 (w), 2851 (w), 2798 (w), 1726 (w), 1618 (s), 1582 (s), 1540 (m), 1494 (w), 1438 (s), 1405 (m), 1377 (m), 1351 (m), 1284 (m), 1253 (w), 1222 (m), 1154 (w), 1095 (m), 1028 (s), 988 (m), 954 (w), 916 (w), 850 (w), 761 (s), 729 (m), 694 (s), 667 (m), 623 (w), 581 (w), 531 (w), 495 (w), 447 (w) cm^{–1}.

HR-MS (LIFDI): m/z calcd. for C₅₇H₄₅FIrN₅O₂S₂ [M]⁺: 1107.2628, found 1107.2611.

CD (MeCN): λ ($\Delta\epsilon$, M^{–1}·cm^{–1}) = 216 (–92), 230 (–47), 234 (–49), 266 (+47), 347 (–12) 494 (+9) nm.

Diastereomers Λ -(S)-C2g



According to procedure B, dimer **rac-C1f** (30.0 mg, 18.6 μ mol, 1.00 eq.), ancillary ligand **(S)-AL1** (8.2 mg, 37.2 μ mol, 1.00 eq.), AgOTf (9.6 mg, 37.2 μ mol, 2.00 eq.), Et₃N (18 μ L, 13.0 mg, 13.1 μ mol, 10.0 eq.), and EtOH (0.4 mL) were used. The crude product was purified by flash chromatography (basic aluminium oxide, *n*-hexane:CH₂Cl₂ 1:1 \rightarrow 1:8) to yield diastereomer **Λ -(S)-C2g** (13.0 mg, 13.1 μ mol, 35%) as a red solid.

TLC (CH₂Cl₂/*n*-hexane 10:1): R_f = 0.29.

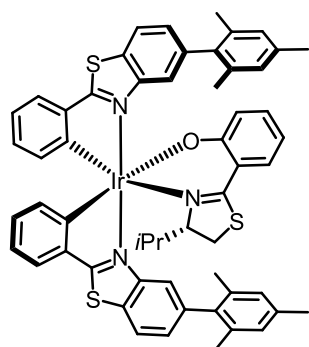
¹H NMR (300 MHz, CD₂Cl₂): δ = 9.04 (d, *J* = 1.8 Hz, 1H, *H*_{Ar}), 7.90 (d, *J* = 1.7 Hz, 1H, *H*_{Ar}), 7.80 (d, *J* = 8.5 Hz, 1H, *H*_{Ar}), 7.76 (d, *J* = 7.9 Hz, 1H, *H*_{Ar}), 7.71 (d, *J* = 8.6 Hz, 1H, *H*_{Ar}), 7.64 (dd, *J* = 7.3, 0.4 Hz, 1H, *H*_{Ar}), 7.53 (dt, *J* = 8.2, 1.8 Hz 1H, *H*_{Ar}), 7.27 (dd, *J* = 7.3, 0.8 Hz, 1H, *H*_{Ar}), 7.07–7.01 (m, 1H, *H*_{Ar}), 6.95–6.89 (m, 2H, *H*_{Ar}), 6.77–6.67 (m, 3H, *H*_{Ar}), 6.61 (dd, *J* = 8.0, 0.5 Hz, 1H, *H*_{Ar}), 6.21–6.11 (m, 2H, *H*_{Ar}), 4.54–4.50 (m, 1H, *H*_{aliph}), 3.63–3.56 (m, 1H, *H*_{aliph}), 3.03 (dd, *J* = 11.8, 1.6 Hz, 1H, *H*_{aliph}), 0.72–0.65 (m, 1H, *H*_{aliph}), 0.36 (d, *J* = 7.0 Hz, 3H, *H*_{aliph}), 0.22 (d, *J* = 6.9 Hz, 3H, *H*_{aliph}) ppm.

¹³C NMR (75 MHz, CD₂Cl₂): δ = 183.6, 182.4, 171.6, 168.8, 153.1, 152.8, 151.8, 151.4, 141.9, 141.8, 135.9, 133.8, 133.4, 132.5, 131.7, 130.9, 130.6, 129.0, 128.5, 127.1, 126.7, 125.5, 124.3, 124.2, 123.7, 122.5, 122.3 (2C), 122.0, 121.5, 121.3, 119.3, 113.9, 84.4, 31.9, 30.1, 28.2, 19.7, 14.8 ppm.

IR (ATR): $\tilde{\nu}$ = 3089 (w), 3051 (w), 3004 (w), 2954 (w), 2920 (w), 2856 (w), 1582 (m), 1549 (m), 1517 (m), 1435 (m), 1401 (m), 1355 (s), 1281 (m), 1245 (m), 1188 (m), 1146 (m), 1098 (m), 1057 (m), 995 (m), 946 (w), 901 (m), 846 (m), 794 (m), 731 (s), 652 (m), 556 (m), 522 (m), 448 (m) cm⁻¹.

HR-MS (ESI): *m/z* calcd. for C₃₈H₂₈Br₂IrN₃OS₃ [M+H]⁺: 991.9434, found 991.9444.

Cross-Coupling Product Λ -(*S*)-C3k



According to procedure C, iridium(III) complex Λ -(*S*)-C2g (40.0 mg, 40.4 μmol, 1.00 eq.), 2,4,6-trimethylphenylboronic acid (26.0 mg, 161 μmol, 4.00 eq.), K₃PO₄ (34.0 mg, 161 μmol, 4.00 eq.), Pd(OAc)₂ (0.9 mg, 4.04 μmol, 10 mol%), SPhos (3.3 mg, 8.08 μmol, 20 mol%), and toluene (200 μL) were used. The crude product was purified by flash chromatography CH₂Cl₂/*n*-hexane (10:1) to yield the iridium(III) complex Λ -(*S*)-C3k (25.0 mg, 23.4 μmol, 64%) as an orange solid.

TLC (CH₂Cl₂/*n*-hexane 10:1): *R*_f = 0.36.

¹H NMR (300 MHz, CD₂Cl₂): δ = 8.59 (d, *J* = 1.8 Hz, 1H, *H*_{Ar}), 7.93 (d, *J* = 6.8 Hz, 1H, *H*_{Ar}), 7.91 (d, *J* = 6.7 Hz, 1H, *H*_{Ar}), 7.77–7.71 (m, 1H, *H*_{Ar}), 7.65 (dd, *J* = 7.6, 0.9 Hz, 1H, *H*_{Ar}), 7.55 (d, *J* = 1.1 Hz, 1H, *H*_{Ar}), 7.28–7.19 (m, 2H, *H*_{Ar}), 7.17 (dd, *J* = 8.2, 1.7 Hz, 1H, *H*_{Ar}), 7.00–6.71 (m, 7H, *H*_{Ar}), 6.71–6.50 (m, 3H, *H*_{Ar}), 6.30 (d, *J* = 7.6 Hz, 1H, *H*_{Ar}), 6.24 (dd, *J* = 8.6, 1.0 Hz,

^1H , H_{Ar}), 6.17–6.08 (m, 1H, H_{Ar}), 4.38–4.28 (m, 1H, H_{aliph}), 2.54–2.46 (m, 1H, H_{aliph}), 2.31 (s, CH_3), 2.27–2.17 (m, 4H, H_{aliph}), 2.04 (s, 3H, CH_3), 1.98 (s, 6H, $2\times\text{CH}_3$), 1.49 (s, 3H, CH_3), 0.68–0.55 (m, 1H, H_{aliph}), 0.23 (d, $J = 7.0$ Hz, 3H, CH_3), 0.08 (d, $J = 6.7$ Hz, 3H, CH_3) ppm.

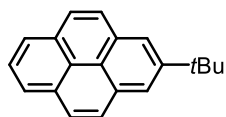
^{13}C NMR (75 MHz, CD_2Cl_2): $\delta = 181.3, 180.9, 170.5, 167.5, 152.7, 151.9, 151.4, 151.1, 142.6, 142.3, 141.2, 138.1, 138.0, 137.4, 137.0, 136.8, 136.3, 135.9, 135.7, 135.4, 133.4, 133.3, 132.9, 131.0, 130.2, 130.0, 128.6, 128.4, 128.3, 128.1, 127.8, 126.8, 126.6, 126.2, 124.3, 124.0, 123.1, 122.2, 122.0, 121.0, 120.6, 118.5, 113.3, 84.4, 31.7, 27.2, 21.4, 21.2, 21.2, 21.1, 20.9, 20.3, 19.6, 14.7$ ppm.

IR (ATR): $\tilde{\nu} = 3047$ (w), 2959 (w), 2915 (w), 2852 (w), 2052 (w), 1989 (w), 1899 (w), 1730 (w), 1598 (w), 1581 (m), 1552 (m), 1521 (m), 1491 (w), 1457 (w), 1435 (s), 1408 (w), 1375 (w), 1349 (w), 1284 (m), 1238 (w), 1195 (m), 1151 (m), 1121 (w), 1044 (w), 1009 (m), 989 (w), 945 (w), 908 (w), 880 (w), 849 (m), 813 (m), 791 (w), 735 (s), 694 (w), 675 (w), 633 (w), 616 (w), 588 (w), 556 (w), 528 (w), 451 (m), 423 (w) cm^{-1} .

HR-MS (ESI): m/z calcd. for $\text{C}_{56}\text{H}_{51}\text{IrN}_3\text{OS}_3$ $[\text{M}+\text{H}]^+$: 1070.2823, found 1070.2818.

3.4.15 Pyreneboronic Ester P2

2-(*tert*-Butyl)pyrene (P1)



P1 was synthesized according to literature known conditions.^[20] A 100 ml flask equipped with nitrogen inlet, septum and stir bar was charged with pyrene (5.00 g, 24.7 mmol, 1.00 eq.) and dissolved in dry CH_2Cl_2 (50 ml).

Tert-butyl chloride (2.52 g, 27.2 mmol, 1.10 eq.) was added to the pale-yellow solution. The reaction mixture was cooled to 0 °C and AlCl_3 (3.29 g, 24.7 mmol, 1.00 eq.) was added portion wise yielding a red suspension. After complete addition, the reaction was allowed to warm up to rt and stirred for 4 h after which TLC indicated full conversion. The reaction was quenched by careful addition of water at 0 °C. After stirring vigorously for 10 min, the aqueous layer was diluted with 100 mL water and the organic layer was separated. The aqueous layer was extracted with CH_2Cl_2 (3x100 mL), the combined organic layers were washed with brine (2x150 mL), dried over Na_2SO_4 , and concentrated under reduced pressure. The brown crude product was recrystallized from MeOH to yield compound **P1** (3.01 g, 11.7 mmol, 49%) as a beige solid.

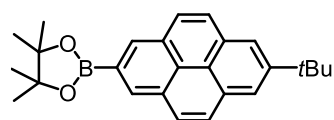
¹H NMR (300 MHz, CDCl₃): δ = 8.24–8.13 (m, 4H, *H*_{Ar}), 8.08–7.93 (m, 5H, *H*_{Ar}), 1.59 (s, 9H, C(CH₃)₃) ppm.

¹³C NMR (75 MHz, CDCl₃): δ = 149.2, 131.2, 131.2, 127.7, 127.6, 127.4, 125.6, 124.9, 122.4, 122.2, 35.4 (C(CH₃)₃), 32.1 (3C, C(CH₃)₃) ppm.

IR (ATR): $\tilde{\nu}$ = 3785 (w), 3092 (w), 3040 (m), 2952 (m), 2896 (m), 2863 (m), 2174 (w), 1852 (w), 1751 (w), 1633 (m), 1596 (w), 1466 (m), 1383 (m), 1356 (m), 1283 (w), 1217 (m), 1175 (m), 1140 (w), 1065 (w), 1023 (w), 956 (w), 918 (w), 874 (s), 838 (s), 810 (s), 750 (m), 707 (s), 553 (w), 524 (w), 496 (w), 445 (w) cm⁻¹.

HR-MS (ESI): *m/z* calcd. for C₂₀H₁₈ [M+H]⁺: 259.1492, found 259.1487.

2-(7-(*tert*-Butyl)pyren-2-yl)-4,4,5,5-tetramethyl-1,3,2-dioxaborolane (**P2**)



The reaction was performed according to a slightly modified literature procedure.^[20] A flame-dried SCHLENK tube (10 mL; threaded PTFE plug) equipped with stir bar was charged with [Ir(μ-OMe)(cod)₂] (33.7 mg, 50.8 μmol, 1.3 mol%), dtbpy (27.3 mg, 102 μmol, 2.6 mol%) and B₂Pin₂ (50.0 mg, 197 μmol, 5.0 mol%). The reactants were suspended in dry *n*-hexane (2 mL) and heated to 50 °C until the yellow suspension turned into a red solution. This solution was transferred into another SCHLENK tube containing a solution of 2-*t*Bu-pyrene (**P1**; 1.01 g, 3.91 mmol, 1.00 eq.) and B₂Pin₂ (1.27 g, 5.00 mmol, 1.28 eq.) in dry *n*-hexane (10 mL). The resulting mixture was stirred at 80 °C for 16 h under nitrogen atmosphere. The reaction mixture was filtered through a pad of silica gel and the filter cake was rinsed with CH₂Cl₂ (500 mL). The solvent was removed under reduced pressure to furnish a yellow residue, which was further purified by recrystallization from *n*-hexane. The beige solid was washed with cold *n*-hexane to obtain pinacolboronic ester **P2** (0.49 mg, 1.08 mmol, 52%) as a colorless solid.

¹H NMR (300 MHz, CDCl₃): δ = 8.61 (s, 2H, *H*_{Ar}), 8.21 (s, 2H, *H*_{Ar}), 8.09 (d, *J* = 9.0 Hz, 2H, *H*_{Ar}), 8.04 (d, *J* = 9.0 Hz, 2H, *H*_{Ar}), 1.59 (s, 9H, C(CH₃)₃), 1.47 (s, 12H, 4xCH₃) ppm.

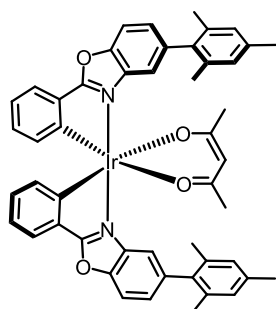
¹³C NMR (75 MHz, CDCl₃): δ = 149.8, 131.7, 131.3, 130.4, 127.8, 127.5, 126.5, 123.0, 122.3, 84.3 (2C, (C(CH₃)₂)₂), 35.4 (C(CH₃)₃), 32.1 (3C, CH₃), 25.2 (4C, CH₃) ppm.

IR (ATR): $\tilde{\nu}$ = 3038 (w), 2966 (m), 1629 (w), 1565 (m), 1460 (m), 1420 (s), 1357 (s), 1322 (m), 1293 (m), 1230 (s), 1134 (s), 1000 (m), 964 (m), 899 (m), 886 (m), 846 (m), 807 (m), 740 (s), 714 (w), 662 (w), 558 (w), 499 (w), 441 (w) cm⁻¹.

HR-MS (ESI): m/z calcd. for $C_{26}H_{29}B_1O_2Na_1$ $[M+Na]^+$: 407.2157, found 407.2161.

3.4.16 Acetylacetonate Complex 4d and 4e

Acac complex Λ -C4e



A flame-dried SCHLENK tube (10 mL; threaded PTFE plug) equipped with stir bar was charged with a suspension of iridium(III) complex Λ -(**S**)-**3a** (40.0 mg, 38.6 μ mol, 1.00 eq.) in CH_3CN (5 mL). Upon addition of TfOH (17.0 μ L, 193 μ mol, 5.0 eq.) the solid dissolved and turned from orange to yellow in a matter of seconds. After 5 min the solution was concentrated and subjected to silica gel flash chromatography (*n*-hexane/EtOAc/ CH_3CN 4:2:1).

The collected intermediate acetonitrile complex was directly dissolved in EtOH and freshly distilled acetylaceton and Et_3N were added. After stirring for 24 h at rt, all volatiles were removed under reduced pressure. The crude product was purified by flash chromatography (*n*-hexane/EtOAc 10:1 \rightarrow 5:1) and Λ -**C4e** (30.0 mg, 32.7 μ mol, 85%) obtained as an orange solid.

1H NMR (300 MHz, CD_2Cl_2): δ = 7.78–7.67 (m, 4H, H_{Ar}), 7.32 (dd, J = 1.5, 0.6 Hz, 2H, H_{Ar}), 7.23 (dd, J = 8.2, 1.7 Hz, 2H, H_{Ar}), 6.98–6.88 (m, 6H, H_{Ar}), 6.82–6.74 (m, 2H, H_{Ar}), 6.66–6.60 (m, 2H, H_{Ar}), 5.25 (s, 1H, CH_{Acac}), 2.30 (s, 6H, $2 \times CH_3$), 2.00 (s, 12H, $4 \times CH_3$). 1.62 (s, 6H, $2 \times CH_3$) ppm.

IR (ATR): $\tilde{\nu}$ = 2962 (w), 2914 (w), 1583 (w), 1513 (w), 1422 (w), 1385 (w), 1257 (m), 1085 (m), 1016 (s), 911 (w), 853 (w), 796 (s), 735 (w), 702 (w), 661 (w), 538 (w), 510 (w), 453 (w), 392 (w) cm^{-1} .

HR-MS (LIFDI): m/z calcd. for $C_{49}H_{43}IrN_2O_4$ $[M]^+$: 916.2856, found 916.2838.

HPLC (Daicel Chiralpak IB column (250 \cdot 4.6 mm), water + 0.1% TFA/ CH_3CN 18:82, flow rate = 0.5 mL \cdot min $^{-1}$, column temperature = 40 $^{\circ}C$, λ = 254 nm): t_R = 23.8 min (major), 27.9 min (minor); 99%ee.

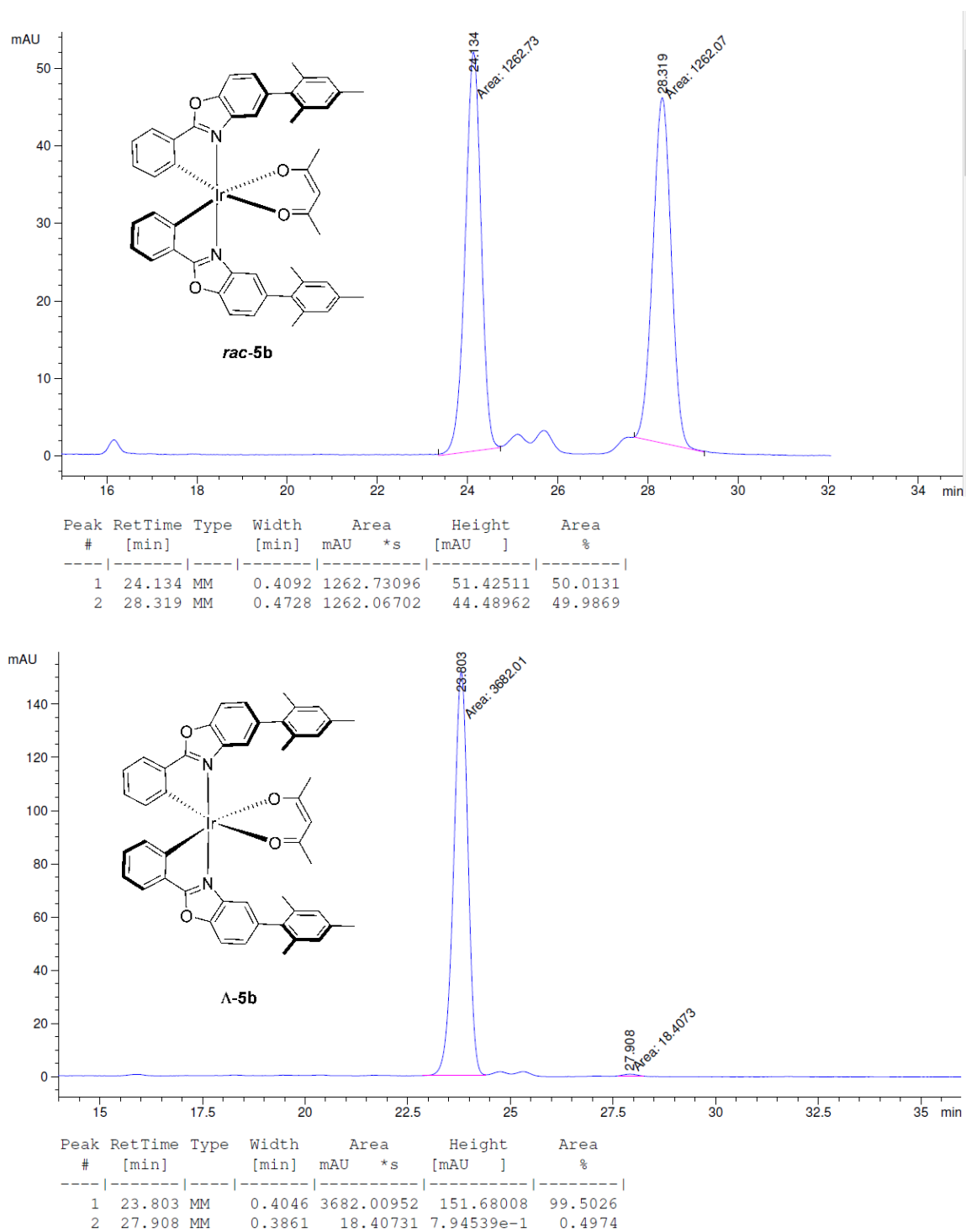
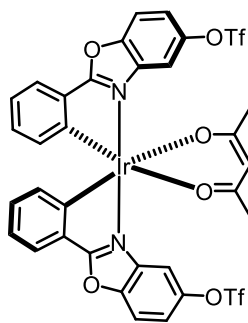


Figure 36: Chiral HPLC traces of *rac*-C4e (top) Λ -C4e (bottom). HPLC conditions: Daicel Chiralpak IB column (250 \times 4.6 mm), solvent A: 0.1% TFA in water, solvent B: MeCN, isocratic ratio A/B 18:82, flow rate: 0.5 mL \cdot min $^{-1}$, column temperature: 40 $^{\circ}$ C, UV absorption detected at λ = 254 nm.

Complex *rac-4d*

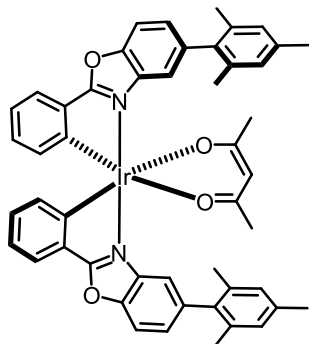


According to procedure B, dimer ***rac-C1a*** (370 mg, 203 μmol , 1.00 eq.), acetylacetone (62.2 μL , 609 μmol , 3.00 eq.), AgOTf (104 mg, 406 μmol , 2.00 eq.), Et₃N (281 μL , 2.03 mmol, 10.0 eq.), EtOH (3.0 mL), and CH₂Cl₂ (3.0 mL) were used. The mixture was stirred at rt for 24 h. After reaction control by TLC indicated full conversion, the solvent was removed under reduced pressure, and the crude product was purified by flash column chromatography (*n*-hexane/EtOAc 10:1 \rightarrow 5:2) to obtain complex ***rac-5a*** as a yellow-green solid (317 mg, 325 μmol , 80%). Single crystals for X-ray analysis were obtained by layering a CH₂Cl₂ solution of complex ***rac-4d*** with *n*-hexane.

¹H NMR (300 MHz, CD₂Cl₂): δ = 7.80 (d, J = 8.9 Hz, 2H, H_{Ar}), 7.77–7.71 (m, 2H, H_{Ar}), 7.47 (d, J = 2.5 Hz, 2H, H_{Ar}), 7.42 (dd, J = 8.9, 2.6 Hz, 2H, H_{Ar}), 7.02–6.94 (m, 2H, H_{Ar}), 6.85–6.77 (m, 2H, H_{Ar}), 6.55–6.48 (m, 2H, H_{Ar}), 5.39 (s, 1H, CH_{acac}), 1.86 (s, 6H, 2xCH₃) ppm

¹³C NMR (75 MHz, CD₂Cl₂): δ = 186.7, 181.1, 149.8, 147.8, 147.7, 140.0, 135.0, 132.4, 130.2, 127.0, 122.2, 119.2 (q, J = 321 Hz, CF₃), 119.0, 113.2, 110.4, 101.9, 28.1 ppm.

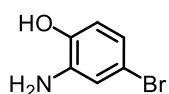
Complex *rac-C4e*



According to procedure C, iridium(III) acac complex ***rac-C4d*** (43.4 mg, 44.5 μmol , 1.00 eq.), 2,4,6-trimethylphenylboronic acid (21.9 mg, 134 μmol , 3.00 eq.), K₃PO₄ (28.3 mg, 134 μmol , 3.00 eq.), Pd(OAc)₂ (1.0 mg, 4.5 μmol , 10 mol%), SPhos (3.8 mg, 9.0 μmol , 20 mol%), and toluene (223 μL) were used. The crude product was purified by flash chromatography *n*-hexane/EtOAc (10:1 \rightarrow 5:1) to yield the racemic iridium(III) acac complex ***rac-5b*** (26.0 mg, 28.3 μmol , 64%) as a yellow solid. For analytical data see **Λ -C4e**.

3.4.17 Ligand L0a

2-Amino-4-bromo-phenol



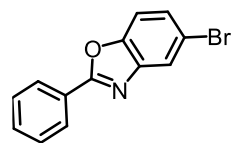
The reaction was performed according to a slightly modified reported procedure. A 100 mL flask equipped with septum and stir bar was charged with $\text{SnCl}_2 \cdot 2\text{H}_2\text{O}$ (6.90 g, 30.6 mmol, 5.00 eq.), MeOH (28 mL), aqueous HCl (15 mL, 36% w/w) and cooled to 0 °C. To this suspension, 4-bromo-2-nitrophenol (1.33 g, 6.12 mmol, 1.00 eq.) was added and the yellow solution was stirred vigorously for 6 h at rt until it become colorless, indicating full conversion. The mixture was neutralized to pH 7 with saturated aqueous NaOH solution, the formed colorless precipitate was filtered through a plug of celite and rinsed with MeOH and EtOAc until the filtrate remained colorless. The aqueous filtrate was extracted with EtOAc (3x100 mL), the combined organic layer dried over MgSO_4 , filtered and concentrated under reduced pressure to obtain phenol (0.94 g, 5.00 mmol, 82%) as a colorless solid, which darkens upon standing. The product was used without further purification.

TLC (*n*-hexane/EtOAc 6:1): R_f = 0.24.

^1H NMR (300 MHz, CD_3OD): δ = 6.83 (d, J = 2.3 Hz, 1H, H_{Ar}), 6.63 (dd, J = 8.3, 2.3 Hz, 1H, H_{Ar}), 6.56 (d, J = 8.3 Hz, 1H, H_{Ar}), 4.85 (s br, 3H, NH_2 , OH) ppm.

^{13}C NMR (75 MHz, CD_3OD): δ = 145.4, 138.7, 121.7, 119.1, 116.6, 112.7 ppm.

5-Bromo-2-phenylbenzo[d]oxazole (L0a)



The reaction was performed according to a slightly modified reported procedure.^[5a] A 250 mL flask equipped with condenser and stir bar was charged with phenol (940 mg, 5.00 mmol, 1.00 eq.), benzaldehyde (0.51 mL, 5.00 mmol, 1.00 eq.), *m*-xylene (25 mL) and stirred at 120 °C for 1 h before 4-MeO-TEMPO (46.6 mg, 0.25 mmol, 5.0 mol%) was added. The solution was vigorously stirred at 120 °C under O_2 -atmosphere (O_2 -balloon) for 24 h. The mixture was cooled to rt, concentrated, adsorbed on silica gel and purified by flash chromatography (*n*-hexane/EtOAc 10:1) yielding product **L0a** as a white solid (671 mg, 2.45 mmol, 50%).

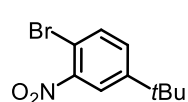
TLC (*n*-hexane/EtOAc 13:1): R_f = 0.40.

^1H NMR (300 MHz, CD_2Cl_2): δ = 8.26–8.22 (m, 2H, H_{Ar}), 7.91–7.89 (m, 1H, H_{Ar}), 7.60–7.48 (m, 5H, H_{Ar}) ppm.

HR-MS (ESI): m/z calcd. for $C_{13}H_9Br_1N_1O_1$ $[M+H]^+$: 275.9843, found 275.9854.

3.4.18 Ligand L9, Dimer *rac*-C1h, Diastereomers Λ -(*S*)-C2n, Λ -(*S*)-C2n and Cat. Λ -C5d

1-Brom-4-*tert*-butyl-2-nitrobenzene (S4a)

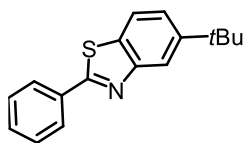


The reaction was performed according to a slightly modified reported procedure.^[56] A 10 mL flask equipped with septum and stir bar was charged with HNO_3 (2.2 mL, 53.3 mmol, 2.50 eq), H_2SO_4 (2.5 mL, 46.8 mmol, 2.20 eq) and cooled to 0 °C. To the cooled acid mixture, 4-*tert*-butyl-bromobenzene (4.54 g, 21.3 mmol, 1.00 eq) was added dropwise. The biphasic mixture was vigorously stirred for 14 h and slowly warmed up to rt. Complete conversion was indicated by TLC. The yellow suspension was the purred unto ice (15 g) and extracted with Et_2O (4x100 mL). The combined organic layers were dried over $MgSO_4$, concentrated and purified by flash column chromatography (*n*-hexane/ $EtOAc$ 20:1) to furnish nitrobenzene **S4a** as yellow oil (3.94 g, 14.9 mmol, 70%).

TLC (*n*-hexane/ $EtOAc$ 20:1): R_f = 0.34.

1H NMR (300 MHz, $CDCl_3$): δ = 7.83 (d, J = 8.5 Hz, 1H, H_{Ar}), 7.64 (d, J = 2.4 Hz, 1H, H_{Ar}), 7.44 (d, J = 8.5, 2.4 Hz, 1H, H_{Ar}), 1.34c (s, 9H, *t*Bu) ppm.

5-*tert*-Butyl-2-phenylbenz[d]thiazole (L9)



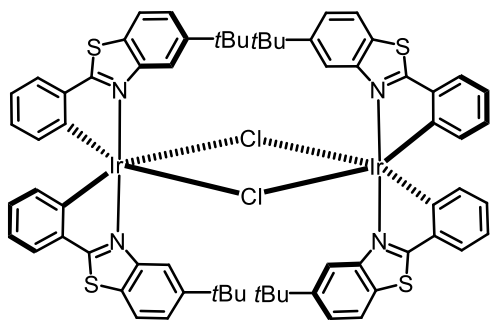
The reaction was performed according to a slightly modified literature procedure.^[5b] A 25 mL flask equipped with nitrogen inlet, condenser and a strong stir bar was charged with a suspension of 1-Brom-4-*tert*-butyl-2-nitrobenzene (**S4a**, 3.94 g, 15.3 mmol, 1.00 eq.), benzylamine (4.2 mL, 38.2 mmol, 2.50 eq.), sulfur (5.87 g, 22.9 mmol, 1.50 eq.), and pyridine (3 mL; freshly distilled). The resulting black suspension was heated to 100 °C and stirred at reflux for 24 h. After cooling the mixture to rt, the solidified red mixture was triturated with CH_2Cl_2 . The insoluble remains were filtered, rinsed with CH_2Cl_2 until colorless, and discarded. The filtrate was concentrated under reduced pressure, adsorbed on silica gel, and purified by flash column chromatography (*n*-hexane/ $EtOAc$ 50:1). The obtained yellow solid was recrystallized from *n*-hexane to afford ligand **L9** as colorless, crystalline solid (1.80 g, 6.73 mmol, 44%).

TLC (*n*-hexane/ $EtOAc$ 50:1): R_f = 0.20.

^1H NMR (300 MHz, CD_2Cl_2): δ = 8.13–8.06 (m, 3H, H_{Ar}), 7.85 (dd, J = 8.5, 0.5 Hz, 1H, H_{Ar}), 7.54–7.47 (m, 4H, H_{Ar}), 7.77 (d, J = 8.9 Hz, 1H, H_{Ar}), 1.42 (s, 9H, $t\text{Bu}$) ppm.

HR-MS (ESI): m/z calcd. for $\text{C}_{17}\text{H}_{18}\text{N}_1\text{S}_1$ $[\text{M}+\text{H}]^+$: 268.1154, found 268.1160.

Dimer *rac*-C1h



According to procedure A, ligand **L9** (1.80 g, 6.73 mmol, 2.00 eq.) and iridium(III) chloride hydrate (1.20 g, 3.37 mmol, 1.00 eq.) were used. Instead of pure ethoxyethanol a 3:1 mixture of ethoxyethanol (100 mL) and water (30 mL) was used to provide a cleaner reaction. To completely consume the ligand, additional iridium(III)chlorate hydrate (120 mg) was added. After cooling to rt, the mixture was diluted with CH_2Cl_2 (100 mL) and filtered through a plug of celite which was rinsed with CH_2Cl_2 (600 mL). After purification by silica gel filter column (CH_2Cl_2) dimer *rac*-C1h was obtained as an orange solid that was rinsed with *n*-hexane to dimer *rac*-C1h (1.83 g, 1.22 mmol, 73% based on the amount of starting ligand **L9**).

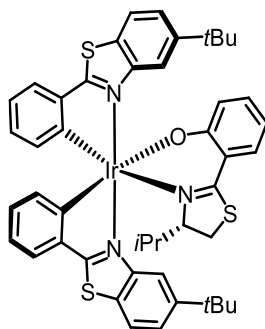
^1H NMR (300 MHz, CD_2Cl_2): δ = 8.88 (d, J = 1.7 Hz, 1H, H_{Ar}), 7.51–7.46 (m, 1H, H_{Ar}), 7.44 (d, J = 8.5, 1H, H_{Ar}), 7.29 (d, J = 8.6, 1.9 Hz, 1H, H_{Ar}), 6.80–6.72 (m, 1H, H_{Ar}), 6.43–6.34 (m, 1H, H_{Ar}), 5.97–5.91 (m, 1H, H_{Ar}), 5.90 (s, 9H, $t\text{Bu}$) ppm.

HR-MS (ESI): m/z calcd.: $\text{C}_{68}\text{H}_{64}\text{Cl}_1\text{Ir}_2\text{N}_4\text{S}_4$ $[\text{M}-\text{Cl}]^+$: 1485,2961, found 1485,2962.

Diastereomers Λ -(*S*)-C2n and Δ -(*S*)-C2n

According to procedure B, dimer *rac*-C1h (850 mg, 560 μ mol, 1.00 eq.), ancillary ligand (*S*)-AL1 (248 mg, 1.12 mmol, 2.00 eq.), AgOTf (288 mg, 1.12 mmol, 2.00 eq.), Et₃N (0.77 mL, 566 mg, 5.59 mmol, 10.0 eq.), and EtOH (32.5 mL) were used. The resulting diastereomers were separated by flash column chromatography (*n*-hexane/EtOAc 6:1). Both diastereomers were once again purified by flash column chromatography (*n*-hexane/EtOAc 6:1 for Λ -(*S*)-C2n and *n*-hexane/EtOAc 5:1 for Δ -(*S*)-C2n) to yield Λ -(*S*)-C2n (428 mg, 453 μ mol, 40%) and Δ -(*S*)-C2n (432 mg, 457 μ mol, 41%) as a red solid.

Diastereomer Λ -(*S*)-C2n

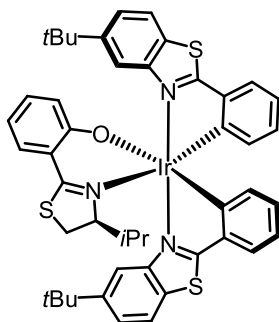


TLC (*n*-hexane/EtOAc 6:1) *R*_f = 0.34.

¹H NMR (300 MHz, CD₂Cl₂): δ = 8.91 (d, *J* = 1.5 Hz, 1H, *H*_{Ar}), 8.12 (d, *J* = 1.7 Hz, 1H, *H*_{Ar}), 7.74 (d, *J* = 8.6 Hz, 1H, *H*_{Ar}), 7.66–7.63 (m, 1H, *H*_{Ar}), 7.57–7.53 (m, 2H, *H*_{Ar}), 7.50 (dd, *J* = 8.6, 1.8 Hz, 1H, *H*_{Ar}), 7.47–7.44 (m, 1H, *H*_{Ar}), 6.98–6.86 (m, 4H, *H*_{Ar}), 6.78–6.64 (m, 5H, *H*_{Ar}), 6.42–6.37 (m, 3H, *H*_{Ar}), 5.97 (d, *J* = 7.7 Hz, 1H, *H*_{Ar}), 5.94–5.89 (m, 1H, *H*_{Ar}), 5.00 (t, *J* = 9.3 Hz, 1H, *H*_{aliph}), 4.89 (dd, *J* = 9.4, 3.5 Hz, 1H, *H*_{aliph}), 4.15 ppm (dd, *J* = 9.3, 3.5 Hz, 1H, *H*_{aliph}) ppm.

HR-MS (LIFDI): *m/z* calcd. for C₄₁H₂₅Br₂F₁IrN₃O₂S₂ [*M*]⁺: 1026.9341, found 1026.9355.

Diastereomer Δ -(*S*)-C2n

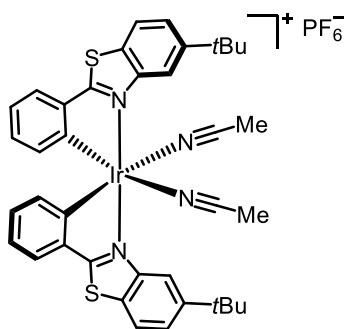


TLC (*n*-hexane/EtOAc 6:1) R_f = 0.24.

^1H NMR (300 MHz, CD_2Cl_2): δ = 9.13 (d, J = 1.8 Hz, 1H, H_{Ar}), 8.25 (d, J = 1.7 Hz, 1H, H_{Ar}), 7.89 (d, J = 8.5 Hz, 1H, H_{Ar}), 7.70–7.67 (m, 1H, H_{Ar}), 7.64–7.58 (m, 3H, H_{Ar}), 7.45 (dd, J = 8.6, 1.8 Hz, 1H, H_{Ar}), 7.07–7.05 (m, 3H, H_{Ar}), 6.92–6.68 (m, 6H, H_{Ar}), 6.27–6.21 (m, 1H, H_{Ar}), 6.18–6.15 (m, 2H, H_{Ar}), 6.03 (d, J = 7.7 Hz, 1H, H_{Ar}), 5.93–5.87 (m, 1H, H_{Ar}), 4.53 (dd, J = 9.1, 6.2 Hz, 1H, H_{aliph}), 4.34 (dd, J = 10.0, 9.1 Hz, 1H, H_{aliph}), 4.08 ppm (dd, J = 10.0, 6.2 Hz, 1H, H_{aliph}) ppm.

HR-MS (LIFDI): m/z calcd. for $\text{C}_{41}\text{H}_{25}\text{Br}_2\text{F}_1\text{IrN}_3\text{O}_2\text{S}_2$ $[\text{M}]^{+}$: 1026.93413, found 1026.9253.

Catalyst Δ -C5d



A solution of complex Δ -(*S*)-C2n (300 mg, 323 μmol , 1.00 eq.) in acetonitrile (60 mL) was treated with NH_4PF_6 (2.90 g, 17.8 mmol, 55.1 eq.) for 16 h under nitrogen atmosphere and exclusion of light. The mixture was concentrated to a thick suspension and purified by column chromatography ($\text{CH}_2\text{Cl}_2/\text{CH}_3\text{CN}$ 100:1 to 30:1) to obtain a yellow solid. The solid was dissolved in CH_2Cl_2 and layered with *n*-hexane to recrystallize by slow liquid-liquid diffusion to form Δ -C5f as yellow, crystalline solid (261 mg, 275 μmol , 85%).

^1H NMR (300 MHz, CD_2Cl_2): δ = 8.41 (d, J = 1.6 Hz, 1H, H_{Ar}), 8.01 (d, J = 8.6 Hz, 1H, H_{Ar}), 7.73 (d, J = 8.6, 1.6 Hz, 1H, H_{Ar}), 7.70–7.62 (m, 1H, H_{Ar}), 7.00–6.92 (m, 1H, H_{Ar}), 6.78–6.70 (m, 1H, H_{Ar}), 6.20–6.14 (m, 1H, H_{Ar}), 2.34 (s, 3H, NCCCH_3), 1.46 (s, 9H, *t*Bu) ppm.

3.4.19 Procedure D): Synthesis of Nazarov Substrates **N1** and **N3**

A round-bottom flask (10 mL) was charged with a solution of β -ketoester **S13a-c** (600–950 μ mol, 1.00 eq.) in CH_2Cl_2 (0.3 M) followed by the addition of piperidine (1.20 eq.), acetic acid (1.00 eq.), and 4 Å molecular sieves (MS; ~500 mg). The mixture was stirred for 30 min at rt before the indicated aldehyde (1.20 eq.; freshly distilled) was added. The mixture was then stirred at rt for 16 h after which TLC indicated full conversion. All volatiles were removed under reduced pressure and the remaining residue purified by flash chromatography (*n*-hexane/EtOAc or *n*-pentane/diethyl ether as eluent as indicated in the individual procedure) to obtain desired substrate **N1** or **N3** as an *E/Z* mixture. The *E/Z* ratio was determined by ^1H NMR analysis after flash chromatography. ^1H NMR assignment is exclusively provided for the *E*-configured products.^[50]

3.4.20 Procedure E): Synthesis of Nazarov Substrates **N1** and **N3**

A round-bottom flask (10 mL) was charged with a solution of β -ketoester **S13a-c** (600–950 μ mol, 1.00 eq.) in CH_2Cl_2 (0.1 M) followed by the addition of piperidine (1.00 eq.), acetic acid (0.50 eq.), and 4 Å molecular sieves (MS; ~500 mg). The mixture was stirred for 30 min at rt before the indicated aldehyde (1.30 eq.; freshly distilled) was added. The mixture was then stirred at rt for 16 h after which TLC indicated full conversion. All volatiles were then removed under reduced pressure and the residue purified by flash chromatography (*n*-hexane/EtOAc or *n*-pentane/diethyl ether as eluent as indicated in the individual procedure) to obtain desired substrate **N1** or **N3** as an *E/Z* mixture. The *E/Z* ratio was determined by ^1H NMR analysis after flash chromatography. ^1H NMR assignment is exclusively provided for the *E*-configured products.^[50]

3.4.21 Procedure F): Nazarov Cyclizations **N1**→**N2**

A vial (1.5 mL) was charged with an *E/Z* mixture of 3,4-dihydropyran-functionalized α -unsaturated β -ketoester **N1** (80–90 μ mol), catalyst **A-C5f** (2 mol%), and a stock solution of DCE containing 1 eq. of HFIP (with respect to substrate **N1**). The vial was then tightly capped with a rubber sealed screw cap, homogenized by sonication (1 min), and kept in a preheated oil bath at 40 °C for the indicated time after which TLC analysis indicated full cyclization. The solvent was removed under reduced pressure and the crude product purified by flash column (*n*-hexane/EtOAc or *n*-pentane/diethyl ether as eluent as indicated in the individual procedure) to

furnish the desired NAZAROV cyclization product **N2** as a viscous oil or solid. NMR assignment is exclusively provided for the *trans* products.

3.4.22 Procedure G): Nazarov Cyclizations **N3**→**N4**

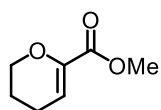
A vial (1.5 mL) was charged with catalyst **Δ-C5f** (or in selected cases **Δ-C5g**; in both cases 2.0 mol% were used), an *E/Z* mixture of indole-functionalized α -unsaturated β -ketoester **N3** (70–90 μ mol), and HFIP (0.3 M). The vial was then tightly capped with a rubber sealed screw cap, homogenized by sonication (1 min), and kept in a preheated oil bath at 50 °C for the indicated time after which TLC analysis indicated full cyclization. The solvent was removed under reduced pressure and the d.r. of the crude product determined by ^1H NMR analysis. The crude product was then transferred into an empty flask (10 mL), dissolved in CH_2Cl_2 (7 mL), basic Al_2O_3 (*Sigma Aldrich*, powder, 58 Å pore size, pH 9.5 ± 0.5 in water, 140 mg) was added, and the mixture stirred at rt for 24 h. Next, the crude mixture was filtered through a short plug of silica gel with EtOAc and MeOH as eluents (removal of Al_2O_3 powder) and the d.r. of the crude equilibrated product determined by ^1H NMR analysis. Finally, the crude product was purified by flash chromatography (*n*-hexane/EtOAc or *n*-pentane/diethyl ether as eluent as indicated in the individual procedure) which gave desired NAZAROV cyclization product **N4** as an off-white solid. NMR assignment is exclusively provided for the *trans* products.

3.4.23 Procedure H): Synthesis of Racemic References

A vial (1.5 mL) was charged with an *E/Z* mixture of 3,4-dihydropyran-functionalized α -unsaturated β -ketoester **N1** or indole-functionalized α -unsaturated β -ketoester **N3** (30–45 μ mol), $\text{Cu}(\text{OTf})_2$ or $\text{Fe}(\text{OTf})_3$ (10 mol%), and DCE (for **N1**) or HFIP (for **N3**). The vial was then tightly capped with a rubber sealed screw cap, homogenized by sonication (1 min), and kept in a preheated oil bath at 40 °C for the indicated time after which TLC analysis indicated full cyclization. The solvent was removed under reduced pressure and the crude product purified by flash column chromatography (*n*-hexane/EtOAc or *n*-pentane/diethyl ether as eluent as indicated in the individual procedure) which gave the desired NAZAROV cyclization product *rac*-**N2** or *rac*-**N4**.

3.4.24 3,4-Dihydropyran-Functionalized α -Unsaturated β -Ketoesters

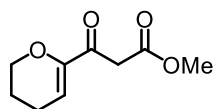
Methyl 3,4-dihydro-2*H*-pyran-6-carboxylate (**S12b**)



The title compound was prepared according to a slightly modified literature-known procedure.^[50] A flask (250 mL) equipped with a septum, a nitrogen inlet, and a stir bar was charged with dry 3,4-dihydro-2*H*-pyran (2.90 mL, 32.1 mmol, 1.26 eq.) and dry THF (40 mL) and cooled to $-78\text{ }^{\circ}\text{C}$. To this solution, *t*-BuLi (1.7 M in pentane, 15.0 mL, 25.5 mmol, 1.00 eq.) was added dropwise, which initially resulted in a yellow solution that turned orange upon heating to rt. After stirring for 30 min at rt, the orange solution was cooled to $-78\text{ }^{\circ}\text{C}$ and a stream of CO_2 gas was bubbled through it for 10 min upon which the reaction turned colorless and viscous. The reaction was then allowed to warm up to $0\text{ }^{\circ}\text{C}$ and further flushed with CO_2 gas for 10 min until the mixture again became viscous. The reaction was then warmed up to rt and further flushed with CO_2 gas for 10 min. Overall, the mixture was flushed with CO_2 gas for a total time of 30 min. The resulting mixture was then diluted with diethyl ether (60 mL) and water (60 mL), the organic layer separated and extracted with water (2x60 mL), and the combined aqueous layers acidified with aqueous HCl (2 M, 60 mL) to pH = 2. The acidified aqueous layer was then extracted with EtOAc (5x50 mL), dried over Na_2SO_4 , filtered, concentrated, and dried under reduced pressure. The obtained brown oil (free acid **S12a**; 1.70 g crude material obtained) was dissolved in dry CH_2Cl_2 (25 mL), treated with excess thionyl chloride (7 mL, 96.5 mmol) and stirred at rt for 12 h. CH_2Cl_2 and excess thionyl chloride were then removed under reduced pressure and the remaining viscous residue dissolved in dry MeOH (25 mL) and stirred at rt for 30 min. The resulting mixture was concentrated under reduced pressure and purified by flash chromatography (*n*-hexane/EtOAc 9:1) to obtain product **S12b** as a colorless oil (1.10 g, 7.74 mmol, 30% based on *t*-BuLi).

^1H NMR (300 MHz, CDCl_3): δ = 6.08 (t, J = 4.1 Hz, 1H, H_{Olef}), 4.17–4.07 (m, 2H, H_{Aliph}), 3.79 (s, 3H, OCH_3), 2.24–2.14 (m, 2H, H_{Aliph}), 1.93–1.81 (m, 2H, H_{Aliph}) ppm.

Methyl 3-(3,4-dihydro-2*H*-pyran-6-yl)-3-oxopropanoate (**S12c**)



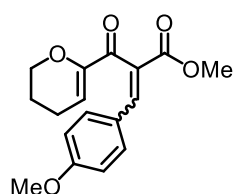
Compound **S12c** was prepared according to a slightly modified literature-known procedure.^[50] A flask (10 mL) equipped with a septum, a nitrogen inlet, and a stir bar was charged with ester **S12b** (1.10 g, 7.74 mmol,

1.00 eq.), dry THF (6.5 mL), and 4 Å molecular sieves (~1 g). In order to prepare the required enolate, a second flask (100 mL) equipped with a septum and a nitrogen inlet was charged with a solution of dry MeOAc (1.85 mL, 23.3 mmol, 3.01 eq.) in dry THF (10 mL) and cooled to –78 °C. To the chilled solution, LiHMDS (1 M in THF; 23.4 mL, 23.4 mmol, 3.02 eq.) was added dropwise at –78 °C. The solution was stirred at this temperature for 30 min, and then additional 30 min at rt. The enolate solution was then again cooled to –78 °C and the solution of ester **S12b** was added dropwise via cannula. The resulting mixture was stirred at this temperature for 30 min and then for additional 30 min at rt. After reaction control by TLC indicated full conversion, the mixture was diluted with EtOAc and water (50 mL each), the aqueous layer separated and extracted with EtOAc (4x50 mL). The combined organic layers were washed with brine (50 mL), dried over Na₂SO₄, filtered, concentrated, and purified by flash chromatography (*n*-hexane/EtOAc 9:1) to obtain desired β -ketoester **S12c** as a colorless oil (680 mg, 3.69 mmol, 48%, keto/enol ratio 5:1).

Analytical data for the keto form of S12c:

¹H NMR (300 MHz, CDCl₃): δ = 6.03 (t, *J* = 4.3 Hz, 1H, *H*_{Olef}), 4.11–4.05 (m, 2H, *H*_{Aliph}), 3.73 (s, 3H, OCH₃), 3.62 (s, 2H, CH₂), 2.26–2.17 (m, 2H, *H*_{Aliph}), 1.91–1.81 (m, 2H, *H*_{Aliph}) ppm.

Methyl (*E*)-2-(3,4-dihydro-2*H*-pyran-6-carbonyl)-3-(4-methoxyphenyl)acrylate (**N1a**)



According to procedure D, β -ketoester **S12c** (113 mg, 613 μ mol, 1.00 eq.), piperidine (72.6 μ L, 733 μ mol, 1.20 eq.), acetic acid (36.1 μ L, 631 μ mol, 1.03 eq.), 4 Å MS (~500 mg), CH₂Cl₂ (2.0 mL), and *p*-methoxyphenyl (89.4 μ L, 735 μ mol, 1.20 eq.) were used. Product **N1a** was obtained after column chromatography (*n*-pentane/Et₂O 2:1) as a yellow viscous oil (131 mg, 433 μ mol, 71%, *E/Z* 20:1).^[50]

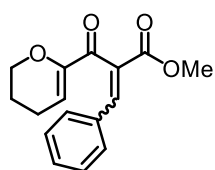
¹H NMR (300 MHz, CDCl₃): δ = 7.76 (s, 1H, *H*_{Olef}), 7.33 (d, *J* = 8.8 Hz, 2H, *H*_{Ar}), 6.83 (d, *J* = 8.8 Hz, 2H, *H*_{Ar}), 6.08 (t, *J* = 4.2 Hz, 1H, *H*_{Olef}), 4.09 (t, *J* = 5.1 Hz, 2H, *H*_{Aliph}), 3.80 (s, 3H, OCH₃), 3.78 (s, 3H, OCH₃), 2.19–2.08 (m, 2H, *H*_{Aliph}), 1.88–1.75 (m, 2H, *H*_{Aliph}) ppm.

¹³C NMR (75 MHz, CDCl₃): δ = 191.1, 165.8, 161.6, 151.4, 143.1, 132.5 (2C), 127.6, 125.7, 116.3, 114.4 (2C), 66.6, 55.5, 52.5, 21.4, 21.2 ppm.

IR (ATR): $\tilde{\nu}$ = 2928 (w), 2846 (w), 1710 (m), 1668 (m), 1597 (m); 1511 (m), 1433 (m), 1305 (w), 1248 (s), 1202 (m), 1169 (s), 1093 (m), 1052 (m), 1026 (m), 995 (m), 910 (m), 829 (m), 761 (m), 698 (m), 521 (m), 404 (m) cm^{-1} .

HR-MS (ESI): m/z calcd. for $\text{C}_{17}\text{H}_{18}\text{O}_5\text{Na}$ $[\text{M}+\text{Na}]^+$: 325.1046, found 325.1043.

Methyl 2-(3,4-dihydro-2H-pyran-6-carbonyl)-3-phenylacrylate (**N1b**)



According to procedure D, β -ketoester **S12c** (113 mg, 613 μmol , 1.00 eq.), piperidine (72.6 μL , 733 μmol , 1.20 eq.), acetic acid (36.1 μL , 631 μmol , 1.03 eq.), 4 Å MS (~500 mg), CH_2Cl_2 (2.0 mL), and benzaldehyde (75.1 μL , 736 μmol , 1.20 eq.) were used. Product **N1b** was obtained after flash chromatography (*n*-pentane/ Et_2O 2:1) as a colorless oil (104 mg, 382 μmol , 62%, *E/Z* 3:1).

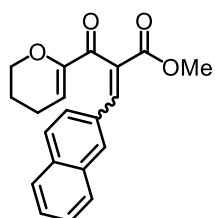
^1H NMR (300 MHz, CDCl_3): δ = 7.84 (s, 1H, H_{Olef}), 7.43–7.29 (m, 5H, H_{Ar}), 6.00 (t, J = 4.3 Hz, 1H, H_{Olef}), 4.14 (t, J = 4.9 Hz, 2H, H_{Aliph}), 3.81 (s, 3H, OCH_3), 2.17–2.09 (m, 2H, H_{Aliph}), 1.86–1.75 (m, 2H, H_{Aliph}) ppm.

^{13}C NMR (75 MHz, CDCl_3): δ = 190.6, 165.5, 151.5, 143.4, 133.2, 130.4 (2C), 129.3, 128.9 (2C), 127.5, 116.4, 66.6, 52.7, 21.5, 21.2 ppm.

IR (ATR): $\tilde{\nu}$ = 2994 (w), 2935 (w), 2877 (w), 1723 (s), 1663 (s), 1622 (s), 1496 (w), 1433 (w), 1300 (w), 1243 (s), 1188 (s), 1094 (m), 1051 (m), 994 (w), 937 (w), 903 (w), 831 (w), 768 (m), 690 (m), 577 (w), 493 (w), 398 (w) cm^{-1} .

HR-MS (ESI): m/z calcd. for $\text{C}_{16}\text{H}_{16}\text{O}_4\text{Na}$ $[\text{M}+\text{Na}]^+$: 295.0941, found 295.0939.

Methyl (*E*)-2-(3,4-dihydro-2H-pyran-6-carbonyl)-3-(naphthalen-2-yl)acrylate (**N1c**)



According to procedure D, β -ketoester **S12c** (113 mg, 613 μmol , 1.00 eq.), piperidine (72.6 μL , 733 μmol , 1.20 eq.), acetic acid (36.1 μL , 631 μmol , 1.03 eq.), 4 Å MS (~500 mg), CH_2Cl_2 (2.0 mL), and 2-naphthaldehyde (115 mg, 736 μmol , 1.20 eq.) were used. Product **N1c** was obtained after column chromatography (*n*-pentane/ Et_2O 2:1) as a colorless viscous oil (96 mg, 298 μmol , 49%, *E/Z* >30:1).

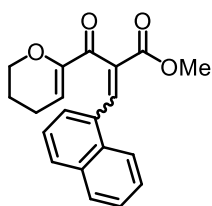
¹H NMR (300 MHz, CDCl₃): δ = 8.00 (s, 1H, *H*_{Ole}), 7.90 (s, 1H, *H*_{Ar}), 7.87–7.72 (m, 3H, *H*_{Ar}), 7.56–7.47 (m, 2H, *H*_{Ar}), 7.46–7.41 (m, 1H, *H*_{Ar}), 6.08 (t, *J* = 4.2 Hz, 1H, *H*_{Ole}), 4.07 (t, *J* = 4.9 Hz, 2H, *H*_{Aliph}), 3.84 (s, 3H, OCH₃), 2.15–2.05 (m, 2H, *H*_{Aliph}), 1.84–1.72 (m, 2H, *H*_{Aliph}) ppm.

¹³C NMR (75 MHz, CDCl₃): δ = 190.6, 165.6, 151.5, 143.4, 134.1, 133.2, 131.9, 130.7, 130.3, 128.3, 128.6, 127.8 (2C), 126.9, 126.2, 116.5, 66.7, 52.7, 21.4, 21.2 ppm.

IR (ATR): $\tilde{\nu}$ = 3049 (w), 2952 (w), 2927 (w), 1712 (s), 1648 (m), 1596 (m); 1511 (w), 1436 (m), 1399 (w), 1327 (s), 1292 (w), 1258 (w), 1201 (w), 1160 (w), 1161 (m), 1120 (m), 1066 (w), 1034 (w), 976 (w), 912 (w), 864 (w), 782 (m), 731 (m), 644 (w), 570 (m), 496 (w), 459 (w), 414 (m) cm⁻¹.

HR-MS (ESI): *m/z* calcd. for C₂₀H₁₈O₄Na₁ [M+Na]⁺: 345.1097, found 345.1097.

Methyl (*E*)-2-(3,4-dihydro-2*H*-pyran-6-carbonyl)-3-(naphthalen-1-yl)acrylate (**N1d**)



According to procedure D, β -ketoester **S12c** (113 mg, 613 μ mol, 1.00 eq.), piperidine (72.6 μ L, 733 μ mol, 1.20 eq.), acetic acid (36.1 μ L, 631 μ mol, 1.03 eq.), 4 Å MS (~500 mg), CH₂Cl₂ (2.0 mL), and 1-naphthaldehyde (99.6 μ L, 733 μ mol, 1.20 eq.) were used. Product **N1d** was obtained after column chromatography (*n*-pentane/Et₂O 2:1) as a colorless solid (110 mg, 341 μ mol, 56%, *E/Z* >30:1).

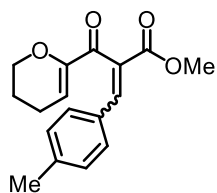
¹H NMR (300 MHz, CDCl₃): δ = 8.61 (s, 1H, *H*_{Ole}), 8.06–7.99 (m, 1H, *H*_{Ar}), 7.89–7.79 (m, 2H, *H*_{Ar}), 7.62–7.48 (m, 2H, *H*_{Ar}), 7.44–7.33 (m, 2H, *H*_{Ar}), 5.86 (t, *J* = 4.3 Hz, 1H, *H*_{Ole}), 3.86 (s, 3H, OCH₃), 3.76 (t, *J* = 5.0 Hz, 2H, *H*_{Aliph}), 1.91–1.82 (m, 2H, *H*_{Aliph}), 1.62–1.50 (m, 2H, *H*_{Aliph}) ppm.

¹³C NMR (75 MHz, CDCl₃): δ = 189.9, 165.2, 151.2, 142.0, 133.5, 132.9, 131.5, 130.9, 130.4, 128.8, 127.7, 127.0, 126.4, 125.5, 124.2, 115.2, 108.0, 66.4, 52.7, 21.3, 20.9 ppm.

IR (ATR): $\tilde{\nu}$ = 2930 (w), 2883 (w), 1719 (s), 1666 (s), 1617 (s), 1508 (w), 1433 (w), 1396 (w), 1346 (w), 1301 (w), 1270 (m), 1227 (s), 1099 (m), 1050 (s), 987 (w), 939 (m), 907 (w), 867 (m), 768 (s), 735 (m), 694 (m), 579 (w), 536 (w), 476 (w), 429 (w) cm⁻¹.

HR-MS (ESI): *m/z* calcd. for C₂₀H₁₈O₄Na₁ [M+Na]⁺: 345.1097, found 345.1098.

Methyl (*E*)-2-(3,4-dihydro-2*H*-pyran-6-carbonyl)-3-(*p*-tolyl)acrylate (N1e)



According to procedure D, β -ketoester **S12c** (113 mg, 613 μ mol, 1.00 eq.), piperidine (72.6 μ L, 733 μ mol, 1.20 eq.), acetic acid (36.1 μ L, 631 μ mol, 1.03 eq.), MS 4 Å (~500 mg), CH_2Cl_2 (2.0 mL), and *p*-methylbenzaldehyde (86.8 μ L, 736 μ mol, 1.20 eq.) were used. Product **N1e** was obtained after column chromatography (*n*-pentane/ Et_2O 2:1) as a yellow viscous oil (83.2 mg, 291 μ mol, 47%, *E/Z* >30:1).

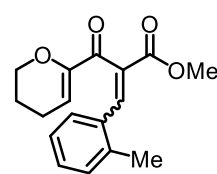
^1H NMR (300 MHz, CDCl_3): δ = 7.87 (s, 1H, H_{Olef}), 7.35 (d, J = 7.8 Hz, 2H, H_{Ar}), 7.20 (m, J = 7.8 Hz, 1H, H_{Ar}), 6.08 (t, J = 4.3 Hz, 1H, H_{Olef}), 4.16 (t, J = 5.1 Hz, 2H, H_{Aliph}), 3.87 (s, 3H, OCH_3), 2.41 (s, 3H, CH_3), 2.26–2.16 (m, 2H, H_{Aliph}), 1.95–1.82 (m, 2H, H_{Aliph}) ppm.

^{13}C NMR (75 MHz, CDCl_3): δ = 190.8, 165.7, 151.4, 143.4, 141.2, 130.5 (2C), 130.3, 129.7 (2C), 129.2, 116.4, 66.6, 52.6, 21.6, 21.5, 21.2 ppm.

IR (ATR): $\tilde{\nu}$ = 2948 (w), 2926 (w), 2875 (w), 1713 (s), 1670 (s), 1619 (s), 1512 (w), 1434 (m), 1378 (w), 1293 (w), 1249 (s), 1178 (s), 1094 (m), 1051 (m), 994 (m), 910 (m), 813 (m), 762 (w), 706 (w), 570 (w), 499 (m), 399 (w) cm^{-1} .

HR-MS (ESI): m/z calcd. for $\text{C}_{17}\text{H}_{18}\text{O}_4\text{Na}$ [$\text{M}+\text{Na}$] $^+$: 309.1097, found 309.1096.

Methyl (*E*)-2-(3,4-dihydro-2*H*-pyran-6-carbonyl)-3-(*o*-tolyl)acrylate (N1f)



According to procedure D, β -ketoester **S12c** (113 mg, 613 μ mol, 1.00 eq.), piperidine (72.6 μ L, 733 μ mol, 1.20 eq.), acetic acid (36.1 μ L, 631 μ mol, 1.03 eq.), 4 Å MS (~500 mg), CH_2Cl_2 (2.0 mL), and *o*-methylbenzaldehyde (88.4 μ L, 765 μ mol, 1.25 eq.) were used. Product **N1f** was obtained after column chromatography (*n*-pentane/ Et_2O 2:1) as a yellow viscous oil (145 mg, 506 μ mol, 83%, *E/Z* 20:1).

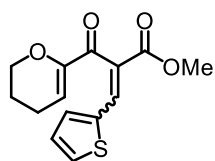
^1H NMR (300 MHz, CDCl_3): δ = 8.09 (s, 1H, H_{Olef}), 7.25–7.14 (m, 1H, H_{Ar}), 7.13–7.06 (m, 1H, H_{Ar}), 5.89 (t, J = 4.2 Hz, 1H, H_{Olef}), 3.94 (t, J = 5.1 Hz, 2H, H_{Aliph}), 3.82 (s, 3H, OCH_3), 2.39 (s, 3H, CH_3), 2.12–2.03 (m, 2H, H_{Aliph}), 1.78–1.67 (m, 2H, H_{Aliph}) ppm.

^{13}C NMR (75 MHz, CDCl_3): δ = 190.2, 165.5, 151.4, 142.5, 137.6, 132.8, 131.5, 130.4, 130.1, 129.1, 126.3, 115.1, 66.5, 52.6, 21.5, 21.1, 20.1 ppm.

IR (ATR): $\tilde{\nu}$ = 2991 (w), 2934 (w), 2882 (w), 1722 (s), 1659 (s), 1618 (s), 1434 (w), 1394 (w), 1348 (w), 1297 (w), 1244 (s), 1204 (s), 1095 (m), 1051 (m), 993 (w), 936 (w), 905 (w), 876 (w), 836 (w), 767 (m), 714 (w), 646 (w), 575 (w), 492 (w), 450 (w), 397 (w) cm^{-1} .

HR-MS (ESI): m/z calcd. for $\text{C}_{17}\text{H}_{18}\text{O}_4\text{Na}$ $[\text{M}+\text{Na}]^+$: 309.1097, found 309.1098.

Methyl (*E*)-2-(3,4-dihydro-2*H*-pyran-6-carbonyl)-3-(thiophen-2-yl)acrylate (N1g**)**



According to procedure D, β -ketoester **S12c** (113 mg, 613 μmol , 1.00 eq.), piperidine (72.6 μL , 733 μmol , 1.20 eq.), acetic acid (36.1 μL , 631 μmol , 1.03 eq.), 4 Å MS (~500 mg), CH_2Cl_2 (2.0 mL), and thiophene-2-carbaldehyde (68.8 μL , 736 μmol , 1.20 eq.) were used. Product **N1g** was obtained after column chromatography (*n*-pentane/ Et_2O 2:1) as a colorless solid (106 mg, 381 μmol , 62%, *E/Z* 14:1).

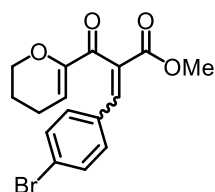
^1H NMR (300 MHz, CDCl_3): δ = 7.91 (s, 1H, H_{Olef}), 7.47 (d, J = 4.8 Hz, 1H, $H_{\text{Thiophene}}$), 7.29 (d, J = 3.7 Hz, 1H, $H_{\text{Thiophene}}$), 7.04 (dd, J = 4.8, 4.0 Hz, 1H, $H_{\text{Thiophene}}$), 6.10 (t, J = 4.3 Hz, 1H, H_{Olef}), 4.14 (t, J = 5.1 Hz, 2H, H_{Aliph}), 3.79 (s, 3H, OCH_3), 2.26–2.17 (m, 2H, H_{Aliph}), 1.93–1.82 (m, 2H, H_{Aliph}) ppm.

^{13}C NMR (75 MHz, CDCl_3): δ = 190.0, 165.6, 151.5, 136.5, 135.3, 134.2, 131.8, 128.0, 127.3, 116.3, 66.7, 52.6, 21.5, 21.3 ppm.

IR (ATR): $\tilde{\nu}$ = 3095 (w), 3075 (w), 2924 (w), 2885 (w), 2855 (w), 1717 (s), 1658 (s), 1613 (s), 1421 (m), 1351 (w), 1298 (w), 1246 (s), 1195 (s), 1092 (s), 1047 (s), 992 (w), 905 (w), 850 (w), 834 (w), 798 (m), 725 (s), 632 (w), 598 (w), 571 (w), 489 (w), 395 (w) cm^{-1} .

HR-MS (ESI): m/z calcd. for $\text{C}_{14}\text{H}_{14}\text{O}_4\text{SNa}$ $[\text{M}+\text{Na}]^+$: 301.0505, found 301.0502.

Methyl (*E*)-3-(4-bromophenyl)-2-(3,4-dihydro-2*H*-pyran-6-carbonyl)acrylate (N1h**)**



According to procedure D, β -ketoester **S12c** (113 mg, 613 μmol , 1.00 eq.), piperidine (72.6 μL , 733 μmol , 1.20 eq.), acetic acid (36.1 μL , 631 μmol , 1.03 eq.), 4 Å MS (~500 mg), CH_2Cl_2 (2.0 mL), and *p*-bromobenzaldehyde (136 mg, 735 μmol , 1.20 eq.) were used. Product **N1h** was obtained after column chromatography (*n*-pentane/ Et_2O 2:1) as a yellow viscous oil (137 mg, 390 μmol , 64%, *E/Z* 30:1).

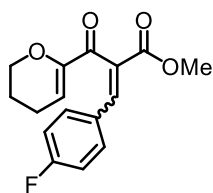
¹H NMR (300 MHz, CDCl₃): δ = 7.74 (s, 1H, *H*_{Olef}), 7.46 (d, *J* = 8.5 Hz, 1H, *H*_{Ar}), 7.23 (d, *J* = 8.5 Hz, 1H, *H*_{Ar}), 5.98 (t, *J* = 4.3 Hz, 1H, *H*_{Olef}), 4.07 (t, *J* = 5.0 Hz, 2H, *H*_{Aliph}), 3.80 (s, 3H, OCH₃), 2.20–2.10 (m, 2H, *H*_{Aliph}), 1.87–1.76 (m, 2H, *H*_{Aliph}) ppm.

¹³C NMR (75 MHz, CDCl₃): δ = 190.1, 165.1, 151.1, 141.7, 132.1 (2C), 131.9, 131.5 (2C), 131.0, 124.9, 116.2, 66.5, 52.6, 21.3, 21.0 ppm.

IR (ATR): $\tilde{\nu}$ = 2951 (w), 2879 (w), 1715 (m), 1669 (m), 1621 (m), 1585 (w), 1487 (w), 1435 (w), 1402 (w), 1351 (w), 1247 (s), 1188 (m), 1097 (m), 1053 (m), 1000 (m), 910 (m), 818 (m), 766 (m), 726 (m); 643 (w), 566 (w), 496 (m), 404 (w) cm⁻¹.

HR-MS (ESI): *m/z* calcd. for C₁₆H₁₅Br₁O₄Na₁ [M+Na]⁺: 373.0046, found 373.0046.

Methyl (*E*)-2-(3,4-dihydro-2*H*-pyran-6-carbonyl)-3-(4-fluorophenyl)acrylate (**N1i**)



According to procedure D, β -ketoester **S12c** (113 mg, 613 μ mol, 1.00 eq.), piperidine (72.6 μ L, 733 μ mol, 1.20 eq.), acetic acid (36.1 μ L, 631 μ mol, 1.03 eq.), 4 Å MS (~500 mg), CH₂Cl₂ (2.0 mL), and *p*-fluorobenzaldehyde (78.9 μ L, 736 μ mol, 1.20 eq.) were used. Product **N1i** was obtained after column chromatography (*n*-pentane/Et₂O 2:1) as a yellow viscous oil (122 mg, 420 μ mol, 69%, *E/Z* >30:1).

¹H NMR (300 MHz, CDCl₃): δ = 7.78 (s, 1H, *H*_{Olef}), 7.44–7.31 (m, 2H, *H*_{Ar}), 7.10–6.95 (m, 2H, *H*_{Ar}), 6.00 (t, *J* = 4.2 Hz, 1H, *H*_{Olef}), 4.08 (t, *J* = 5.1 Hz, 2H, *H*_{Aliph}), 3.81 (s, 3H, OCH₃), 2.20–2.09 (m, 2H, *H*_{Aliph}), 1.87–1.76 (m, 2H, *H*_{Aliph}) ppm.

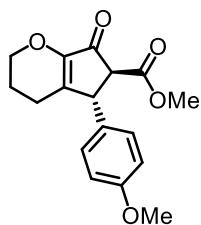
¹³C NMR (75 MHz, CDCl₃): δ = 190.5, 165.4, 164 (d, *J* = 253.8 Hz), 151.3, 142.0, 132.4 (d, *J* = 8.6 Hz, 2C), 130.2 (d, *J* = 1.7 Hz), 129.4 (d, *J* = 3.3 Hz), 116.4, 116.1 (d, *J* = 22.0 Hz, 2C), 66.7, 52.7, 21.4, 21.2 ppm.

IR (ATR): $\tilde{\nu}$ = 3071 (w), 2928 (w), 2871 (w), 1724 (s), 1663 (s), 1662 (s), 1594 (s); 1507 (s), 1427 (w), 1396 (w), 1348 (w), 1300 (w), 1231 (s), 1187 (s), 1161 (s), 1095 (s), 1052 (s), 995 (w), 965 (w), 933 (m), 905 (w), 837 (s), 798 (m), 760 (w), 699 (w), 654 (w), 622 (w), 573 (m), 514 (m), 491 (w), 417 (w) cm⁻¹.

HR-MS (ESI): *m/z* calcd. for C₁₆H₁₅F₁O₄Na₁ [M+Na]⁺: 313.0847, found 313.0845.

3.4.25 Nazarov Cyclizations with α -Unsaturated β -Ketoesters **N1**

Methyl (5*R*,6*S*)-5-(4-methoxyphenyl)-7-oxo-2,3,4,5,6,7-hexahydrocyclopenta[*b*]pyran-6-carboxylate (**N2a**)



According to procedure F, α -unsaturated β -ketoester **N1a** (25.2 mg, 83.5 μ mol, 1.00 eq.) and catalyst **A-C5f** (1.6 mg, 1.7 μ mol, 2.0 mol%) in DCE (280 μ L containing 1 eq. HFIP) were used; reaction time: 14 h. Desired NAZAROV product **N2a** was obtained after column chromatography (*n*-hexane/EtOAc 3:1) as a colorless viscous oil (21.7 mg, 71.8 μ mol, 86%). D.r.

value determined by ^1H NMR analysis of the crude product: *trans/cis* 18:1; enantiomeric excess of the *trans* diastereomer of the isolated product determined by chiral HPLC analysis: 93% ee (AD-H column, $\lambda = 238$ nm, *n*-hexane/2-propanol 70:30, 0.8 mL/min, column temp.: 25 $^\circ\text{C}$; t_R (major) = 10.0 min, t_R (minor) = 12.8 min), $[\alpha]_{\text{D}}^{27} = -228$ (c 1.0, CHCl_3).

^1H NMR (300 MHz, CDCl_3): δ = 7.05 (d, J = 8.6 Hz, 2H, H_{Ar}), 6.87 (d, J = 8.6 Hz, 2H, H_{Ar}), 4.22–4.09 (m, 3H, H_{Aliph}), 3.79 (s, 3H, OCH_3), 3.76 (s, 3H, OCH_3), 3.29 (d, J = 2.2 Hz, 1H, CH), 2.28–2.07 (m, 2H, H_{Aliph}), 2.02–1.83 (m, 2H, H_{Aliph}) ppm.

^{13}C NMR (75 MHz, CDCl_3): δ = 193.2, 169.0, 159.3, 149.8, 147.8, 131.9, 128.5, 114.7, 67.2, 59.6, 55.5, 52.9, 47.1, 22.4, 21.5 ppm.

IR (ATR): $\tilde{\nu}$ = 2952 (w), 2929 (w), 2845 (w), 1739 (m), 1713 (s), 1648 (w), 1611 (w), 1511 (w), 1437 (w), 1400 (w), 1301 (w), 1249 (m), 1166 (w), 1121 (w), 1066 (w), 1032 (w), 978 (w), 915 (w), 836 (w), 567 (w) cm^{-1} .

HR-MS (ESI): m/z calcd. for $\text{C}_{17}\text{H}_{18}\text{O}_5\text{Na}$ $[\text{M}+\text{Na}]^+$: 325.1046, found 325.1048.

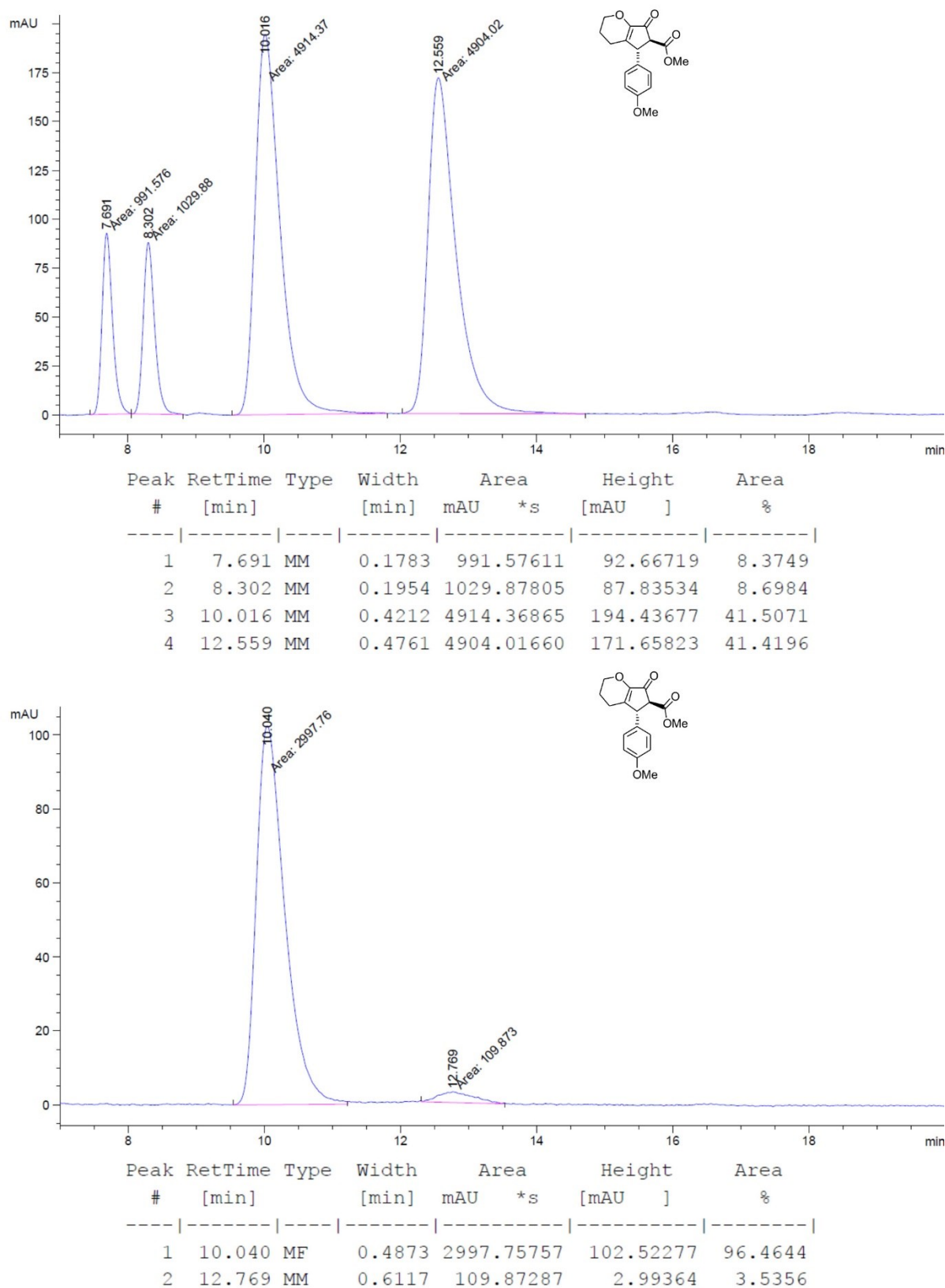
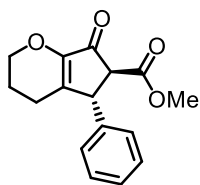


Figure 37: Chiral HPLC traces of **N2a** (racemic top, enriched bottom). HPLC conditions: Daicel Chiralpak AD-H column (250 × 4.6 mm), solvent A: *n*-hexane, solvent B: 2-propanol, isocratic ratio A/B 70:30, flow rate: 0.8 mL·min⁻¹, column temperature: 25 °C, UV absorption detected at $\lambda = 238$ nm.

Methyl (5*R*,6*S*)-7-oxo-5-phenyl-2,3,4,5,6,7-hexahydrocyclopenta[*b*]pyran-6-carboxylate (N2b)



Synthetic steps were carried out by THOMAS CRUCHTER. According to procedure F, α -unsaturated β -ketoester **N1b** (23.2 mg, 85.2 μ mol, 1.00 eq.) with catalyst **A-C5f** (1.6 mg, 1.7 μ mol, 2.0 mol%) in DCE (280 μ L containing 1 eq. HFIP) were used; reaction time: 15 h. Desired NAZAROV cyclization product **N2b** was obtained after column chromatography (*n*-hexane/EtOAc 3:1) as a colorless viscous oil (21.6 mg, 79.3 μ mol, 93%). D.r. value determined by ^1H NMR analysis of the crude product: *trans/cis* 19:1; enantiomeric excess of the *trans* diastereomer of the isolated product determined by chiral HPLC analysis: 97% ee (AS-H column, λ = 238 nm, *n*-hexane/2-propanol 70:30, 0.8 mL/min, column temp.: 25 $^\circ\text{C}$; t_{R} (minor) = 23.0 min, t_{R} (major) = 28.7 min), $[\alpha]_{\text{D}}^{27} = -133$ (c 1.0, CHCl_3).

^1H NMR (300 MHz, CDCl_3): δ = 7.49–7.44 (m, 2H, H_{Ar}), 7.42–7.37 (m, 1H, H_{Ar}), 7.27–7.23 (m, 2H, H_{Ar}), 4.36–4.33 (m, 1H, H_{Aliph}), 4.32–4.23 (m, 2H, H_{Aliph}), 3.88 (s, 3H, OCH_3), 3.44 (d, J = 2.4 Hz, 1H, CH), 2.39–2.30 (m, 1H, H_{Aliph}), 2.26–2.17 (m, 1H, H_{Aliph}), 2.14–1.98 (m, 2H, H_{Aliph}) ppm.

^{13}C NMR (75 MHz, CDCl_3): δ = 193.1, 168.9, 150.0, 147.6, 140.0, 129.3 (2C), 127.8, 127.5 (2C), 67.2, 59.3, 53.0, 47.8, 22.4, 21.4 ppm.

IR (ATR): $\tilde{\nu}$ = 2953 (w), 2924 (w), 1738 (m), 1711 (s), 1647 (m), 1493 (w), 1442 (w), 1401 (w), 1298 (w), 1257 (w), 1214 (w), 1161 (w), 1121 (m), 1067 (w), 1032 (w), 977 (w), 919 (w), 861 (w), 774 (w), 704 (w), 638 (w), 567 (w), 466 (w) cm^{-1} .

HR-MS (ESI): m/z calcd. for $\text{C}_{16}\text{H}_{16}\text{O}_4\text{Na}_1$ $[\text{M}+\text{Na}]^+$: 295.0941, found 295.0941.

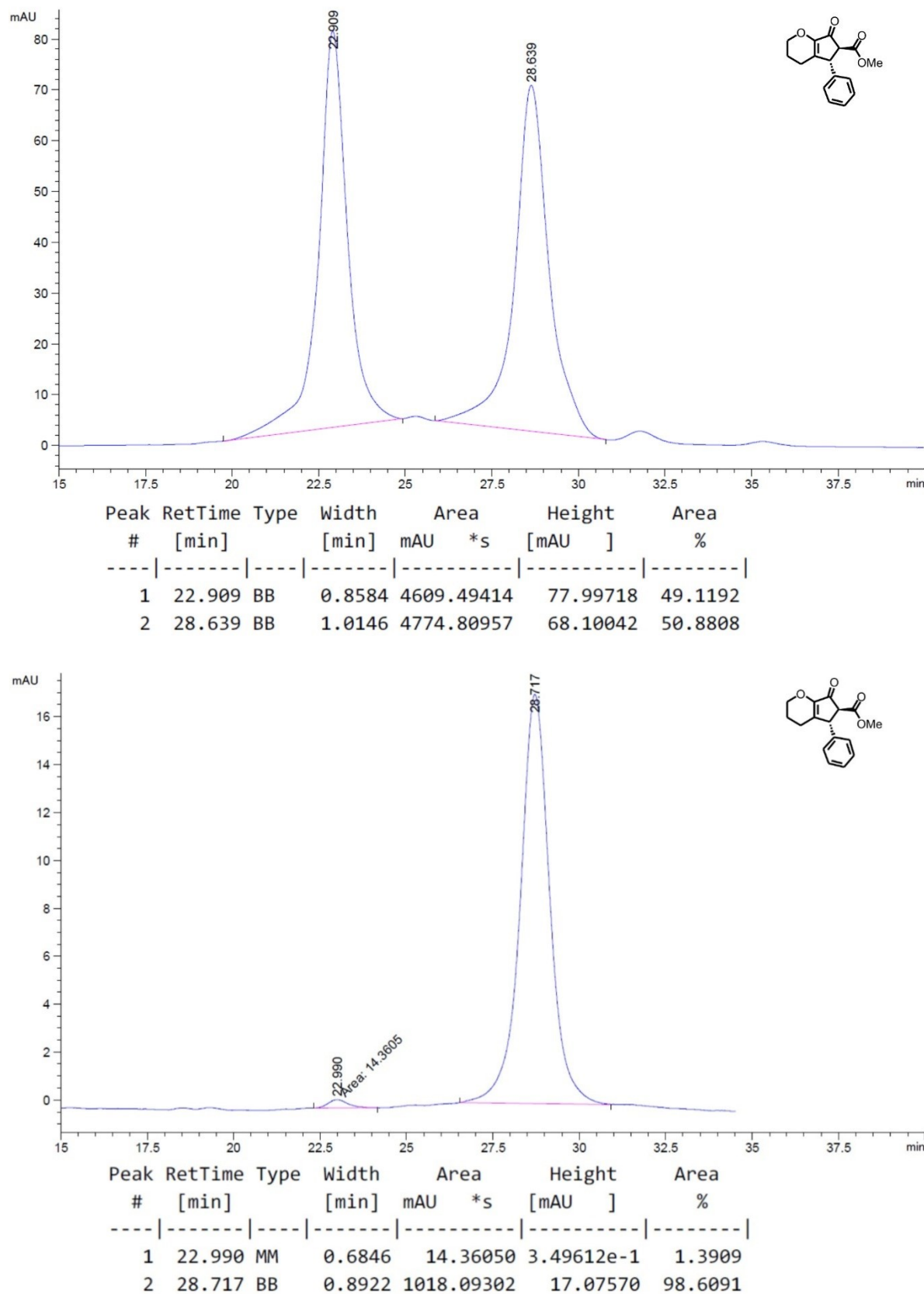
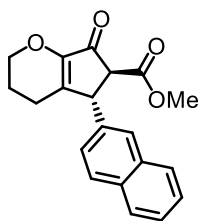


Figure 38: Chiral HPLC traces of **N2b** (racemic top, enriched bottom). HPLC conditions: Daicel Chiralpak AS-H column (250 × 4.6 mm), solvent A: *n*-hexane, solvent B: 2-propanol, isocratic ratio A/B 70:30, flow rate: 0.8 mL·min⁻¹, column temperature: 25 °C, UV absorption detected at λ = 238 nm.

Methyl (5*R*,6*S*)-5-(naphthalen-2-yl)-7-oxo-2,3,4,5,6,7-hexahydrocyclopenta[*b*]pyran-6-carboxylate (N2c)



According to procedure F, α -unsaturated β -ketoester **N1c** (27.4 mg, 85.0 μ mol, 1.00 eq.) and catalyst **A-C5f** (1.6 mg, 1.7 μ mol, 2.0 mol%) in DCE (280 μ L containing 1 eq. HFIP) were used; reaction time: 12 h. Desired NAZAROV product **N2c** was obtained after column chromatography (*n*-hexane/EtOAc 3:1) as a colorless viscous oil (25.4 mg, 81.6 μ mol, 96%). D.r.

value determined by ^1H NMR analysis of the crude product: *trans/cis* 20:1; enantiomeric excess of the *trans* diastereomer of the isolated product determined by chiral HPLC analysis: 95% ee (AD-H column, $\lambda = 238$ nm, *n*-hexane/2-propanol 70:30, 0.8 mL/min, column temp.: 25 °C; t_R (major) = 10.3 min, t_R (minor) = 13.5 min), $[\alpha]_D^{27} = -210$ (c 1.0, CHCl_3).

^1H NMR (300 MHz, CDCl_3): $\delta = 7.86\text{--}7.78$ (m, 3H, H_{Ar}), 7.67–7.65 (m, 1H, H_{Ar}), 7.53–7.46 (m, 2H, H_{Ar}), 7.19 (dd, $J = 8.5, 1.8$ Hz, 1H, H_{Ar}), 4.44–4.39 (m, 1H, H_{Aliph}), 4.23–4.15 (m, 2H, H_{Aliph}), 3.78 (s, 3H, OCH_3), 3.43 (d, $J = 2.3$ Hz, 1H, CH), 2.30–2.21 (m, 1H, H_{Aliph}), 2.14–2.05 (m, 1H, H_{Aliph}), 2.02–1.88 (m, 2H, H_{Aliph}) ppm.

^{13}C NMR (75 MHz, CDCl_3): $\delta = 193.1, 168.9, 150.1, 147.7, 137.1, 133.6, 132.9, 129.4, 127.9, 127.8, 127.0, 126.7, 126.3, 124.5, 67.3, 59.2, 53.0, 47.9, 22.4, 21.4$ ppm.

IR (ATR): $\tilde{\nu} = 3053$ (w), 2949 (w), 1712 (s), 1647 (m), 1601 (w), 1508 (w), 1436 (w), 1401 (w), 1329 (w), 1261 (w), 1161 (w), 1120 (m), 1063 (w), 977 (w), 913 (w), 862 (w), 822 (w), 734 (w), 649 (w), 559 (w), 480 (w) cm^{-1} .

HR-MS (ESI): m/z calcd. for $\text{C}_{20}\text{H}_{18}\text{O}_4\text{Na}_1$ $[\text{M}+\text{Na}]^+$: 345.1097, found 345.1097.

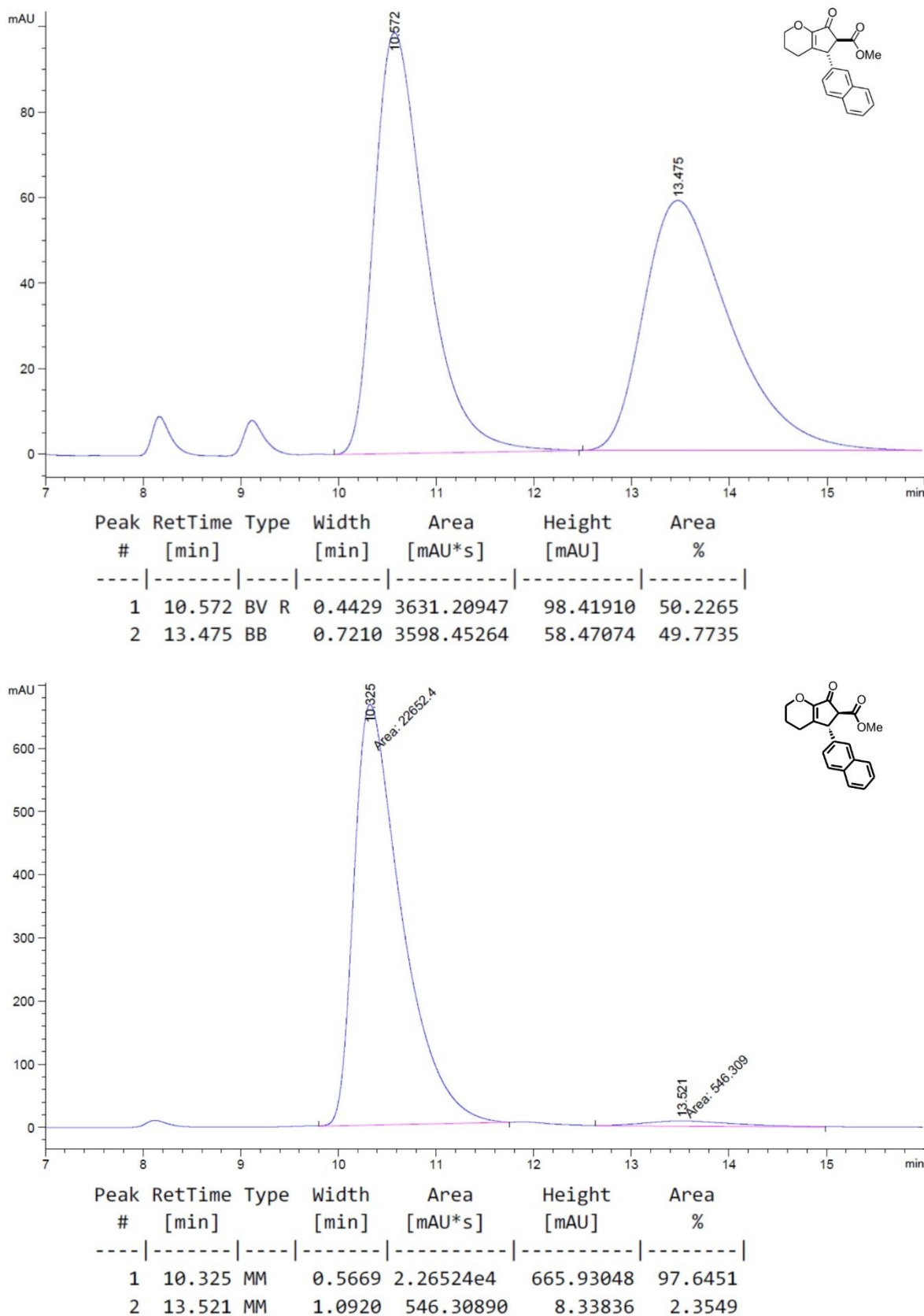
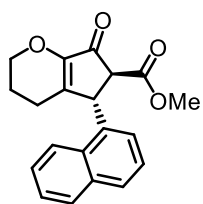


Figure 39: Chiral HPLC traces of **N2c** (racemic top, enriched bottom). HPLC conditions: Daicel Chiralpak AD-H column (250 × 4.6 mm), solvent A: *n*-hexane, solvent B: 2-propanol, isocratic ratio A/B 70:30, flow rate: 0.8 mL·min⁻¹, column temperature: 25 °C, UV absorption detected at λ = 238 nm.

Methyl (5*R*,6*S*)-5-(naphthalen-1-yl)-7-oxo-2,3,4,5,6,7-hexahydrocyclopenta[*b*]pyran-6-carboxylate (N2d)



Synthetic steps were carried out by VLADIMIR LARIONOV. According to procedure F, α -unsaturated β -ketoester **N1d** (27.4 mg, 85.0 μ mol, 1.00 eq.) and catalyst **Λ -C5f** (1.6 mg, 1.7 μ mol, 2.0 mol%) in DCE (280 μ L containing 1 eq. HFIP) were used; reaction time: 14 h. Desired NAZAROV product **N2d** was obtained after column chromatography (*n*-hexane/EtOAc 3:1) as a colorless viscous oil (25.2 mg, 78.2 μ mol, 92%); D.r. value determined by ^1H NMR analysis of the crude product: *trans/cis* 29:1; enantiomeric excess of the *trans* diastereomer of the isolated product determined by chiral HPLC analysis: 95% ee (AS-H column, λ = 254 nm, *n*-hexane/2-propanol 70:30, 1.0 mL/min, column temp.: 25 °C; t_R (major) = 21.9 min, t_R (minor) = 28.7 min), $[\alpha]_D^{27}$ = +16 (*c* 1.0, CHCl_3).

^1H NMR (300 MHz, CDCl_3): δ = 8.28–7.98 (m, 1H, H_{Ar}), 7.96–7.85 (m, 1H, H_{Ar}), 7.85–7.72 (m, 1H, H_{Ar}), 7.62–7.48 (m, 2H, H_{Ar}), 7.48–7.37 (m, 1H, H_{Ar}), 7.21–7.04 (m, 1H, H_{Ar}), 5.20 (s br, 1H, H_{Aliph}), 4.33–4.14 (m, 2H, H_{Aliph}), 3.79 (s br, 3H, OCH_3), 3.28 (s, J = 2.3 Hz, 1H, CH), 2.37–2.17 (m, 2H, H_{Aliph}), 2.10–1.89 (m, 2H, H_{Aliph}) ppm. We observed broadened signals, we assume hindered rotation of the 1-naphthyl moiety.

^{13}C NMR: We observed broadened signals, we assume hindered rotation of the 1-naphthyl moiety.

IR (ATR): $\tilde{\nu}$ = 2924 (w), 2877 (w), 2854 (w), 1719 (s), 1667 (s), 1620 (s), 1434 (w), 1269 (w), 1228 (m), 1204 (w), 1103 (m), 1050 (w), 989 (w), 773 (w) cm^{-1} .

HR-MS (ESI): m/z calcd. for $\text{C}_{20}\text{H}_{18}\text{O}_4\text{Na}$ $[\text{M}+\text{Na}]^+$: 345.1097, found 345.1096.

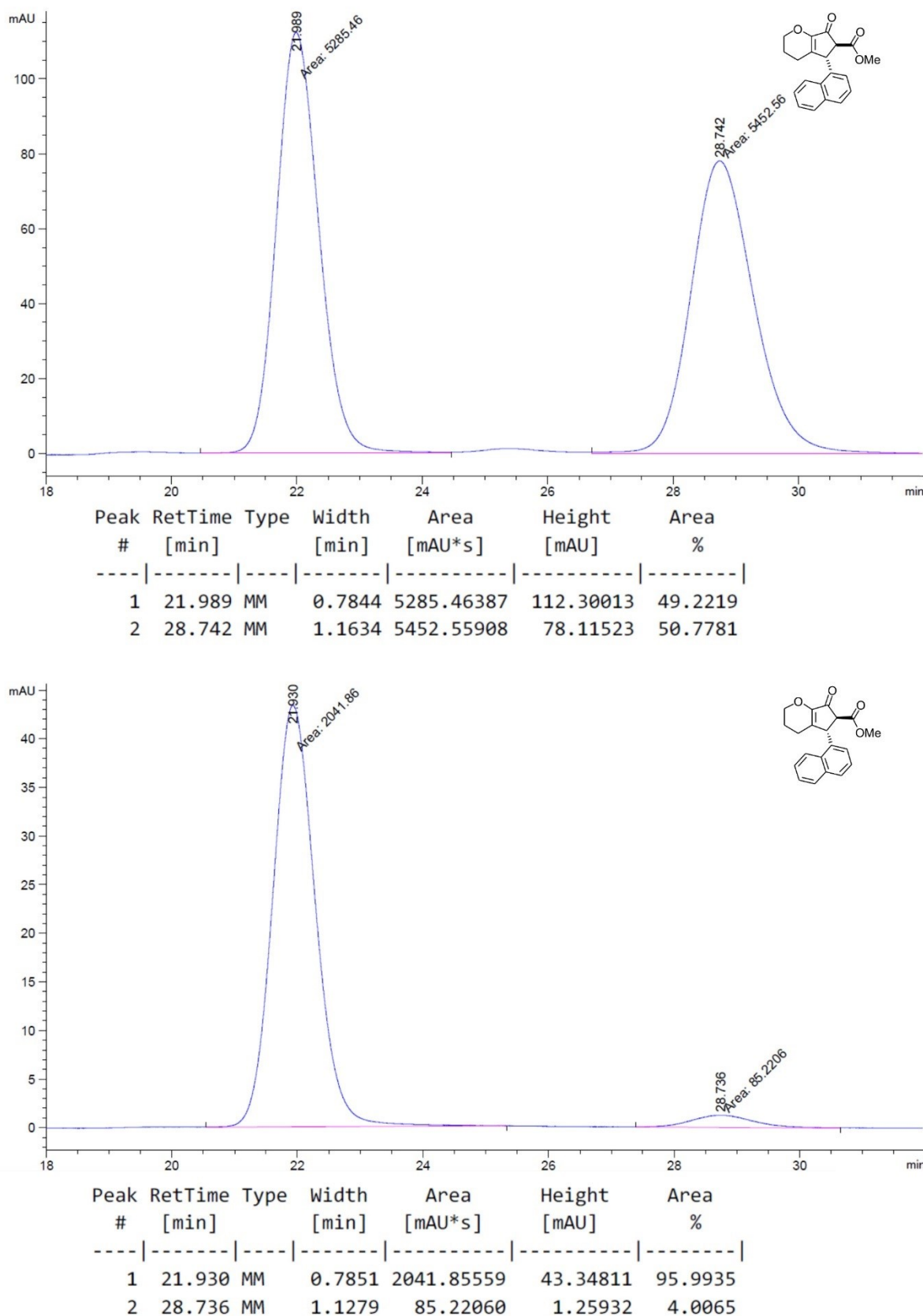
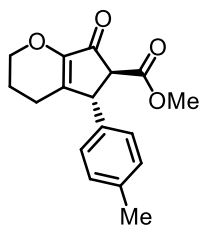


Figure 40: Chiral HPLC traces of **N2d** (racemic top, enriched bottom). HPLC conditions: Daicel Chiralpak AS-H column (250 × 4.6 mm), solvent A: *n*-hexane, solvent B: 2-propanol, isocratic ratio A/B 70:30, flow rate: 1.0 mL·min⁻¹, column temperature: 25 °C, UV absorption detected at $\lambda = 254$ nm.

Methyl (5*R*,6*S*)-7-oxo-5-(*p*-tolyl)-2,3,4,5,6,7-hexahydrocyclopenta[*b*]pyran-6-carboxylate (N2e)



According to procedure F, α -unsaturated β -ketoester **N1e** (25.0 mg, 87.3 μ mol, 1.00 eq.) and catalyst **A-C5f** (1.6 mg, 1.7 μ mol, 2.0 mol%) in DCE (280 μ L containing 1 eq. HFIP) were used; reaction time: 14 h. Desired NAZAROV product **N2e** was obtained after column chromatography (*n*-hexane/EtOAc 3:1) as a colorless viscous oil (23.3 mg, 81.2 μ mol, 93%).

D.r. value determined by ^1H NMR analysis of the crude product: *trans/cis* 28:1; enantiomeric excess of the *trans* diastereomer of the isolated product determined by chiral HPLC analysis: 94% ee (AS-H column, λ = 254 nm, *n*-hexane/2-propanol 70:30, 1.0 mL/min, column temp.: 25 °C; t_R (major) = 13.9 min, t_R (minor) = 19.5 min), $[\alpha]_D^{27} = -177$ (*c* 1.0, CHCl_3).

^1H NMR (300 MHz, CDCl_3): δ = 7.15 (d, J = 7.9 Hz, 2H, H_{Ar}), 7.02 (d, J = 7.9 Hz, 2H, H_{Ar}), 4.25–4.08 (m, 3H, H_{Aliph}), 3.79 (s, 3H, OCH_3), 3.30 (d, J = 2.2 Hz, 1H, CH), 2.33 (s, 3H, CH_3), 2.28–2.08 (m, 2H, H_{Aliph}), 2.03–1.83 (m, 2H, H_{Aliph}) ppm.

^{13}C NMR (75 MHz, CDCl_3): δ = 193.2, 169.0, 149.9, 147.8, 137.6, 136.9, 130.0, 127.4, 67.2, 59.5, 52.9, 47.5, 22.4, 21.5, 21.2 ppm.

IR (ATR): $\tilde{\nu}$ = 2952 (w), 2926 (w), 1739 (m), 1711 (s), 1647 (m), 1513 (w), 1436 (w), 1403 (w), 1297 (w), 1256 (w), 1160 (w), 1119 (m), 1062 (w), 978 (w), 953 (w), 914 (w), 859 (w), 818 (w), 728 (w), 693 (w), 560 (w), 479 (w) cm^{-1} .

HR-MS (ESI): m/z calcd. for $\text{C}_{17}\text{H}_{18}\text{O}_4\text{Na}$ $[\text{M}+\text{Na}]^+$: 309.1097, found 309.1097.

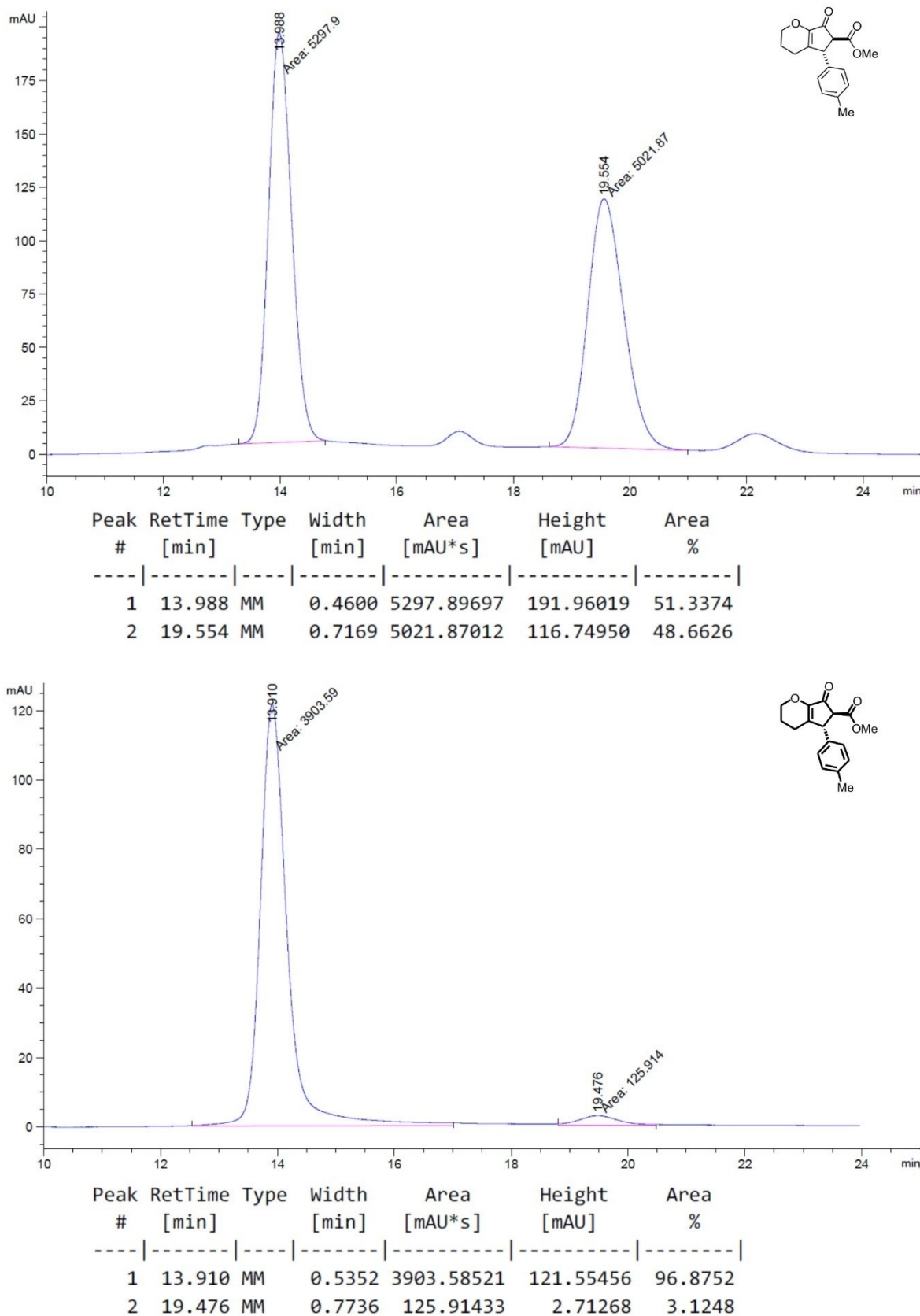
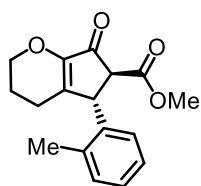


Figure 41: Chiral HPLC traces of **N2e** (racemic top, enriched bottom). HPLC conditions: Daicel Chiralpak AS-H column (250 × 4.6 mm), solvent A: *n*-hexane, solvent B: 2-propanol, isocratic ratio A/B 70:30, flow rate: 1.0 mL·min⁻¹, column temperature: 25 °C, UV absorption detected at λ = 254 nm.

Methyl (5*R*, 6*S*)-7-oxo-5-(*o*-tolyl)-2,3,4,5,6,7-hexahydrocyclopenta[*b*]pyran-6-carboxylate (N2f)



According to procedure F, α -unsaturated β -ketoester **N1f** (23.5 mg, 82.1 μ mol, 1.00 eq.) and catalyst **A-C5f** (1.6 mg, 1.7 μ mol, 2.0 mol%) in DCE (280 μ L containing 1 eq. HFIP) were used; reaction time: 14 h. Desired NAZAROV product **N2f** was obtained after column chromatography (*n*-hexane/EtOAc 3:1) as a colorless viscous oil (22.3 mg, 77.9 μ mol, 95%). D.r. value determined by ^1H NMR analysis of the crude product: *trans/cis* 20:1; enantiomeric excess of the *trans* diastereomer of the isolated product determined by chiral HPLC analysis: 95% ee (AS-H column, λ = 254 nm, *n*-hexane/2-propanol 70:30, 1.0 mL/min, column temp.: 25 $^\circ\text{C}$; t_R (minor) = 25.6 min, t_R (major) = 34.5 min), $[\alpha]_D^{27} = -115$ (*c* 0.3, CHCl_3).

^1H NMR (300 MHz, CDCl_3): δ = 7.21–7.14 (m, 3H, H_{Ar}), 6.95–6.87 (m, 1H, H_{Ar}), 4.58–4.51 (m, 1H, H_{Aliph}), 4.23–4.13 (m, 2H, H_{Aliph}), 3.78 (s, 3H, OCH_3), 3.24 (d, J = 1.5 Hz, 1H, CH), 2.36 (s, 3H, CH_3), 2.23–2.13 (m, 2H, H_{Aliph}), 2.02–1.89 (m, 2H, H_{Aliph}) ppm.

^{13}C NMR (75 MHz, CDCl_3): δ = 193.3, 169.3, 150.3, 148.0, 138.3, 136.7, 131.1, 127.5, 127.0, 67.2, 59.1, 53.0, 22.6, 21.5, 19.8 ppm.

IR (ATR): $\tilde{\nu}$ = 2950 (w), 2926 (w), 1739 (m), 1713 (s), 1648 (m), 1490 (w), 1436 (w), 1400 (w), 1299 (w), 1257 (w), 1162 (w), 1121 (m), 1065 (w), 977 (w), 952 (w), 917 (w), 863 (w), 764 (w), 729 (w) cm^{-1} .

HR-MS (ESI): m/z calcd. for $\text{C}_{17}\text{H}_{18}\text{O}_4\text{Na}$ $[\text{M}+\text{Na}]^+$: 309.1097, found 309.1098.

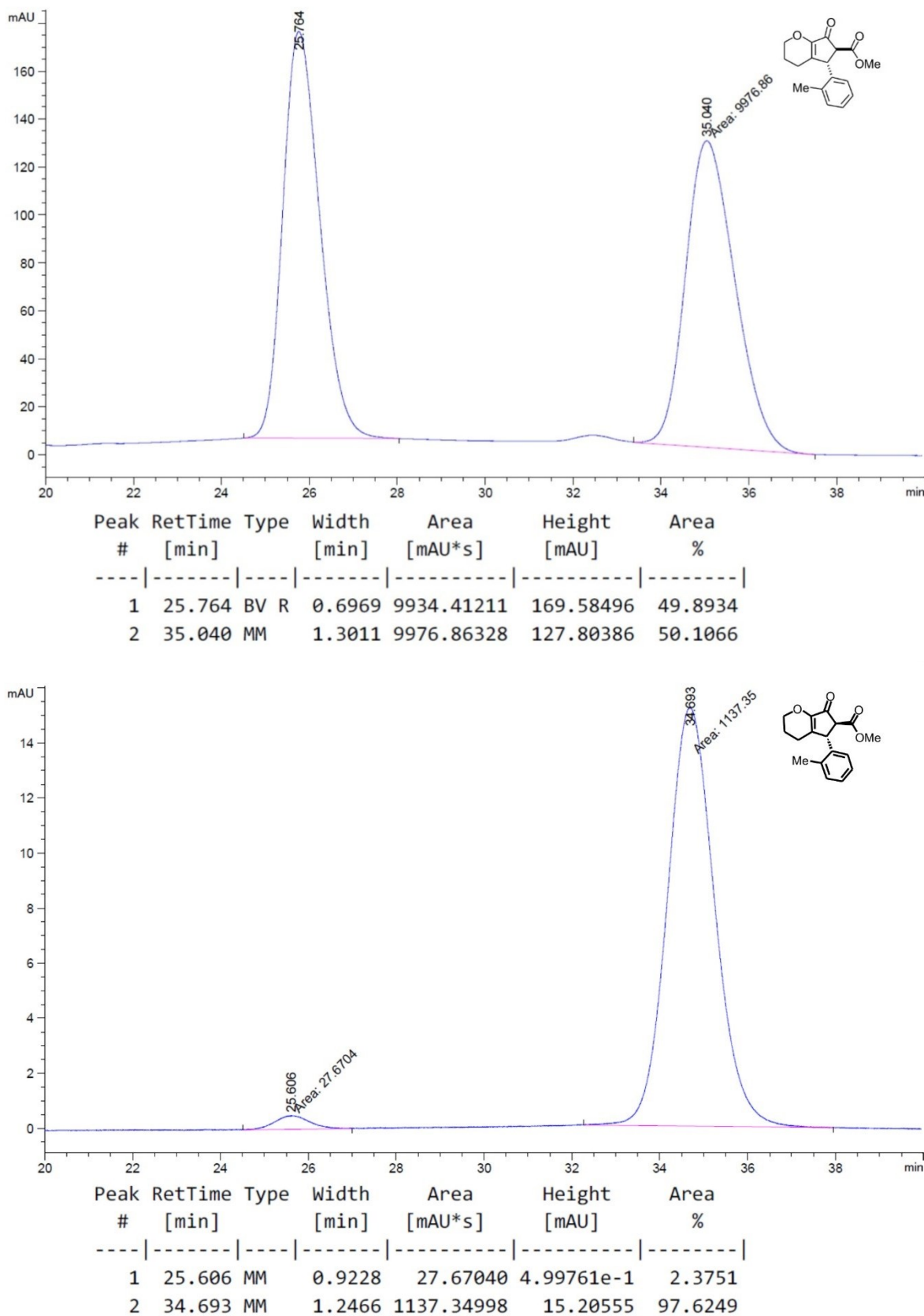
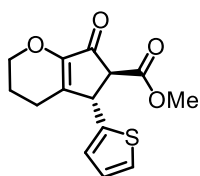


Figure 42: Chiral HPLC traces of **N2f** (racemic top, enriched bottom). HPLC conditions: Daicel Chiralpak AS-H column (250 × 4.6 mm), solvent A: *n*-hexane, solvent B: 2-propanol, isocratic ratio A/B 70:30, flow rate: 1.0 mL·min⁻¹, column temperature: 25 °C, UV absorption detected at $\lambda = 254$ nm.

Methyl (5*S*,6*S*)-7-oxo-5-(thiophen-2-yl)-2,3,4,5,6,7-hexahydrocyclopenta[*b*]pyran-6-carboxylate (N2g)

Note: Switching from R → S is not caused by actual inversion of the stereocenter but by higher priority of the thiophene ring according to CIP rules.



Synthetic steps were carried out by VLADIMIR LARIONOV. According to procedure F, α -unsaturated β -ketoester **N1g** (23.7 mg, 85.2 μ mol, 1.00 eq.) and catalyst **A-C5f** (1.6 mg, 1.7 μ mol, 2.0 mol%) in DCE (280 μ L containing 1 eq. HFIP) were used; reaction time: 23 h. Desired NAZAROV product **N2g** was obtained after column chromatography (*n*-hexane/EtOAc 3:1) as a colorless solid (23.2 mg, 83.5 μ mol, 98%). D.r. value determined by ^1H NMR analysis of the crude product: *trans/cis* 50:1; enantiomeric excess of the *trans* diastereomer of the isolated product determined by chiral HPLC analysis: 89% ee (AD-H column, λ = 238 nm, *n*-hexane/2-propanol 70:30, 1.0 mL/min, column temp.: 25 °C; t_R (major) = 9.0 min, t_R (minor) = 12.7 min), $[\alpha]_D^{27} = -159$ (*c* 1.0, CHCl_3).

^1H NMR (300 MHz, CDCl_3): δ = 7.22 (dd, J = 5.1, 0.7 Hz, 1H, H_{Ar}), 7.19 (dd, J = 5.1, 3.5 Hz, 1H, H_{Ar}), 6.91 (dd, J = 3.5, 0.7 Hz, 1H, H_{Ar}), 4.60–4.57 (m, 1H, H_{Aliph}), 4.21–4.11 (m, 2H, H_{Ar}), 3.78 (s, 3H, OCH_3), 3.44 (d, J = 2.5 Hz, 1H, CH), 2.30–2.25 (m, 2H, H_{Aliph}), 2.02–1.91 (m, 2H, H_{Aliph}) ppm.

^{13}C NMR (75 MHz, CDCl_3): δ = 192.2, 168.5, 149.5, 146.7, 143.4, 127.3, 125.7, 125.1, 67.3, 59.8, 53.1, 42.8, 22.4, 21.4 ppm.

IR (ATR): $\tilde{\nu}$ = 2922 (m), 2855 (m), 1708 (s), 1645 (m), 1436 (w), 1402 (w), 1370 (w), 1327 (w), 1264 (m), 1216 (w), 1156 (w), 1117 (s), 1034 (m), 974 (w), 910 (w), 854 (w), 805 (w), 705 (s), 623 (w), 586 (w), 555 (w), 491 (w) cm^{-1} .

HR-MS (ESI): m/z calcd. for $\text{C}_{14}\text{H}_{14}\text{O}_4\text{S}_1\text{Na}_1$ $[\text{M}+\text{Na}]^+$: 301.0505, found 301.0507.

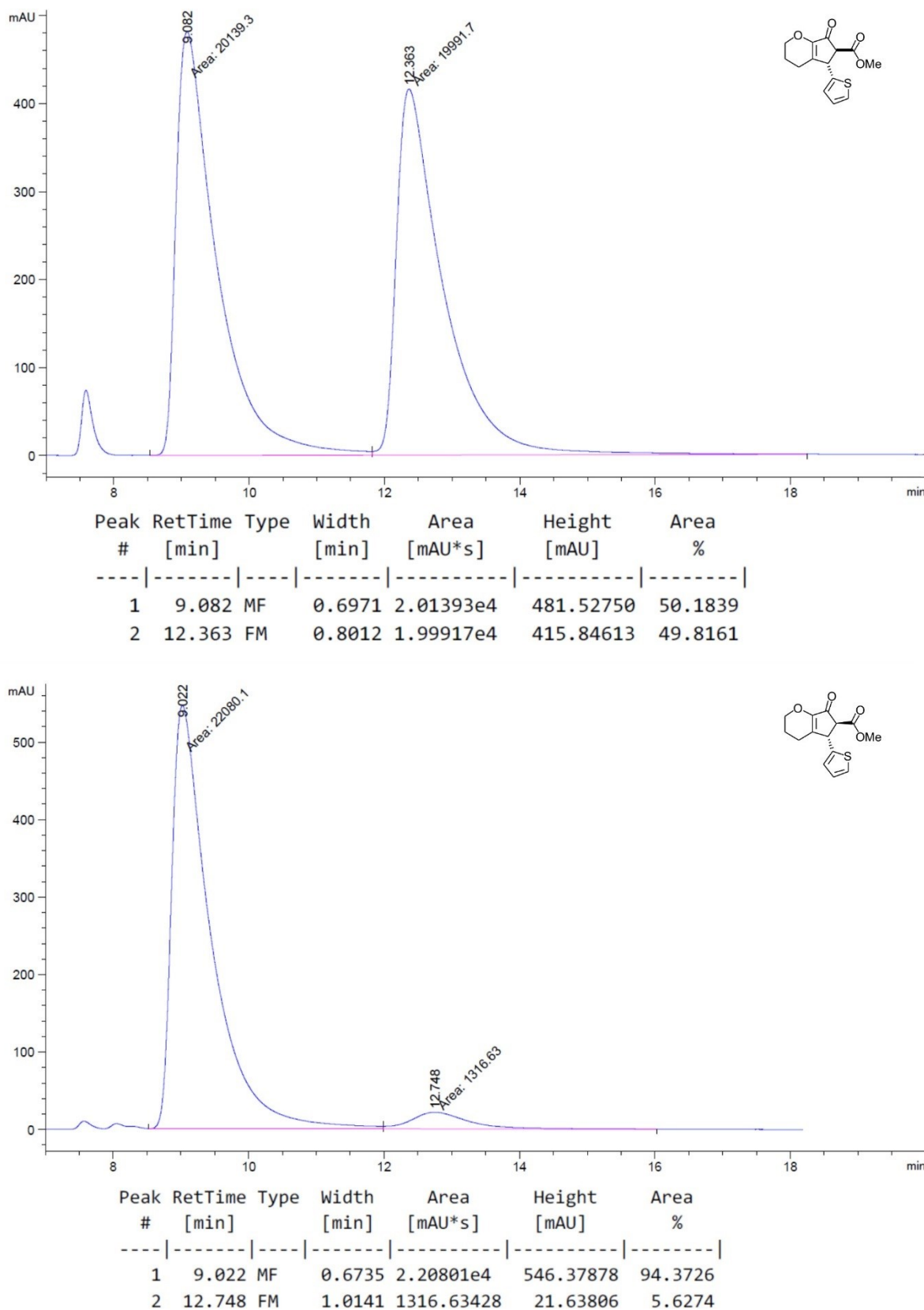
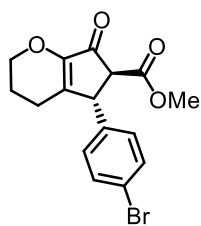


Figure 43: Chiral HPLC traces of **N2g** (racemic top, enriched bottom). HPLC conditions: Daicel Chiralpak AD-H column (250 × 4.6 mm), solvent A: *n*-hexane, solvent B: 2-propanol, isocratic ratio A/B 70:30, flow rate: 1.0 mL·min⁻¹, column temperature: 25 °C, UV absorption detected at $\lambda = 238$ nm.

Methyl (5*R*,6*S*)-5-(4-bromophenyl)-7-oxo-2,3,4,5,6,7-hexahydrocyclopenta[*b*]pyran-6-carboxylate (N2h)



According to procedure F, α -unsaturated β -ketoester **N1h** (30.1 mg, 85.7 μ mol, 1.00 eq.) and catalyst **A-C5f** (1.6 mg, 1.7 μ mol, 2.0 mol%) in DCE (280 μ L containing 1 eq. HFIP) were used; reaction time: 23 h. Desired NAZAROV product **N2h** was obtained after column chromatography (*n*-hexane/EtOAc 3:1) as a colorless solid (25.6 mg, 72.8 μ mol, 85%). D.r. value determined by ^1H NMR analysis of the crude product: *trans/cis* 20:1; enantiomeric excess of the *trans* diastereomer of the isolated product determined by chiral HPLC analysis: 99% ee (AD-H column, λ = 238 nm, *n*-hexane/2-propanol 70:30, 0.8 mL/min, column temp.: 25 $^\circ\text{C}$; t_{R} (major) = 11.1 min, t_{R} (minor) = 26.6 min), $[\alpha]_{\text{D}}^{27} = -213$ (*c* 1.0, CHCl_3).

^1H NMR (300 MHz, CDCl_3): δ = 7.47 (d, J = 8.3 Hz, 2H, H_{Ar}), 7.02 (d, J = 8.3 Hz, 2H, H_{Ar}), 4.26–4.09 (m, 3H, H_{Aliph}), 3.77 (s, 3H, OCH_3), 3.26 (d, J = 2.2 Hz, 1H, CH), 2.30–2.14 (m, 1H, H_{Aliph}), 2.14–1.84 (m, 3H, H_{Aliph}) ppm.

^{13}C NMR (75 MHz, CDCl_3): δ = 192.6, 168.6, 150.2, 146.6, 139.1, 132.5, 129.2, 121.8, 67.3, 59.2, 53.0, 47.2, 22.3, 21.4 ppm.

IR (ATR): $\tilde{\nu}$ = 2951 (w), 2928 (w), 1714 (s), 1649 (m), 1487 (w), 1436 (w), 1404 (w), 1303 (w), 1257 (w), 1162 (w), 1122 (m), 1069 (w), 1012 (w), 978 (w), 913 (w), 829 (w), 727 (w), 535 (w), 479 (w) cm^{-1} .

HR-MS (ESI): m/z calcd. for $\text{C}_{16}\text{H}_{15}\text{Br}_1\text{O}_4\text{Na}_1$ $[\text{M}+\text{Na}]^+$: 375.0027, found 375.0027.

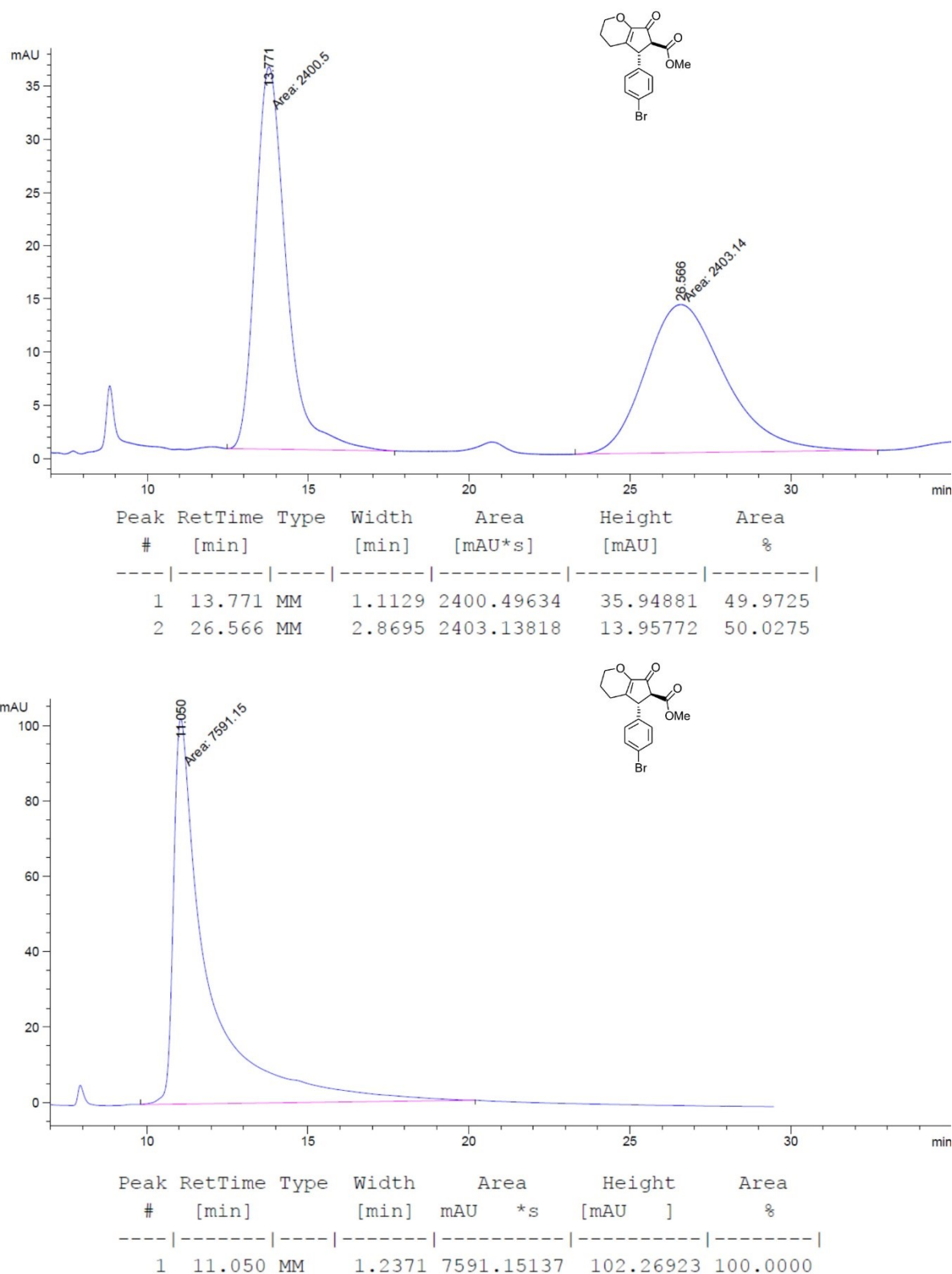
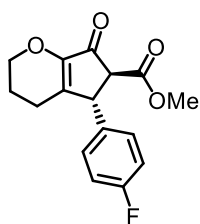


Figure 44: Chiral HPLC traces of N2h (racemic top, enriched bottom). HPLC conditions: Daicel Chiralpak AD-H column (250 × 4.6 mm), solvent A: *n*-hexane, solvent B: 2-propanol, isocratic ratio A/B 70:30, flow rate: 0.8 mL·min⁻¹, column temperature: 25 °C, UV absorption detected at λ = 238 nm.

Methyl (5*R*,6*S*)-5-(4-fluorophenyl)-7-oxo-2,3,4,5,6,7-hexahydrocyclopenta[*b*]pyran-6-carboxylate (N2i)



Synthetic steps were carried out by THOMAS CRUCHTER. According to procedure F, α -unsaturated β -ketoester **N1i** (24.7 mg, 85.1 μ mol, 1.00 eq.) and catalyst **A-C5f** (1.6 mg, 1.7 μ mol, 2.0 mol%) in DCE (280 μ L containing 1 eq. HFIP) were used; reaction time: 14 h. Desired NAZAROV product **N2i** was obtained after column chromatography (*n*-hexane/EtOAc 3:1) as a yellow

viscous oil (22.4 mg, 77.2 μ mol, 91%). D.r. value determined by ^1H NMR analysis of the crude product: *trans/cis* 15:1; enantiomeric excess of the *trans* diastereomer of the isolated product determined by chiral HPLC analysis: 96% ee (OJ-H, 254 nm, *n*-hexane/2-propanol 70:30, 0.8 mL/min, column temp.: 25 °C, t_R (major) = 23.8 min, t_R (minor) = 29.3 min), $[\alpha]_{\text{D}}^{27} = -132$ (*c* 1.0, CHCl_3).

^1H NMR (500 MHz, CDCl_3): δ = 7.13–7.08 (m, 2H, H_{Ar}), 7.06–7.00 (m, 2H, H_{Ar}), 4.24–4.20 (m, 1H, H_{Aliph}), 4.20–4.11 (m, 2H, H_{Aliph}), 3.77 (s, 3H, OCH_3), 3.26 (d, J = 2.3 Hz, 1H, CH), 2.25–2.16 (m, 1H, H_{Aliph}), 2.12–2.03 (m, 1H, H_{Aliph}), 2.02–1.86 (m, 2H, H_{Aliph}) ppm.

^{13}C NMR (125 MHz, CDCl_3): δ = 192.8, 168.7, 162.3 (d, J = 246.9 Hz, 1C), 150.0, 147.1, 135.7 (d, J = 3.2 Hz, 1C), 129.1 (d, J = 8.2 Hz, 2C), 116.3 (d, J = 21.7 Hz, 2C), 116.2, 67.2, 59.4, 53.0, 47.0, 22.3, 21.4 ppm.

^{19}F NMR (282 MHz, CDCl_3): δ = 114.4 ppm.

IR (ATR): $\tilde{\nu}$ = 2954 (w), 2923 (w), 1713 (s), 1648 (m), 1604 (w), 1507 (w), 1437 (w), 1402 (w), 1300 (w), 1258 (m), 1223 (m), 1160 (w), 1121 (m), 1063 (w), 1063 (w), 977 (w), 914 (w), 841 (w), 797 (w), 728 (w), 558 (w), 520 (w), 457 (w), 412 (w) cm^{-1} .

HR-MS (ESI): m/z calcd. for $\text{C}_{16}\text{H}_{15}\text{F}_1\text{O}_4\text{Na}_1$ $[\text{M}+\text{Na}]^+$: 313.0847, found 313.0848.

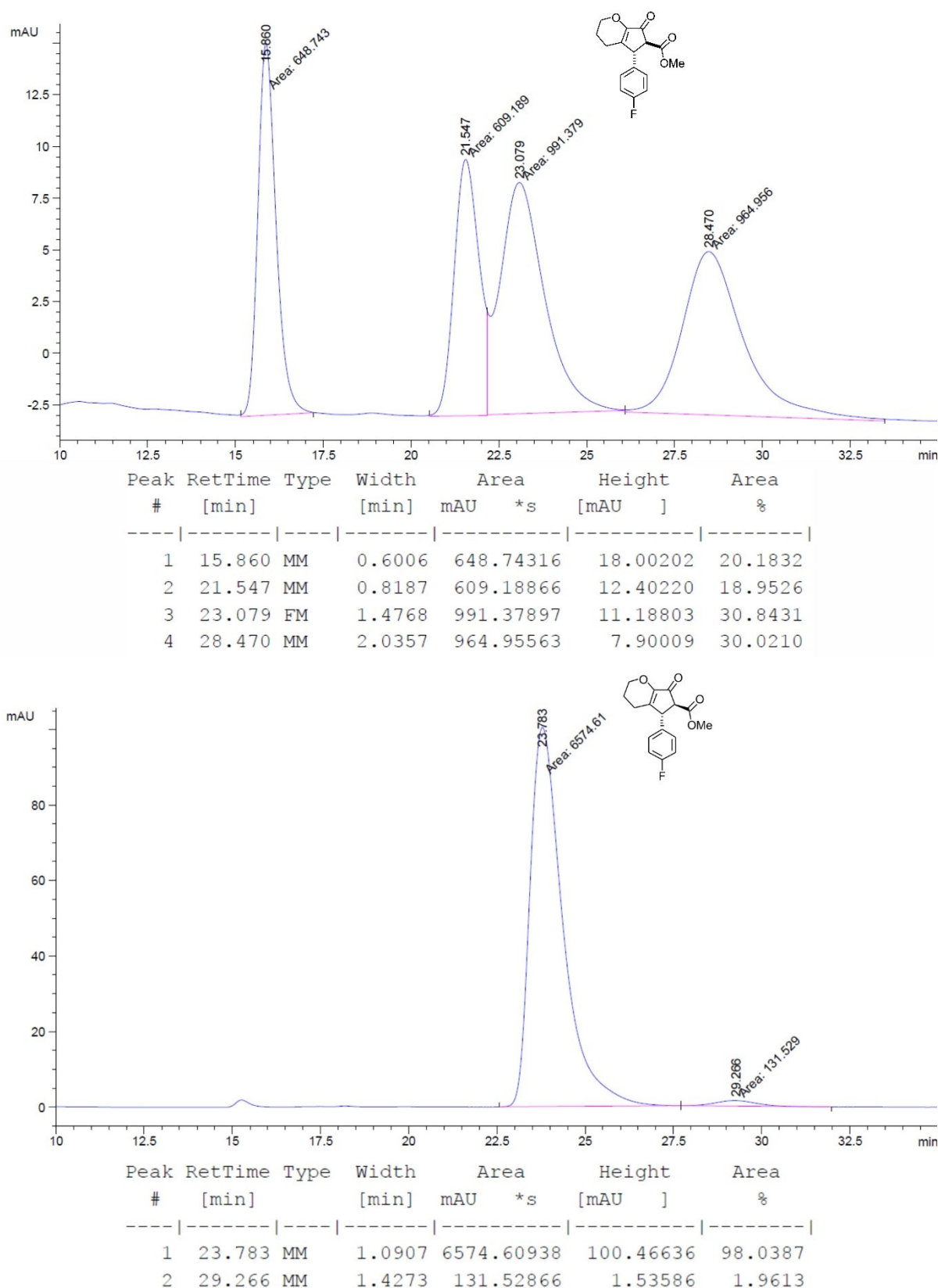
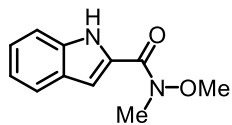


Figure 45: Chiral HPLC traces of **N2i** (racemic top, enriched bottom). HPLC conditions: Daicel Chiralpak OJ-H column (250 × 4.6 mm), solvent A: *n*-hexane, solvent B: 2-propanol, isocratic ratio A/B 70:30, flow rate: 0.8 mL·min⁻¹, column temperature: 25 °C, UV absorption detected at $\lambda = 254$ nm.

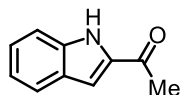
3.4.26 Indole-Functionalized α -Unsaturated β -Ketoesters N3***N*-Methoxy-*N*-methyl-1*H*-indole-2-carboxamide (**S13a**)**

Compound **S13a** was prepared according to a slightly modified literature-known procedure.^[50] A flask (250 mL) equipped with a septum, a nitrogen inlet, and a stir bar was charged with indole-2-carboxylic acid (2.82 g, 17.5 mmol, 1.00 eq.) and dry CH₂Cl₂ (120 mL). To this solution *N,O*-dimethyl hydroxylamine hydrochloride (1.71 g, 17.5 mmol, 1.00 eq.), Et₃N (2.45 mL, 17.7 mmol, 1.01 eq.), and DCC (3.67 g, 17.8 mmol, 1.02 eq.) were added and the solution stirred under nitrogen atmosphere for 4 h. Water (100 mL) was added, the layers separated, and the aqueous layer extracted with CH₂Cl₂ (3x30 mL). The combined organic layers were washed with brine, dried over MgSO₄, filtered, and concentrated under reduced pressure. The crude product was purified by flash chromatography (*n*-hexane/EtOAc 2:1 → 1:1) to furnish WEINREB amide **S13a** (2.19 g, 10.7 mmol, 61%) as a beige solid.

TLC (*n*-hexane/EtOAc 2:1) *R*_f = 0.13.

¹H NMR (300 MHz, CDCl₃): δ = 9.47 (s, 1H, NH), 7.70 (dd, 1H, *J* = 8.1, 0.9 Hz, *H*_{Ar}), 7.44 (dd, 1H, *J* = 8.4, 0.9 Hz, *H*_{Ar}), 7.36–7.26 (m, 1H, *H*_{Ar}), 7.24–7.23 (m, 1H, *H*_{Ar}), 7.14 (m, 1H, *H*_{Ar}), 3.85 (s, 3H, CH₃), 3.44 (s, 3H, CH₃) ppm.

¹³C NMR (75 MHz, CDCl₃): δ = 161.8, 136.0, 128.4, 128.2, 125.0, 122.7, 120.6, 111.9, 108.1, 61.5, 33.4 ppm.

1-(1*H*-Indole-2-yl)ethan-1-one (S13b**)**

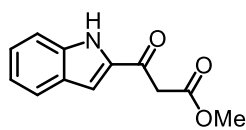
Compound **S13b** was prepared according to a slightly modified literature-known procedure.^[50] A flask (250 mL) equipped with a septum, a nitrogen inlet, and a stir bar was charged with WEINREB amide **S13a** (2.51 g, 12.3 mmol, 1.00 eq.) and dry THF (80.0 mL) and the resulting solution cooled to –78 °C. To this solution MeLi (1.6 M in Et₂O; 30.7 mL, 49.2 mmol, 4.00 eq.) was added dropwise. After 1 h at –78 °C, the cooling bath was removed and water (100 mL) was added at rt and the aqueous layer extracted with Et₂O (3x 30 mL). The combined organic layers were washed with brine (50 mL), dried over Na₂SO₄, filtered, concentrated under reduced pressure, and the crude product subjected to flash chromatography (*n*-hexane/EtOAc 7:3). Desired ketone **S13b** (1.37 g, 8.60 mmol, 70%) was obtained as a colorless solid.

TLC (*n*-hexane/EtOAc 7:3) R_f = 0.44.

^1H NMR (300 MHz, CDCl_3): δ = 8.98 (s, 1H, NH), 7.77–7.67 (m, 1H, H_{Ar}), 7.45–7.39 (m, 1H, H_{Ar}), 7.39–7.32 (m, 1H, H_{Ar}), 7.22–7.20 (m, 1H, H_{Ar}), 7.19–7.13 (m, 1H, H_{Ar}), 2.60 (s, 3H, CH_3) ppm.

^{13}C NMR (75 MHz, CDCl_3): δ = 190.7, 137.6, 135.5, 127.7, 126.4, 123.1, 121.0, 112.4, 110.0, 26.0 ppm.

Methyl 3-(1*H*-Indole-2-yl)-3-oxopropanoate (**S13c**)



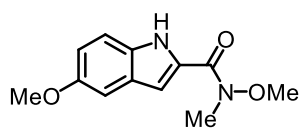
Compound **S13c** was prepared according to a slightly modified literature-known procedure.^[50] A flask (100 mL) equipped with a septum, a nitrogen inlet, and a stir bar was charged with NaH (60% in mineral oil; 308 mg, 7.70 mmol, 1.35 eq.), KH (30% in mineral oil; 931 mg, 6.98 mmol, 1.23 eq.), dry THF (10 mL), and dimethylcarbonate (1.80 mL, 21.4 mmol, 3.75 eq.) and the resulting mixture cooled to 0 °C. To this suspension, a solution of ketone **S13b** (907 mg, 5.70 mmol, 1.00 eq.) in THF (5 mL) was added dropwise (*caution: violent reaction!*). After the gas evolution had ceased (~10 min), the reaction was heated to 40 °C for 19 h after which TLC analysis indicated full conversion. Aqueous HCl (1 M, 15 mL) and water (15 mL) were then added carefully. The layers were separated, and the aqueous layer extracted with EtOAc (6x30 mL). The combined organic layers were washed with brine (50 mL), dried over Na_2SO_4 , filtered, and concentrated under reduced pressure. The crude product was dissolved in CH_2Cl_2 , adsorbed on silica gel, and purified by flash chromatography (*n*-hexane/EtOAc 7:3) to furnish ketoester **S13c** (886 mg, 4.08 mmol, 72%) as a beige, crystalline solid.

TLC (*n*-hexane/EtOAc 7:3) R_f = 0.26.

^1H NMR (300 MHz, CDCl_3): δ = 9.24 (s, 1H, NH), 7.75–7.69 (m, 1H, H_{Ar}), 7.47–7.41 (m, 1H, H_{Ar}), 7.40–7.34 (m, 1H, H_{Ar}), 7.26–7.24 (m, 1H, H_{Ar}), 7.20–7.13 (m, 1H, H_{Ar}), 3.99 (s, 3H, CH_3), 3.77 (s, 3H, CH_3) ppm.

^{13}C NMR (75 MHz, CDCl_3): δ = 184.7, 167.8, 137.6, 134.4, 127.6, 127.2, 123.4, 121.4, 112.5, 111.2, 52.7, 45.4 ppm.

***N*,5-Dimethoxy-*N*-methyl-1*H*-indole-2-carboxamide (S14a)**



The title compound was prepared according to a slightly modified literature-known procedure.^[50] A flask (250 mL) equipped with a septum, a nitrogen inlet, and a stir bar was charged with 5-methoxy-1*H*-indole-2-carboxylic acid (3.00 g, 15.7 mmol, 1.00 eq.) and dry CH₂Cl₂ (100 mL). To this solution *N,O*-dimethylhydroxylamine hydrochloride (1.84 g, 26.5 mmol, 1.69 eq.), Et₃N (3.7 mL, 26.7 mmol, 1.70 eq.), and DCC (3.90 g, 18.9 mmol, 1.20 eq.) were added and the solution was stirred under nitrogen atmosphere for 24 h. The yellow solution was then diluted with dichloromethane/water (1:1), the layers separated, and the aqueous layer extracted with CH₂Cl₂ until it became virtually colorless. The combined organic layers were dried over MgSO₄, filtered, and concentrated under reduced pressure. The crude product was dissolved in CH₂Cl₂, adsorbed on silica gel, and purified by flash chromatography (*n*-hexane/EtOAc 3:2) to furnish WEINREB amide **S14a** (1.89 g, 8.07 mmol, 51%) as a beige solid.

TLC (*n*-hexane/EtOAc 3:2) *R*_f = 0.30.

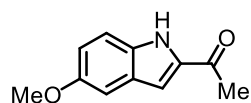
¹H NMR (300 MHz, CDCl₃): δ = 9.16 (s, 1H, *NH*), 7.36–7.30 (m, 1H, *H*_{Ar}), 7.16 (dd, 1H, *J* = 2.2, 0.9 Hz, *H*_{Ar}), 7.10 (d, *J* = 2.4 Hz, 1H, *H*_{Ar}), 6.98 (dd, *J* = 8.9, 2.4 Hz, *H*_{Ar}), 3.86 (s, 3H, *CH*₃), 3.85 (s, 3H, *CH*₃), 3.42 (s, 3H, *CH*₃) ppm.

¹³C NMR (75 MHz, CDCl₃): δ = 161.8, 154.7, 131.3, 128.6, 128.5, 116.6, 112.8, 107.7, 102.8, 61.5, 55.9, 33.4 ppm.

IR (ATR): $\tilde{\nu}$ = 3288 (m), 2993 (w), 2926 (m), 2926 (w), 1596 (m), 1522 (m), 1445 (m), 1400 (m), 1357 (m), 1283 (m), 1228 (m), 1197 (s), 1158 (s), 1105 (m), 1081 (m), 1035 (m), 997 (m), 957 (m), 885 (m), 845 (s), 798 (s), 733 (s), 695 (s), 616 (m), 591 (m), 559 (m), 527 (m), 436 (m) cm⁻¹.

HR-MS (ESI): *m/z* calcd. for C₁₂H₁₄N₂O₃Na₁ [*M*+Na]⁺: 257.0897, found 257.0898.

1-(5-Methoxy-1*H*-indole-2-yl)ethan-1-one (S14b)



Compound **S14b** was prepared according to a slightly modified literature-known procedure.^[50] A flask (250 mL) equipped with a septum, a nitrogen inlet, and a stir bar was charged with WEINREB amide **S14a** (1.85 g, 7.90 mmol, 1.00 eq.) and dry THF (80.0 mL) and the resulting solution cooled to –78 °C. To this solution MeLi (1.6 M in Et₂O; 14.8 mL, 23.7 mmol, 3.00 eq.) was added dropwise. After

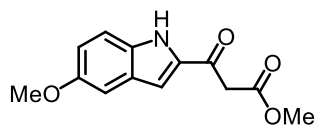
1 h at $-78\text{ }^{\circ}\text{C}$, the cooling bath was removed, water (70 mL) was added at rt and the aqueous layer extracted with Et_2O (3x30 mL). The combined organic layers were washed with brine (30 mL), dried over MgSO_4 , filtered, and concentrated under reduced pressure. The product was dissolved in CH_2Cl_2 , adsorbed on silica gel, and purified by short column chromatography (*n*-hexane/ EtOAc 2:1) to furnish ketone **S14b** (1.33 g, 7.03 mmol, 89%) as a yellow, crystalline solid.

^1H NMR (300 MHz, CDCl_3): δ = 8.95 (s, 1H, NH), 7.35–7.29 (m, 1H, H_{Ar}), 7.12 (dd, 1H, J = 2.1, 0.9 Hz, H_{Ar}), 7.09 (d, J = 2.3 Hz, 1H, H_{Ar}), 7.03 (dd, J = 8.9, 2.5 Hz, H_{Ar}), 3.86 (s, 3H, CH_3), 2.58 (s, 3H, CH_3) ppm;

IR (ATR): $\tilde{\nu}$ = 3303 (m), 2992 (w), 2933 (w), 1629 (s), 1519 (m), 1450 (m), 1409 (m), 1351 (m), 1297 (m), 1210 (s), 1148 (m), 1108 (m), 1024 (m), 977 (m), 929 (m), 820 (m), 787 (m), 745 (m), 704 (s), 633 (m), 588 (m), 546 (m), 433 (m) cm^{-1} ;

HR-MS (ESI): m/z calcd. for $\text{C}_{11}\text{H}_{12}\text{N}_1\text{O}_2$ $[\text{M}+\text{H}]^+$: 190.0863, found 190.0863.

Methyl 3-(5-methoxy-1*H*-indole-2-yl)-3-oxopropanoate (**S14c**)



The title compound was prepared according to a slightly modified literature-known procedure.^[50] A flask (100 mL) equipped with a septum, a nitrogen inlet, and a stir bar was charged with NaH (60% in mineral oil; 478 mg, 12.0 mmol, 1.76 eq.), KH (30% in mineral oil; 1.67 g, 12.5 mmol, 1.84 eq.), dry THF (40 mL), and dimethyl carbonate (4.00 mL, 47.5 mmol, 6.97 eq.) and the resulting mixture cooled to $0\text{ }^{\circ}\text{C}$. To this suspension, a solution of ketone **S14b** (1.29 g, 6.82 mmol, 1.00 eq.) in THF (30 mL) was added dropwise (*caution: violent reaction!*). After the gas evolution had ceased (10 min), the reaction was heated to $40\text{ }^{\circ}\text{C}$ for 65 h after which TLC analysis indicated full conversion. Aqueous HCl (1 M, 15 mL) was added carefully at $0\text{ }^{\circ}\text{C}$ and the mixture further diluted with diethyl ether and water (50 mL each). The organic layer was separated, and the aqueous layer extracted with diethyl ether (3x50 mL). The combined organic layers were washed with brine (50 mL), dried over MgSO_4 , filtered, and concentrated under reduced pressure. The crude product was dissolved in CH_2Cl_2 , adsorbed on silica gel, and purified by flash chromatography (*n*-hexane/ EtOAc 5:2) to furnish ketoester **S14c** (1.36 g, 5.50 mmol, 81%) as a yellow, crystalline solid.

TLC (*n*-hexane/ EtOAc 5:2) R_f = 0.30.

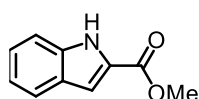
¹H NMR (300 MHz, CDCl₃): δ = 9.23 (s, 1H, NH), 7.36–7.30 (m, 1H, *H*_{Ar}), 7.16 (dd, 1H, *J* = 2.1, 0.8 Hz, H3 *H*_{Ar}), 7.09–7.02 (m, 2H, *H*_{Ar}), 3.96 (s, 2H, CH₂), 3.85 (s, 3H, OCH₃), 3.76 (s, 3H, OCH₃) ppm.

¹³C NMR (75 MHz, CDCl₃): δ = 184.2, 167.8, 155.1, 134.8, 133.6, 128.0, 119.2, 113.4, 110.6, 102.9, 55.8 (OCH₃), 52.7 (OCH₃), 45.4 ppm.

IR (ATR): $\tilde{\nu}$ = 3313 (m), 3001 (w), 2943 (w), 2838 (w), 1736 (m), 1639 (s), 1516 (m), 1456 (m), 1406 (m), 1354 (m), 1290 (m), 1268 (m), 1236 (m), 1203 (s), 1173 (m), 1141 (s), 1053 (m), 1021 (m), 925 (m), 842 (m), 806 (s), 743 (m), 696 (m), 624 (m), 591 (m), 523 (m), 431 (m) cm⁻¹.

HR-MS (ESI): *m/z* calcd. for C₁₃H₁₃N₁O₄Na₁ [M+Na]⁺: 270.0737, found 270.0739.

Methyl 1*H*-indole-2-carboxylate (**S15a**)

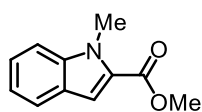


The title compound was prepared according to a slightly modified literature-known procedure. A SCHLENK tube (50 mL) was charged with *N*-indole-2-carboxylic acid (2.00 g, 12.4 mmol, 1.00 eq.) and CH₂Cl₂ (20 mL) and the resulting mixture cooled to 0 °C. DMF (80.0 μ L, 1.03 mmol, 8.0 mol%) and oxalyl chloride (1.1 mL, 12.8 mmol, 1.03 eq.) were carefully added (*caution: violent gas evolution!*) and the reaction mixture allowed to slowly warm up to rt. After the gas evolution had ceased, all volatiles were removed from the yellow solution under reduced pressure. The yellow residue was dissolved in dry toluene (3 mL) and again all volatiles removed in vacuo (removal of traces of oxalyl chloride and DMF by co-evaporation). The resulting green solid was dissolved in MeOH and heated to 70 °C for 1 h. All volatiles were removed in vacuo and the desired ester **S15a** (2.14 g, 12.2 mmol, 98%) was obtained as a solid without the need for further purification.

¹H NMR (300 MHz, CDCl₃): δ = 8.83 (s, 1H, NH), 7.73–7.67 (m, 1H, *H*_{Ar}), 7.44–7.41 (m, 1H, *H*_{Ar}), 7.37–7.29 (m, 1H, *H*_{Ar}), 7.24–7.21 (m, 1H, *H*_{Ar}), 7.20–7.12 (m, 1H, *H*_{Ar}), 3.95 (s, 3H, OCH₃) ppm.

¹³C NMR (75 MHz, CDCl₃): δ = 162.6, 137.0, 127.7, 127.3, 125.6, 122.8, 121.0, 112.0, 109.0, 52.1 (OCH₃) ppm.

Methyl *N*-methyl-indole-2-carboxylate (**S15b**)



The title compound was prepared according to a slightly modified literature-known procedure. A SCHLENK tube (50 mL) was charged with ester **S15a** (2.19 g, 12.5 mmol, 1.00 eq.) and dry THF (10.0 mL) and the resulting mixture cooled to 0 °C. Next, NaH (60% in mineral oil; 732 mg, 18.3 mmol, 1.46 eq.) and dry THF (6 mL) were carefully added (*caution: violent gas evolution!*). After the gas development had ceased, methyl iodide (1.0 mL, 16.1 mmol, 1.29 eq) was added and the resulting red reaction mixture was allowed to warm up to rt slowly. After 14 h at rt, full conversion was indicated by TLC analysis and the mixture was diluted with aqueous HCl (6 M; 20 mL) and EtOAc (20 mL). The layers were separated, and the aqueous layer extracted with EtOAc (5x50 mL). The combined organic layers were washed with brine (50 mL), dried over MgSO₄, filtered, and concentrated under reduced pressure. The crude product was dissolved in CH₂Cl₂, adsorbed on silica gel, and subjected to flash chromatography (*n*-hexane/CH₂Cl₂ 1:1) to yield desired ester **S15b** (1.48 g, 7.82 mmol, 63%) as a brownish solid.

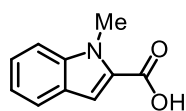
¹H NMR (300 MHz, CDCl₃): δ = 7.68 (d, *J* = 8.0 Hz, 1H, *H*_{Ar}), 7.43–7.33 (m, 2H, *H*_{Ar}), 7.30 (s, 1H, *H*_{Ar}), 7.20–7.12 (m, 1H, *H*_{Ar}), 4.09 (s, 3H, CH₃), 3.92 (s, 3H, CH₃) ppm.

¹³C NMR (75 MHz, CDCl₃): δ = 162.8, 139.8, 127.9, 126.1, 125.2, 122.8, 120.7, 110.4, 51.7 (OCH₃), 31.7 (CH₃) ppm.

IR (ATR): $\tilde{\nu}$ = 3041 (w), 2948 (w), 1701 (s), 1512 (m), 1466 (m), 1436 (m) 1390 (m), 1359 (w), 1318 (w), 1250 (s), 1222 (s), 1155 (m), 1134 (m), 1085 (m), 961 (m), 896 (m), 838 (m), 807 (m), 745 (s), 596 (m), 571 (m), 538 (m), 434 (m) cm⁻¹.

HR-MS (ESI): *m/z* calcd. for C₁₁H₁₂N₁O₂ [M+H]⁺: 190.0863, found 190.0863.

N-Methyl-indole-2-carboxylic acid (**S15b**)



The title compound was prepared according to a slightly modified literature-known procedure. A flask (50 mL) was charged with ester (700 mg, 3.70 mmol, 1.00 eq.), MeOH (14 mL), and aqueous KOH solution (12% w/w, 7.0 mL) and the resulting mixture stirred at reflux for 16 h. MeOH was removed under reduced pressure to furnish a yellow paste. Aqueous HCl (6 M; 80 mL) was added, and the resulting mixture stirred for 30 min. The aqueous layer then was extracted with EtOAc (6x30 mL), the combined organic layers washed with brine (30 mL), dried over MgSO₄, filtered, and

concentrated under reduced pressure. After drying in vacuo, desired acid **S15b** (645 mg, 3.68 mmol, >99%) was obtained as a colorless solid without the need for further purification.

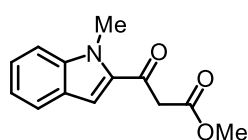
¹H NMR (300 MHz, DMSO-*d*₆): δ = 12.89 (s 1H, COOH), 7.71–7.64 (m, 1H, *H*_{Ar}), 7.60–7.53 (m, 1H, *H*_{Ar}), 7.37–7.29 (m, 1H, *H*_{Ar}), 7.15–7.07 (m, 1H, *H*_{Ar}), 4.02 (s, 3H, CH₃) ppm.

¹³C NMR (75 MHz, DMSO-*d*₆): δ = 162.9, 139.2, 128.5, 125.3, 124.5, 122.1, 120.3, 110.7, 109.3, 31.4 ppm.

IR (ATR): $\tilde{\nu}$ = 2920 (m), 2854 (m), 2592 (br), 1662 (s), 1518 (m), 1437 (m), 1357 (m) 1316 (m), 1257 (s), 1131 (m), 883 (m), 814 (m), 731 (s), 580 (m), 541 (m), 471 (m), 425 (m) cm⁻¹.

HR-MS (EI): *m/z* calcd. for C₁₀H₉N₁O₂ [M]⁺: 175.06333, found 175.06229.

Methyl 3-(*N*-methyl-indole-2-yl)-3-oxopropanoate (**S15c**)



The title compound was prepared according to a slightly modified literature-known procedure. A SCHLENK tube (50 mL) was charged with free acid **S15b** (500 mg, 2.85 mmol, 1.00 eq.) and CH₂Cl₂ (5.0 mL) and the resulting mixture cooled to 0 °C. DMF (220 μ L, 2.83 mmol, 0.99 eq.) and oxalyl chloride (269 μ L, 3.14 mmol, 1.10 eq.) were carefully added (*caution: violent gas evolution!*) and the reaction mixture was allowed to slowly warm up to rt. After the gas development had ceased, all volatiles were removed from the yellow solution under reduced pressure. The yellow residue was then dissolved in dry toluene (3 mL) and again all volatiles removed in vacuo (removal of traces of oxalyl chloride and DMF by co-evaporation) and the resulting residue dissolved in dry CH₂Cl₂ (5 mL) for later use. A separate flask (100 mL) was charged with dry methyl acetate (230 μ L, 2.89 mmol, 1.00 eq.) and dry THF (10 mL) and the resulting solution cooled to –78 °C. LiHMDS (1 M in THF; 5.8 mL, 5.80 mmol, 2.04 eq.) was slowly added (enolate preparation) and the resulting red solution stirred at –78 °C for 2 h. Then, the prepared acid chloride solution was added dropwise via cannula at –78 °C to this solution. After 1 h at –78 °C, complete conversion was indicated by TLC analysis and the reaction mixture diluted with saturated aqueous NH₄Cl solution and Et₂O (30 mL each). The layers were separated, and the aqueous layer extracted with Et₂O (3x30 mL). The combined organic layers were dried over MgSO₄, filtered, and dried under reduced pressure. After column chromatography (*n*-hexane/EtOAc 5:1) desired ketoester **S15c** (545 mg, 2.36 mmol, 83%) was obtained as an off-white solid.

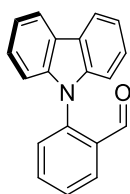
¹H NMR (300 MHz, CDCl₃): δ = 7.73–7.67 (m, 1H, *H*_{Ar}), 7.44–7.36 (m, 2H, *H*_{Ar}), 7.30 (s, 1H, *H*_{Ar}), 7.20–7.13 (m, 1H, *H*_{Ar}), 4.08 (s, 3H, CH₃), 4.00 (s, 2H, CH₂), 3.76 (s, 3H, CH₃) ppm.

¹³C NMR (75 MHz, CDCl₃): δ = 185.4, 168.1, 140.7, 134.0, 126.7, 125.9, 123.3, 121.2, 113.0, 110.6, 52.6 (OCH₃), 47.1, 32.3 ppm.

IR (ATR): $\tilde{\nu}$ = 2927 (w), 2854 (w), 1728 (s), 1661 (s), 1509 (m), 1466 (m), 1432 (m), 1396 (m), 1357 (m), 1319 (m), 1271 (s), 1209 (s), 1173 (s), 1148 (s), 1124 (s), 1036 (m), 1004 (s), 940 (m), 895 (m), 835 (m), 795 (m), 740 (s), 684 (m), 649 (m), 582 (m), 549 (m), 512 (m), 433 (m) cm⁻¹.

HR-MS (ESI): *m/z* calcd. for C₁₃H₁₃N₁O₃Na₁ [*M*+Na]⁺: 254.0788, found 254.0788.

2-(Carbazol-9-yl)benzaldehyde (**S1c**)



The reaction was performed according to a slightly modified reported procedure.

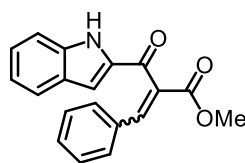
A 50 mL two-necked flask equipped with nitrogen inlet and stir bar was charged with carbazole (1.00 g, 5.98 mmol, 1.00 eq.), KO^tBu (1.00 g, 8.97 mmol, 1.5 eq.), DMF (24 mL) and heated to 110 °C. 2-fluorobenzaldehyde (0.95 mL, 8.97 mmol, 1.5 eq.) was added dropwise. The mixture was stirred at 110 °C for 17 h until reaction control by TLC indicated full conversion. The product mixture was diluted with water and CH₂Cl₂ (100 mL each), the aqueous layer was extracted with CH₂Cl₂ (4x100 mL), the combined organic layers washed with brine (100 mL), dried over MgSO₄, concentrated and dried under reduced pressure at 70 °C. The sticky, brown mixture was dissolved in CH₂Cl₂/acetone (1:1), adsorbed on silica gel and purified by flash chromatography (*n*-hexane/EtOAc 20:1) to yield product **S1c** as an off white, solid (1.13 g, 4.19 mmol, 70%).

TLC (*n*-hexane/EtOAc 6:1): *R*_f = 0.24.

¹H NMR (300 MHz, CDCl₃): δ = 9.61 (d, *J* = 0.9 Hz, 1H), 8.23 (dd, *J* = 7.8 Hz, *J* = 1.8 Hz, 1H), 8.21–8.15 (m, 2H), 7.85 (ddd, *J* = 7.7 Hz, *J* = 7.5 Hz, *J* = 1.7 Hz, 1H), 7.68 (tt, *J* = 7.6 Hz, *J* = 1.0 Hz, 1H), 7.55 (dd, *J* = 7.9 Hz, *J* = 0.8 Hz, 1H), 7.48–7.39 (m, 2H), 7.38–7.30 (m, 2H), 7.22–7.15 (m, 2H) ppm.

HRMS (ESI): *m/z* calcd for C₁₉H₁₃N₁O₁Na₁: 294.0889 [*M*+Na]⁺; found: 294.0902.

Methyl 2-(indole-2-carbonyl)-3-phenylacrylate (**N3a**)



According to procedure D, β -ketoester **S13c** (200 mg, 921 μ mol, 1.00 eq.), piperidine (109 μ L, 1.10 mmol, 1.20 eq.), acetic acid (52.7 μ L, 921 μ mol, 1.00 eq.), 4 Å MS (~750 mg), CH_2Cl_2 (3.0 mL), and benzaldehyde (112 μ L, 1.10 mmol, 1.20 eq.) were used. Product **N3a** was obtained after flash chromatography (*n*-pentane/Et₂O 2:1) as a yellow solid (222 mg, 727 μ mol, 79%, *E/Z* 20:1).

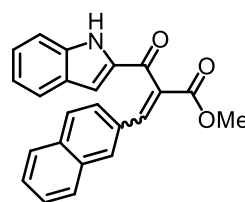
¹H NMR (300 MHz, CDCl_3): δ = 9.15 (br s, 1H, *NH*), 8.02 (s, 1H, *H*_{Olef}), 7.64–7.57 (m, 1H, *H*_{Ar}), 7.47–7.32 (m, 5H, *H*_{Ar}), 7.26–7.19 (m, 3H, *H*_{Ar}), 7.15–7.07 (m, 1H, *H*_{Ar}), 7.04–7.00 (m, 1H, *H*_{Ar}), 3.79 (s, 3H, *CH*₃) ppm.

¹³C NMR (75 MHz, CDCl_3): δ = 186.8, 165.7, 143.7, 138.3, 135.1, 133.1, 130.6, 130.4 (2C), 129.0 (2C), 127.7, 127.2, 123.6, 121.3, 112.9, 112.5, 52.8 ppm.

IR (ATR): $\tilde{\nu}$ = 3355 (m), 3063 (m), 2999 (m), 2949 (m), 1709 (s), 1622 (s), 1518 (m), 1425 (m), 1338 (m), 1312 (m), 1256 (s), 1194 (s), 1160 (s), 1092 (s), 1015 (s), 961 (m), 900 (m), 826 (s), 785 (s), 749 (s), 685 (s), 645 (w), 577 (s), 492 (s), 456 (s), 430 (s) cm^{-1} .

HR-MS (ESI): *m/z* calcd. for $\text{C}_{19}\text{H}_{15}\text{N}_1\text{O}_3\text{Na}_1$ [*M*+*Na*]⁺: 328.0944, found 328.1944.

Methyl 2-(indole-2-carbonyl)-3-(naphthalen-2-yl)acrylate (**N3b**)



According to procedure E, β -ketoester **S13c** (129 mg, 594 μ mol, 1.00 eq.), piperidine (58.8 μ L, 595 μ mol, 1.00 eq.), acetic acid (18.8 μ L, 329 μ mol, 0.55 eq.), 4 Å MS (~500 mg), CH_2Cl_2 (5.9 mL), and 2-naphthaldehyde (120 mg, 768 μ mol, 1.29 eq.) were used. Product **N3b** was obtained after column chromatography (*n*-hexane/EtOAc 7:2) as a yellow solid (128 mg, 360 μ mol, 61%, *E/Z* 20:1).

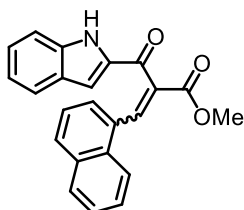
¹H NMR (300 MHz, CDCl_3): δ = 9.19 (br s, 1H, *NH*), 8.19 (s, 1H, *H*_{Olef}), 7.98–7.93 (m, 1H, *H*_{Ar}), 7.80–7.73 (m, 1H, *H*_{Ar}), 7.72–7.64 (m, 1H, *H*_{Ar}), 7.65–7.59 (m, 1H, *H*_{Ar}), 7.59–7.53 (m, 1H, *H*_{Ar}), 7.49–7.39 (m, 4H, *H*_{Ar}), 7.37–7.30 (m, 1H, *H*_{Ar}), 7.12–7.00 (m, 2H, *H*_{Ar}), 3.81 (s, 3H, *OCH*₃) ppm.

^{13}C NMR (75 MHz, CDCl_3): δ = 186.8, 165.8, 143.8, 138.3, 135.3, 134.1, 133.2, 132.1, 130.7, 130.3, 128.9, 128.7, 127.8, 127.8, 127.8, 127.2, 126.8, 126.0, 123.7, 121.3, 112.9, 112.4, 52.8 (OCH_3) ppm.

IR (ATR): $\tilde{\nu}$ = 3378 (br, w), 1697 (m), 1612 (m), 1515 (m), 1422 (m), 1336 (m), 1308 (m), 1273 (m), 1239 (s), 1215 (m), 1186 (m), 1154 (m), 1085 (m), 1013 (m), 957 (m), 890 (m), 855 (m), 803 (m), 740 (s), 694 (m), 651 (m), 620 (m), 569 (m), 513 (m), 471 (s), 425 (m) cm^{-1} .

HR-MS (ESI): m/z calcd. for $\text{C}_{23}\text{H}_{17}\text{N}_1\text{O}_3\text{Na}_1$ $[\text{M}+\text{Na}]^+$: 378.1101, found 378.1102.

Methyl-2-(indole-2-carbonyl)-3-(naphthalen-1-yl)acrylate (**N3c**)



According to procedure E, β -ketoester **S13c** (129 mg, 594 μmol , 1.00 eq.), piperidine (58.8 μL , 595 μmol , 1.00 eq.), acetic acid (18.8 μL , 329 μmol , 0.55 eq.), 4 Å MS (~500 mg), CH_2Cl_2 (5.9 mL), and 1-naphthaldehyde (105 μL , 773 μmol , 1.30 eq.) were used. Product **N3c** was obtained after column chromatography (n -hexane/EtOAc 7:2) as a yellow solid (165 mg, 464 μmol , 78%, E/Z 20:1).

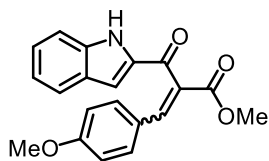
^1H NMR (300 MHz, CDCl_3): δ = 9.03 (br s, 1H, NH), 8.78 (s, 1H, H_{Olef}), 8.22–8.11 (m, 1H, H_{Ar}), 7.83–7.77 (m, 1H, H_{Ar}), 7.77–7.59 (m, 1H, H_{Ar}), 7.68–7.59 (m, 1H, H_{Ar}), 7.57–7.50 (m, 2H, H_{Ar}), 7.49–7.44 (m, 1H, H_{Ar}), 7.36–7.30 (m, 1H, H_{Ar}), 7.30–7.26 (m, 1H, H_{Ar}), 7.26–7.24 (m, 1H, H_{Ar}), 7.23–7.20 (m, 1H, H_{Ar}), 7.05–6.99 (m, 1H, H_{Ar}), 6.91 (dd, J = 2.1, 0.8 Hz, 1H, H_{Ar}), 6.94 (dd, J = 2.1, 0.9 Hz, 1H, H_{Ar}), 3.85 (s, 3H, OCH_3) ppm.

^{13}C NMR (75 MHz, CDCl_3): δ = 186.1, 165.4, 141.9, 138.1, 135.2, 133.6, 132.8, 131.7, 130.8, 130.6, 129.0, 127.8, 127.6, 127.2, 127.0, 126.5, 125.4, 124.0, 123.6, 121.1, 112.3, 112.2, 52.9 (OCH_3) ppm.

IR (ATR): $\tilde{\nu}$ = 3347 (br, w), 2922 (w), 2852 (m), 1700 (m), 1616 (m), 1519 (m), 1431 (m), 1338 (m), 1309 (m), 1274 (m), 1228 (s), 1167 (m), 1139 (m), 1087 (m), 1015 (m), 959 (m), 934 (w), 903 (m), 859 (m), 826 (m), 798 (m), 768 (m), 734 (m), 700 (m), 662 (m), 627 (m), 570 (m), 533 (m), 460 (m), 429 (m), 399 (m) cm^{-1} .

HR-MS (ESI): m/z calcd. for $\text{C}_{23}\text{H}_{17}\text{N}_1\text{O}_3\text{Na}_1$ $[\text{M}+\text{Na}]^+$: 378.1101, found 378.1101.

Methyl 2-(1*H*-indole-2-carbonyl)-3-(4-methoxyphenyl)acrylate (**N3d**)



According to procedure E, β -ketoester **S13c** (129 mg, 594 μ mol, 1.00 eq.), piperidine (58.8 μ L, 595 μ mol, 1.00 eq.), acetic acid (18.8 μ L, 329 μ mol, 0.55 eq.), 4 Å MS (~500 mg), CH₂Cl₂ (5.9 mL), and 4-methoxybenzaldehyde (94.0 μ L, 774 μ mol, 1.30 eq.) were used. Product **N3d** was obtained after column chromatography (*n*-hexane/EtOAc 5:2) as a yellow solid (185 mg, 552 μ mol, 93%, *E/Z* 20:1).

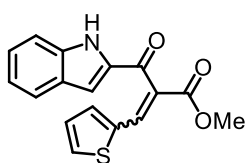
¹H NMR (300 MHz, CDCl₃): δ = 9.33 (br s, 1H, *NH*), 7.97 (s, 1H, *H*_{Olef}), 7.64–7.57 (m, 1H, *H*_{Ar}), 7.47–7.41 (m, 1H, *H*_{Ar}), 7.41–7.30 (m, 3H, *H*_{Ar}), 7.15–7.07 (m, 1H, *H*_{Ar}), 6.77–6.69 (m, 2H, *H*_{Ar}), 3.77 (s, 3H, *CH*₃), 3.72 (s, 3H, *CH*₃) ppm.

¹³C NMR (75 MHz, CDCl₃): δ = 187.4, 166.0, 161.6, 143.4, 138.4, 135.3, 132.5, 127.7, 127.1, 125.6, 123.6, 121.3, 114.5, 112.8, 112.5, 55.4 (OCH₃), 52.6 (OCH₃) ppm.

IR (ATR): $\tilde{\nu}$ = 3329 (m), 3068 (w), 2954 (w), 2849 (w), 1714 (s), 1617 (s), 1574 (m), 1518 (s), 1422 (m), 1390 (m), 1319 (s), 1255 (s), 1201 (s), 1167 (s), 1117 (s), 1062 (s), 1015 (s), 965 (m), 934 (m), 901 (m), 828 (s), 746 (s), 710 (s), 660 (m), 590 (s), 503 (m), 458 (m), 429 (m) cm⁻¹.

HR-MS (ESI): *m/z* calcd. for C₂₀H₁₇N₁O₄Na₁ [*M*+Na]⁺: 358.1050, found 358.1054.

Methyl 2-(indole-2-carbonyl)-3-(thiophen-2-yl)acrylate (**N3e**)



According to procedure E, β -ketoester **S13c** (129 mg, 594 μ mol, 1.00 eq.), piperidine (58.8 μ L, 595 μ mol, 1.00 eq.), acetic acid (18.8 μ L, 329 μ mol, 0.55 eq.), 4 Å MS (~500 mg), CH₂Cl₂ (5.9 mL), and thiophene-2-carbaldehyde (70.9 μ L, 772 μ mol, 1.30 eq.) were used. Product **N3e** was obtained after column chromatography (*n*-hexane/EtOAc 7:2) as a yellow solid (132 mg, 424 μ mol, 72%, *E/Z* 21:1).

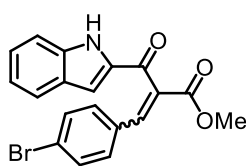
¹H NMR (300 MHz, CDCl₃): δ = 9.21 (br s, 1H, *NH*), 8.11 (s, 1H, *H*_{Olef}), 7.49–7.43 (m, 1H, *H*_{Ar}), 7.49–7.44 (m, 1H, *H*_{Ar}), 7.40–7.33 (m, 2H, *H*_{Ar}), 7.33–7.28 (m, 1H, *H*_{Ar}), 7.17–7.10 (m, 2H, *H*_{Ar}), 6.99–6.94 (m, 1H, *H*_{Ar}), 3.78 (s, 3H, OCH₃) ppm.

¹³C NMR (75 MHz, CDCl₃): δ = 186.3, 165.7, 138.6, 136.4, 135.8, 135.2, 134.4, 132.0, 127.9, 127.7, 127.3, 127.2, 123.7, 121.3, 113.0, 112.8, 52.7 (OCH₃) ppm.

IR (ATR): $\tilde{\nu}$ = 3357 (br, m), 1700 (m), 1601 (s), 1517 (m), 1415 (m), 1337 (m), 1251 (m), 1200 (s), 1150 (m), 1085 (m), 1043 (m), 1016 (m), 953 (m), 901 (m), 849 (m), 793 (m), 733 (s), 680 (m), 630 (m), 572 (m), 494 (m), 456 (m), 424 (m) cm^{-1} .

HR-MS (ESI): m/z calcd. for $\text{C}_{17}\text{H}_{13}\text{N}_1\text{O}_3\text{S}_1\text{Na}_1$ $[\text{M}+\text{Na}]^+$: 334.0508, found 334.0508.

Methyl 3-(4-bromophenyl)-2-(indole-2-carbonyl)acrylate (N3f)



According to procedure D, β -ketoester **S13c** (200 mg, 921 μmol , 1.00 eq.), piperidine (109 μL , 1.10 mmol, 1.20 eq.), acetic acid (52.7 μL , 921 μmol , 1.00 eq.), 4 Å MS (~500 mg), CH_2Cl_2 (2 mL), and 4-bromobenzaldehyde (204 mg, 1.10 mmol, 1.20 eq.) were used. Product **N3f** was obtained after column chromatography (*n*-pentane/ Et_2O 2:1 \rightarrow 1:1) as a yellow solid (228 mg, 594 μmol , 64%, *E/Z* 22:1).

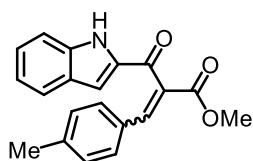
^1H NMR (300 MHz, CDCl_3): δ = 9.13 (br s, 1H, NH), 7.86 (s, 1H, H_{Olef}), 7.56–7.50 (m, 1H, H_{Ar}), 7.40–7.33 (m, 1H, H_{Ar}), 7.33–7.25 (m, 3H, H_{Ar}), 7.24–7.16 (m, 3H, H_{Ar}), 7.08–7.01 (m, 1H, H_{Ar}), 6.97–6.89 (m, 1H, H_{Ar}), 3.71 (s, 3H, OCH_3) ppm.

^{13}C NMR (75 MHz, CDCl_3): δ = 186.3, 165.4, 142.2, 138.4, 134.9, 132.3, 132.0, 131.7, 131.1, 127.7, 127.4, 125.2, 123.7, 121.5, 113.0, 112.5, 52.9 (OCH_3).

IR (ATR): $\tilde{\nu}$ = 3331 (m), 2950 (w), 2926 (w), 2852 (w), 1712 (m), 1614 (s), 1579 (m), 1514 (m), 1490 (m), 1420 (m), 1342 (m), 1312 (m), 1249 (s), 1193 (m), 1164 (m), 1134 (m), 1072 (m), 1011 (m), 961 (w), 900 (w), 818 (m), 727 (m), 667 (m), 627 (m), 572 (m), 496 (m), 431 (w), 407 (w) cm^{-1} .

HR-MS (ESI): m/z calcd. for $\text{C}_{19}\text{H}_{14}\text{Br}_1\text{N}_1\text{O}_3\text{Na}_1$ $[\text{M}+\text{Na}]^+$: 408.0031, found 408.0033.

Methyl 2-(indole-2-carbonyl)-3-*p*-tolylacrylate (N3g)



According to procedure D, β -ketoester **S13c** (129 mg, 594 μmol , 1.00 eq.), piperidine (58.8 μL , 595 μmol , 1.00 eq.), acetic acid (18.8 μL , 329 μmol , 0.55 eq.), 4 Å MS (~500 mg), CH_2Cl_2 (5.9 mL), and 4-methylbenzaldehyde (91.3 μL , 774 μmol , 1.30 eq.) were used. Product **N3g** was obtained after column chromatography (*n*-hexane/ EtOAc 7:2) as a yellow solid (144 mg, 451 μmol , 76%, *E/Z* 20:1).

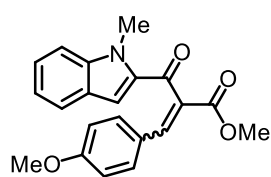
¹H NMR (300 MHz, CDCl₃): δ = 9.25 (br s, 1H, NH), 7.99 (s, 1H, *H*_{Olef}), 7.64–7.55 (m, 1H, *H*_{Ar}), 7.48–7.40 (m, 1H, *H*_{Ar}), 7.38–7.28 (m, 3H, *H*_{Ar}), 7.14–7.06 (m, 1H, *H*_{Ar}), 7.06–6.98 (m, 3H, *H*_{Ar}), 3.78 (s, 3H, OCH₃), 2.25 (s, 3H, CH₃) ppm.

¹³C NMR (75 MHz, CDCl₃): δ = 187.1, 165.8, 143.7, 141.3, 138.3, 135.2, 130.5 (2C), 130.3, 129.7 (2C), 129.3, 127.8, 127.1, 123.6, 121.3, 112.8, 112.5, 52.7 (OCH₃), 21.5 (CH₃).

IR (ATR): $\tilde{\nu}$ = 3314 (m), 3111 (w), 3064 (w), 3003 (w), 2949 (w), 2839 (w) 1706 (s), 1597 (s), 1513 (s), 1428 (m), 1340 (m), 1309 (s), 1254 (s), 1206 (s), 1169 (s), 1089 (m), 1022 (s), 960 (m), 899 (m), 826 (s), 746 (s), 668 (m), 629 (m), 572 (m), 522 (s), 458 (w), 432 (m), 408 (m) cm⁻¹.

HR-MS (ESI): *m/z* calcd. for C₂₀H₁₇N₁O₃Na₁ [M+Na]⁺: 342.1101, found 342.1101.

Methyl 3-(4-methoxyphenyl)-2-(*N*-methyl-indole-2-carbonyl)acrylate (**N3h**)



A SCHLENK tube (10 mL) was charged with β -ketoester **S15c** (400 mg, 1.73 mmol, 1.00 eq), 4-methoxybenzaldehyde (210 μ L, 1.73 mmol, 1.00 eq), AcOH (50.0 μ L, 874 μ mol, 0.50 eq), piperidine (20.0 μ L, 202 μ mol, 0.12 eq), and toluene (0.70 mL) and the mixture heated to 80 °C for 36 h. The reaction mixture was allowed to cool to rt and then diluted with water and EtOAc (30 mL each). The organic layer was separated, and the aqueous layer extracted with EtOAc (2x30 mL). The combined organic layers were dried over MgSO₄, filtered, concentrated, and purified by flash chromatography (*n*-hexane/EtOAc 5:1) to furnish NAZAROV substrate **N3h** (157 mg, 0.45 mmol, 26%, *E/Z* 7:1) as a pale-yellow solid.

TLC *R*_f = 0.39 (*n*-hexane/EtOAc 3:1).

¹H NMR (300 MHz, CDCl₃): δ = 7.88 (s, 1H, *H*_{Olef}), 7.61–7.55 (m, 1H, *H*_{Ar}), 7.45–7.36 (m, 4H, *H*_{Ar}), 7.16–7.09 (m, 2H, *H*_{Ar}), 6.76 (d, *J* = 8.8 Hz, 2H, *H*_{Ar}), 4.22 (s, 3H, CH₃), 3.76 (s, 3H, CH₃), 3.75 (s, 3H, CH₃) ppm.

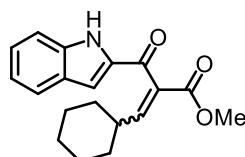
¹³C NMR (75 MHz, CDCl₃): δ = (75 MHz, CDCl₃): δ = 188.4, 166.3, 161.6, 142.3, 141.2, 135.1, 132.5, 129.5, 126.8, 126.3, 126.0, 123.7, 121.1, 115.1, 114.6, 110.7, 55.5 (OCH₃), 52.7 (OCH₃), 32.4 (CH₃) ppm.

IR (ATR): $\tilde{\nu}$ = 2948 (w), 2837 (w), 1708 (m), 1637 (m), 1597 (m), 1507 (m), 1462 (m), 1428 (m) 1395 (m), 1355 (m), 1310 (m), 1250 (s), 1200 (m), 1167 (m), 1122 (m), 1076 (m), 1025

(m), 982 (m), 924 (m), 825 (m), 743 (m), 698 (m), 743 (m), 698 (m), 649 (m), 620 (m), 583 (m), 527 (m), 488 (m), 431 (m) cm^{-1} .

HR-MS (ESI): m/z calcd. for $\text{C}_{21}\text{H}_{19}\text{N}_1\text{O}_4\text{Na}_1$ $[\text{M}+\text{Na}]^+$: 372.1206, found 372.1206.

Methyl 3-cyclohexyl-2-(indole-2-carbonyl)acrylate (**N3i**)



According to procedure D, β -ketoester **S13c** (200 mg, 921 μmol , 1.00 eq.), piperidine (109 μL , 1.10 mmol, 1.20 eq.), acetic acid (52.7 μL , 921 μmol , 1.00 eq.), 4 Å MS (~750 mg), CH_2Cl_2 (3.0 mL), and cyclohexane carboxaldehyde (133 μL , 1.10 mmol, 1.20 eq.) were used.

Product **N3i** was obtained after column chromatography (*n*-pentane/ Et_2O 2:1) as a colorless solid (175 mg, 562 μmol , 61%, *E/Z* 7:1).

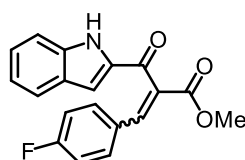
^1H NMR (300 MHz, CDCl_3): δ = 9.31 (br s, 1H, NH), 7.73–7.67 (m, 1H, H_{Ar}), 7.50–7.44 (m, 1H, H_{Ar}), 7.41–7.34 (m, 1H, H_{Ar}), 7.20–7.12 (m, 1H, H_{Ar}), 7.08–7.00 (m, 2H, H_{Ar}), 3.72 (s, 3H, OCH_3), 2.31–2.14 (m, 1H, H_{Aliph}), 1.75–1.55 (m, 5H, H_{Aliph}), 1.31–1.01 (m, 1H, H_{Aliph}) ppm.

^{13}C NMR (75 MHz, CDCl_3): δ = 185.9, 165.5, 153.5, 138.2, 135.8, 130.9, 127.7, 127.1, 123.6, 112.5, 52.4 (OCH_3), 38.9, 32.0 (2C), 25.7, 25.1 (2C) ppm.

IR (ATR): $\tilde{\nu}$ = 3307 (m), 2929 (w), 2853 (w), 1723 (s), 1615 (s), 1574 (w), 1515 (m), 1416 (w), 1344 (w), 1304 (w), 1244 (m), 1218 (s), 1176 (w), 1138 (m), 1082 (w), 1015 (m), 977 (m), 942 (m), 826 (s), 797 (m), 780 (m), 744 (m), 720 (m), 697 (m), 639 (m), 573 (m), 533 (m), 468 (w), 436 (m), 406 (m) cm^{-1} .

HR-MS (ESI): m/z calcd. for $\text{C}_{19}\text{H}_{21}\text{N}_1\text{O}_3\text{Na}_1$ $[\text{M}+\text{Na}]^+$: 334.1414, found 334.1416.

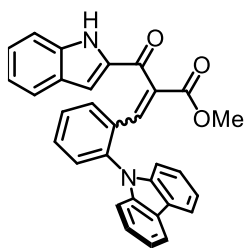
Methyl 3-(4-fluorophenyl)-2-(indole-2-carbonyl)acrylate (**N3j**)



According to procedure D, β -ketoester **S13c** (129 mg, 594 μmol , 1.00 eq.), piperidine (58.8 μL , 595 μmol , 1.00 eq.), acetic acid (18.8 μL , 329 μmol , 0.55 eq.), 4 Å MS (~500 mg), CH_2Cl_2 (5.9 mL), and 4-fluorobenzaldehyde (83.0 μL , 774 μmol , 1.30 eq.) were used. Product

N3j was obtained after column chromatography (*n*-hexane/ EtOAc 7:2) as a yellow solid (153 mg, 473 μmol , 80%, *E/Z* 20:1).

Methyl 3-(2-(carbazol-9-yl)phenyl)-2-(indole-2-carbonyl)acrylate (**N3l**)



According to procedure E, β -ketoester **S13c** (129 mg, 594 μ mol, 1.00 eq.), piperidine (58.8 μ L, 595 μ mol, 1.00 eq.), acetic acid (18.8 μ L, 329 μ mol, 0.55 eq.), 4 Å MS (~500 mg), CH_2Cl_2 (5.9 mL), and 2-(carbazol-9-yl)benzaldehyde **S1c** (209 mg, 772 μ mol, 1.30 eq.) were used. Product **N3l** was obtained after column chromatography (*n*-hexane/EtOAc 7:2) as a yellow solid (204 mg, 434 μ mol, 73%, *E/Z* 20:1).

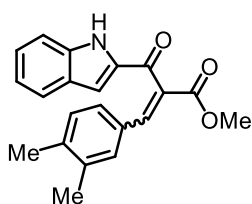
^1H NMR (300 MHz, CDCl_3): δ = 9.02 (br s, 1H, *NH*), 8.07–8.00 (m, 2H, H_{Ar}), 7.66–7.54 (m, 3H, $H_{\text{Ar/Olef}}$), 7.41–7.33 (m, 3H, H_{Ar}), 7.31–7.21 (m, 6H, H_{Ar}), 7.12–7.05 (m, 1H, H_{Ar}), 7.04–7.02 (m, 1H, H_{Ar}), 7.02–6.99 (m, 1H, H_{Ar}), 6.73–6.67 (m, 1H, H_{Ar}), 3.47 (s, 3H, OCH_3) ppm.

^{13}C NMR (75 MHz, CDCl_3): δ = 185.6, 165.0, 141.6, 139.5, 138.3, 137.5, 135.0, 133.0, 131.8, 131.0, 129.8, 128.9, 127.6, 127.2, 126.3 (2C), 123.8, 123.6, 121.4, 120.6 (2C), 120.4 (2C), 113.0, 112.5, 110.1 (2C), 52.6 (OCH_3) ppm.

IR (ATR): $\tilde{\nu}$ = 3313 (br, m), 3054 (w), 1724 (m), 1623 (m), 1516 (m), 1488 (m), 1448 (m), 1344 (m), 1310 (m), 1229 (m), 1196 (m), 1167 (m), 1139 (m), 1109 (m), 1091 (m), 1008 (m), 967 (m), 906 (m), 828 (m), 796 (m), 741 (s), 723 (s), 649 (m), 618 (m), 570 (m), 524 (m), 456 (m), 427 (m) cm^{-1} .

HR-MS (ESI): *m/z* calcd. for $\text{C}_{31}\text{H}_{22}\text{N}_1\text{O}_3\text{Na}$ [$\text{M}+\text{Na}$] $^+$: 493.1523, found 493.1523.

Methyl 3-(3,4-dimethylphenyl)-2-(indole-2-carbonyl)acrylate (**N3m**)



According to procedure D, β -ketoester **S13c** (100 mg, 460 μ mol, 1.00 eq.), piperidine (54.6 μ L, 553 μ mol, 1.20 eq.), acetic acid (26.3 μ L, 460 μ mol, 1.00 eq.), 4 Å MS (~500 mg), CH_2Cl_2 (2 mL), and 3,4-dimethylbenzaldehyde (72.7 μ L, 548 μ mol, 1.19 eq.) were used. Product

N3m was obtained after column chromatography (*n*-pentane/ Et_2O 2:1 to 1:1) as a yellow solid (115 mg, 345 μ mol, 75%, *E/Z* 20:1).

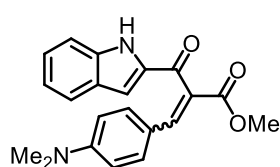
^1H NMR (300 MHz, CDCl_3): δ = 9.56 (br s, 1H, *NH*), 7.99 (s, 1H, H_{Olef}), 7.64–7.56 (m, 1H, H_{Ar}), 7.46–7.40 (m, 1H, H_{Ar}), 7.36–7.29 (m, 1H, H_{Ar}), 7.22–7.14 (m, 2H, H_{Ar}), 7.13–7.06 (m, 1H, H_{Ar}), 7.06–7.03 (m, 1H, H_{Ar}), 6.97–6.90 (m, 1H, H_{Ar}), 3.78 (s, 3H, OCH_3), 2.13 (s, 3H, CH_3), 2.08 (s, 3H, CH_3) ppm.

^{13}C NMR (75 MHz, CDCl_3): δ = 187.3, 165.9, 144.0, 140.0, 138.4, 137.2, 135.3, 132.0, 130.6, 130.3, 129.1, 127.9, 127.7, 127.0, 123.5, 121.2, 112.8, 112.5, 52.7 (OCH_3), 19.8 (CH_3), 19.7 (CH_3) ppm.

IR (ATR): $\tilde{\nu}$ = 3318 (br, m), 2949 (w), 2855 (w), 1711 (m), 1616 (s), 1572 (w), 1520 (m), 1430 (m), 1384 (m), 1342 (w), 1301 (w), 1264 (m), 1230 (s), 1168 (m), 1139 (m), 1092 (m), 1021 (m), 969 (m), 906 (m), 817 (m), 736(m), 657 (m), 581 (w), 553 (w), 436 (m) cm^{-1} .

HR-MS (ESI): m/z calcd. for $\text{C}_{21}\text{H}_{19}\text{N}_1\text{O}_3\text{Na}_1$ $[\text{M}+\text{Na}]^+$: 356.1257, found 356.1257.

Methyl 3-(4-(dimethylamino)phenyl)-2-(indole-2-carbonyl)acrylate (**N3n**)



According to procedure E, β -ketoester **S13c** (129 mg, 594 μmol , 1.00 eq.), piperidine (58.8 μL , 595 μmol , 1.00 eq.), acetic acid (18.8 μL , 329 μmol , 0.55 eq.), 4 Å MS (~500 mg), CH_2Cl_2 (5.9 mL), and 4-(dimethylamino)benzaldehyde (115 mg, 771 μmol , 1.30 eq.) were used. Product **N3n** was obtained after column chromatography (*n*-hexane/EtOAc 7:2) as a red solid (148 mg, 425 μmol , 72%, *E/Z* >30:1).

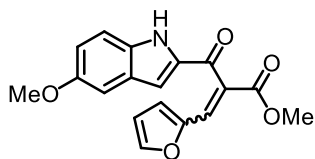
^1H NMR (300 MHz, CDCl_3): δ = 9.39 (br s, 1H, NH), 7.88 (s, 1H, H_{Olef}), 7.64–7.58 (m, 1H, H_{Ar}), 7.50–7.44 (m, 1H, H_{Ar}), 7.38–7.31 (m, 1H, H_{Ar}), 7.29 (d, J = 9.0 Hz, 2H, H_{Ar}), 7.14–7.08 (m, 1H, H_{Ar}), 7.07 (dd, J = 2.1, 0.9 Hz, 1H, H_{Ar}), 6.50 (d, J = 9.0 Hz, 2H, H_{Ar}), 3.73 (s, 3H, OCH_3), 2.91 (s, 6H, $\text{N}(\text{CH}_3)_2$) ppm.

^{13}C NMR (75 MHz, CDCl_3): δ = 188.4, 166.5, 151.8, 144.4, 138.3 (2C), 135.7, 132.8, 127.8, 126.8, 124.1, 123.6, 121.0, 120.4, 112.5, 112.5, 111.7 (2C), 52.4 (OCH_3), 40.0 (2C, $2\times\text{CH}_3$) ppm.

IR (ATR): $\tilde{\nu}$ = 3299 (br, m), 2900 (w), 1701 (m), 1606 (m), 1573 (s), 1518 (s), 1430 (m), 1369 (m), 1343 (m), 1315 (m), 1262 (m), 1226 (m), 1180 (m), 1131 (s), 1086 (m), 1012 (m), 941 (m), 896 (m), 796(m), 734 (m), 696 (s), 637 (s), 572 (m), 513 (m), 461 (m), 420 (m) cm^{-1} .

HR-MS (ESI): m/z calcd. for $\text{C}_{21}\text{H}_{20}\text{N}_2\text{O}_3\text{Na}_1$ $[\text{M}+\text{Na}]^+$: 371.1366, found 371.1366.

Methyl 3-(furan-2-yl)-2-(6-methoxy-indole-2-carbonyl)acrylate (N3o)



According to procedure D, β -ketoester **S14c** (124 mg, 502 μ mol, 1.00 eq.), piperidine (59.1 μ L, 598 μ mol, 1.19 eq.), acetic acid (29.3 μ L, 512 mmol, 1.02 eq.), 4 Å MS (~1.6 g), CH₂Cl₂ (1.7 mL), and furan-2-carbaldehyde (50.1 μ L, 605 μ mol, 1.21 eq.) were used.

Product **N3o** was obtained after column chromatography (*n*-hexane/EtOAc 2:1 to 2:1) as a yellow solid (113 mg, 347 μ mol, 69%, *E/Z* 20:1).

¹H NMR (300 MHz, CDCl₃): δ = 9.03 (br s, 1H, *NH*), 7.72 (s, 1H, *H*_{Olef}), 7.38–7.33 (m, 1H, *H*_{Ar}), 7.31 (d, *J* = 1.7 Hz, 1H, *H*_{Furan}), 7.05 (dd, *J* = 8.9, 2.5 Hz, 1H, *H*_{Ar}), 7.00 (d, *J* = 2.5 Hz, 1H, *H*_{Ar}), 6.94 (dd, *J* = 2.1, 0.9 Hz, 1H, *H*_{Ar}), 6.69 (d, *J* = 3.5 Hz, 1H, *H*_{Furan}), 6.37 (dd, *J* = 3.5, 1.8 Hz, *H*_{Ar}), 3.81 (s, 3H, OCH₃), 3.77 (s, 3H, OCH₃) ppm.

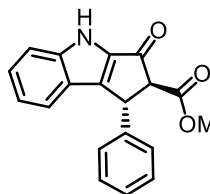
¹³C NMR (75 MHz, CDCl₃): δ = 185.8, 165.8, 155.1, 149.5, 146.6, 136.0, 133.8, 129.2, 128.2, 126.4, 119.0, 118.4, 113.5, 112.7, 111.8, 103.2, 55.9 (OCH₃), 52.8 (OCH₃) ppm.

IR (ATR): $\tilde{\nu}$ = 3304 (br, m), 2953 (w), 1715 (m), 1621 (m), 1552 (w), 1518 (m), 1459 (w), 1409 (w), 1356 (m), 1288 (w), 1242 (m), 1204 (s), 1174 (m), 1143 (m), 1086 (w), 1020 (m), 964 (w), 929 (w), 893 (w), 845 (m), 803 (m), 748 (m), 698 (m), 612 (m), 584 (m), 530 (m), 429 (m) cm⁻¹.

HR-MS (ESI): *m/z* calcd. for C₁₈H₁₆N₁O₅ [M+H]⁺: 326.1023, found 326.1023.

3.4.27 Nazarov Cyclizations with α -Unsaturated β -Ketoesters N3

Methyl (1*R*,2*S*)-2-phenyl-3-oxo-1,2,3,4-tetrahydrocyclopenta[*b*]indole-2-carboxylate (N4a)



According to procedure G, α -unsaturated β -ketoester **N3a** (26.0 mg, 85.2 μ mol, 1.00 eq.) and catalyst **A-C5f** (1.6 mg, 1.7 μ mol, 2.0 mol%) in HFIP (280 μ L) were used; reaction time: 7 h (excluding time for Al_2O_3 -induced equilibration). Desired NAZAROV product **N4a** was obtained after column chromatography (*n*-hexane/EtOAc 3:1) as a colorless solid (19.4 mg, 63.5 μ mol, 75%). D.r. value determined by ^1H NMR analysis of the crude product: *trans/cis* 1:1.8 *before* and 15:1 *after* Al_2O_3 -induced equilibration. Enantiomeric excess of the *trans* diastereomer of the isolated product determined by chiral HPLC analysis: 93% ee (AD-H column, $\lambda = 254$ nm, *n*-hexane/2-propanol 90:10, 0.6 mL/min, column temp.: 25 $^\circ\text{C}$, t_R (major) = 23.0 min, t_R (minor) = 32.1 min), $[\alpha]_D^{27} = -102$ (*c* 1.0, CH_2Cl_2).

^1H NMR (300 MHz, CDCl_3): δ = 9.29 (br s, 1H, *NH*), 7.55–7.48 (m, 1H, H_{Ar}), 7.45–7.21 (m, 8H, H_{Ar}), 7.14–7.05 (m, 1H, H_{Ar}), 5.08 (d, $J = 2.9$ Hz, 1H, H_{Aliph}), 3.92 (d, $J = 2.9$ Hz, 1H, H_{Aliph}), 3.85 (s, 3H, CH_3) ppm.

^{13}C NMR (75 MHz, CDCl_3): δ = 186.8, 169.6, 148.0, 144.6, 140.9, 137.2, 129.2 (2C), 128.3, 127.6, 127.5 (2C), 123.1, 122.4, 121.4, 113.8, 67.9, 52.9, 44.2 ppm.

IR (ATR): $\tilde{\nu}$ = 3266 (br m), 3067 (w), 3028 (w), 2950 (w), 1733 (m), 1676 (s), 1620 (w), 1541 (w), 1486 (w), 1438 (w), 1370 (w), 1320 (m), 1246 (m), 1158 (m), 1101 (w), 1063 (w), 1016 (w), 910 (w), 851 (w), 743 (m), 702 (m), 618 (w), 506 (w), 430 (w) cm^{-1} .

HR-MS (ESI): m/z calcd. for $\text{C}_{19}\text{H}_{15}\text{N}_1\text{O}_3\text{Na}_1$ $[\text{M}+\text{Na}]^+$: 328.0944, found 328.0944.

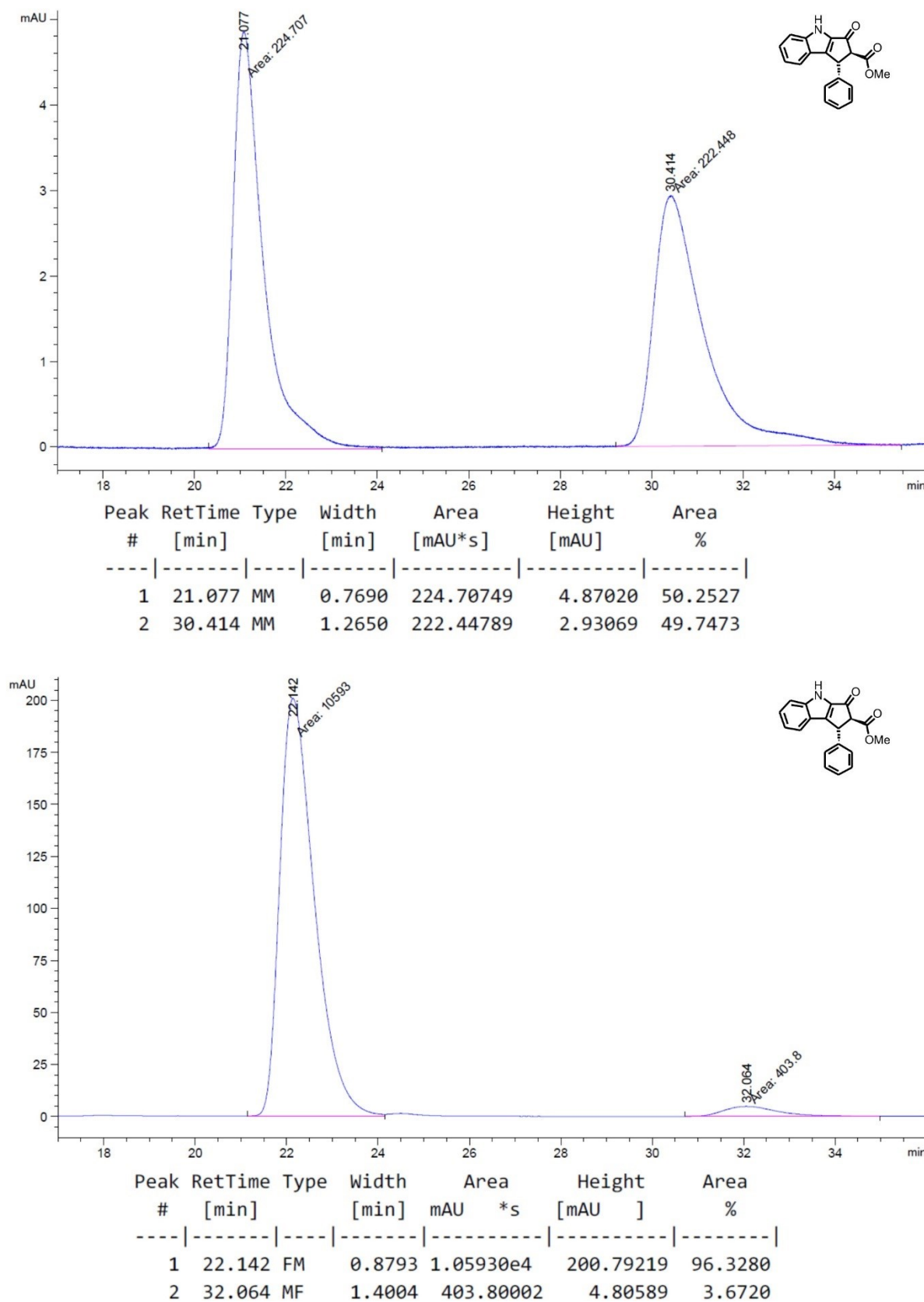
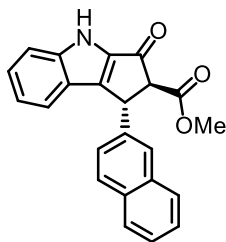


Figure 46: Chiral HPLC traces of **N4a** (racemic top, enriched bottom). HPLC conditions: Daicel Chiralpak AD-H column (250 × 4.6 mm), solvent A: *n*-hexane, solvent B: 2-propanol, isocratic ratio A/B 90:10, flow rate: 0.6 mL·min⁻¹, column temperature: 25 °C, UV absorption detected at λ = 254 nm.

Methyl (1*R*,2*S*)-1-(naphthalen-2-yl)-3-oxo-1,2,3,4-tetrahydrocyclopenta[*b*]indole-2-carboxylate (N4b)



Synthetic steps were carried out by VLADIMIR LARIONOV. According to procedure G, α -unsaturated β -ketoester **N3b** (30.2 mg, 85.0 μ mol, 1.00 eq.) and catalyst **Λ -C5f** (1.6 mg, 1.7 μ mol, 2.0 mol%) in HFIP (280 μ L) were used; reaction time: 12 h (excluding time for Al_2O_3 -induced equilibration).

Desired NAZAROV product **N4b** was obtained after column chromatography (*n*-hexane/EtOAc 3:1) as a colorless solid (27.1 mg, 76.3 μ mol, 90%). D.r. value determined by ^1H NMR analysis of the crude product: *trans/cis* 3.7:1 *before* and 18:1 *after* Al_2O_3 -induced equilibration. Enantiomeric excess of the *trans* diastereomer of the isolated product determined by chiral HPLC analysis: 93% ee (AD-H column, $\lambda = 254$ nm, *n*-hexane/2-propanol 90:10, 0.6 mL/min, column temp.: 25 $^\circ\text{C}$, t_R (major) = 33.5 min, t_R (minor) = 50.0 min), $[\alpha]_{\text{D}}^{27} = -131$ (*c* 1.0, CH_2Cl_2).

^1H NMR (300 MHz, CDCl_3): δ = 9.20 (br s, 1H, *NH*), 7.86–7.72 (m, 4H, H_{Ar}), 7.56–7.51 (m, 1H, H_{Ar}), 7.50–7.45 (m, 2H, H_{Ar}), 7.44–7.37 (m, 1H, H_{Ar}), 7.36–7.29 (m, 2H, H_{Ar}), 7.10–7.03 (m, 2H, H_{Ar}), 5.24 (d, $J = 2.9$ Hz, 1H, H_{Aliph}), 4.00 (d, $J = 2.9$ Hz, 1H, H_{Aliph}), 3.87 (s, 3H, CH_3) ppm.

^{13}C NMR (75 MHz, CDCl_3): δ = 186.7, 169.6, 147.9, 144.5, 138.3, 137.3, 133.7, 133.0, 129.2, 128.3, 128.0, 127.9, 126.6, 126.3, 126.2, 125.4, 123.2, 122.5, 121.5, 113.8, 67.8, 53.0, 44.4 ppm.

IR (ATR): $\tilde{\nu}$ = 3262 (br m), 3058 (w), 2951 (w), 1734 (m), 1679 (s), 1621 (w), 1542 (w), 1481 (w), 1436 (w), 1367 (w), 1321 (m), 1247 (w), 1157 (w), 1100 (w), 1062 (w), 1017 (w), 906 (w), 861 (w), 742 (m), 654 (w), 608 (w), 535 (w), 480 (w), 430 (w) cm^{-1} .

HR-MS (ESI): m/z calcd. for $\text{C}_{23}\text{H}_{17}\text{N}_1\text{O}_3\text{Na}_1$ $[\text{M}+\text{Na}]^+$: 378.1101, found 378.1101.

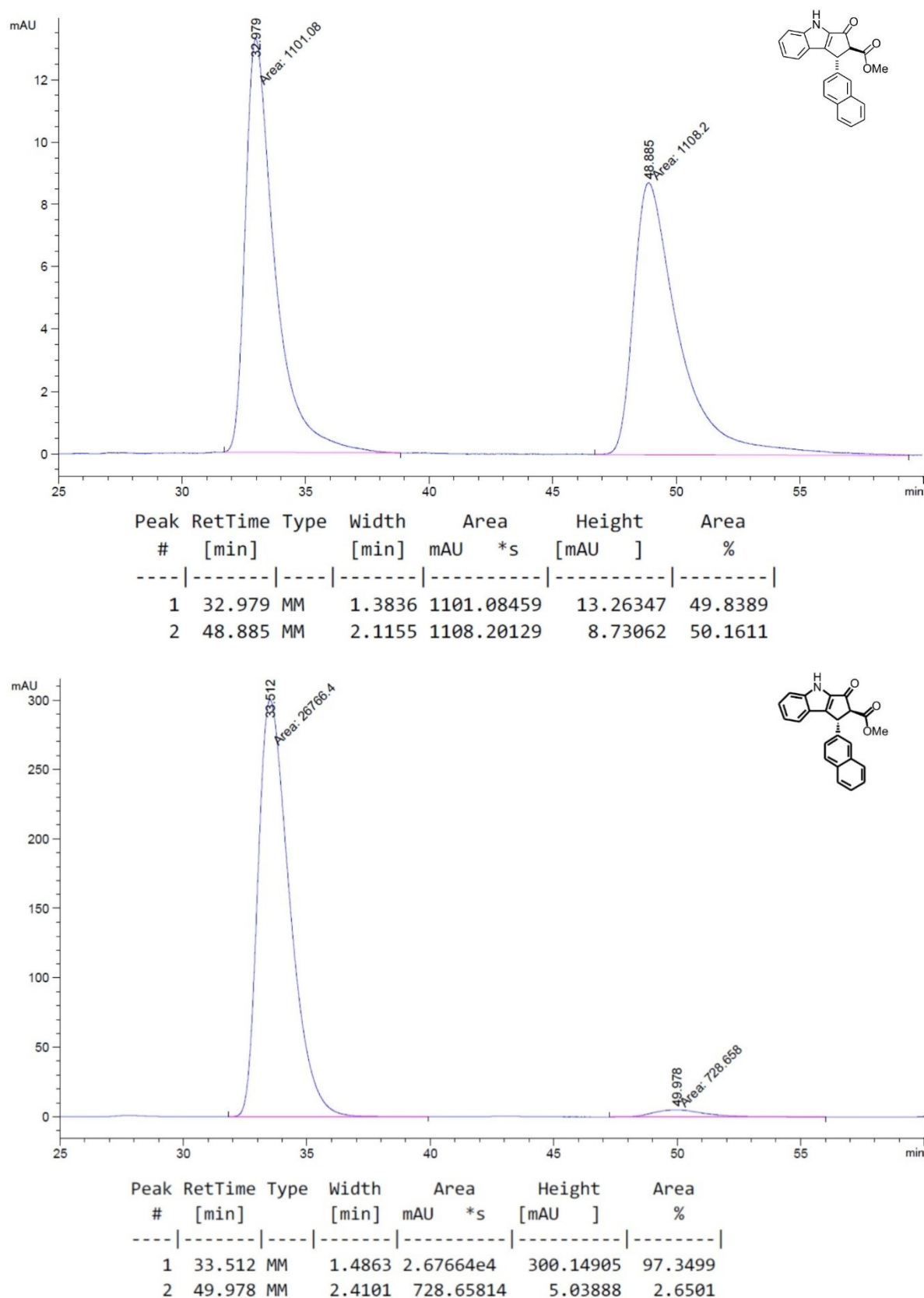
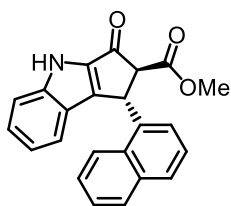


Figure 47: Chiral HPLC traces of **N4b** (racemic top, enriched bottom). HPLC conditions: Daicel Chiralpak AD-H column (250 × 4.6 mm), solvent A: *n*-hexane, solvent B: 2-propanol, isocratic ratio A/B 90:10, flow rate: 0.6 mL·min⁻¹, column temperature: 25 °C, UV absorption detected at λ = 254 nm.

Methyl (1*R*,2*S*)-1-(naphthalen-1-yl)-3-oxo-1,2,3,4-tetrahydrocyclopenta[*b*]indole-2-carboxylate (N4c)



Synthetic steps were carried out by THOMAS CRUCHTER. According to procedure G, α -unsaturated β -ketoester **N3c** (26.4 mg, 74.3 μ mol, 1.00 eq.) and catalyst **A-C5f** (1.6 mg, 1.7 μ mol, 2.3 mol%) in HFIP (250 μ L) were used; reaction time: 12 h (excluding time for Al_2O_3 -induced equilibration).

Desired NAZAROV product **N4c** was obtained after column chromatography (*n*-hexane/EtOAc 3:1) as a colorless solid (18.5 mg, 52.1 μ mol, 70%). D.r. value determined by ^1H NMR analysis of the crude product: *trans/cis* 1:6 *before* and 18:1 *after* Al_2O_3 -induced equilibration. Enantiomeric excess of the *trans* diastereomer of the isolated product determined by chiral HPLC analysis: 96% ee (AD-H column, λ = 254 nm, *n*-hexane/2-propanol 90:10, 0.6 mL/min, column temp.: 25 $^\circ\text{C}$, t_R (major) = 20.0 min, t_R (minor) = 56.1 min), $[\alpha]_{\text{D}}^{27} = +117$ (*c* 1.0, CH_2Cl_2).

^1H NMR (300 MHz, CDCl_3): δ = 9.29 (br s, 1H, NH), 8.32–8.13 (br m, 1H, H_{Ar}), 8.00–7.90 (m, 1H, H_{Ar}), 7.84–7.75 (m, 1H, H_{Ar}), 7.68–7.49 (m, 3H, H_{Ar}), 7.47–7.37 (m, 1H, H_{Ar}), 7.36–7.27 (br m, 2H, H_{Ar}), 7.47–7.01 (br m, 2H, H_{Ar}), 6.02–5.82 (br m, 1H, H_{Ar}), 3.97 (s, 4H, CH_3 , CH) ppm.

^{13}C NMR (75 MHz, CDCl_3): δ = 186.8, 170.0, 144.7, 137.4 (br), 134.3, 131.9, 129.3, 128.4, 128.3 (br), 126.8, 126.1 (br), 125.8, 124.5 (br), 123.3, 123.2, 122.7 (br), 121.5, 113.9, 68.0 (br), 53.1 (OCH_3), 39.7 (br) ppm.

IR (ATR): $\tilde{\nu}$ = 3278 (br m), 3061 (w), 2950 (w), 1732 (m), 1677 (s), 1621 (w), 1542 (w), 1481 (w), 1436 (w), 1367 (w), 1320 (m), 1241 (m), 1157 (m), 1101 (w), 1065 (w), 1000 (w), 910 (w), 868 (w), 779 (m), 736 (m). 641 (w), 533 (w), 493 (w), 428 (w) cm^{-1} .

HR-MS (ESI): m/z calcd. for $\text{C}_{23}\text{H}_{17}\text{N}_1\text{O}_3\text{Na}_1$ $[\text{M}+\text{Na}]^+$: 378.1101, found 378.1100.

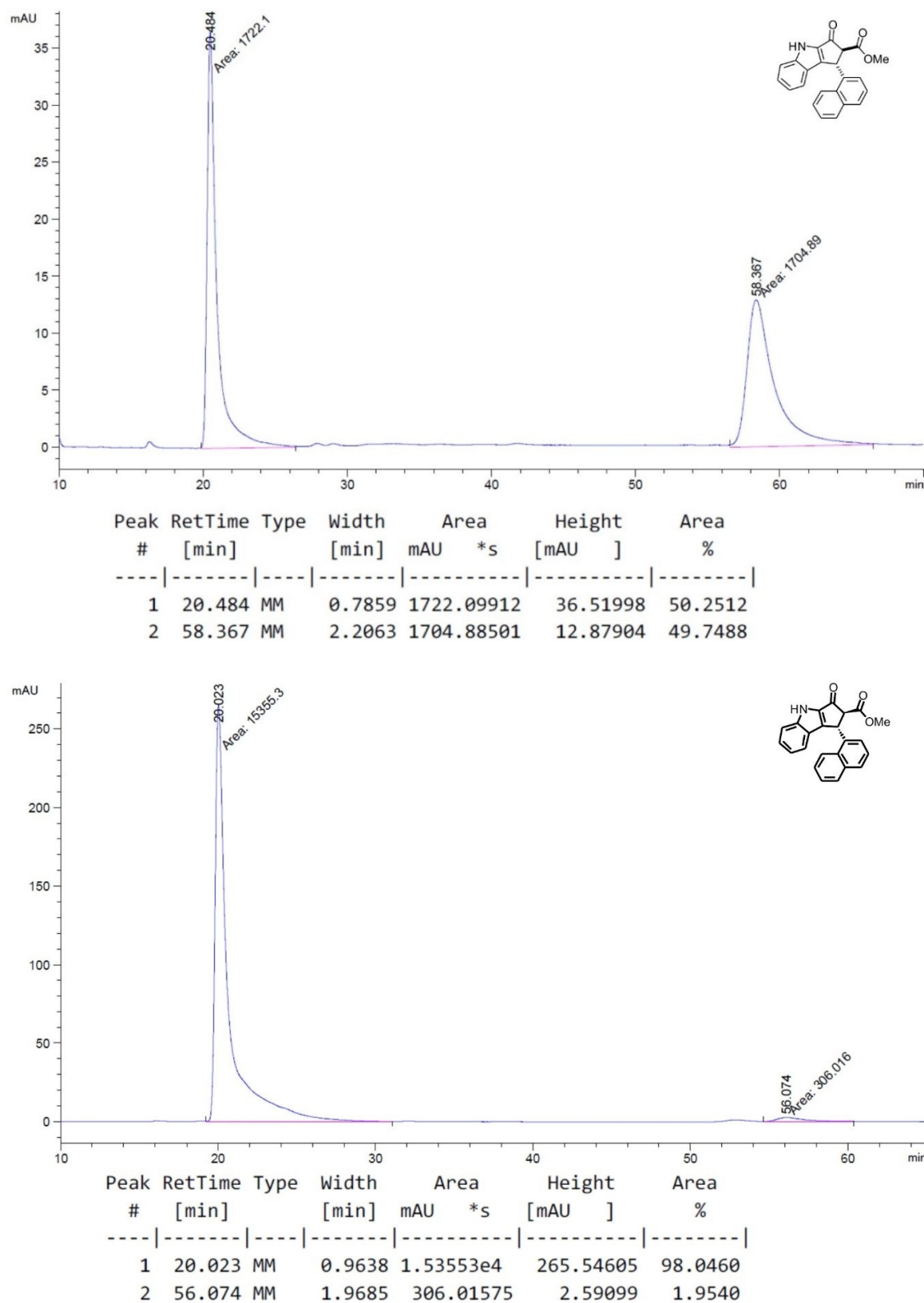
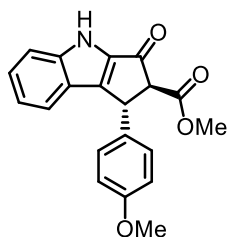


Figure 48: Chiral HPLC traces of **N4c** (racemic top, enriched bottom). HPLC conditions: Daicel Chiralpak AD-H column (250 × 4.6 mm), solvent A: n-hexane, solvent B: 2-propanol, isocratic ratio A/B 90:10, flow rate: 0.6 mL·min⁻¹, column temperature: 25 °C, UV absorption detected at $\lambda = 254$ nm.

Methyl (1*R*,2*S*)-1-(4-methoxyphenyl)-3-oxo-1,2,3,4-tetrahydrocyclopenta[*b*]indole-2-carboxylate (N4d)

a) With catalyst **A-C5f**:



According to procedure G, α -unsaturated β -ketoester **N3d** (28.5 mg, 85.0 μ mol, 1.00 eq.) and catalyst **A-C5f** (1.6 mg, 1.7 μ mol, 2.0 mol%) in HFIP (280 μ L) were used; reaction time: 4.5 h (excluding time for Al_2O_3 -induced equilibration). Desired NAZAROV product **N4d** was obtained after column chromatography (*n*-hexane/EtOAc 3:1) as a colorless solid (24.4 mg, 72.8 μ mol, 86%). D.r. value determined by ^1H NMR analysis of the crude product: *trans/cis* 1:2.5 *before* and 13:1 *after* Al_2O_3 -induced equilibration. Enantiomeric excess of the *trans* diastereomer of the isolated product determined by chiral HPLC analysis: 89% ee (AS-H column, $\lambda = 254$ nm, *n*-hexane/2-propanol 85:15, 1.0 mL/min, column temp.: 25 $^\circ\text{C}$, t_R (major) = 17.2 min, t_R (minor) = 40.4 min), $[\alpha]_{\text{D}}^{27} = -138$ (*c* 1.1, CH_2Cl_2).

^1H NMR (300 MHz, CDCl_3): δ = 9.29 (br s, 1H, NH), 7.54–7.48 (m, 1H, H_{Ar}), 7.43–7.32 (m, 2H, H_{Ar}), 7.16 (d, $J = 8.7$ Hz, 2H, H_{Ar}), 7.12–7.05 (m, 1H, H_{Ar}), 6.85 (d, $J = 8.7$ Hz, 2H, H_{Ar}), 5.02 (d, $J = 2.8$ Hz, 1H, H_{Aliph}), 3.88 (d, $J = 2.8$ Hz, 1H, H_{Aliph}), 3.85 (s, 3H, OCH_3), 3.80 (s, 3H, CH_3) ppm.

^{13}C NMR (75 MHz, CDCl_3): δ = 187.0, 169.6, 159.1, 148.3, 144.6, 137.1, 132.9, 128.6 (2C), 128.2, 123.1, 122.4, 121.4, 114.5 (2C), 113.8, 68.1, 55.4, 52.9, 43.6 ppm.

IR (ATR): $\tilde{\nu}$ = 3302 (br, w), 3067 (w), 3002 (w), 2949 (w), 2841 (w), 1733 (m), 1675 (s), 1614 (m), 1542 (m), 1510 (m), 1437 (w), 1370 (w), 1317 (m), 1242 (s), 1159 (m), 1101 (w), 1092 (w), 1024 (m), 927 (w), 838 (m), 739 (m), 702 (m), 608 (m), 570 (w), 524 (w), 428 (m) cm^{-1} .

HR-MS (ESI): m/z calcd. for $\text{C}_{20}\text{H}_{17}\text{N}_1\text{O}_4\text{Na}_1$ $[\text{M}+\text{Na}]^+$: 358.1050, found 358.1050.

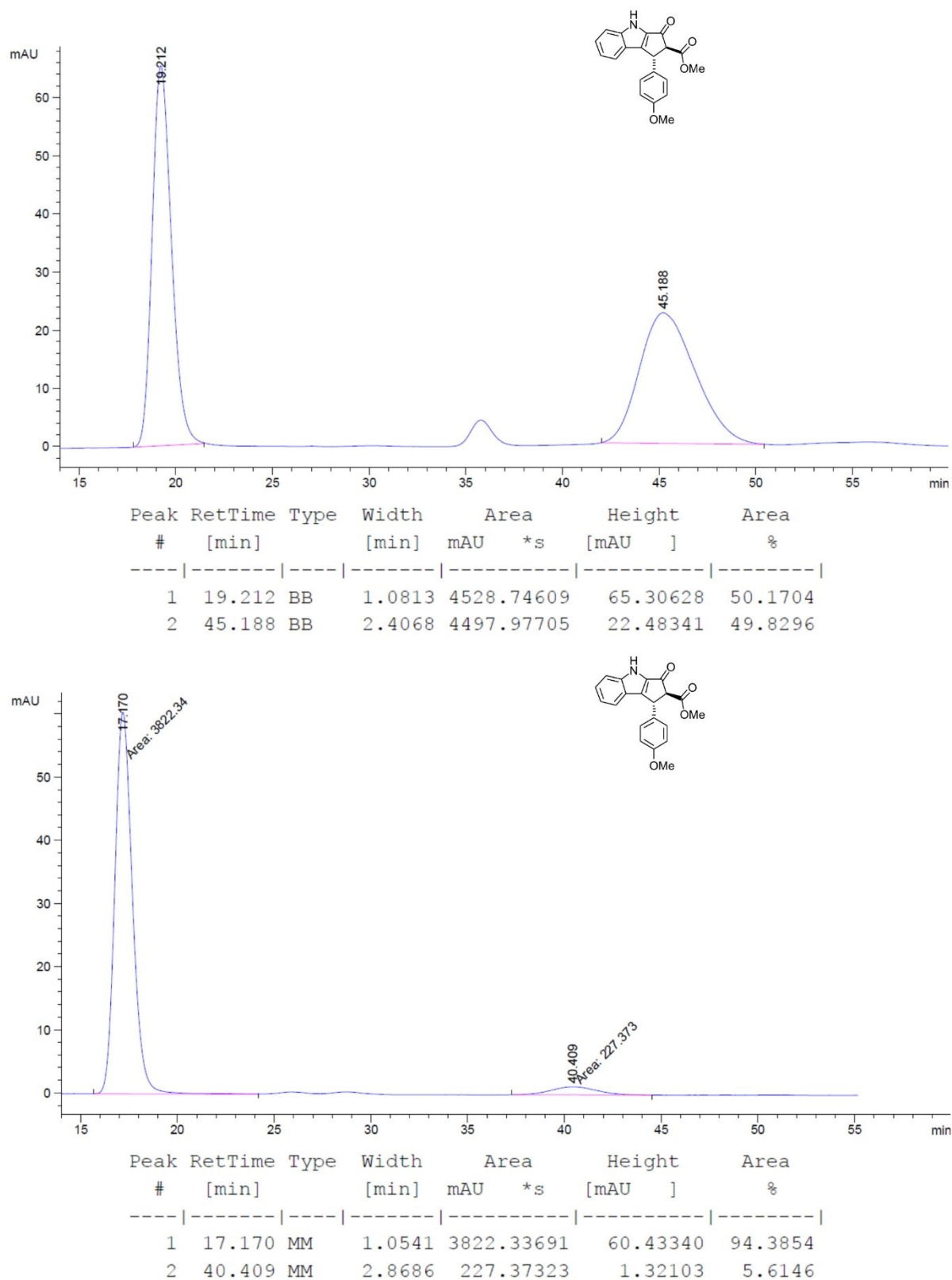
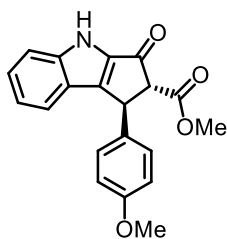


Figure 49: Chiral HPLC traces of **N4d** (racemic top, enriched bottom, catalyst **A-C5f**). HPLC conditions: Daicel Chiralpak AS-H column (250 × 4.6 mm), solvent A: *n*-hexane, solvent B: 2-propanol, isocratic ratio A/B 85:15, flow rate: 1.0 mL·min⁻¹, column temperature: 25 °C, UV absorption detected at $\lambda = 254$ nm.

Methyl (1*S*,2*R*)-1-(4-methoxyphenyl)-3-oxo-1,2,3,4-tetrahydrocyclopenta[*b*]indole-2-carboxylate (N4d)

b) With catalyst **Δ-C5g**:



Synthetic steps were carried out by VLADIMIR LARIONOV. According to procedure G, α -unsaturated β -ketoester **N3e** (28.5 mg, 85.0 μ mol, 1.00 eq.) and catalyst **Δ-C5g** (1.4 mg, 1.7 μ mol, 2.0 mol%) in HFIP (280 μ L) were used; reaction time: 2.5 h (excluding time for Al_2O_3 -induced equilibration).

Desired NAZAROV product **N4d** was obtained after column chromatography (*n*-hexane/EtOAc 3:1) as a colorless solid (24.1 mg, 71.9 μ mol, 85%). D.r. value determined by ^1H NMR analysis of the crude product: *trans/cis* 1:1 *before* and 12:1 *after* Al_2O_3 -induced equilibration. Enantiomeric excess of the *trans* diastereomer of the isolated product determined by chiral HPLC analysis: –89% ee (AS-H column, λ = 254 nm, *n*-hexane/2-propanol 85:15, 1.0 mL/min, column temp.: 25 °C, t_R (minor) = 19.5 min, t_R (major) = 46.4 min), $[\alpha]_D^{27} = +138$ (*c* 1.1, CH_2Cl_2).

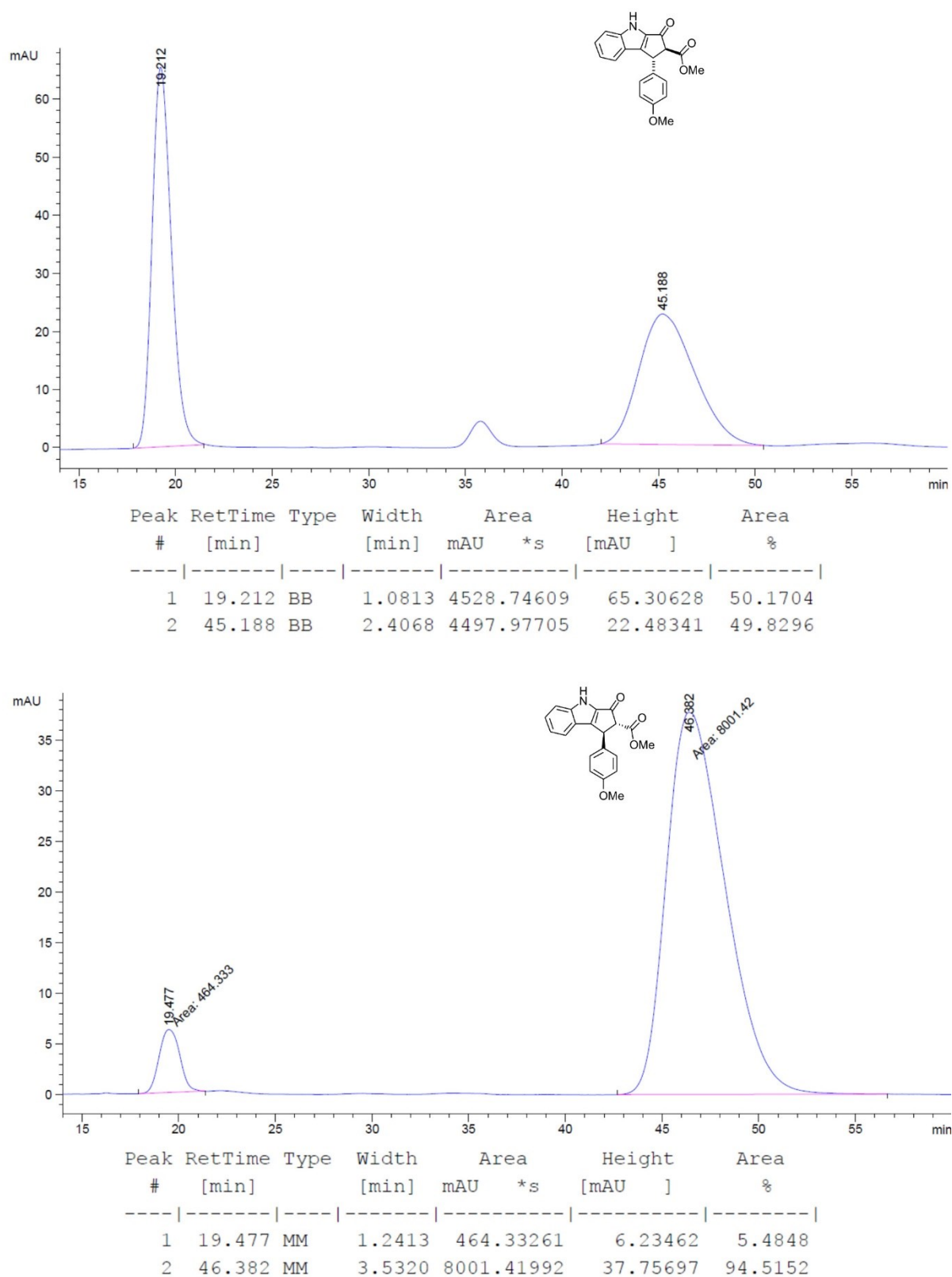
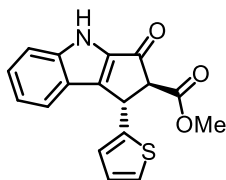


Figure 50: Chiral HPLC traces of N4d (racemic top, enriched bottom, catalyst Δ -C5g). HPLC conditions: Daicel Chiralpak AS-H column (250 \times 4.6 mm), solvent A: n-hexane, solvent B: 2-propanol, isocratic ratio A/B 85:15, flow rate: 1.0 mL \cdot min $^{-1}$, column temperature: 25 $^{\circ}$ C, UV absorption detected at λ = 254 nm.

Methyl (1*S*,2*S*)-3-oxo-1-(thiophen-2-yl)-1,2,3,4-tetrahydrocyclopenta[*b*]indole-2-carboxylate (N4e)

Note: Switching from R → S is not caused by actual inversion of the stereocenter but by higher priority of the thiophene ring according to CIP rules.



Synthetic steps were carried out by VLADIMIR LARIONOV. According to procedure G, α -unsaturated β -ketoester **N3e** (26.5 mg, 85.1 μ mol, 1.00 eq.) and catalyst **A-C5f** (1.6 mg, 1.7 μ mol, 2.0 mol%) in HFIP (280 μ L) were used; reaction time: 24 h (excluding time for Al₂O₃-induced equilibration).

Desired NAZAROV product **N4e** was obtained after column chromatography (*n*-hexane/EtOAc 3:1) as a colorless solid (21.1 mg, 67.8 μ mol, 80%). D.r. value determined by ¹H NMR analysis of the crude product: *trans/cis* 2.6:1 *before* and 17:1 *after* Al₂O₃-induced equilibration. Enantiomeric excess of the *trans* diastereomer of the isolated product determined by chiral HPLC analysis: 93% ee (AD-H column, λ = 254 nm, *n*-hexane/2-propanol 90:10, 0.6 mL/min, column temp.: 25 °C, *t*_R (major) = 26.0 min, *t*_R (minor) = 37.7 min), [α]_D²⁷ = −41 (*c* 1.0, CH₂Cl₂).

¹H NMR (300 MHz, CDCl₃): δ = 9.19 (br s, 1H, *NH*), 7.55–7.48 (m, 2H, *H*_{Ar}), 7.46–7.38 (m, 1H, *H*_{Ar}), 7.84–7.75 (m, 1H, *H*_{Ar}), 7.68–7.49 (m, 3H, *H*_{Ar}), 7.47–7.37 (m, 1H, *H*_{Ar}), 7.22 (dd, *J* = 4.5, 1.9 Hz, 1H, *H*_{Thiophene}), 7.18–7.11 (m, 1H, *H*_{Ar}), 7.01–6.93 (m, 2H, *H*_{Ar}), 5.36 (d, *J* = 2.9 Hz, 1H, *H*_{Aliph}), 4.02 (d, *J* = 2.9 Hz, 1H, *H*_{Aliph}), 3.86 (s, 3H, CH₃) ppm.

¹³C NMR (75 MHz, CDCl₃): δ = 185.8, 169.1, 147.1, 144.4, 144.2, 136.6, 128.3, 127.2, 125.3, 124.9, 123.0, 122.5, 121.6, 113.9, 68.2, 53.0 (OCH₃), 39.3 ppm.

IR (ATR): $\tilde{\nu}$ = 3312 (br w), 2951 (w), 1734 (m), 1682 (s), 1620 (w), 1541 (w), 1482 (w), 1436 (w), 1367 (w), 1321 (w), 1236 (w), 1157 (m), 1100 (w), 1060 (w), 1012 (w), 914 (w), 851 (w), 748 (w), 704 (w), 630 (w), 502 (w), 431 (w) cm^{−1}.

HR-MS (ESI): *m/z* calcd. for C₁₇H₁₃N₁O₃SN_a1 [M+Na]⁺: 334.0508, found 334.0509.

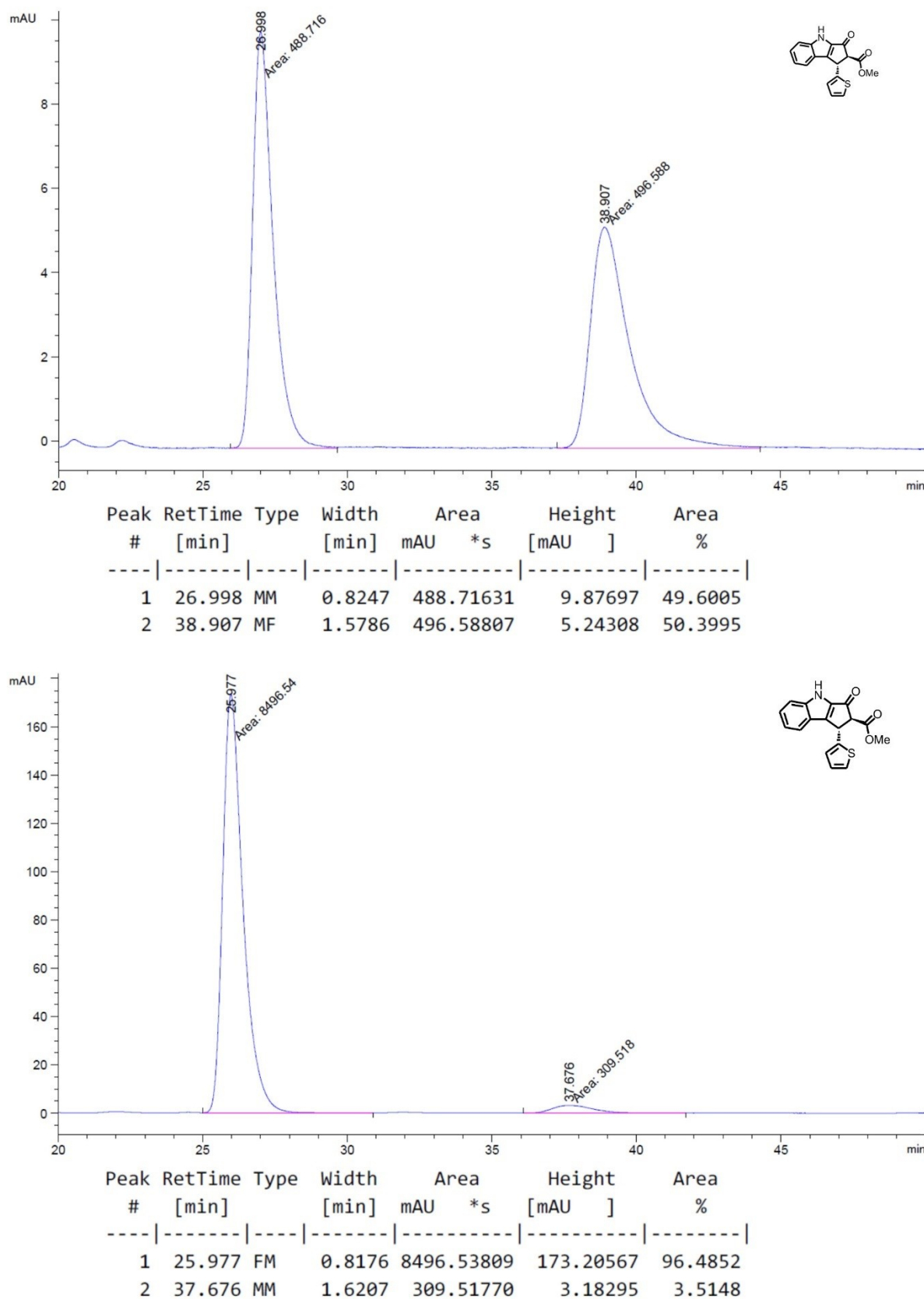
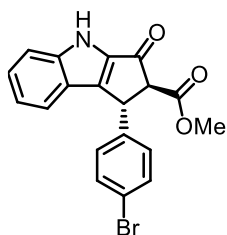


Figure 51: Chiral HPLC traces of **N4e** (racemic top, enriched bottom). HPLC conditions: Daicel Chiralpak AD-H column (250 × 4.6 mm), solvent A: *n*-hexane, solvent B: 2-propanol, isocratic ratio A/B 90:10, flow rate: 0.6 mL·min⁻¹, column temperature: 25 °C, UV absorption detected at $\lambda = 254$ nm.

Methyl (1*R*,2*S*)-1-(4-bromophenyl)-3-oxo-1,2,3,4-tetrahydrocyclopenta[*b*]indole-2-Carboxylate (N4f)



Synthetic steps were carried out by THOMAS CRUCHTER. According to procedure G, α -unsaturated β -ketoester **N3f** (33.0 mg, 85.9 μ mol, 1.00 eq.) and catalyst **Λ -C5f** (1.6 mg, 1.7 μ mol, 2.0 mol%) in HFIP (280 μ L) were used; reaction time: 24 h (excluding time for Al₂O₃-induced equilibration).

Desired NAZAROV product **N4f** was obtained after column chromatography (*n*-hexane/EtOAc 3:1) as a colorless solid (27.0 mg, 70.3 μ mol, 82%). D.r. value determined by ¹H NMR analysis of the crude product: *trans/cis* 12:1 *before* and 12:1 *after* Al₂O₃-induced equilibration. Enantiomeric excess of the *trans* diastereomer of the isolated product determined by chiral HPLC analysis: 96% ee (AD-H column, λ = 254 nm, *n*-hexane/2-propanol 90:10, 0.6 mL/min, column temp.: 25 °C, *t*_R (major) = 26.5 min, *t*_R (minor) = 42.2 min), [α]_D²⁷ = −52 (*c* 0.8, CH₂Cl₂).

¹H NMR (300 MHz, CDCl₃): δ = 9.46 (br s, 1H, *NH*), 7.57–7.49 (m, 1H, *H*_{Ar}), 7.48–7.36 (m, 3H, *H*_{Ar}), 7.36–7.28 (m, 1H, *H*_{Ar}), 7.17–7.09 (m, 3H, *H*_{Ar}), 5.03 (d, *J* = 2.0 Hz, 1H, *H*_{Aliph}), 3.85 (br s, 4H, *CH*₃+*CH*) ppm.

¹³C NMR (75 MHz, CDCl₃): δ = 186.4, 169.3, 147.1, 144.6, 139.9, 137.2, 132.3 (2C), 130.8, 129.3 (2C), 128.4, 122.9, 122.2, 121.6, 114.0, 67.7, 53.0, 43.6 ppm.

IR (ATR): $\tilde{\nu}$ = 3284 (br w), 2955 (w), 1733 (m), 1677 (s), 1620 (w), 1541 (w), 1484 (w), 1436 (w), 1370 (w), 1320 (w), 1251 (w), 1157 (w), 1099 (w), 1069 (w), 1012 (m), 910 (w), 803 (w), 729 (m), 646 (w), 607 (w), 577 (w), 539 (w), 504 (w), 430 (w) cm^{−1}.

HR-MS (ESI): *m/z* calcd. for C₁₉H₁₄BrN₁O₃Na₁ [*M*+Na]⁺: 406.0049, found 406.0047.

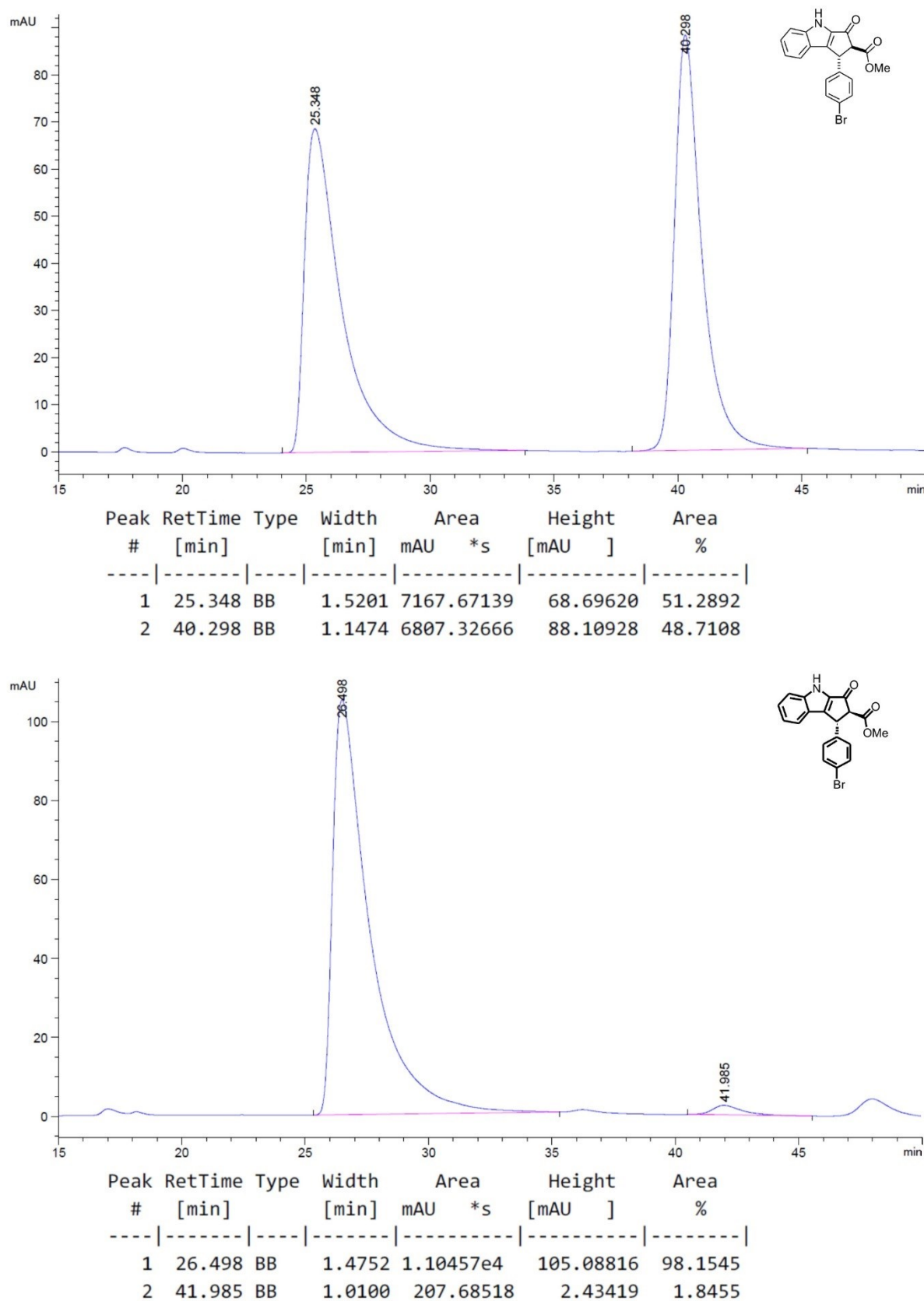
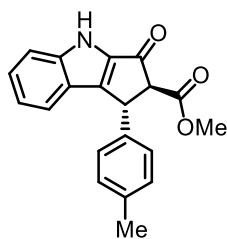


Figure 52: Chiral HPLC traces of **N4f** (racemic top, enriched bottom). HPLC conditions: Daicel Chiralpak AD-H column (250 × 4.6 mm), solvent A: *n*-hexane, solvent B: 2-propanol, isocratic ratio A/B 90:10, flow rate: 0.6 mL·min⁻¹, column temperature: 25 °C, UV absorption detected at λ = 254 nm.

Methyl (1*R*,2*S*)-3-oxo-1-(*p*-tolyl)-1,2,3,4-tetrahydrocyclopenta[*b*]indole-2-carboxylate (N4g)



Synthetic steps were carried out by THOMAS CRUCHTER. According to procedure G, α -unsaturated β -ketoester **N3g** (26.7 mg, 83.6 μ mol, 1.00 eq.) and catalyst **A-C5f** (1.6 mg, 1.7 μ mol, 2.0 mol%) in HFIP (280 μ L) were used; reaction time: 12 h (excluding time for Al₂O₃-induced equilibration).

Desired NAZAROV product **N4g** was obtained after column chromatography (*n*-hexane/EtOAc 3:1) as a colorless solid (22.8 mg, 71.4 μ mol, 85%). D.r. value determined by ¹H NMR analysis of the crude product: *trans/cis* 1:1 *before* and 15:1 *after* Al₂O₃-induced equilibration. Enantiomeric excess of the *trans* diastereomer of the isolated product determined by chiral HPLC analysis: 91% ee (AD-H column, λ = 254 nm, *n*-hexane/2-propanol 90:10, 0.6 mL/min, column temp.: 30 °C, *t*_R (major) = 22.1 min, *t*_R (minor) = 37.5 min), [α]_D²⁷ = −89 (*c* 1.1, CH₂Cl₂).

¹H NMR (300 MHz, CDCl₃): δ = 9.44 (br s, 1H, *NH*), 7.55–7.49 (m, 1H, *H*_{Ar}), 7.43–7.38 (m, 1H, *H*_{Ar}), 7.38–7.32 (m, 1H, *H*_{Ar}), 7.16–7.04 (m, 5H, *H*_{Ar}), 5.03 (d, *J* = 2.8 Hz, 1H, *H*_{Aliph}), 3.90 (d, *J* = 2.8 Hz, 1H, *H*_{Aliph}), 3.85 (s, 3H, OCH₃), 2.34 (s, 3H, CH₃) ppm.

¹³C NMR (75 MHz, CDCl₃): δ = 187.2, 169.7, 148.4, 144.6, 137.8, 137.3, 137.1, 129.8 (2C), 128.2, 127.4 (2C), 123.0, 122.4, 121.3, 113.9, 68.0, 53.0, 43.9, 21.2 ppm.

IR (ATR): $\tilde{\nu}$ = 3258 (br w), 2953 (w), 2921 (w), 2856 (w), 1735 (m), 1676 (s), 1620 (w), 1540 (w), 1511 (w), 1437 (w), 1371 (w), 1319 (w), 1246 (w), 1156 (m), 1100 (w), 1062 (w), 910 (w), 810 (w), 733 (m), 647 (w), 609 (w), 576 (w), 538 (w), 506 (w), 429 (w) cm^{−1}.

HR-MS (ESI): *m/z* calcd. for C₂₀H₁₇N₁O₃Na₁ [M+Na]⁺: 342.1101, found 342.1109.

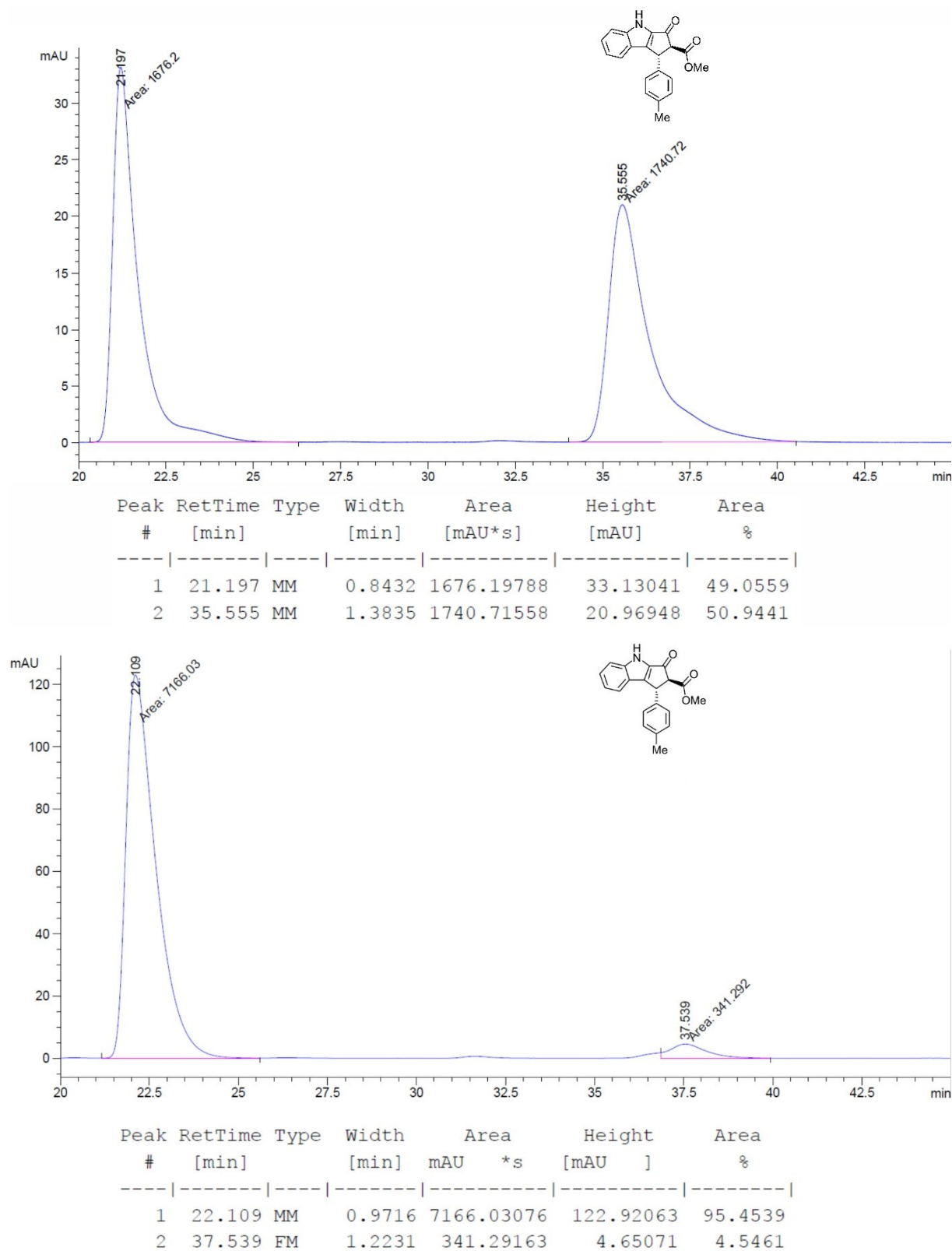
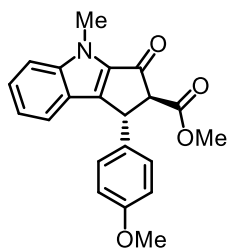


Figure 53: Chiral HPLC traces of **N4g** (racemic top, enriched bottom). HPLC conditions: Daicel Chiralpak AD-H column (250 × 4.6 mm), solvent A: *n*-hexane, solvent B: 2-propanol, isocratic ratio A/B 90:10, flow rate: 0.6 mL·min⁻¹, column temperature: 30 °C, UV absorption detected at $\lambda = 254$ nm.

Methyl (1*R*,2*S*)-1-(4-methoxyphenyl)-4-methyl-3-oxo-1,2,3,4-tetrahydrocyclopenta[*b*]indole-2-carboxylate (N4h)



According to procedure G, α -unsaturated β -ketoester **N3h** (29.7 mg, 85.0 μ mol, 1.00 eq.) and catalyst **A-C5f** (1.6 mg, 1.7 μ mol, 2.0 mol%) in HFIP (280 μ L) were used; reaction time: 6 h (excluding time for Al_2O_3 -induced equilibration). Desired NAZAROV product **N4h** was obtained after column chromatography (*n*-hexane/EtOAc 2:1) as a colorless solid (24.9 mg, 71.3 μ mol, 84%). D.r. value determined by ^1H NMR analysis of the crude product: *trans/cis* 1.7:1 *before* and 13:1 *after* Al_2O_3 -induced equilibration. Enantiomeric excess of the *trans* diastereomer of the isolated product determined by chiral HPLC analysis: 88% ee (IA column, $\lambda = 254$ nm, *n*-hexane/2-propanol 90:10, 1.0 mL/min, column temp.: 25 $^\circ\text{C}$, t_R (minor) = 10.6 min, t_R (major) = 15.5 min), $[\alpha]_{\text{D}}^{27} = -105$ (c 1.0, CH_2Cl_2).

^1H NMR (300 MHz, CDCl_3): δ = 7.44–7.38 (m, 2H, H_{Ar}), 7.36–7.31 (m, 1H, H_{Ar}), 7.15 (d, $J = 8.7$ Hz, 2H, H_{Ar}), 7.12–7.05 (m, 1H, H_{Ar}), 6.84 (d, $J = 8.7$ Hz, 2H, H_{Ar}), 4.97 (d, $J = 2.9$ Hz, 1H, H_{Aliph}), 3.97 (s, 3H, CH_3), 3.86–3.81 (m, 4H, H_{Aliph}), 3.79 (s, 3H, OCH_3) ppm.

^{13}C NMR (75 MHz, CDCl_3): δ = 187.0, 169.8, 159.1, 145.9, 145.7, 137.3, 133.2, 128.5 (2C), 127.6, 122.6, 120.9, 114.5 (2C), 111.2, 68.5, 55.4, 52.8 (OCH_3), 43.1, 30.4 ppm.

IR (ATR): $\tilde{\nu}$ = 2948 (w), 2838 (w), 1735 (m), 1686 (s), 1611 (w), 1547 (m), 1510 (m), 1432 (w), 1345 (w), 1310 (m), 1244 (s), 1160 (m), 1030 (m), 975 (w), 925 (w), 894 (m), 833 (m), 738 (s), 610 (w), 557 (w), 518 (w), 429 (w) cm^{-1} .

HR-MS (ESI): m/z calcd. for $\text{C}_{21}\text{H}_{19}\text{N}_1\text{O}_4\text{Na}_1$ $[\text{M}+\text{Na}]^+$: 372.1206, found 372.1206.

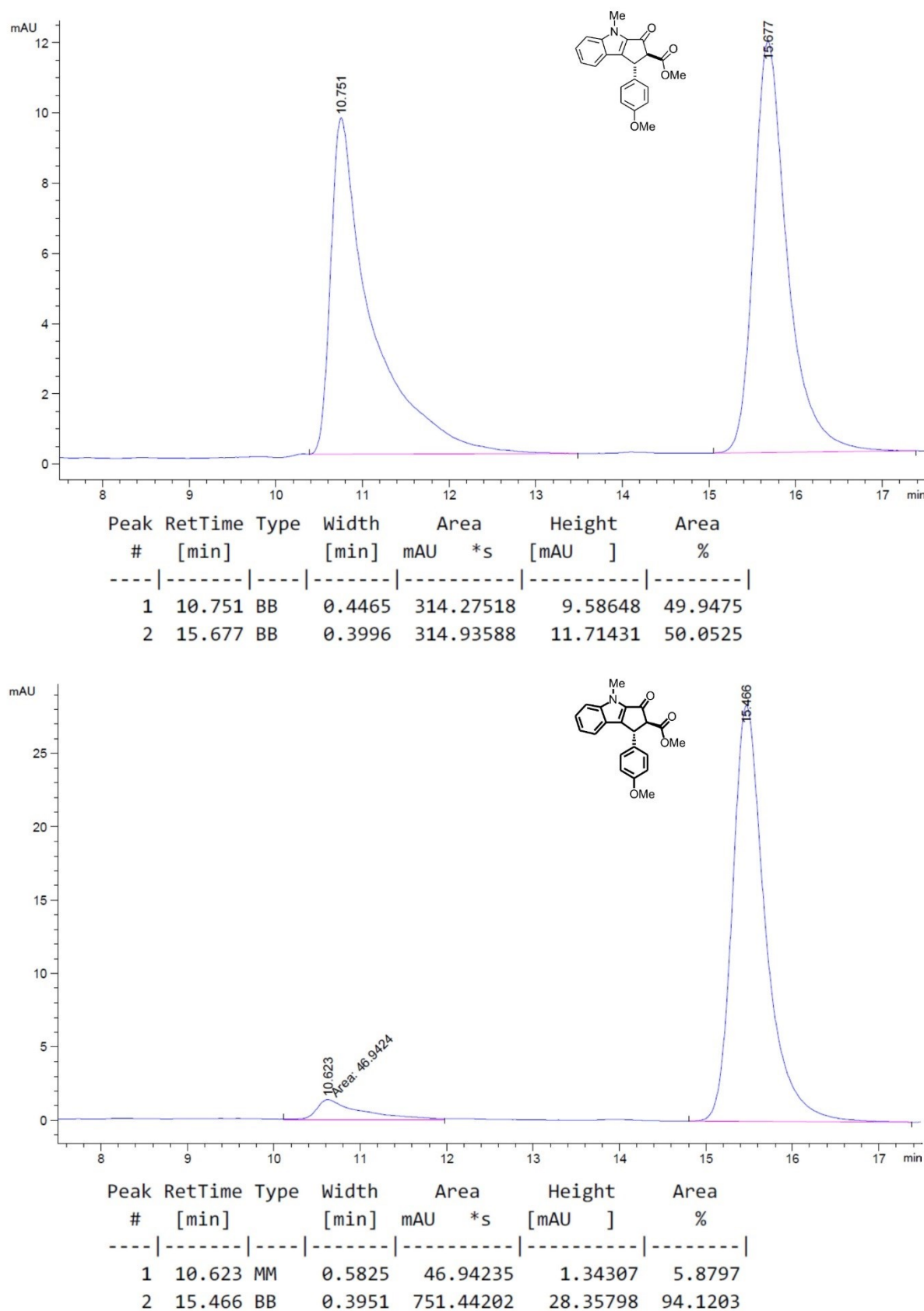
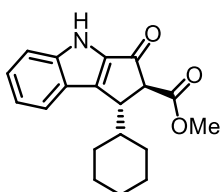


Figure 54: Chiral HPLC traces of **N4h** (racemic top, enriched bottom). HPLC conditions: Daicel Chiralpak IA column (250 × 4.6 mm), solvent A: *n*-hexane, solvent B: 2-propanol, isocratic ratio A/B 90:10, flow rate: 1.0 mL·min⁻¹, column temperature: 25 °C, UV absorption detected at λ = 254 nm.

Methyl (1*S*,2*S*)-1-cyclohexyl-3-oxo-1,2,3,4-tetrahydrocyclopenta[*b*]indole-2-carboxylate (N4i)

Note: Switching from R → S is not caused by actual inversion of the stereocenter but by higher priority of the thiophene ring according to CIP rules.

a) With catalyst **Λ-C5f**:



Synthetic steps were carried out by THOMAS CRUCHTER. According to procedure G, α -unsaturated β -ketoester **N3i** (26.0 mg, 83.5 μ mol, 1.00 eq.) and catalyst **Λ-C5f** (1.6 mg, 1.7 μ mol, 2.0 mol%) in HFIP (280 μ L) were used; reaction time: 168 h (excluding time for Al₂O₃-induced equilibration). Desired NAZAROV product **N4i** was obtained after column chromatography (*n*-hexane/EtOAc 3:1) as a colorless solid (22.1 mg, 71.0 μ mol, 85%). D.r. value determined by ¹H NMR analysis of the crude product: *trans/cis* >20:1 *before* and >20:1 *after* Al₂O₃-induced equilibration. Enantiomeric excess of the *trans* diastereomer of the isolated product determined by chiral HPLC analysis: 41% ee (AD-H column, λ = 254 nm, *n*-hexane/2-propanol 90:10, 0.7 mL/min, column temp.: 25 °C, *t_R* (major) = 15.5 min, *t_R* (minor) = 22.2 min), [α]_D²⁷ = −73 (*c* 1.1, CH₂Cl₂).

¹H NMR (300 MHz, CDCl₃): δ = 9.52 (br s, 1H, NH), 7.77–7.73 (m, 1H, *H*_{Ar}), 7.53–7.48 (m, 1H, *H*_{Ar}), 7.43–7.38 (m, 1H, *H*_{Ar}), 7.21–7.16 (m, 1H, *H*_{Ar}), 3.84 (d, *J* = 2.1 Hz, 1H, *H*_{Aliph}), 3.79 (dd, *J* = 5.2, 2.8 Hz, 1H, *H*_{Aliph}), 3.78 (s, 3H, OCH₃), 2.02–1.92 (m, 1H, *H*_{Aliph}), 1.89–1.82 (m, 1H, *H*_{Aliph}), 1.82–1.75 (m, 1H, *H*_{Aliph}), 1.75–1.64 (m, 2H, *H*_{Aliph}), 1.56–1.49 (m, 1H, *H*_{Aliph}), 1.31–1.07 (m, 5H, *H*_{Aliph}) ppm.

¹³C NMR (75 MHz, CDCl₃): δ = 187.9, 170.7, 149.2, 144.6, 137.3, 128.0, 123.5, 122.8, 121.1, 114.0, 61.5, 52.8, 45.7, 41.8, 31.6, 29.4, 26.5, 26.4, 26.4 ppm.

IR (ATR): $\tilde{\nu}$ = 3250 (br w), 2925 (w), 2852 (w), 1734 (m), 1673 (s), 1596 (w), 1536 (w), 1479 (w), 1441 (w), 1371 (w), 1320 (w), 1256 (m), 1169 (m), 1096 (w), 1016 (w), 806 (w), 743 (m), 679 (w), 613 (w), 575 (w), 541 (w), 506 (w), 433 (w) cm^{−1}.

HR-MS (ESI): *m/z* calcd. for C₁₉H₂₁N₁O₃Na₁ [*M*+Na]⁺: 334.1414, found 334.1413.

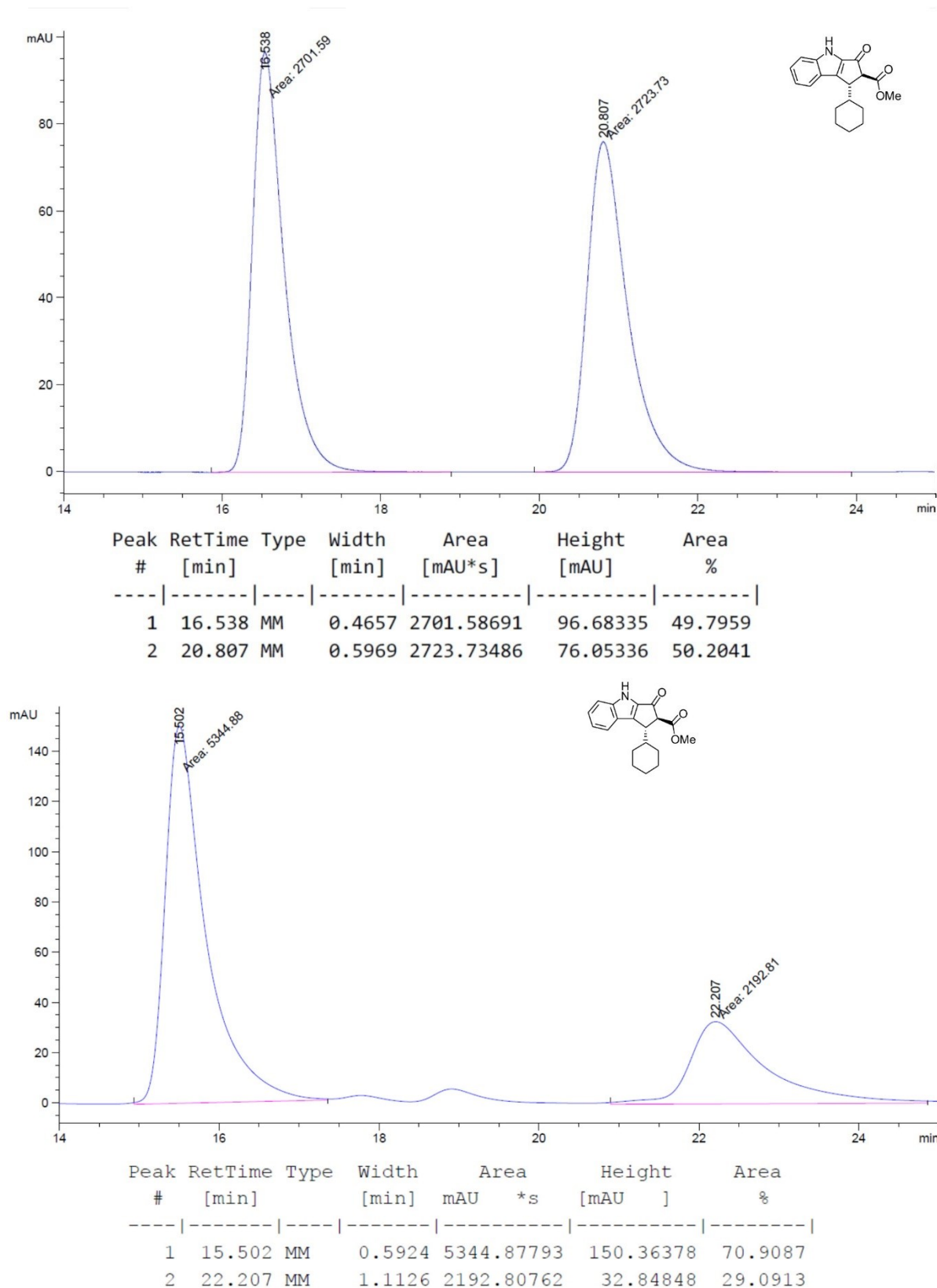
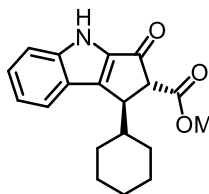


Figure 55: Chiral HPLC traces of **N4i** (racemic top, enriched bottom, catalyst **A-C5f**). HPLC conditions: Daicel Chiralpak AD-H column (250 × 4.6 mm), solvent A: *n*-hexane, solvent B: 2-propanol, isocratic ratio A/B 90:10, flow rate: 0.7 mL·min⁻¹, column temperature: 25 °C, UV absorption detected at $\lambda = 254$ nm.

Methyl (1*R*,2*R*)-1-cyclohexyl-3-oxo-1,2,3,4-tetrahydrocyclopenta[*b*]indole-2-carboxylate (N4i)

b) With catalyst **Δ-C5g**:



According to procedure G, α -unsaturated β -ketoester **N3i** (26.2 mg, 84.1 μ mol, 1.00 eq.) and catalyst **Δ-C5g** (1.4 mg, 1.7 μ mol, 2.0 mol%) in HFIP (280 μ L) were used; reaction time: 96 h (excluding time for Al_2O_3 -induced equilibration). Desired NAZAROV product **N4i** was obtained after column chromatography (*n*-hexane/EtOAc 3:1) as a colorless solid (23.3 mg, 74.8 μ mol, 89%). D.r. value determined by ^1H NMR analysis of the crude product: *trans/cis* >20:1 *before* and >20:1 *after* Al_2O_3 -induced equilibration. Enantiomeric excess of the *trans* diastereomer of the isolated product determined by chiral HPLC analysis: 58% ee (AD-H column, λ = 254 nm, *n*-hexane/2-propanol 90:10, 0.7 mL/min, column temp.: 25 $^\circ\text{C}$, t_{R} (minor) = 16.6 min, t_{R} (major) = 20.8 min), $[\alpha]_{\text{D}}^{27}$ = +65 (*c* 1.1, CH_2Cl_2).

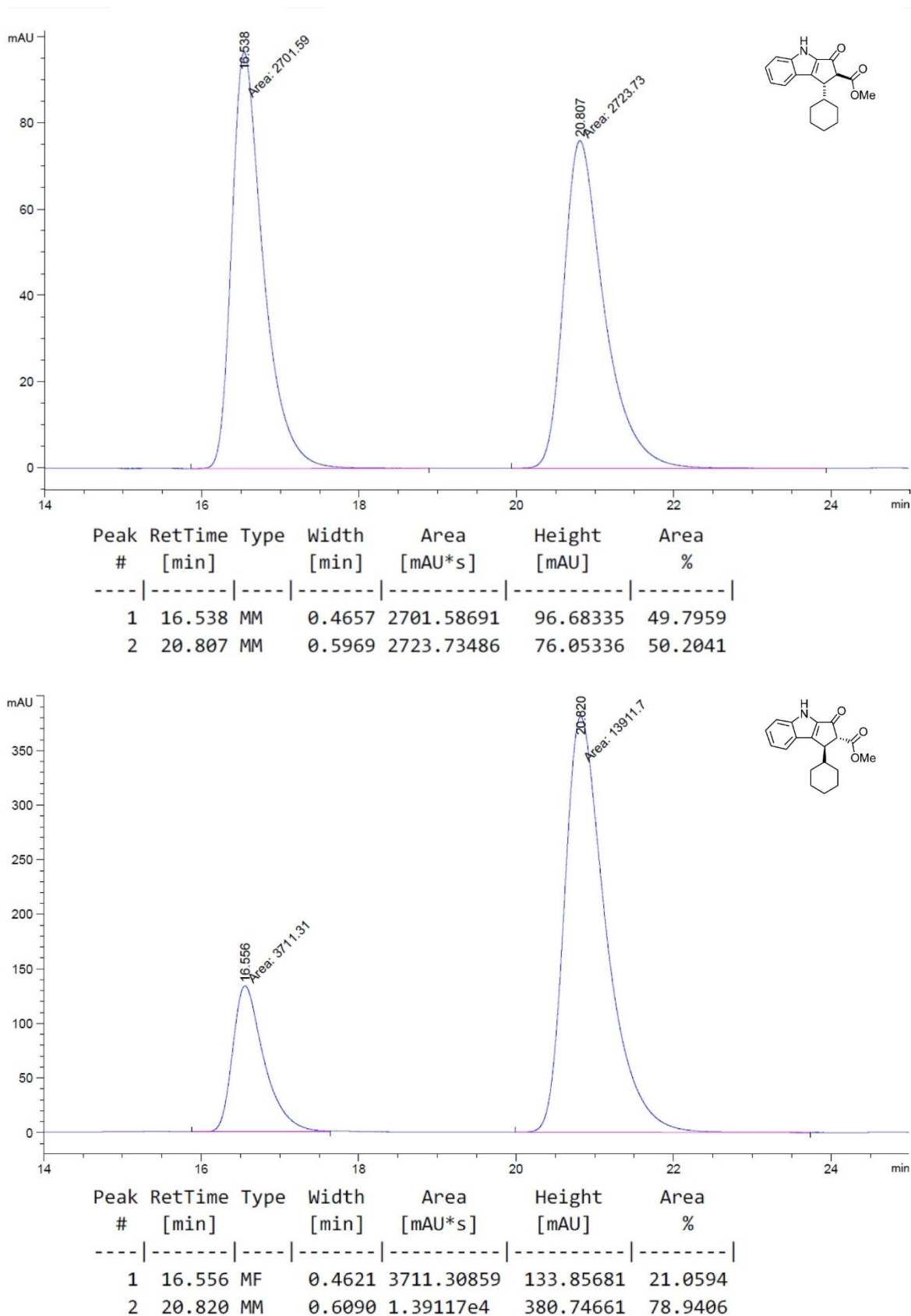
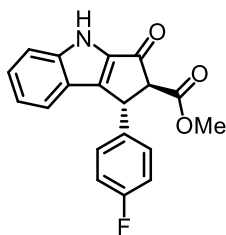


Figure 56: Chiral HPLC traces of **N4i** (racemic top, enriched bottom, catalyst **Δ -C5g**). HPLC conditions: Daicel Chiralpak AD-H column (250 \times 4.6 mm), solvent A: *n*-hexane, solvent B: 2-propanol, isocratic ratio A/B 90:10, flow rate: 0.7 mL \cdot min $^{-1}$, column temperature: 25 $^{\circ}$ C, UV absorption detected at λ = 254 nm.

Methyl (1*R*,2*S*)-1-(4-fluorophenyl)-3-oxo-1,2,3,4-tetrahydrocyclopenta[*b*]indole-2-carboxylate (N4j)



According to procedure G, α -unsaturated β -ketoester **N3j** (27.0 mg, 83.5 μ mol, 1.00 eq.) and catalyst **A-C5f** (1.6 mg, 1.7 μ mol, 2.0 mol%) in HFIP (280 μ L) were used; reaction time: 24 h (excluding time for Al_2O_3 -induced equilibration). Desired NAZAROV product **N4j** was obtained after column chromatography (*n*-pentane/Et₂O 1:1) as a colorless solid (21.3 mg, 66.0 μ mol, 79%). D.r. value determined by ¹H NMR analysis of the crude product: *trans/cis* >13:1 *before* and >13:1 *after* Al_2O_3 -induced equilibration. Enantiomeric excess of the *trans* diastereomer of the isolated product determined by chiral HPLC analysis: 97% ee (AD-H column, λ = 254 nm, *n*-hexane/2-propanol 90:10, 0.6 mL/min, column temp.: 25 °C, *t*_R (major) = 23.0 min, *t*_R (minor) = 36.3 min), [α]_D²⁷ = −48 (*c* 1.0, CH₂Cl₂).

¹H NMR (300 MHz, CDCl₃): δ = 9.44 (br s, 1H, NH), 7.55–7.49 (m, 1H, *H*_{Ar}), 7.43–7.38 (m, 1H, *H*_{Ar}), 7.38–7.32 (m, 1H, *H*_{Ar}), 7.16–7.04 (m, 5H, *H*_{Ar}), 5.03 (d, *J* = 2.8 Hz, 1H, *H*_{Aliph}), 3.90 (d, *J* = 2.8 Hz, 1H, *H*_{Aliph}), 3.85 (s, 3H, OCH₃), 2.34 (s, 3H, CH₃) ppm.

¹³C NMR (75 MHz, CDCl₃): δ = 186.5, 169.4, 147.6, 144.5, 137.2, 136.6 (d, *J* = 3.1 Hz, 1C), 129.1 (d, *J* = 8.2 Hz, 2C), 128.4, 122.9, 122.3, 121.5, 116.2, 115.9 (d, *J* = 21.7 Hz, 2C), 113.9, 67.9, 53.0, 43.4 ppm.

IR (ATR): $\tilde{\nu}$ = 3257 (br w), 2923 (w), 2854 (w), 1734 (m), 1674 (s), 1613 (w), 1541 (w), 1506 (m), 1480 (m), 1435 (w), 1369 (w), 1318 (w), 1221 (w), 1154 (m), 1098 (w), 1061 (w), 988 (w), 928 (w), 840 (w), 804 (w), 745 (m), 644 (w), 606 (w), 575 (w), 537 (w), 512 (w), 423 (w) cm^{−1}.

MR-MS (ESI): *m/z* calcd. for C₁₉H₁₄N₁O₃Na₁ [M+Na]⁺: 346.0850, found 346.0852.

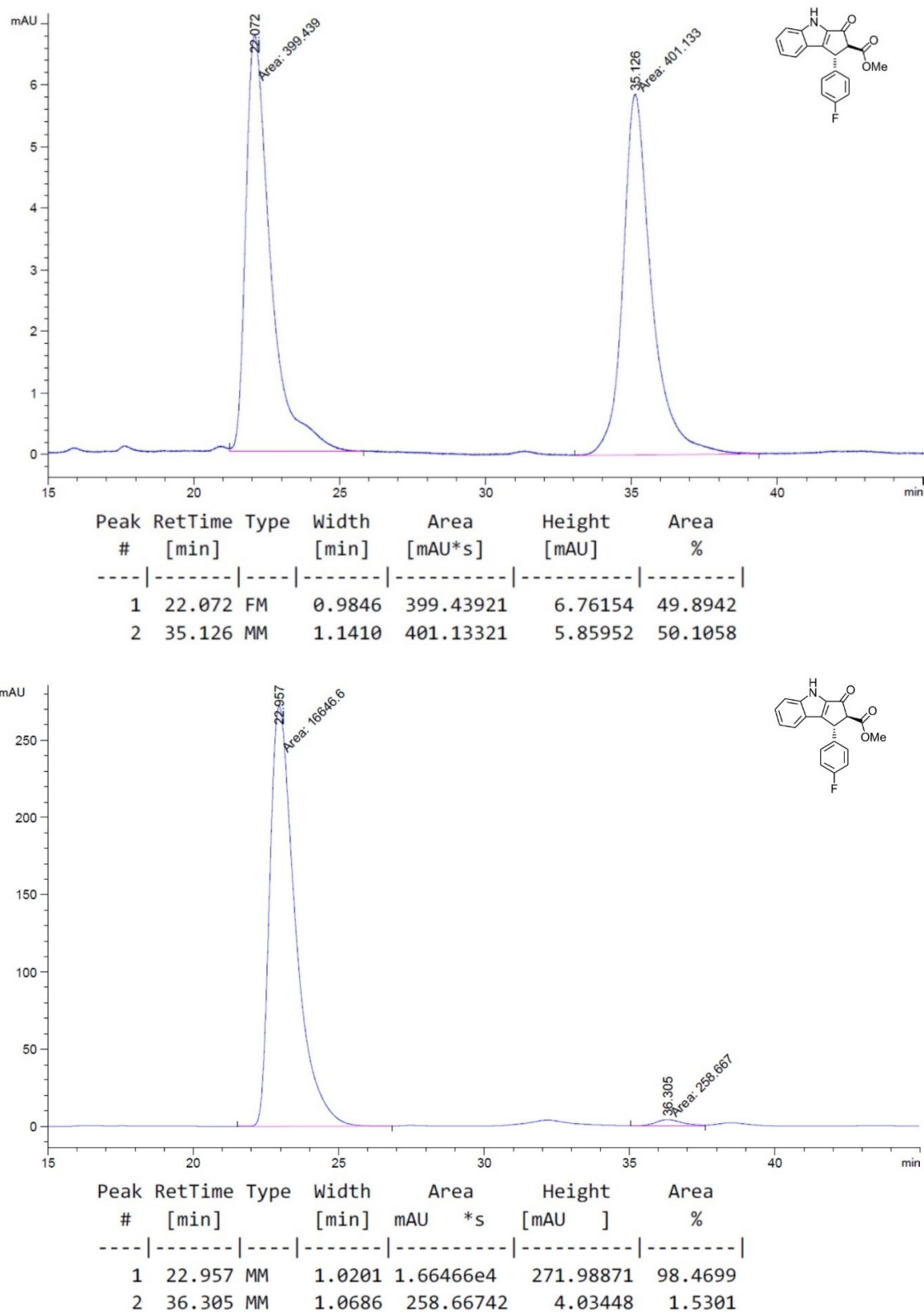
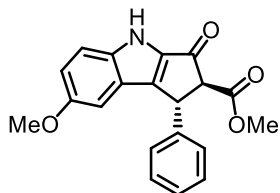


Figure 57: Chiral HPLC traces of **N4j** (racemic top, enriched bottom). HPLC conditions: Daicel Chiralpak AD-H column (250 × 4.6 mm), solvent A: *n*-hexane, solvent B: 2-propanol, isocratic ratio A/B 90:10, flow rate: 0.6 mL·min⁻¹, column temperature: 25 °C, UV absorption detected at λ = 254 nm.

Methyl (1*R*,2*S*)-6-methoxy-3-oxo-1-phenyl-1,2,3,4-tetrahydrocyclopenta[*b*]indole-2-carboxylate (N4k)



Synthetic steps were carried out by THOMAS CRUCHTER. According to procedure G, α -unsaturated β -ketoester **N3k** (28.3 mg, 84.4 μ mol, 1.00 eq.) and catalyst **A-C5f** (1.6 mg, 1.7 μ mol, 2.0 mol%) in HFIP (280 μ L) were used; reaction time: 12 h (excluding time for Al_2O_3 -induced equilibration). Desired NAZAROV product **N4k** was obtained after column chromatography (*n*-hexane/EtOAc 3:1) as a colorless solid (21.2 mg, 63.2 μ mol, 75%). D.r. value determined by ^1H NMR analysis of the crude product: *trans/cis* 4.5:1 *before* and 13:1 *after* Al_2O_3 -induced equilibration. Enantiomeric excess of the *trans* diastereomer of the isolated product determined by chiral HPLC analysis: ee = 97% (OD-H column, λ = 254 nm, *n*-hexane/2-propanol 90:10, 0.6 mL/min, column temp.: 25 $^\circ\text{C}$, t_R (major) = 28.9 min, t_R (minor) = 40.9 min), $[\alpha]_{\text{D}}^{27} = -68$ (*c* 0.7, CH_2Cl_2).

^1H NMR (300 MHz, CDCl_3): δ = 9.43 (br s, 1H, NH), 7.43 (d, J = 9.1 Hz, 1H, H_{Aliph}), 7.35–7.22 (m, 5H, H_{Ar}), 7.08 (dd, J = 9.1, 2.4 Hz, 1H, H_{Ar}), 6.67 (d, J = 2.4 Hz, 1H, H_{Ar}), 5.05 (d, J = 2.8 Hz, 1H, H_{Aliph}), 3.89 (d, J = 2.8 Hz, 1H, H_{Aliph}), 3.86 (s, 3H, OCH_3), 3.70 (s, 3H, OCH_3) ppm.

^{13}C NMR (75 MHz, CDCl_3): δ = 186.7, 169.7, 154.9, 147.0, 140.9, 140.0, 137.5, 129.1 (2C), 127.6, 127.5 (2C), 123.3, 119.8, 114.8, 102.2, 67.9, 55.8, 53.0, 44.1 ppm.

IR (ATR): $\tilde{\nu}$ = 3263 (br w), 2953 (w), 2924 (w), 2846 (w), 1734 (m), 1675 (s), 1536 (w), 1493 (m), 1441 (w), 1370 (w), 1305 (w), 1260 (w), 1213 (m), 1163 (w), 1098 (w), 1064 (w), 1023 (w), 910 (w), 810 (w), 730 (m), 701 (w), 634 (w), 526 (w), 432 (w) cm^{-1} .

HR-MS (ESI): m/z calcd. for $\text{C}_{20}\text{H}_{17}\text{N}_1\text{O}_4\text{Na}_1$ $[\text{M}+\text{Na}]^+$: 358.1050, found 358.1050.

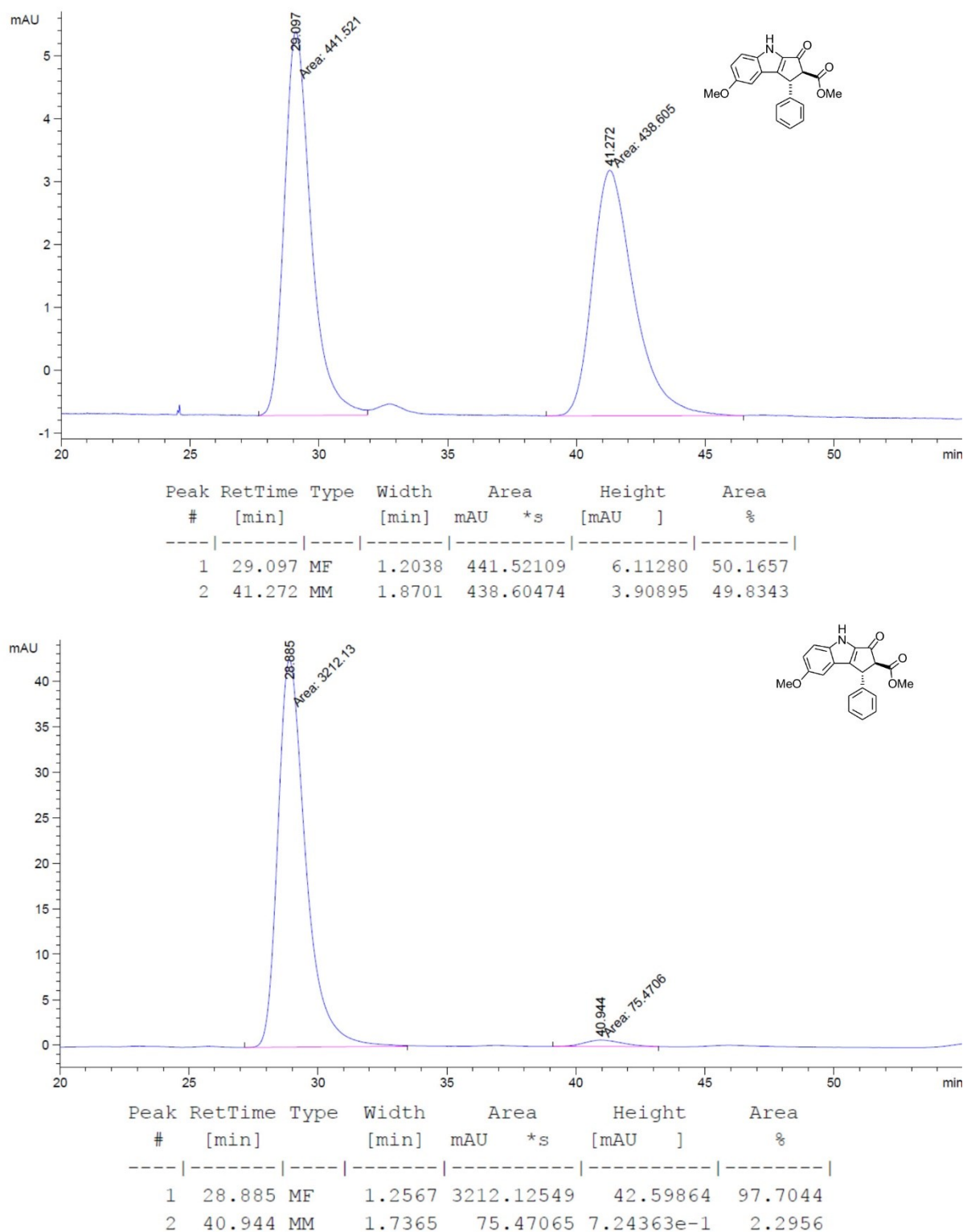
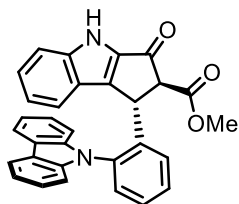


Figure 58: Chiral HPLC traces of **N4k** (racemic top, enriched bottom). HPLC conditions: Daicel Chiralpak OD-H column (250 × 4.6 mm), solvent A: *n*-hexane, solvent B: 2-propanol, isocratic ratio A/B 90:10, flow rate: 0.6 mL·min⁻¹, column temperature: 25 °C, UV absorption detected at λ = 254 nm.

Methyl (1*R*,2*S*)-2-(carbazol-9-yl)phenyl)-3-oxo-1,2,3,4-tetrahydrocyclopenta[*b*]indole-2-carboxylate (N4l)



Synthetic steps were carried out by THOMAS CRUCHTER. According to procedure G, α -unsaturated β -ketoester **N3l** (39.5 mg, 83.9 μ mol, 1.00 eq.) and catalyst **A-C5f** (1.6 mg, 1.7 μ mol, 2.0 mol%) in HFIP (280 μ L) were used; reaction time: 48 h (excluding time for Al₂O₃-induced equilibration).

Desired NAZAROV product **N4l** was obtained after column chromatography (*n*-hexane/EtOAc 3:1) as a colorless solid (36.6 mg, 77.8 μ mol, 93%). D.r. value determined by ¹H NMR analysis of the crude product: *trans/cis* 2.5:1 *before* and 28:1 *after* Al₂O₃-induced equilibration. Enantiomeric excess of the *trans* diastereomer of the isolated product determined by chiral HPLC analysis: 95% ee (AD-H column, λ = 254 nm, *n*-hexane/2-propanol 90:10, 0.6 mL/min, column temp.: 25 °C, *t*_R (major) = 21.0 min, *t*_R (minor) = 34.8 min), [α]_D²⁷ = −500 (*c* 0.2, CH₂Cl₂).

¹H NMR (300 MHz, CDCl₃): δ = 9.30 (br s, 1H, *NH*), 8.24–8.12 (m, 2H, *H*_{Ar}), 7.55–7.28 (m, 12H, *H*_{Ar}), 7.20–7.09 (m, 2H, *H*_{Ar}), 7.08–7.03 (m, 1H, *H*_{Ar}), 4.85 (d, *J* = 2.3 Hz, 1H, *H*_{Aliph}), 3.67 (d, *J* = 2.3 Hz, 1H, *H*_{Aliph}), 2.90 (s, 3H, *CH*₃) ppm.

¹³C NMR (75 MHz, CDCl₃): δ = 186.5, 167.6, 147.6, 144.7, 142.3, 141.3, 141.0, 137.4, 136.0, 130.3, 129.9, 129.4, 128.8, 128.2, 126.4, 126.4, 123.7, 123.4, 122.7, 122.1, 121.4, 120.8, 120.4, 120.2, 120.0, 114.0, 109.7, 109.4, 68.0, 52.2, 38.9 ppm.

IR (ATR): $\tilde{\nu}$ = 3327 (br m), 3057 (w), 2955 (w), 2923 (w), 2853 (w), 1737 (m), 1688 (s), 1621 (w), 1596 (w), 1543 (w), 1486 (w), 1451 (m), 1369 (w), 1316 (w), 1257 (m), 1233 (w), 1195 (w), 1155 (w), 1096 (w), 1051 (w), 1014 (w), 929 (w), 845 (w), 807 (w), 748 (s), 626 (w), 565 (w), 526 (w), 500 (w), 424 (w) cm^{−1}.

HR-MS (ESI): *m/z* calcd. for C₃₁H₂₂N₂O₃Na₁ [*M*+Na]⁺: 493.1523, found 493.1528.

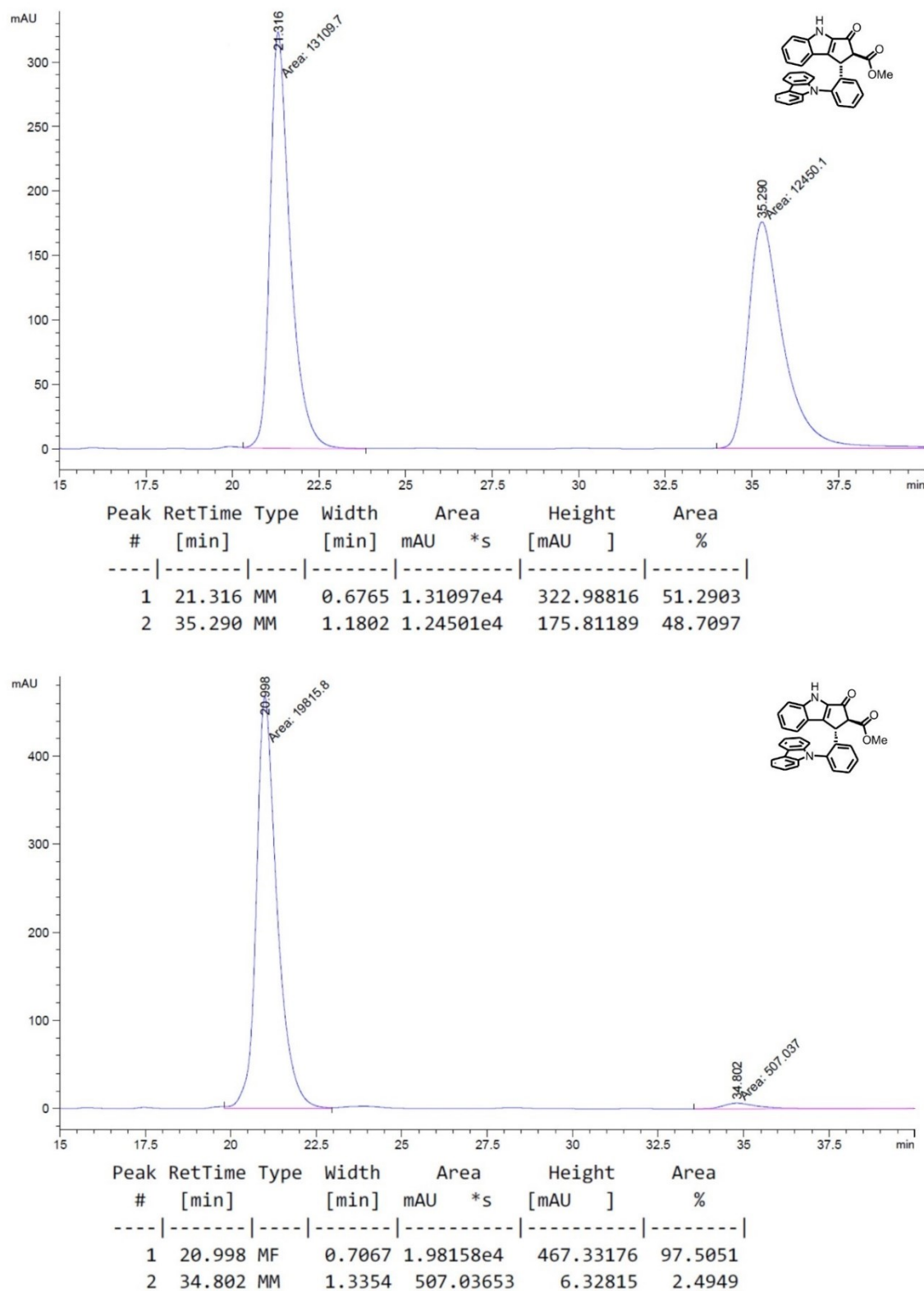
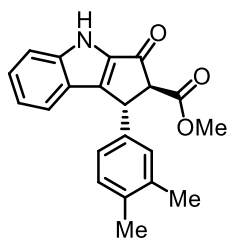


Figure 59: Chiral HPLC traces of **N4I** (racemic top, enriched bottom). HPLC conditions: Daicel Chiralpak AD-H column (250 × 4.6 mm), solvent A: *n*-hexane, solvent B: 2-propanol, isocratic ratio A/B 90:10, flow rate: 0.6 mL·min⁻¹, column temperature: 25 °C, UV absorption detected at λ = 254 nm.

Methyl (1*R*,2*S*)-1-(3,4-dimethylphenyl)-3-oxo-1,2,3,4-tetrahydrocyclopenta[*b*]indole-2-carboxylate (N4m)



Synthetic steps were carried out by THOMAS CRUCHTER. According to procedure G, α -unsaturated β -ketoester **N3m** (28.2 mg, 84.6 μ mol, 1.00 eq.) and catalyst **A-C5f** (1.6 mg, 1.7 μ mol, 2.0 mol%) in HFIP (280 μ L) were used; reaction time: 15 h (excluding time for Al₂O₃-induced equilibration). Desired NAZAROV product **N4m** was obtained after column chromatography (*n*-hexane/EtOAc 3:1) as a colorless solid (23.5 mg, 70.5 μ mol, 83%). D.r. value determined by ¹H NMR analysis of the crude product: *trans/cis* 2.2:1 *before* and 16:1 *after* Al₂O₃-induced equilibration. Enantiomeric excess of the *trans* diastereomer of the isolated product determined by chiral HPLC analysis: 95% ee (AS-H column, λ = 254 nm, *n*-hexane/2-propanol 90:10, 0.6 mL/min, column temp.: 25 °C, *t_R* (major) = 20.4 min, *t_R* (minor) = 34.4 min), [α]_D²⁷ = −117 (*c* 1.0, CH₂Cl₂).

¹H NMR (300 MHz, CDCl₃): δ = 9.50 (br s, 1H, *NH*), 7.54–7.51 (m, 1H, *H_{Ar}*), 7.42–7.38 (m, 1H, *H_{Ar}*), 7.38–7.35 (m, 1H, *H_{Ar}*), 7.10–7.06 (m, 2H, *H_{Ar}*), 7.03–7.00 (m, 1H, *H_{Ar}*), 6.98–6.94 (m, 1H, *H_{Ar}*), 5.00 (d, *J* = 2.8 Hz, 1H, *H_{Aliph}*), 3.92 (d, *J* = 2.8 Hz, 1H, *H_{Aliph}*), 3.85 (s, 3H, OCH₃), 2.24 (s, 3H, CH₃), 2.22 (s, 3H, CH₃) ppm.

¹³C NMR (75 MHz, CDCl₃): δ = 187.3, 169.7, 148.6, 144.6, 138.2, 137.3, 137.0, 135.9, 130.3, 128.7, 128.2, 124.8, 123.0, 122.5, 121.2, 113.9, 68.0, 52.9, 43.9, 20.0, 19.6 ppm.

IR (ATR): $\tilde{\nu}$ = 3254 (br w), 2925 (w), 1736 (m), 1677 (s), 1619 (w), 1571 (w), 1540 (w), 1505 (w), 1480 (w), 1438 (w), 1372 (w), 1320 (w), 1250 (w), 1157 (w), 1099 (w), 1062 (w), 1017 (w), 910 (w), 821 (w), 741 (w), 622 (w), 577 (w), 540 (w), 493 (w), 433 (w) cm^{−1}.

HR-MS (ESI): *m/z* calcd. for C₂₁H₁₉N₁O₃Na₁ [M+Na]⁺: 356.1257, found 356.1257.

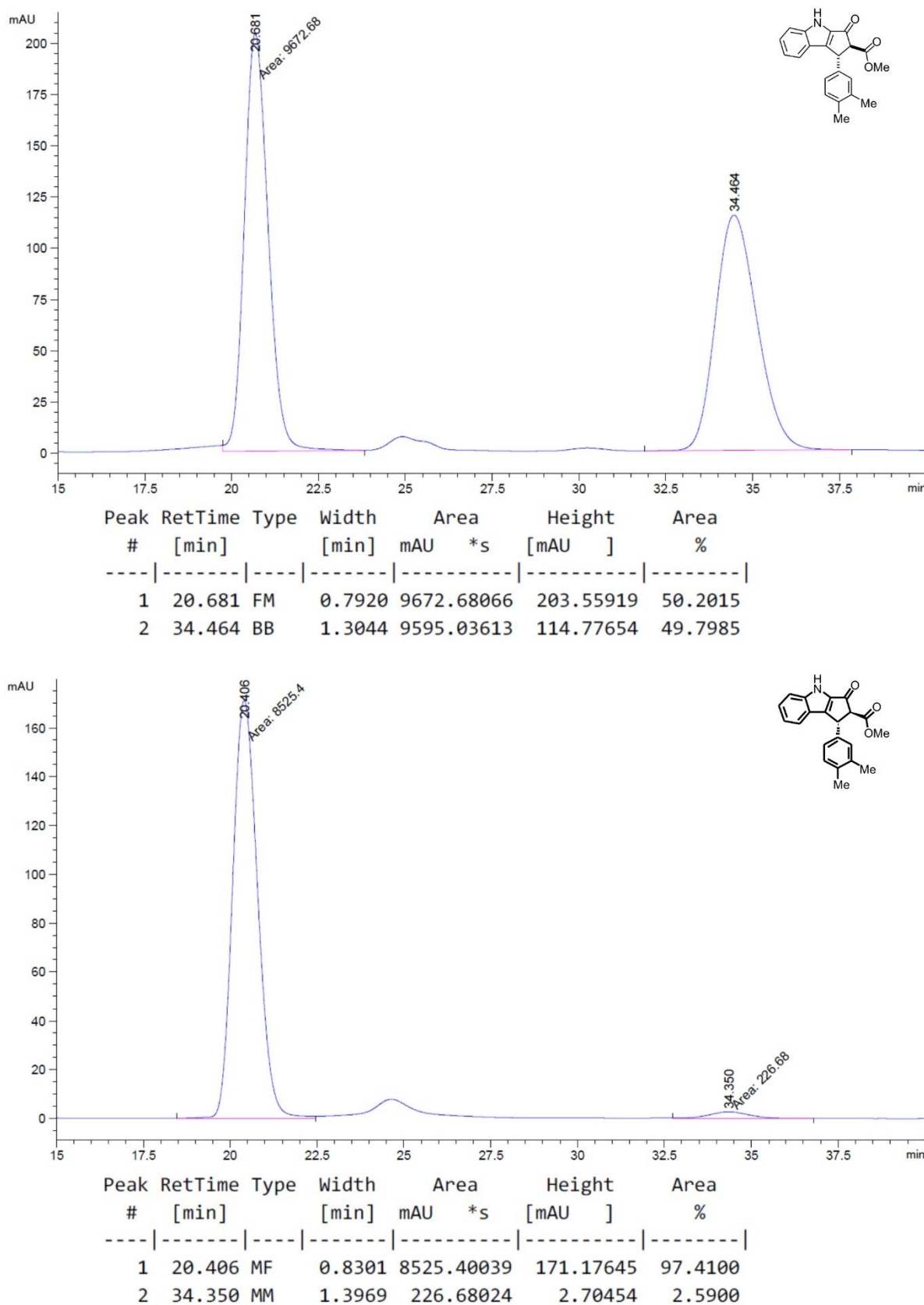
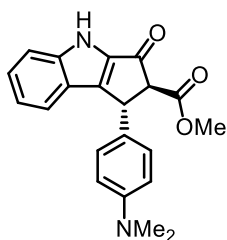


Figure 60: Chiral HPLC traces of **N4m** (racemic top, enriched bottom). HPLC conditions: Daicel Chiralpak AS-H column (250 × 4.6 mm), solvent A: *n*-hexane, solvent B: 2-propanol, isocratic ratio A/B 90:10, flow rate: 0.6 mL·min⁻¹, column temperature: 25 °C, UV absorption detected at λ = 254 nm.

Methyl (1*R*,2*S*)-1-(4-(dimethylamino)phenyl)-3-oxo-1,2,3,4-tetrahydrocyclopenta[*b*]indole-2-carboxylate (N4n)



Synthetic steps were carried out by VLADIMIR LARIONOV. According to procedure G, α -unsaturated β -ketoester **N3n** (29.6 mg, 85.0 μ mol, 1.00 eq.) and catalyst **A-C5f** (1.6 mg, 1.7 μ mol, 2.0 mol%) in HFIP (280 μ L); reaction time: 24 h (excluding time for Al_2O_3 -induced equilibration).

Desired NAZAROV product **N4n** was obtained after column chromatography (*n*-hexane/EtOAc 3:1) as a colorless solid (24.2 mg, 69.5 μ mol, 82%). D.r. value determined by ^1H NMR analysis of the crude product: *trans/cis* 9.4:1 *before* and 12:1 *after* Al_2O_3 -induced equilibration. Enantiomeric excess of the *trans* diastereomer of the isolated product determined by chiral HPLC analysis: 60% ee (AD-H column, $\lambda = 254$ nm, *n*-hexane/2-propanol 90:10, 0.6 mL/min, column temp.: 25 $^\circ\text{C}$, t_R (major) = 42.9 min, t_R (minor) = 70.5 min), $[\alpha]_D^{27} = -93$ (*c* 1.0, CH_2Cl_2).

^1H NMR (300 MHz, CDCl_3): δ = 9.21 (br s, 1H, NH), 7.52–7.47 (m, 1H, H_{Ar}), 7.42–7.35 (m, 2H, H_{Ar}), 7.15–7.05 (m, 3H, H_{Ar}), 6.78–6.67 (m, 2H, H_{Ar}), 4.89 (d, $J = 2.8$ Hz, 1H, H_{Aliph}), 3.88 (d, $J = 2.8$ Hz, 1H, H_{Aliph}), 3.84 (s, 3H, OCH_3), (s, 6H, $\text{N}(\text{CH}_3)_2$) ppm.

^{13}C NMR (75 MHz, CDCl_3): δ = 187.2, 169.8, 149.8 (br), 148.8, 144.5, 137.1, 128.3 (2C), 128.1, 123.2, 122.6, 121.7, 113.8, 113.4 (br), 68.2, 52.8, 43.6, 40.9 ppm.

IR (ATR): $\tilde{\nu}$ = 3258 (br w), 2948 (w), 2803 (w), 1735 (m), 1681 (s), 1616 (w), 1522 (w), 1480 (w), 1440 (w), 1322 (w), 1249 (w), 1158 (w), 1100 (w), 1061 (w), 1015 (w), 914 (w), 822 (w), 747 (w), 611 (w), 529 (w), 430 (w) cm^{-1} .

HR-MS (ESI): m/z calcd. for $\text{C}_{21}\text{H}_{21}\text{N}_1\text{O}_3$ $[\text{M}+\text{H}]^+$: 349.1547, found 349.1549.

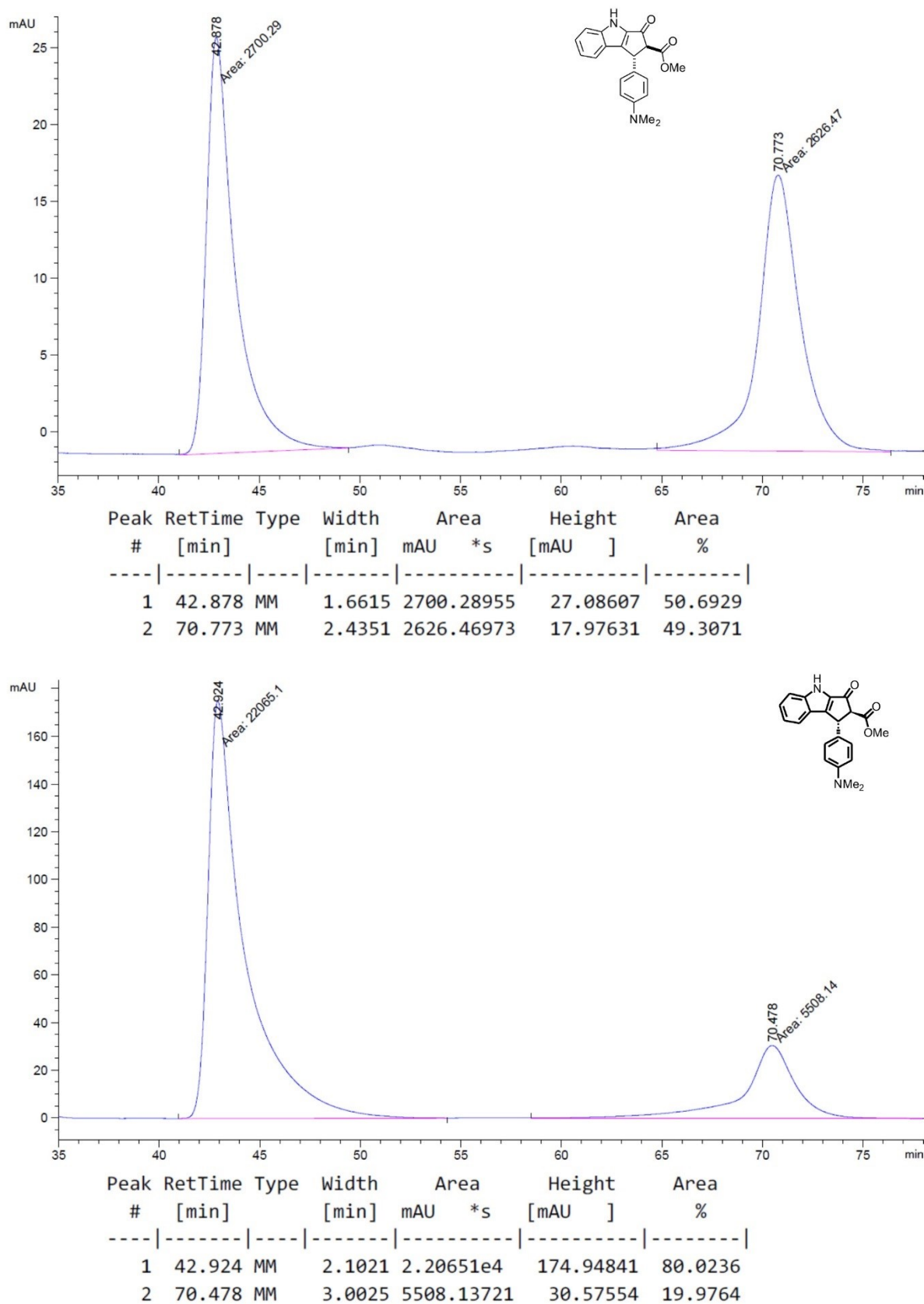
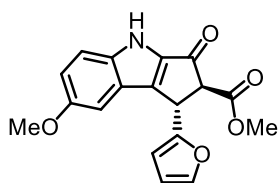


Figure 61: Chiral HPLC traces of **N4n** (racemic top, enriched bottom). HPLC conditions: Daicel Chiralpak AD-H column (250 × 4.6 mm), solvent A: *n*-hexane, solvent B: 2-propanol, isocratic ratio A/B 90:10, flow rate: 0.6 mL·min⁻¹, column temperature: 25 °C, UV absorption detected at $\lambda = 254$ nm.

Methyl (1*S*,2*S*)-1-(furan-2-yl)-6-methoxy-3-oxo-1,2,3,4-tetrahydrocyclopenta[*b*]indole-2-carboxylate (N4o)

Note: Switching from R → S is not caused by actual inversion of the stereocenter but by higher priority of the furan ring according to CIP rules.



Synthetic steps were carried out by VLADIMIR LARIONOV. According to procedure G, α -unsaturated β -ketoester **N3o** (27.2 mg, 83.5 μ mol, 1.00 eq.) and catalyst **A-C5f** (3.2 mg, 3.4 μ mol, 4.0 mol%) in HFIP (280 μ L) were used; reaction time: 96 h (excluding time for Al_2O_3 -induced equilibration). Desired NAZAROV product **N4o** was obtained after column chromatography (*n*-hexane/EtOAc 3:1) as a colorless solid (12.5 mg, 38.4 μ mol, 46%). D.r. value determined by ^1H NMR analysis of the crude product: *trans/cis* 10:1 *before* and 20:1 *after* Al_2O_3 -induced equilibration. Enantiomeric excess of the *trans* diastereomer of the isolated product determined by chiral HPLC analysis: 50% ee (AD-H column, $\lambda = 254$ nm, *n*-hexane/2-propanol 90:10, 0.7 mL/min, column temp.: 25 °C, t_R (major) = 19.0 min, t_R (minor) = 22.5 min).

^1H NMR (300 MHz, CDCl_3): δ = 9.05 (br s, 1H, NH), 7.43–7.36 (m, 2H, H_{Ar}), 7.10 (dd, $J = 9.1, 2.5$ Hz, 1H, H_{Ar}), 7.10 (d, $J = 2.5$ Hz, 1H, H_{Ar}), 6.32 (dd, $J = 3.0, 2.0$ Hz, 1H, H_{Ar}), 6.17 (d, $J = 3.1$ Hz, 1H, H_{Ar}), 5.12 (d, $J = 2.7$ Hz, 1H, H_{Aliph}), 4.09 (d, $J = 2.7$ Hz, 1H, H_{Aliph}), 3.86 (s, 3H, CH_3), 3.81 (s, 3H, CH_3) ppm.

^{13}C NMR (75 MHz, CDCl_3): δ = 185.7, 169.3, 155.1, 153.4, 144.5, 142.6, 139.8, 137.0, 123.3, 119.9, 114.7, 110.5, 106.5, 102.2, 64.3, 55.9, 53.1, 37.6 ppm.

IR (ATR): $\tilde{\nu}$ = 3317 (br w), 2954 (w), 2923 (w), 2852 (w), 1737 (m), 1686 (s), 1537 (w), 1495 (w), 1441 (w), 1371 (w), 1300 (w), 1257 (w), 1213 (m), 1172 (w), 1095 (w), 1021 (w), 923 (w), 810 (w), 742 (w), 706 (w), 675 (w), 574 (w), 541 (w), 433 (w) cm^{-1} .

HR-MS (ESI): m/z calcd. for $\text{C}_{18}\text{H}_{15}\text{N}_1\text{O}_5\text{Na}_1$ $[\text{M}+\text{Na}]^+$: 348.0842, found 348.0841.

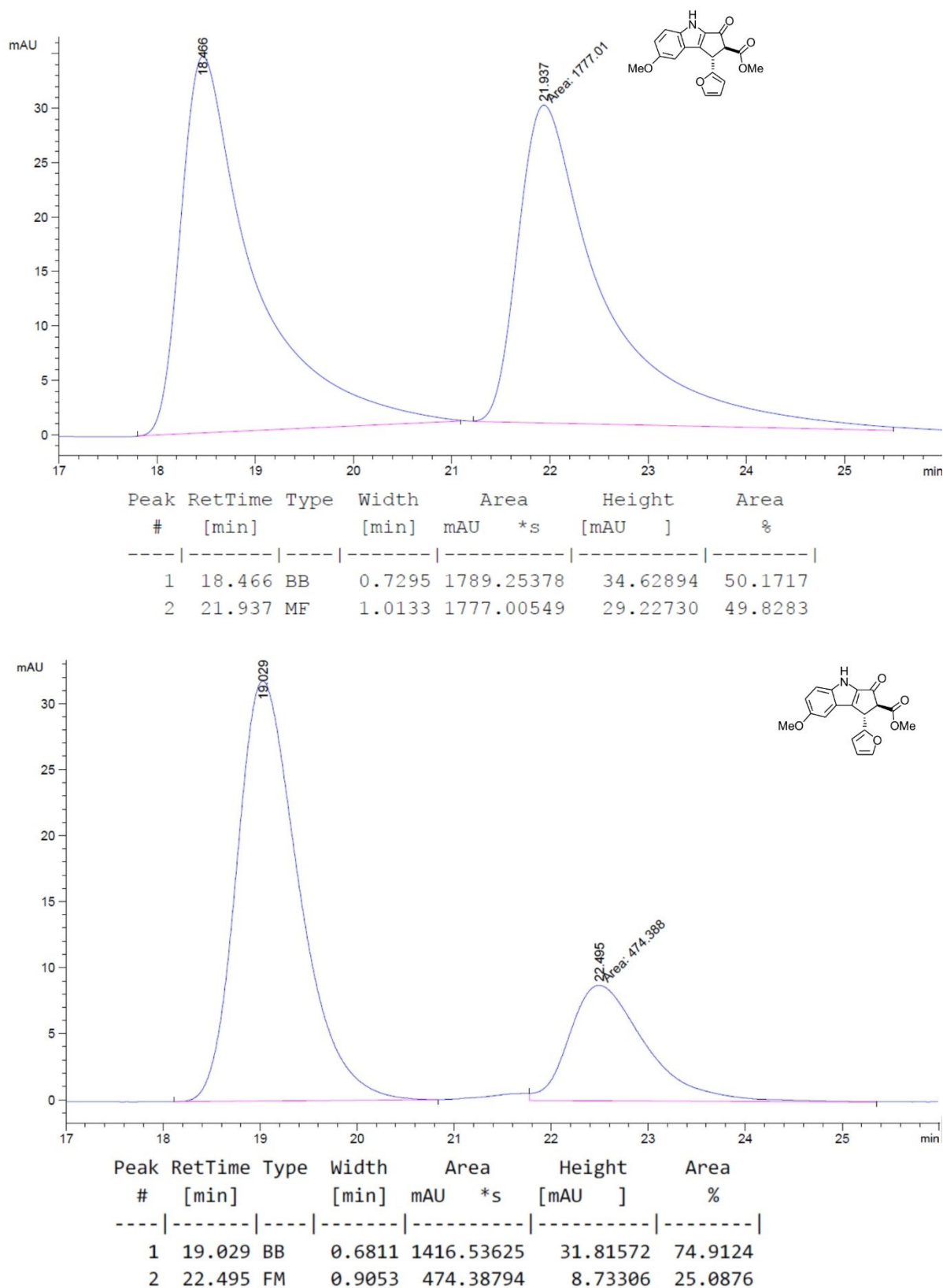


Figure 62: Chiral HPLC traces of **N4o** (racemic top, enriched bottom). HPLC conditions: Daicel Chiralpak AD-H column (250 × 4.6 mm), solvent A: *n*-hexane, solvent B: 2-propanol, isocratic ratio A/B 90:10, flow rate: 0.7 mL·min⁻¹, column temperature: 25 °C, UV absorption detected at $\lambda = 254$ nm.

4 Appendix

4.1 Representative ^1H NMR and ^{13}C NMR Spectra

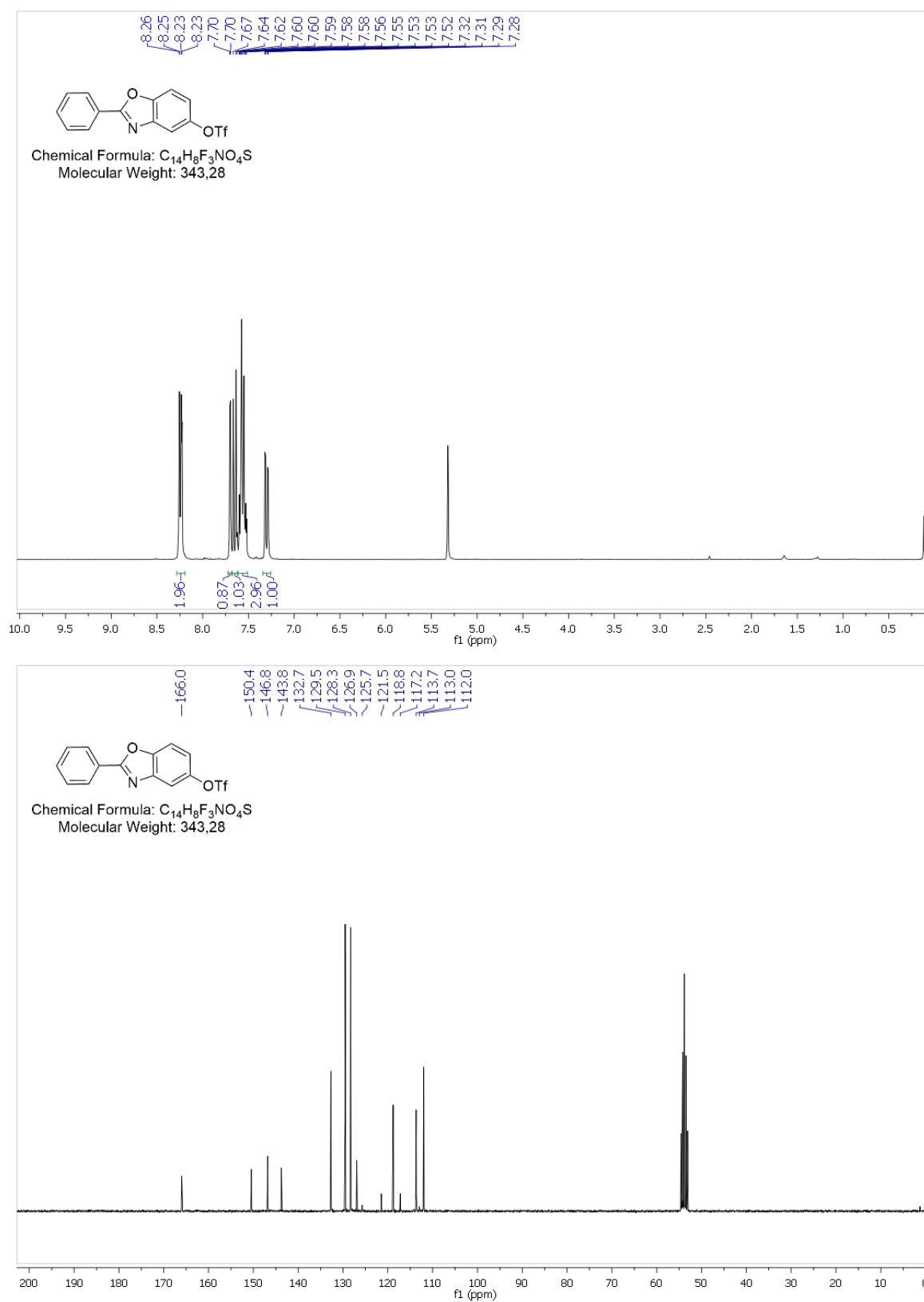


Figure 63: ^1H NMR spectra of compounds **L1c** in CD_2Cl_2 recorded with a *Bruker Avance III* at 300 MHz (top) and ^{13}C NMR spectra of compounds **L1c** in CD_2Cl_2 recorded with a *Bruker Avance III* at 75 MHz (bottom).

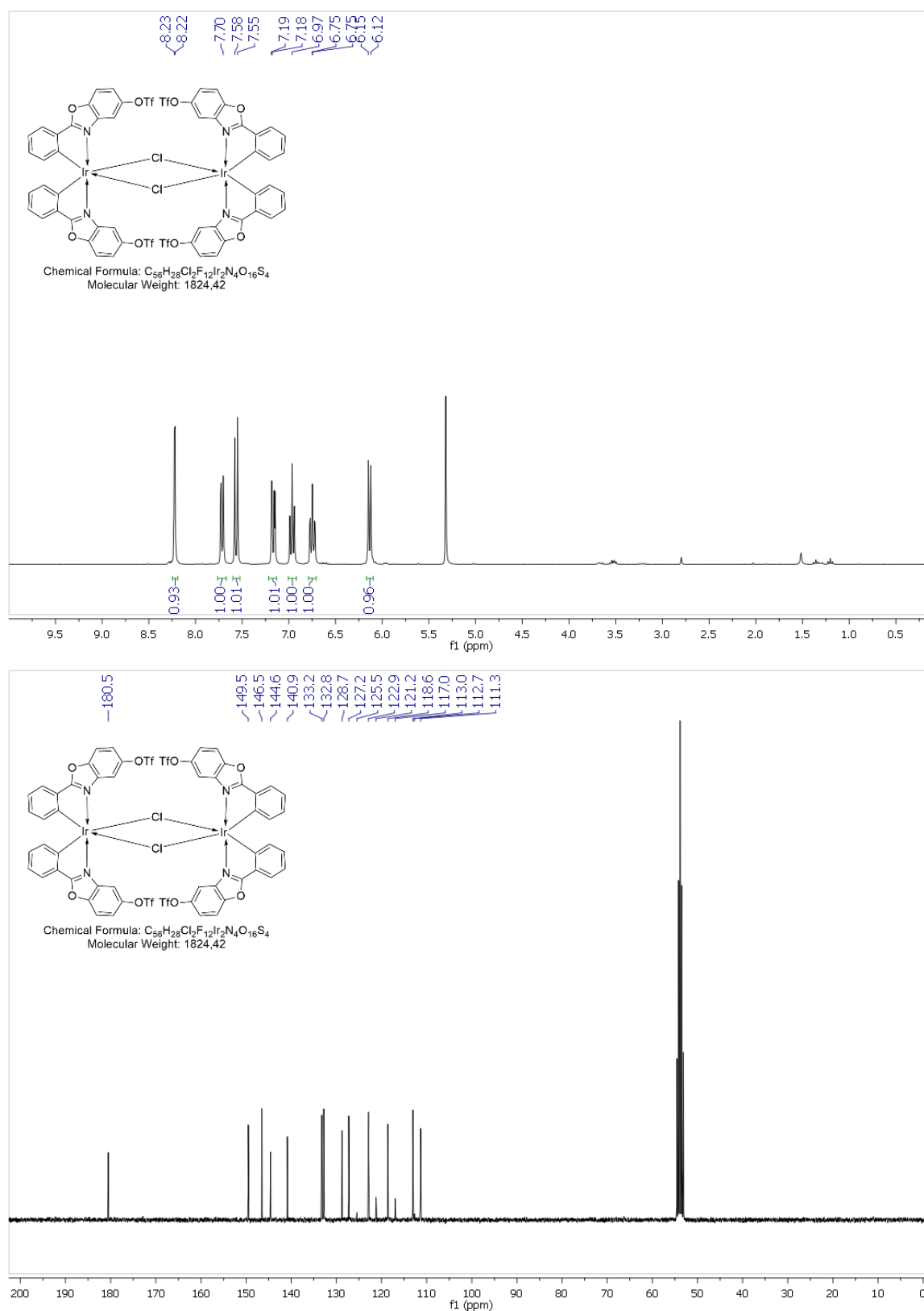


Figure 64: ¹H NMR spectra of compounds *rac*-C1a in CD₂Cl₂ recorded with a Bruker Avance III at 300 MHz (top) and ¹³C NMR spectra of compounds *rac*-C1a in CD₂Cl₂ recorded with a Bruker Avance III at 75 MHz (bottom).

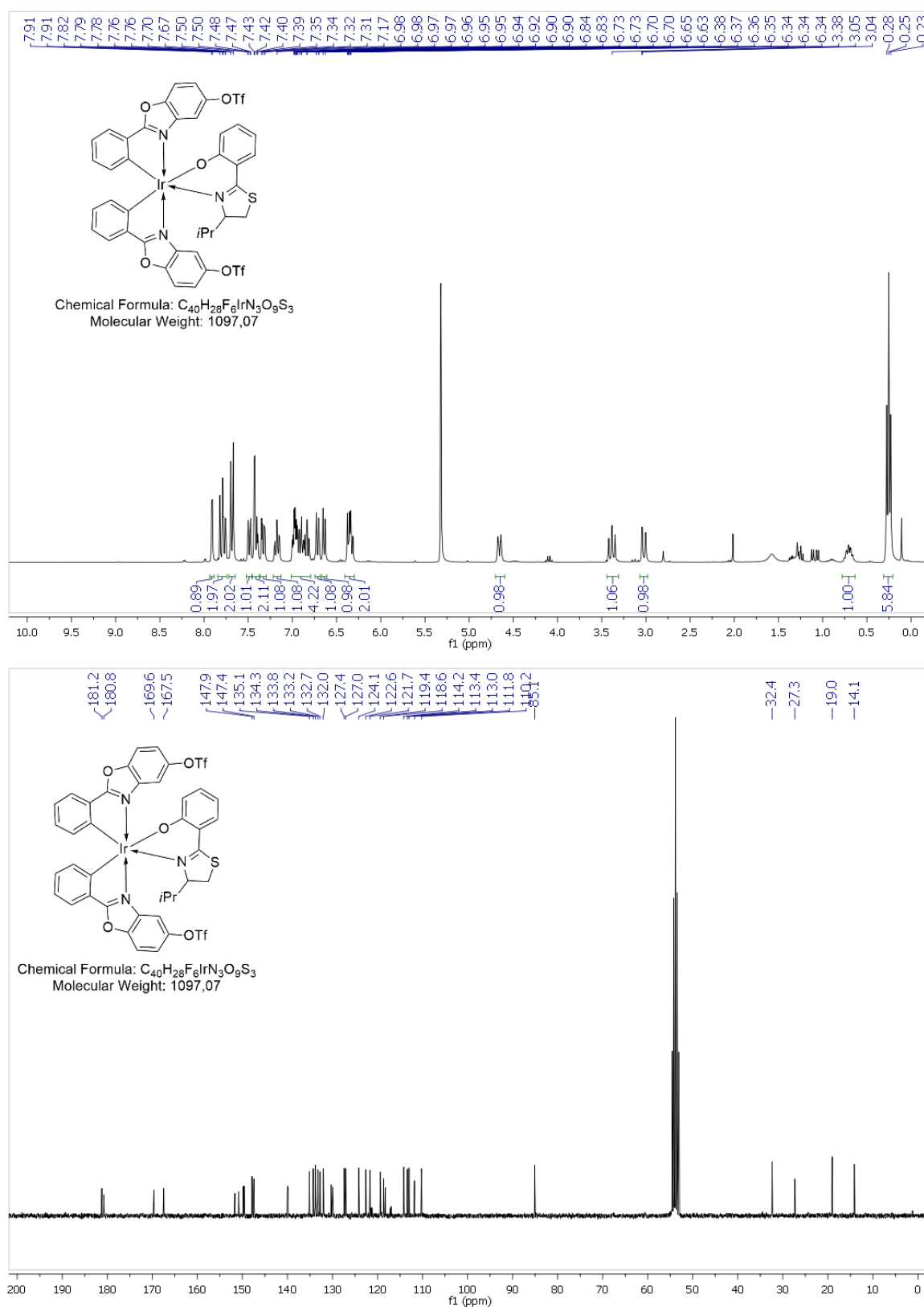


Figure 65: ¹H NMR spectra of compounds **A-(S)-C2a** in CD₂Cl₂ recorded with a Bruker Avance III at 300 MHz (top) and ¹³C NMR spectra of compounds **A-(S)-C2a** in CD₂Cl₂ recorded with a Bruker Avance III at 75 MHz (bottom).

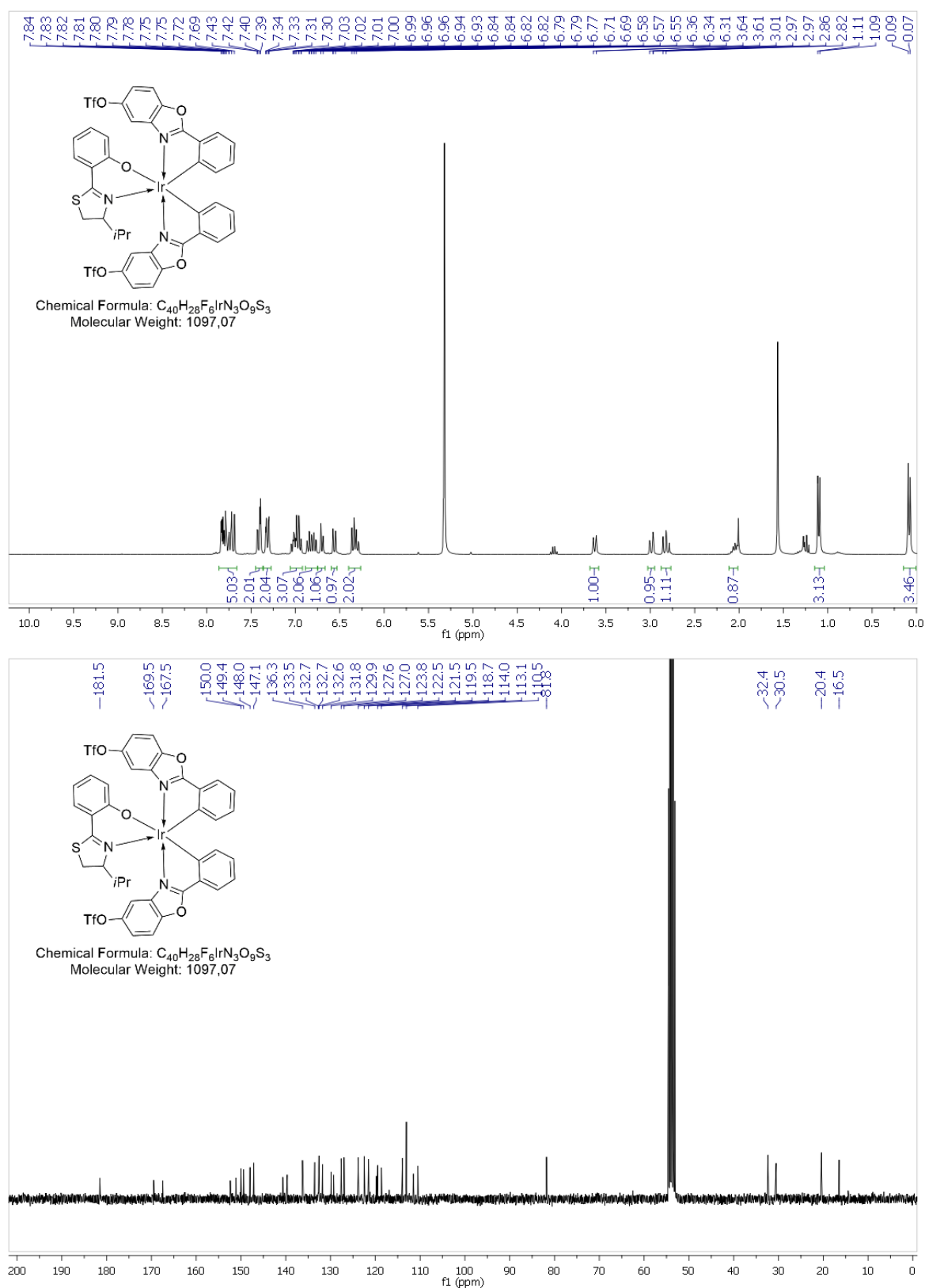


Figure 66: ¹H NMR spectra of compounds Δ -(S)-C2a in CD₂Cl₂ recorded with a Bruker Avance III at 300 MHz (top) and ¹³C NMR spectra of compounds Δ -(S)-C2a in CD₂Cl₂ recorded with a Bruker Avance III at 75 MHz (bottom).

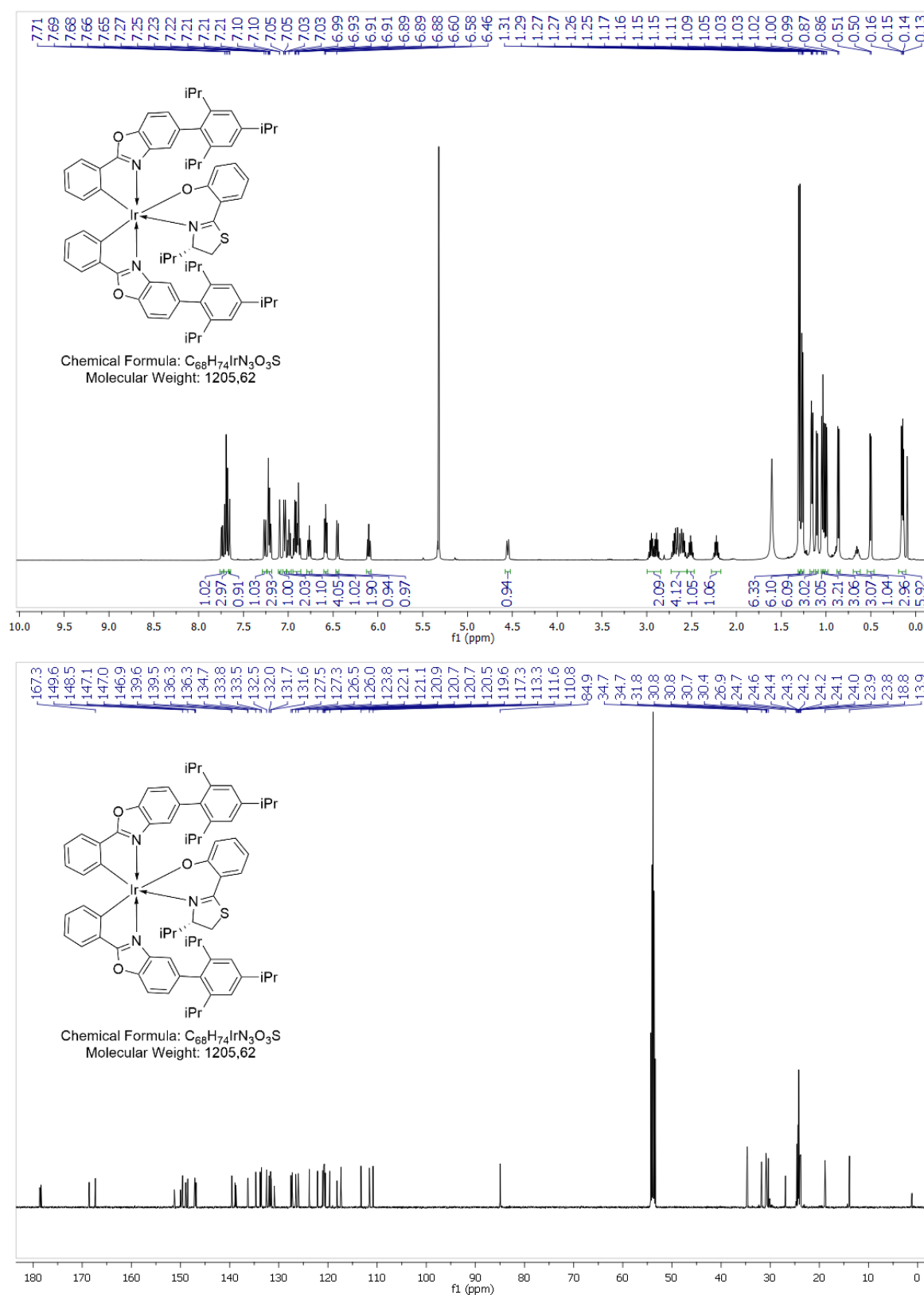


Figure 67: ¹H NMR spectra of compounds **A-(S)-C3c** in CD₂Cl₂ recorded with a *Bruker Avance III* at 500 MHz (top) and ¹³C NMR spectra of compounds **A-(S)-C3c** in CD₂Cl₂ recorded with a *Bruker Avance III* at 125 MHz (bottom).

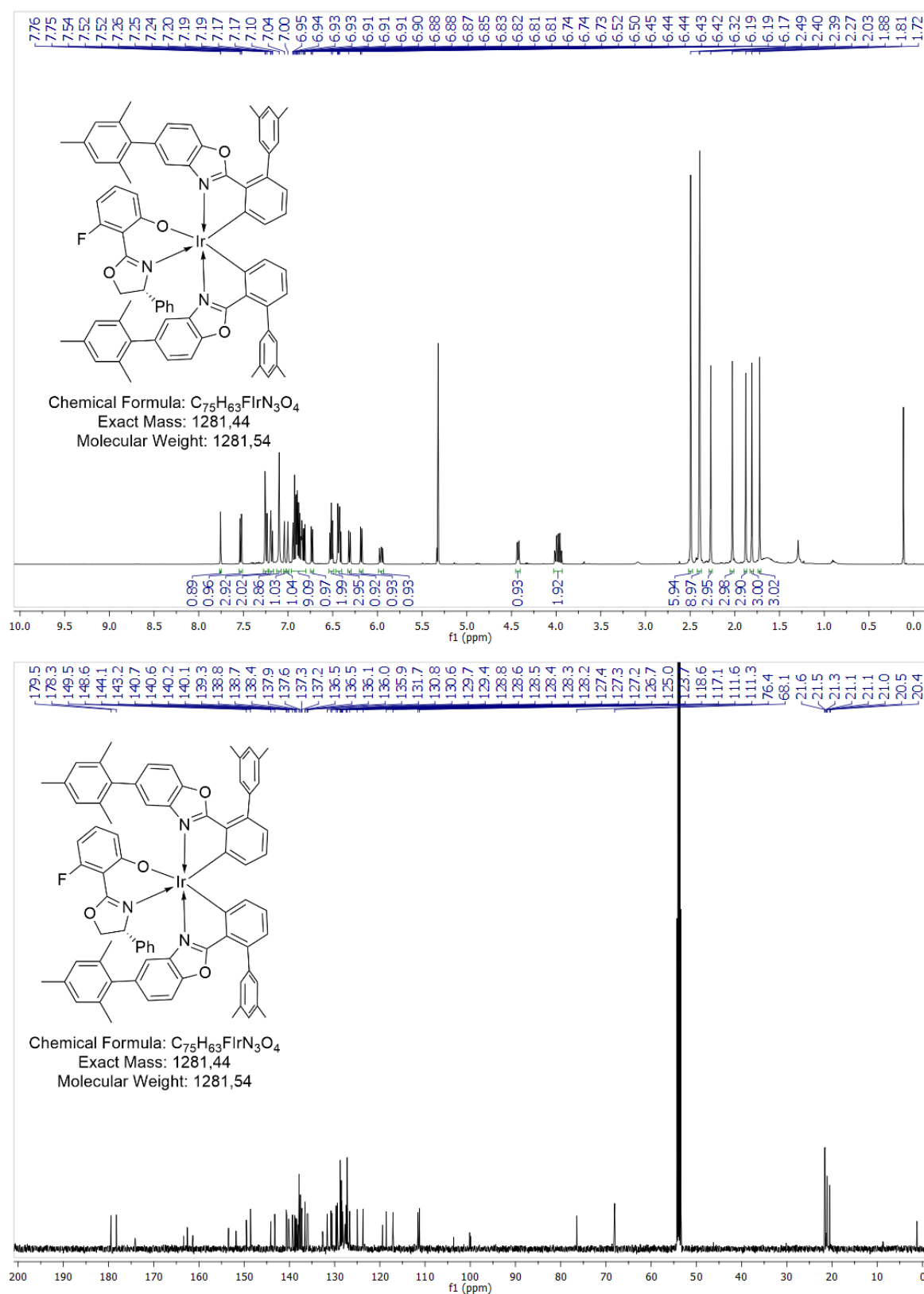


Figure 68: ¹H NMR spectra of compounds **Δ-(S)-C3i** in CD₂Cl₂ recorded with a *Bruker Avance III* at 500 MHz (top) and ¹³C NMR spectra of compounds **Δ-(S)-C3i** in CD₂Cl₂ recorded with a *Bruker Avance III* at 125 MHz (bottom).

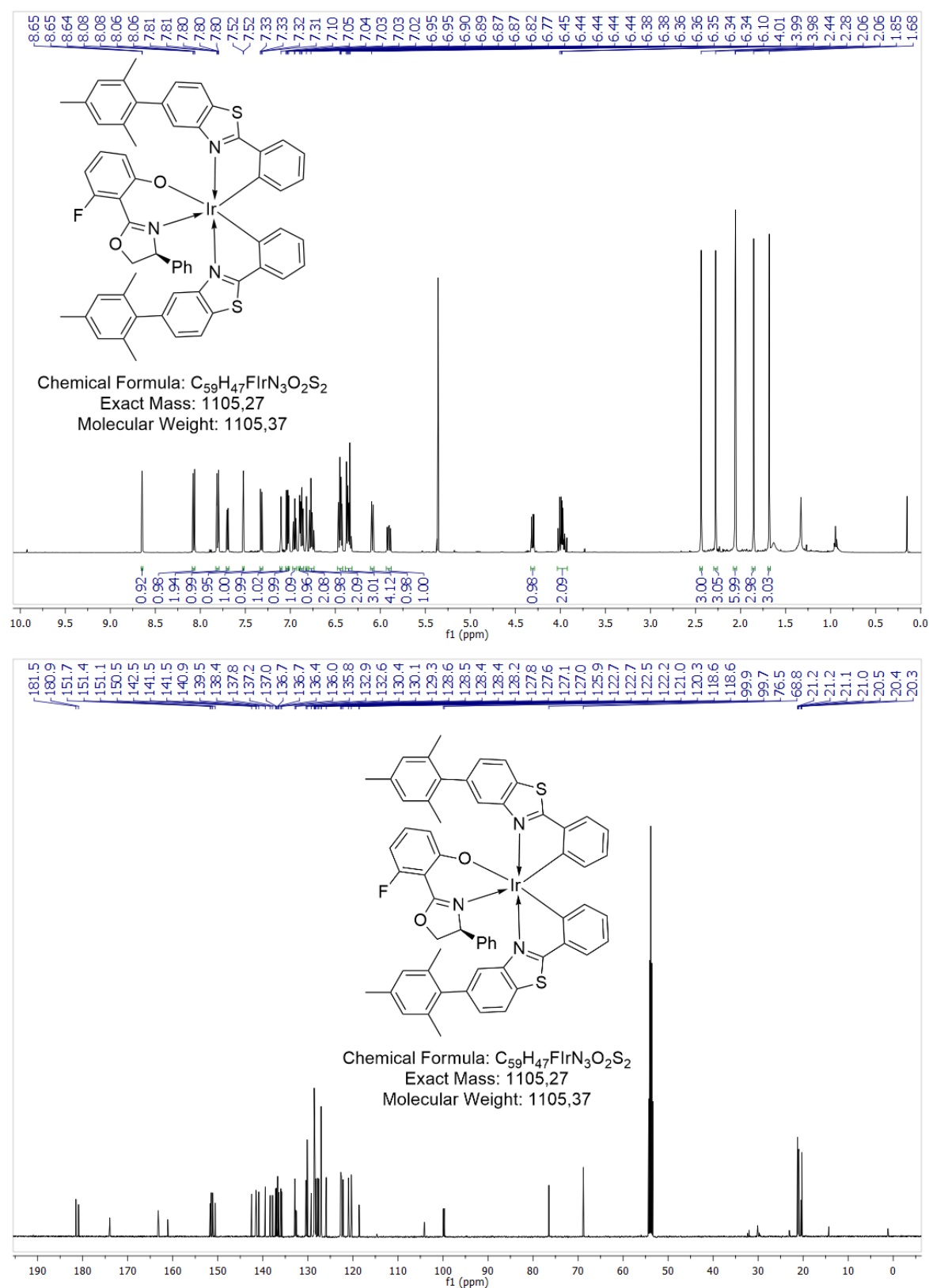


Figure 69: ¹H NMR spectra of compounds **Δ-(S)-C3m** in CD₂Cl₂ recorded with a *Bruker Avance III* at 500 MHz (top) and ¹³C NMR spectra of compounds **Δ-(S)-C3m** in CD₂Cl₂ recorded with a *Bruker Avance III* at 125 MHz (bottom).

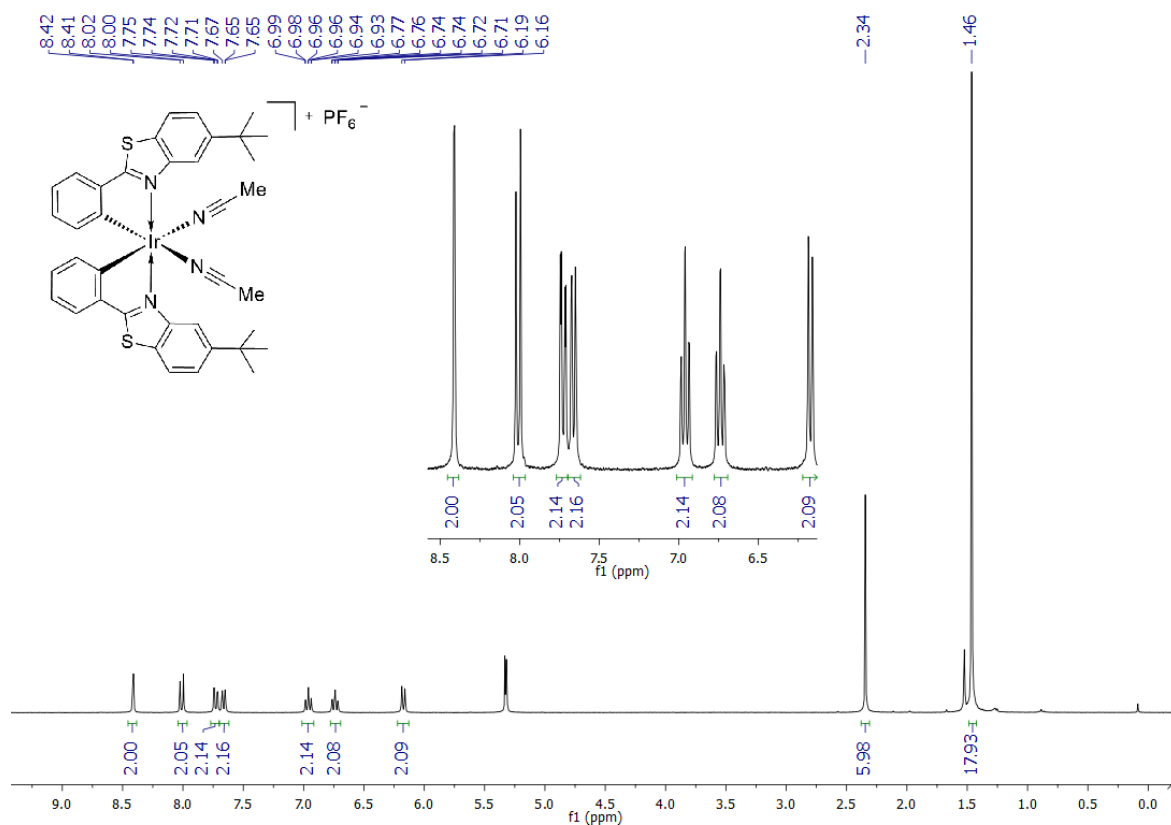


Figure 70: ¹H NMR spectra of compounds A-C5f in CD₂Cl₂ recorded with a *Bruker Avance III* at 300 MHz.

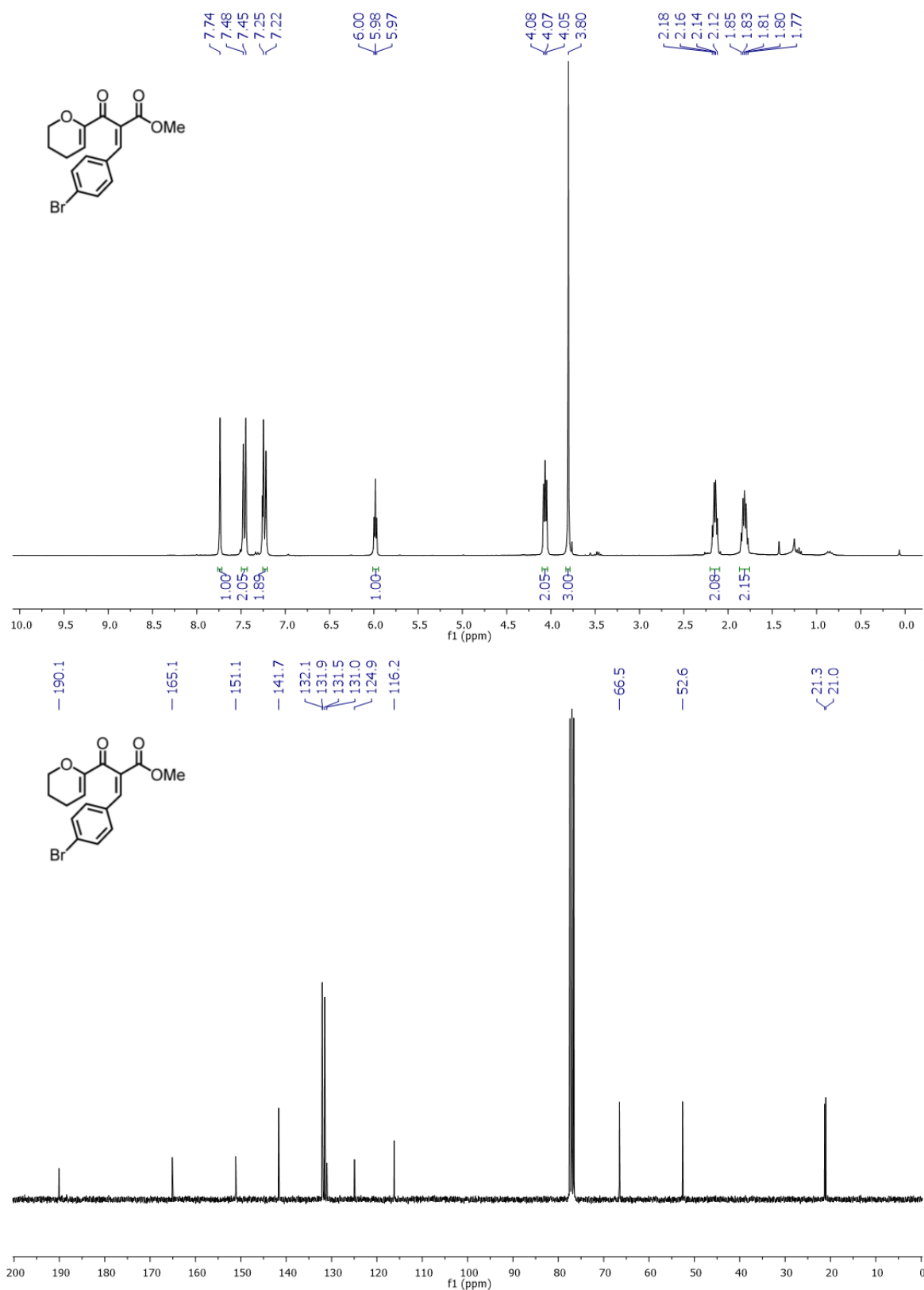


Figure 71: ^1H NMR spectra of compounds **N1h** in CDCl_3 recorded with a *Bruker Avance III* at 300 MHz (top) and ^{13}C NMR spectra of compounds **N1h** in CDCl_3 recorded with a *Bruker Avance III* at 75 MHz (bottom).

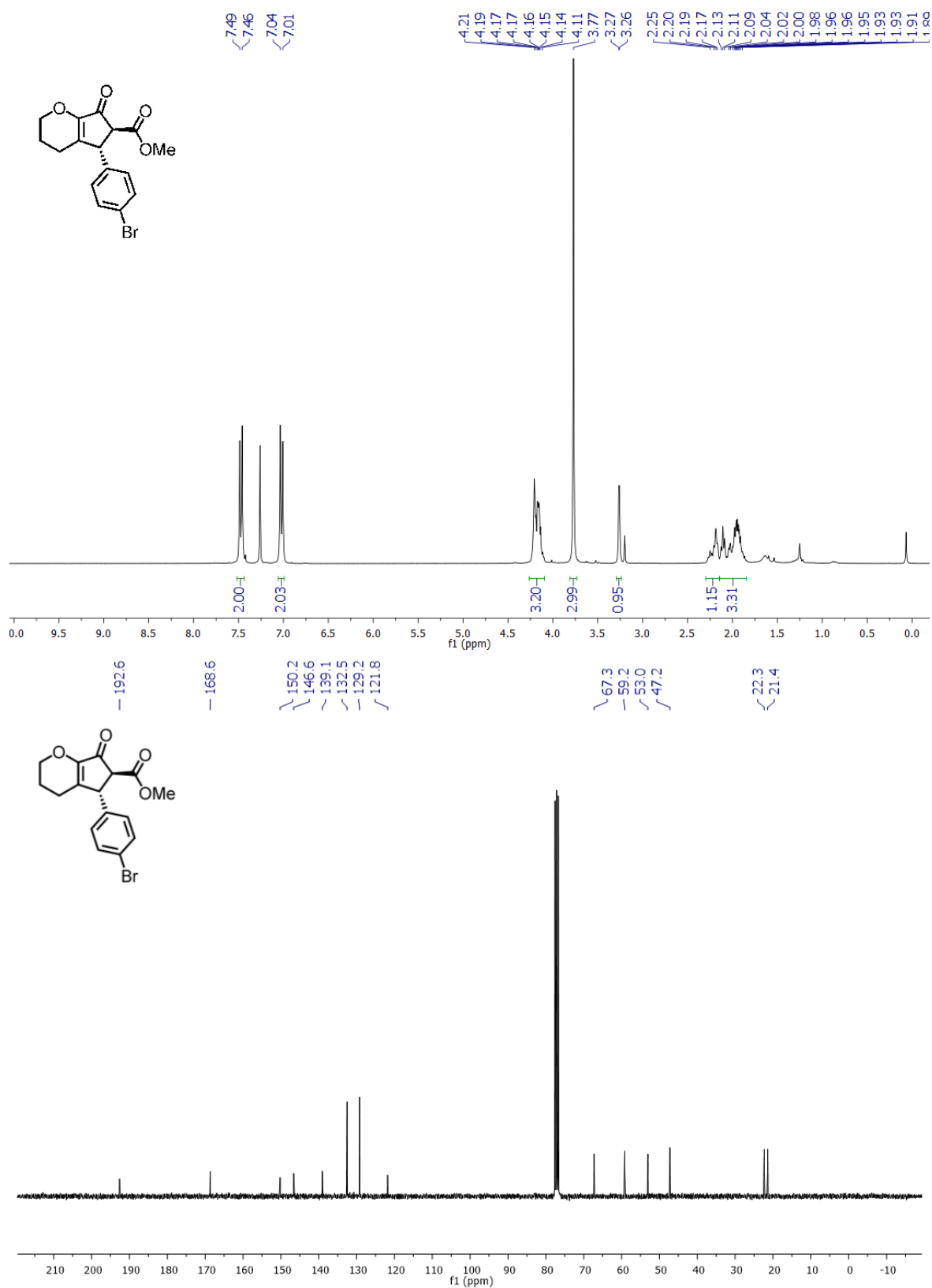


Figure 72: ¹H NMR spectra of compounds **N2h** in CDCl₃ recorded with a *Bruker Avance III* at 300 MHz (top) and ¹³C NMR spectra of compounds **N2h** in CDCl₃ recorded with a *Bruker Avance III* at 75 MHz (bottom).

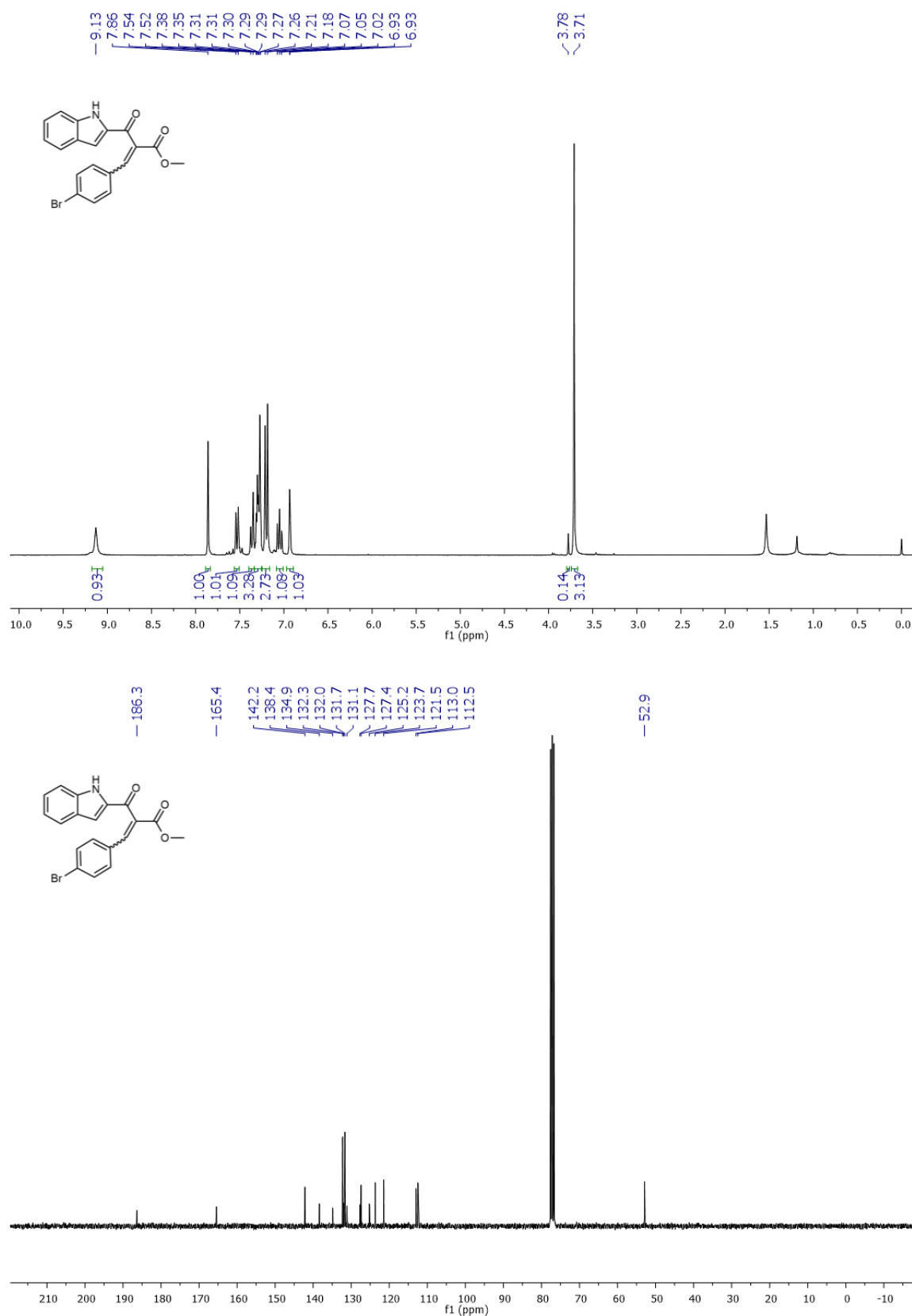


Figure 73: ¹H NMR spectra of compounds **N3f** in CDCl₃ recorded with a *Bruker Avance III* at 300 MHz (top) and ¹³C NMR spectra of compounds **N3f** in CDCl₃ recorded with a *Bruker Avance III* at 75 MHz (bottom).

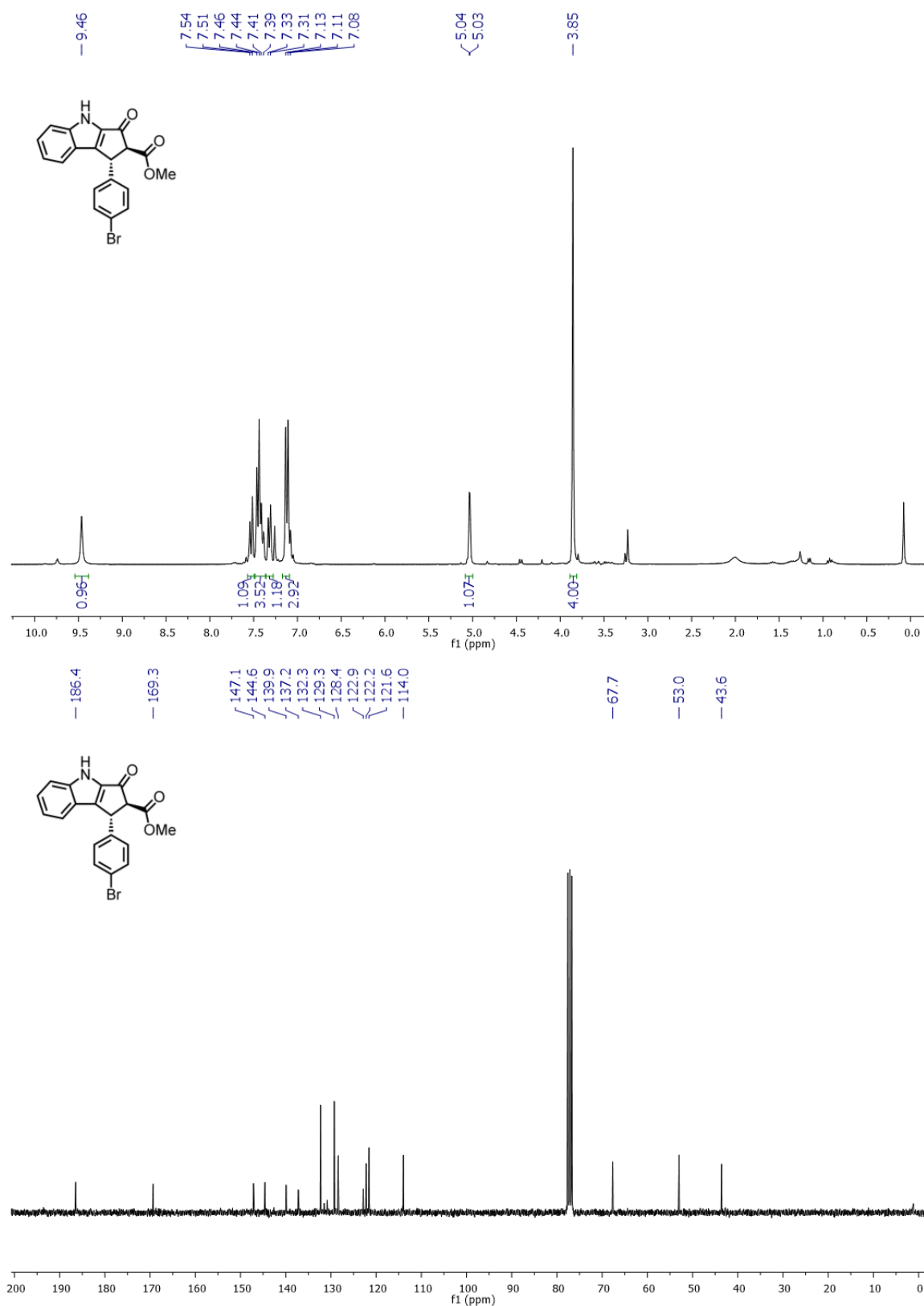


Figure 74: ^1H NMR spectra of compounds **N4f** in CDCl_3 recorded with a *Bruker Avance III* at 300 MHz (top) and ^{13}C NMR spectra of compounds **N4f** in CDCl_3 recorded with a *Bruker Avance III* at 75 MHz (bottom).

4.2 Crystallographic Data

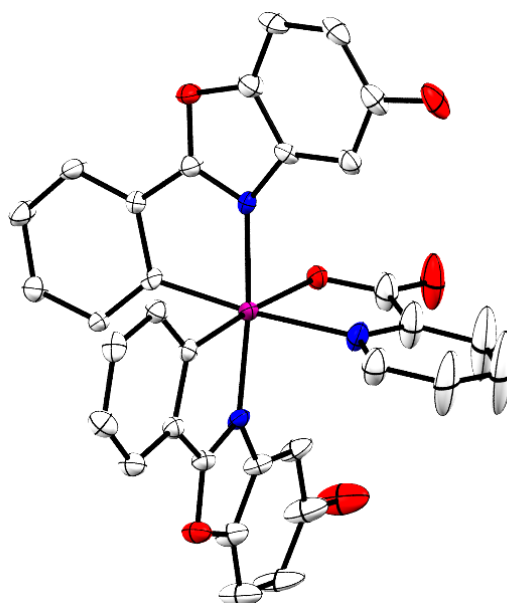


Table 10: Crystal data for *rac*-C4a (TM031a_0m_sq).

Crystal Data		
Identification code	TM031a_0m_sq	
Habitus, color	needle, yellow	
Crystal size	0.36 x 0.05 x 0.03 mm ³	
Crystal system	Monoclinic	
Space group	C 2/c	Z = 8
Unit cell dimensions	a = 34.0863(7) Å	$\alpha = 90.000(2)^\circ$
	b = 8.4988(19) Å	$\beta = 102.57^\circ$
	c = 24.897 Å	$\gamma = 90^\circ$
Volume	7039.6(16) Å ³	
Cell determination	2525 peaks with Theta 1.7° to 23.3°.	
Empirical formula	C ₃₂ H ₁₈ Ir N ₃ O ₆	
Formula weight	732.69	
Density (calculated)	1.383 Mg/m ³	
Absorption coefficient	3.834 mm ⁻¹	
F(000)	2848	

Table 11: Data Collection for *rac*-C4a (TM031a_0m_sq).

Data Collection	
Diffractometer type	Bruker D8 QUEST area detector
Wavelength	0.71073 Å
Temperature	100(2) K
Theta range for data collection	2.281 to 25.499°.
Index ranges	$-41 \leq h \leq 41$, $-10 \leq k \leq 10$, $-30 \leq l \leq 28$
Data collection software	BRUKER APEX II
Cell refinement software	APEX2 v2013.10-0 (Bruker AXS)
Data reduction software	SAINT V8.34A (Bruker AXS Inc., 2013)

Table 12: Structure refinement for *rac*-C4a (TM031a_0m_sq).

Solution and Refinement	
Reflections collected	64556
Independent reflections	6548 [R(int) = 0.1011]
Completeness to Theta = 25.242°	99.9%
Observed reflections	5080[II > 2(I)]
Reflections used for refinement	6548
Absorption correction	Semi-empirical from equivalents
Max. and min. transmission	0.89 and 0.64
Largest diff. peak and hole	0.776 and -1.045 e.Å^{-3}
Solution	Direct methods
Refinement	Full-matrix least-squares on F ²
Treatment of hydrogen atoms	Calc. posit., constr. Ref.
Programs used	SHELXS-97 (Sheldrick, 2008)
	SHELXL-2013 (Sheldrick, 2013)
	DIAMOND (Crystal Impact)
Data / restraints / parameters	6548 / 0 / 382
Goodness-of-fit on F ²	1.022
R index (all data)	wR2 = 0.0779
R index conventional I>2sigma(I)]	R1 = 0.0334

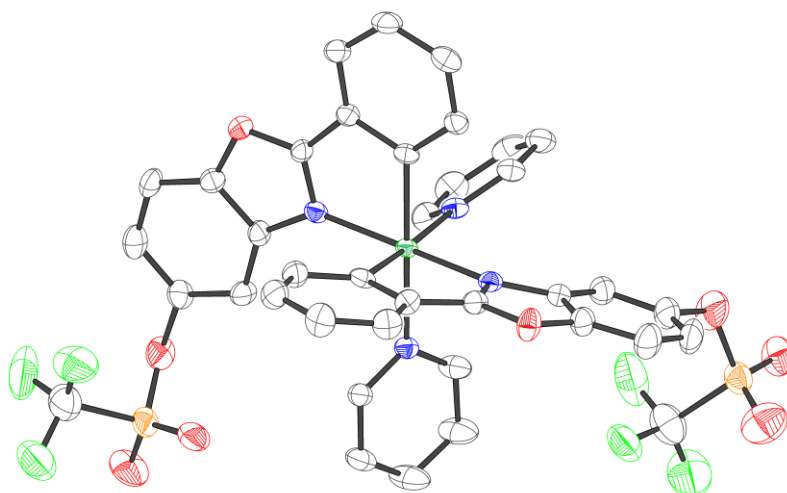


Table 13: Crystal data and structure refinement for *rac*-**C4b** (tm033_0m).

Crystal Data		
Identification code	tm033_0m	
Habitus, color	block, yellow	
Crystal size	0.30 x 0.09 x 0.06 mm ³	
Crystal system	Triclinic	
Space group	P-1	Z = 2
Unit cell dimensions	a = 11.3790(4) Å	α = 88.3250(10)°
	b = 12.6224(3) Å	β = 77.263(2)°
	c = 15.6326(5) Å	γ = 77.152(2)°
Volume	2134.77(12) Å ³	
Cell determination	9997 peaks with Theta 2.5 to 29.8°.	
Empirical formula	C _{39.50} H ₂₅ Cl F ₉ Ir N ₄ O ₁₁ S ₃	
Moiety formula	C ₃₈ H ₂₄ F ₆ Ir N ₄ O ₈ S ₂ , C F ₃ O ₃ S, 0.5(C H ₂ Cl ₂)	
Formula weight	1226.46	
Density (calculated)	1.908 Mg/m ³	
Absorption coefficient	3.442 mm ⁻¹	
F(000)	1202	

Table 14: Data Collection for *rac*-C4b (tm033_0m).

Data Collection	
Diffractometer type	Bruker D8 QUEST area detector
Wavelength	0.71073 Å
Temperature	100(2) K
Theta range for data collection	2.149 to 25.497°.
Index ranges	−13≤h≤13, −15≤k≤15, −18≤l≤18
Data collection software	APEX3 (Bruker AXS Inc., 2015) ^[57]
Cell refinement software	SAINT V8.37A (Bruker AXS Inc., 2015) ^[58]
Data reduction software	SAINT V8.37A (Bruker AXS Inc., 2015)

Table 15: Structure refinement for *rac*-C4b (tm033_0m).

Solution and Refinement	
Reflections collected	32883
Independent reflections	7946 [R(int) = 0.0382]
Completeness to Theta = 25.242°	99.9%
Observed reflections	7133[I > 2σ(I)]
Reflections used for refinement	7946
Absorption correction	Semi-empirical from equivalents ^[59]
Max. and min. transmission	0.82 and 0.42
Largest diff. peak and hole	0.972 and −0.598 e.Å ^{−3}
Solution	dual space algorithm
Refinement	Full-matrix least-squares on F ²
Treatment of hydrogen atoms	Calculated positions, constr. ref.
Programs used	XT V2014/1 (Bruker AXS Inc., 2014) ^[60]
	SHELXL-2014/7 (Sheldrick, 2014) ^[61]
	DIAMOND (Crystal Impact) ^[63]
	ShelXle (Hübschle, Sheldrick, Dittrich, 2011) ^[64]
Data / restraints / parameters	7946 / 744 / 760
Goodness-of-fit on F ²	1.061
R index (all data)	wR2 = 0.0671
R index conventional I>2sigma(I)]	R1 = 0.0265

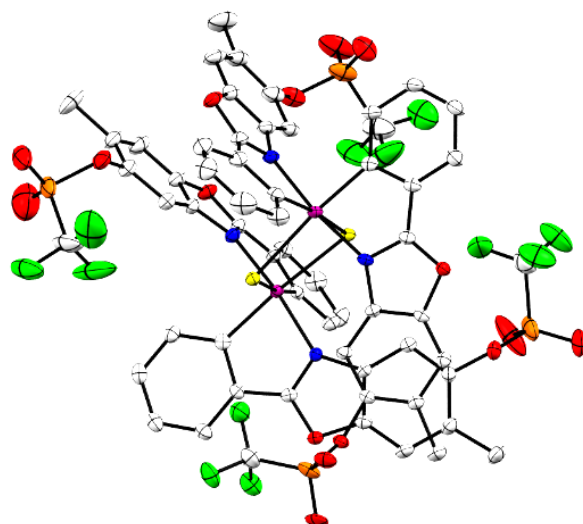


Table 16: Crystal data and structure refinement for *rac*-**C1b** (FNTC18_0m).

Crystal Data		
Identification code	FNTC18_0m	
Habitus, color	block, yellow	
Crystal size	0.41 x 0.24 x 0.08 mm ³	
Crystal system	Monoclinic	
Space group	P2 _{1/n}	Z = 4
Unit cell dimensions	a = 12.8854(5) Å	α = 90°
	b = 30.4371(11) Å	β = 103.220(1)°
	c = 18.3800(7) Å	γ = 90°
Volume	7017.5(5) Å ³	
Cell determination	9840 peaks with Theta 2.3 to 27.5°.	
Empirical formula	C _{60.36} H _{36.72} Cl _{2.72} F ₁₂ Ir ₂ N ₄ O ₁₆ S ₄	
Moiety formula	C ₆₀ H ₃₆ Cl ₂ F ₁₂ Ir ₂ N ₄ O ₁₆ S ₄ , 0.36(C H ₂ Cl ₂)	
Formula weight	1910.92	
Density (calculated)	1.809 Mg/m ³	
Absorption coefficient	4.110 mm ⁻¹	
F(000)	3708	

Table 17: Data Collection for *rac*-**C1b** (FNTC18_0m).

Data Collection	
Diffractometer type	Bruker D8 QUEST area detector
Wavelength	0.71073 Å
Temperature	100(2) K
Theta range for data collection	2.186 to 27.534°.
Index ranges	−16≤h≤16, −39≤k≤39, −23≤l≤23
Data collection software	APEX3 (Bruker AXS Inc., 2015)[57]
Cell refinement software	SAINT V8.35A (Bruker AXS Inc., 2015)[58]
Data reduction software	SAINT V8.35A (Bruker AXS Inc., 2015)

Table 18: Structure refinement for *rac*-**C1b** (FNTC18_0m).

Solution and Refinement	
Reflections collected	96921
Independent reflections	16142 [R(int) = 0.0306]
Completeness to Theta = 25.242°	99.9%
Observed reflections	14440[I > 2σ(I)]
Reflections used for refinement	16142
Extinction coefficient	X = 0.000179(12)
Absorption correction	Semi-empirical from equivalents[59]
Max. and min. transmission	0.73 and 0.54
Largest diff. peak and hole	0.756 and −0.786 e.Å ^{−3}
Solution	direct methods
Refinement	Full-matrix least-squares on F ²
Treatment of hydrogen atoms	Calculated positions, constr. ref.
Programs used	XT V2014/1 (Bruker AXS Inc., 2014)[60]
	SHELXL-2014/7 (Sheldrick, 2014)[62]
	DIAMOND (Crystal Impact)[63]
	ShelXle (Hübschle, Sheldrick, Dittrich, 2011)[64]
Data / restraints / parameters	16142 / 165 / 1052
Goodness-of-fit on F ²	1.045
R index (all data)	wR2 = 0.0458
R index conventional I>2sigma(I)]	R1 = 0.0211

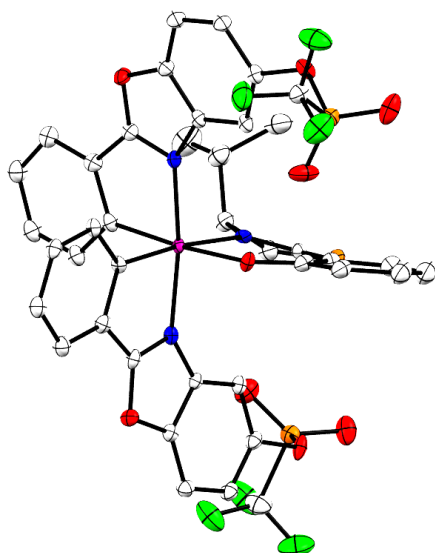


Table 19: Crystal data and structure refinement for Λ -(*S*)-C2a (EMTM03Dia1_twin5).

Crystal Data		
Identification code	EMTM03Dia1_twin5	
Habitus, color	needle, yellow	
Crystal size	0.29 x 0.08 x 0.05 mm ³	
Crystal system	Monoclinic	
Space group	P2 ₁	Z = 4
Unit cell dimensions	a = 12.2632(5) Å	$\alpha = 90^\circ$
	b = 27.1492(11) Å	$\beta = 91.8760(10)^\circ$
	c = 12.6372(6) Å	$\gamma = 90^\circ$
Volume	4205.1(3) Å ³	
Cell determination	9788 peaks with Theta 2.3 to 25.3°.	
Empirical formula	C ₄₁ H ₃₀ Cl ₂ F ₆ Ir N ₃ O ₉ S ₃	
Moiety formula	C ₄₀ H ₂₈ F ₆ Ir N ₃ O ₉ S ₃ , C H ₂ Cl ₂	
Formula weight	1181.96	
Density (calculated)	1.867 Mg/m ³	
Absorption coefficient	3.539 mm ⁻¹	
F(000)	2328	

Table 20: Data Collection for **Λ -(S)-C2a** (EMTM03Dia1_twin5).

Data Collection	
Diffractometer type	Bruker D8 QUEST area detector
Wavelength	0.71073 Å
Temperature	100(2) K
Theta range for data collection	2.239 to 25.297°.
Index ranges	$-14 \leq h \leq 14$, $-32 \leq k \leq 32$, $-15 \leq l \leq 15$
Data collection software	BRUKER APEX2 2014.9-0 ^[65]
Cell refinement software	BRUKER SAINT ^[62]
Data reduction software	SAINT V8.34A (Bruker AXS Inc., 2013) ^[62]

Table 21: Structure refinement for **Λ -(S)-C2a** (EMTM03Dia1_twin5).

Solution and Refinement	
Reflections collected	50494
Independent reflections	15068 [R(int) = 0.0516]
Completeness to Theta = 25.242°	99.9 %
Observed reflections	14383 [$I > 2\sigma(I)$]
Reflections used for refinement	15068
Absorption correction	Multiscan (Twinabs ^[63])
Max. and min. transmission	0.74 and 0.55
Flack parameter (absolute struct.)	0.013(4)
Largest diff. peak and hole	1.147 and -1.315 e.Å^{-3}
Solution	Direct methods ^[66,67]
Refinement	Full-matrix least-squares on F^2 ^[63,66]
Treatment of hydrogen atoms	Calculated positions, constr. ref.
Programs used	XT V2014/1 (Bruker AXS Inc., 2014) ^[67]
	SHELXL-2014/7 (Sheldrick, 2014) ^[67]
	DIAMOND (Crystal Impact) ^[63]
Data / restraints / parameters	15068 / 2239 / 1178
Goodness-of-fit on F^2	1.073
R index (all data)	wR2 = 0.0710
R index conventional $I > 2\sigma(I)$	R1 = 0.0365

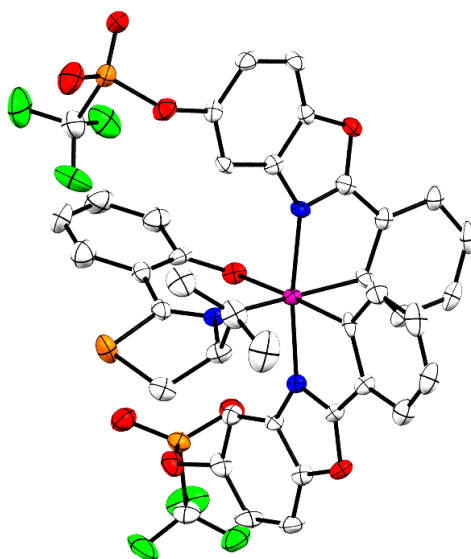


Table 22: Crystal data and structure refinement for Δ -(S)-C2a (EWTM03_0m).

Crystal Data		
Identification code	EWTM03_0m	
Habitus, color	plate, colorless	
Crystal size	0.16 x 0.13 x 0.04 mm ³	
Crystal system	Monoclinic	
Space group	P2 ₁	Z = 2
Unit cell dimensions	a = 11.6324(4) Å	$\alpha = 90^\circ$
	b = 14.6353(5) Å	$\beta = 108.492(1)^\circ$
	c = 12.2944(5) Å	$\gamma = 90^\circ$
Volume	1984.98(13) Å ³	
Cell determination	9871 peaks with Theta 2.2 to 25.3°.	
Empirical formula	C ₄₀ H ₂₈ F ₆ Ir N ₃ O ₉ S ₃	
Moiety formula	C ₄₀ H ₂₈ F ₆ Ir N ₃ O ₉ S ₃	
Formula weight	1097.03	
Density (calculated)	1.835 Mg/m ³	
Absorption coefficient	3.611 mm ⁻¹	
F(000)	1080	

Table 23: Data Collection for Δ -(S)-C2a (EWTM03_0m).

Data Collection	
Diffractometer type	Bruker D8 QUEST area detector
Wavelength	0.71073 Å
Temperature	110(2) K
Theta range for data collection	2.233 to 25.321°.
Index ranges	$-13 \leq h \leq 11$, $-17 \leq k \leq 17$, $-14 \leq l \leq 14$
Data collection software	BRUKER APEX2 2014.9-0 ^[65]
Cell refinement software	BRUKER SAINT ^[62]
Data reduction software	SAINT V8.34A (Bruker XS Inc., 2013) ^[62]

Table 24: Structure refinement for Δ -(S)-C2a (EWTM03_0m).

Solution and Refinement	
Reflections collected	42825
Independent reflections	7200 [R(int) = 0.0528]
Completeness to Theta = 25.242°	99.9%
Observed reflections	6735[I>2sigma(I)]
Reflections used for refinement	7200
Absorption correction	Numerical ^[68]
Max. and min. transmission	0.87 and 0.64
Flack parameter (absolute struct.)	0.027(3)
Largest diff. peak and hole	0.774 and -0.499 e.Å ⁻³
Solution	Direct methods ^[66,67]
Refinement	Full-matrix least-squares on F ² ^[66]
Treatment of hydrogen atoms	Calculated positions, constr. refinement
Programs used	XT V2014/1 (Bruker AXS Inc., 2014) ^[66,67]
	SHELXL-2014/7 (Sheldrick, 2014) ^[66,67]
	DIAMOND (Crystal Impact) ^[63]
Data / restraints / parameters	7200 / 103 / 625
Goodness-of-fit on F ²	0.947
R index (all data)	wR2 = 0.0411
R index conventional I>2sigma(I)]	R1 = 0.0197

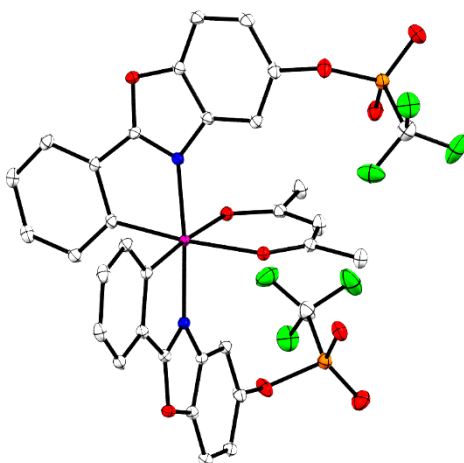


Table 25: Crystal data and structure refinement for *rac*-**C4d** (TM233_0m).

Crystal Data		
Identification code	TM233_0m	
Habitus, color	prism, green	
Crystal size	0.26 x 0.10 x 0.08 mm ³	
Crystal system	Monoclinic	
Space group	C2/c	Z = 4
Unit cell dimensions	a = 10.4525(4) Å	$\alpha = 90^\circ$
	b = 20.9837(8) Å	$\beta = 107.328(1)^\circ$
	c = 15.7265(6) Å	$\gamma = 90^\circ$
Volume	3292.8(2) Å ³	
Cell determination	9718 peaks with Theta 2.3 to 27.6°.	
Empirical formula	C ₃₃ H ₂₁ F ₆ Ir N ₂ O ₁₀ S ₂	
Moiety formula	C ₃₃ H ₂₁ F ₆ Ir N ₂ O ₁₀ S ₂	
Formula weight	975.84	
Density (calculated)	1.968 Mg/m ³	
Absorption coefficient	4.280 mm ⁻¹	
F(000)	1904	

Table 26: Data Collection for *rac*-C4d (TM233_0m).

Data Collection	
Diffractometer type	Bruker D8 QUEST area detector
Wavelength	0.71073 Å
Temperature	100(2) K
Theta range for data collection	2.260 to 27.552°.
Index ranges	−13≤h≤13, −27≤k≤27, −20≤l≤20
Data collection software	BRUKER APEX2 2014.9-0 ^[65]
Cell refinement software	BRUKER SAINT ^[62]
Data reduction software	SAINT V8.34A (Bruker AXS Inc., 2013) ^[62]

Table 27: Structure refinement for *rac*-C4d (TM233_0m).

Solution and Refinement	
Reflections collected	43831
Independent reflections	3812 [R(int) = 0.0251]
Completeness to Theta = 25.242°	99.9%
Observed reflections	3678[I>2sigma(I)]
Reflections used for refinement	3812
Absorption correction	Semi-empirical from equivalents ^[68]
Max. and min. transmission	0.73 and 0.57
Largest diff. peak and hole	0.515 and −0.842 e.Å ^{−3}
Solution	Direct methods ^[66]
Refinement	Full-matrix least-squares on F ² ^[66]
Treatment of hydrogen atoms	Calculated positions, constr. ref.
Programs used	XT V2014/1 (Bruker AXS Inc., 2014) ^[66,67]
	SHELXL-2014/7 (Sheldrick, 2014) ^[66,67]
	DIAMOND (Crystal Impact) ^[63]
Data / restraints / parameters	3812 / 0 / 246
Goodness-of-fit on F ²	1.086
R index (all data)	wR2 = 0.0345
R index conventional I>2sigma(I)]	R1 = 0.0136

Crystal Data		
Identification code	XyPhboOTf_0m	
Habitus, color	block, yellow	
Crystal size	0.19 x 0.18 x 0.15 mm ³	
Crystal system	Monoclinic	
Space group	C2/c	Z = 4
Unit cell dimensions	a = 14.2619(5) Å	α = 90°
	b = 28.8162(11) Å	β = 105.1370(10)°
	c = 23.2088(9) Å	γ = 90°
Volume	9207.3(6) Å ³	
Cell determination	9729 peaks with Theta 2.6 to 27.5°.	
Empirical formula	C ₉₄ H ₇₄ Cl ₂ F ₁₂ Ir ₂ N ₄ O ₁₆ S ₄	
Moiety formula	C ₈₈ H ₆₀ Cl ₂ F ₁₂ Ir ₂ N ₄ O ₁₆ S ₄ , C ₆ H ₁₄	
Formula weight	2327.11	
Density (calculated)	1.679 Mg/m ³	
Absorption coefficient	3.129 mm ⁻¹	
F(000)	4616	

Table 29: Data Collection for *rac*-**C1d** (XyPhboOTf_0m).

Data Collection	
Diffractometer type	Bruker D8 QUEST area detector
Wavelength	0.71073 Å
Temperature	110(2) K
Theta range for data collection	2.303 to 27.551°.
Index ranges	$-17 \leq h \leq 18$, $-37 \leq k \leq 37$, $-29 \leq l \leq 30$
Data collection software	APEX3 (Bruker AXS Inc., 2015) ^[57]
Cell refinement software	SAINT V8.37A (Bruker AXS Inc., 2015) ^[58]
Data reduction software	SAINT V8.37A (Bruker AXS Inc., 2015) ^[58]

Table 30: Structure refinement for *rac*-**C1d** (XyPhboOTf_0m).

Solution and Refinement	
Reflections collected	66733
Independent reflections	10619 [R(int) = 0.0296]
Completeness to Theta = 25.242°	99.9%
Observed reflections	9307 [I > 2σ(I)]
Reflections used for refinement	10619
Absorption correction	Semi-empirical from equivalents ^[68]
Max. and min. transmission	0.73 and 0.57
Largest diff. peak and hole	1.025 and −0.842 e.Å ^{−3}
Solution	dual space algorithm
Refinement	Full-matrix least-squares on F ²
Treatment of hydrogen atoms	Calculated positions, constr. ref.
Programs used	XT V2014/1 (Bruker AXS Inc., 2014) ^[60]
	SHELXL-2014/7 (Sheldrick, 2014) ^[62]
	DIAMOND (Crystal Impact) ^[63]
	ShelXle (Hübschle, Sheldrick, Dittrich, 2011) ^[64]
Data / restraints / parameters	10619 / 32 / 683
Goodness-of-fit on F ²	1.020
R index (all data)	wR2 = 0.0534
R index conventional I>2sigma(I)]	R1 = 0.0219

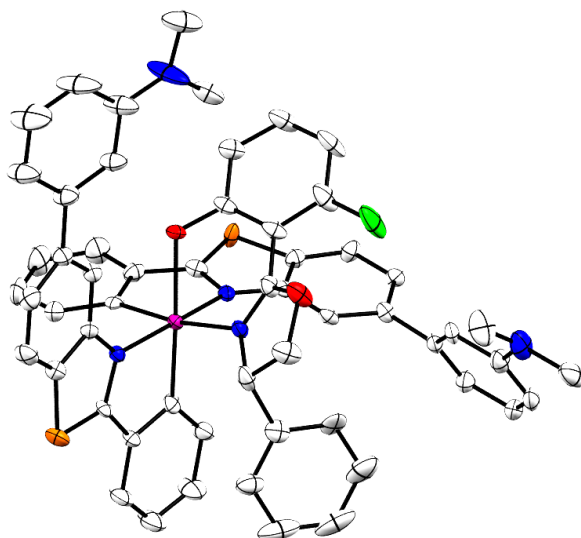


Table 31: Crystal data and structure refinement for Δ -(S)-C3o (TMNI25_0m).

Crystal Data		
Identification code	TMNI25_0m	
Habitus, color	needle, orange	
Crystal size	0.40 x 0.05 x 0.04 mm ³	
Crystal system	Orthorhombic	
Space group	P212121	Z = 4
Unit cell dimensions	a = 14.8897(7) Å	$\alpha = 90^\circ$
	b = 16.2824(7) Å	$\beta = 90^\circ$
	c = 20.5659(8) Å	$\gamma = 90^\circ$
Volume	4986.0(4) Å ³	
Cell determination	9337 peaks with Theta 2.3 to 26.2°.	
Empirical formula	C ₅₈ H _{48.28} Cl ₂ F Ir N ₅ O _{2.64} S ₂	
Moiety formula	C ₅₇ H ₄₅ F Ir N ₅ O ₂ S ₂ , CH ₂ Cl ₂ , 0.64 (H ₂ O)	
Formula weight	1203.71	
Density (calculated)	1.604 Mg/m ³	
Absorption coefficient	2.924 mm ⁻¹	
F(000)	2418	

Table 32: Data Collection for Δ -(S)-C3o (TMNI25_0m).

Data Collection	
Diffractometer type	Bruker D8 QUEST area detector
Wavelength	0.71073 Å
Temperature	100(2) K
Theta range for data collection	2.101 to 26.452°.
Index ranges	$-18 \leq h \leq 18$, $-20 \leq k \leq 20$, $-25 \leq l \leq 24$
Data collection software	APEX3 (Bruker AXS Inc., 2015) ^[69]
Cell refinement software	SAINT V8.35A (Bruker AXS Inc., 2015) ^[58]
Data reduction software	SAINT V8.35A (Bruker AXS Inc., 2015) ^[58]

Table 33: Structure refinement for Δ -(S)-C3o (TMNI25_0m).

Solution and Refinement	
Reflections collected	57721
Independent reflections	10225 [R(int) = 0.0711]
Completeness to Theta = 25.242°	99.9%
Observed reflections	9106 [I > 2σ(I)]
Reflections used for refinement	10225
Absorption correction	Semi-empirical from equivalents ^[68]
Max. and min. transmission	0.91 and 0.70
Flack parameter (absolute struct.)	0.000(4) ^[70]
Largest diff. peak and hole	0.568 and -0.664 e.Å ⁻³
Solution	Direct methods
Refinement	Full-matrix least-squares on F ²
Treatment of hydrogen atoms	Calcd. positions, constr. ref.
Programs used	XT V2014/1 (Bruker AXS Inc., 2014) ^[60]
	SHELXL-2014/7 (Sheldrick, 2014) ^[62]
	DIAMOND (Crystal Impact) ^[63]
	ShelXle (Hübschle, Sheldrick, Dittrich, 2011) ^[64]
Data / restraints / parameters	10225 / 600 / 838
Goodness-of-fit on F ²	1.040
R index (all data)	wR2 = 0.0521
R index conventional I>2sigma(I)]	R1 = 0.0298

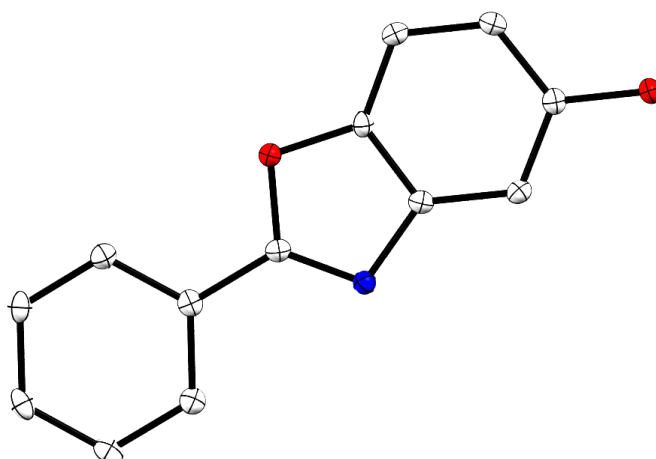


Table 34: Crystal data and structure refinement for **L1b** (TM020_0m).

Crystal Data		
Identification code	TM020_0m	
Habitus, color	prism, colorless	
Crystal size	0.291 x 0.287 x 0.282 mm ³	
Crystal system	Monoclinic	
Space group	P 2 _{1/n}	Z = 4
Unit cell dimensions	a = 5.7835(3) Å	$\alpha = 90^\circ$
	b = 19.2410(9) Å	$\beta = 94.0795(15)^\circ$
	c = 8.7173(4) Å	$\gamma = 90^\circ$
Volume	967.61(8) Å ³	
Cell determination	7574 peaks with Theta 2.6 to 27.5°.	
Empirical formula	C ₁₃ H ₉ N O ₂	
Formula weight	211.21	
Density (calculated)	1.450 Mg/m ³	
Absorption coefficient	0.099 mm ⁻¹	
F(000)	440	

Table 35: Data Collection for **L1b** (TM020_0m).

Data Collection	
Diffractometer type	Bruker D8 QUEST area detector
Wavelength	0.71073 Å
Temperature	100(2) K
Theta range for data collection	2.570 to 25.498°.
Index ranges	$-7 \leq h \leq 7$, $-23 \leq k \leq 23$, $-10 \leq l \leq 10$
Data collection software	BRUKER APEX II
Cell refinement software	SAINT V8.34A (Bruker AXS Inc., 2013)
Data reduction software	SAINT V8.34A (Bruker AXS Inc., 2013)

Table 36: Structure refinement for **L1b** (TM020_0m).

Solution and Refinement	
Reflections collected	11148
Independent reflections	1796 [R(int) = 0.0203]
Completeness to Theta = 25.242°	99.9%
Observed reflections	1666[I > 2σ(I)]
Reflections used for refinement	1796
Absorption correction	Semi-empirical from equivalents ^[63]
Max. and min. transmission	0.97 and 0.94
Largest diff. peak and hole	0.168 and -0.213 e.Å ⁻³
Solution	Direct methods ^[17, 18]
Refinement	Full-matrix least-squares on F ² ^[63,66]
Treatment of hydrogen atoms	CH calcd., constr., OH located, isotr. ref.
Programs used	SHELXS-97 (Sheldrick, 2008)
	SHELXL-2013 (Sheldrick, 2013)
	DIAMOND (Crystal Impact)
Data / restraints / parameters	1796 / 0 / 149
Goodness-of-fit on F ²	1.054
R index (all data)	wR2 = 0.0806
R index conventional I>2sigma(I)]	R1 = 0.0317

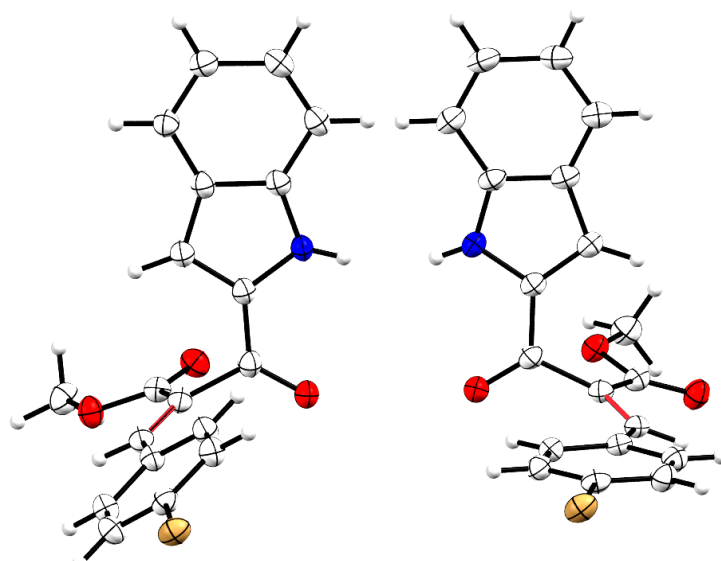


Table 37: Crystal data and structure refinement for **N3f** TMFM1K.

Crystal Data		
Identification code	TMFM1K	
Habitus, color	nugget, colorless	
Crystal size	0.160 x 0.150 x 0.090 mm ³	
Crystal system	Triclinic	
Space group	P-1	Z = 4
Unit cell dimensions	a = 11.3862(2) Å	α = 81.462(2)°
	b = 12.1388(2) Å	β = 71.267(2)°
	c = 12.6017(3) Å	γ = 79.814(2)°
Volume	1615.61(6) Å ³	
Cell determination	39372 peaks with Theta 3.7 to 78.3°	
Empirical formula	C ₁₉ H ₁₄ Br N O ₃	
Moiety formula	C ₁₉ H ₁₄ Br N O ₃	
Formula weight	384.22	
Density (calculated)	1.580 Mg/m ³	
Absorption coefficient	3.615 mm ⁻¹	
F(000)	776	

Table 38: Data Collection for **N3f** TMFM1K.

Data Collection	
Diffraction type	STOE STADIVARI
Wavelength	1.54178 Å
Temperature	100(2) K
Theta range for data collection	3.718 to 75.855°
Index ranges	−14≤h≤13, −14≤k≤15, −10≤l≤15
Data collection software	X-Area Pilatus3_SV 1.31.127.0 (STOE, 2016) ^[71]
Cell refinement software	X-Area Recipe 1.33.0.0 (STOE, 2015) ^[72]
Data reduction software	X-Area Integrate 1.71.0.0 (STOE, 2016) ^[73]
	X-Area LANA 1.68.2.0 (STOE, 2016) ^[74]

Table 39: Structure refinement for **N3f** TMFM1K.

Solution and Refinement	
Reflections collected	28558
Independent reflections	6464 [R(int) = 0.0263]
Completeness to Theta = 25.242°	97.8%
Observed reflections	5967[I > 2σ(I)]
Reflections used for refinement	6464
Extinction coefficient	X = 0.0039(4)
Absorption correction	Semi-empirical from equivalents ^[74]
Max. and min. transmission	0.4267 and 0.1870
Largest diff. peak and hole	0.562 and −0.763 e.Å ^{−3}
Solution	Dual Space Algorithm ^[60]
Refinement	Full-matrix least-squares on F ² ^[65]
Treatment of hydrogen atoms	CH ‘riding model’, NH located, isotropic ref.
Programs used	XT V2014/1 (Bruker AXS Inc., 2014) ^[60]
	SHELXL-2017/1 (Sheldrick, 2017) ^[65]
	DIAMOND (Crystal Impact) ^[62]
	ShelXle (Hübschle, Sheldrick, Dittrich, 2011) ^[63]
Data / restraints / parameters	6464 / 0 / 444
Goodness-of-fit on F ²	1.147
R index (all data)	wR2 = 0.1432
R index conventional I>2sigma(I)]	R1 = 0.0487

4.3 CD Spectra

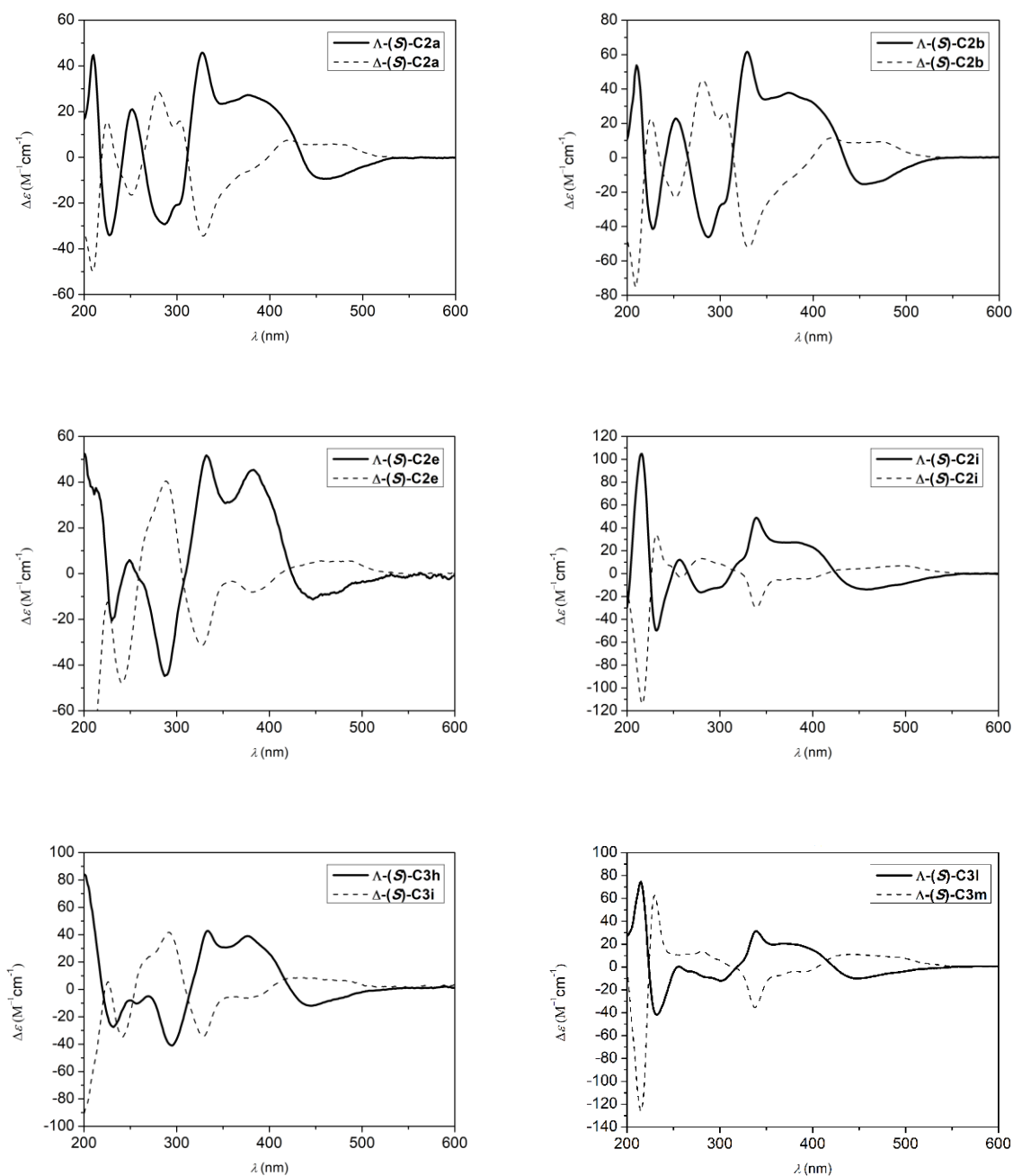


Figure 75: CD Spectra of Λ -(*S*) and Δ -(*S*) diastereomer complexes of **C2a** (top left), **C2b** (top right), **C2e** (center left), **C2i** (center right), **C3h-i** (bottom left), and **C3l-m** (bottom right) in comparison. Λ -(*S*) diastereomers are illustrated as continuous lines. Δ -(*S*) diastereomers are illustrated as dashed lines.

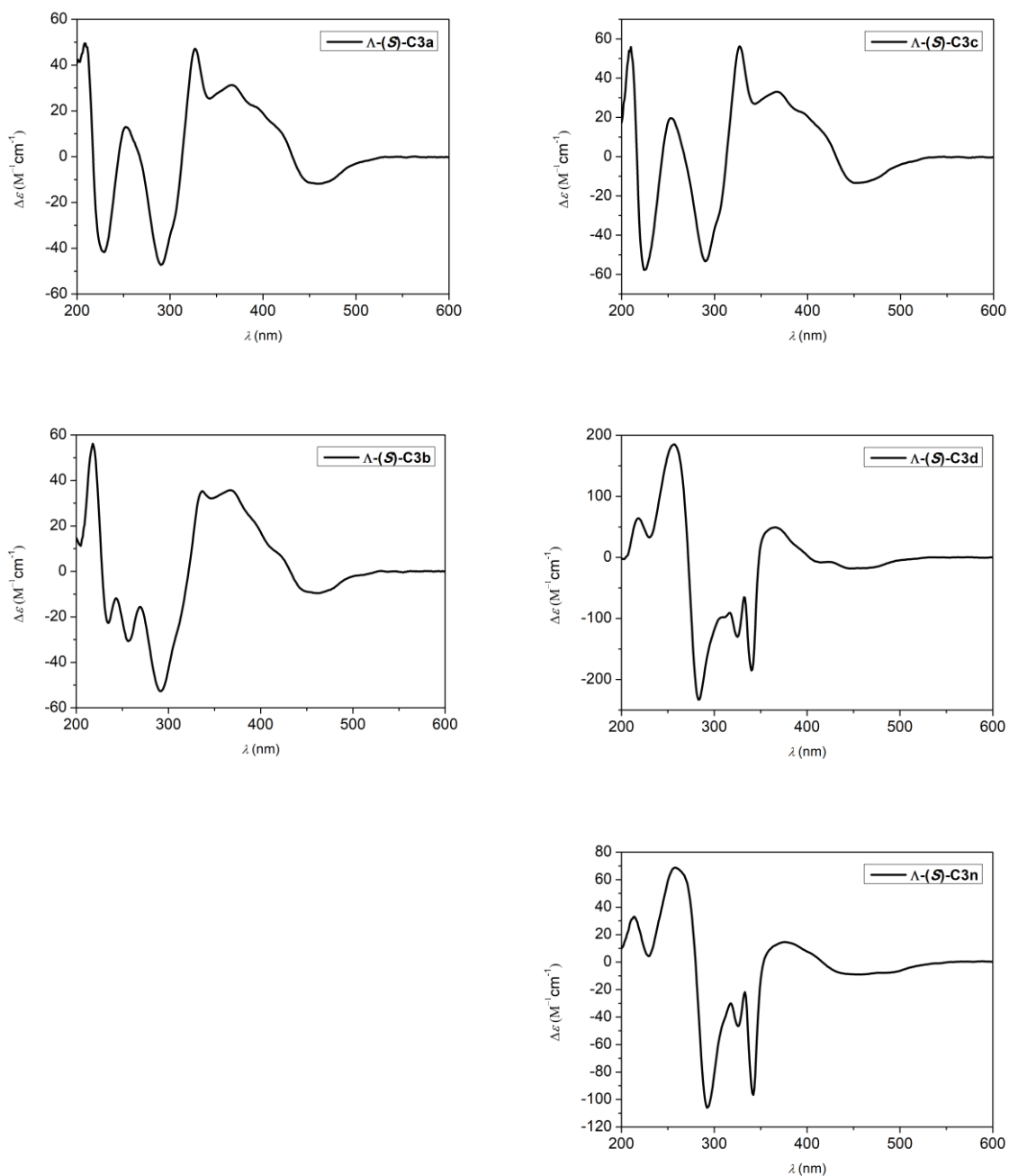


Figure 76: CD Spectra of complexes Λ -(S)-C3a (top left), Λ -(S)-C3c (top right), Λ -(S)-C3b (center left), Λ -(S)-C3d (center right) and Λ -(S)-C3n (bottom right) after cross-coupling. Λ -(S) diastereomers are illustrated exclusively.

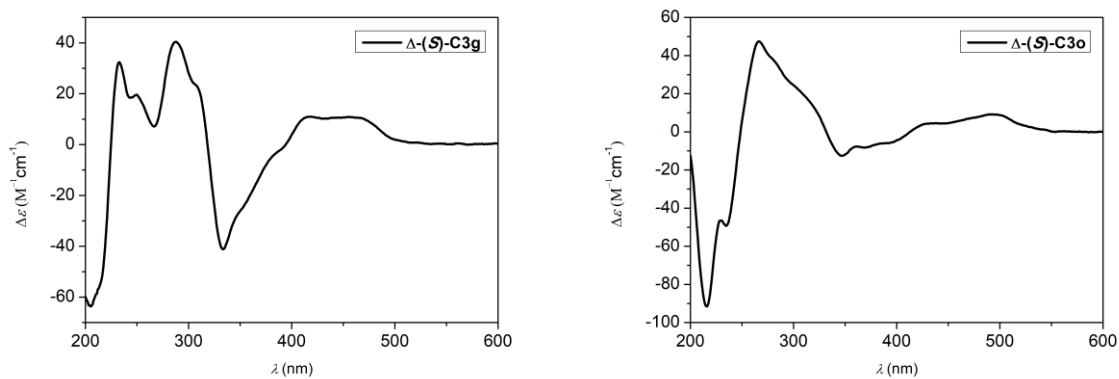


Figure 77: CD Spectra of complexes Δ -(S)-C3g (left) and Δ -(S)-C3o (right) after cross-coupling. Δ -(S)-diastereomere is illustrated exclusively.

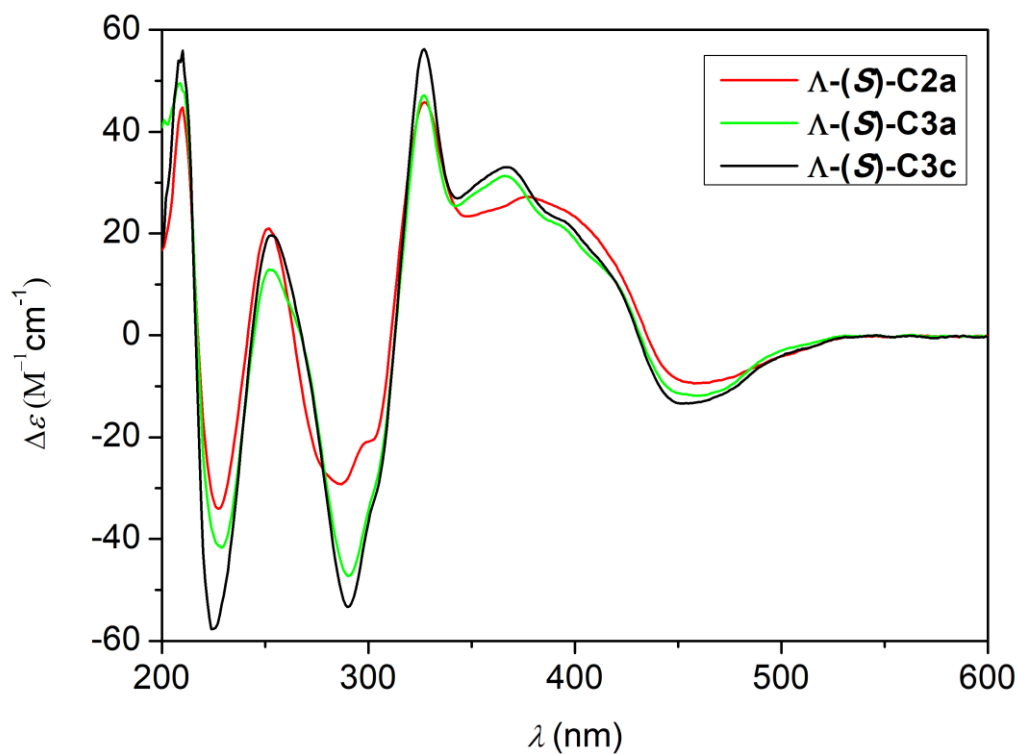
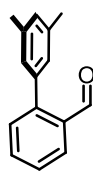
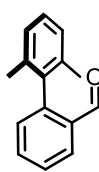


Figure 78: CD Spectra of triflated precursor complex Δ -(S)-C2a (red) overlaid with the cross-coupling products Δ -(S)-C3a (green) and Δ -(S)-C3c (black).

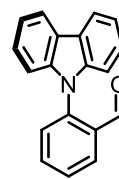
4.4 Synthesized Ligands L and Building Blocks S



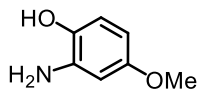
S1a, 95%



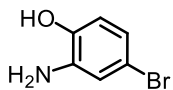
S1b, quant



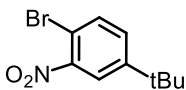
S1c, 70%



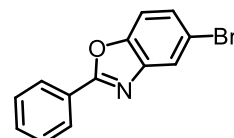
S2a, 99%



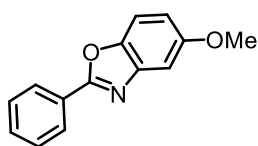
S2c, 82%



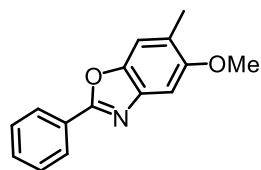
S4a, 70%



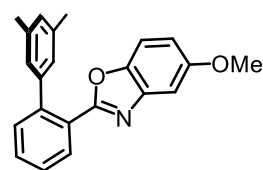
L0a, 50%



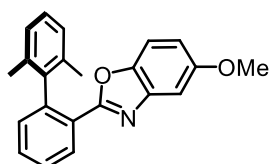
L1a, 90%



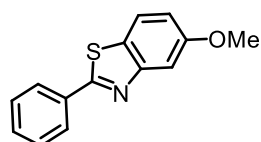
L2a, 86%



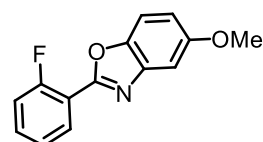
L3a, 75%



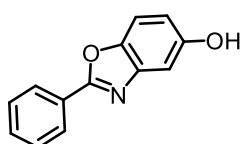
L4a, 91%



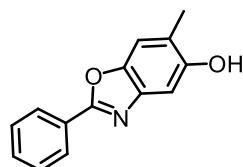
L6a, 80%



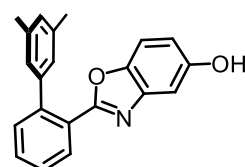
L7a, 89%



L1b, 98%

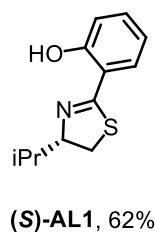
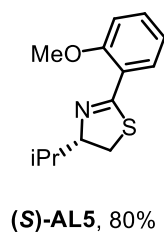
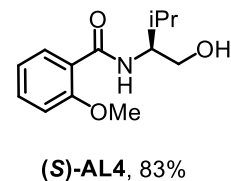
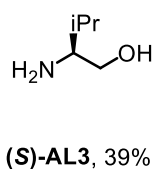
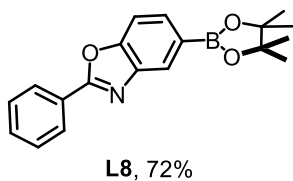
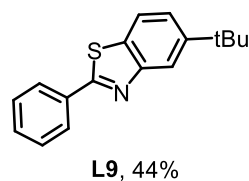
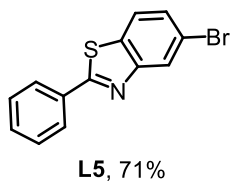
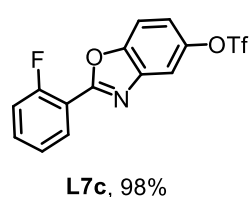
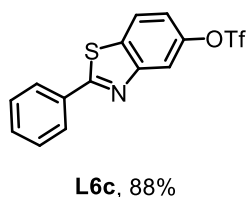
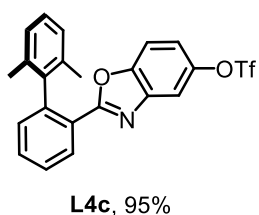
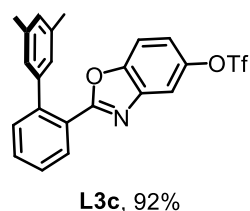
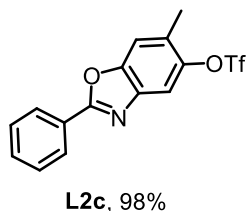
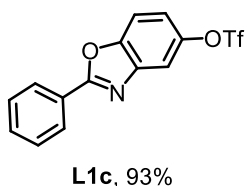
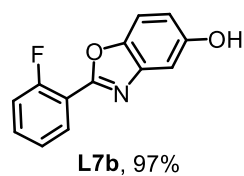
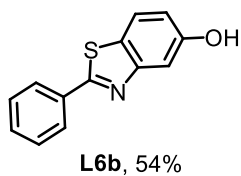
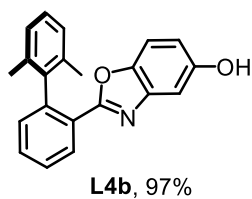


L2b, 99%

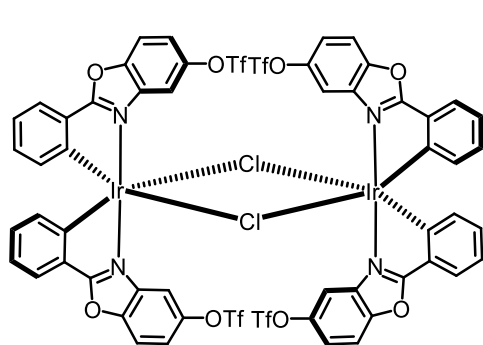


L3b, 95%

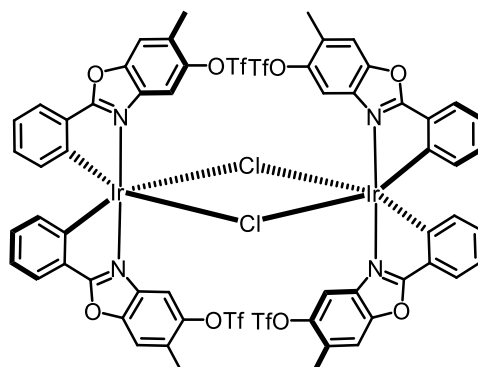
4.5 Synthesized Ligands L, Ancillary Ligands AL and Building Blocks



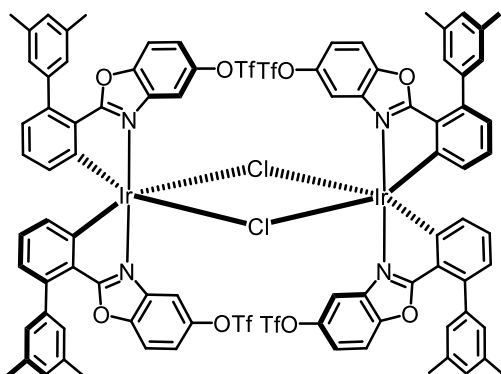
4.6 Synthesized Racemic Complexes *rac*-C1



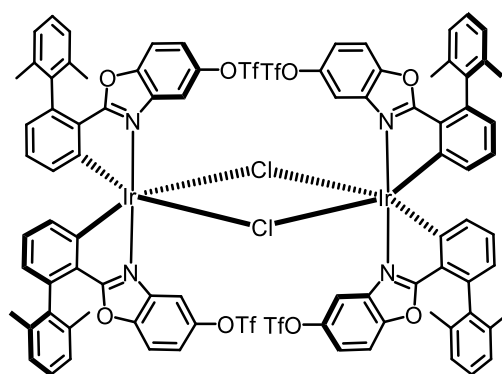
***rac*-C1a**, 87%



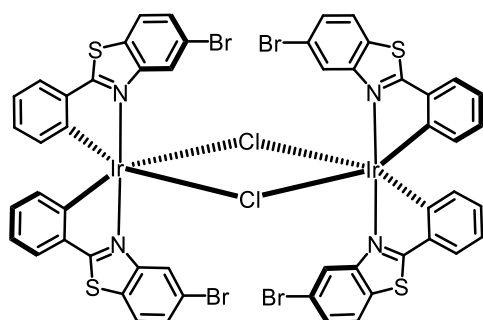
***rac*-C1b**, 89%



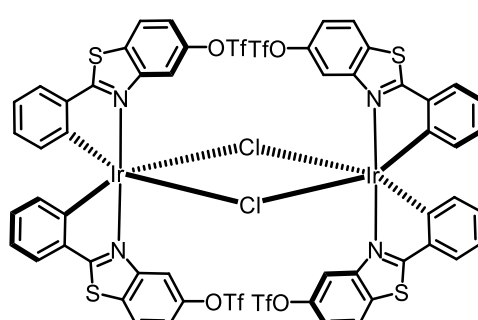
***rac*-C1c**, 79%



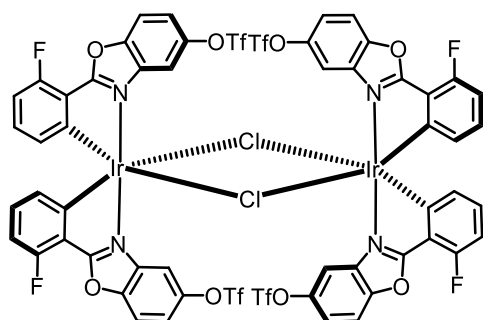
***rac*-C1d**, 39%



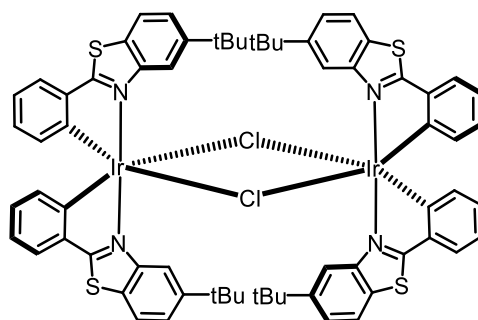
***rac*-C1e**, 70%



***rac*-C1f**, 7%

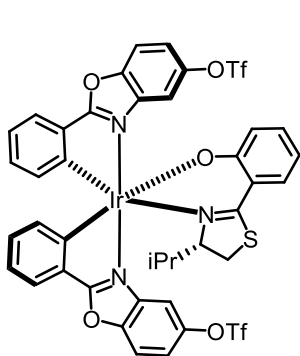


***rac*-C1g**, 79%



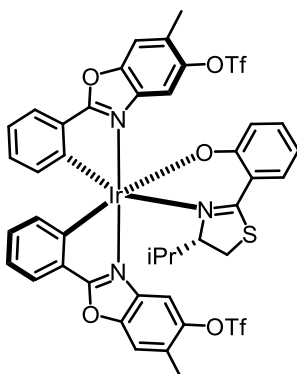
***rac*-C1i**, 73%

4.7 Synthesized Diastereomer Complexes Λ -(S)-C2 and Δ -(S)-C2



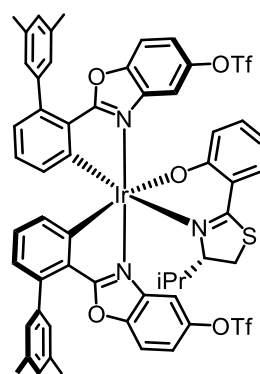
Λ -(S)-C2a, 40%

Δ -(S)-C2a, 38%

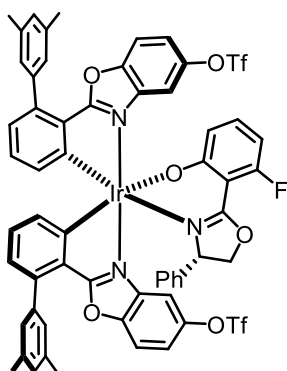


Λ -(S)-C2b, 40%

Δ -(S)-C2b, 37%

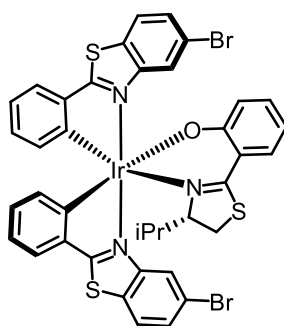


Λ -(S)-C2c, 35%

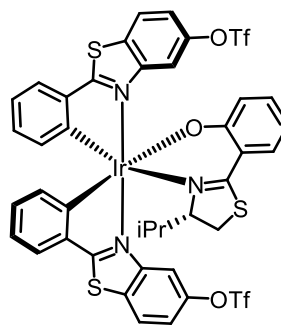


Λ -(S)-C2e, 39%

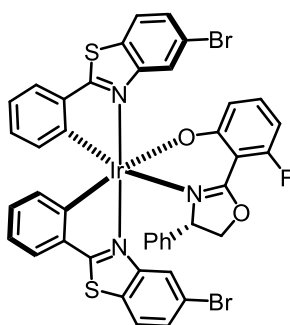
Δ -(S)-C2e, 35%



Λ -(S)-C2g, 35%

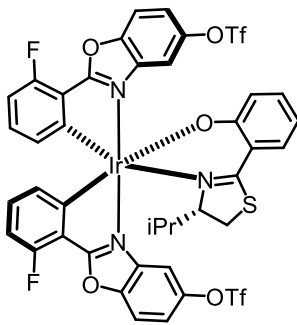


Λ -(S)-C2h, 28%



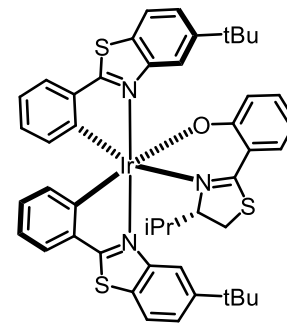
Λ -(S)-C2i, 46%

Δ -(S)-C2i, 44%



Λ -(S)-C2j, 44%

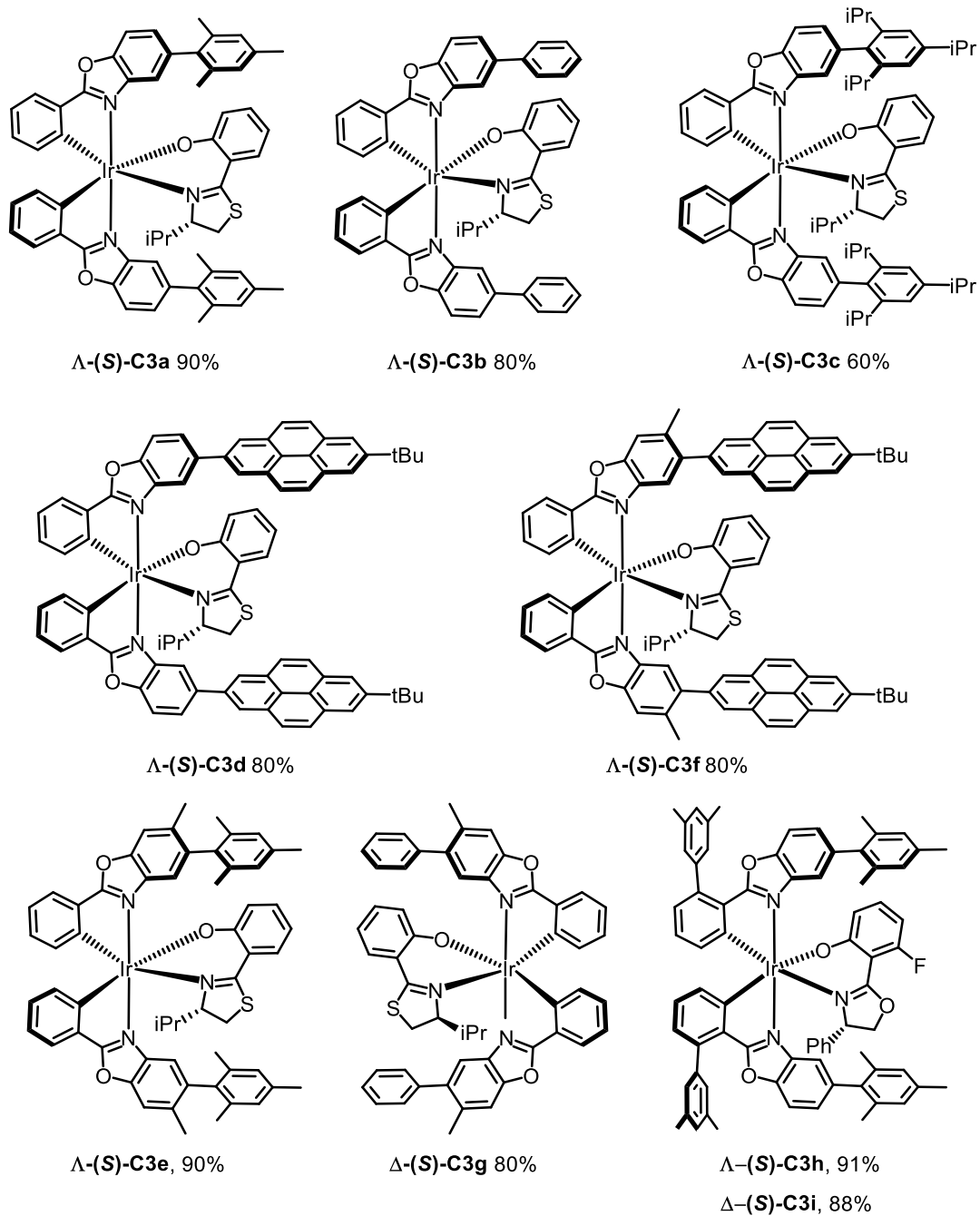
Δ -(S)-C2j, 28%



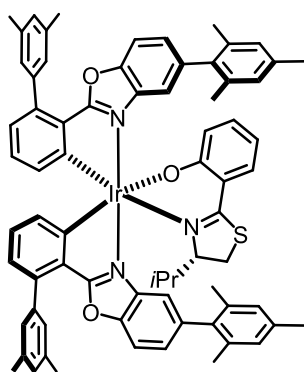
Λ -(S)-C2j, 40%

Δ -(S)-C2j, 41%

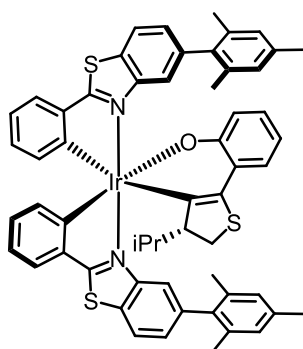
4.8 Cross-Coupling Product Complexes Λ -(S)-C3 and Δ -(S)-C3



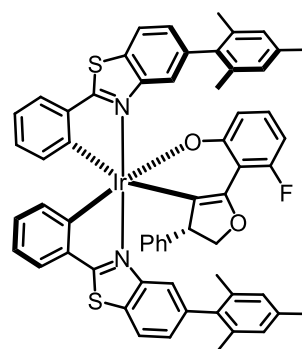
4.9 Cross-Coupling Product Complexes Λ -(S)-C3, Δ -(S)-C3 and C4e



Λ -(S)-C3j, 88%

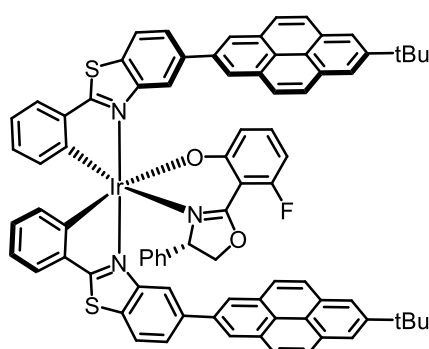


Λ -(S)-C3k, 64%

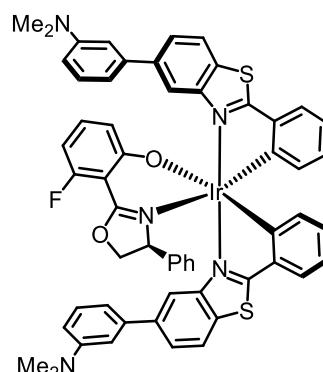


Λ -(S)-C3l, 94%

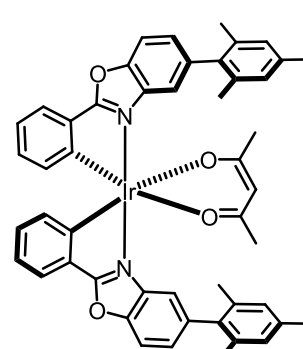
Δ -(S)-C3m, 92%



Λ -(S)-C3n, 92%



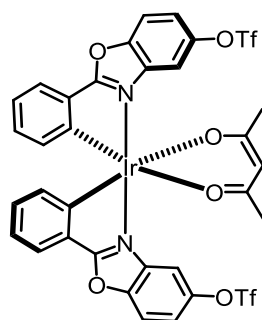
Δ -(S)-C3o, 55%



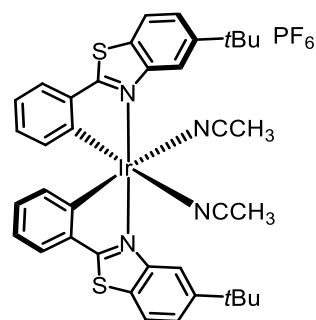
rac-C4e, 64%

Λ -C4e, 85%, 99%ee

4.10 Other Complexes *rac*-C4d and Λ -C5d

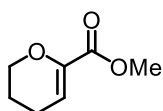


rac-C4d, 80%

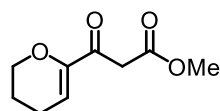


Λ -C5f, 85%

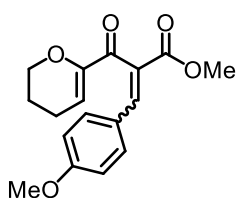
4.11 Synthesized Nazarov Substrates N1 and Building Blocks S12



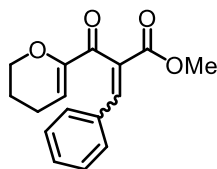
S12b, 30%
over 2 steps



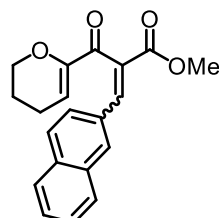
S12c, 48%



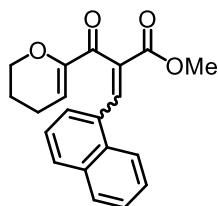
N1a; 71% yield
E/Z 20:1



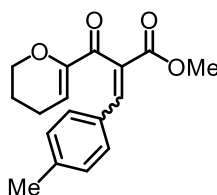
N1b; 62% yield
E/Z 3:1



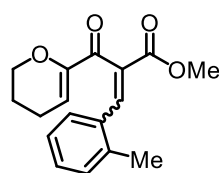
N1c; 49% yield
E/Z >30:1



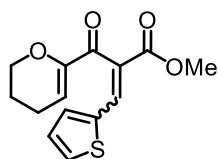
N1d; 56% yield
E/Z >30:1



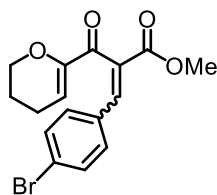
N1e; 47% yield
E/Z >30:1



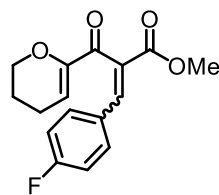
N1f; 83% yield
E/Z 20:1



N1g; 62% yield
E/Z 14:1

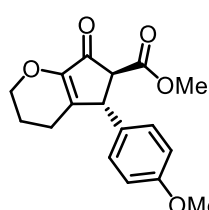


N1h; 64% yield
E/Z 30:1

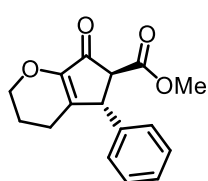


N1i; 69% yield
E/Z >30:1

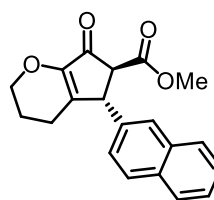
4.12 Synthesized Nazarov Products N2



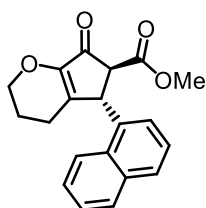
N2a, 14 h, 86% yield
93% ee, *trans/cis* 18:1



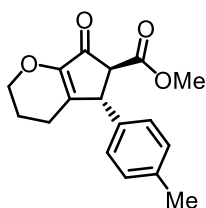
N2b, 15 h, 93% yield
97% ee, *trans/cis* 19:1



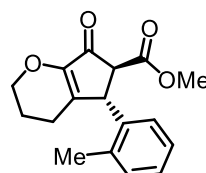
N2c, 12 h, 96% yield
95% ee, *trans/cis* 20:1



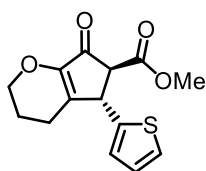
N2d, 14 h, 92% yield
92% ee, *trans/cis* 29:1



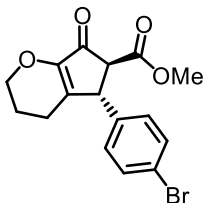
N2e, 14 h, 93% yield
94% ee, *trans/cis* 28:1



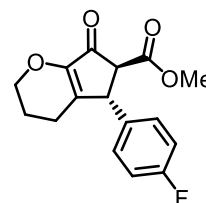
N2f, 14 h, 95% yield
95% ee, *trans/cis* 20:1



N2g, 23 h, 98% yield
89% ee, *trans/cis* 50:1

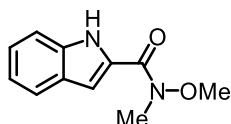


N2h, 23 h, 85% yield
>99% ee, *trans/cis* 20:1

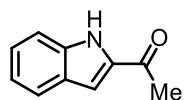


N2i, 14 h, 91% yield
96% ee, *trans/cis* 15:1

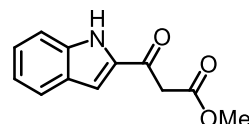
4.13 Synthesized Building Blocks S13 to S15



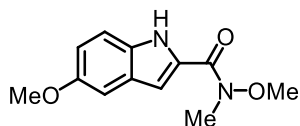
S13a, 61%



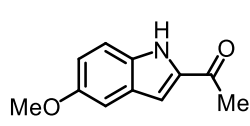
S13b, 70%



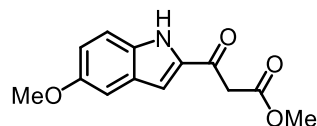
S13c, 72%



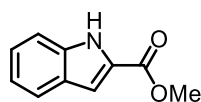
S14a, 51%



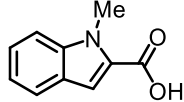
S14b, 89%



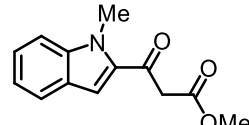
S14c, 81%



S15a, 98%

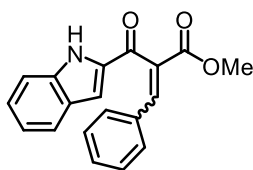


S15b, 63%

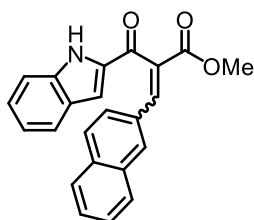


S15c, 83%

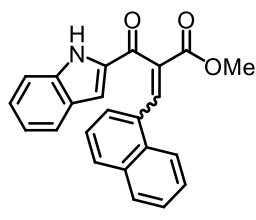
4.14 Synthesized Nazarov Substrates N3



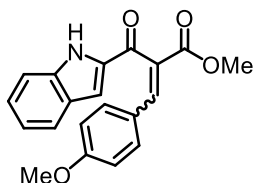
N3a; 79% yield
E/Z 20:1



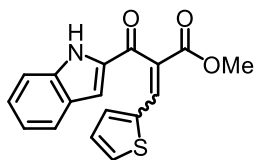
N3b; 61% yield
E/Z 20:1



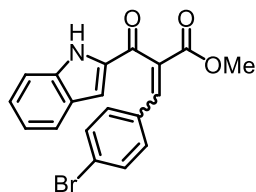
N3c; 78% yield
E/Z 20:1



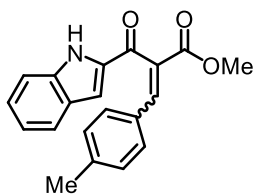
N3d; 93% yield
E/Z 20:1



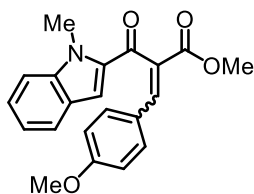
N3e; 72% yield
E/Z 21:1



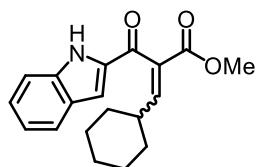
N3f; 64% yield
E/Z 22:1



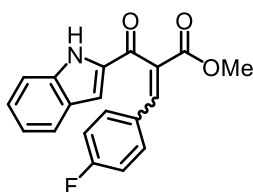
N3g; 76% yield
E/Z 20:1



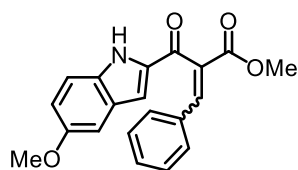
N3h; 26% yield^a
E/Z 7:1



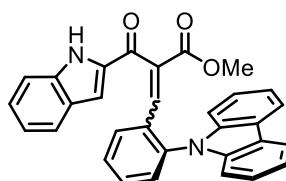
N3i; 61% yield
E/Z 7:1



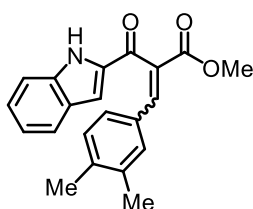
N3j; 80% yield
E/Z 20:1



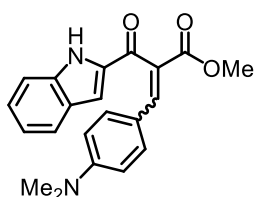
N3k; 60% yield
E/Z 14:1



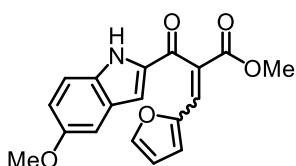
N3l; 73% yield
E/Z 20:1



N3m; 75% yield
E/Z 20:1

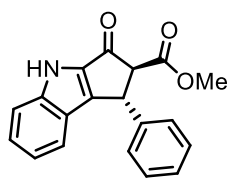


N3n; 71% yield
E/Z >30:1

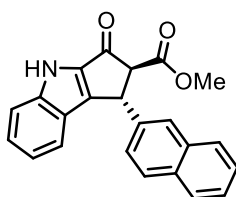


N3o; 69% yield
E/Z 20:1

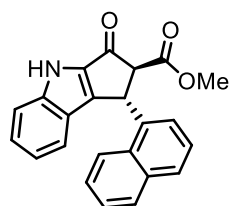
4.15 Synthesized Nazarov Products N4



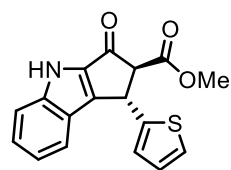
N4a; 75% yield
93% ee, *trans/cis* 15:1
(1:1.8)



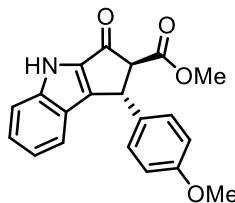
N4b; 12 h; 90% yield
95% ee, *trans/cis* 18:1
(3.7:1)



N4c; 12 h; 70% yield
96% ee, *trans/cis* 18:1
(1:6)



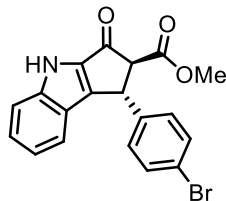
N4e; 24 h; 80% yield
93% ee, *trans/cis* 17:1
(2.6:1)



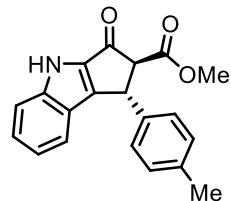
N4d

With Δ -**C5f**: 4.5 h; 86% yield,
89% ee, *trans/cis* 13:1 (1:2.5)

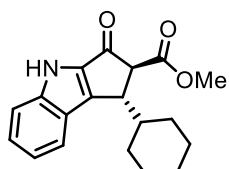
With Δ -**C5g**: 2.5 h; 85% yield,
–89% ee, *trans/cis* 12:1 (1:1)



N4f; 24 h; 82% yield
96% ee, *trans/cis* 12:1
(12:1)



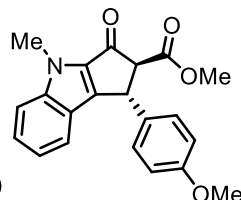
N4g; 12 h; 85% yield
93% ee, *trans/cis* 15:1
(1:1)



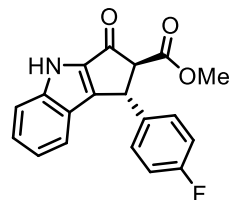
N4i

With Δ -**C5f**: 168 h; 85% yield,
58% ee, *trans/cis* >20:1 (>20:1)

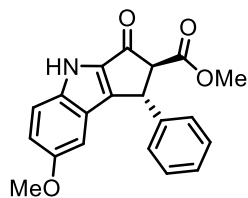
With Δ -**C5g**: 96 h; 89% yield
–58% ee, *trans/cis* >20:1 (>20:1)



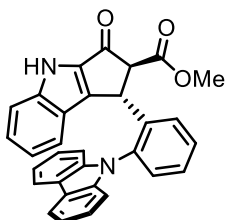
N4h; 6 h; 84% yield
88% ee, *trans/cis* 13:1
(1.7:1)



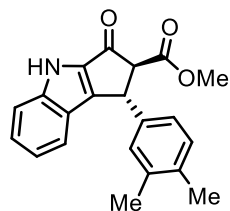
N4j; 24 h; 79 yield
97% ee, *trans/cis* 13:1
(13:1)



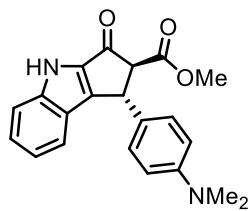
N4k; 12 h; 75% yield
97% ee, *trans/cis* 13:1
(4.5:1)



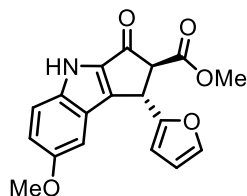
N4l; 48 h; 93% yield
95% ee, *trans/cis* 28:1
(2.5:1)



N4m; 15 h; 83% yield
95% ee, *trans/cis* 16:1
(2.2:1)



N4n; 24 h, 82%, yield
60% ee, *trans/cis* 12:1
(9.4:1)



N4o; 96 h, 46% yield
50% ee, *trans/cis* 20:1
(10:1)

4.16 List of Abbreviations

°	degree
°C	degrees celsius
$[\alpha]_D^{27}$	specific rotation for a given temperature (27 °C) and wavelength (D line)

A

Å	angstrom
A ⁺	acid
α	alpha position
<i>Acac</i>	acetylacetonato ligand acetylacetone
ACDC	asymmetric counterion directed catalysis
AcOH	acetic acid
AgBr	silver bromide
AgCl	silver chloride
AgOTf	Silver trifluoromethanesulfonate or silver triflate
AgSbF ₆	silver hexafluoroantimonate
AL	ancillary ligand
Al ₂ O ₃	aluminium oxide
ArBr	aryl bromide
ArMgBr	aryl magnesium bromide, a GRIGNARD reagent
ATR	attenuated total reflection

B

β	beta position
Ba(OH) ₂	barium hydroxide
BArF ₂₄ ⁻	tetrakis(3,5-bis(trifluoromethyl)phenyl)borate
BBr ₃	boron tribromide
BH ₃ · THF	borane THF complex

BI DIME	(<i>S</i>)-3- <i>tert</i> -Butyl-4-(2,6-dimethoxyphenyl)-2,3-dihydrobenzo-[<i>d</i>]-[1,3]oxaphosphole
Bo	benzoxazole
B(OH) ₂	boronic acid
<i>BOX</i>	bisoxazoline ligand
Bpin	pinacolato boron
br	broad signal
Bt	benzthiazole
C	
<i>c</i>	concentration: in the context of polarimetry the unit are: g/100 mL
C1	racemic dimer complex
C2	diastereomer complex
C3	diastereomer complex after cross-coupling reaction
cat.	catalyst
CD	circular dichroism
CDCl ₃	deuterated chloroform
CD ₂ Cl ₂	deuterated dichloromethane
CD ₃ NO ₂	deuterated nitromethane
CFC1 ₃	trichlorofluoromethane
CH	carbon-hydrogen bond
CH ₂ Cl ₂	dichloromethane
CHCl ₃	chloroform
CH ₃ CN	acetonitrile
C ₆ H ₆	benzene
ClO ₄ ⁻	chlorate
CO ₂	carbon dioxide
Co(ClO ₄) ₂	cobalt(II) chlorate
cod	1,5-cyclooctadiene
conc.	concentration

conv.	Conversion
CuBr ₂	copper bromide
CuCl ₂	copper(II) chloride
Cu(ClO ₄) ₂	copper(II) chlorate
D	
D	sodium line ($\lambda = 589$ nm)
<i>d</i>	days in the context of time
	doublet in the context of NMR spectroscopy
dd	double doublet
DABCO	1,4-diazabicyclo[2.2.2]octan
DCC	<i>N,N'</i> -dicyclohexylcarbodiimid
DCE	1,2-dichloroethane
DIBAL-H	diisobutylaluminiumhydrid
DIPEA	<i>N,N</i> -diisopropylethylamine
DME	dimethoxyethane
DMSO	dimethyl sulfoxide
DMSO- <i>d</i> ₆	deuterated dimethyl sulfoxide
dppf	1,1'-bis(diphenylphosphino)ferrocene
d.r.	diastereomeric ratio
dtbpy	4,4'-Di- <i>tert</i> -butyl-2,2'-bipyridine
E	
<i>E</i>	moieties with highest priority are on opposite side of a double bond
E ⁺	electrophile
ee	enantiomeric excess
eq.	equivalent
ESI	electrospray ionization
Et ₃ N	triethylamine
Et ₂ O	diethyl ether

~ Appendix – List of Abbreviations ~

EtOAc ethyl acetate

EtOH ethanol

F

Fe(ClO₄)₂ iron(II) chlorate

Fe(OTf)₂ iron(II) triflate

FT-IR fourier-transform infrared spectroscopy

H

h hour

H hydrogen

H₂ gaseous hydrogen

HCl hydrochloric acid

HCO₂H formic acid

HCO₂Na sodium formate

HFIP hexafluoro-*iso*-propanol

H₂O Water

H₂O₂ hydrogen peroxide

HPLC high performance liquid chromatography

HR-MS high-resolution mass spectrometry

Hz hertz

I

*i*Pr propyl

Ir(III) iridium(III)

IR infrared spectroscopy

IrCl₃·XH₂O iridium(III) chloride hydrate

J

J coupling constant

K

K	kelvin
K ₂ CO ₃	potassium carbonate
KH	potassium hydride
KOH	potassium hydroxide
KOtBu	potassium <i>tert</i> -butoxide
K ₃ PO ₄	tripotassium phosphate

L

L	ligand
LDA	lithium diisopropylamide
LED	light-emitting diode
LiHMDS	lithium bis(trimethylsilyl)amide
LIFDI	liquid injection field desorption ionization

M

μ	micro when used as a prefix for units
	hapticity in the context of complex naming conventions
μm	micrometer
m	multiplet in the context of NMR spectroscopy
	medium in the context of IR spectroscopy
<i>m</i>	<i>meta</i>
M	metal in the context of metal complexes.
	molecular weight in the context of mass spectrometry
Me	methyl
MeI	iodomethane
MeO	methoxy group
MeOCH ₂ CH ₂ OH	methoxyethanol
MeOH	methanol
Min	minute

~ Appendix – List of Abbreviations ~

mL	milli liter
μM	micromolar
mM	millimolar
MS	molecular sieve
MsCl	mesyl chloride
MTBE	methyl- <i>tert</i> -butyl ether
N	
N	nitrogen
N ₂	molecular nitrogen
n.a.	
NaBH ₄	sodium borohydride
Na ₂ CO ₃	sodium carbonate
NaH	sodium hydride
NaOH	sodium hydroxide
n.d.	not determined
NHC	N-heterocyclic carbene
NH ₄ PF ₆	ammonium hexafluorophosphate
Ni(NTf ₂) ₂	nickel(II) bistriflimide
Ni(PPh ₃)Cl ₂	dichlorobis(triphenylphosphine)nickel(II)
nm	nanometer
NMe ₂	dimethylamin
NMR	nuclear magnetic resonance
<i>N,O</i>	bidentate ligand coordinating with one oxygen atom and nitrogen atom
NO ₂	nitrogroup
NTf ₂	bistriflimide
Nu ⁻	nucleophile
O	
<i>o</i>	<i>ortho</i>

O	oxygen
O ₂	molecular oxygen
<i>O,O</i>	bidentate ligand coordinating with two oxygen atoms
ORTEP	Oak Ridge Thermal Ellipsoid Plot
TfO	trifluoromethanesulfonate or triflate
 P	
<i>p</i>	<i>para</i>
Pd/C	palladium on activated charcoal
Pd ₂ (dba) ₃	tris(dibenzylideneacetone)dipalladium(0)
Pd(OAc) ₂	palladium acetate
Pd(PPh ₃) ₄	tetrakis(triphenylphosphine)palladium(0)
PF ₆ ⁻	hexafluorophosphate
Ph	phenyl
Pigiphos	
PMP	<i>para</i> -methoxyphenyl
ppm	parts per million
P(<i>t</i> Bu) ₃	<i>tert</i> -butyl phosphane
PTFE	polytetrafluoroethylene
PyBOX	pyridine bisoxazoline ligand
 Q	
quant.	quantitative
 R	
R	residue
<i>rac.</i>	Racemic
Ru(II)	rhodium(III)
rt	room temperature

S

S	sulfur
	selectivity factor in the context of kinetic resolution
s	singlet in the context of NMR spectroscopy
	strong in the context of IR spectroscopy
S ₈	sulfur, crown
SOCl ₂	thionyl chloride
SPhos	2-dicyclohexylphosphino-2',6'-dimethoxybiphenyl

T

t	triplet
T	temperature
TAA	<i>tert</i> -amylalkohol or 2-Methyl-2-butanol
TADDOL	$\alpha,\alpha,\alpha',\alpha'$ -tetraaryl-2,2-disubstituted 1,3-dioxolane-4,5-dimethanol
<i>t</i> Bu	<i>tert</i> -butyl
<i>t</i> -BuLi	<i>tert</i> -Butyllithium
TLC	thin layer chromatography
<i>TMP</i>	trimethoxyphenyl
t _R	retention time
TEMPO	(2,2,6,6-Tetramethylpiperidin-1-yl)oxyl
TFA	trifluoroacetic acid
Tf ₂ O	trifluoromethanesulfonate anhydrid
TfOH	trifluoromethanesulfonic acid or triflic acid
THF	tetrahydrofuran
TMS	trimethylsilane in context of protecting groups for alcohols
	tetramethylsilane in context of NMR analysis

U

UV	ultraviolet light
----	-------------------

~ Appendix – List of Abbreviations ~

V

$\tilde{\nu}$ wavenumber in the unit cm^{-1}

Vis visible

v/v volume to volume ratio

W

w weak

X

XPhos 2-Dicyclohexylphosphino-2',4',6'-triisopropylbiphenyl

XRD X-ray diffraction

Xy xylyl or dimethylphenyl

Z

Z moieties with highest priority are on the same side of a double bond

5 Literature

- [1] Kilian Muñiz, *Chem. Unserer Zeit*, **2006**, *40*, 112–124.
- [2] a) M. Chavarot, S. Ménage, O. Hamelin, F. Charnay, J. Pécaut, M. Fontecave, *Inorg. Chem.* **2003**, *42*, 4810–4816; b) O. Hamelin, M. Rimboud, J. Pécaut, M. Fontecave, *Inorg. Chem.* **2007**, *46*, 5354–5360.
- [3] C. Ganzmann, J. A. Gladysz, *Chem. - Eur. J.* **2008**, *14*, 5397–5400.
- [4] a) L.-A. Chen, W. Xu, B. Huang, J. Ma, L. Wang, J. Xi, K. Harms, L. Gong, E. Meggers, *J. Am. Chem. Soc.* **2013**, *135*, 10598–10601; b) H. Huo, C. Fu, C. Wang, K. Harms, E. Meggers, *Chem. Commun.* **2014**, *50*, 10409–10411.
- [5] Synthesis of the benzoxazole and benzothiazole core moiety: a) Y.-X. Chen, L.-F. Quian, W. Zhang, B. Han, *Angew. Chem., Int. Ed.* **2008**, *47*, 9330–9333; b) T. B. Nguyen, L. Ermolenko, P. Retailleau, A. Al-Mourabit, *Angew. Chem., Int. Ed.* **2014**, *53*, 13808–13812.
- [6] M. Nonoyama, *Bull. Chem. Soc. Jpn.* **1974**, *47*, 767–768.
- [7] Auxiliary-mediated method for the synthesis of octahedral transition metal complexes: a) E. Meggers, *Chem. Eur. J.* **2010**, *16*, 752–758; b) O. Chepelin, J. Ujma, X. Wu, A. M. Z. Slawin, M. B. Pitak, S. J. Coles, J. Michel, A. C. Jones, P. E. Barran, P. J. Lusby, *J. Am. Chem. Soc.* **2012**, *134*, 19334–19337; c) E. Marchi, R. Sinisi, G. Bergamini, M. Tragni, M. Monari, M. Bandini, P. Ceroni, *Chem. Eur. J.* **2012**, *18*, 8765–8773; d) L. Gong, M. Wenzel, E. Meggers, *Acc. Chem. Res.* **2013**, *46*, 2635–2644; e) M. Helms, Z. Lin, L. Gong, K. Harms, E. Meggers, *Eur. J. Inorg. Chem.* **2013**, 4164–4172; f) D. L. Davies, K. Singh, S. Singh, B. Villa-Marcos, *Chem. Commun.* **2013**, *49*, 6546–6548; g) M. Helms, C. Wang, B. Orth, K. Harms, E. Meggers, *Eur. J. Inorg. Chem.* **2016**, 2896–2901; h) S.-Y. Yao, Y.-L. Ou, B.-H. Ye, *Inorg. Chem.* **2016**, *55*, 6018–6026. See also ref. [4] and [9].
- [8] Selected examples dealing with the racemic synthesis of bis-cyclometalated iridium(III) complexes: a) S. Lamansky, P. Djurovich, D. Murphy, F. Abdel-Razzag, H. Lee, C. Adachi, P. E. Burrows, S. R. Forrest, M. E. Thompson, *J. Am. Chem. Soc.* **2001**, *123*, 4304–4312; b) M. S. Lowry, W. R. Hudson, R. A. Pascal, Jr., S. Bernhard, *J. Am. Chem. Soc.* **2004**, *126*, 14129–14135; c) M. Xu, W. Li, Z. An, Q. Zhou, G. Wang, *Appl. Organomet. Chem.* **2005**, *19*, 1225–1231; d) A. S. Ionkin, W. J. Marshall, B. M. Fish, *Organometallics* **2006**, *25*, 1461–1471; e) M. Lepeltier, T. Lee, K. Lo, L. Toupet, H. Bozec, V. Guerschais, *Eur. J. Inorg. Chem.* **2007**, (18), 2734–2747; f) T. Chen, *J. Organomet. Chem.* **2008**, *693*, 3117–3170; g) J. J. Kim, Y. You, Y.

Park, J. Kim, S. Y. Park, *J. Mater. Chem.* **2009**, *19*, 8347–8359; h) E. Baranoff, B. F. E. Curchod, F. Monti, F. Steimer, G. Accorsi, I. Tavernelli, U. Rothlisberger, R. Scopelliti, M. Grätzel, M. K. Nazeeruddin, *Inorg. Chem.* **2012**, *51*, 799–811; i) A. M. Prokhorov, A. Santoro, J. A. G. Williams, D. W. Bruce, *Angew. Chem. Int. Ed.* **2012**, *51*, 95–98; *Angew. Chem.* **2012**, *124*, 99–102; j) J. Dai, K. Zhou, M. Li, H. Sun, Y. Chen, S. Su, X. Pu, Y. Huang, Z. Lu, *Dalton Trans.* **2013**, *42*, 10559–10571; k) B. Liang, S. Hu, Y. Liu, Z. Fan, X. Wang, W. Zhu, H. Wu, Y. Cao, *Dyes and Pigments* **2013**, *99*, 41–51; l) D. R. Whang, K. Sakai, S. Y. Park, *Angew. Chem. Int. Ed.* **2013**, *52*, 11612–11615; *Angew. Chem.* **2013**, *125*, 11826–11829; m) E. Baranoff, B. F. E. Curchod, F. Monti, F. Steimer, G. Accorsi, I. Tavernelli, U. Rothlisberger, R. P. Lanoe, C. M. Tong, R. W. Harrington, M. R. Probert, W. Clegg, J. A. G. Williams, V. N. Kozhevnikov, *Chem. Commun.* **2014**, *50*, 6831–6834; n) Z. Niu, T. Zheng, Y. Su, P. Wang, X. Li, F. Cui, J. Liang, G. Li, *New J. Chem.* **2015**, *39*, 6025–6033; o) C. Pei, P. Cui, C. Mc Cleese, S. Kilina, C. Burda, W. Sun, *Dalton trans.* **2015**, *44*, 2176–2190; p) A. Paul, N. Das, Y. Halpin, J. G. Vos, M. T. Pryce, *Dalton Trans.* **2015**, *44*, 10423–10430; q) J. Kim, K. H. Lee, S. J. Lee, H. W. Lee, Y. K. Kim, Y. S. Kim, S. S. Yoon, *Chem. Eur. J.* **2016**, *22*, 4036–4045.

[9] T. Cruchter, M. G. Medvedev, X. Shen, T. Mietke, K. Harms, M. Marsch, E. Meggers *ACS Catal.* **2017**, *7*, 5151–5162.

[10] Examples for cross-coupling on axial chiral binaphthol derivatives: a) P. Wipf, J. K. Jung, *J. Org. Chem.* **2000**, *65*, 6319–6337; b) W. C. P. Tsang, R. R. Schrock, A. H. Hoveyda *Organometallics* **2001**, *20*, 5658–5669; c) R. I. Storer, D. E. Carrera, Y. Ni, D. W. C. MacMillan, *J. Am. Chem. Soc.* **2006**, *128*, 84–86; d) M. Yamanaka, J. Itoh, K. Fuchibe, T. Akiyama, *J. Am. Chem. Soc.* **2007**, *129*, 6756–6764; e) X. Cheng, R. Goddard, G. Buth, B. List, *Angew. Chem. Int. Ed.* **2008**, *47*, 5079–5081; *Angew. Chem.* **2008**, *120*, 5157–5159; f) M. Klussmann, L. Ratjen, S. Hoffmann, V. Wakchaure, R. Goddard, B. List, *Synlett* **2010**, (14), 2189–2192; g) B. Li, P. Chiu, *Eur. J. Org.* **2011**, 3932–3937; h) F. Romanov–Michailidis, L. Guénée, A. Alexakis, *Angew. Chem. Int. Ed.* **2013**, *52*, 9266–9270; *Angew. Chem.* **2013**, *125*, 9436–9440; i) D. Parmar, E. Sugiono, S. Raja, M. Rueping, *Chem. Rev.* **2014**, *114*, 9047–9153; j) B. Qu, N. Haddad, S. Rodriguez, J. D. Sieber, J. Desrosiers, N. D. Patel, Y. Zhang, N. Grinberg, H. Lee, S. Ma, U. J. Ries, N. K. Yee, C. H. Senanayake, *J. Org. Chem.* **2016**, *81*, 745–750.

[11] Examples for cross-coupling on planar chiral cyclophanes: a) Y. Morisaki, Y. Chujo, *Macromolecules* **2003**, *36*, 9319–9324; b) Y. Morisaki, Y. Chujo, *Macromolecules* **2004**, *37*, 4099–4103; c) Y. Morisaki, Y. Chujo, *Chem. Lett.* **2012**, *41*, 840–846; d) M. Cakici, Z. Gu, M.

Nieger, J. Bürck, L. Heinke, S. Bräse, *Chem. Commun.* **2015**, 51, 4790–4798; e) D. Enders, M. Ludwig, G. Raabe, *Chirality* **2012**, 24, 215–222; f) M. Cakici, S. Bräse, *Eur. J. Org. Chem.* **2012**, 6132–6135; g) C. Braun, E. Spurling, N. B. Heine, M. Cakici, M. Nieger, S. Bräse, *Adv. Synth. Catal* **2016**, 358, 1664–1670.

[12] For precedence on the cross-coupling at iridium(III) complexes: a) *New J. Chem.* **2001**, 25, 1136–1147 b) W. Leslie, A. S. Batsanov, J. A. K. Howard, J. A. G. Williams, *Dalton Trans.* **2004**, 623–631; c) J. A. G. Williams, *Chem. Commun.* **2005**, 230–232; d) K. J. Arm, J. A. G. Williams, *Dalton Trans.* **2006**, 2172–2174; e) H. A. Bronstein, C. E. Finlayson, K.R. Kirov, R. H. Friend, C. K. Williams, *Organometallics* **2008**, 27, 2980–2989; f) J. A. G. Williams, A. J. Wilkinson, V. L. Whittle, *Dalton Trans.* **2008**, 2081–2099; g) K. J. Arm, V. L. Whittle, J. A. G. Williams, *Inorg. Chem.* **2008**, 47, 6596–6607; h) J. A. G. Williams, *Chem. Soc. Rev.* **2009**, 38, 1783–1801; i) V. L. Whittle, J. A. G. Williams, *Dalton Trans.* **2009**, 3929–3940; j) N. Akino, R. Okamura, *Metal complex, polymer compound and device containing those*, EP 2128168 A1, **2009**; k) G. Liaptsis, D. Hertel, K. Meerholz, *Angew. Chem. Int. Ed.* **2013**, 52, 9563–9567; *Angew. Chem.* **2013**, 125, 9742–9746; l) A. Liang, K. Zhang, J. Zhang, F. Huang, X. Zhu, Y. Cao, *Chem. Mater.* **2013**, 25, 1013–1019; m) M. Lian, Y. Yu, J. Zhao, Z. Huang, X. Yang, G. Zhou, Z. Wu, D. Wang, *J. Mater Chem. C* **2014**, 2, 9523–9535; n) J. Pérez-Miqueo, A. Telleria, M. Muñoz- Olasagasti, A. Altube, E. Garcia-Lecina, A. de Cózar, Z. Freixa, *Dalton Trans.* **2015**, 2075–2091; o) A. Telleria, J. Pérez-Miqueo, A. Altube, E. Garcia-Lecina, A. de Cózar, Z. Freixa, *Organometallics* **2015**, 34, 5513–5529; p) Z. Huang, B. Liu, Y. He, X. Yan, X. Yang, X. Xu, G. Zhou, Y. Ren, Z. Wu, *J. Organomet. Chem.* **2015**, 794, 1–10; q) R. Muñoz-Rodríguez, E. Buñuel, N. Fuentes, J. A. G. Williams, D. J. Cárdenas, *Dalton Trans.* **2015**, 44, 8394–8405.

[13] Examples for bis-cyclometalated iridium complexes as (photoactive) chiral Lewis acid catalysts: a) H. Huo, C. Fu, K. Harms, E. Meggers, *J. Am. Chem. Soc.* **2014**, 136, 2990–2993; b) H. Huo, X. Shen, C. Wang, L. Zhang, P. Röse, L. Chen, K. Harms, M. Marsch, G. Hilt, E. Meggers, *Nature* **2014**, 515, 100–103; c) X. Shen, H. Huo, C. Wang, B. Zhang, K. Harms, E. Meggers, *Chem. Eur. J.* **2015**, 21, 9720–9726; d) H. Huo, C. Wang, K. Harms, E. Meggers, *J. Am. Chem. Soc.* **2015**, 137, 9551–9554; e) C. Wang, Y. Zheng, H. Huo, P. Röse, L. Zhang, K. Harms, G. Hilt, E. Meggers, *Chem. Eur. J.* **2015**, 21, 7355–7359; f) C. Wang, J. Qin, X. Shen, R. Riedel, K. Harms, E. Meggers, *Angew. Chem. Int. Ed.* **2016**, 55, 685–688; *Angew. Chem.* **2016**, 128, 695–698; g) G.-Q. Xu, H. Liang, J. Fang, Z.-L. Jia, J.-Q. Chen, P.-F. Xu, *Chem. Asian J.* **2016**, 11, 3355–3358.

- [14] Examples for oxidative addition steps in cross-coupling with TfO: a) S. E. Denmark, R. F. Sweis, *Org. Lett.* **2002**, *4*, 3771–3774; b) S. Riggleman, P. DeShong, *J. Org. Chem.* **2003**, *68*, 8106–8109; c) M. Bonaterra, R. A. Rossi, S. E. Martin, *Organometallics* **2008**, *28*, 933–936; d) A. He, J. R. Falck, *J. Am. Chem. Soc.* **2009**, *132*, 2524–2525.
- [15] Triflating agents: a) W. J. Scott, J. E. Mc Murry, *Tetrahedron Lett.* **1983**, *24*, 979–982; b) A. Dehghani, D. L. Comins, *Tetrahedron Lett.* **1992**, *33*, 6299–6302.
- [16] M. Cui, X. Wang, P. Yu, J. Zhang, Z. Li, X. Zhang, Y. Yang, M. Ono, H. Jia, H. Saji, B. Liu, *J. Med. Chem.* **2012**, *55*, 9283–9296.
- [17] For air sensitivity of organozinc and moisture sensitivity organomagnesium compounds see: a) T. R. Crompton, *Analysis of Organoaluminium and Organozinc Compounds*, Pergamon Press, Oxford **1968**; b) K. P. C. Vollhardt, N. E. Schore, *Organische Chemie*, 4.ed. Wiley–VCH, Weinheim **2011**.
- [18] For toxicologic studies on organotin and organoboron compounds see: a) A.H. Soloway, *Science*, **1958**, *128*, 1572–1574; b) A. H. Soloway, B. Whitman, J. R. Messer, *J. Med. Pharm. Chem.* **1962**, *7*, 640; c) D. S. Matteson, A. H. Soloway, D. W. Tomlinson, J. D. Campbell, and G. A. Nixon, *J. Med. Chem.* **1964**, *7*, 640–643; d) M. R. Krigman, A. P. Silverman, *Neurotoxicology* **1984**, *5*, 129–139; e) M. Benderdour, T. Bui-Van, A. Dicko, F. Belleville, *J. Trace Elem. Med. Biol.* **1998**, *12*, 2–7; f) J. N. Cambre, B. S. Sumerlin *Polymer* **2011**, *52*, 4631–4643; g) M. A. Soriano-Ursúa, E. D. Farfán-García, Y. López-Cabrera, E. Querejeta, J. G. Trujillo-Ferrara, *Neurotoxicology* **2014**, *40*, 8–15.
- [19] For biaryl phosphine ligands in palladium-catalyzed cross-coupling reactions see: a) S. D. Walker, T. E. Barder, J. R. Martinelli, S. L. Buchwald, *Angew. Chem. Int. Ed.* **2004**, *43*, 1871–1876; *Angew. Chem.* **2004**, *116*, 1907–1912; b) T. E. Barder, S. D. Walker, J. R. Martinelli, S. L. Buchwald, *J. Am. Chem. Soc.* **2005**, *127*, 4685–4696; c) D. S. Surry, S. L. Buchwald, *Angew Chem Int Ed.* **2008** *47* 338–6361; d) P. G. Gildner, T. J. Colacot, *Organometallics* **2015**, *34*, 5497–5508; e) R. Martin, S. L. Buchwald, *Acc. Chem. Res.* **2008**, *41*, 1461–1473; f) Q. Zhao, C. Li, C. H. Senanayake, W. Tang, *Chem. Eur. J.* **2013**, *19*, 2261–2265 g) B. Qu, N. Haddad, S. Rodriguez, J. D. Sieber, J.-N. Desrosiers, N. D. Patel, Y. Zhang, N. Grinberg, H. Lee, S. Ma, U. J. Ries, N. K. Yee, C. H. Senanayake, *J. Org. Chem.* **2016**, *81*, 745–750; h) Nitinchandra D. Patel Daniel Rivalti, Frederic G. Buono, Arindom Chatterjee, Bo Qu, Stefan Braith, Jean-Nicolas Desrosiers, Sonia Rodriguez, Joshua D. Sieber, Nizar Haddad, Keith R. Fandrick, Heewon Lee, Nathan K. Yee, Carl A. Busacca, Chris H. Senanayake, *Asian J. Org. Chem.* **2017**, *6*, 1285–1291.

- [20] A. G. Crawford, Z. Liu, I. A. I. Mkhaliid, M. Thibault, N. Schwarz, G. Alcaraz, A. Steffen, J. C. Collings, A. S. Batsanov, J. A. K. Howard, T. B. Marder, *Chem. Eur. J.* **2012**, *18*, 5022–5035.
- [21] a) X. Chen, Y. Okamoto, T. Yano, J. Otsuki, *J. Sep. Sci.* **2007**, *30*, 713–716; b) H. Sato, K. Tamura, M. Taniguchi, A. Yamagishi, *New J. Chem.* **2010**, *34*, 617–622.
- [22] For an excerpt on reactions catalized by stereogenic-at-metal rhodium(III) complexes see: a) X. Shen, K. Harms, M. Marsch, E. Meggers, *Chem. Eur. J.* **2016**, *22*, 9102–910; b) S. Luo, X. Zhang, Y. Zheng, K. Harms, L. Zhang, E. Meggers, *J. Org. Chem.* **2017**, *82*, 8995–9005; c) S. Chen, X. Huang, E. Meggers, K. N. Houk, *J. Am. Chem. Soc.* **2017**, *139*, 17902–17907; d) J. Ma, A. R. Rosales, X. Huang, K. Harms, R. Riedel, O. Wiest, and E. Meggers, *J. Am. Chem. Soc.* **2017**, *139*, 17245–17248; e) X. Huang, X. Li, X. Xie, R. Riedel, E. Meggers, *Nat. Commun.* **2017**, *8*, 2245; f) J. Ma, X. Xie, E. Meggers, *Chem. Eur. J.* **2018**, *24*, 259–265; see also reference [53].
- [23] M. J. Neeb, C. A. Sehon, A. Q. Viet, K. B. Goodman, G. Z. Wang, *Morpholinyl and pyrrolidinyl analogs*, WO 2008011551 A1, **2008**.
- [24] Cross-coupling on benzaldehydes **S1a-b**: a) V. Mamane, P. Hannen, A. Fürstner, *Chem. Eur. J.* **2004**, *10*, 4556–4575; b) T. E. Barder, S. D. Walker, J. R. Martinelli, S. L. Buchwald, *J. Am. Chem. Soc.* **2005**, *127*, 4685–4696.
- [25] R. H. Contreras, T. Llorente, L. C. Ducati, C. F. Tormena, *J. Phys. Chem. A* **2014**, *118*, 5068–5075.
- [26] E. Winterling, *Synthese chiraler Iridiumkomplexe via late-stage Suzuki-Kupplung als asymmetrische Katalysatoren*, unv. Diss., Philipps-University of Marburg, Marburg **2015**.
- [27] J. Meinecke, *Synthese sterisch anspruchsvoller Iridiumkomplexe via late-stage Suzuki-Kupplung mit Anwendung in der asymmetrischen Organokatalyse*, unv. Diss., Philipps-University of Marburg, Marburg **2015**.
- [28] M. Murata, T. Oyama, S. Watanabe, Y. Masuda, *J. Org. Chem.* **2000**, *65*, 164–168.
- [29] Application of the cross-coupling protocol: a) A. Larionov, T. Cruchter, T. Mietke, E. Meggers *Organometallics* **2017**, *36*, 1457–1460; b) T. Cruchter, *Design, Synthesis, and Application of a Nucleophilic Octahedral Stereogenic-Only-at-Metal Iridium(III) Catalyst*, unv. Diss., Philipps-University of Marburg, Marburg **2018**. See also reference [9]; c) J. Ma, A.

R. Rosales, X. Huang, K. Harms, R. Riedel, O. Wiest, E. Meggers, *J. Am. Chem. Soc.* **2017**, *139*, 17245–17248.

[30] a) S. Handa, M. P. Andersson, Fabrice Gallou, J. Reilly, B. H. Lipshutz, *Angew. Chem. Int. Ed.* **2016**, *55*, 4914–4918; *Angew. Chem.* **2016**, *128*, 4998–5002.

[31] a) E. Davies, R. Renner, *Chem. World* **2011**, *1*, 50–54; b) P. Mike, *New Sci.* **2011**, *2*, 2799.

[32] Examples for palladium catalyzed cross-coupling reactions using catalyst on a part per million scale: a) R. K. Arvela, N. E. Leadbeater, M. S. Sangi, V. A. Williams, P. Granados, R. D. Singer, *J. Org. Chem.* **2005**, *70*, 161–168; b) N. E. Leadbeater, V. A. Williams, T. M. Barnard, M. J. Collins, *Org. Process Res. Dev.* **2006**, *10*, 833–837; c) S. M. Wong, C. M. So, K. H. Chung, C. P. Lau, F. Y. Kwong, *Eur. J. Org. Chem.* **2012**, 4172–4177; d) Z. Dong, Z. Ye, *Adv. Synth. Catal.* **2014**, *356*, 3401–3414; e) C. Deraedt, L. Salmon, D. Astruc, *Adv. Synth. Catal.* **2014**, *356*, 2525–2538.

[33] For an overview on nickel catalysts in cross-coupling reactions: a) F.-S. Han, *Chem. Soc. Rev.* **2013**, *42*, 5270–5298; b) S. Z. Tasker, E. A. Standley, T. F. Jamison, *Nature* **2014**, *509*, 299–309; c) S. Handa, E. D. Slack, B. H. Lipshutz, *Angew. Chem. Int. Ed.* **2015**, *54*, 11994–11998; *Angew. Chem.* **2015**, *127*, 12162–12166.

[34] For an overview on supported copper catalysts in cross-coupling reactions: a) M. B. Thathagar, J. Beckers, G. Rothenberg, *J. Am. Chem. Soc.* **2002**, *124*, 11858–11859; b) J. Mao, J. Huo, F. Fang, S.-J. Ji, *Tetrahedron* **2008**, *64*, 3905–3911.

[35] S. K. Gurung, S. Thapa, A. Kafle, D. A. Dickie, R. Giri, *Org. Lett.* **2014**, *16*, 1264–1267.

[36] For more details on immobilized homogenous catalysts see: a) W. Keima, *Green Chemistry* **2003**, *5*, 105–111; b) C. E. Songa, *Annu. Rep. Prog. Chem., Sect. C: Phys. Chem.* **2005**, *101*, 143–173; c) K. Ding, Y. Uozumi, *Handbook of Asymmetric Heterogeneous Catalysis*, Wiley–VCH: New York, **2008**;

[37] For reviews on the NAZAROV cyclization, see: a.) A. J. Frontier, C. Collison, *Tetrahedron* **2005**, *61*, 7577–7606; b.) T. Vaidya, R. Eisenberg, A. J. Frontier, *ChemCatChem* **2011**, *3*, 1531–1548; c.) T. Itoh, T. Nokami, M. Kawatsura, *Chem. Rec.* **2016**, *16*, 1676–1689; d.) M. G. Vinogradov, O. V. Turova, S. G. Zlotin, *Org. Biomol. Chem.* **2017**, *15*, 8245–8269.

[38] For a review on the synthesis of chiral cyclopentenones, see: S. P. Simeonov, J. P. M. Nunes, K. Guerra, V. B. Kurteva, C. A. M. Afonso, *Chem. Rev.* **2016**, *116*, 5744–5893.

[39] For applications of the NAZAROV cyclization for natural product synthesis, see: a.) P. E. Harrington, M. A. Tius, *J. Am. Chem. Soc.* **2001**, *123*, 8509–8514; b.) Y. Abdallah, B. Frontier, A. J. Frontier, *Org. Lett.* **2009**, 49–52; c) J. A. Malona, K. Cariou, W. T. Spencer III, A. J. Frontier, *J. Org. Chem.* **2012**, *77*, 1891–1908; d) P. N. Carlsen, T. J. Mann, A. H. Hoveyda, A. J. Frontier, *Angew. Chem. Int. Ed.* **2014**, *53*, 9334–9338; *Angew. Chem.* **2014**, *126*, 9488–9492; e) Z. Zhou, M. A. Tius, *Angew. Chem. Int. Ed.* **2015**, *54*, 6037–6040; f.) G. Sudhakar, K. Satish, *Chem. Eur. J.* **2015**, *21*, 6475–6480; g.) Z. Zhou, D. D. Dixon, A. Jolitt, M. A. Tius, *Chem. Eur. J.* **2016**, *22*, 15929–15936.

[40] For a recent review on asymmetric NAZAROV cyclizations, see: N. Shimada, C. Stewart, M. A. Tius, *Tetrahedron* **2011**, *67*, 5851–5870.

[41] T. Vivekanand, B. Satpathi, S. K. Bankar, S. S. V. Ramasastry, *RSC Adv.* **2018**, *8*, 18576–18588.

[42] Z. Xu, H. Ren, L. Wang, Y. Tang, *Org. Chem. Front.* **2015**, *2*, 811–814.

[43] a) G. Liang, S. N. Gradl, D. Trauner, *Org. Lett.* **2003**, *5*, 4931–4934.

[44] For NAZAROV cyclization with substrates of type A see: a) V. K. Aggarwal, A. J. Belfield, *Org. Lett.* **2003**, *5*, 5075–5078; b) I. Walz, A. Bertogg, A. Togni, *Eur. J. Org. Chem.* **2007**, 2650–2658; c) I. Walz, A. Togni, *Chem. Commun.* **2008**, 4315–4317; d) M. Kawatsura, K. Kajita, S. Hayase, T. Itoh, *Synlett* **2010**, 1243–1246; e) see reference [42].

[45] For NAZAROV cyclization with substrates of type B see: a) A. K. Basak, N. Shimada, W. F. Bow, D. A. Vicic, M. A. Tius, *J. Am. Chem. Soc.* **2010**, *132*, 8266–8267; b) A. H. Asari, Y.-H. Lam, M. A. Tius, and K. N. Houk, *J. Am. Chem. Soc.* **2015**, *137*, 13191–13199; c) K. Kitamura, N. Shimada, C. Stewart, A. C. Atesin, T. A. Atesin, M. A. Tius, *Angew. Chem. Int. Ed.* **2015**, *54*, 6288–6291.

[46] For NAZAROV cyclization with substrates of type C: a) M. Rueping, W. Ieawsuwan, A. P. Antonchick, B. J. Nachtsheim, *Angew. Chem. Int. Ed.* **2007**, *46*, 2097–2100; b) G. E. Hutson, Y. E. Turkmen, V. H. Rawal, *J. Am. Chem. Soc.* **2013**, *135*, 4988–4991.

[47] For NAZAROV cyclization with substrates of type D: a) P. Cao, C. Deng, Y.-Y. Zhou, X.-L. Sun, J.-C. Zheng, Z. Xie, Y. Tang, *Angew. Chem. Int. Ed.* **2010**, *49*, 4463–4466; b) S. Raja, M. Nakajima, M. Rueping, *Angew. Chem. Int. Ed.* **2015**, *54*, 2762–2765; c) T. Takeda, S. Harada, A. Nishida, *Org. Lett.* **2015**, *17*, 5184–5187.

- [48] Example for asymmetric NAZAROV cyclization reactions using chiral iridium complexes: T. Vaidya, A. C. Atesin, I. R. Herrick, A. J. Frontier, R. Eisenberg, *Angew. Chem. Int. Ed.* **2010**, *49*, 3363–3366.
- [49] Examples for reactions from the MEGGERS group using *N,O*-coordinating substrates and iridium(III) complexes as photoredox catalysts: a) see reference [13b]: b) H. Hou, C. Wang, K. Harms, E. Meggers, *J. Am. Chem. Soc.* **2015**, *137*, 9551–9554; c) H. Huo, X. Huang, X. Shen, K. Harms, E. Meggers, *Synlett* **2016**, *27*, 749–753.
- [50] J. Davies, D. Leonori, *Chem. Commun.* **2014**, *50*, 15171–15174.
- [51] C. Wang, L.-A. Chen, H. Huo, X. Shen, K. Harms, L. Gong, E. Meggers, *Chem. Sci.* **2015**, *6*, 1094–1100.
- [52] M. Karplus, *J. Am. Chem. Soc.* **1963**, *85*, 2870–2871.
- [53] L. Zhang, E. Meggers, *Acc. Chem. Res.* **2017**, *50*, 320–330.
- [54] a) I. Colomer, A. E. R. Chamberlain, M. B.- Haughey, T. J. Donohoe, *Nat. Chem. Rev.* **2017**, *1*, 0088; b) D. Leboeuf, L. Marin, B. Michelet, A. Perez-Luna, R. Guillot, E. Schulz, V. Gandon, *Chem. Eur. J.* **2016**, *22*, 16165–16171.
- [55] M. J. McKennon, A. I. Meyers, K. Drauz, M. Schwarm, *J. Org. Chem.* **1993**, *58*, 3568–3571.
- [56] H. A. Wegner, H. Reisch, K. Rauch, A. Demeter, K. A. Zachariasse, A. de Meijere, L. T. Scott, *J. Org. Chem.* **2006**, *71*, 9080-9087.
- [57] APEX3, Bruker AXS Inc., Madison, Wisconsin, USA, **2016**.
- [58] SAINT, Bruker AXS Inc., Madison, Wisconsin, USA, **2015**.
- [59] SADABS. Bruker AXS area detector scaling and absorption correction, Bruker AXS Inc., Madison, Wisconsin, USA, **2016**.
- [60] G. M. Sheldrick, *Acta Crystallogr A Found Adv* **2015**, *71*, 3–8.
- [61] G. M. Sheldrick, T. R. Schneider in *Methods in Enzymology*, Elsevier, **1997**.
- [62] G. M. Sheldrick, *Acta crystallographica. Section C, Structural chemistry* **2015**, *71*, 3–8.
- [63] K. Brandenburg, *Diamond - Crystal and Molecular Structure Visualization*, Crystal Impact, Dr. H. Putz & Dr. K. Brandenburg GbR, Bonn, Germany, **2014**.

- [64] C. B. Hübschle, G. M. Sheldrick, B. Dittrich, *Journal of applied crystallography* **2011**, *44*, 1281–1284.
- [65] [14] APEX2, Bruker AXS Inc., Madison, Wisconsin, USA, **2014**.
- [66] G. M. Sheldrick, *Acta crystallographica. Section A* **2008**, *64*, 112–122.
- [67] G. M. Sheldrick, SHELXT, Universität Göttingen, Germany, **2014**.
- [68] SADABS, Bruker AXS area detector scaling and absorption correction, Bruker AXS Inc., Madison, Wisconsin, USA, **2014**.
- [69] APEX3, Bruker AXS Inc., Madison, Wisconsin, USA, **2015**.
- [70] S. Parsons, H. D. Flack, T. Wagner, *Acta crystallographica. Section B* **2013**, *69*, 249–259.
- [71] X-Area Pilatus3_SV, STOE & Cie GmbH, Darmstadt, Germany, **2016**.
- [72] X-Area Recipe, STOE & Cie GmbH, Darmstadt, Germany, **2015**.
- [73] X-Area Integrate, STOE & Cie GmbH, Darmstadt, Germany, **2016**.
- [74] X-Area LANA, *STOE & Cie GmbH*, Darmstadt, Germany, **2016**.